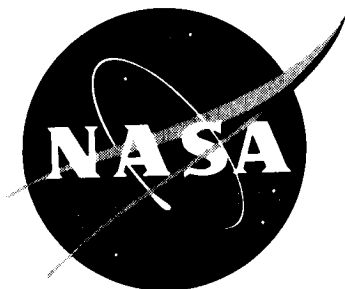


6875-P. 4  
*NASA Conference Publication 3258*

# **Second NASA Aerospace Pyrotechnic Systems Workshop**

*Compiled by*  
William W. St. Cyr  
*John C. Stennis Space Center*  
*Stennis Space Center, Mississippi*

Proceedings of a workshop sponsored by the  
Pyrotechnically Actuated Systems Program  
Office of Safety and Mission Quality  
National Aeronautics and Space Administration  
Washington, D.C., and held at  
Sandia National Laboratories  
Albuquerque, New Mexico  
February 8-9, 1994



National Aeronautics and  
Space Administration  
Office of Management  
Scientific and Technical  
Information Program  
**1994**

# **Workshop Management**

## **NASA Pyrotechnically Actuated Systems Program**

**Norman R. Schulze, NASA Headquarters - Program Manager**

### **Host Representative**

**Jere Harlan - Sandia National Laboratories**

### **Workshop Coordinator**

**William W. St. Cyr - NASA, John C. Stennis Space Center**

## **Workshop Program Committee**

**Norman R. Schulze**  
National Aeronautics and Space Administration  
Code QW  
Washington, DC 20546

**James Gageby**  
The Aerospace Corporation  
P. O. Box 92957  
Los Angeles, CA 90009

**Laurence J. Bement**  
National Aeronautics and Space Administration  
Langley Research Center  
Code 433  
Hampton, VA 23665

**Anthony Agajanian**  
Jet Propulsion Laboratory  
Code 158-224  
4800 Oak Grove Drive  
Pasadena, CA 91109

**William W. St. Cyr**  
National Aeronautics and Space Administration  
John C. Stennis Space Center  
Code KA60 - Building 1100  
Stennis Space Center, MS 39529



## Table of Contents

|   |         |
|---|---------|
| WELCOMING ADDRESS .....   | 1 - 9   |
| <i>Dr. John Stichman, Director, Surety Components and Instrumentation Center,<br/>Sandia National Laboratories</i>  |         |
| NASA Pyrotechnically Actuated Systems Program .....   | 13 - 81 |
| <i>Norman R. Schulze, NASA, Washington DC</i>   |         |
| <br><b>SESSION 1 - Laser Initiation and Laser Systems</b>   |         |
| Laser Initiated Ordnance Activities in NASA .....   | 29 - 2  |
| <i>Norman R. Schulze, NASA, Washington DC</i>   |         |
| Laser-Ignited Explosive and Pyrotechnic Components .....  | 49 - 0  |
| <i>Al Munger, Tom Beckman, Dan Kramer and Ed Spangler,<br/>EG&amp;G Mound Applied Technology</i>  |         |
| A Low Cost Ignitor Utilizing an SCB and Titanium Sub-Hydride Potassium Perchlorate<br>Pyrotechnic .....   | 61 - 3  |
| <i>Robert W. Bickes, Jr. and M. C. Grubelich, Sandia National Laboratories<br/>J. K. Hartman and C. B. McCampbell, SCB Technologies, Inc.<br/>J. K. Churchill, Quantic-Holox</i>  |         |
| Optical Ordnance System for Use in Explosive Ordnance Disposal Activities .....   | 65 - 4  |
| <i>John A. Merson, F. J. Salas and F. M. Helsel, Sandia National Laboratories</i>   |         |
| Laser Diode Ignition .....  | 71 - 5  |
| <i>William J. Kass, Larry A. Andrews, Craig M. Boney, Weng W. Chow,<br/>James W. Clements, Chris Colburn, Scott C. Holswade, John A. Merson,<br/>Fredrick J. Salas, and Randy J. Williams, Sandia National Laboratories<br/>Lane Hinkle, Martin Marietta Specialty Components</i> |         |
| Standardized Laser Initiated Ordnance System .....  | 79 - 6  |
| <i>James V. Gageby, The Aerospace Corporation</i>   |         |
| Miniature Laser Ignited Bellows Motor .....   | 83 - 7  |
| <i>Steven L. Renfro, The Ensign-Bickford Co.</i>  |         |
| Performance Characteristics of a Laser-Initiated NASA Standard Initiator .....  | 93 - 8  |
| <i>John A. Graham, The Ensign-Bickford Co.</i>  |         |
| Four Channel Laser Firing Unit (LFU) Using Laser Diodes .....   | 101 - 9 |
| <i>David Rosner and Edwin Spomer<br/>Pacific Scientific, Energy Dynamics Division</i>   |         |
| LIO Validation on Pegasus (Oral Presentation Only) .....  | 115 - 0 |
| <i>Arthur D. Rhea, The Ensign-Bickford Co.</i>  |         |

## SESSION 2 - Electric Initiation

|  |     |     |
|--|-----|-----|
| EBWs and EFIs - The Other Electric Detonators . . . . .  | 117 | -10 |
| <i>Ron Varosh, Reynolds Industries Systems, Inc.</i>   |     |     |
| Low Cost, Combined RF and Electrostatic Protection for Electroexplosive Devices . . .                    | 125 | -11 |
| <i>Robert L. Dow, Attenuation Technology, Inc.</i>   |     |     |
| Unique Passive Diagnostic for Slapper Detonators . . . . .   | 131 | -12 |
| <i>William P. Brigham and John J. Schwartz, Sandia National Laboratories</i>                             |     |     |
| Applying Analog Integrated Circuits for HERO Protection . . . . .  | 143 | -13 |
| <i>Kenneth E. Willis, Quantic Industries, Inc.</i><br><i>Thomas J. Blachowski, NSWC, Indian Head MD</i>  |     |     |
| Cable Discharge System for Fundamental Detonator Studies . . . . .                                       | 149 | -14 |
| <i>Steven G. Barnhart, Gregg R. Peevy and William P. Brigham,</i><br><i>Sandia National Laboratories</i> |     |     |
| Improved Test Method for Hot Bridgewire All-fire/No-fire Data . . . . .                                  | 165 | -15 |
| <i>Gerald L. O'Barr, Retired (formerly with General Dynamics)</i>  |     |     |

## SESSION 3 - Mechanisms & Explosively Actuated Devices

|  |     |     |
|--|-----|-----|
| Development and Demonstration of an NSI Derived Gas Generating Cartridge (NSGG) . . . . .  | 177 | -16 |
| <i>Laurence J. Bement, NASA, Langley Research Center</i><br><i>Harold Karp, Hi Shear Technology Corp.</i><br><i>Michael C. Magenot, Universal Propulsion Co.</i><br><i>Morry L. Schimmel, Schimmel Company</i> |     |     |
| Development of the Toggle Deployment Mechanism . . . . .   | 191 | -17 |
| <i>Christopher W. Brown, NASA, Johnson Space Center</i>  |     |     |
| The Ordnance Transfer Interrupter, A New Type of S&A Device . . . . .  | 213 | -18 |
| <i>John T. Greenslade, Pacific Scientific, Energy Dynamics Division</i>  |     |     |
| A Very Low Shock Alternative to Conventional, Pyrotechnically Operated Release Devices . . . . .   | 223 | -19 |
| <i>Steven P. Robinson, Boeing Defense &amp; Space Group</i>  |     |     |
| Investigation of Failure to Separate an Inconel 718 Frangible Nut . . . . .  | 233 | -20 |
| <i>William C. Hoffman III and Carl W. Hohmann, NASA, Johnson Space Center</i>  |     |     |

## SESSION 4 - Analytical Methods & Studies

|  |     |     |
|--|-----|-----|
| Bolt Cutter Functional Evaluation . . . . .  | 243 | -21 |
| <i>S. Goldstein, S. W. Frost, J. B. Gageby, T. E. Wong, and R. B. Pan,</i><br><i>The Aerospace Corporation</i> |     |     |
| Choked Flow Effects in the NSI Driven Pin-Puller . . . . .   | 269 | -22 |
| <i>Joseph M. Powers and Keith A. Gonthier, University of Notre Dame</i>  |     |     |

|   |     |     |
|---|-----|-----|
| Finite Element Analysis of the 2.5 Inch Frangible Nut for the Space Shuttle . . . . .                     | 285 | -23 |
| <i>Darin McKinnis, NASA, Johnson Space Center</i>   |     |     |
| Analysis of a Simplified Frangible Joint System . . . . .   | 297 | -24 |
| <i>Steven L. Renfro and James E. Fritz, The Ensign-Bickford Co.</i>                                       |     |     |
| <i>Steven L. Olson, Orbital Sciences Corp.</i>  |     |     |
| Portable, Solid State, Fiber Optic Coupled VISAR for High Speed Motion and Shock<br>Diagnostics . . . . . | 309 | -25 |
| <i>Kevin J. Fleming and O. B. Crump, Jr., Sandia National Laboratories</i>                                |     |     |
| Development and Qualification of a Laser-Ignited, All-Secondary (DDT) Detonator . . .                     | 317 | -26 |
| <i>Steve Tipton, Air Logistics Center (AFMC)</i>  |     |     |
| <i>Thomas J. Blachowski and Darrin Krivitsky, NSWC, Indian Head MD</i>                                    |     |     |

## SESSION 5 - Miscellaneous

|   |     |
|---|-----|
| Pyrotechnically Actuated Systems Database and Catalog . . . . . | 331 |
| <i>Paul Steffes, Analex Corporation</i>                         |     |
| Fire As I've Seen It . . . . .                                  | 337 |
| <i>Dick Stresau, Stresau Laboratory</i>                         |     |

## SESSION 6 - Panel Discussion/Open Forum

Moderator: William W. St. Cyr, NASA, John C. Stennis Space Center

Panel Members:

Norm Schulze, NASA Headquarters - Code QW  
 Larry Bement, NASA Langley Research Center  
 Tom Seeholzer, NASA Lewis Research Center  
 Jere Harlan, Sandia National Laboratories  
 Jim Gageby, The Aerospace Corporation  
 Ken VonDerAhe, Pacific Scientific Corporation

Discussion topics:

Topics submitted from the audience.  
 What's the future of pyrotechnics?  
 What are the predominant issues pertaining to pyrotechnics?  
 Pyrotechnic failures - lessons learned.  
 Pyrotechnic coordination - is it needed?  
 Are standards and standard specifications needed?

**Note: The panel discussion and open forum commenets were not recorded and are not included in this conference publication.**

|   |     |
|---|-----|
| APPENDIX A - List of Participants . . . . . | A-1 |
|---|-----|

**1994 NASA AEROSPACE  
PYROTECHNIC SYSTEMS WORKSHOP**

February 8-9, 1994  
Sandia National Laboratories  
Albuquerque, NM

Welcoming Address - John Stichman, Director  
Surety components and Instrumentation Center  
Sandia National Laboratories

# Welcome

---

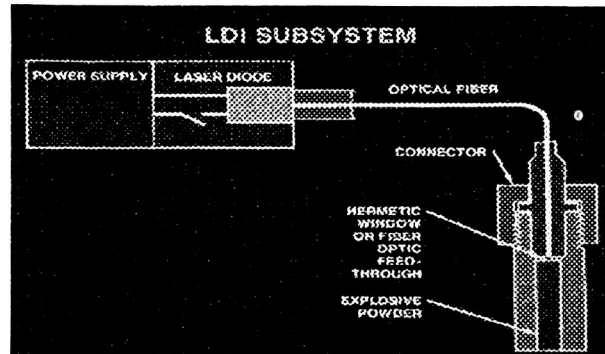


Primary purpose of this conference is to promote communications between government agencies and private industry.



# Conference is Organized in Four Sessions

---

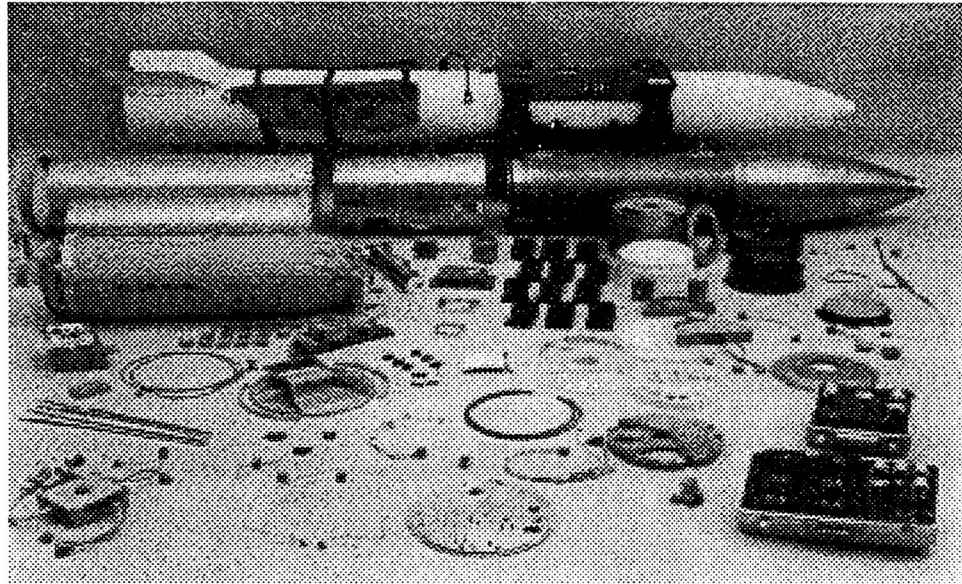


- **Optical Ordnance**
  - New, exciting and potentially significant safety improvements.
- **Electrical Initiation**
  - Backbone of pyrotechnics.
  - Continued safety improvements (ESD & EMR).
- **Mechanisms & Explosive Activated Devices**
  - Details of device designs are important for specific technology transfer.
- **Analytic Methods & Studies**
  - Computer analysis & improved test methods lead to a deeper understanding & improved performance characterization



# Five Decades of National Service

---

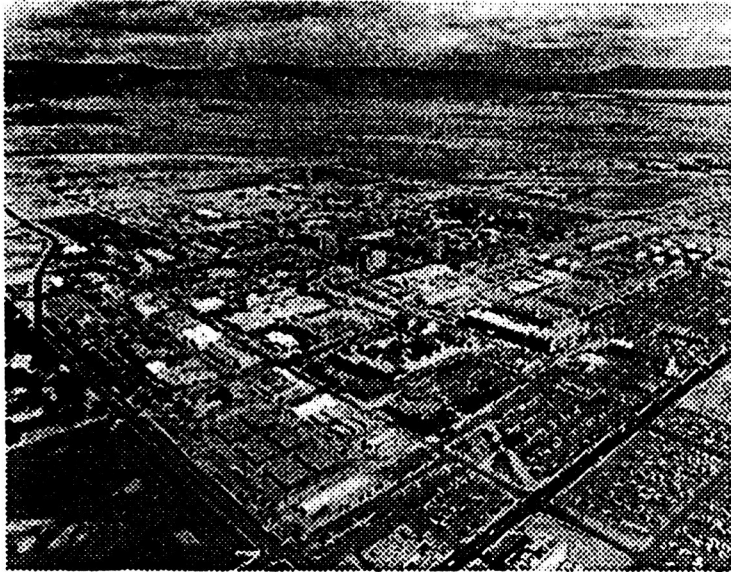


**National Laboratories have had opportunity & privilege to support U.S. nuclear weapons programs where we must provide long life & high reliability components. Performance is characterized by studies of fundamental mechanisms of explosive & pyrotechnic phenomena.**

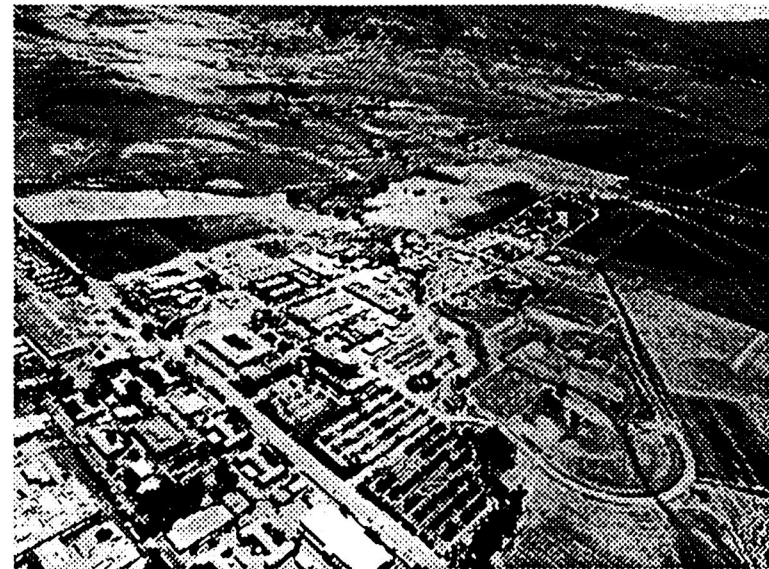


Sandia has two major laboratory locations . . .

---



New Mexico

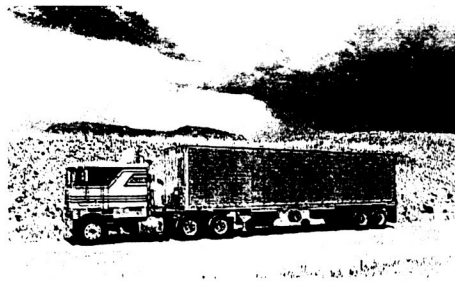
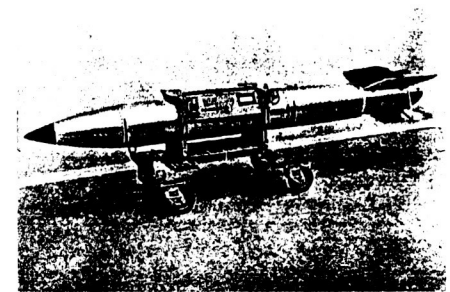
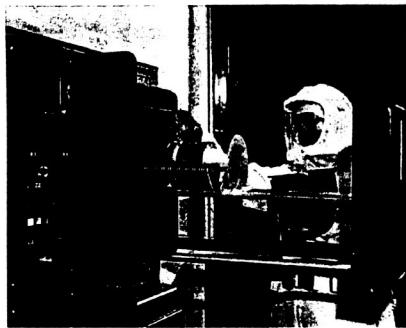
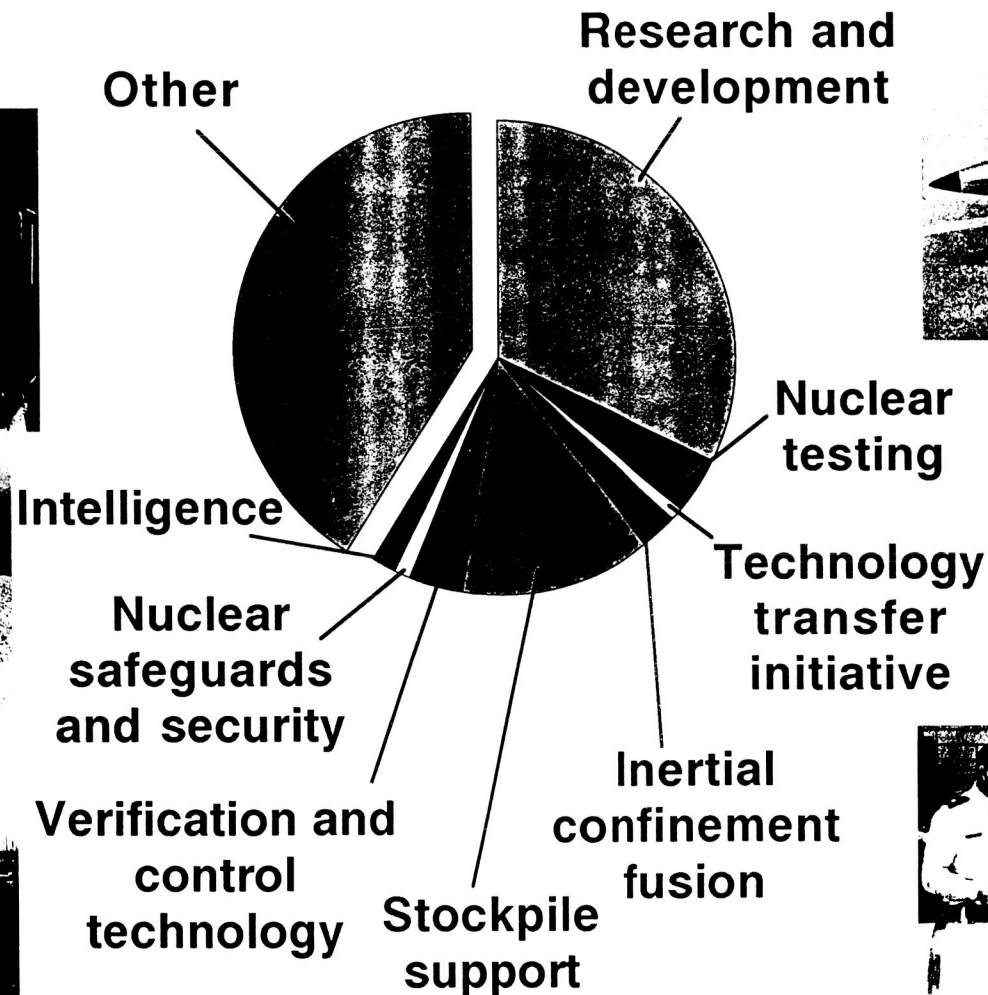


California





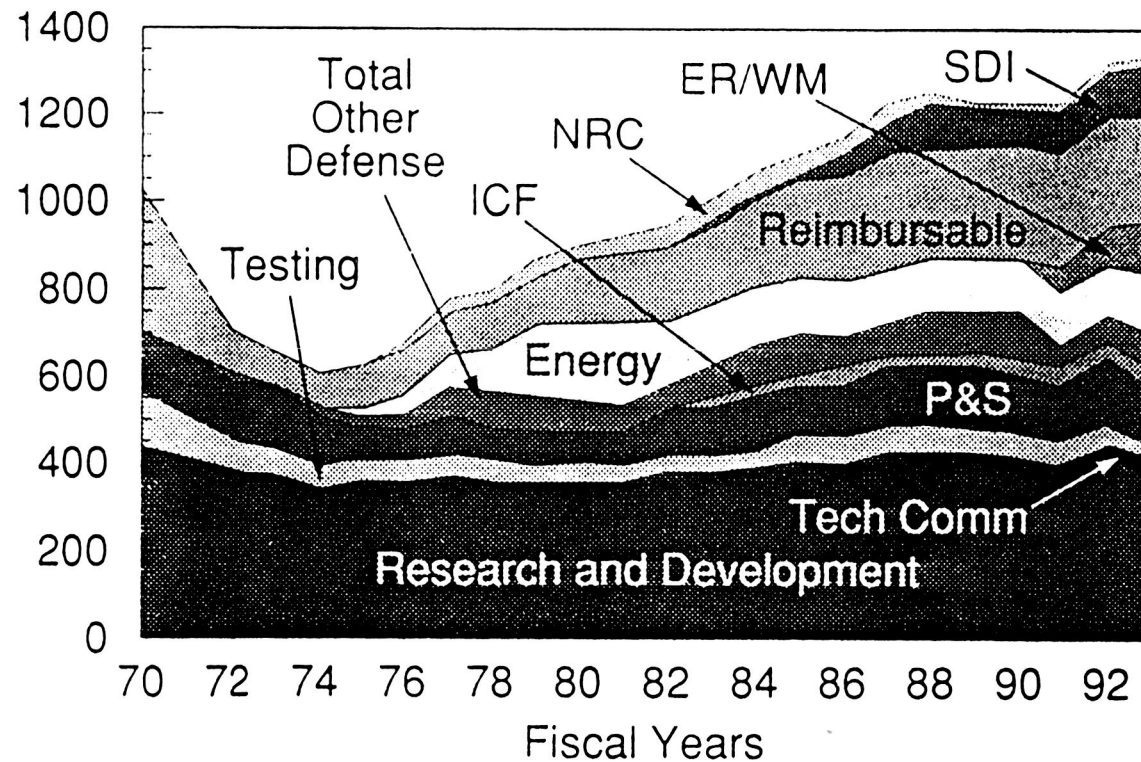
# The Defense Programs Sector is responsible for a significant fraction of the Laboratories' activities



## Our programmatic efforts address changing national needs

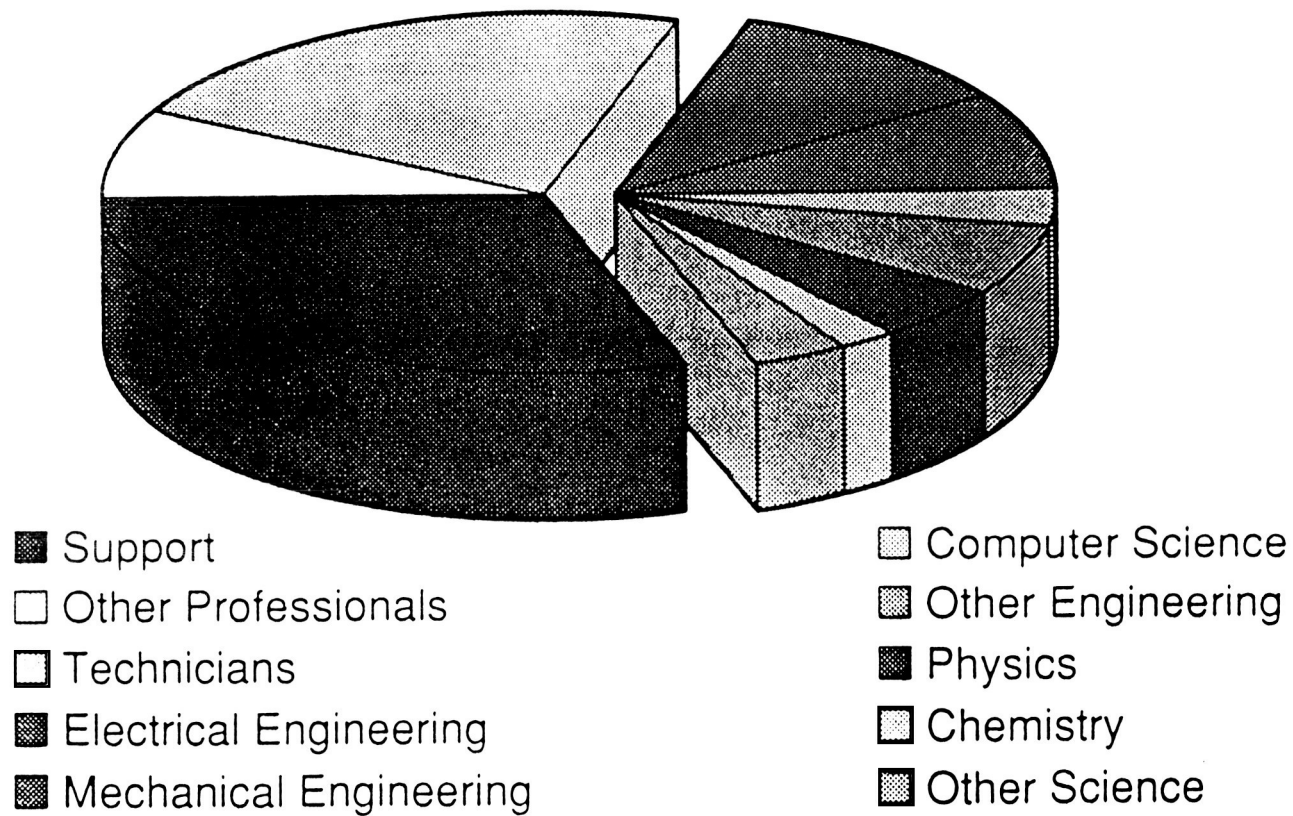
---

DOLLARS IN MILLIONS



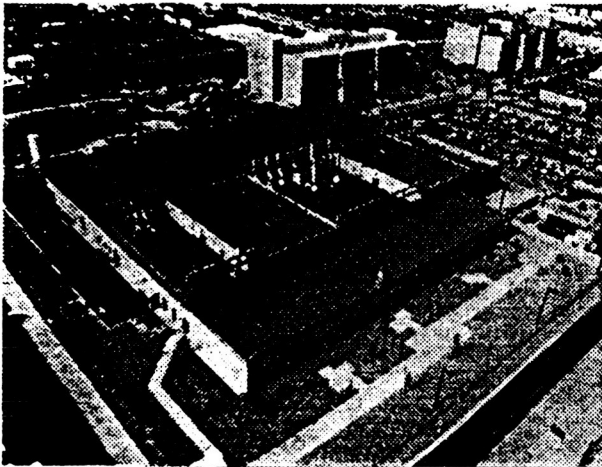
## Engineering and physical sciences are the backbone of our multidiscipline laboratories

---



## Modern process development and prototype fabrication facilities

---



Process  
Development  
Laboratory



Manufacturing  
Technologies Facility

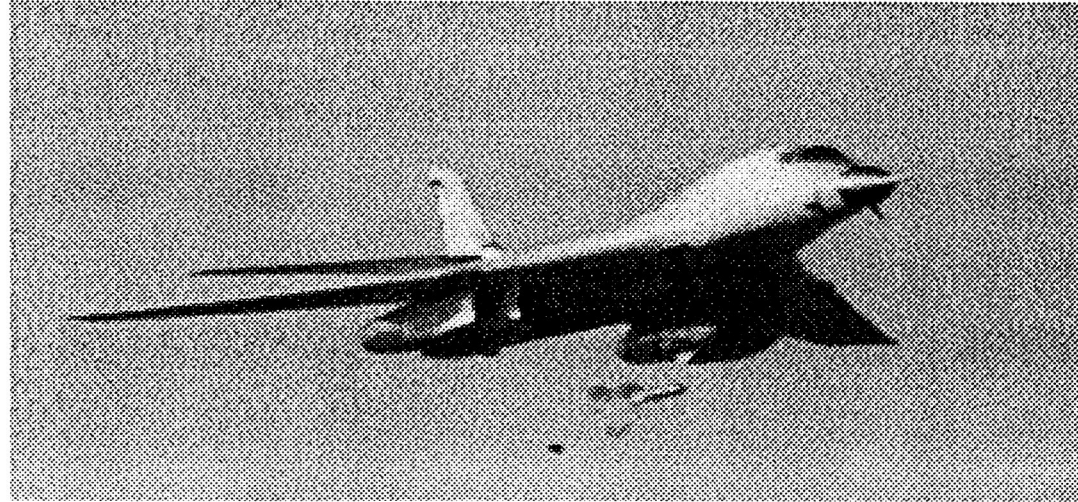


Integrated  
Manufacturing  
Technologies  
Laboratory



# Improved Industrial Competitiveness

---

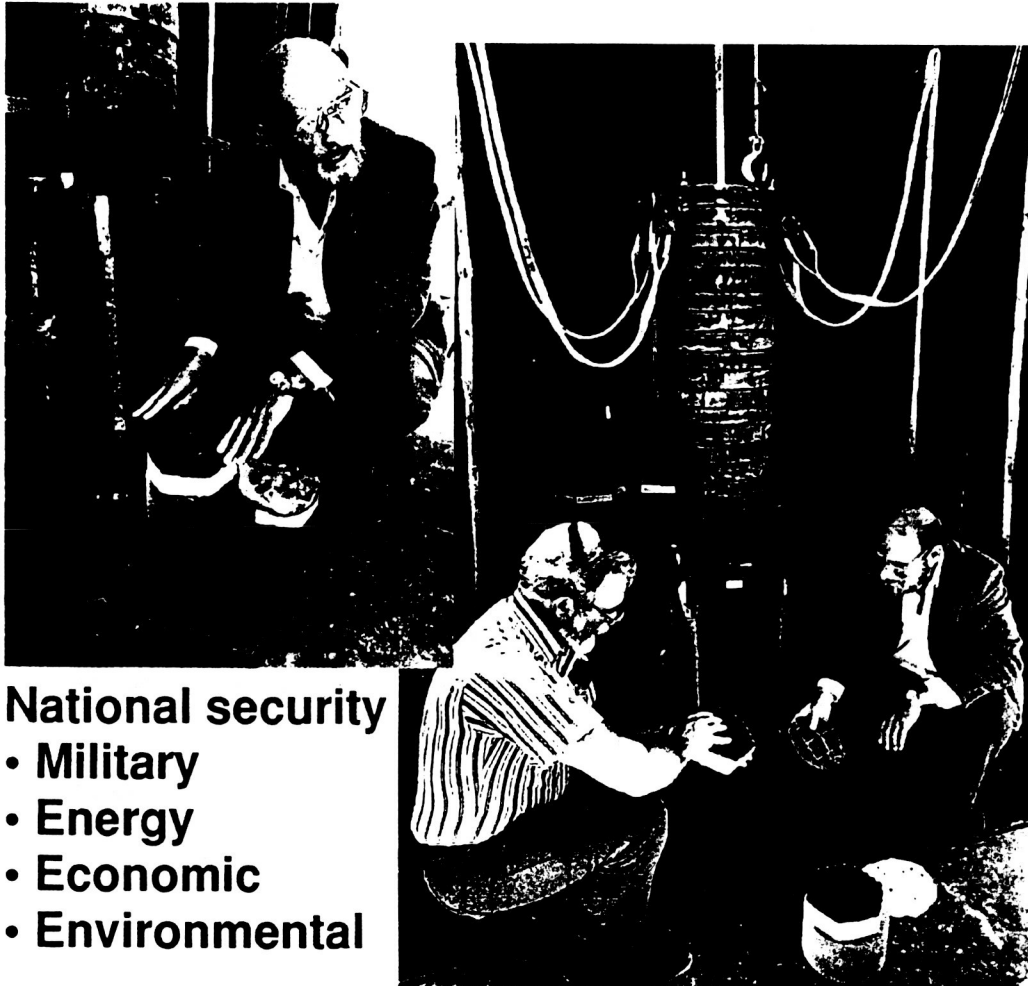


**Technology transfer in the past has been controlled for security reasons, however, today it is becoming a mission of the national laboratories to help other government agencies and private industry in order to improve our economic security.**



# Sandia undertakes new programs that enhance national security and industrial competitiveness

---



## National security

- Military
- Energy
- Economic
- Environmental



## Teaming with industry



**“All federal R&D agencies will be encouraged to act as partners with industry wherever possible. All laboratories managed by the Department of Defense that can make a productive contribution to the civilian economy will be reviewed with the aim of devoting at least 10-20 percent of their budgets to R&D partnerships with industry. In this way, federal investments can be managed to benefit both government’s needs and the needs of U.S. Business”**

**President Bill Clinton**

**“Technology for America's Economic Growth”**

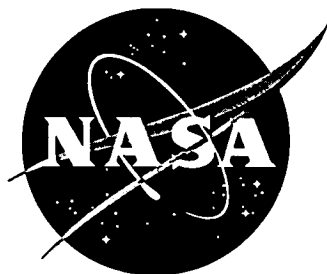
**February 22, 1993**



S1-81

6981

P-16



# **Update: NASA Pyrotechnically Actuated Systems Program**

**Norman R. Schulze, NASA Headquarters  
Second NASA Aerospace Pyrotechnic Systems Workshop  
Sandia National Laboratory, Albuquerque, NM  
February 8, 1994**



# Agenda

~~OSMA~~

- I. Program Origin
- II. Program Description
- III. Summary

February 8, 1994

2

~~OSMA~~

## I. Program Origin

# Introduction – Pyrotechnic Systems

~~OSMA~~

- Routinely perform wide variety of mechanical functions:
  - Staging
  - Jettison
  - Control flow
  - Escape
  - Severance
- Mission Critical
- Are required to have near perfect reliability
- But failures continue, some repeatedly

February 8, 1994

4

## Definition

~~OSMA~~

- By example, pyrotechnic devices and systems include:
  - Ignition devices
  - Explosive charges and trains
  - Functional component assemblies, e.g., pin pullers, cutters, explosive valves, escape systems
  - Systems, i.e., component assembly, ignition circuitry, plus the interactions with the environment such as structure, radio waves, etc.

February 8, 1994

5

# Summary of Survey

OSMA

- 23 year span covered
- Failure categories
  - Initiation
  - Mechanisms
  - Spacecraft separation systems and linear explosives
  - Firing circuits
- Reviewed by Steering Committee
- Report prepared
  - Bement, L. J., "Pyrotechnic System Failures: Causes and Prevention," NASA TM 100633, Langley Research Center, Hampton, VA, June 1988

February 8, 1994

6

# Assessment of Survey Results

OSMA

| Deficient Areas   | Recommended Tasks  |
|---|--|
| <ul style="list-style-type: none"><li>• Design Approaches<ul style="list-style-type: none"><li>– generic specification</li><li>– standard devices</li></ul></li></ul>   | <ul style="list-style-type: none"><li>• Design Approaches<ul style="list-style-type: none"><li>– prepare NASA specification handbook</li><li>– select/verify existing hardware types</li></ul></li></ul>   |
| <ul style="list-style-type: none"><li>• Pyrotechnic Technology<ul style="list-style-type: none"><li>– research/development technology base</li><li>– recognized engineering discipline</li><li>– training/education</li><li>– test methodology/capabilities</li><li>– new standard hardware</li></ul></li></ul> | <ul style="list-style-type: none"><li>• Pyrotechnic Technology<ul style="list-style-type: none"><li>– endorse and fund plan's technology tasks</li><li>– fund training and academic efforts</li><li>– R&amp;D for new measurement techniques</li><li>– develop new h/w for standard applications</li></ul></li></ul> |
| <ul style="list-style-type: none"><li>• Communications<ul style="list-style-type: none"><li>– technology exchange</li><li>– data bank &amp; lessons learned</li><li>– intercenter program support</li></ul></li></ul>   | <ul style="list-style-type: none"><li>• Communications<ul style="list-style-type: none"><li>– continue Steering Committee meetings</li><li>– initiate symposia</li><li>– establish pyro reporting requirements for NASA PRACA</li><li>– perform as a Steering Committee function</li></ul></li></ul>                 |
| <ul style="list-style-type: none"><li>• Resources<ul style="list-style-type: none"><li>– funds</li><li>– research/development staff and facilities</li></ul></li></ul>  | <ul style="list-style-type: none"><li>• Resources<ul style="list-style-type: none"><li>– implement pyrotechnic program plan</li></ul></li></ul>  |

February 8, 1994

## II. Program

- **PAS Program Goals**
- **Program Flow**
- **PAS Program Organization**

### 1.0 Program Requirements and Assessments Element

- **Implement projects necessary to address management aspects of the Program's objectives**
- **Emphasize documentation and communications**
- **Prepare policy and planning documents to ensure products used**
- **Analyze NASA's future program requirements and current problems**
- **Provide computerized data base**
- **Produce documentation related to reviews, proceedings, analyses, etc.**

## 1.1 Future Pyrotechnic Requirements

OSMA

**Project Mgr: N. Schulze, Headquarters**

- **Determine new pyrotechnic technology requirements**
- **Define efforts to:**
  - Improve PAS quality
  - Meet more demanding environments
  - Extend service requirements
- **Evaluate new diagnostic techniques**
- **Provide functional understanding using computational modeling capabilities – enhance specifications**
- **Product:**
  - Report on analysis of future requirements

**STATUS:**

On hold pending program review

February 8, 1994

10

## 1.3 PAS Technical Specification

OSMA

**Project Mgr: B. Wittschen, Johnson Space Center**

- **Develop common procurement specifications**
- **Provide consistent technical reference for common technologies**
- **Use shared experience**
- **Make applicable to design, development, demonstration, environmental qualification, lot acceptance testing, and documentation**
- **Assure critical concerns addressed using expertise of pyro community**
- **Provide common in-process quality assurance measures**
- **Product:**
  - NASA Handbook (NHB)

**STATUS:**

On hold pending action by Pyrotechnic Steering Committee to complete review of the document

February 8, 1994

## 1.4 PAS Data Base

**OSMA**

**Project Mgr: T. Seeholzer, Lewis Research Center**

- **Include past and current programs in terms of a hardware database incorporating system requirements, designs developed, performance achieved, specifications, lessons learned, and qualification status**
- **Present sufficient detail to provide guidance for users**

**Pyrotechnic Catalogue:**

- Describe PAS devices used on prior programs
- Make available single data source to provide information on applications of pyrotechnic devices including:
  - their requirements
  - physical envelopes
  - weights
  - functional performance
  - lessons learned
  - environmental qualification
  - flight history

February 8, 1994

12

## 1.4 PAS Data Base (continued)

**OSMA**

- **Provide available information on pyrotechnic flight failures**
- **Coordinate with industry**
- **Product:**
  - Catalogue to be made available upon request

**STATUS:**

- Project is underway, content selected, data being compiled, first draft submitted to Committee for review, comments being incorporated
- Workshop paper to provide details
- Project completion expected in 1995

February 8, 1994

13

## 1.7 NASA PAS Manual

OSMA

**Project Mgr: L. Bement, Langley Research Center**

- Develop detailed "how-to" document to provide guidance on all aspects of design, development, demonstration, qualification (environmental), common test methods, margin demonstrations, etc. of pyrotechnically actuated devices and systems
- Scope: Applies to pyro life cycle from creation of PAS/component design to final disposition of device
- Product:
  - NASA Handbook (NHB) for reference

**STATUS:**

- Project is underway, content selected, text/data being compiled
- Project completion expected in approximately one year

February 8, 1994

14

## 1.8 Pyrotechnically Actuated Systems Workshop

OSMA

**Project Mgr: W. St. Cyr, Stennis Space Center**

- Create opportunity for technology exchanges at national level
- Perform planning for review by the Steering Committee
- Presentations by government and industry personnel on latest developments
- Informal to facilitate communications
- Product:
  - Workshop organization, preparations, implementation, and preparation of proceedings in a timely manner

**STATUS:**

- First Workshop held on June 9-10, 1992
- Workshop proceedings published and distributed, NASA CP-3169

February 8, 1994

- 20 -

15

## 2.0 Design Methodology Program Element

~~OSMA~~

- **Applied technology focus**
- **Hardware developed**
- **Emphasize design standards and analytical techniques**
- **Decrease chance of failure of new hardware design approaches or of proven hardware in new operational regimes**
- **All aspects of pyrotechnic component and systems applications covered**
- **Provide guidelines, handbooks, and specifications for design and development of pyrotechnic components and systems**

February 8, 1994

16

## 2.1 NASA Standard Gas Generator (NSGG)

~~OSMA~~

**Project Mgr: L. Bement, Langley Research Center**

- **Develop where the use of gas output is needed to perform a function rather than serving as ignitor:**
  - Separation nuts, valves, cutters, switches, pin pullers, thrusters, mortars, bolts, etc.
- **Common NASA GG**
  - Based on NSI (NASA Standard Initiator) to provide pedigree
  - Important for safety
  - Saves \$, NSI
  - Wide variety of cartridges - lack "pedigree" inherent with a "Standard"

February 8, 1994

17



## 2.1 NSGG (continued)

OSMA

- **Develop sizes to meet wide range of performance requirements**
- **Products:**
  - Qualified NSGG
  - Design specification (NHB)
  - Test reports

### **STATUS:**

- **Project has been successfully completed**
- **Two sources**
- **Workshop paper to provide details**

February 8, 1994

18

## 2.2.1 NASA Standard Linear Separation System (NSLSS)

OSMA

**Project Mgr: Joe B. Davis. Marshall Space Flight Center**

- **Develop standard linear separation system**
  - Improved, more reliable, high performance hardware
  - Lower cost
- **Characterize functional performance, effects of system variables, including scaling**
- **Specify process controls to assure consistency and reliability**
- **Qual test for flight**
- **Establish operational functional margin**
- **Solicit design approaches from industry**
  - Prepare NASA-wide technical specification

### **STATUS:**

- **Project has been terminated due to lack of funds**

February 8, 1994

19

## 2.5 Advanced Pyrotechnically Actuated Systems (PAS)

~~OSMA~~

---

- Define and pursue advanced design concepts to bring NASA programs up to the state-of-the-art in pyrotechnic technology
- Maintain currency

### STATUS:

- Project has been terminated due to lack of funds

February 8, 1994

20

## 3.0 Test Techniques Program Element

~~OSMA~~

---

- Address all aspects of testing: manufacturing, lot acceptance, qualification, margin validation, accelerated life, ground checkout, and in-flight checkout
- Provide better characterization of component and system performance

February 8, 1994

21

## 3.1 NSGG Performance

OSMA

**Project Mgr: L. Bement, Langley Research Center**

- **Test to demonstrate NSGG for flight**
- **Develop test procedures**
- **Quantify performance**
- **Qualify NSGG**
- **Prepare design and test specifications**
- **Products:**
  - Design and test specification
  - NSGG qualification test report

**STATUS:**

- **Project has been successfully completed**
- **Functional performance and qualification completed**
- **Workshop paper to provide details**

February 8, 1994

22

## 3.2 Standard System Designs

OSMA

- Provide improved, more reliable, high performance standard hardware designs
- Establish functional performance, effects of system variables, scaling
- Prioritized selection of candidate hardware to become "standards"
- **Products:**
  - System designs flight qualified and reports
  - Process controls specified in a technical specification

February 8, 1994

## 3.2.1 NSLSS Performance

OSMA

**Project Mgr: L. Bement, Langley Research Center/J. Davis, MSFC**

- **Demonstrate functional performance of the NSLSS developed in Project 2.2.1.**
- **Develop test procedures for the NSLSS that confirm its intended operation**
- **Quantify performance output and update design specifications**
- **Products:**
  - System design(s) flight qualified
  - Process controls specified in a technical specification
  - Comprehensive final report

**STATUS:**

- **Project has been terminated due to lack of funds**

February 8, 1994

24

## 3.6 Service Life Aging Evaluations

OSMA

**Project Mgr: L. Bement, Langley Research Center**

- **Evaluate effects of aging on pyrotechnic devices and degradation from storage in the intended operational environments**
- **Determine relationships between storage environments and device shelf life**
- **Evaluate accelerated life test approaches**
- **Find performance characteristics that can be measured during qualification to ensure that function and margins are not impaired by long periods of storage**
- **Product:**
  - Guidelines for estimating service life

February 8, 1994

## 3.6.1 Service Life Evaluations – Shuttle Flight Hardware

OSMA

**Project Mgr: L. Bement, Langley Research Center**

- **Determine effects of aging on Shuttle flight pyrotechnic devices**
  - Ensure that function and margins not impaired by long periods of storage
  - 42 units tested
- **Compare actual space flight hardware with older hardware stored on the ground under controlled conditions**
- **Test phase recently completed**
  - Results look good. Five year extension.

**STATUS:**

- **Project has been successfully completed**
- **Service life extended**

February 8, 1994

26

## 4.0 Process Technology Program Element

OSMA

- **Put science into design and analysis of pyros**
- **Develop approaches for analytically characterizing device performance sensitivities to manufacturing tolerances and “faults,” or deviations, in component ingredients**
- **Perform tests that verify analysis**
- **Address problems caused by inadequately controlled specifications or introduction of unanticipated substances into manufacturing process**
- **Establish proper degree of controls for assuring product quality and reliability**
- **Emphasize process understanding and controls to assure that specified hardware performance is realized during manufacturing processes**
- **Support product inspection criteria and acceptance testing criteria**

February 8, 1994

27

## 4.2 NSI Model Development

OSMA

**Project Mgr: R. Stubbs, Lewis Research Center**

- **Provide better understanding of NSI's sensitivities to the effects of process variables on performance**
- **Develop model**
  - Contract with Dr. J. Powers and Dr. K. Gonthier, U. of Notre Dame
- **Verify by testing**
- **Present necessary technical details to control device's function providing consistently high reliability level of performance**
- **Products:**
  - Validated model
  - Report describing model in specification format

### **STATUS:**

- **Project has been successfully completed**
- **Feasibility of modeling demonstrated**
- **Workshop paper to provide details**
- **Work given international recognition: International Pyrotechnics Society Award, to be presented February 20-25, 1994 at Christchurch New Zealand**

February 8, 1994

28

## III. Summary

OSMA

- **Program presented in the 1992 has been substantially phased down**
- **Funded projects in work/completed as planned within cost and schedule constraints:**
  - Data Base (in work)
  - Pyro manual (in work)
  - Workshop (no funds)
  - NSI Derived Gas Generating Cartridge
  - Shuttle Pyrotechnics Service Life Extension
  - Laser ordnance demonstration (Pegasus) (in work)
  - Laser ordnance demonstration (Shuttle Cargo Bay) (in work)
  - Modeling NSI
  - Modeling Linear Separation System (in work)

February 8, 1994

29

### III. Summary (continued)

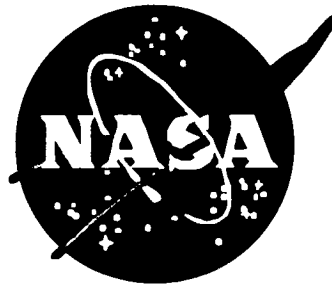
**OSMA**

- **Programs eliminated:**
  - Linear Separation System
  - Improved safe and arm system
  - Advanced standard hardware
  - Standard components and detonator
  - Training
- **Goal was to reduce risks on future programs through better engineering understandings of pyrotechnic devices**
- **Pyrotechnic problems persist – one of the most likely causes for the failure of the Mars Observer**
- **New program initiatives may be forthcoming as a result of that failure**
- **Plan to be given senior management attention**
- **Only advocacy at NASA Headquarters for pyrotechnics resides in Code Q**

February 8, 1994

30

52-28  
6982  
P-20



# **Laser Initiated Ordnance (LIO) Activities in NASA**

**Norman R. Schulze, NASA Headquarters  
Second NASA Aerospace Systems Workshop  
Sandia National Laboratory, Albuquerque, NM  
February 8, 1994**



## **LASER INITIATED ORDNANCE BENEFITS**

### **[GOALS FOR ANY PROGRAM]**

- **GREATER RELIABILITY**
- **ENHANCED SAFETY**
- **LIGHTER WEIGHT**
- **LESS COSTLY PRODUCTS**
- **IMPROVEMENTS IN DESIGN LEADING TO HIGHER OPERATIONAL EFFICIENCY**

## **APPLICATIONS**

- **INITIATION OF SEQUENCING FUNCTIONS**
- **FLIGHT TERMINATION**
- **PROGRAM APPLICATIONS**
  - new launch vehicles
  - selected use on existing fleet designs
  - spacecraft
- **LASERS HAVE LONG DEVELOPMENTAL HISTORY BUT LACK OPERATIONAL PEDIGREE**
  - ~15+ years
  - small ICBM rod lasers, first laser ordnance flight test

## ADVANTAGES OF LASER ORDNANCE

- PHYSICS OF PHOTON NOT SUSCEPTIBLE TO HAZARDS OF ELECTRON: ELECTROSTATICS, EMI, RF
- LASER DIODES HAVE THE POTENTIAL FOR DESIGN OF ALL SOLID STATE SYSTEM
- POTENTIAL FOR BUILT-IN-TEST (BIT)
- PERMITS LESS SENSITIVE INITIATION ORDNANCE
- ELIMINATES POSSIBLE HAZARD TO ELECTRONIC EQUIPMENT FROM FIRING OF HOT BRIDGEWIRE CARTRIDGE
  - Mars Observer failure option
  - Magellan
- BOTTOM LINE: THE ABOVE FEATURES, WE SAY, FOR LASER DIODES EQUATE TO IMPROVEMENTS IN SAFETY, RELIABILITY, OPERATIONS, COST, POWER, MASS

\*\*\*\*\*

- CONCLUSION: ADDRESS LASER DIODE ORDNANCE DEVELOPMENT FOR OPERATIONAL FEASIBILITY

## DISADVANTAGES OF LASER DIODE INITIATED ORDNANCE

- TECHNICAL
  - Low voltage to activate laser
    - concern over electronics setting off laser accidentally
  - BIT not proven
    - development of requirements necessary
- MANAGERIAL:
  - Hardware not proven with operational experience
    - application not mandatory for program success
    - new programs wait for others to "break the ice" to reduce risks with cost, performance, schedule
  - Incomplete understanding of requirements

## **IN THE BEGINNING .....**

### **PAS PROGRAM PLAN**

#### **LIO PROGRAMS**

- 2.4 NASA STANDARD LASER DIODE SAFE AND ARM**
- 2.5.1 NASA STANDARD LASER DETONATOR**
- 3.4 LASER DIODE SAFE/ARM PERFORMANCE**

### **PAS PROGRAM PLAN FOR LIO**

#### **2.4 NASA STANDARD LASER DIODE SAFE AND ARM**

Project Mgr: B. Wittschen, Johnson Space Center

- Develop, qualify, and demonstrate in flight a standardizable solid state laser safe and arm system
  - Flight demonstration – TBD
  - Joint HQS. activity with JSC
- Determine criteria for what constitutes an acceptable S&A
  - Closely involve range safety in the design and testing
  - Place operational considerations up front in the design
- Enhance safety and reduce risk
  - Enhance functional reliability
  - Simplify design
  - Eliminate problems with current electromechanical designs
- Reduce power, explosive containment, and costs
- Make design more easy to manufacture/checkout
- Products:
  - Flight performance demonstration-TBD
  - Guidelines for incorporating features into flight units
  - Design specification for standard safe/arm devices

#### **STATUS:**

- Project has been terminated

### **2.5.1 NASA STANDARD LASER DETONATOR**

Phase I – Developmental Investigations

Project Mgr: B. Wittschen, Johnson Space Center

- Advance pyrotechnic technology - develop laser detonators
  - Supports Project 2.4, NASA Standard Laser Diode Safe and Arm
  - Conduct off-limits testing of developmental hardware
  - Phase II task qualifies a NASA Standard Laser Detonator
- Goals include optimizing optical interface between the fiber and the pyrotechnic charge, publishing a specification, and the procurement and test of devices to provide a data base
- Products: Qualified NASA Standard Laser Detonator and design/test specification

STATUS:

- Project has been terminated

### **3.4 LASER DIODE SAFE/ARM PERFORMANCE**

Project Mgr: B. Wittschen, Johnson Space Center

- Develop test procedures
- Quantify performance
- Confirm specification performance
- Demonstrate safe/arm devices for flight
- Update design and test specifications
- Products:
  - Publish test specification for use by programs
  - Prepare qualification report

STATUS:

- Project has been terminated

***THEN .....***  
***RE-EVALUATE***

10

January 30, 1994

**IMPLEMENTATION of a FEASIBILITY APPROACH: -  
BACKGROUND-**

- **EVALUATED BY STEERING COMMITTEE FOR MANY YEARS**
  - concern about maturity
- **AUGUST 1991: OSC/EBCO UNSOLICITED PROPOSAL TO CONDUCT DEMONSTRATION ABOARD PEGASUS**
  - NASA performs one-time mission demonstration for a complete vehicle ordnance change
  - OSC performs fleet change
- **OBJECTIVE WAS "QUICK DEMONSTRATION" USING AVAILABLE TECHNOLOGY**
  - delayed for two years
    - Pegasus vehicle contracted under services contract, not R&D
    - lacked clear contractual means to conduct a technology demonstration

## **IMPLEMENTATION APPROACH**

- **MANAGERIAL ASPECTS OF LIO INITIATION POINTED TOWARD:**
  - lack of technical requirements for LIO systems
  - no practical operational experience
  - lack of quick, simple, contractual instrument to implement new technology
- **MANAGERIAL SOLUTION NECESSARY TO PURSUE TECHNICAL ISSUES**
- **ABOVE ANALYSIS POINTED NEED FOR NEW LIO PROGRAMMATIC PATH**

## **STEPS REQUIRED FOR LIO IMPLEMENTATION**

### **1. VALIDATE FEASIBILITY**

- a. **ARE THE TECHNOLOGY CLAIMS CORRECT?**
- b. **WHAT ARE THE SAFETY, RELIABILITY PROGRAMMATIC DESIGN REQUIREMENTS TO FLY LASER ORDNANCE?**

**IF FEASIBLE WITHIN COST COMPETITION OF EXISTING ELECTROMECHANICAL SYSTEMS, THEN ADDRESS THE:**

### **2. IMPLEMENTATION OF LIO INTO OPERATIONS**

## **A. VALIDATE LIO FEASIBILITY:**

### **« REDUCE THE RISK «**

#### **1. PERFORM FLIGHT DEMONSTRATIONS**

##### **PHILOSOPHY:**

- a. TAKE THE MANAGERIAL APPROACH OF COMMENCING WITH A MINIMUM SAFETY IMPACT PROJECT – THEN PROGRESS TO THE MOST DEMANDING:**
    - low hazard level in a controllable application, but safety impact exists and is such that the LIO hazard must be controlled
    - LIO serves an active function in flight - not along just for the ride
    - ultimate application range is from unmanned to manned applications
    - ultimate system range is from flight sequencing to flight termination
  - b. PERFORM SIMPLE, QUICK, DO-ABLE PROJECTS, ADDRESSING ISSUES AS PROGRESSION OCCURS**
- #### **2. DEVELOP REQUIREMENTS**
- a. PREPARE SPECIFICATION REQUIREMENTS**
  - b. DEVELOP RANGE REQUIREMENTS**

## **B. OPERATIONAL IMPLEMENTATION**

### **« REMOVE THE RISK «**

- 1. DEVELOP A “STANDARD”**
  - discussions held with Aerospace/Air Force:
  - definition of “Standard” – build to print or to performance specification
- 2. QUALIFY FOR TOTAL OPERATIONAL ENVIRONMENTAL SPECTRUM: – CAPTURE MARKET**
- 3. HAVE A PRODUCT READY FOR PROGRAMMATIC USE, ACCEPTED BY THE PYRO TECHNICAL COMMUNITY**
- 4. MAINTAIN TWO QUALIFIED SOURCES AS A MINIMUM-NO SFP'S**

**STATUS:**

**THIS IS WHAT WE DID AND ARE DOING WITH  
REGARD TO THE ABOVE PROCESS**

16

January 30, 1994

**1. PERFORM FLIGHT DEMONSTRATIONS**

**a. DEVELOP A NEW PROCUREMENT PROCESS:**

***COOPERATIVE AGREEMENT***

***WITH PROFIT MAKING ORGANIZATIONS***

**b. IMPLEMENT VIA QUICK, CHEAP FLIGHT DEMONSTRATION  
PROGRAM**



## **COOPERATIVE AGREEMENT WITH PROFIT MAKING ORGANIZATIONS (CAWPMO)**

- **NEW PROCUREMENT PROCESS**
  - grants normally performed with universities
  - cooperative agreement previously limited by policy to non-profit organizations e.g. think-tanks, universities, etc.
- **CAWPMO: FROM FIRST THOUGHT UNTIL SIGNATURE = 2 MONTHS**
- **FROM: RECEIPT OF PROPOSAL UNTIL SIGNATURE = 1 MONTH**
- **THIS INSTRUMENT IS BASICALLY A PARTNERSHIP WITH BOTH GRANTEE WITH GOVERNMENT HAVING ACTIVE ROLES**
- **COOPERATIVE AGREEMENT ACCOMPLISHES COMMON BENEFIT**
- **NO HARDWARE IS DELIVERED**
- **NO FEE**
- **INTERNAL COMPANY FUNDING HELPS BUT NOT REQUIRED**
- **RED TAPE REDUCED**

18

January 30, 1994

## **PROJECTS**

### **A. PEGASUS EXPERIMENT**

### **B. SOUNDING ROCKET FTS DEMONSTRATION**

### **C. SHUTTLE**

#### **EFFORTS AIMED AT THE DEVELOPMENT OF REQUIREMENTS:**

- Specification
- Range Safety

## **A. PEGASUS EXPERIMENT**

### **TWO TESTS OF LIO CONDUCTED DURING ORBCOMM MISSION:**

- **CONDUCT A FLIGHT SEQUENCING FUNCTION: IGNITE TWO OF THE NINE FIN ROCKET MOTORS USING LIO**
  - safety hazard to operational personnel: accidental motor ignition. Control by design and procedure
  - not mission success dependent. Fin rocket motors not required for mission success
  - qualitative information. Go-no go information.
- **FIRE LIO INTO A CLOSED BOMB**
  - not a safety hazard. Accidental ignition pressurizes a metal container designed to take the load
  - not mission success dependent. Separate experiment
  - quantitative information. Pressure measurements performed during flight will be compared with ground test data.
- **FLY ABOARD COMMERCIAL MISSION**
  - current date is June 1994

## **ENSIGN BICKFORD COMPANY TASKS:**

1. Conduct necessary design and research to demonstrate feasibility of LIO
2. Manufacture equipment
3. Perform testing in coordination with NASA testing
4. Conduct analyses
5. Coordinate program activities closely with NASA
6. Conduct program tasks per E-B Proposal

## NASA TASKS:

As necessary:

1. Perform technical review, analyses, and test support
2. Involve Range Safety Offices
3. Conduct off-limits/overstress tests & evaluations to support Range Safety objectives
4. Establish requirements for NASA-wide application
5. Provide test equipment support such as OTDR
6. Provide overall planning for incorporation of LIO into flight programs
7. Conduct analyses sneak circuit analyses
8. Conduct validation testing of sneak circuit analysis
9. Perform FMEA, safety, and reliability analyses
10. Conduct evaluations of program test planning
11. Conduct safety and reliability ordnance initiation evaluations
12. Provide consultation regarding operational processes
13. Provide guidance on generic flight operational procedures
14. Assist in technology transfer

## B. SOUNDING ROCKET FTS DEMONSTRATION

- **OBJECTIVE: TAKE THE NEXT STEP WITH UNDERSTANDING REQUIREMENTS AND GAINING CONFIDENCE**
- **INSTALL A FLIGHT TERMINATION SYSTEM ABOARD A TWO STAGE SOUNDING ROCKET AND DESTROY DURING THRUST**
  - Nike Orion - second stage destroy flown out of Wallops
- **IGNITE FIRST AND SECOND STAGES USING LIO**
  - maximize experience
- **ACTIVATE FTS BY TIMER-THIS DEMONSTRATION NOT A TEST TO VALIDATE NEW RF COMMAND SYSTEM**
- **HIGHER LEVEL OF SAFETY REQUIRED BEYOND PEGASUS**
- **6 MONTH PROGRAM**
- **AWAIT UNSOLICITED PROPOSAL FOR CAWPMO**

## **COMPANY TASKS:**

1. Design and manufacture termination ordnance
2. Provide LIO ignition for Nike and Orion motors
3. Provide laser firing unit, the fiber optic cable, connectors, detonators, and initiators
4. Perform testing in coordination with NASA testing
5. Conduct analyses
6. Install ordnance and integrate FTS/payload into launch vehicle
7. Participate in flight operations and post flight analysis
8. Testing at company's discretion but expected for demonstrating compatibility of laser initiation with current motor ignition system

## **NASA TASKS:**

1. Launch vehicle: Nike-Orion
2. Vehicle drawings
3. Provide environmental test requirements and WFF range safety requirements
4. Pyro interface such as mounting platform for LIO electronics
5. Instrumentation defining key events and body accelerations
6. 3-axis accelerometer
7. FTS activation timer
8. FM-FM transmitter
9. Build-up and integration of the motor and stage assembly
10. Flight performance analysis
11. Radar coverage
12. Launch operations
13. Post flight analysis support
14. Photographic coverage

### **C. SHUTTLE**

- Payload (Solar Exposure to Laser Ordnance Device)
  - LIO opens shutter in space
  - Exposure of LIDS and LIS:
    - 4 different initiators
    - 2 different detonators
    - 2 different laser firing units
  - Exposure to solar radiation:
    - direct exposure to sun
    - 10:1 magnified exposure to sun
    - no exposure to sun
  - LIO subjected to Shuttle payload safety review process
- STS Equipment (potential project not started - hazardous gas detection bottles)
  - Will subject LIO to Shuttle vehicle safety review process

## **EFFORTS AIMED AT THE DEVELOPMENT OF REQUIREMENTS:**

- **SPECIFICATION: UNFUNDED IN-HOUSE ACTIVITY**
- **COORDINATION WITH RANGE SAFETY STAFF**
  - preliminary set of requirements developed
  - work continues

## PRELIMINARY

# RANGE REQUIREMENTS FOR LIOS:

## GENERAL CATEGORY "A" REQUIREMENTS:

### System Level Requirements:

1. Single fault tolerant (two independent safeties) before and after installation of SAFE/ARM type connectors  
Cleared pad during power switching, power-on, and RF radiation operations  
To allow operations during these conditions, LIOS must be at least two-fault tolerant and meet the Man-Rated design requirements defined in RSM-93 Paragraph 5.3.4.4.5
2. At least one of safety controllable from pad
3. Design to allow power-control operations remotely from blockhouse
4. Component (if electrical type) adjacent to the laser system must be single/double fault tolerant
5. Component adjacent to the lasing device (either in the power or return leg of electrical circuit), shall not be activated until programmed initiation event
6. LIOS must not be susceptible to external energy sources, such as stray light energy, static and RF
7. Design to preclude inadvertent initiation due to singular energy sources, such as unplanned energy in power leg of circuit or due to short circuits or ground loops.
8. Design to allow for ordnance connection at the latest possible time in the countdown process

### Trigger Circuit Requirements

9. Design such that voltage required to initiate laser is at least 4 times the VCC of solid state logic circuits
10. Design to output energy after application of a 20 ms pulse

### Monitor and Test Capability:

11. Provide circuits to allow for remote control and monitor of all components in the Category "A" system. Application of  $\pm 35V$  in the monitor circuit shall not affect the Category "A" circuit
12. Recommend Built-in-Test (BIT)  
Allow remote testing at energy levels of  $10^{-2}$  below no fire for both normal and failure modes. Use different wavelength than main firing laser, separated by at least 100 nm
13. Design to allow for "no-stray energy" type of tests prior to performing ordnance connection
14. Employ pulse catcher system to detect inadvertent actuation of laser prior to ordnance connection  
Monitor 1/100 no-fire and be capable of determining a valid all-fire (power, energy density, frequency, pulse-width)

### Laser Output Requirements:

15. Energy delivered to LID shall be 2x all-fire

### Ordnance Requirements:

16. All ordnance used with LIOS must be secondary explosive.

**Power Supply Requirements:**

17. Install charged ("Hot") batteries into Category "A" circuits only if at least one of the following design approaches is utilized. Otherwise, charge battery at latest feasible point in countdown process with no personnel in danger area
  - 17.1 Electromechanical device utilized which mechanically misalign ordnance train
  - 17.2 Optical barriers utilized which mechanically misalign initiation power from either LID or laser
  - 17.3 Capacitive Discharge Ignition (CDI) system used meeting circuit criteria in RSM-93 Paragraph 5.3.4.4.4
  - 17.4 Designed to be Man-Rated and meets circuit requirements in RSM-93 Paragraph 5.3.4.4.5

**PRELIMINARY**

**SPECIFIC CATEGORY "A" REQUIREMENTS (PARTIAL LIST):**

1. Shielding for electrical firing circuits shall meet:
  - 1.1 Minimum of 20 dB safety margin below minimum rated function current to initiate laser and provide a minimum of 85% optical coverage. (A solid shield = 100% optical coverage)
  - 1.2 Shielding shall be continuous and terminated to the shell of connectors and/or components. Electrically join shield to shell of connector/component around 360° of shield. Shell of connectors/components shall provide attenuation at least equal to that of shield
  - 1.3 Shield should be grounded to a single point ground at power source
  - 1.4 Otherwise, employ static bleed resistors to drain all RF power on shield
2. Wires should be capable of handling 150% of design load. Design shall assure that latched command will remain latched with a 50 ms dropout pulse
3. Bent pin analysis shall be performed to assure no failure modes
4. Analysis/Testing shall be performed to determine debris contamination for blind connection sensitivity on optical connectors
5. All components in the Category "A" initiation system shall be sealed to  $10^{-6}$ cc/sec

30

January 30, 1994

**PRELIMINARY**

**FTS REQUIREMENTS:**

1. FTS circuit must meet all requirements defined under Category "A" requirements
2. Circuit must requirements in RCC STANDARD-319-92, FTS Commonalty Standard, Chapters 1, 2, 3, and 4
3. All LIOS components must meet test requirements in RCC STANDARD-31992, FTS Commonalty Standard, Chapters 5.1 and 5.2
4. Meet design requirements specified in WRR-127.1 (June 30, 1993) Chapter 4:
  - a. Circuit requirements in Sections 4.6.7.4.5, 4.6.7.4.8, and 4.6.7.4.9
  - b. Optical connector requirements in Section 4.7.5.2
  - c. LFU requirements in Section 4.7.7.4.1
  - d. LID requirements in Section 4.7.8.3
5. System must meet test requirements specified in WRR-127.1 (June 30, 1993) Chapter 4:
  - a. Appendix 4A.7: LFU Acceptance testing
  - b. Appendix 4A.7: LFU Qualification testing
  - c. Appendix 4A.7: Fiber Optic Cable Assembly Lot Acceptance Testing
  - d. Appendix 4A.7: Fiber Optic Cable Assembly Qualification Testing
  - e. Appendix 4A.7: LID Lot Acceptance Testing
  - f. Appendix 4A.7- LID Qualification; Testing (need to revise numbers)
  - g. Appendix 4A.7: LID Aging Surveillance Test
  - h. Appendix 4B: Common Tests Requirement

6. Incorporate a Built-in-Test (BIT) feature which allow remote testing at energy levels of  $10^{-2}$  below no-fire for both normal and failure modes and must also be at a different wavelength than main firing laser. The wavelengths for the main firing laser and the test laser must be separated by at least 100 nm
7. Piece parts shall be IAW ELV specs
8. All ordnance interfaces shall allow for 4 times (axial, angular max. gap) or 0.15" and 50% minimum design gap
9. Connectors per IAW MIL-C-38999J
10. Perform analysis/design on: LIOS FTS-FMECA, bent-pin analysis, LID heat dissipation due to SPF's

## **SAFETY POINTS**

- **GENERAL REQUIREMENTS:**
  - avoid introduction of new hazards,
  - avoid inadvertent ignition,
  - functions upon demand
- **LOW VOLTAGE FOR DIODE TO LASE CONCERN**
- **POSITIVE CONTROL OF PERSONNEL SAFETY AT PAD ESSENTIAL**
- **RANGE STRAWMAN REQUIREMENTS**



## **ISSUES TO WORK**

- **SAFETY REQUIREMENTS**
- **BUILT-IN-TEST**
- **COSTS**
- **DEMONSTRATED RELIABILITY UNDER VARIETY OF APPLICATIONS AND ENVIRONMENTS**

## **WHERE DO WE GO FROM HERE?**

### **WORK NEEDED AND NEXT STEPS**

- **BUILT-IN-TEST**
- **SPECIFICATION**
- **DEMONSTRATED RELIABILITY UNDER A VARIETY OF APPLICATIONS AND ENVIRONMENTS**
- **STANDARD DESIGN: BUILD TO PRINT VERSUS BUILD TO SPECIFICATION**
- **MARKET ANALYSIS**

## **SUMMARY**

- **PROGRAMS MORE LIKELY TO USE IF CONCEPT IS PROVEN VIA DEMONSTRATION**
- **PROGRAMS WILL USE LIO IF QUALIFIED AND IS COST COMPETITIVE**
- **NO PROGRAM DESIRES TO MAKE USE OF LIO AND PROCEED DOWN THE LEARNING ROAD, UNLESS MANDATORY FOR PROGRAM SUCCESS OR SAFETY**
- **WITHOUT A PROCESS WHEREBY THIS TECHNOLOGY IS DEMONSTRATED AND COST FACTORS VERIFIED, THERE IS NOT ANTICIPATED TO BE A DEMAND**

## **CONCLUDING THOUGHTS**

- **A TECHNICAL COMMUNITY NOT UNITED IS NOT ANTICIPATED TO MEET WITH THE SUCCESS NECESSARY FOR LIO IMPLEMENTATION ON A REASONABLE TIME FRAME.**
- **A WELL-COORDINATED, JOINTLY-CONDUCTED, AND CO-FUNDED INITIATIVE BETWEEN GOVERNMENT AND INDUSTRY OFFERS THE BEST OPPORTUNITY FOR TECHNOLOGY IMPLEMENTATION.**
  - One example is the Pegasus demonstration.
  - Another is laser gyro demonstration.
- **THERE ARE ISSUES TO BE WORKED WITH SUCH AN APPROACH SUCH AS: PROPRIETARY INFORMATION, DEGREE OF FUNDING PARTICIPATION VERSUS RETURN EXPECTED, WHO DOES WHAT, GETTING AGREEMENT ON TECHNICAL ISSUES, ETC.**
- **BUT THESE MUST BE CONSIDERED WORKABLE WHEN VIEWED FROM THE PERSPECTIVE OF THE VALUE OF THE EFFORT AND THE IMPACT OF SUCCESS.**

## **LASER-IGNITED EXPLOSIVE AND PYROTECHNIC COMPONENTS**

**A. C. MUNGER, T. M. BECKMAN, D. P. KRAMER  
AND E. M. SPANGLER**

**AEROSPACE PYROTECHNIC SYSTEMS WORKSHOP  
FEBRUARY 8, 1994**



## EG&G MOUND APPLIED TECHNOLOGIES HAS PURSUED LASER - IGNITION TECHNOLOGIES SINCE 1980

- EVALUATED FUNDAMENTAL EXPLOSIVE PROPERTIES
- TESTED OPTICAL FEED-THROUGH DESIGNS
- SHOWN FEASIBILITY OF PROTOTYPE DEVICES
- FABRICATED & TESTED PRE-PRODUCTION QUANTITIES



MOUND HAS PERFORMED LASER IGNITION TESTS ON A  
VARIETY OF PYROTECHNIC AND EXPLOSIVE MATERIALS

### EXPLOSIVES

BARIUM STYPHNATE

CP<sup>a</sup>

CP/CARBON BLACK

HMX<sup>b</sup>

HMX/CARBON BLACK

HMX/GRAPHITE

HNS<sup>c</sup>

### PYROTECHNICS

BCTK<sup>d</sup>

Ti/KClO<sub>4</sub>

TiH<sub>0.65</sub>/KClO<sub>4</sub>

TiH<sub>1.65</sub>/KClO<sub>4</sub>

ZrKClO<sub>4</sub>/GRAPHITE/VITON

a) 2-(5-CYANOTETRAZOLATO) PENTAAMINE COBALT (III) PERCHLORATE

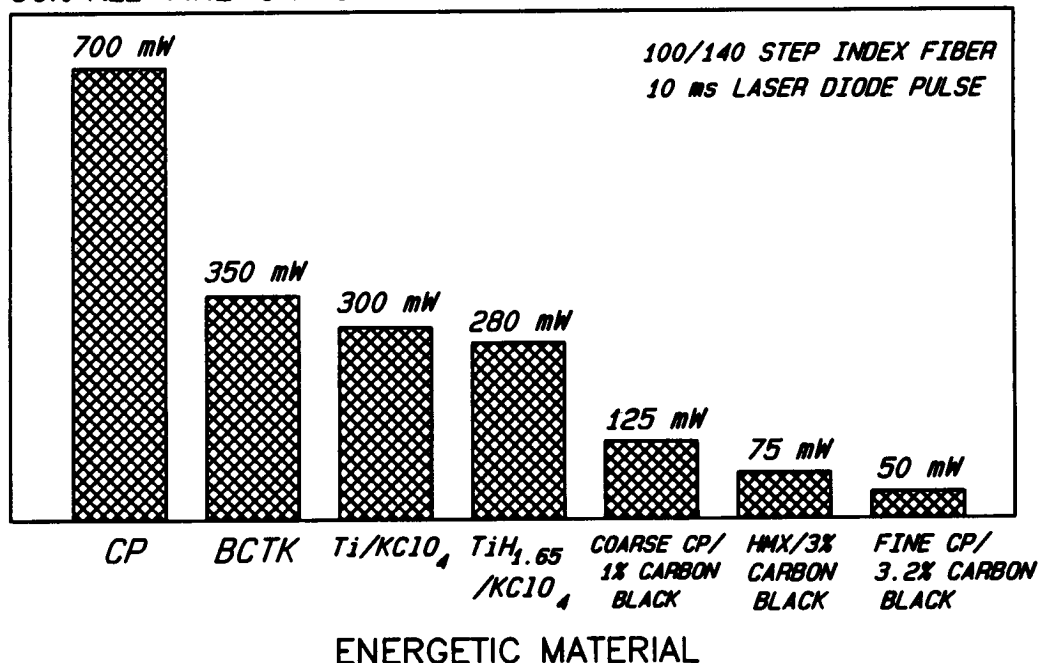
b) CYCLOTETRAMETHYLENETETRANITRAMINE

c) HEXA-NITRO-STILBENE

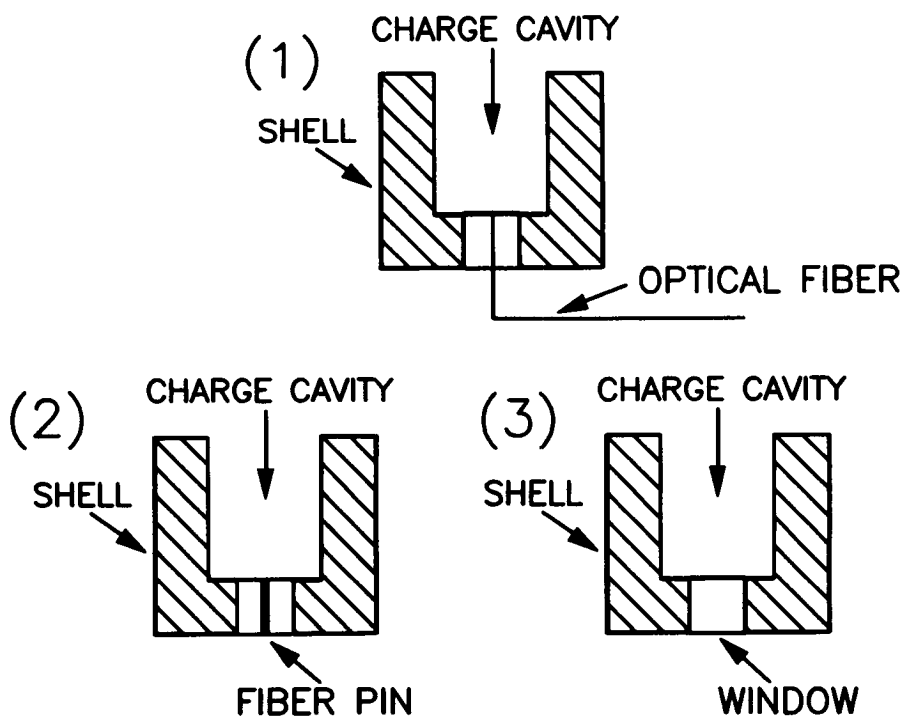
d) BORON CALCIUM CHROMATE TITANIUM POTASSIUM PERCHLORATE

# COMPARISON OF THE IGNITION THRESHOLDS OBTAINED ON VARIOUS ENERGETIC MATERIALS

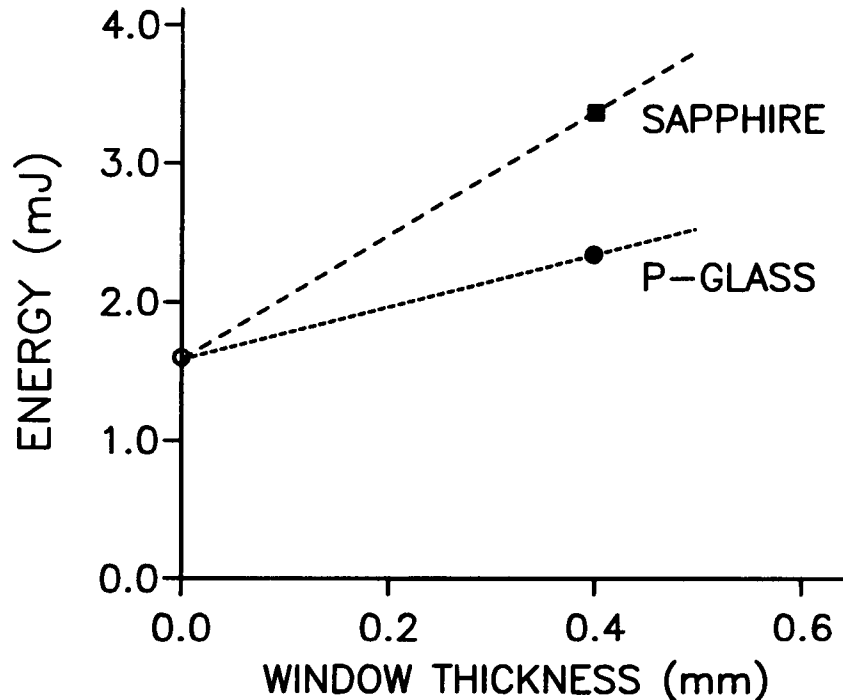
50% ALL-FIRE IGNITION THRESHOLD



## COMPARISON OF THE THREE PRINCIPAL DESIGNS UNDER CONSIDERATION FOR LASER-IGNITED COMPONENTS



## COMPARISON OF THE 50% ALL-FIRE THRESHOLDS USING SAPPHIRE AND P-GLASS WINDOW DEVICES



**MOUND HAS DESIGNED AND FABRICATED OVER  
TEN DIFFERENT LASER-IGNITED COMPONENTS**

- **3 “FIBER PIGTAIL” PROTOTYPES**
- **5 “WINDOW”**
- **6 “FIBER PIN”**
- **LOT SIZES - UP TO 400 COMPONENTS**



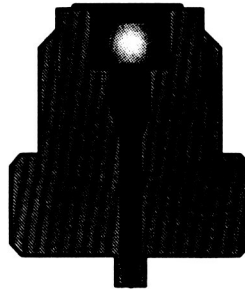
## MOUND IS ACTIVELY ENGAGED IN LASER DIODE IGNITION (LDI) COMPONENT DEVELOPMENT



**SEALED  
WINDOW  
DETONATOR**



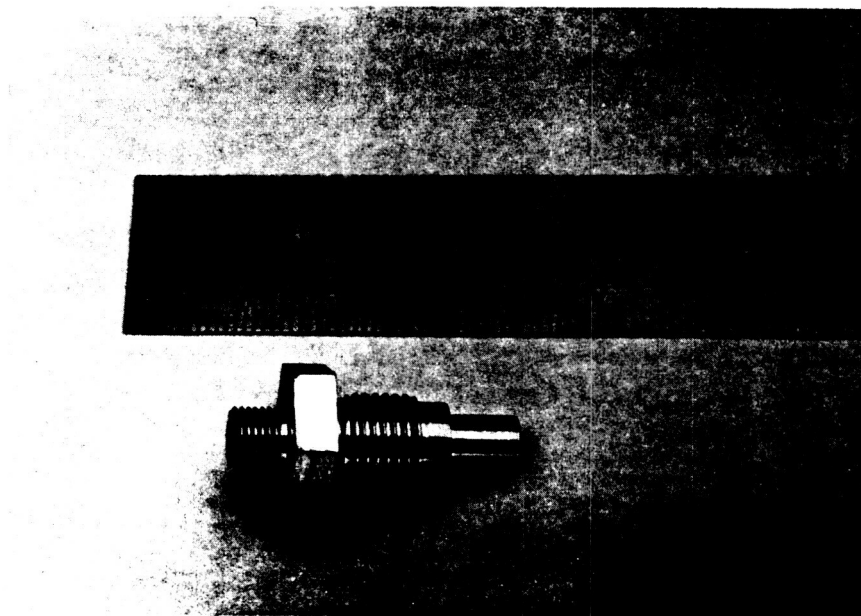
**SEALED  
FIBER  
DETONATOR**



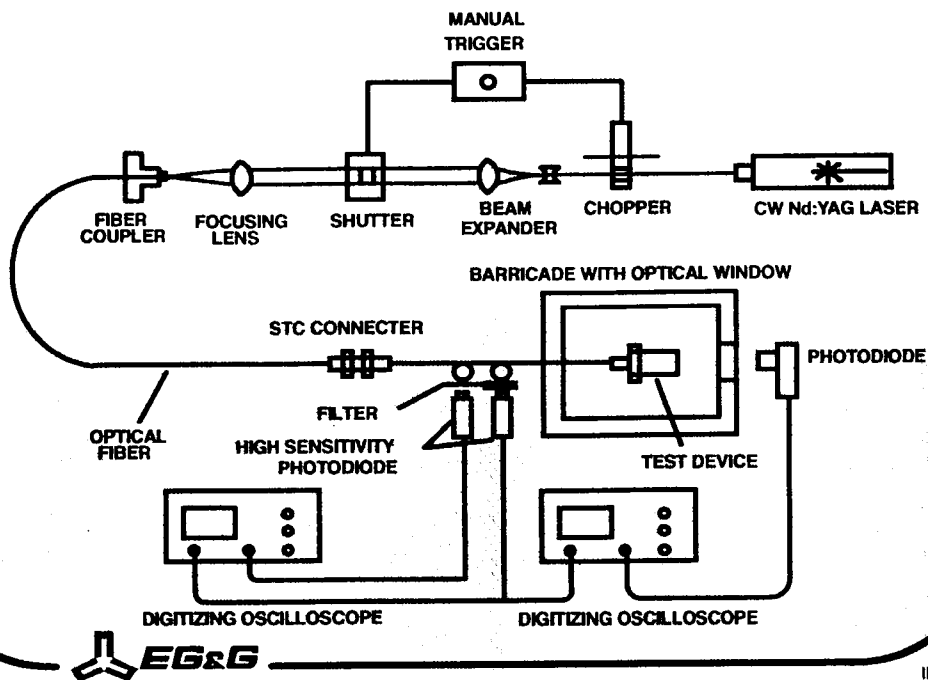
**HIGH  
STRENGTH  
ACTUATOR**



## HERMETIC, LASER-IGNITED DEFLAGRATION TO DETONATION TRANSITION (DDT) DETONATOR



## IGNITION THRESHOLD DATA ACQUISITION SYSTEM



SEVERAL PARAMETERS MUST BE CONSIDERED WHEN REFERRING TO COMPONENT THRESHOLD VALUES

- LASER BEAM/POWDER INTERFACE
  - SPOT SIZE
  - SPOT SHAPE
- LASER BEAM
  - PULSE LENGTH
  - PULSE SHAPE
  - WAVELENGTH
- THERMAL CONDUCTIVITY
  - POWDER/FIBER/SHELL/WINDOW



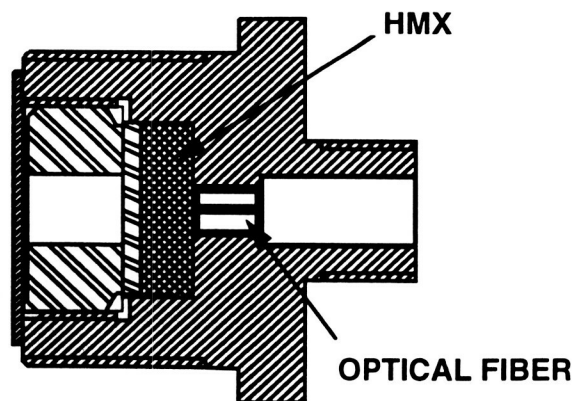
# THE DDT DETONATOR HAS BEEN SUCCESSFULLY LASER-FIRED USING A VARIETY OF TEST PARAMETERS

| <u>Laser</u> | <u>Fiber Dia.</u> | <u>N.A.</u> | <u>Maximum<br/>Pulse Length</u> | <u>50% All-Fire<br/>Threshold</u> | <u>Standard<br/>Deviation</u> |
|--------------|-------------------|-------------|---------------------------------|-----------------------------------|-------------------------------|
| Nd:YAG       | 1000 $\mu$        | 0.22        | 12 msec                         | 30 mJ                             | 8 mJ                          |
| Nd:YAG       | 200 $\mu$         | 0.37        | 150 $\mu$ sec                   | 34 mJ                             | 16 mJ                         |
| Nd:YAG       | 200 $\mu$         | 0.22        | 12 msec                         | 50 mJ                             | 11 mJ                         |



## ONE OF THE SEALED FIBER DEVICES HAS BEEN SUCCESSFULLY CHARACTERIZED

- HMX/CARBON BLACK
- HERMETIC
- 50% ALL-FIRE IGNITION  
THRESHOLD ~1.4mJ
- MAINTAINED STRUCTURAL INTEGRITY  
MAXIMUM PRESSURE ~20,000 psi

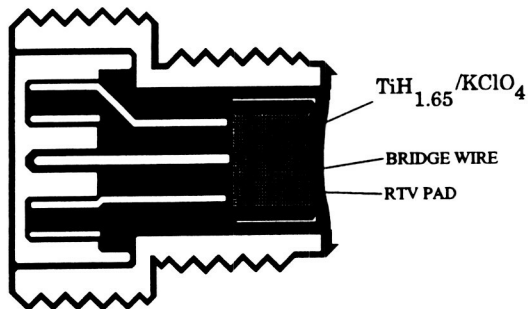


HMX LASER SQUIB

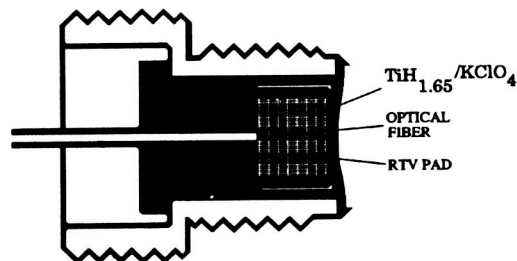


**The Laser Fired Pyrotechnic device  
was derived from the well tested  
" Hot-Wire" Device**

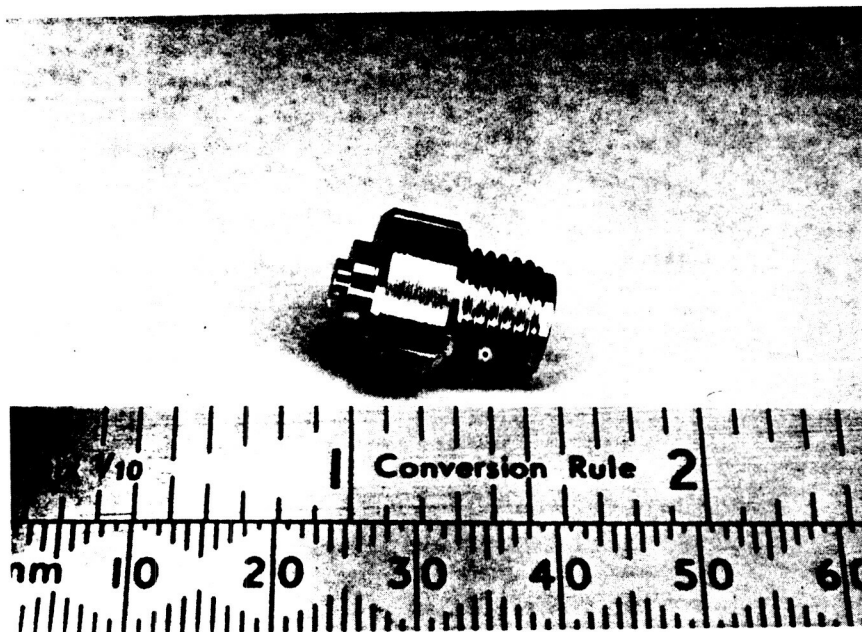
ELECTRIC PYROTECHNIC SQUIB



LASER PYROTECHNIC SQUIB



**EXAMPLE OF A HIGH-STRENGTH LASER  
IGNITED PYROTECHNIC ACTUATOR**



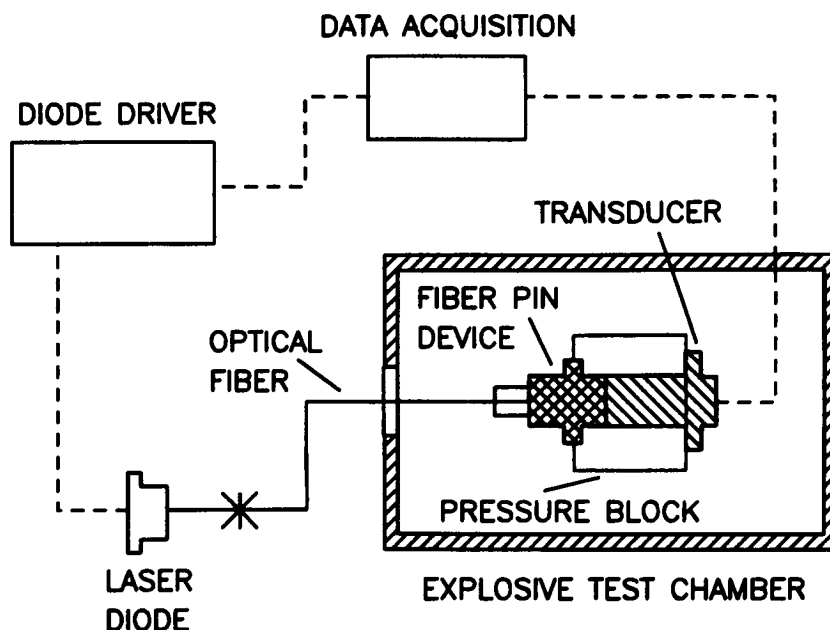
# THRESHOLD PERFORMANCE INDICATES THAT A RELIABLE DEVICE CAN BE FABRICATED

## THRESHOLD DATA WITH 10 ms PULSE

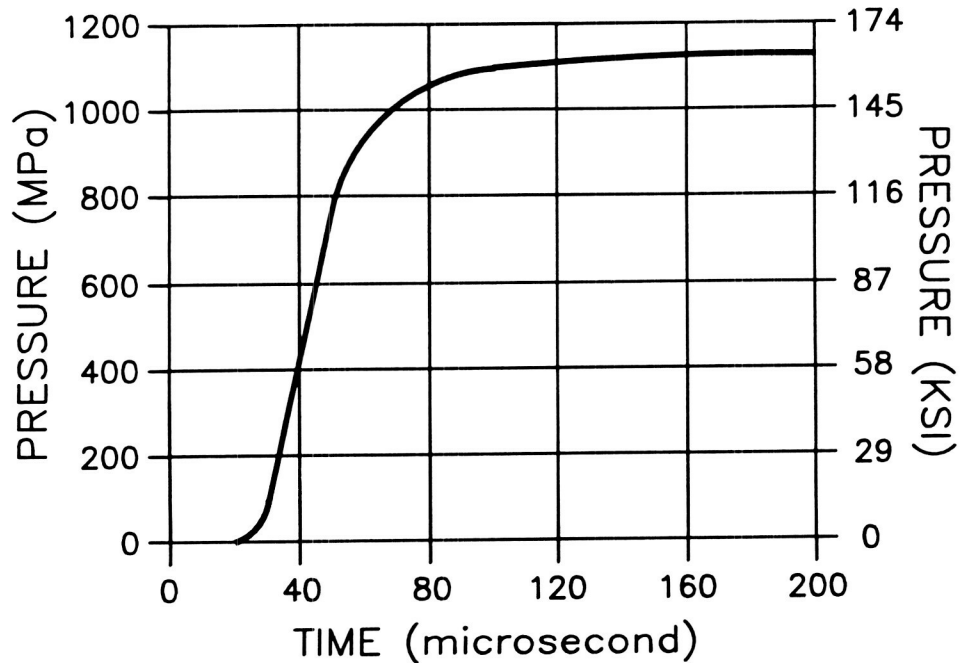
| <u>ENVIRONMENT</u> | <u>ENERGY</u> | <u>TEMP_C</u> |
|--------------------|---------------|---------------|
| NONE               | 5.3 mJ (0.05) | -55           |
| TS, TC             | 5.02 mJ (0.7) | -55           |
| TC, TS             | 4.50 mJ (0.2) | -55           |
| NONE, MYLAR        | 3.3 mJ (1.2)  | -55           |
| TC, MYLAR          | 2.7 mJ (0.5)  | -55           |



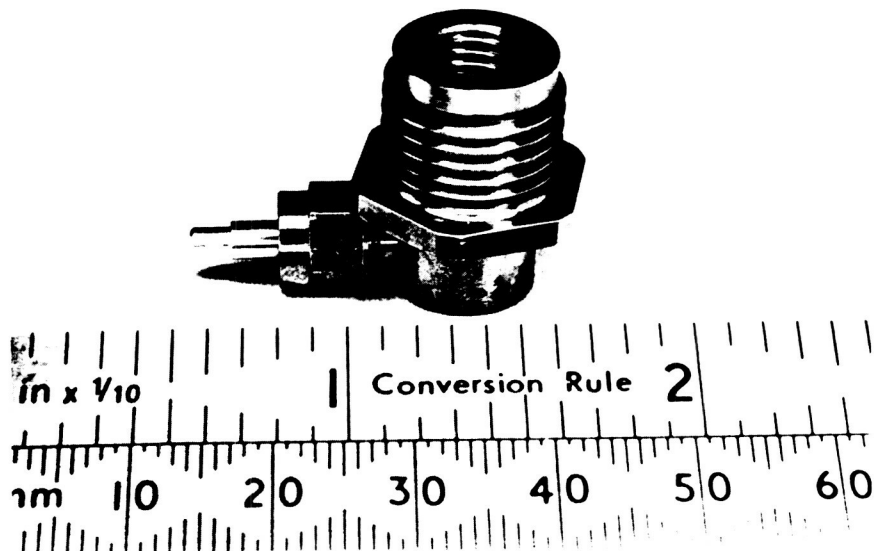
## ZERO VOLUME FIRING TEST SETUP USED TO DETERMINE PRESSURE OUTPUT OF LASER-IGNITED FIBER PIN DEVICE



# ZERO VOLUME FIRING TEST RESULT OBTAINED ON A LASER-IGNITED FIBER PIN DEVICE



"COMPACT" RIGHT-ANGLE LASER-IGNITED  
DEVICES CAN BE MANUFACTURED



# **LASER-IGNITED DETONATORS HAVE BEEN DESIGNED TO BE BON-FIRE SAFE**

- **TWO PROTOTYPE STYLES HAVE BEEN TESTED**
- **TESTS HAVE SHOWN THAT DETONATION DID NOT  
OCCUR DURING THERMAL EXCURSION**
- **DEVICE WILL NOT RECOVER**



## **LDI COMPONENTS HAVE BEEN FABRICATED AT MOUND TO SUPPORT A VARIETY OF TESTING**

### **MOUND TESTING**

**THRESHOLD DETERMINATION  
HOT, COLD, AMBIENT**

**ENVIRONMENTAL CONDITIONING  
THERMAL AND MECHANICAL**

**KED TESTING ( ZERO VOLUME )  
VALVE ACTUATOR**

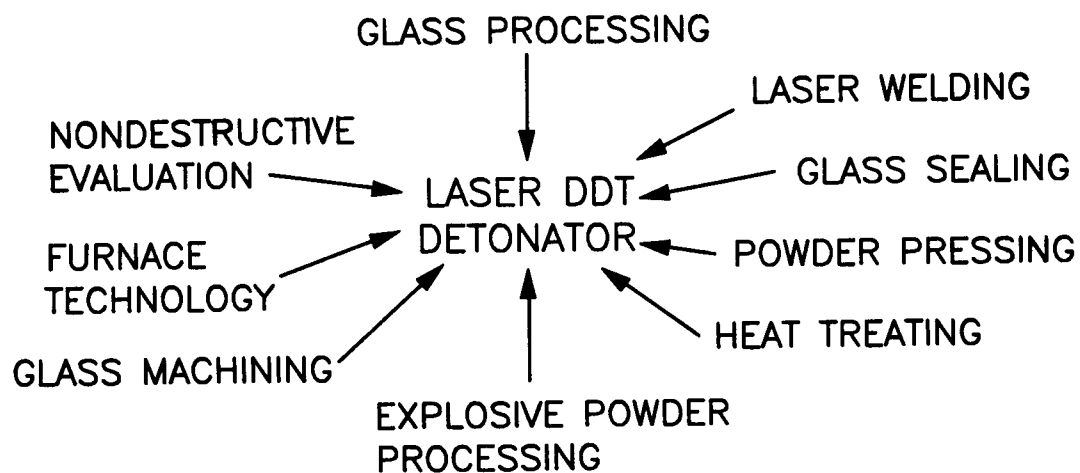
### **SANDIA TESTING**

**LIGHTNING STRIKE**

**ESD - FISHER MODEL  
- SANDIA STANDARD MAN**



LASER DETONATOR MANUFACTURING REQUIRES  
THE APPLICATION OF SEVERAL KEY TECHNOLOGIES



53-28  
6483  
174

## 1994 NASA PYROTECHNIC SYSTEMS WORKSHOP

# A LOW COST IGNITER UTILIZING AN SCB AND TITANIUM SUB-HYDRIDE POTASSIUM PERCHLORATE PYROTECHNIC

R. W. Bickes, Jr. and M. C. Grubelich  
Sandia National Laboratories  
Albuquerque, NM 87185-0326

J. K. Hartman and C. B. McCampbell  
SCB Technologies, Inc.  
Albuquerque, NM 87106

J. K. Churchill  
Quantic-Holex  
Hollister, CA

### ABSTRACT

A conventional NSI (NASA Standard Initiator) normally employs a hot-wire ignition element to ignite ZPP (zirconium potassium perchlorate). With minor modifications to the interior of a header similar to an NSI device to accommodate an SCB (semiconductor bridge), a low cost initiator was obtained. In addition, the ZPP was replaced with THKP (titanium subhydride potassium perchlorate) to obtain increased overall gas production and reduced static-charge sensitivity. This paper reports on the all-fire and no-fire levels obtained and on a dual mix device that uses THKP as the igniter mix and a thermite as the output mix.

### 1. INTRODUCTION

The Explosive Components Department at Sandia National laboratories was assigned the task of designing actuators for several different functions for a Department of Energy (DOE) program. The actuators will be exposed to personnel as well as to a wide variety of mechanical, temperature and electromagnetic environments. In addition, required outputs vary from a high pressure gas pulse for piston actuation to a high temperature thermal output for propellant ignition. In order to minimize complexity, the firing sets for all the actuators must be the same, and the firing signal must be transmitted via a cable over lengths as long as thirty feet.

Our solution was to modify an existing Quantic-Holex component (similar to a conventional NSI device) with a semiconductor bridge, SCB. Our prototype device used titanium subhydride potassium perchlorate (THKP) as the pyrotechnic. Our second (dual mix) design used THKP as the igniter mix and CuO/Al thermite as the output charge. The low firing energy requirements of the SCB substantially reduced the demands on the firing system; indeed, the present firing system design could not accommodate conventional hot-wire devices. The reduced static sensitivity of THKP<sup>1</sup> helped mitigate the electromagnetic environment requirements for exposure to radio frequency

\*This work performed at Sandia National Laboratories is supported by the U. S. Department of Energy under contract DE-AC04-76DP00789. Approved for public release; distribution unlimited.

(RF) signals and human-body electrostatic discharges (ESD).

## 2. SCB DESCRIPTION

An SCB is a heavily doped polysilicon volume approximately 100  $\mu\text{m}$  long by 380  $\mu\text{m}$  wide and 2  $\mu\text{m}$  thick with a nominal resistance of 1  $\Omega$ . It is formed out of the polysilicon layer on a polysilicon-on-silicon wafer. Aluminum lands are defined over the doped polysilicon; wires are bonded onto the lands connecting the lands to the electrical feed-throughs of the explosive header. The firing signal is a short (30  $\mu\text{s}$ ) current pulse that flows from land-to-land through the bridge. The current melts and vaporizes the bridge producing a bright plasma discharge that quickly ignites the THKP pressed against the bridge.<sup>2</sup>

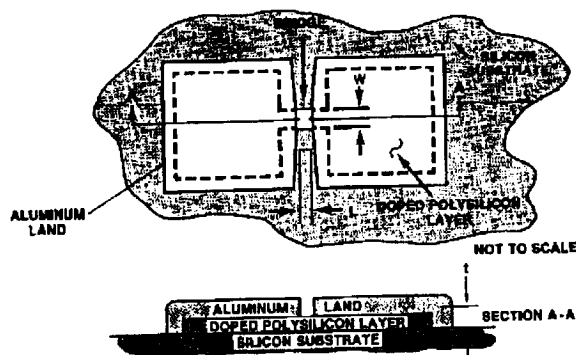


Figure 1. Simplified sketch of an SCB.

The main advantages of an SCB igniter versus conventional hot-wire igniters are that (1) the input energy required to obtain powder ignition is a decade less than for hot wires; (2) the no-fire levels are improved due to the large heat sinking of the silicon substrate; and (3) the function times (i.e. the time from the onset of the firing pulse to the explosive output of the devices) are only a few tens of microseconds or less.<sup>3</sup>

## 3. IGNITER DESIGN

Our SCB igniter is similar to the NSI device. It consists of a metal body containing a glass header, charge holder and pyrotechnic material. 3/8-24 UNF threads allow the device to be installed into test hardware and an O-ring under the hexagonal head provides the gas seal. The

internal charge cavity was reduced to a diameter of 0.156" by utilizing a threaded fiber glass composite (G10) charge holder. The threads help prevent separation of the powder from the bridge due to mechanical shock. The pins are hermetically sealed by glass-to-metal seals and extend approximately 0.020" past the header base into the charge holder. The SCB chip is bonded to the header base between the pins with a thermally conductive epoxy. Aluminum wires, 0.005" in diameter, are thermalsonically bonded to the header pins and the aluminum lands on the chip. For the prototype device, a charge of 85 mg of THKP is pressed at 12,500 psi into the charge holder. A G10 disk, 0.156" diameter and 0.010" thick, is placed on top of the pressed powder, followed by an RTV disk, 0.150" diameter and 0.016" thick. A G10 plug, 0.065" thick, is then pressed on top of the RTV at a pressure sufficient to compress the RTV pad to half its thickness, which maintains a pressure of approximately 5,000 psi on top of the THKP column. A high temperature epoxy seals the interference fit G10 plug in place.

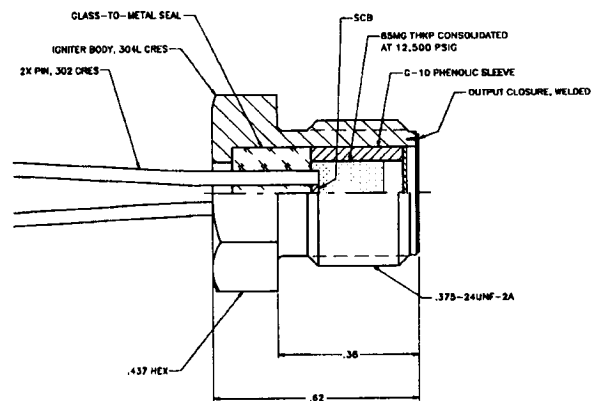


Figure 2. The SCB igniter outline.

## 4. FIRING SET DESCRIPTION

The firing set for our application is low voltage capacitor discharge unit (CDU) with a 50  $\mu\text{F}$  capacitor charged to 28 V (nominal).<sup>4</sup> Because the SCB dynamic impedance changes significantly during the process that produces the plasma discharge, two FET switches in parallel are required to discharge the 35 A current pulse into the SCB. In addition a test current pulse is included that passes a 10 mA pulse through the bridge to verify igniter integrity.



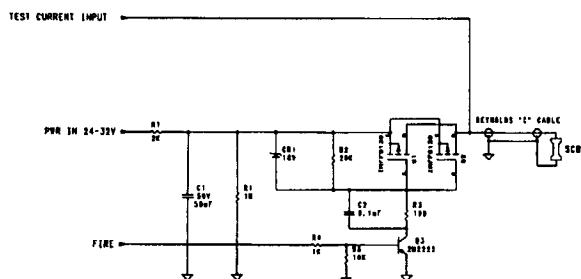


Figure 3. Wiring schematic for the SCB low voltage CDU firing set.

As noted in section 1., some of the igniters may be located as far as thirty feet from the firing set. The use of either large diameter wire pairs or ordinary BNC cable reduced the transmitted current pulses to levels below threshold for ignition. However, Reynolds Industries "C" cable was able to transmit the current pulse with only a small attenuation of the peak current.

## 5. PROTOTYPE TESTS

Figure 4. shows the voltage, current and

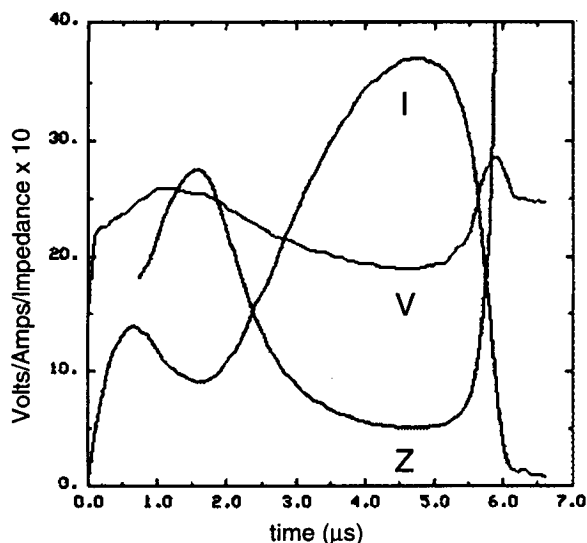


Figure 4. Current (I), voltage (V) and impedance (Z) wave forms across the SCB. At 4.8  $\mu$ s the peak current was 37.4 A, the corresponding voltage was 19.1 V and the impedance 0.5  $\Omega$ .

impedance wave forms across a device fired when connected to the firing set through 30 feet of "C" cable. At ambient conditions, the device functioned in 83  $\mu$ s (determined by a

photomultiplier tube looking at the end of the device through a fiber optic cable).

Ten units were tested using the NEYER/SENSIT scheme.<sup>5</sup> The units were fired at ambient and connected to the firing set with 30 feet of "C" cable. An ASENT<sup>6</sup> analysis of the data indicated a mean all-fire voltage of 17.8 V  $\pm$  0.2 V; confidence limits on the mean were 17.7 to 19.2 V at a 95% confidence level and a probability of function of 0.999. See table I for a listing of the data in the shot order prescribed by SENSIT.

TABLE I: ALL-FIRE DATA

| Cap Voltage<br>(V) | Go/Nogo<br>(X/O) | Energy<br>(mJ) |
|--------------------|------------------|----------------|
| 18.0               | X                | 5.01           |
| 17.0               | O                | 4.36           |
| 17.5               | O                | 4.63           |
| 18.2               | X                | 4.63           |
| 17.7               | X                | 4.77           |
| 17.2               | O                | 4.54           |
| 17.9               | O                | 4.90           |
| 17.3               | O                | 4.54           |
| 18.2               | X                | 5.08           |
| 17.4               | O                | 4.66           |

All Fire: 17.8  $\pm$  0.2 V, 4.8  $\pm$  0.1 mJ

Six THKP units underwent 3 temperature cycles over a twenty-four hour period. Each cycle consisted of 4 hours a 74C and 4 hours at -54C. The devices were fired as soon as possible after the cold cycle at approximately -15C. All of the units function when fired using the firing set without the 30 foot cable.

We subjected a THKP unit to a 1 A current for 5 minutes. There was no indication of device degradation and the unit functioned properly when tested. Based on the no-fire tests in Ref. 3, which used the same bridge as tested in this paper, we are confident that these units will have similar no-fire levels similar to those reported in Ref. 3 (1.39 $\pm$ 0.03A).

## 6. DUAL MIX DEVICE

Because composite propellants require a relatively large amplitude long duration thermal

input for reliable ignition, we developed an SCB igniter employing two discrete pyrotechnic compositions. First, 25 mg of THKP is pressed at 12.5 kpsi against the SCB and is used as a starter mix to pyrotechnically amplify the low energy SCB signal. The THKP in turn ignites and ejects 150 mg of a high density thermite composition composed of CuO and Al pressed onto the THKP.

We briefly describe the advantages of this device over a device composed of only a single load of THKP or CuO/Al. THKP has excellent and well known interface, ignition and pyrotechnic propagation properties. It also is an excellent gas producer providing zero volume pressures greater than 150 kpsi. Unfortunately, the short, high pressure output pulse of THKP is not ideally suited for the ignition of a composite propellant. CuO/Al on the other hand is an ideal material for the ignition of composite propellants. Hot copper vapor condensing and molten copper impacting on the surface of the propellant provides an excellent source of thermal energy for ignition. Furthermore, copper and copper oxides catalytically enhance the ignition and combustion of ammonium perchlorate. Unfortunately, CuO/Al thermites exhibit poor ignition characteristics at high density and are sensitive to header and charge holder thermal losses. Thus, CuO/Al at high density requires large input energies for ignition and the reaction once started can be quenched as a result of radial heat losses. The THKP ignition charge eliminates both of these problems by providing an overwhelming thermal input to the CuO/Al. Although the CuO/Al is itself a poor gas producer (the copper vapor rapidly condenses), the THKP produces a sufficient gas pulse for this device to be used to operate small, lightly loaded, piston type actuators. In addition, the thermal output of the CuO/Al helps to maintain the temperature of the gases produced by the THKP. We have tested both piston actuator and propellant loaded gas generators with this dual mix device with good results.

## 7. SUMMARY

We have developed two SCB igniters housed in an assembly with an outline similar to the standard NSI component. Our prototype design utilized THKP to provide for a pressure output static-insensitive device. Our second design used a THKP and thermite mix to provide an output sufficient for piston actuators as well as propellant loaded gas generators. All-fire voltage

using a 50  $\mu$ F CDU firing set was 17.8 V; the 5 minute no-fire level is estimated to be greater than 1 A with no device degradation. Future research will examine the tolerance of this device to mechanical shock and electromagnetic environments.

## 8. ACKNOWLEDGMENT

The testing expertise of Dave Wackerbarth, Sandia National Labs, is acknowledged with grateful thanks.

## 9. REFERENCES

- <sup>1</sup>E. A. Kjelgaard, "Development of a Spark Insensitive Actuator/Igniter," Fifth International Pyrotechnics Seminar, Vail Colorado (July 1976).
- <sup>2</sup>See for example, D. A. Benson, M. E. Larson, A. M. Renlund, W. M. Trott and R. W. Bickes, Jr., "Semiconductor Bridge (SCB): A Plasma Generator for the Ignition of Explosives," Journ. Appl. Phys. 62, 1622(1987)
- <sup>3</sup>R. W. Bickes, Jr., S. L. Schlobohm and D. W. Ewick, "Semiconductor Bridge (SCB) Igniter Studies: I. Comparison of SCB and Hot-Wire Pyrotechnic Actuators," Thirteenth International Pyrotechnic Seminar, Grand Junction Colorado (July 1988).
- <sup>4</sup>Firing set designed by J. H. Weinlein of the Firing Set and Mechanical Design Department, Sandia National Laboratories.
- <sup>5</sup>B. T. Neyer, "More Efficient Sensitivity Testing," EG&G Mound Applied Technologies, MLM-3609, (October 20, 1989)
- <sup>6</sup>H. E. Anderson, "STATLIB," Sandia National Laboratories, SAND82-1976, (September 1982).

54 28  
6984  
P 6

## Optical Ordnance System For Use In Explosive Ordnance Disposal Activities\*

J. A. Merson, F. J. Salas, and F. M. Helsel  
Explosives Subsystems and Materials Department 2652  
P. O. Box 5800  
Sandia National Laboratories  
Albuquerque, NM 87185-0329

### ABSTRACT

A portable hand-held solid state rod laser system and an optically-ignited detonator have been developed for use in explosive ordnance disposal (EOD) activities. Laser prototypes from Whittaker Ordnance and Universal Propulsion have been tested and evaluated. The optical detonator contains 2-(5 cyanotetrazolato) pentaamine cobalt III perchlorate (CP) as the DDT column and the explosive Octahydro - 1,3,5,7 - tetranitro - 1,3,5,7 - tetrazocine (HMX) as the output charge. The laser is designed to have an output of 150 mJ in a 500 microsecond pulse. This output allows firing through 2000 meters of optical fiber. The detonator can also be ignited with a portable laser diode source through a shorter length of fiber.

### 1.0 INTRODUCTION

Sandia National Laboratories has been actively pursuing the development of optically ignited explosive subsystems for several years concentrating on developing the technology through experiment<sup>1-3</sup> and numerical modeling of optical ignition.<sup>4,5</sup> Several other references dealing with various aspects of optical ordnance development are also available in the literature.<sup>6-10</sup> Our primary motivation for this development effort is one of safety, specifically reducing the potential of device premature that can occur with a low energy electrically ignited explosive device (EED). Using laser ignition of the energetic material provides the opportunity to remove the bridgewire and electrically conductive pins from the

charge cavity, thus isolating the explosive from stray electrical ignition sources such as electrostatic discharge (ESD) or electromagnetic radiation (EMR). The insensitivity of the explosive devices to stray ignition sources allows the use of these ordnance systems in environments where EED use is a safety risk.

The Office of Special Technologies under the EOD/LIC program directed the development of a portable hand-held solid state rod laser system and an optically-ignited detonator to be used as a replacement of electric blasting caps for initiating Comp C-4 explosive or detonation cord in explosive ordnance disposal (EOD) activities. The prototype systems that have been tested are discussed in this paper. Laser prototypes were procured from both Whittaker Ordnance (now Quantic) and Universal Propulsion Company and tests were conducted at Sandia National Laboratories. An optical detonator was designed at Sandia National Laboratories and built by Pacific Scientific - Energy Dynamics Division formerly Unidynamics in Phoenix (UPI).

### 2.0 THEORY OF OPERATION

The intent of the optical firing system is to provide the same functional output performance of an electrically fired blasting cap without the use of primary explosives. Electrical detonation systems use current to heat a bridgewire which in turn heats an explosive powder to its auto-ignition temperature through conduction. In contrast, an optical system uses light energy from a laser source that is absorbed

\*This work was sponsored by the Office of Special Technologies under funding documents NO464A92WR07053 and NO464A91WR10380 and supported by the United States Department of Energy under Contracts DE-ACO4-76DP00789 and DE-ACO4-94AL85000.

by the powder, thus raising its temperature to the auto-ignition temperature. The primary advantage of optical ignition is that there are no electrically conductive bridgewires and pins in direct contact with the explosive powder. This removes the potential electrostatic discharge pathways and eliminates premature initiations which can be caused by stray electrical signals. This is illustrated by the comparison of the electrically and optically ignited ordnance systems shown in Figure 1.

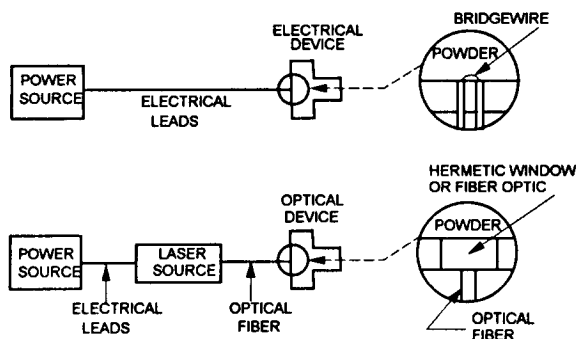


Figure 1. Comparison of electrically and optically ignited ordnance systems.

### 3.0 SYSTEM DESCRIPTION

The optical system is intended to be an additional tool for EOD applications which provides a HERO (Hazards of Electromagnetic Radiation to Ordnance) safe system with a detonation output sufficient to directly initiate Comp C-4 or detonation cord without the use of primary explosives such as Lead Azide. The system contains an optical detonator, a portable, battery operated laser, and optical fiber to couple the laser output to the detonator. Each part of the system will be discussed individually.

#### 3.1 Detonator Description

A drawing of the detonator design is shown in Figure 2. The detonator relies upon the deflagration to detonation transition or DDT. The detonator contains approximately 90 mg of 2-(5-cyanotetrazolato) pentaamine cobalt III perchlorate or CP (see Figure 3 for chemical structure) for the DDT column and 1 g of HMX for the output charge. The detonator wall around the HMX output charge is thin in order to minimize the attenuation of the shock produced by the detonation of the HMX. The detonator incorporates threads that will accept a

standard SMA 906 optical connector. The connector positions the optical fiber in contact with a sapphire window as shown in Figure 2. This optical interface and the use of optical fibers instead of electrical wires completely de-couples stray electrical sources from the detonator by removing any electrical path to the explosive.

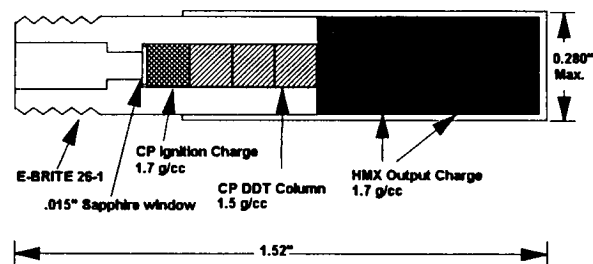


Figure 2. SMA compatible optical detonator with doped CP ignition charge, undoped CP DDT column and a HMX output charge.

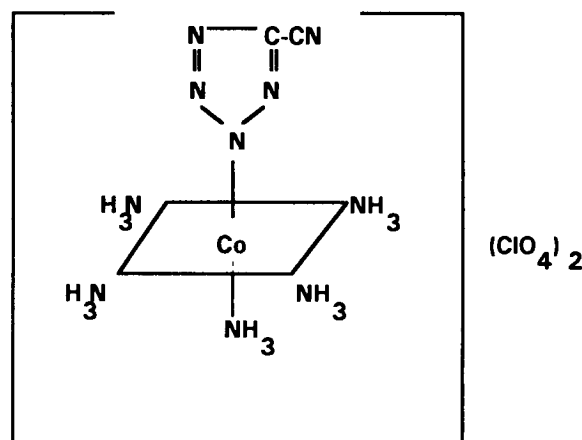


Figure 3. 2-(5-cyanotetrazolato) pentaamine cobalt III perchlorate or CP.

The optical ignition of explosives depends on the optical power delivered and the energy absorbed by the explosive. This dependence is important at low power as shown Figure 4.

At low power, it is necessary to dope some explosives with other materials such as carbon black or graphite in order to increase their absorptance of the optical energy and thus lower their ignition threshold. We have chosen to use CP doped with 1% carbon black so that these detonators can be fired from lower power laser sources such as laser diodes.

At high powers, such as that provided by the Navy EOD system, a minimum energy must be delivered to the explosive in order for it to ignite. As seen in Figure 4, this minimum energy for doped CP is on the order of 0.25 mJ. The Navy EOD system uses a solid state rod laser capable of delivering 100 to 200 mJ of optical energy in a fraction of a millisecond. Explosive doping is not required in this detonator when utilizing the high power rod laser but was implemented so that the detonator could be used for a wide range of applications.

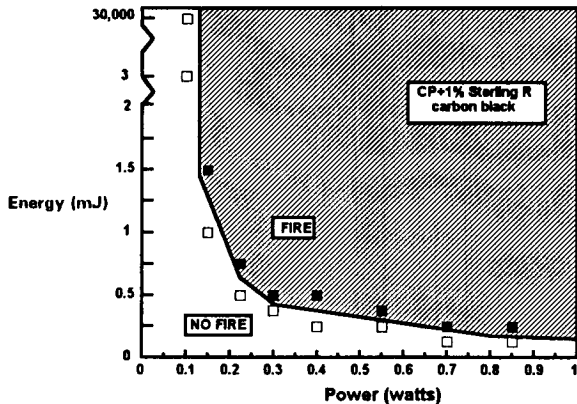


Figure 4. Optical ignition threshold for doped CP at low laser powers.

Successful ignition and function of the optical detonator has been achieved with both portable solid state rod laser systems powered by a 9 V supply and by a portable semiconductor laser diode system powered by five 9 V batteries (45 V total). The operational goals of the detonation system require the use of long optical fiber lengths (up to 2000 m) which may have optical attenuation or loss near 90 percent with fibers that have 4 - 5 dB/km loss. Fibers with higher loss per kilometer will enhance the optical attenuation problem. The portable laser diode is capable of delivering 2 W of optical power, well within the ignition requirements, but insufficient to overcome the cable losses in 2000 m of optical cable. For this reason, the EOD system uses solid state rods for the optical energy supply which are discussed in the next section.

### 3.2 Solid State Rod Laser

Two laser firing unit designs have been built by Whittaker Ordnance (now Quantic) and by Universal Propulsion Company in Phoenix. The Whittaker design was the first generation prototype followed by

the second generation prototype design from Universal Propulsion. Both systems have been shown to be effective at igniting the optical detonator through 1000 meters of optical fiber. Both laser designs are discussed below.

The first laser firing unit for the Navy EOD laser ordnance system was built by Whittaker Ordnance and was designed to be portable, rugged, water-proof during transport, and battery operated. The laser unit contains a 9-volt battery which supplies voltage to a DC/DC converter to step up the voltage to approximately 500 volts. This voltage charges the 300  $\mu$ f capacitor which supplies current to the flash lamps. The functioning of the flashlamps excites the laser rod material, Nd doped YAG, and causes the laser to function. The system is designed to deliver between 100 and 200 mJ of optical energy during a 500 microsecond pulse. This exceeds the energy required for the ignition of the detonator by at least 2 orders of magnitude. The laser output is coupled into a 200  $\mu$ m optical fiber which can be connected to the laser firing unit using the SMA 905 connector port on the top of the laser.

The laser can be easily transported in the field. It is contained in a cylindrical container which is approximately 3.5 inches in diameter and 6 inches tall. The package weighs about 2 pounds. The laser is not eye safe and care must be taken to properly protect the operator and any casualties from exposure to the beam. Laser safety glasses with an optical density of 4.6 or greater are required for personnel within 10 feet or 3 meters of the laser or the output end of a fiber when it is coupled to the laser. During operations, one person maintains positive control of the laser and the optical detonators. It is the responsibility of that person to assure that all personnel within the exposure radius of 3 meters have the proper eye protection. Once this is verified, the laser can be armed by depressing the arm button on the top of the laser firing unit. After 10 to 30 seconds, the fire light will begin to blink. The laser can then be fired by depressing the fire button. The optical fiber can then be disconnected from the laser and the protective cover placed back on the optical port on the laser.

The second generation laser was designed and built by Universal Propulsion Company. It improved upon the packaging, specifically with respect to environmental protection, and maintained a comparable laser output to the Whittaker laser. This

laser uses either six 1.5 V AA batteries or three 3 V AA batteries to power the laser with a 9 V supply. The 9 V supply is stepped up to 360 V to charge a 200  $\mu$ f capacitor. The body of the laser is more rugged and environmentally sealed. The housing is similar to a flashlight housing and is 10.1 inches long and 2.75 inches in diameter. The laser weighs 2.1 pounds. Operation of the laser is similar to that of the Whittaker design. The design utilizes a rotary arm/fire switch located in the rear of the laser housing. The laser delivers 200 - 300 mJ optical energy in a 200  $\mu$ sec pulse. The optical energy is coupled into a 200  $\mu$ m fiber using a press fit SMA 906 connector which attaches to the front of the laser housing.

### 3.3 Optical Fiber and Connections

The optical energy from the laser is coupled to the optical detonator with the use of optical fiber. The fiber contains a core glass and either a glass or plastic cladding depending on the manufacturer. The mismatch of the index of refraction of the core and cladding is such that all of the optical energy in the core glass is internally reflected by the cladding in a process known as total internal reflectance. Each optical fiber is described by a size and numerical aperture (NA). The size of the fiber is determined by the core glass diameter. The Navy EOD system uses 200  $\mu$ m fiber and could easily be adapted to larger diameters such as 400  $\mu$ m. The NA of the fiber describes the acceptance angle of the light that can be coupled into the fiber such that the light in the fiber does not exceed the critical angle and is totally internally reflected. The core and cladding are coated with an organic buffer to add strength. Additional layers of plastic and other strength members including Kevlar are used in the optical fiber cable to give it additional strength. The overall cable diameter can vary depending upon the jacketing and strength member materials but is on the order of 0.125 inches.

The optical fiber is relatively durable, however it can be broken. Care should be taken to avoid sharp bends less than 0.5 inch radius. Using a visible light source which should be eye safe, the operator can check for breaks in the optical cable by shining the light through the fiber. During system setup, the light can be transmitted through the fiber to verify continuity. If the light does not appear at the other end, then there is a break in the fiber cable. Only an

eye safe, low power, light source should be used for checking fiber continuity. The fiber continuity cannot be checked by the laser firing unit as it is not eye safe, and the laser light is invisible to the human eye.

Connections to optical fibers can be made with standard optical connectors. This procedure can be done in the field if required but is easier if done ahead of time. The polish on the optical fiber is important on the laser end. The polish on the detonator end is not as critical and a simple cleave of the fiber is sufficient. During explosive shots, the last portion of the optical fiber is destroyed. Therefore, it is recommended that optical cable jumpers be prepared ahead of time and used in the field to minimize the number of connectors that are made in the field.

### 4.0 SUMMARY

The optical ordnance system utilizes laser light energy to ignite an explosive powder contained in a detonator. The detonator is HERO safe and produces a detonation output sufficient to detonate Comp C-4 or detonation cord. The detonator does not contain primary explosives. The laser is portable and powered by batteries. The optical energy from the laser is coupled into standard optical fiber which is connected to the detonator. Jumpers are used to minimize the number of optical fiber terminations that must be made in the field with multiple shots. The system has been shown to be effective at detonating Comp C-4 through 1000 meters of optical fiber.

### 5.0 REFERENCES

1. S. C. Kunz and F. J. Salas, "Diode Laser Ignition of High Explosives and Pyrotechnics", Proceedings of the Thirteenth International Pyrotechnics Seminar, Grand Junction, CO, 11-15 July 1988, p. 505.
2. R. G. Jungst, F. J. Salas, R. D. Watkins and L. Kovacic, "Development of Diode Laser-Ignited Pyrotechnic and Explosive Components", Proceedings of the Fifteenth International Pyrotechnics Seminar, Boulder, CO, 9-13 July 1990, p. 549.
3. J. A. Merson, F. J. Salas and J. G. Harlan, "The Development of Laser Ignited Deflagration-to-Detonation Transition (DDT) Detonators and

Pyrotechnic Actuators", to be published in Proceedings of the Nineteenth International Pyrotechnics Seminar, Christchurch, New Zealand, 20-25 February, 1994.

4. M. W. Glass, J. A. Merson, and F. J. Salas, "Modeling Low Energy Laser Ignition of Explosive and Pyrotechnic Powders", Proceedings of the Eighteenth International Pyrotechnics Seminar, Breckenridge, CO, 12-17 July 1992, p. 321.
5. R. D. Skocypec, A. R. Mahoney, M. W. Glass, R. G. Jungst, N. A. Evans and K. L. Erickson, "Modeling Laser Ignition of Explosives and Pyrotechnics: Effects and Characterization of Radiative Transfer", Proceedings of the Fifteenth International Pyrotechnics Seminar, Boulder, CO, 9-13 July 1990, p. 877.
6. D. W. Ewick, "Improved 2-D Finite Difference Model for Laser Diode Ignited Components", Proceedings of the Eighteenth International Pyrotechnics Seminar, Breckenridge, CO, 12-17 July 1992, p. 255.
7. D. W. Ewick, T. M. Beckman, J. A. Holy and R. Thorpe, "Ignition of HMX Using Low Energy Laser Diodes", Proceedings of the Fourteenth Symposium on Explosives and Pyrotechnics, Philadelphia, PA, 1990, p. 2-1.
8. D. W. Ewick, T. M. Beckman and D. P. Kramer, "Feasibility of a Laser-Ignited HMX Deflagration-to-Detonation Device for the U. S. Navy LITES Program", Rep. No. MLM-3691, EG&G Mound Applied Technologies, Miamisburg, OH, June 1991, 21 pp.
9. C. M. Woods, E. M. Spangler, T. M. Beckman and D. P. Kramer, "Development of a Laser-Ignited All-Secondary Explosive DDT Detonator", Proceedings of the Eighteenth International Pyrotechnics Seminar, Breckenridge, CO, 12-17 July 1992, p. 973.
10. D. W. Ewick, "Finite Difference Modeling of Laser Diode Ignited Components", Proceedings of the Fifteenth International Pyrotechnics Seminar, Boulder, CO, 9-13 July 1990, p. 277.

55-28  
6985  
1-8

**Laser Diode Ignition (LDI)**  
 William J. Kass, Larry A. Andrews, Craig M. Boney, Weng W. Chow,  
 James W. Clements, John A. Merson, F. Jim Salas, Randy J. Williams  
 Sandia National Laboratories  
 Albuquerque, NM  
 and  
 Lane R. Hinkle  
 Martin Marietta Speciality Components  
 Clearwater, FL

**ABSTRACT**

This paper reviews the status of the Laser Diode Ignition (LDI) program at Sandia National Labs. One watt laser diodes have been characterized for use with a single explosive actuator. Extensive measurements of the effect of electrostatic discharge (ESD) pulses on the laser diode optical output have been made. Characterization of optical fiber and connectors over temperature has been done. Multiple laser diodes have been packaged to ignite multiple explosive devices and an eight element laser diode array has been recently tested by igniting eight explosive devices at predetermined 100 ms intervals. A video tape of these tests will be shown.

**INTRODUCTION.**

Laser diode ignition of explosive ordnance [1],[2] is an active program at Sandia [3]. Optical ignited ordnance enhances safety both on a component and system level. Electrically initiated devices can be sensitive to electrostatic discharges which dictate special handling care. Accidental initiation could cause personal injury or death. Optical ignition eliminates the possibility of this occurrence. Other advantages of optical ignition are resistance to triggering by electromagnetic radiation, no electrical conductance after fire and the absence of corrodible electrodes or bridgewires.

The goal of this program is to develop a laser diode based optical firing system to ignite an octahydro-1,3,5,7-tetranitro-1,3,5,7-tetrazocine (HMX) /carbon mixture in an explosive actuator. Several components and systems have been built and tested. Among these are a single laser diode system, a three laser diode system, a high power laser diode igniting several actuators

"simultaneously", and an addressable array of laser diodes used to ignite multiple detonators. The building blocks of these systems, environmental testing of the components and the various systems and their function will be described.

**SINGLE LASER DIODE FIRING SYSTEM.**

The simplest system which we have developed consists of a single laser diode, an optical fiber, a connector and an explosive

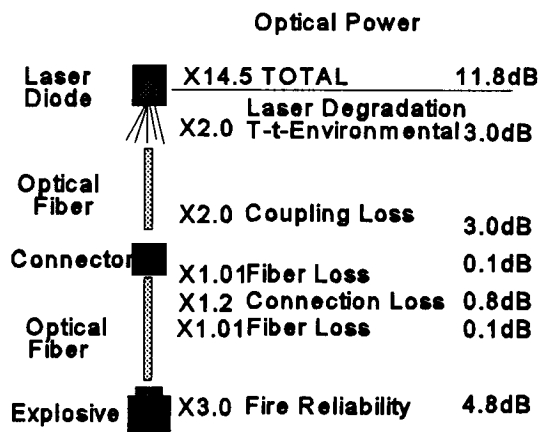


**Figure 1. Power budget for laser diode ignition.**



actuator. This system along with a power budget for each loss element is shown schematically in **Figure 1**.

The losses indicated in **Figure 1** are referenced to the nominal (50%) fire level of the explosive actuator. A factor of 3.0 (4.8dB) is arbitrarily used to achieve a higher fire reliability. The actual fire reliability will require a measure of the spread in the measurement of the fire threshold. Fiber losses (0.1 dB) and connector losses (0.8dB) are estimated from our experience with commercial connectors and fibers. The coupling loss (3.0 dB) represents the worst case coupling between the laser diode chip and the integrated optical fiber with which it is packaged. Degradation over time, temperature and thermal and mechanical environments is taken as a factor of two (3.0 dB) over the expected lifetime (20+ years) of the laser diode ignition system. The result of this analysis is that the laser diode chip power, before coupling, necessary to ignite the explosive is approximately 15 times the nominal fire threshold. For HMX/C, the nominal threshold for a 10ms optical pulse is 70 mW, hence, a 1.0+ watt uncoupled laser diode chip is required. Commercially available laser diode chips delivering greater than 1.0 W coupled power have been

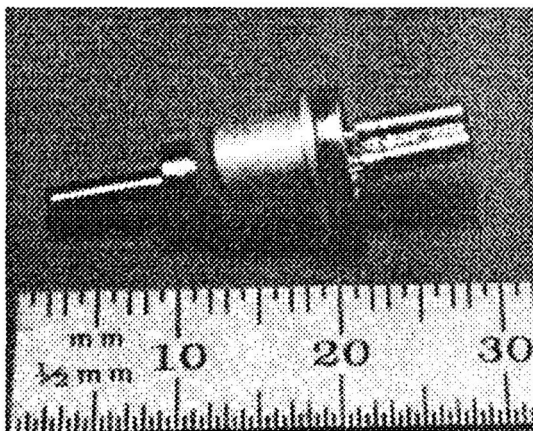


**Figure 2** Hermetically sealed-fiber optic coupled 1W laser diode for optical ignition.

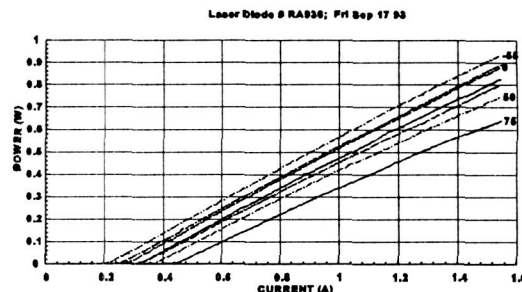


**Figure 3.** Optical power vs. drive current at temperatures between -55C and 75C for a typical 1W laser diode.

obtained and evaluated.

The single laser diode firing system also includes an electronic drive circuit used to convert 28 V-10 ms input power pulse to the 1.6-2.0 A-10 ms drive current pulse required to deliver 1 W optical power from the fiber coupled laser diode.

#### LASER DIODE.

The laser diodes used for these tests have an optical output of approximately 1 W in the spectral range of 800-850 nm. The laser diode is an AlGaAs single quantum well device manufactured by Spectra Diode Labs. The laser diode is hermetically packaged with an integrally coupled 0.22 numerical aperture-100  $\mu$ m diameter optical fiber which is terminated in a commercial optical connector ferrule. A photo of this device is shown in **Figure 2**.

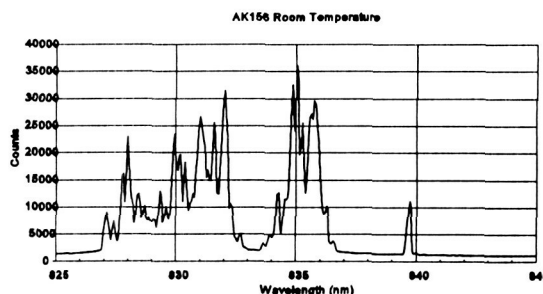


**Figure 4** Spectrum for a typical AlGaAs quantum well laser diode.

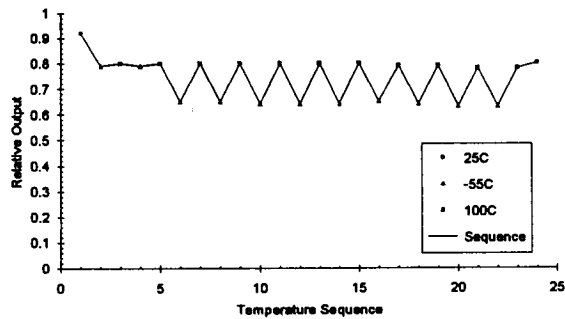


**Figure 5** Optical transmission during temperature cycling for an ST type connector.

**Figure 3** shows the optical power vs. drive current for a typical 1 W laser diode used for this system. The coupling efficiency from the chip to the fiber is greater than 50% and the nominal power at room temperature is about 0.8 W at 1.5 A drive current. At 75°C, however, the power has been degraded to 0.6 W, still in excess of the power required from the power budget.

Because of the broad band absorptance of the HMX/carbon [4] mixture used for LDI, the output spectrum of the laser diode is less important than the output power. However, the spectrum is an indicator of the proper function of the diode [5]. **Figure 4** shows the spectrum for a typical diode laser.

#### OPTICAL FIBER AND CONNECTORS.

The diode package fiber is connected to the explosive actuator via commercial optical connectors and fiber. The optical connectors have been tested over temperature by cycling between -55°C and 100°C multiple times. As can be seen in **Figure 5**, the transmittance degrades through the first two cycles and then oscillates between high and low temperature values. The optical fiber used was 0.22 NA, 100  $\mu$ m diameter, pure silica core, doped silica cladding obtained from Polymicro Technologies. The results of temperature testing only this fiber are shown

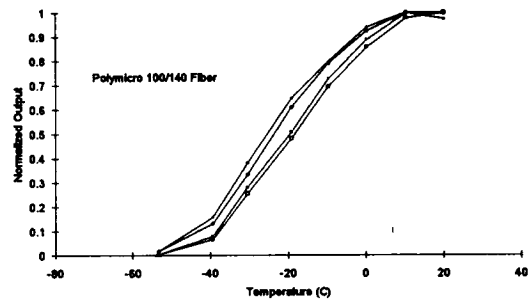


**Figure 6** Optical transmission vs. temperature for Polymicro optical fiber.

in **Figure 6**. It can be seen that a reversible transmission loss occurs as the fiber is cycled to low temperature. The loss is consistent with losses predicted from microbending due to the mismatch in thermal expansion between the fiber and the polyimide coating [6]. A larger diameter Polymicro fiber and a fiber from General Optics (with a loose acrylate buffer) were also tested as shown in **Figure 7**. The losses from the 400  $\mu$ m Polymicro fiber were less pronounced than the 100  $\mu$ m while the losses from the General Fiber were negligible.

#### EXPLOSIVE ACTUATOR.

The majority of the explosive

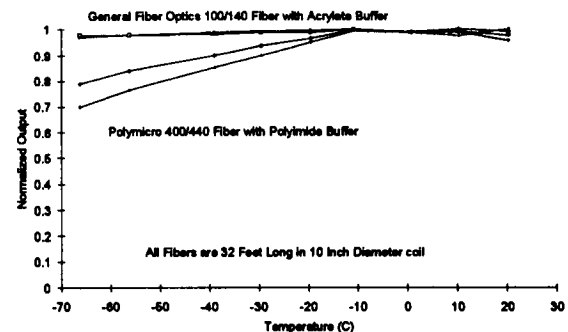


**Figure 7** Optical transmittance vs. temperature for two kinds of optical fiber.

characterization done at Sandia National Labs has been for 2-(5 cyanotetrazolato) pentaamine cobalt III perchlorate (CP) and  $\text{TiH}_{1.65}\text{KClO}_4$  ignition charges. The CP ignition charges are normally the first element in a detonation column consisting of  $1.7 \text{ g/cm}^3$  CP doped with carbon black,  $1.5 \text{ g/cm}^3$  CP,  $1.7 \text{ g/cm}^3$  HMX. The charges are 20 mg of material in a 2.1 mm diameter by 2.5 mm long cylinder. They are unsealed and the fiber is placed in direct contact with the explosive powder. The LDI system was designed to operate with explosive actuators to generate gas and perform mechanical work. The actuators consist entirely of a mixture of HMX and 3% carbon black. The carbon increases the material absorbance in the near IR where the laser diode emits.

#### ESD TESTING

Laser diode ignition derives its immunity to ESD and electromagnetic radiation (EMR) because of the absence of electrical conductors within the region where the energetic material is located. A related issue in ESD safety, however, is what the optical output of the laser diode is when it is subjected to an ESD pulse. Is the optical energy or power generated sufficient to ignite the energetic material? To address this issue we measured the optical output while subjecting the laser diode to an ESD pulse. This pulse is defined by an electrical circuit

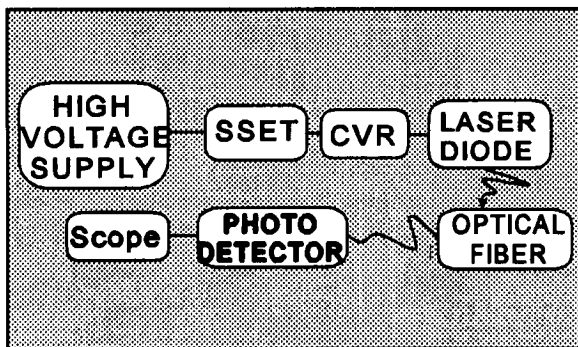


**Figure 8** Test setup for measuring laser diode output power with an ESD pulse current input.

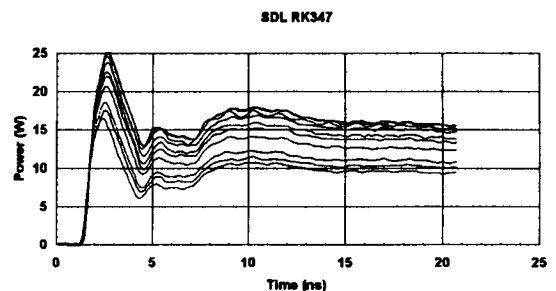


**Figure 9** Optical output power for a laser diode subjected to a series of Sandia Severe Human Body ESD pulses.

designed to simulate a human body spark including a hand (small capacitance) and body discharge [7]. The schematic of the measuring equipment is shown in **Figure 8**.

A series of measurements were made by increasing the voltage on the SSET (Sandia Severe ESD Tester) circuit and monitoring the current through the laser diode. The optical output from the laser diode was coupled to an optical fiber and measured with a fast response photodetector. The early time results are shown in **Figure 9**. The peak output is reached in 2 ns followed by signal decay with two time constants. The first decay constant is a few nanoseconds and the second is 300 ns. These decay constants result in a total signal

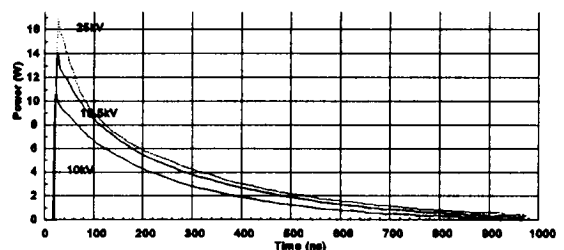


**Figure 10** Long time decay of optical output for 25kV, 15.5kV and 10kV circuit input voltages.

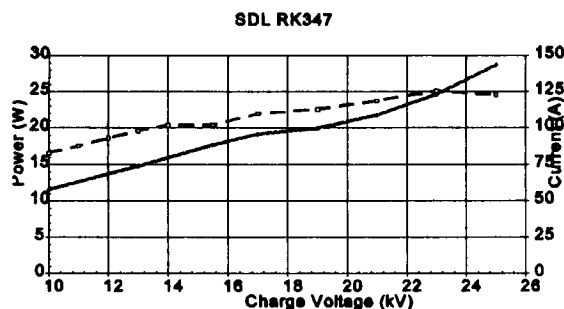


**Figure 11** Peak output power (broken line) and current (solid line) vs. charge voltage on ESD test circuit.

decay in about 1000 ns. As the input voltage to the ESD circuit is increased from 10 kV to 25 kV, the peak current increases from 60 A to 140 A. The optical output tracks this current until degradation of the diode begins. This occurs at about 125 A with a circuit input voltage of 23 kV. The peak optical output power is 25 W while the

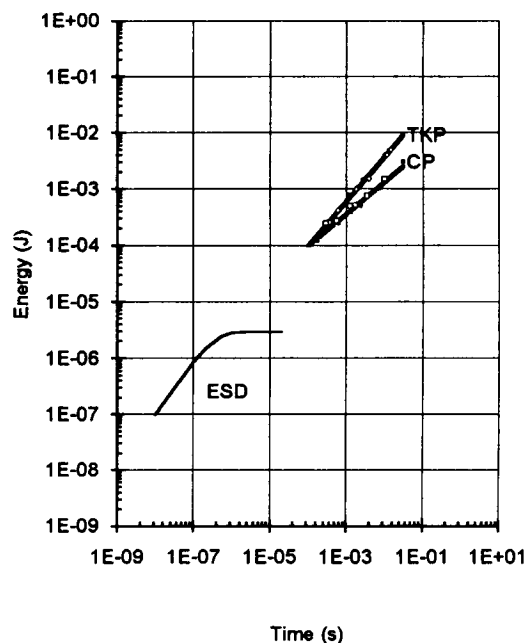


**Figure 13** Comparison of optical energy necessary to ignite TKP and CP with the maximum optical energy available from an ESD source.

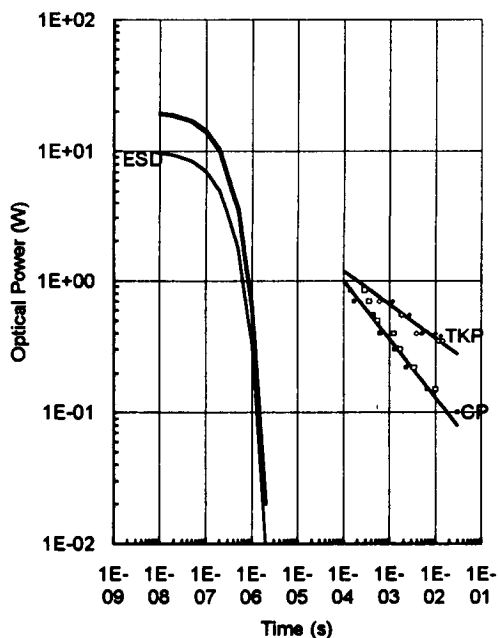


**Figure 12** Optical power necessary for explosive ignition and optical power generated by ESD pulses vs. time.

maximum energy found from integration of the complete decay is 5  $\mu$ J. The optical decay until 1000 ns is shown in **Figure 10**.

**Figure 11** shows peak optical power and diode current plotted vs. circuit input voltage. The behavior of this laser diode and others tested indicates that even though the current through the diode continues to increase with higher circuit drive voltages, the optical power levels off and begins to decay as the laser diode is degraded. This phenomenon becomes a safety advantage because the diode will not be able to deliver sufficient power to ignite the explosive.

**Figure 12** shows the optical power available from a laser diode driven by an ESD source

vs. time and compared to the power-time combination required to ignite titanium potassium perchlorate or CP. The HMX threshold falls slightly below that for CP. It can be seen from this plot that even though there is ample power for ignition, the duration is too short to ignite the explosive material.

The integration of the power vs. time curves gives a maximum available optical energy of 3-5  $\mu$ J from this type of ESD pulse. This energy also probably represents the maximum energy available under other high current conditions. Figure 13 shows the available optical energy plotted vs. time compared to the energy required to ignite CP or TKP. When plotted in this manner it is apparent that too little ESD generated optical energy is available to ignite these explosives.

## CONCLUSION

A complete laser diode ignition system has

been built and tested in various configurations. We have estimated a power budget for reliable ignition and the individual loss terms are being characterized. Fiber losses and connector losses can be accommodated with proper choices of connectors and fibers. Currently available commercial high power laser diodes provide ample power to ignite a variety of explosives under extremes in temperature and mechanical environments. The behavior of these laser diodes is being characterized over temperature, mechanical environments and time (aging). ESD testing demonstrates that the laser diode is inherently safe from producing optical power or energy which exceeds the explosive ignition threshold.

## ACKNOWLEDGMENT

The authors would like to express their appreciation to John Barnum for making the ESD measurements.

## REFERENCES

1. S. C. Kunz and F. J. Salas, "Diode Laser Ignition of High Explosives and Pyrotechnics, Proc. of 13th International Pyrotechnics Seminar, Grand Junction, CO, 11-15 July 1988, pp505
2. D. W. Ewick, L. R. Dosser, S. R. McComb and L. P. Brodsky, "Feasibility of a Laser Ignited Pyrotechnic Device", Proc of the 13th International Pyrotechnic Seminar, Grand Junction CO, 11-15 July 1988, pp 263
3. J. A. Merson, F. J. Salas, W. W. Chow, J. W. Clements and W. J. Kass, "Laser Diode Ignition Activities at Sandia National Laboratories", Proceedings of the First NASA Aerospace Pyrotechnic Systems Workshop, Houston, TX, 9-10 June 1992, pp179-196.
4. R. J. Jungst, F. J. Salas, R. D. Watkins and T. L. Kovacic, "Development of Diode Laser-Ignited Pyrotechnic and Explosive Components," Proc. of the 15th International Pyrotechnics Seminar, Boulder, CO, 9-13 July 1990, pp549-568.
5. L. F. DeChiaro, S. Ovadia, L. M. Schiavone, C. J. Sandroff, "Quantitative spectral analysis in semiconductor laser reliability," SPIE Technical Conference 2148A, Los Angeles, CA, 24-26 January, 1994.

6. Powers Garmon, "Analysis of Excess Attenuation in Optical Fibers Subjected to Low Temperatures", Proc. of the International Wire and Cable Symposium, 1983, pp134-143.

7. R. J. Fisher, "The Electrostatic Discharge Threat Environment Data Base and Recommended Baseline Stockpile-to-Target Sequence Specifications," SAND88-2658, November 1988.

56-28  
6986

## **STANDARDIZED** **LASER INITIATED ORDNANCE**

**James V. Gageby**  
Engineering Specialist  
Explosive Ordnance Office  
**The Aerospace Corporation**

### **Abstract**

Launch vehicles and spacecraft use explosively initiated devices to effect numerous events from lift-off to orbit. These explosive devices are electrically initiated by way of electro-mechanical switching networks. Today's technology indicates that upgrading to solid state control circuits and laser initiated explosive devices can improve performance, streamline operations and reduce costs. This paper describes a plan to show that these technology advancements are viable for Air Force Space and Missile System Center (SMC) program use, as well as others.

### **Introduction**

A plan to develop, qualify and flight demonstrate a laser initiated ordnance system (LIOS) has been accepted by the SMC Chief Engineer and The Aerospace Corp. Corporate Chief Engineer as part of their horizontal engineering program. The Chief Engineers' horizontal engineering effort includes a task for standardization of systems and components common to a variety of programs. The objective of standardization is to reduce costs by eliminating duplications in development and qualification often seen when vertical engineering prevents cross pollination.

The LIOS is intended as a state-of-the-art solid state replacement for the present day electrically initiated ordnance firing circuits for future space launch vehicle and satellite systems. The LIOS eliminates the need for electro-mechanical safe and arm devices and latching relays that are presently used in today's ordnance firing circuits.

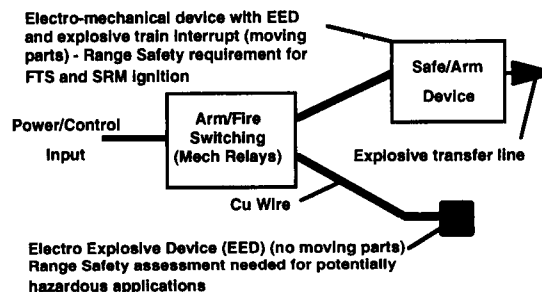
This plan will result in confirmation of LIOS suitability for SMC applications. It will establish a performance and requirements specification for standardization on SMC programs. Flight system performance enhancements and cost savings will result from the safety improvements, streamlined operational flow, weight savings, improved reliability and hardware interchangeability features of this new technology. It is expected that a family of LIOS's having various multiple output configurations will be developed to fit SMC program needs.

A typical SMC launch vehicle and satellite uses at least 40 explosively initiated events to get into proper orbit. The majority of these are redundant, therefore, 80 explosive initiations can

occur from engine ignition and lift-off to final appendage deployments in orbit. At the extreme NASA's space shuttle uses more than 400 explosive events from lift-off through deployment and release of their drag parachute on landing.

Shown below is a simplified description of the conventional ordnance firing circuits used on most SMC programs to effect these explosive initiations.

### **Conventional Ordnance Firing Circuit**



In the conventional system, sequenced power and control inputs from system computers are routed to a switching network that allows safe, arm and fire commands to be sent to the explosive devices. Mechanical latching relays are used to effect these commands.

The commands are sent via copper wire to either an electro explosive device (EED) or to a safe and arm device that contains an EED. The EED has an electrically conductive path directly to the explosive materials internal to it. Electrical energy in this path, at predetermined thresholds, causes EED ignition. The EED contains no moving parts.

The safe and arm device (S/A) is an electro mechanical component required for

compliance with safety regulations in flight termination and solid rocket motor ignition systems only. It contains moving parts. It provides a barrier, or interrupt, in the explosive train so that premature ignition of the EED will not cause an unplanned event. This interrupt is remotely removed during the mission sequence to allow end item function. The safe and arm device also contains a component called a safing pin which must be manually removed before remote arming and firing can be effected. Removal of the safing pin is done late in the pre-launch cycle and usually requires the launch site to be cleared of all but essential personnel.

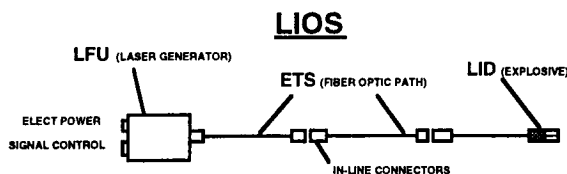
The LIOS replaces the EED used in the conventional ordnance system with a device that uses laser diode energy to ignite the same explosives. The primary advantage is the elimination of electrically conductive paths to the explosive mixes. This drastically reduces concerns of premature ignition since external environments like static electricity, electro-magnetic interferences as well as radio frequency (R-F) fields are isolated from the explosives.

The new explosive component is called a laser initiated device or LID. The LID will be designed to use secondary explosive materials as ignition sources rather than primaries as used in EED's. This reduces handling concerns. The LID could be considered in the same category as small arms ammunition for handling and shipping purposes. This will result in a significant, although indeterminate, cost savings.

The LID outputs can be configured to be nearly identical to the EED outputs; therefore, interfaces with present day explosively actuated components will be compatible. Requalification of explosively actuated components with LID's, that were previously qualified with EED's, should be minimal.

### LIOS Concept

A description of the LIOS is given below.



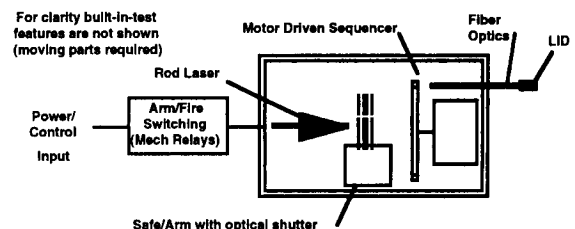
- Laser firing unit (LFU) - receives control signals and power (28VDC) for sequencing. Laser diodes in LFU produce single or multiple laser outputs. Contains no moving parts.
- Energy transfer system (ETS) - conveys laser light through fiber optics and connectors to LID.
- Laser initiated device (LID) - allows laser energy (heat) to be absorbed into chemical mixture causing deflagration/detonation of explosive.

The LIOS contains no moving parts. The switching network in the LIOS uses solid state electronics to accomplish the functions mechanical latching relays and S/A's provide in the conventional ordnance system.

Advantages of LIOS are in reduced handling and safety concerns during ground operations. During most pre-launch operational cycles, R-F silence and limited access conditions are in effect while ordnance installations are in progress. These down times could be eliminated or drastically reduced by use of the proposed LIOS. The reduced safety concerns may allow for installation of ordnance items at the factory instead of the launch site, thus reducing pre-launch operational costs by streamlining ground operations.

The use of lasers for ignition of explosives is not new. Research in this area began more than twenty-five years ago. In fact, the small intercontinental ballistic missile (SICBM) program developed and flight demonstrated a crystalline rod laser system a few years ago. The SICBM laser ordnance concept is shown below.

### SICBM Laser Ordnance Concept



The SICBM concept served its purpose well. Unfortunately, it is more complicated than the conventional ordnance firing system. It requires numerous electro-mechanical components for safety and operational reasons.

Power to the rod laser is sequenced through an electro-mechanical switching network similar to that used in the conventional system. For system function an optical shutter is remotely actuated to allow lased light to be directed onto a motor driven sequencer. The sequencer has optical prisms on a rotating wheel that allow for splitting of the laser beam for multiple output functions.

Included in the system, but not shown in the schematic, is a built-in-test (BIT) feature. The BIT feature requires additional electro-mechanical devices to bypass the rod laser and let a light emitting diode (LED) be pulsed into the fiber optic transmission line. To verify health of the transmission line, the LED's pulse is reflected at



the LID and it's total travel time measured by means of an optical time domain reflectometer (OTDR). This transmission line check-out is done as late in the pre-launch cycle as practical. The OTDR is not part of the flight hardware.

The use of semiconductor laser diodes as an ignition source is a new, emerging technology. Their use is, by all indications, a viable alternative not only to the present day electrically initiated systems but also to the SICBM approach. At the onset of the SICBM effort, laser diode technology had not developed sufficiently to provide output energies needed to meet LID ignition margin requirements. Today the technology has progressed to a point that laser diodes can provide high energies with ample margin.

Using laser diodes in place of crystalline rod lasers is a quantum leap in miniaturization. This miniaturization allows for multiple outputs without having to use a mechanical prism sequencer as in the SICBM system. All mechanical components are removed. It also allows for the introduction of solid state control logic circuits to further advance explosive ignition technology in space applications.

## **SMC LIOS**

The SMC LIOS standardization plan is broken down into six major tasks shown below.

### **LIOS Major Tasks**

| Task  | Accomplishment   | Exit Criteria  |
|---|--|--|
| 1. Acquire Range Cmdrs Council approval for use of solid state LIOS | Eliminate mechanical components in ordnance firing circuits                          | LIOS not approved or use of moving components with LIOS mandated   |
| 2. System and circuit modeling                                      | Validate circuit performance<br>Validate system energy margins<br>Assess BIT designs | Solid state logic cannot meet performance/safety requirements<br>Lack of margin<br>BIT not compatible with designs |
| 3. Determine system compatibility with RF/EM/ESD                    | Compatibility validated  | System not compatible  |
| 4. Verify compatibility with SMC programs                           | Interfaces validated   | LIOS not compatible  |
| 5. Determine cost benefit of LIOS use                               | Cost benefits defined  | No cost savings  |
| 6. Qualify and flight demo an SMC compatible LIOS                   | LIOS technology ready for SMC use  | Funding not available  |

The following discussion will outline the key points of each task. Note that the exit criteria shown for each task is not task completion. It is criteria that will prevent LIOS from becoming a standard for SMC programs, i.e., criteria that would cause cessation of the SMC LIOS standardization effort.

3

The first Task is to obtain an agreement with the Range Commanders Council allowing use of LIOS at all launch sites. To be specific, the agreement must allow use of a LIOS, without moving parts, i.e., remotely controlled shutters, etc., on any ordnance system, at any launch site. This includes both flight termination and operational ordnance firing systems.

If the Task 1 agreement cannot be attained the SMC LIOS effort will stop. The cost advantages of a LIOS using mechanical components compared to the cost of today's conventional ordnance firing system are not of sufficient magnitude to warrant implementation.

The remaining tasks will provide technical rational to support safety and performance requirements of the Task 1 agreement. These must satisfy any Range Commanders Council or SMC program concerns.

The second task is to analyze the solid state circuits to verify that they can meet safety and performance requirements. This will be followed by an effort to model the entire LIOS and assess performance margins. The margin analysis must show that there is at least 50% more energy available than necessary to ignite the LID when all system parameters and external environments are at their extremes. If the designs can not show sufficient margins for safety and performance needs, the SMC LIOS effort will be stopped.

Circuit concepts will be analyzed and be validated by bench tests of designs that are representative of the optimum configurations. These tests are considered a key element in the validation of the LIOS concept. Contributing expertise to these tasks are Dave Landis and Don Herbert of the Electronics Division.

During the course of the modeling BIT designs will be evaluated. The BIT feature will be used to check continuity of the ETS path between the laser diode and the LID only. Full power system checks will be done prior to final connection of the LID and be performed as late in the pre-launch cycle as deemed practical. A key feature of the LIOS implementation is an ability to perform remote check-out of system health without interfering with other pre-launch activities. Therefore, the LIOS effort will be stopped if an adequate BIT feature cannot be found.

The third task is to determine the LIOS compatibility with external environments that may cause premature ignition or prevent ignition of the LID. These environments include lightning induced electro-static discharges (ESD), R-F and electro-magnetic interferences (EMI). These are the same

environments that are concerns for conventional ordnance firing circuit designs. As previously noted, current designs are influenced by these while the LIOS is not. Verification of LID compatibility with reasonable limits of these environments is obtainable. Much work has been done in this area and will be evaluated for applicability.

The LFU must also be shown to adequately shield these environments from the sensitive components within it. If the LID or the LFU can not be shown to survive reasonable limits of these environments, and designs cannot be altered to do so, the SMC LIOS effort will be stopped.

The fourth task examines the compatibility of LIOS with common SMC program interfaces. An attempt will be made to determine the optimum LIOS configuration in terms of the number of LID outputs, control circuit configurations and BIT options. This will, more than likely, result in several configurations and create a family of LIOS options. Determining the number of changes to the LIOS design to suit interface needs and maximize standardization will be a major part of the task.

All of the above will have a direct impact on Task 5 which will evaluate cost benefits of LIOS implementation. Task 5 is also affected by other factors including ground operations and flight performance improvements. In ground operations costs, procedural changes in handling and check out of conventional ordnance systems versus LIOS need to be assessed.

It is anticipated that use of LIOS on SMC programs will be limited to new programs and to those undergoing major changes. The non recurring costs of a blanket change to use a LIOS on existing programs is prohibitive. No other justification would outweigh these cost differences.

If the fifth task indicates that there is no cost savings the effort will be stopped. Likewise, if Task 4 shows that the LIOS is not compatible with SMC programs the LIOS effort will be stopped.

The sixth task will be the ultimate proof of the LIOS concept and its compatibility with SMC programs. The work of the other tasks will result in creation of a performance and requirements document that will be used to solicit multiple suppliers for qualification of LIOS designs. This will be followed by a flight demonstration on an SMC program. Success will demonstrate the usefulness of LIOS for space and launch applications. Task 6 will not be executed if funding is not made available.

## **Acknowledgments**

The author wishes to thank Col. J. Randmaa, Col W. Riles, Maj. K. Johnson, Capt. R. Anderson and W. Evans of the SMC Chief Engineers office, and Dr. J Meltzer, Dr. R. Hall and J. Gower of The Aerospace Corp. Chief Engineers office for sponsoring the pursuit of the LIOS plan. I also need to thank Norm Schulze of NASA Hqtrs for the opportunity of being a member of his NASA/DOD/DOE Pyrotechnic Steering Committee where the LIOS concept was initiated.

57-28  
6487  
10

## MINIATURE LASER IGNITED BELLOWS MOTOR

Steven L. Renfro  
The Ensign-Bickford Company  
Simsbury, CT

Tom M. Beckman  
The Ensign-Bickford Company  
Simsbury, CT

### Abstract

A miniature optically ignited actuation device has been demonstrated using a laser diode as an ignition source. This pyrotechnic driven motor provides between 4 and 6 lbs of linear force across a 0.090 inch diameter surface. The physical envelope of the device is 1/2 inch long and 1/8 inch diameter. This unique application of optical energy can be used as a mechanical link in optical arming systems or other applications where low shock actuation is desired and space is limited.

An analysis was performed to determine pyrotechnic materials suitable to actuate a bellows device constructed of aluminum or stainless steel. The aluminum bellows was chosen for further development and several candidate pyrotechnics were evaluated. The velocity profile and delivered force were quantified using an non-intrusive optical motion sensor.

### Introduction

A small optical to mechanical link has been developed for uses where low velocity force is required. This device uses a small B/KNO<sub>3</sub> charge to actuate a miniature rolling bellows. This laser diode ignited system provides approximately 4 lbs of force over 0.1 inches of displacement. The device was designed to move a small barrier either into or out of the way to provide means for a miniature optical arming feature. The overall size of the device is less than 1/2 inches long and 1/8 inches in

diameter. A mounting feature allows simplified integration into new or existing systems.

### Design Analysis

The challenges of this development program are to balance the gas output to desired force, ignite with a 1 Watt rated laser diode, and to downsize processes to manufacture such a small complex device.

The force is dictated by the material used for the bellows. This analysis assumes that in order to sufficiently move the bellows, plastic deformation must occur. This requires that the yield point of the selected material be exceeded without violating the ultimate strength. Following these guidelines, the pressure required for actuation can be calculated. The results are summarized in Table 1.

The burst pressure for hardened aluminum alloys is less than the pressure required for actuation. Annealed 302 Stainless Steel, Aluminum 1100-0, or Aluminum 3003-0 are suitable bellows candidate materials. Using this information, the resultant force developed by a fully actuated bellows can be calculated. The force results are listed in Table 2.

In order to produce the desired force,

several candidate pyrotechnic materials and stoichiometries were considered. Size restraints required that the selected pyrotechnic use the space allocated for the charge holder precisely. This analysis was crucial due to space restraints for the charge allocated given the overall size envelope.

The amount and type of pyrotechnic material was calculated based on the pressure required for actuation using the NASA-Lewis equilibrium thermochemistry code. The results of this analysis are normalized to  $\text{Ti/KClO}_4$  and are listed in Table 3.

The mass calculations were used to select materials for prototype testing. Based on these mass calculations, the first candidates selected for prototype testing were  $\text{B/KNO}_3$ ,  $\text{Ti/KClO}_4$ , and  $\text{B/BaCrO}_4/\text{KClO}_4$ .

#### Initial Prototype Testing

In order to gain information isolated to function of the bellows, larger prototypes were used for the initial test series. The results of the first two groups of five prototypes each are listed in Table 4.

The  $\text{B/KNO}_3$  resulted in an acceptable charge weight for the desired extension. The other candidates did not perform successfully. The  $\text{B/BaCrO}_4/\text{KClO}_4$  loaded devices would not ignite using the output from a 1 W laser diode. The  $\text{Ti/KClO}_4$  loaded devices resulted in burst of the bellows. The burn rate of the  $\text{Ti/KClO}_4$  did not provide the low velocity required for this application.

#### Sensitivity of $\text{B/KNO}_3$

The  $\text{B/KNO}_3$  material ignites consistently

using full power 840 nm diode with a 10 ms pulse width. An interface sensitivity test was used to verify reliability. The results of this testing using 200 micron fiber are listed in Table 5. These results are listed based on the calibrated output from the diode and do not include line losses.

#### Process Development

The success of this miniature component depends highly on an integral charge holder / fiber optic subassembly. In order to offset losses expected in fiber optic interfaces, a smaller core fiber was chosen to increase the power density of the available optical energy. This allows for the fiber to be prepared prior to final assembly into the charge holder. Polishing would not be possible given the restricted space. The Ensign-Bickford Company developed a cleaving technique capable of limiting losses to less than 1dB at the final assembly level. These losses are acceptable for reliable ignition without polishing the fiber in the final assembly.

The charge for the test units was pressed directly onto the fiber to ensure intimate contact between the fiber and the  $\text{B/KNO}_3$ .

The development units were assembled using processes developed for miniaturization. These early development units were then functionally tested to verify analysis and prototype work and to determine force and velocity output.

#### Force Output Testing

The units are designed to function under axial load, therefore, it is desirable to test them in that mode. A crushable foam

was selected to determine the approximate output force developed by each test unit. The bellows must develop at least 2.64 lbs to actuate. The goal for total nominal developed force is 4.02 lbs. A polyurethane foam was selected with a minimum compressive strength to require at least 2.0 lbs to crush in order to assess the total nominal force output. Figure 2 illustrates the test setup and Figure 3 illustrates the results of the four units tested using this method.

Each of the test articles were bonded to the test block utilizing the existing mounting flange and two part epoxy. This bonding method successfully held each test unit during function. Three of the units extended approximately 0.060 inches into the foam block and the fourth did not actuate. The failed unit was inspected and revealed that the bellows had been inadvertently bonded in place during assembly. This unit burst under the developed pressure. This lesson learned resulted in careful inspection of the bellows area after final assembly. The area filled with epoxy cannot be readily viewed with the unaided eye. Future assembly will necessarily require magnification.

#### Velocity Testing

To assess the overall impulse of the delivered force, a simple velocity measurement sensor was devised. This article is illustrated in Figure 2.

The velocity fixture is quite simple. Two donor fiber optics are aligned across a channel with acceptor fiber optics. Each donor / acceptor pair is placed at a known distance from the unextended bellows. Using white light as a source, the acceptor fiber picks up the light and

is then connected to a photo-diode to produce a small voltage. Upon function of the unit, this optical path is broken resulting in a voltage drop across the photo-diode. This voltage is monitored using an oscilloscope to determine a time difference between the donor / acceptor pairs. This measurement scheme allows for determination of average bellows velocity without interrupting the function.

The results of three of these test units are presented in Figure 4. During function of the bellows motor into air, the test bellows for the first unit did not stay intact. This indicated that the unit probably is producing too much gas for function without axial load. The resultant velocity is not for the entire bellows for this test unit, but for the aluminum end free from the assembly. The second and third units functioned correctly and the velocities measured are for the bellows.

#### Further Development Work

The Ensign-Bickford Company is continuing to develop this product under contract for Los Alamos National Laboratory. The ideal miniature bellows will function under load to produce the desired force and be able to function in air without expelling products of reaction. The final development phase is to concentrate on optimizing the charge size in order to meet these goals.

#### Discussion

The analysis and prototype phase contributed to development of the miniature bellows motor. More work needs to be done to refine the design. A pyrotechnic device to deliver a small amount of force is possible and has been demonstrated.

**Table 1. Pressure Requirements for Bellows Actuation and Burst**

| Bellows Material | Alloy and Temper | Minimum Actuation Pressure (psi) | Burst Pressure (psi) |
|------------------|------------------|----------------------------------|----------------------|
| Aluminum         | 1100-0           | 389                              | 577                  |
| Aluminum         | 1100-H12         | 1089                             | 689                  |
| Aluminum         | 1100-H14         | 1555                             | 977                  |
| Aluminum         | 3003-0           | 467                              | 711                  |
| Stainless Steel  | 302, Annealed    | 2722                             | 4000                 |

**Table 2. Force Developed for Various Bellows Materials**

| Bellows Material | Alloy and Temper | Actuation Force (lbs) | Target Force (lbs) |
|------------------|------------------|-----------------------|--------------------|
| Aluminum         | 1100-0           | 2.64                  | 4.02               |
| Stainless Steel  | 302, Annealed    | 17.32                 | 25.45              |

**Table 3. NASA Lewis Calculation Results**

| Candidate Pyrotechnic Formulation       | Calculated Flame Temperature (K) | Normalized Mass Required to Produce 500 psi |
|---|----------------------------------|---|
| Ti/KClO <sub>4</sub>                    | 5006                             | 1.00  |
| Ti/KClO <sub>4</sub> + RDX              | 4155                             | 0.63  |
| RDX + C                                 | 3083                             | 0.67  |
| B/BaCrO <sub>4</sub> /KClO <sub>4</sub> | 3872                             | 1.19  |
| BKNO <sub>3</sub>                       | 4044                             | 0.79  |

**Table 4. Results of Initial Prototype Testing**

| Pyrotechnic Material                    | Charge Mass (mg) | Ignition Source | Maximum Extension |
|---|------------------|-----------------|-------------------|
| BKNO <sub>3</sub>                       | 6                | Laser Diode     | 0.08              |
| Ti/KClO <sub>4</sub>                    | 6                | Laser Diode     | Bellows Burst     |
| B/BaCrO <sub>4</sub> /KClO <sub>4</sub> | 6                | Nd:YAG          | 0                 |

**Table 5. Ignition Threshold Test Results Using 840 nm Diode**

|                           | Test Results |
|---------------------------|--------------|
| No. of Tests              | 10           |
| Threshold (50% Level)     | 536 mW       |
| Standard Deviation        | 56 mW        |
| All-Fire Level (.999/95%) | 909 mW       |

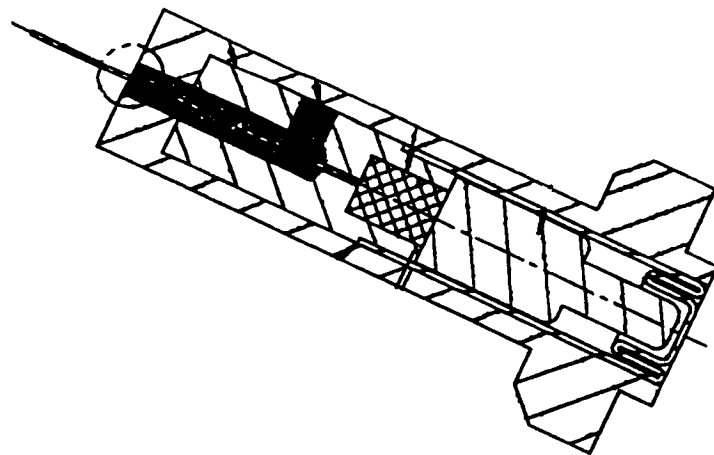


**Figure 1** Minature Laser Ignited Bellows



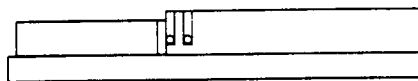
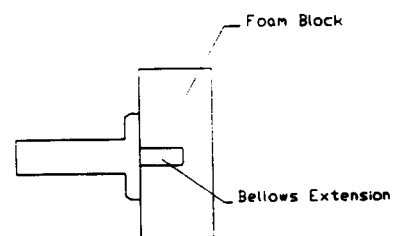
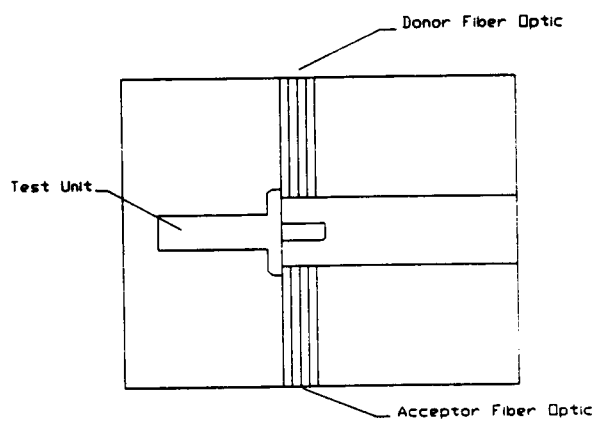


**Figure 2** Force and Velocity Test Setup

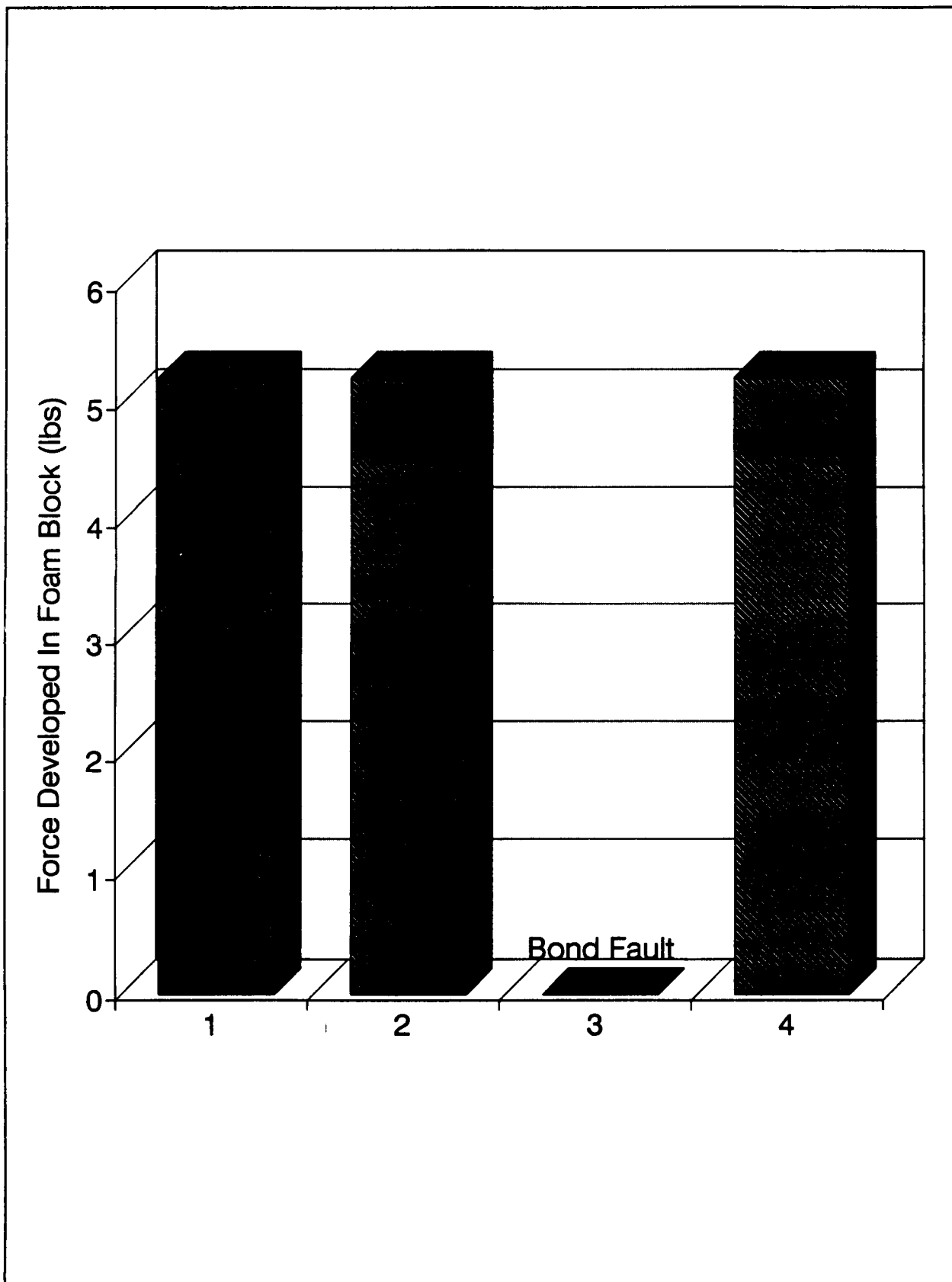


**Figure 3** Force Output Test Results

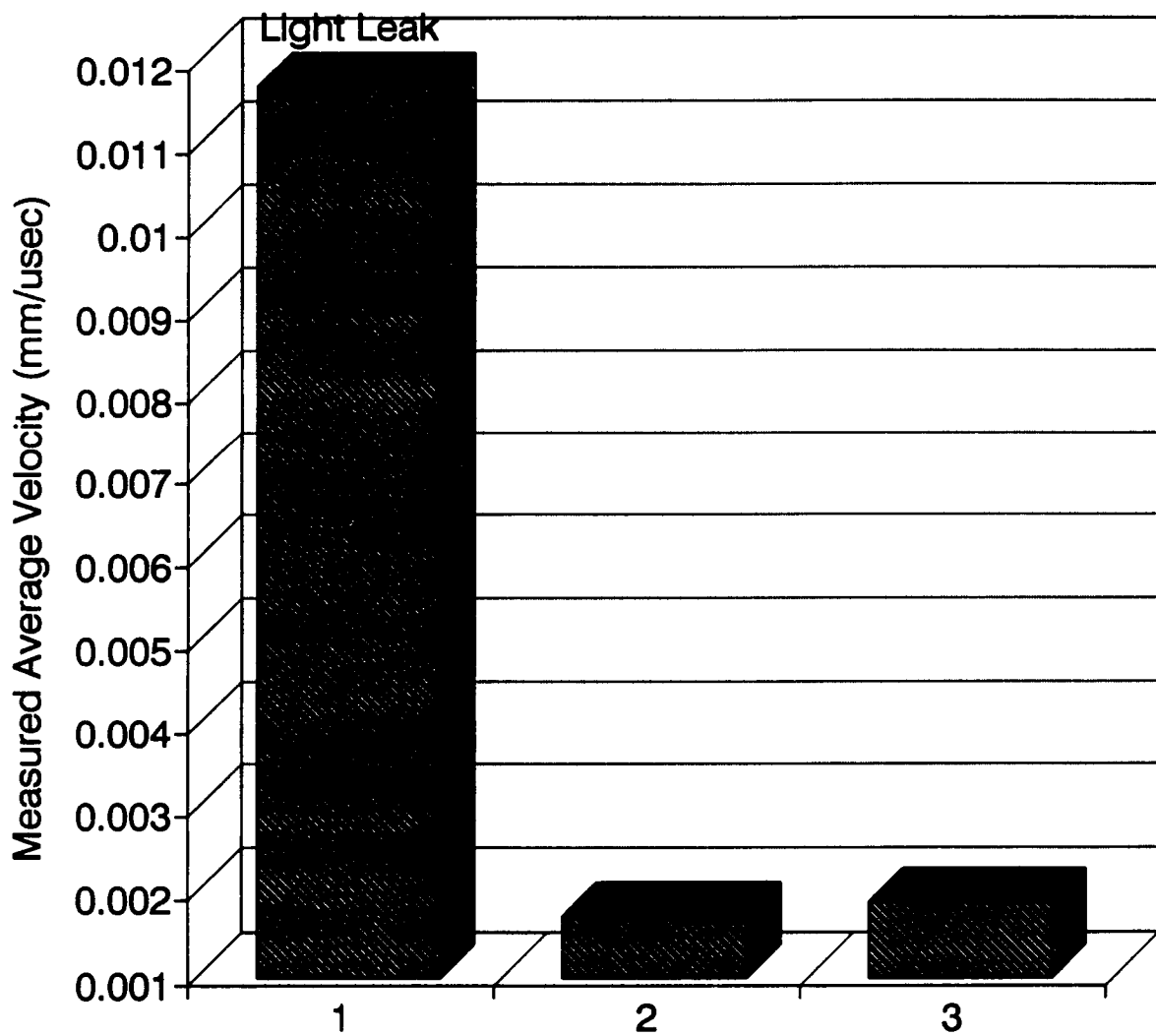


**Figure 4** Results of Velocity Tests



58-28  
6988  
P-8

## PERFORMANCE CHARACTERISTICS OF A LASER-INITIATED NASA STANDARD INITIATOR

John A. Graham  
Senior Project Engineer  
The Ensign-Bickford Company  
Aerospace and Specialty Products

### INTRODUCTION

The Ensign-Bickford Company has been actively involved in the design and development of a laser equivalent to the electrically initiated NASA Standard Initiator (NSI). The purpose of this paper is to describe the present design and its performance characteristics. Recommendations for advancement of this program are also presented.

### DESIGN DESCRIPTION

The Ensign-Bickford Laser-initiated NASA Standard Initiator (LNSI) design consists of an Optical Connector, Optical Fiber and a Propellant that is hermetically sealed in a Squib Housing (see Figure 1). The LNSI is equivalent to the NSI, using the NSI propellant and matching the installation envelope so that it can be used to function present NSI initiated devices.

A standard ST or SMA connector is used and attached to the optical fiber with a pot and polish technique. The present design uses 200 micron Hard Clad Silica optical fiber but is not limited to that size; larger or smaller diameter fiber can be incorporated if dictated by system level requirements. The fiber is installed and sealed into an optical header using Ensign-Bickford proprietary fiber seal technology. The Ensign-Bickford seal has demonstrated hermeticity after exposure to a 40,000 psi proof pressure; also hermeticity is

maintained post-function. This seal technology has been successfully employed in devices functioned from  $-62^{\circ}\text{C}$  to  $+93^{\circ}\text{C}$  ( $-80^{\circ}\text{F}$  to  $+200^{\circ}\text{F}$ ) and has successfully endured exposure to the same level of thermal shock without performance degradation.

The propellant is the NSI-defined blend of Zirconium, Potassium Perchlorate, Graphite and Viton "B". Powdered raw materials are wet blended in a high shear blender followed by application of Viton "B" via a precipitation process. The mix has been examined by Scanning Electron Microscope and found to be uniform. The blending process does not alter particle morphology.

The optical fiber is polished *in situ* and dB loss characteristics verified prior to propellant loading. The propellant is in direct contact with the exposed polished fiber face thus allowing laser diode power to reach the propellant without power density loss due to beam divergence.

Hermetic sealing is provided by laser welds. A closure disc is laser welded onto the output end of the squib housing. The disc has a chemical milled "flower pattern" which "blossoms" when the device is functioned. The flower pattern prevents expulsion of large metallic particles from the squib and into devices which would be detrimental in some applications.

Two versions are available, one using a stainless steel housing and another using Inconel 718. In either design, the charge cavity is proof pressure tested at 15,000 psi prior to loading propellant.

### **ALL-FIRE POWER**

Reliability testing has been done to establish the all-fire power requirement at room temperature. Testing was done using 200 $\mu$ m fiber. The "pass" criteria was that the time from the start of the laser pulse to first pressure had to be less than or equal to 10 milliseconds, although the actual laser diode pulse width was 50 milliseconds. The long duration pulse was used to get a better characterization of the relationship between power and time to ignition (Figure 2). The 0.9999 all-fire power at 95% confidence is 595 milliwatts. This corresponds to an all-fire power density of 1900 watts/cm<sup>2</sup>.

### **LASER IGNITION TRANSIENT THERMAL FINITE ELEMENT ANALYSIS (FEA)**

The reliability test data suggests that ignition time repeatability is a function of the laser power. At high laser power, the function time (i.e. time to ignition) is short and repeatable, but as power is decreased, function time slows and is less predictable.

Transient FEA was done over a range of input powers to gain a qualitative understanding of this phenomena. The computer model included the propellant, fiber optic core/cladding, epoxy and surrounding metal structure. Upon initial application of laser energy, the heating rate is high, but slows and asymptotically approaches a limit that is a measure of the LNSI's ability to reject heat to the surrounding environment. If the

autoignition temperature of the mix is reached quickly, then the function time will be very repeatable because only the propellant is heated and therefore only the variability of the propellant comes into play (eg mix homogeneity, density gradient within the pressed powder, etc). As the time to ignition increases, the thermal effects of the surrounding materials become significant. Sources of variation include the amount of epoxy and the concentricity of the optical fiber to the ferrule. Conditions such as these increase the variability of the thermal time constant resulting in greater function time jitter.

This has system level implications. The specification for the laser diode firing unit pulse duration needs to balance the output power of presently available laser diodes versus the inherent increase of non-repeatability of function time as the pulse duration is lengthened to allow for lower net laser diode power. Another way to state this is function time jitter will be minimized when the laser diode with the highest output power is used. Also, thermal isolation of the propellant from surrounding materials will result in more repeatable ignition and, therefore, lower all-fire power level which in turn means laser diode output power requirements are reduced.

### **PRESSURE PERFORMANCE**

For many NSI users, the interest is in output pressure characterization since the NSI is used as a cartridge to actuate pressure driven devices (eg bolt cutters, pin pullers, etc). The LNSI has demonstrated a nominal output pressure of 654 psi over the last several lots of LNSI's; within each lot, the Coefficient of Variation has ranged from 3 to 5%.

Also of concern is the response time and time to peak pressure. At 800 milliwatts net power applied at the opto-propellant interface, function times (i.e. time from application of laser diode power to first pressure) has been 1.5 milliseconds with a Coefficient of Variation of 12%; time to peak pressure has been 0.13 milliseconds with a Coefficient of Variation of 20%.

This data is difficult to compare with the NSI specification since requirements are tied to the applied current level. What can be said first of all is the energy source, whether it be a hot bridge wire or a laser diode, does not effect the pressure performance of the NSI propellant. Secondly, the pressure rise rate to 525 psi can be inferred to be equal to or better than the rise rate performance reported above for attaining peak pressure. Further, all of the NSI pressure-time requirements at 3.5 amps can be met:

- (1) Time to first pressure of greater than 1.0 milliseconds
- (2) Time to 525 psig shall not exceed 6.0 milliseconds
- (3) Peak pressure shall be 525 to 775 psig
- (4) Range of time to first pressure shall not exceed 3.5 milliseconds
- (5) Range of pressure rise from first pressure to 525 psig shall not exceed 0.5 milliseconds

## **PLANNED TESTING**

Development testing is on-going at Ensign-Bickford. The next test series includes exposure to random vibration and thermal cycling along with high and low temperature all-fire power reliability tests. The requirements were customer driven based upon satellite requirements. The test matrix is shown in Table 1.

Random Vibration will consist of 1 min/axis exposures to the level indicated on Figure 3 .

Thermal cycle exposure will be from -16°C to +56°C (3°F to 133°F) for a total of 6 cycles with a 2 hours minimum dwell at temperature.

The final two test groups will be used in reliability tests to establish all-fire power at hot and cold temperatures.

## **RECOMMENDATIONS FOR FUTURE DEVELOPMENT**

Further development of the LNSI is needed to expand the performance envelope. No problems are anticipated from vibration due to the mechanical similarities between the NSI and the LNSI. The thermal environment does however raise some questions regarding low temperature performance of optical fibers.

A parallel task is to develop a specification for an LNSI. Specific areas needing attention are: (1) all-fire power and pulse width, (2) no-fire power and pulse width (which also requires credible stray light sources to be identified and quantified) and, (3) pressure versus time performance.

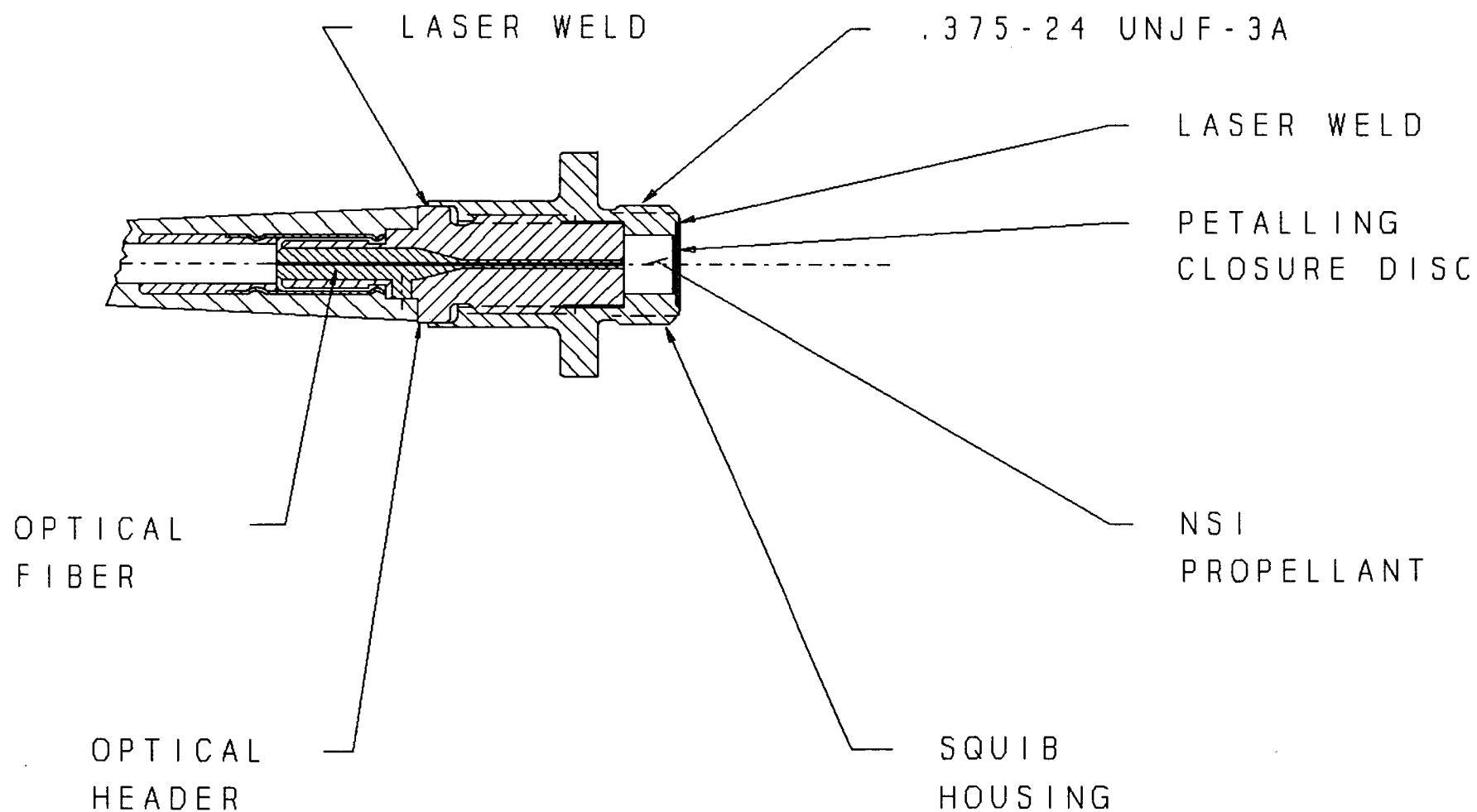




**TABLE 1 -- FLIGHT READINESS TEST MATRIX**

| <b>TEST</b>                 | <b>GROUP</b>         |                      |                      |                      |                       |                       |
|-----------------------------|----------------------|----------------------|----------------------|----------------------|-----------------------|-----------------------|
|                             | <b>A<br/>9 Units</b> | <b>B<br/>9 Units</b> | <b>C<br/>9 Units</b> | <b>D<br/>9 Units</b> | <b>E<br/>20 Units</b> | <b>F<br/>20 Units</b> |
| <b>INSPECTION</b>           | ●                    | ●                    | ●                    | ●                    | ●                     | ●                     |
| <b>THERMAL<br/>CYCLE</b>    |                      |                      | ●                    | ●                    |                       |                       |
| <b>RANDOM<br/>VIBRATION</b> |                      | ●                    |                      | ●                    |                       |                       |
| <b>FUNCTION</b>             |                      |                      |                      |                      |                       |                       |
| <b>High Temp</b>            | <b>3</b>             | <b>3</b>             | <b>3</b>             | <b>3</b>             |                       | <b>20</b>             |
| <b>Ambient</b>              | <b>3</b>             | <b>3</b>             | <b>3</b>             | <b>3</b>             |                       |                       |
| <b>Low Temp</b>             | <b>3</b>             | <b>3</b>             | <b>3</b>             | <b>3</b>             | <b>20</b>             |                       |

**Figure 2**  
**LASER INITIATED NSI PERFORMANCE**  
**200 $\mu$  Optical Fiber Pigtail**  
**Room Temperature Data**

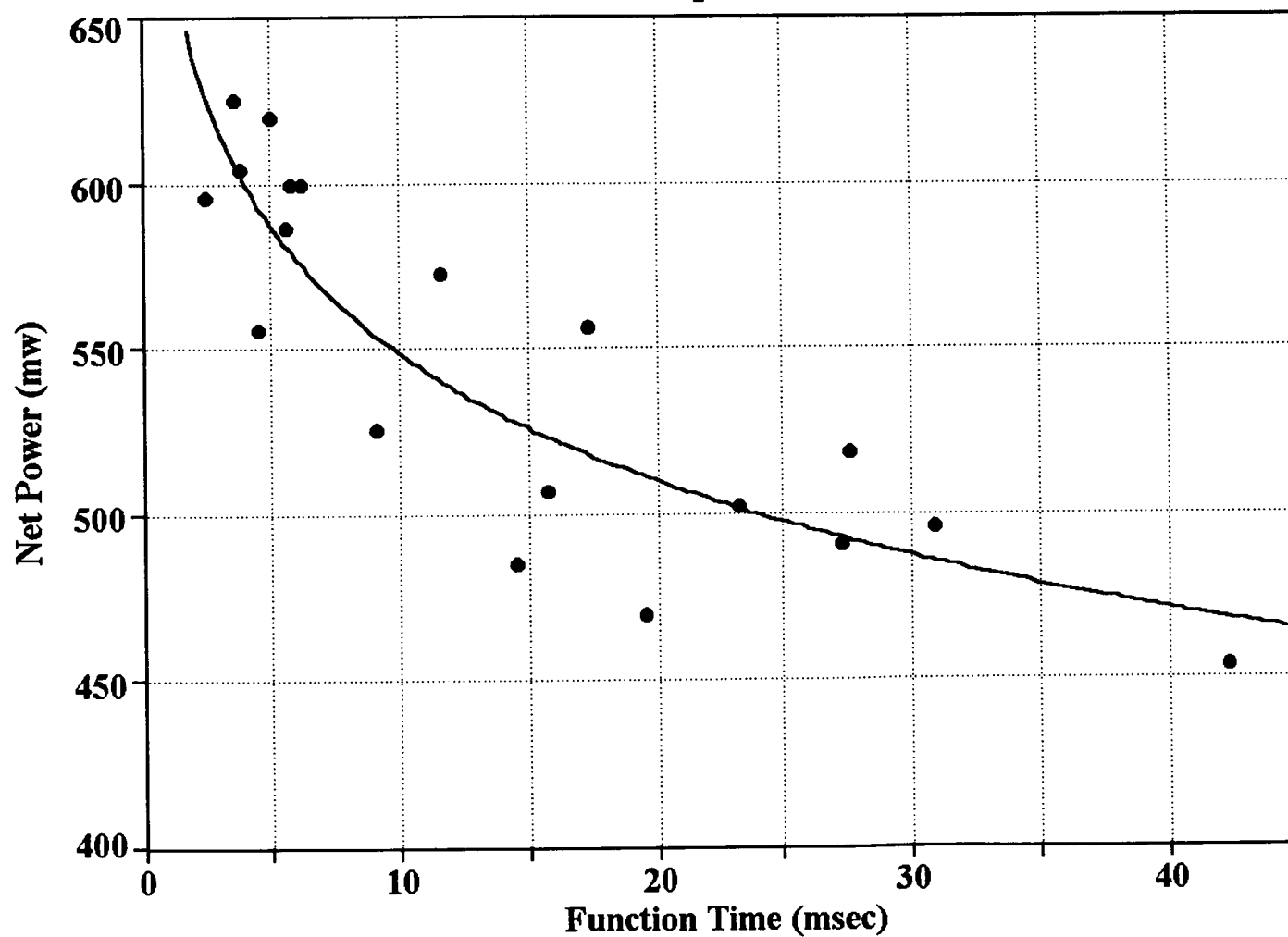
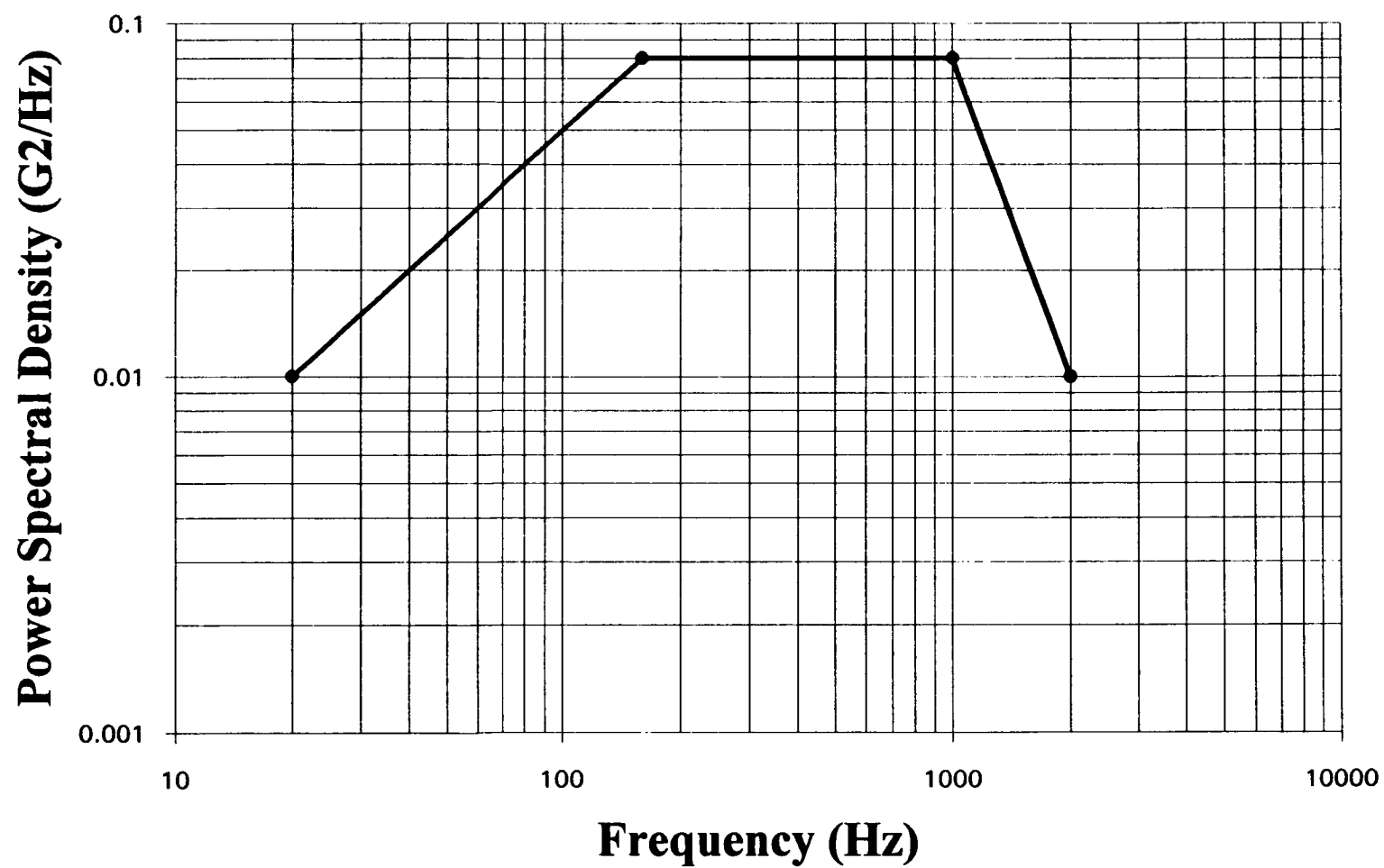


**Figure 3 -- Random Vibration Spectrum**



59-28  
6284  
14

## Four Channel Laser Firing Unit Using Laser Diodes

David Rosner, Sr. Electrical Development Engineer  
Edwin Spomer, Sr. Electrical Development Engineer  
Pacific Scientific/ Energy Dynamics Division

### ABSTRACT

This paper describes the accomplishments and status of PS/EDD's internal research and development effort to prototype and demonstrate a practical four channel laser firing unit (LFU) that uses laser diodes to initiate pyrotechnic events. The LFU individually initiates four ordnance devices using the energy from four diode lasers carried over fiber optics. The LFU demonstrates end-to-end optical built in test (BIT) capabilities. Both Single Fiber Reflective BIT and Dual Fiber Reflective BIT approaches are discussed and reflection loss data is presented.

This paper includes detailed discussions of the advantages and disadvantages of both BIT approaches, all-fire and no-fire levels, and BIT detection levels. The following topics are also addressed: electronic control and BIT circuits, fiber optic sizing and distribution, and an electromechanical shutter type safe/arm device. This paper shows the viability of laser diode initiation systems and single fiber BIT for typical military applications.

### 1. INTRODUCTION.

**1.1 Purpose.** This paper presents the accomplishments and status of Pacific Scientific/Energy Dynamics Division (PS/EDD) internal research and development effort to prototype and demonstrate a practical Four Channel Laser Firing Unit (LFU) incorporating laser diodes. In this program, PS/EDD is developing and demonstrating laser diode initiated safe/arm technology for commercial, space, and defense applications.

**1.2 Design Goals.** PS/EDD designed the LFU as a Safe and Arm Device (SAD) shown in

Figure 1 for a typical missile application requiring flight functions like stage separation, motor ignition, and shroud removal. We designed it to operate in typical missile environments. EMI/EMP protection features, and systems for built-in-test (BIT) of the optical and electronic subsystems were incorporated. We chose a simple electronic interface using redundant electronic controllers that can be tailored to support a more sophisticated interface.

As much as practical, we designed the LFU to address the typical Military safety specifications and guidelines for in-line SAD. The LFU uses one electromechanical energy barrier in the optical path, several static switches in the arm and firing circuits, and no mechanical barrier in the ordnance train.

**1.3 Typical Safety Requirements.** Ordnance subsystems must often meet certain documented safety criteria. The following documents are some of the specifications that can be applied to ordnance subsystems in military and aerospace systems:

- MIL-STD-1316D titled "Military Standard, Fuze Design, Safety Criteria For"
- MIL-STD-1512 titled "Military Standard, Electroexplosive Subsystem, Electrically Initiated, Design Requirements and Test Methods"
- MIL-STD-1576 titled "Military Standard, Electroexplosive Subsystem Safety Requirements and Test Methods For Space Systems"
- MIL-STD-1901 titled "Military Standard, Munition Rocket and Missile Motor Ignition System Design, Safety Criteria For"
- WSERB Guidelines Titled "WSERB Technical Manual For Electronic Safety and Arming Devices with Non-Interrupted Explosive Trains"

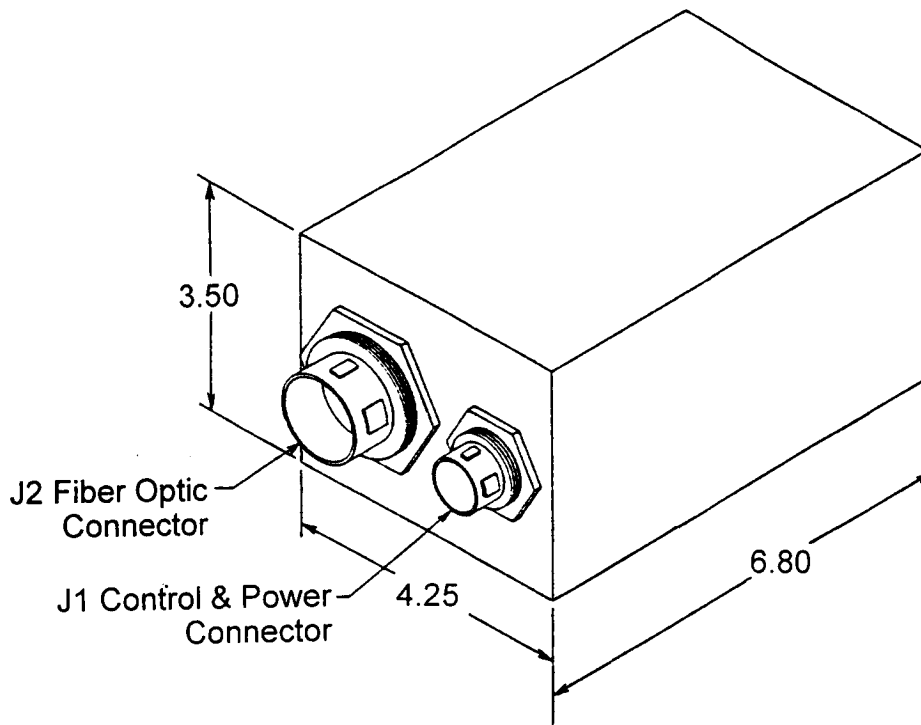


Figure 1. Four Channel Laser Firing Unit

Both MIL-STD-1316D and MIL-STD-1901 address interruption type and in-line ordnance subsystems. The WSERB Guidelines specifically address in-line ordnance systems and are often specified in addition to MIL-STD-1316D and MIL-STD-1901. However, these specifications do not directly address laser initiation systems. The LFU is designed to address these requirements and guidelines as much as practical.

## 2. LFU OVERVIEW.

**2.1 Introduction.** The LFU uses laser diodes and solid state electronics to initiate ordnance devices via fiber optics. It contains a Laser Diode Safe/Arm Module (LDSAM) to provide the safety-reliability of a movable barrier or shutter. It also contains a built-in test system that performs an end-to-end test of the fiber optic paths.

The size of the LFU shown in Figure 1 is 6.80 in. x 4.25 in. x 3.50 in. and it weighs 3.8 lb excluding connectors and cables. The LFU is

equipped with MIL-C-38999 Class IV connectors for both electrical and fiber optic interfaces. The input power requirements are 28 Vdc at 0.4 Adc average and 3.6 Apeak for 10 ms when firing a laser.

The input commands enter the LFU through J1. Each uses an opto-isolated pair of connections that can be driven by 5 V TTL logic. The input commands are:

- Master Reset Command resets the LFU logic and starts operation in the selected Test/Launch mode. This is essentially a powerup reset without cycling power.
- Test/Launch Mode Command instructs the LFU either to perform an automatic BIT sequence (Test) or to execute the normal operational sequence (Launch) after power-up or master reset.
- Pre-arm Command energizes the Pre-arm Switch Circuit to make electrical power available to the electronic switches for the high power laser diodes and LDSAM arming solenoid.

- Arm Command energizes the Arm Switch Circuit to power the LDSAM arming solenoid using power available via the Pre-arm Switch Circuit.
- Select 1, Select 2, and Select 3 Commands act as a three bit code to select between the four LFU outputs before each fire command.
- Fire Command commands the LFU to supply the high power laser pulse from the selected output provided that the LFU is armed.

The two output status signals, BIT Pass and BIT Fail, exit the LFU through J1. Each uses an opto-isolated pair of connections providing an electronic switch closure.

The four laser outputs exit the LFU through J2. Each uses 100  $\mu\text{m}$  core 0.37 numerical aperture (NA) fiber and provides a 904 nm wavelength 10 ms pulse of approximately 1.0 watt.

**2.2 LDSAM Characteristics.** The LDSAM is a 24 output electromechanical shutter assembly with only four outputs fully assembled. It provides an optomechanical safety feature for ordnance initiation power. As show in Figure 2, all critical optical elements in the LDSAM are rigidly mounted to eliminate misalignment in harsh environments.

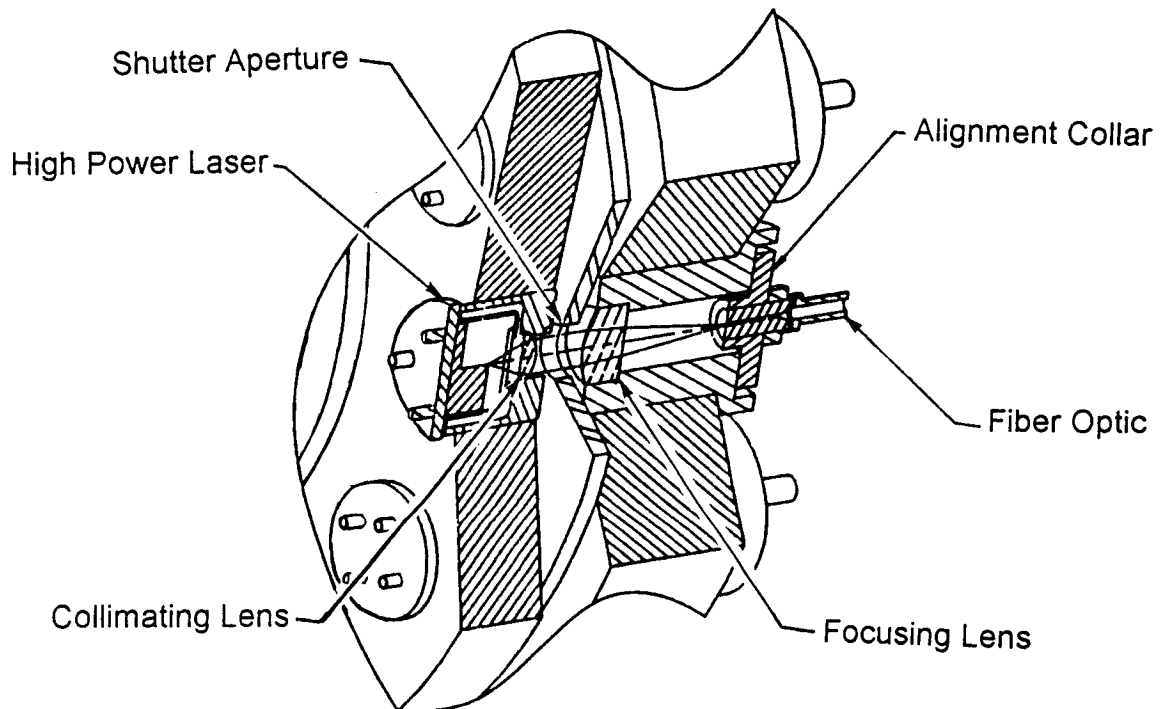


Figure 2. LDSAM Cutaway View

For each output, a rigidly mounted laser diode and collimating lens illuminates a rigidly mounted focusing lens and 100  $\mu\text{m}$  core fiber optic cable. An aluminum shutter, located between the collimating and focusing optics, acts as an energy barrier. A solenoid rotates the shutter between Safe and Arm positions with a spring loaded return to Safe.

An electro-optical sensor monitors the Safe position of shutter. Visual indication is provided by a shutter driven flag and window. The flag is labeled "S" for safe and "A" for Armed. A removable safing pin locks the shutter into the Safe position when installed.

**2.3 Built-In-Test (BIT) System.** The LFU also contains a BIT system that performs the following tests on the LFU subsystems:

- Continuity of fiber optic paths between the LFU and ordnance devices
- Firing of high power laser diodes
- Operation of Pre-arm circuits
- Operation of LDSAM.

To develop an optimal design, PS/EDD investigated two different approaches to performing the optical continuity BIT. The LFU is equipped with two channels of each type. They are:

- **Single Fiber Reflective BIT.** A low power laser signal is sent to the ordnance device through the same fiber optic used to initiate that device. This signal reflects off the dichroic mirror deposited on the window in the ordnance device and returns to the BIT system through the same fiber optic. A photodiode and electronic circuit measure its intensity.
- **Dual Fiber Reflective BIT.** A low power laser signal is sent to the ordnance device using the same high power diode laser and fiber optic used to initiate that device. The output power of the high power laser diode is limited to a level safely below the no-fire level by an aperture in the shutter. A small fraction of this signal reflects off the ordnance device window and returns to the BIT system through a second fiber optic. The BIT system uses a photodiode and electronic

circuit to measure the intensity of this reflection.

**2.4 Electronic Subsystem.** The Electronic Subsystem controls and sequences the BIT features and the laser initiation system. It also interfaces to other missile systems. The Electronic Subsystem consists of the following elements shown in the LFU Functional Block Diagram (Figure 3):

- Input and Output Circuits
- Power Converters
- Redundant Controllers
- Pre-arm Switch Circuit
- Arm Switch Circuit
- High Power Laser Drive Circuit
- BIT Laser Drive Circuit
- BIT Sense Circuits

**2.4.1 Input and Output Circuits.** We used optocouplers and transient suppressors for all electronic input and output (I/O) signals. Each input command enters the LFU through J1 and uses an opto-isolated pair of connections that can be driven by 5 V TTL logic.

Each output signal exits the LFU through J1 and uses an opto-isolated pair of connections providing electronic switch closure. All electrical inputs and outputs, including power, are equipped with semiconductor transient suppressors to protect against electrostatic discharge (ESD) and electromagnetic pulse (EMP).

**2.4.2 Power Converters.** The LFU is equipped with two DC/DC power converters that provide regulated sources of 5 Vdc for logic circuits, and of 15 Vdc for the analog circuits and the BIT lasers. Unregulated 28 Vdc provides power to both DC/DC converters and to the Pre-arm Circuit. Note, the DC/DC Converters operate when 28 Vdc is present no matter whether the Pre-arm Switch Circuit is open or closed.

The power returns for the 28 Vdc, 5 Vdc, and 15 Vdc sources are separately routed. They are connected to the chassis at a single point through 47 k $\Omega$  resistors bypassed by 0.01  $\mu\text{F}$  capacitors. This minimizes cross talk between the digital, analog, and laser fire circuits.

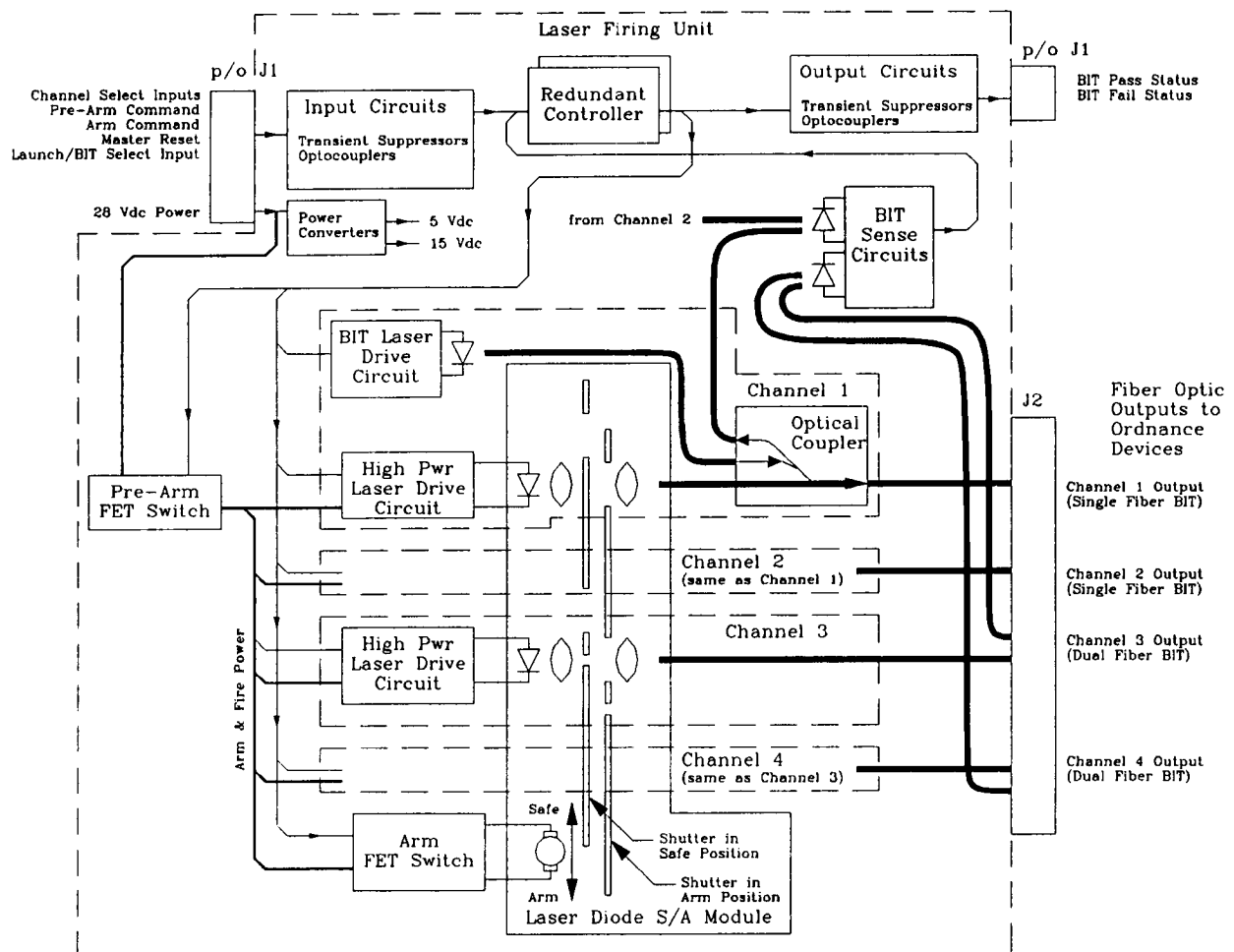


Figure 3. LFU Functional Block Diagram

**2.4.3 Redundant Controllers.** PS/EDD chose to use hard logic implemented with application specific integrated circuits (ASIC) instead of using microprocessors or stored program devices. This choice eliminates the costs involved in developing, debugging, and eventually qualifying software.

Each Redundant Controller consists of a single ACTEL brand factory programmable logic array (FPGA). Both controllers are identical and operate from a common clock. A common power-up reset circuit resets the logic circuits in each FPGA and initiates the automatic BIT testing of the LFU.

The BIT logic circuit part of each FPGA is basically a string of latches fed by logic gates. This forms a state machine that sequences through a set of predefined steps. Each step sets the FPGA's outputs to predefined levels and performs a boolean logic test of all inputs. If the test passes then the logic proceeds to the next state, if it fails the logic indicates a BIT failure and stops.

The fire control logic circuit part of each FPGA consists of logic circuits to decode the channel selection and fire commands originating from outside the LFU. It also consists of timing circuits to control the duration of the High Power Laser outputs.



Each FPGA monitors the following commands originating from outside the LFU: Master Reset Command; Test/Launch Mode Command; Pre-arm Command; Arm Command; Channel Select Inputs (Select 1, Select 2, and Select 3 Commands); and Fire Command. Each FPGA also monitors the following internal signals: Pre-arm Switch Circuit monitor; Arm Switch Circuit monitor; Safe position status of LDSAM; and output of the Bit Sense Circuit.

Each FPGA generates the Bit Pass and Bit Fail status commands for use by missile systems outside the LFU. Each also generates commands to arm the Arm Switch Circuit and to fire High Power Laser Diode Drive Circuits. The FPGA's command outputs are ANDed together by the subsystems they control. In other words, both FPGAs must issue identical output commands before a subsystem uses that output command. The BIT Fail status outputs are ORed together so that either controller can issue a BIT failure signal.

**2.4.4 Pre-arm and Arm Switch Circuits.** The LFU uses unregulated 28 Vdc to energize the LDSAM solenoid and to power the High Power Laser Diodes. The unregulated power is first routed through the Pre-arm Switch Circuit to provide the first static switch function for arming and ordnance initiation power.

The Pre-arm Switch Circuit uses MOSFET switches to switch both the +28 Vdc and 28 Vdc return lines, and is commanded by the Redundant Controllers through two series connected optocouplers. This arrangement requires that both Redundant Controllers issue the Pre-arm command to turn on the Pre-arm Switch Circuit. The Pre-arm Switch Circuit also provides a single monitor signal to both Redundant Controllers through an optocoupler.

The switched +28 Vdc and 28 Vdc return outputs of the Pre-arm Switch Circuit is then routed to the High Power Laser Drive Circuits and to the Arm Switch Circuit.

The Arm Switch Circuit provides the second static switch function for arming power. It uses

MOSFET switches to control both the +28 Vdc and 28 Vdc return lines, and to energize the LDSAM solenoid. It is also commanded by the Redundant Controllers through two series connected optocouplers and provides a single monitor signal to both Redundant Controllers through an optocoupler.

**2.4.5 High Power Laser Drive Circuit.** This drive circuit consists of four individual MOSFET switches to control each of the four High Power Laser Diodes. These MOSFET switches receive switched +28 Vdc power from the Pre-arm Switch Circuit through a common current regulator circuit. The current regulator compensates for variations in the unregulated 28 Vdc power source and provides a constant current to the High Power Laser Diodes. It is designed to operate the lasers within their rated power limits.

The MOSFET switches provide the second static switch function for ordnance initiation power and are controlled by the Redundant Controllers through two series connected optocouplers. As with the Pre-arm and Arm Switch Circuits, this arrangement requires that both Redundant Controllers issue the fire command to turn on a laser diode.

**2.4.6 BIT Laser Drive Circuits.** This drive circuit consists of two individual MOSFET switches to control each of the two BIT Laser Diodes used in the single fiber BIT system. These MOSFET switches receive regulated 15 Vdc from the Power Converters through a common current regulator circuit. The current regulator provides a constant current to the BIT Laser Diodes and operates the lasers within their rated power limits.

The MOSFET switches are controlled by the Redundant Controllers through two series connected optocouplers. As with the High Power Laser Drive Circuits, this arrangement requires that both Redundant Controllers issue the fire command to turn on a laser diode.

**2.4.7 BIT Sense Circuit.** This circuit supports the optical continuity BIT function by sensing

the reflected light and by providing a simple digital signal to Redundant Controllers. The BIT Sense Circuit supports both Single and Dual Fiber BIT systems, and consists of:

- Photo diodes to sense the reflected BIT signals
- Analog circuits for amplification and level detection
- Optocouplers for output to the Redundant Controllers

The sensitivity of the BIT Sense Circuit is limited by the photo diode's rated dark current while the response time is limited by the photo diode's total capacitance rating. In other words, the optical BIT signal must be bright enough to be reliably detected above the photo diode's worst case dark current and must be present long enough for the photo diode's capacitance to charge up.

### 3. LASER DIODE INITIATION SUBSYSTEM.

**3.1 Introduction.** The basic mechanism for laser ignition is thermal in nature. The laser ignition system must deliver a sufficient intensity to raise the temperature of the ordnance compound above its ignition temperature. This depends on the properties of the ordnance compound such as: ignition temperature, thermal diffusivity, specific heat, surface optical properties, and particle size.

The Laser Diode Initiation Subsystem uses continuous type lasers that are typically rated in watts. For this reason, it is best to specify the all-fire and no-fire levels in units of power (milliwatts) instead of units of energy (millijoules). Since the all-fire and no-fire levels depend on spot size, the type of fiber used to deliver the laser energy to the ordnance device must be specified.

For this design we used a 100  $\mu\text{m}$  core step index fiber optic inside the LFU and 110  $\mu\text{m}$  core step index fiber for the external cables. This conserves the intensity of the laser diode as it is delivered to the ordnance device.

The optical path starts with a 920 nm wavelength High Power Laser Diode coupled to a collimating lens and mounted in the LDSAM, shown in the Initiation Subsystem Functional Block Diagram Figure 4. The collimated laser light passes through the LDSAM shutter and is refocused into a 100  $\mu\text{m}$  fiber using another lens in the LDSAM. For channels one and two, the coupler is the next item in the optical path. Finally the J2 connector on the LFU is the last item in the optical path. Table 1 lists the typical output delivered to an ordnance device through the external 110  $\mu\text{m}$  cables.

**3.2 Requirements.** There are no established industry-wide all-fire and no-fire standards for laser ordnance. However, PS/EDD has designed several diode initiated devices. As an example, we designed and manufactured a miniature piston actuator that had a 320 mw all-fire and a 130 mw no-fire using 110  $\mu\text{m}$  diameter fiber. We used these levels as a guide in developing the LFU.

This actuator used titanium potassium perchlorate for the ignition/output charge and incorporates a fiber optic pigtail. A Neyer statistical analysis was used to determine the all-fire and no-fire levels. Table 2 shows the test data from the Neyer test performed on the piston actuator. The power levels listed in the table were measured prior to each test shot using the fiber that connects to the pigtail of the device.

**3.3 Design Trades.** The main goal in designing the LFU is to maximize the efficiency of delivering power to the ordnance devices. This usually requires selecting a fiber optic cable with the smallest diameter practical and usually becomes a trade between launch efficiency and spot size. In other words, one must select a combination of laser diodes and fibers that supply the largest power per unit area. Minimizing the quantity of connector interfaces is another design goal.

In designing ordnance devices, the main goal is to minimize the spot size at the ordnance compound while meeting other requirements like cost, proof pressure, and sealing. Fiber optic

Table 1. Measured LFU Output

| Output Channel | Typical Output Power | Margin<br>(based on 320 mw all-fire) |
|----------------|----------------------|--------------------------------------|
| 1              | 27.1 dBm<br>(517 mw) | 162%                                 |
| 2              | 26.6 dBm<br>(452 mw) | 141%                                 |
| 3              | 27.0 dBm<br>(500 mw) | 156%                                 |
| 4              | 26.8 dBm<br>(482 mw) | 151%                                 |

cables emit light in a diverging cone that causes the spot size to grow with distance. To minimize the spot size, the ordnance device must either put a fiber in contact with the ordnance compound or use optics to refocus the spot onto the ordnance compound. Plane parallel windows are not typically used in devices initiated by laser diodes. However, a gradient index (GRIN) lens or an integral fiber can efficiently couple a fiber's output to the ordnance compound.

**3.4 Output Tests.** We measured the LFU outputs at the ordnance end of external 110  $\mu$ m cables. The results are listed in Table 1. Note, the LFU can deliver sufficient laser intensity to initiate ordnance devices with 141% to 162% margins above an 320 mw all-fire requirement. This margin means that the LFU operates from 4.3 to 6.4 times the 30.7 mw sigma over the 0.999 reliability all-fire level shown in Table 2.

Table 2. Neyer Analysis of Laser Initiated Piston Actuator

| Stimulus in milliwatts | Successes |
|------------------------|-----------|
| 133.0                  | 0         |
| 172.0                  | 0         |
| 190.0                  | 0         |
| 213.0                  | 1         |
| 241.0                  | 0         |
| 243.5                  | 1         |
| 279.0                  | 1         |
| 289.0                  | 1         |
| 298.0                  | 1         |
| 460.0                  | 1         |

Note:

The Mu was 222.9 mw with a sigma of 30.7 mw. The calculated 0.999 all-fire level is 317.8 mw and the 0.001 no-fire level is 128.1 mw.

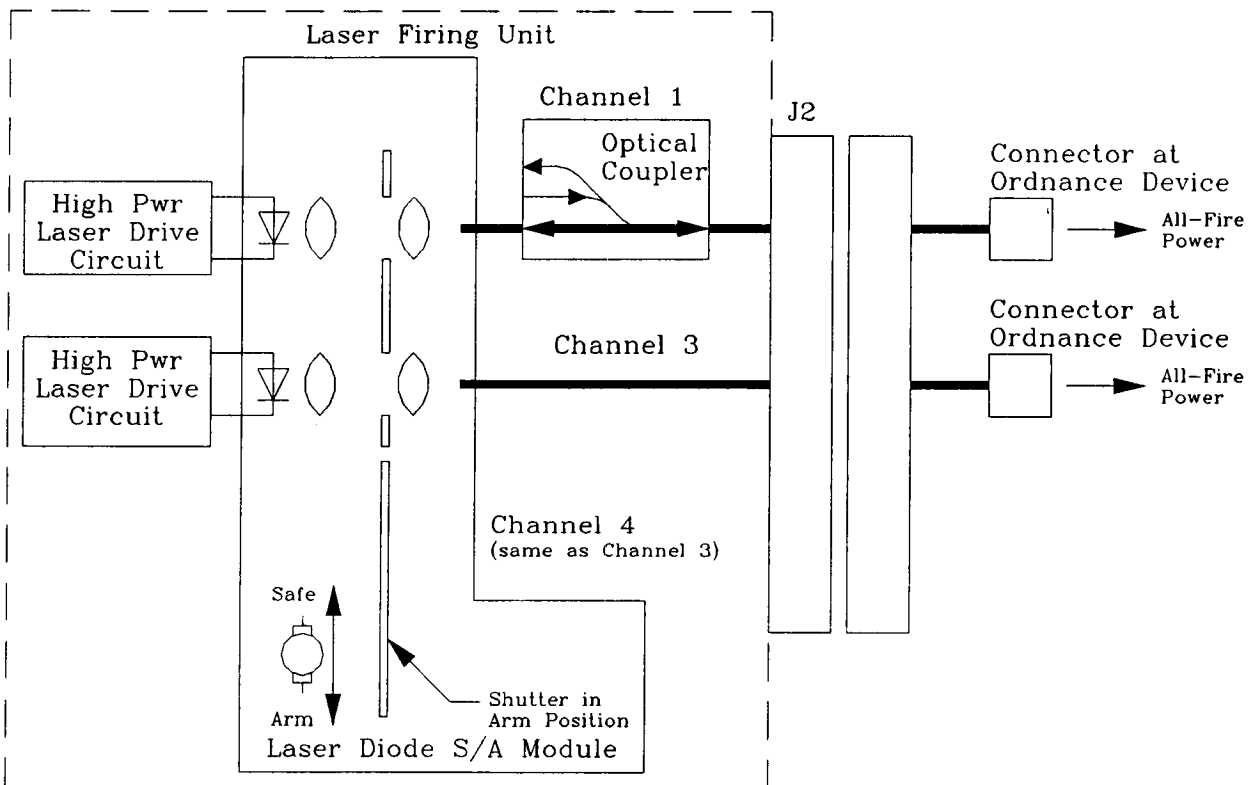


Figure 4. Initiation Subsystem Functional Block Diagram

#### 4. SINGLE FIBER BIT SUBSYSTEM.

**4.1 Introduction.** The Single Fiber BIT Subsystem is meant to detect broken fiber optics or mismatched and contaminated optical connections. Each Single Fiber BIT channel consists of following elements shown in Figure 5:

- A 1.0 mw BIT Laser Diode operating at 780 nm wavelength
- A fiber coupler that has three inputs and one output
- A common BIT Sense Circuit to detect the reflected optical BIT signal.
- An ordnance device with a dichroic coating on the window that reflects 780 nm wavelength light.

The Optical Coupler provides paths for injecting the BIT laser signal into the output fiber and for extracting the return signal from the output fiber. The three inputs of the coupler are connected to the High Power laser diode, BIT laser diode, and the BIT photodiode.

During Single Fiber BIT operation, the LDSAM is in the safe position with the output of the High Power Laser Diodes blocked by the closed LDSAM shutter. A BIT laser is fired to provide a low power laser pulse to illuminate the ordnance device through the single output cable. The dichroic coating on the ordnance device window reflects 90% of the BIT laser output back to the LFU through the same cable. The fiber coupler directs this reflected signal to the BIT Sense Circuit.

**4.2 Requirements.** To keep with the spirit of the monitor circuit requirements of MIL-STD-1516, the power of the BIT signal should be kept 20 dB below the rated no-fire of the ordnance device. Note, MIL-STD-1516 paragraph 5.10.7 limits the monitor current for electroexplosive devices to one tenth of the no-fire level. This corresponds to a one hundredth factor for power or a margin of 20 dB.

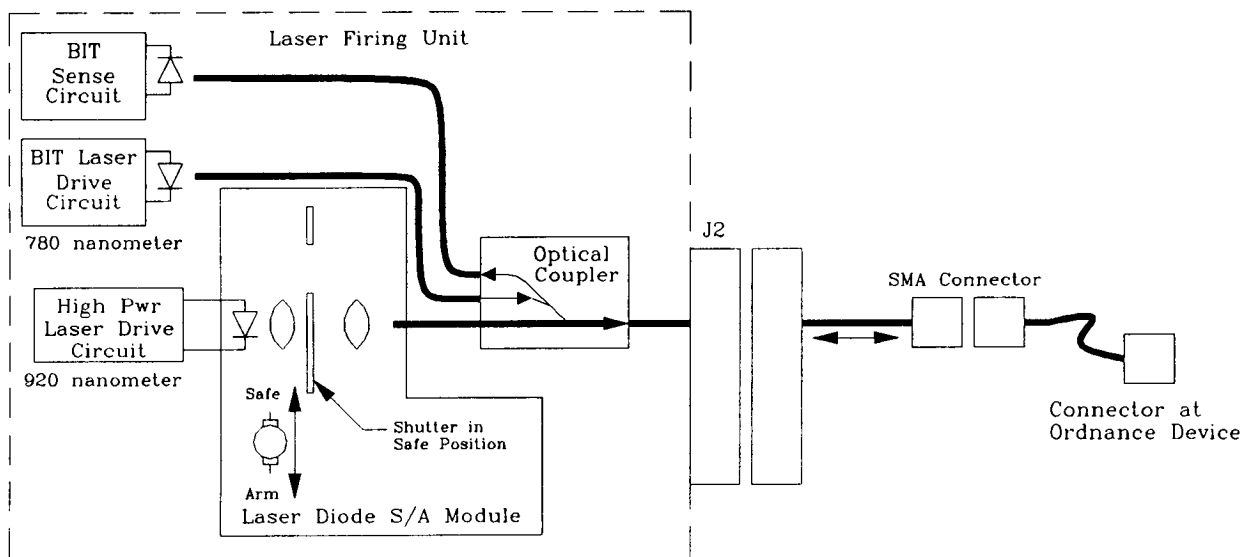


Figure 5. Single Fiber BIT Subsystem Functional Block Diagram

The BIT Laser Diodes are rated at 1.0 mw which is 21 dB below the no-fire level of 130 mw. This 1.0 mw output is attenuated by the 11 dB loss in the coupler and the coupling loss to the fiber. In other words, the laser intensity at the ordnance device is at least 31 dB below the no-fire level of 130 mw or 12 dB lower than the MIL-STD-1516 requirement. Note, this does not include the losses associated with the connectors (typically 0.7 dB to 1.5 dB loss per connector) and with the dichroic coating (10 dB loss i.e. it passes 10% at 780 nm).

**4.3 Design Trades.** Unwanted reflections are the main limiting factor for the Single Fiber BIT system. These are caused by the connectors in the optical path and by the coupler's internal reflections. These reflections are sensed by the BIT Sense Circuit and appear as background noise that the BIT reflection must overcome. For connectors, the fresnel reflection at each glass-to-air interface is 4.0% of the incident light. The intensity of the coupler's internal reflections are approximately 25 dB below (or 0.32% of) the BIT Laser intensity. The main design trade is to optimize the coupler design to minimize reflections while still providing an adequate optical path for initiation energy.

**4.4 BIT Tests.** We performed some testing to determine the reflection losses that we can expect at the ordnance device during Single Fiber BIT. A mirror and GRIN lens simulated the ordnance device with dichroic coating. A 110  $\mu\text{m}$  fiber optic with an SMA connector was routed from the LFU and mated with the GRIN lens/mirror combination. Using an optics breadboard we could vary the gap distance between the SMA connector and the GRIN lens. Using a HeNe laser in place of the BIT laser diode, we measured the reflection loss for a variety of gaps. Figure 6 is a plot of the relative loss versus gap distance. The loss values are referenced to the BIT output intensity of the LFU.

As Figure 6 shows, there is a 1.5 dB dynamic range for discriminating between pass and fail. However the intensity of the reflection is only about 22 dB to 24 dB below the LFU's BIT output. In the spirit of MIL-STD-1516, the BIT reflection could be as bright as 44 dB below the rated no-fire of the ordnance device. This could be as much as 5.2  $\mu\text{w}$  for a system using 130 mw no-fire ordnance devices. Silicon photodetectors have a typical sensitivity of 0.5  $\mu\text{A}/\mu\text{w}$  and would generate a 2.6  $\mu\text{A}$  signal that is easily detectable.

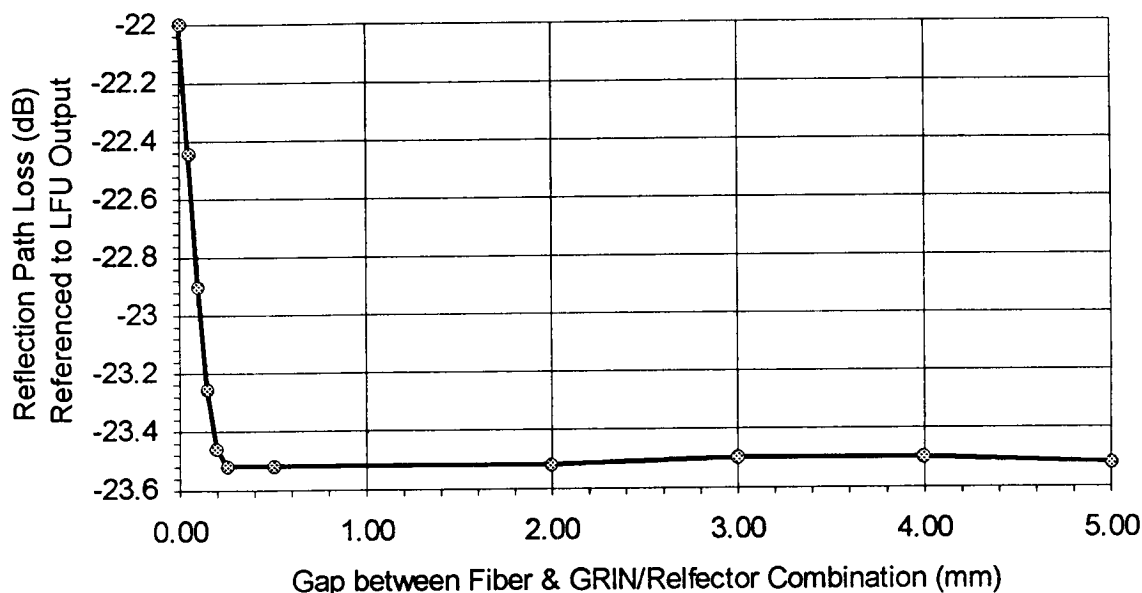


Figure 6. Reflection Loss Verses Gap Distance for Single Fiber BIT

## 5. DUAL FIBER BIT SUBSYSTEM.

**5.1 Introduction.** The Dual Fiber BIT Subsystem is meant to detect mismatched and contaminated optical connections. It uses two separate fibers from the LFU that are terminated together in the connector that mates with the ordnance device. One fiber connects to a LDSAM output while the other connects to a PIN diode photodetector in the BIT Sense Circuit as shown in Figure 7.

During BIT, the LDSAM is in the safe position and a high power laser diode is fired to provide a low power laser pulse to illuminate the ordnance device. Note, the output power of the high power laser diode is limited by an aperture in the shutter. A small fraction of this signal reflects off the ordnance device and returns to the BIT Sense Circuit through a second fiber optic.

We wanted to minimize costs by making the ordnance interface simple fabricate. The cable interface at the ordnance device consists of an

SMA type fiber optic connector with two fibers bonded side-by-side and polished. The fiber core diameter was 110 $\mu$ m with an overall diameter of 125  $\mu$ m, and a numerical aperture (NA) of 0.37.

**5.2 Requirements.** To keep with the spirit of the monitor circuit requirements of MIL-STD-1516, the power of the BIT signal should be kept 20 dB below the rated no-fire of the ordnance device. Note, MIL-STD-1516 paragraph 5.10.7 limits the monitor current for electroexplosive devices to one tenth of the no-fire level. This corresponds to a one hundredth factor for power or a margin of 20 dB.

The High Power Laser Diodes have a 13 dB dynamic range from 0.1 W at threshold to a maximum of 2.0 W. This dynamic range is not large enough to use current limiting alone to reach the 20 dB safety margin. Therefore a shutter with either an aperture or other type of optical attenuator was required. We found that an aperture of about 0.005 in. provides 27 db to 30 dB of attenuation.

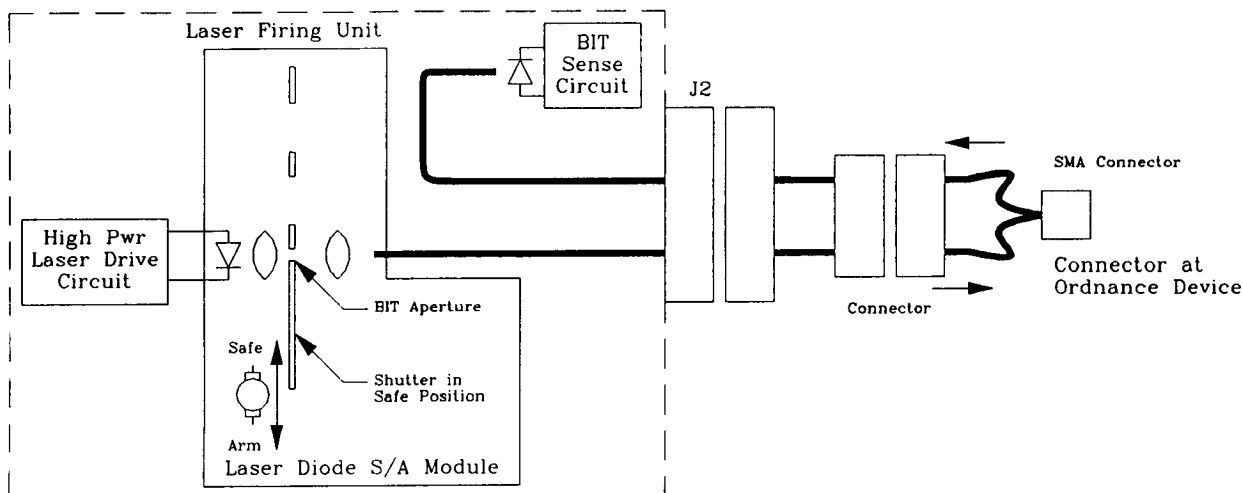


Figure 7. Dual Fiber BIT Subsystem Functional Block Diagram

**5.3 Design Trades.** The main design trade for a Dual Fiber BIT systems is cost verses the intensity of reflected signal. For example, we could have used a coupler, a separate BIT laser operating at 780 nm, and a dichroic coating on the ordnance device. This would have increased the reflected signal however the system cost and configuration are very similar to the Single Fiber BIT configuration. Alternately, we could have complicated the ordnance interface to improve the intensity of the reflected signal. However this would significantly increase the cost of the ordnance devices.

For our low cost approach, the critical design trade is to maximize the reflected BIT signal while providing adequate initiation power. Figure 8 shows the ray diagram associated with a pair of fibers up against a reflector. The reflecting surface represents the ordnance compound and fresnel reflections from and imaging optics associated with a practical ordnance device. Unlike the single fiber BIT approach, dichroic coatings can not be used since this approach uses the same laser for BIT and initiation.

As mentioned in section 3.3, any laser diode initiated ordnance device would use optics between the fiber and the ordnance compound to

re-image the laser spot while providing a seal. Ideally, the net effect of such optics would be the same as not having any optics. For simplicity, Figure 8 does not show any re-imaging optics.

The bottom fiber illuminates the reflector while the top fiber gathers the reflected light. Both fibers emit or accept light in diverging 43.4 degree cones that overlap at the reflecting surface. The intensity of the reflected BIT laser signal is directly effected by this overlap area and by reflectivity of the ordnance compound.

Note that the area of this overlap varies with the gap between the reflector and the fiber ends. For a given set of fiber core diameters and fiber spacing, there is a range of usable gaps with specific minimum and maximum gap distances. One can expect the intensity of the reflected BIT to increase with gap distance to a peak value and then decrease with larger gap distances. To avoid the ambiguity of having an intensity value indicate two different gap distances, a designer would select a gap that is at or beyond the peak.

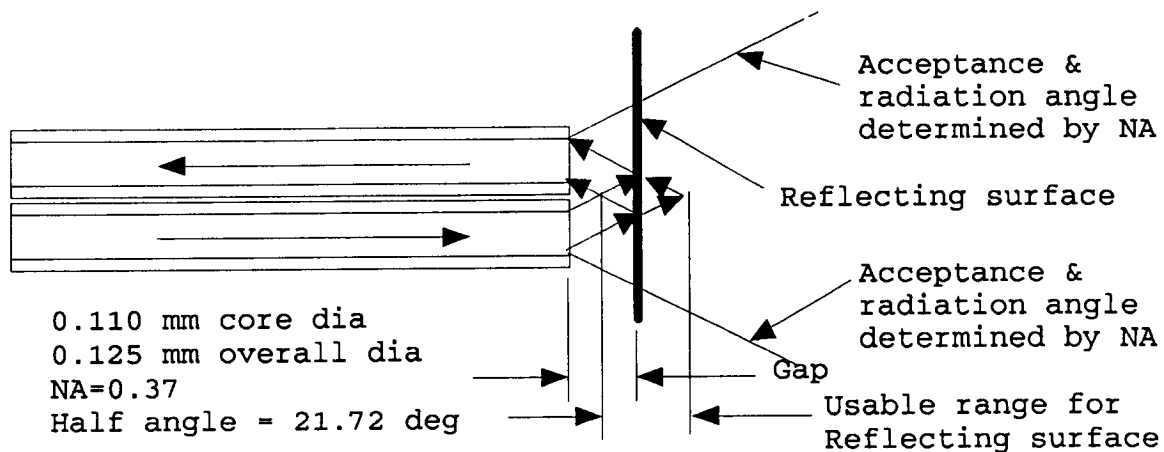


Figure 8. Dual Fiber BIT Sense Geometry

As mentioned in section 3.1, any gap in the fiber-to-ordnance interface increases spot size requiring more all-fire power from the High Power Laser Diodes. With this type of fiber geometry, one must select the BIT laser, fiber size, and ordnance interface geometry to maximize the reflected BIT signal while providing adequate initiation power for the resulting spot size.

**5.4 BIT Tests.** We performed some testing to determine the reflection losses that we can expect at the ordnance device during Dual Fiber BIT. A flat black surface and GRIN lens simulated the ordnance device. A pair of 110  $\mu\text{m}$  fibers were terminated in an SMA connector mated with the GRIN lens/black surface combination. One fiber was routed from a HeNe laser to simulate the LFU's BIT output and the other fiber was monitored by an optical wattmeter.

Using an optics breadboard we could vary the gap distance between the SMA connector and the GRIN lens. Figure 9 is a plot of the relative loss versus gap distance. The loss values are referenced to the output intensity of the LFU. The loss curve starts at a low level, peaks at -25 dB, and the gradually drops to -40 dB. Note that losses between -25 dB to -40 dB correspond to two different gap values.

As discussed in section 5.3, the selected fiber geometry has a range of usable gaps with specific minimum and maximum gaps. The effect of the minimum gap can be seen in the steep rise while the effect of the maximum gap is seen in the curve's fall.

However, one would expect a steeper fall than shown. We believe that the gradual drop is caused by reflections from the test setup. Similar reflections might be expected from a connector that is partially mated to an ordnance device with its clean reflective connector interface. In any case, the such reflections effect the sensitivity of this BIT approach.

As Figure 9 shows, there is a 15 dB dynamic range for discriminating between pass and fail. However the intensity of the reflection ranges from 26 dB to 40 dB below the LFU output. In the spirit of MIL-STD-1516, the BIT reflection could be as bright as 46 dB to 60 dB below the rated no-fire of the ordnance device. This could be as much as 3.3  $\mu\text{w}$  to 130 nW for a system using 130 mW no-fire ordnance devices. Silicon photodetectors have a typical sensitivity of 0.5  $\mu\text{A}/\mu\text{W}$  and would generate a 1.7  $\mu\text{A}$  to 65 nA signal that is not easily detectable.



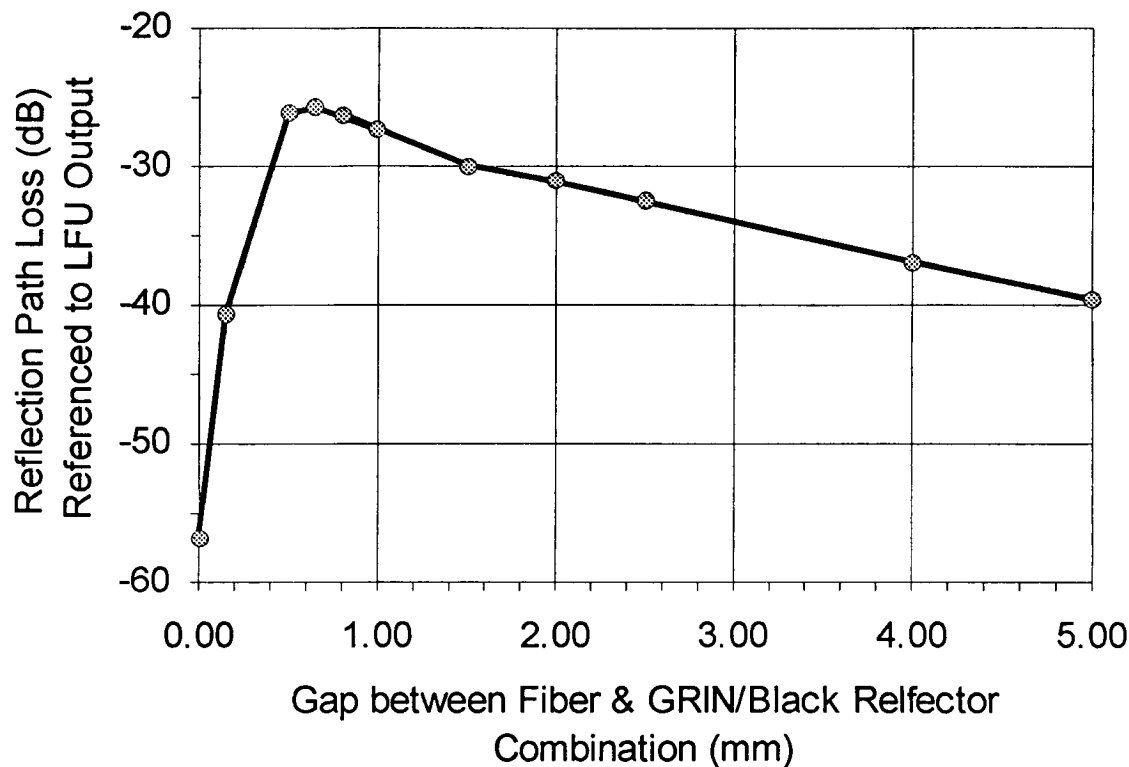


Figure 9. Reflection Loss versus Gap Distance for Dual Fiber BIT

## 6. SUMMARY .

**6.1 Conclusions.** With this effort, PS/EDD is demonstrating a viable laser diode based initiation system that uses Single Fiber BIT and a high degree of automatic operation. The LFU delivers sufficient laser power with 141% to 162% margins above an 320 mw all-fire requirement. This margin is 4.3 to 6.4 times the 30.7 mw sigma over the 0.999 reliability all-fire level shown in Table 2. PS/EDD is demonstrating a workable Single Fiber BIT System that requires only one fiber per ordnance device for both initiation and BIT.

Our aggressive approach to Dual Fiber BIT is proving to be unsuitable for diode based initiation systems. For simplicity, we used an extremely simple fiber-to-ordnance device interface that requires a gap to obtain reasonable BIT return signals. This gap degrades the delivery of initiation energy. Our approach, is better suited for solid state laser initiation systems that use

two different wavelengths and dichroic coatings on the ordnance devices.

**6.2 What's Remains.** In general, PS/EDD plans to apply this technology to simpler and lower cost units. We will perform some environmental testing on LDSAM and BIT verification tests of the Single Fiber BIT system. In future laser diode initiation systems we will reselect laser diodes to take advantage of the newer high power lasers that have are now available. In future Single Fiber BIT Subsystems we will update the coupler design to further reduce internal reflections.

**LIO Validation on Pegasus  
(Oral Presentation Only)**

**Arthur D. Rhea**

**The Ensign-Bickford Company  
Simsbury, CT**

510-28  
6419  
8

## EBW'S AND EFI'S THE OTHER ELECTRIC DETONATORS

RON VAROSH  
RISI

### INTRODUCTION

Exploding BridgeWire Detonators (EBW) and Exploding Foil Initiators (EFI) which were originally developed for military applications, have found numerous uses in the non-military commercial market while still retaining their military uses.

While not as common as the more familiar hot wire initiators, EBW's and EFI's have definite advantages in certain applications. These advantages, and disadvantages, are discussed for typical designs.

### HISTORY

EBW's were invented in the early 1940's by Luis Alvarez as part of the Manhattan project (1). Alvarez's insight was to use a rapidly discharging capacitor to fire a hot wire detonator and thus obtain the required simultaneity for a nuclear device. Further research showed that this "exploding wire concept" could also be used to initiate secondary explosives such as PETN and RDX. The concept remained classified for many years until a patent was issued in 1962 to Lawrence Johnston, one of Alvarez's co-workers. These detonators were studied and used extensively by the former Atomic Energy Commission. Although many of these studies have never been declassified, a good sampling of what was learned was published in the proceedings of the Exploding Wire Conferences (2).

Of particular interest in these conference proceedings are many of the reports of T.J. Tucker, especially his formulation of the "action" concept (3). The "action" concept

remains the basis for the design and evaluation of both EBW's and EFI's.

EFI's (or slappers as they are frequently called) were invented by John Stroud of Lawrence Livermore National Laboratory in 1965 (4). In a report on the acceleration of thin plates by exploding foils, Stroud noted that the pressures produced by these "slappers" appeared to be sufficient to initiate high density secondary explosives.

### DEFINITIONS OF EBW'S AND EFI'S

The same basic definition can be applied to both EBW's and EFI's.

An EBW (or EFI) is an all secondary explosive detonator that requires a unique, high amplitude, short duration electrical pulse for proper functioning.

Both EBW's and EFI's require a unique high amplitude electrical pulse, and each contains only secondary explosives. The differences are that the explosive in an EBW is directly against the bridgewire and is usually at 50% of crystal density. The explosive is "believed" to be shock initiated by the exploding wire. In an EFI, the exploding foil accelerates a disc across a gap and the high density explosive (90% crystal density) is initiated by the kinetic energy of the flying disc. For the EFI, the explosive is not in direct contact with the exploding foil.

### WHY BOTHER?

These electric detonators appear to be so much more complicated than

simple hot wire devices, that the question must be addressed as to why bother with this added complication? Three major reasons why people bother with EBW's and EFI's are:

Safety  
Repeatability  
Reliability.

Safety comes primarily from the fact that no primary explosives are used in either device. Both are electrostatically safe as demonstrated by the "standard man test (5). Nominal values of RF are also not a problem (6). Stray currents do not affect the devices since approximately 3 amps DC are required to melt open a common type bridgewire and about 5 amps to open a typical foil.

The second major reason for using EBW's and EFI's is their excellent shot to shot repeatability. Even with different firing systems, shot to shot repeatabilities under 5 microseconds are easily obtained.

Finally for applications where simultaneity is a requirement, both EBW's and EFI's are easily fabricated with standard deviations under 25 nanoseconds.

#### APPLICATIONS

Following are some of the applications where EBW's and EFI's have found substantial acceptance:

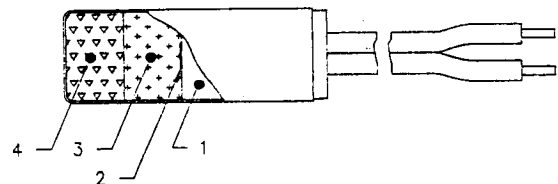
Military Ordnance  
Military R & D  
Explosive Welding  
Explosive Hardening  
Seismic  
Oil Fields  
Forest Service  
Mining  
Power Plants

Military Ordnance is an obvious application, although most conventional weapons still use hot wire initiators. The reverse is true with Ordnance R & D. The need to synchro-

nize cameras, flash X-Rays, etc. with detonations makes good use of the inherent repeatability of EBW's and EFI's. Much of the explosive welding is performed on-site to electric power plant boilers - a location notorious for stray voltages. Not only is the safety important here, but in addition many of the welds require the simultaneous detonation of two charges. Safety is the primary requirement for the majority of the other applications. Mining applications are limited since most mining requires "ripple" firing - something extremely difficult to accomplish with either EBW's or EFI's.

#### EBW CONSTRUCTION

Figure 1 shows a typical EBW detonator and compares it with a typical



1-HEAD  
2-BRIDGEWIRE  
3-INITIAL PRESSING  
4-OUTPUT PELLETT

HOT-WIRE  
Plastic  
Hi-resist  
Lead Azide  
PETN/RDX

EBW  
Plastic  
Lo-resist  
PETN  
PETN/RDX

Figure 1. Typical Bridgewire Detonators

hot wire detonator. Heads and output pellets are the same for both detonators. The major differences are in the bridgewires and initial pressings. EBW's generally use gold or platinum wires, primarily for their inertness, while hot wire devices use high resistance materials such as Nichrome. The explosive against the bridgewire in an EBW is generally PETN although RDX and "thermites" have been used. Hot wire devices generally have Lead Azide or Lead Styphnate against the bridge wire.

In addition, the explosive in an EBW is generally at about 50 percent of crystal density. In the EBW, the "explosion" of the wire starts a detonation without any intervening deflagration as is the case with a hot wire detonator.

#### SAFETY DATA

Since EBW's have been around for almost 50 years a great deal of test data has been accumulated by various organizations. Everyone has an opinion on which safety tests are most important, but the US Forest Service is probably the most imaginative. In their testing, which was conducted for them by China Lake (7), detonators were subjected to the following "potential" hazards:

- 110 vac, 60 cycle
- 220 vac, 60 cycle
- 12 vdc battery
- truck ignition coil
- camera flash unit
- chain saw magneto
- campfire.

In all the above testing, all detonators dudded and none detonated. These are obviously hazards which they believe could occur in their work areas.

The National Laboratories at Los Alamos, Sandia and Livermore have performed the most design studies on both EBW's and EFI's and obviously have the most test data on these devices.

#### EFI CONSTRUCTION

Figure 2 illustrates the major components of an EFI. Tamper can be any rigid dielectric material: plastics, metals, sapphire, etc. have all been used successfully. Next comes the bridge foil. These may be any conductor. Copper and aluminum are the most common. Thicknesses are usually about 0.0002 inch thick. The thinnest width nowadays is about 0.008 inch wide, although previously foils as wide as 0.025 were used.

The length of the narrow section is approximately equal to the width i.e. about 0.008 inch long.

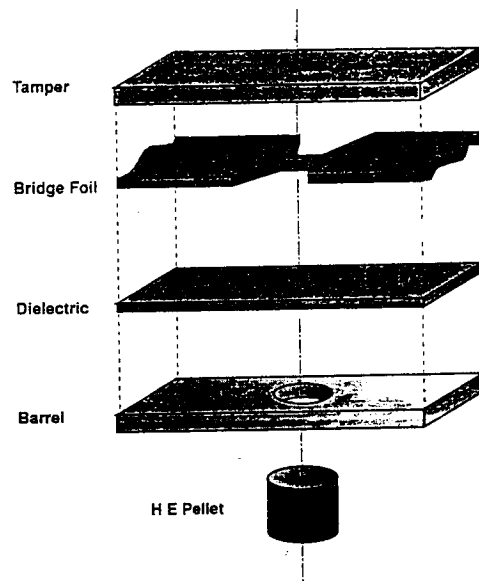


Figure 2. EFI Major Components

The dielectric flyer is usually polyimide, .001 inch thick, but other materials have been used.

The barrel is usually a dielectric, but a conductor could also be used. If the diameter of the barrel hole equals the length of the narrow bridge foil length (0.008 inch), the design is called a "finite barrel design". If the diameter of the barrel hole is 2+ times the narrow bridge foil length, the design is called an "infinite barrel design".

The above four components are laminated into one sub assembly, and clamped against a high density explosive pellet - usually HNS.

In operation, for the finite barrel design, a high current explodes the narrow section of the bridge foil, which shears out a disc of dielectric which accelerates down the barrel and by means of kinetic energy initiates the high explosive pellet. An infinite barrel design works exactly the

same way except the rapid expansion of the dielectric "bubble" is the source of the kinetic energy.

Both, EBW bridgewires and EFI foils "explode" because the electric current is heating the conductor which is trying to expand, but the conductor is being heated faster than it can physically expand.

#### FIRING CIRCUITS

A typical firing circuit for either EBW's or EFI's is shown in Figure 3. The circuits are similar except

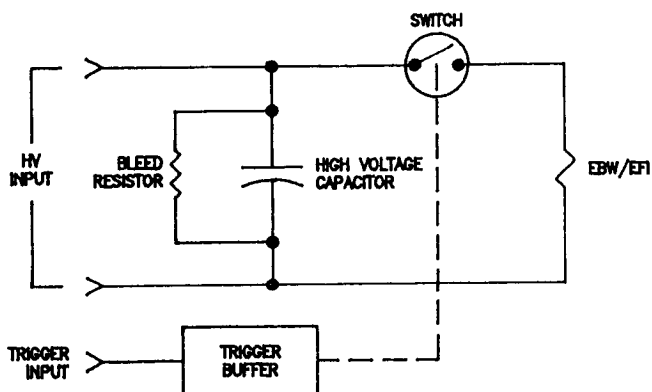


Figure 3. Typical EBW/EFI Firing Circuit

EFI's tend to use lower capacitance values (0.1 microfarad) because of their requirement for low low inductance while EBW's usually use about 1.0 microfarad. The low inductance is necessary to "explode" the foil rapidly enough to accelerate the flyer to a high enough velocity to initiate the explosive.

A wide variety of switches have been used for both EFI's and EBW's. These have included:

- overvoltage switches
- vacuum triggered switches
- gas filled triggered switches
- solid state switches
- crush switches
- etc.

Power supplies have included systems

such as:

- batteries
- line voltage
- piezoelectric generators
- fluidic generators
- etc.

Most circuits also have "safety" type features such as bleeder resistors to discharge the capacitor in case of an aborted test, features to prevent repetitive firing, etc.

#### TYPICAL CURRENT TRACES

Figure 4 shows typical current traces through a bridgewire and a foil.

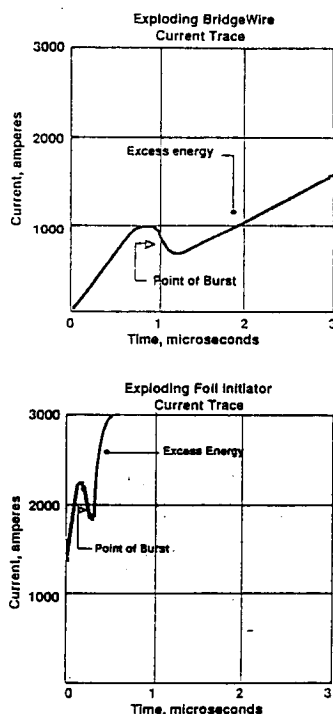


Figure 4. Typical Current Traces

Both work exactly the same way. Current flows through the device, when the bridge starts to heat the resistance increases and the current falls. At the inflection point, burst occurs and an arc is created. The arc being of lower resistance, allows the current to recover.

Burst occurs when a constant action (integral of current squared, from zero to burst time) is accumulated.

Also, the current at threshold is constant regardless of circuit parameters whereas the threshold voltage varies with circuit parameters.

Burst, preferably should occur at about 1 microsecond for an EBW, and 0.1 microsecond for an EFI. Longer times allow the wire or foil to melt open before exploding.

#### EXPLOSIVES

Most EBW's use PETN which has a reasonable threshold firing current (200 amps). RDX has a significantly higher threshold firing current (450 amps) but is frequently used where higher operating temperatures are required. These threshold firing currents work out to be 500 and 800 volts respectively on a 1 microfarad capacitor. EBW's (and EFI's) can also shock initiate (?) "Thermites" to produce an initiator with a deflagrating output (8). Other explosives tested to date with EBW's have too high a threshold voltage to make a reasonable system (above 5000 volts on a 1 microfarad capacitor).

EFI's can initiate just about any explosive although PETN and HNS have acceptably low thresholds (9). PETN is frequently chosen as a "weak link" in an explosive train because of its ability to sublime away at moderate temperatures and dud the weapon system. Most DOD systems use HNS for two major reasons - its relatively low threshold and its acceptability by MIL-STD-1316.

Figure 5 shows one of the main reasons why HNS is so popular as an initiating explosive for EFI's. Plotting EFI threshold voltage versus a measure of explosive sensitivity such as Drop Hammer Height shows most explosives following a straight line (PETN-RDX-PBX9407). HNS does not follow the same general trend. Instead it is quite insensitive as indicated by its large drop height, but still has a low threshold to EFI initiation.

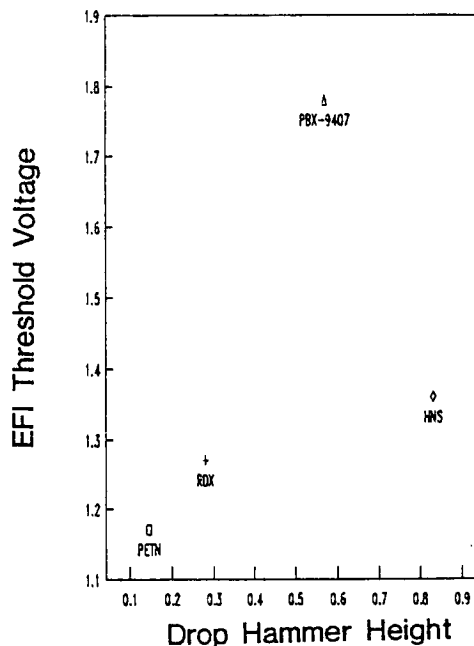


Figure 5. EFI Threshold vs Drop Hammer

MIL-STD-1316 which covers the safety criteria for fuzes and Safety and Arming Devices applies to all munitions except:

- Nuclear Weapons
- Hand Grenades
- Flares
- Manually emplaced ordnance
- Pyrotechnic countermeasures.

For an in-line device, the only permissible explosives are:

- Comp A3
- Comp A4
- Comp A5
- Comp CH6
- PBX 9407
- PBXN-5
- PBXM-6
- DIPAM
- HNS Type 1
- HNS Type 2
- HNS-IV.

Note that PETN is not an acceptable explosive. Of the listed explosives, HNS appears to be the best choice for an in-line device.

# ELECTRIC DETONATOR COMPARISON

Table 1 compares some of the electrical characteristics of three different types of electric detonators.

|                      | <u>Hot Wire</u> | <u>EBW</u>    | <u>EFI</u>      |
|----------------------|-----------------|---------------|-----------------|
| <b>Current</b>       |                 |               |                 |
| Threshold            | 1 amp           | 200 amps      | 2000 amps       |
| Operating            | 5 amps          | 500 amps      | 3000 amps       |
| <b>Voltage</b>       |                 |               |                 |
| Threshold            | 20 volts        | 500 volts     | 1500 volts      |
| <b>Energy</b>        |                 |               |                 |
| Threshold            | 0.2 joule       | 0.2 joule     | 0.2 joule       |
| <b>Power</b>         |                 |               |                 |
| Threshold            | 1 watt          | 100,000 watts | 3,000,000 watts |
| <b>Function Time</b> |                 |               |                 |
| Typical              | 1 millisecc.    | 1 microsec.   | 0.1 microsec.   |

Table 1. Electric Detonator Comparison

The values listed are nominal and obviously detonators have been built with lower energy and power requirements, but the comparison is still useful.

For the EBW, values assume a 1 microfarad capacitor while a .15 microfarad is assumed for the EFI. The 1 amp 1 watt hot wire device is what is generally required for DOD devices although detonators with an all fire current of 50 milliamps have been fabricated (10).

Of particular interest, is the fact that all the energy values are approximately equal. This implies that the same physical size fire set can be used for all three types of detonators. The major difference between the three detonators is the power. The higher power levels of the EBW's and EFI's are related to the very short energy spike associated with these devices. A typical bridgewire

burst time is 1 microsecond for an EBW and 100 nanoseconds for an EFI.

The equality of the energy has been utilized in a recently developed "Power Multiplier" which takes the energy output of a normal capacitive hot wire firing unit and steps up the power to fire an EBW (11).

## SUMMARY

Both EBW's and EFI's tend to have definite advantages where safety, reliability and repeatability are required but EFI's have a clear advantage in being able to initiate HNS and PBX-9407 and thus are Mil-Std-1316 acceptable.

As disadvantages, both tend to be more expensive than hot-wire blasting caps, but this is primarily because of the limited manufacturing base. Blasting caps are manufactured in the 10's of millions annually while the total annual fabrication of EBW's is about 100,000. Only about 10 - 20,000 EFI's are currently manufactured annually in the US.

Two other major disadvantages of EBW's and EFI's, are the small number of detonators which can be fired per shot and the difficulty in delaying individual detonators. The ability to delay individual detonators is very important in the mining industry where "ripple" firing is necessary for efficient earth movement.

The final disadvantage is the requirement for low inductance. This is much more severe for EFI's than for EBW's. EBW's can be reliably fired over 100 feet of twin lead or 300 feet of coax at 3.5kv from a 1 microfarad capacitor. To fire EFI's over 10 feet, generally requires a flat cable, or some other method of obtaining the low inductance required for a fast rise time.

## REFERENCES

- (1) Luis W. Alvarez, "Alvarez: Adven-



tures of a Physicist," Basic Books, Inc., New York, 1987, pp. 132-135.

(2) "Exploding Wires," Vol. 1-4, edited by W.G. Chace and H.K. Moore, Plenum Press, New York, 1959 - 1968.

(3) T.J. Tucker, "Exploding Wire Detonators: The Burst Current Criteria of Detonator Performance," in Exploding Wires, Vol. 3, edited by W.G. Chace and H.K. Moore, Plenum Press, New York, 1964, p. 175.

(4) "History," RISI Technical Topics, San Ramon, CA., Issue 05-93.

(5) R.S. Lee and R.E. Lee, "Electrostatic Discharge Effects on EBW Detonators," UCRL-ID-105644, Lawrence Livermore National Lab, August 1991.

(6) Letter Report, R.H. Joppa, Los Alamos National Laboratory to Eglin Air Force Base, July 10, 1973.

(7) Carl F. Austin and Carl C. Halsey, "Safety and Durability Tests of the Fireline Explosive Cord," TS 74-47

(8) "Secondary Explosive Initiators & Accessories," RISI Product Catalog, San Ramon, CA., April 1992.

(9) H.A. Golopol, et al., "A New Booster Explosive, LX-15," UCRL-52175, Lawrence Livermore National Laboratory, March 1977.

(10) Richard M. Joppa, et al, "Response of Airborne Electroexplosive Devices to Electromagnetic Radiation," Technical Report ASD-TR-73-10, Los Alamos Scientific Laboratory, February 1973.

(11) "PM-25 and PM-100," RISI Data Sheet, San Ramon, CA., 1994.

S11-28  
691  
A6

LOW COST, COMBINED RADIO FREQUENCY AND ELECTROSTATIC PROTECTION  
FOR ELECTROEXPLOSIVE DEVICES

Robert L. Dow  
President, Attenuation Technology Incorporated

Attenuation Technology Incorporated  
9674 Charles Street  
La Plata, Maryland 20646

---

**Abstract:** Attenuation Technology Inc. (ATI) has developed a series of ferrite attenuators for protecting electroexplosive devices (EEDs) from inadvertent actuation due to RF exposure. ATI's first attenuator was fabricated using the MN 67 ferrite formulation. That attenuator protected EEDs from both pin-to-pin and pin-to-case RF exposure. Those attenuators passed MIL STD 1385B testing when used in electric blasting caps (EBC), electric squibs, and firing line filters made for the US Navy.

An improved attenuator, fabricated using ferrite formulation MN 68<sup>TM</sup>, protects EEDs from both RF and electrostatic inadvertent actuation. The pin-to-pin and pin-to-case combination protection previously demonstrated with MN 67 attenuators was maintained for the RF and extended to the electrostatic protection area. In-house testing indicates that the EED protection can be extended to near-by lightning protection using these new attenuators.

Franklin Research Center independently confirmed the increased protection provided by MN 68<sup>TM</sup> Ferrite Devices using the Mk 11 Mod 0 EBC which uses a conventional bridgewire initiator. A new R&D MN 68<sup>TM</sup>

Ferrite Device combined with a Semiconducting Bridge (SCB) passed MIL STD 1385B testing for the first time. ATI is continuing to extend the protection technology to other EED initiator designs and uses other than EEDs.

ATI has issued USA Patents on the MN 67 and MN 68<sup>TM</sup> protection technologies and for many individual applications. USA patent applications are pending on SCB protection and other newer EED applications. US and overseas patent applications are pending on the extended coverage.

ATI developed the technology for supplying ATI Certified MN 68<sup>TM</sup> Ferrite Devices for each application that has passed the required qualification testing. ATI has the Trade Mark on MN 68<sup>TM</sup>. The Certification Mark application is pending at the US Patent and Trademark Office. Production tooling is available to manufacture the .25 caliber MN 68<sup>TM</sup> Ferrite Devices.

---

**Introduction:** Attenuation Technology Inc. (ATI) has developed a series of ferrite protection devices using a new and different basic technical approach. That approach is to modify the basic MN 68<sup>TM</sup> Ferrite Formulation in order to

get the desired combined RF and electrostatic (ES) protection characteristics in the final ferrite protection device, and then to place that ferrite device inside the electroexplosive devices (EEDs) in direct contact with and electrically grounded to the conductive case.

**Background:** Prior to our new efforts in this area, prior art EED RF protection applications used ferrite devices with Curie Temperatures as low as 150°C. The Curie Temperature of these prior art devices was exceeded within a few seconds when the EED was exposed to RF energy levels called out in MIL STD 1385. The early prior art ferrite devices also had cutoff frequencies above 3 megahertz, which made them unacceptable when MIL STD 1385 required RF protection at one megahertz.

These early failures gave generic ferrite protection devices a bad reputation that they still have difficulty overcoming. Many people still automatically revert to thinking of these early failures when the subject of EED protection using any ferrite devices is discussed. As a consequence, they are still excluded as alternative EED protection options even though the technology has changed significantly. As far as ATI can determine, we are the first company to specially formulate a specific ferrite formulation, MN 68<sup>TM</sup>, for EED protection and then make specific formulation modifications for individual EED applications.

**New Technology:** The first ferrite formulation characteristic that was changed was the Curie Temperature. This physical property characteristic is important because, when the lossy ferrite device is exposed to RF energy, it converts that RF energy to heat. If that heat cannot be removed effectively, the ferrite device will increase in temperature. When the ferrite device reaches its Curie Temperature, it stops converting the RF energy to heat. If the ferrite device reaches its Curie Temperature, it can not protect the EED. The RF attenuation property is reversible in that once the ferrite device cools below its Curie Temperature, it resumes attenuating RF energy until it repeats the temperature cycle.

ATI has consistently increased the Curie Temperatures of its lossy, soft ferrite formulation with 250 to 280°C modifications currently available for manufacture. ATI is working toward a goal of at least approaching 400°C on a second ferrite formulation series. Progress has been slow on this new ferrite formulation, since ATI appears to be the only customer in the USA with interest in the very high Curie Temperature, lossy ferrites. There is some interest developing in Europe in using these very high Curie Temperature formulations.

The second lossy ferrite formulation characteristic that was changed was to provide a controlled DC resistance in the ferrite device. Most of the previous art EED ferrite protective device applications used lossy ferrites that were

not DC conductive. Further, most of these prior art lossy ferrite devices were potted in place in the EEDs with nonconductive adhesives. We made the conscious effort to go in the opposite direction and provide lossy, high Curie Temperature ferrite device with a controlled DC resistance within an acceptable range.

The third lossy ferrite formulation physical property that is included in all our ferrite formulations is cut off frequencies below one megahertz. MN 68<sup>TM</sup> Ferrite Devices successfully attenuate RF energy at 10 kilohertz.

Our lossy ferrite devices have a sufficiently low DC resistance to equalize the electrostatic energy that can build up between the firing leads of an EED (pin-to-pin) and/or between the firing leads and the conductive case of an EED (pin-to-case). Our lossy ferrite devices have sufficiently high DC resistance so that they do not act as a DC shunt for the EED's DC firing pulse. Each EED application must be tailored to work within those DC limits. ATI has developed the technology to provide this acceptable range for each EED application.

**Improved EED Design:** Once the three ferrite device requirements were met, the design of the RF protective device and assembly methods used for securing it in the EED could be greatly simplified. Nonconductive potting materials were no longer required during EED assembly. The electrical insulation previously used on the firing leads passing through the ferrite device was

eliminated. One lossy ferrite device could provide both RF and ES protection for the EED for both pin-to-pin and pin-to-case RF and ES energy exposure modes.

It was also determined that the ferrite device could be inserted into EEDs, such as electric blasting caps (EBC) thin conductive case, without excessive breakage. It was further determined that a good electrical ground could be achieved between the lossy ferrite device and the conductive case using just the insertion assembly method. All of this work was done with ferrite devices that were right circular cylinders. New manufacturing methods have recently been developed, so that a chamfer can be molded into the finished ferrite device to make assembly of other EED designs easier.

**Benefits of Design:** The first synergistic effect of this assembly procedure was that once all of the electrically insulating potting material was removed from the EED design, the heat conduction path available to cool the RF attenuating ferrite device were greatly improved. Thus, subsequent EED designs that contained the higher Curie Temperature lossy ferrite devices, actually stabilized at lower temperatures when exposed to comparable amounts of RF energy than prior art EED designs.

This observation was attributed to an improved heat removal path directly to the EED's conductive case, providing better cooling of the attenuating, lossy ferrite

device. Thus, the safety factor of these new EED designs were improved by two mechanisms instead of the original approach of simply using the higher Curie Temperature, lossy ferrite devices.

The second synergistic effect was that tying the conductive EED case to the firing leads through the controlled circuit ferrite allowed large amounts of ES energy to be safely dissipated without firing the EED. Laboratory tests of the ATI ferrite devices showed that repeated exposures of the wound ferrite devices with up to 12 Joules of ES energy did not destroy the ferrite device or change its RF attenuation properties. Most other components in the EED when exposed to that level of ES energy only once, were completely disintegrated, destroyed, or failed to the duded mode.

The final discovery was that the level of RF protection could be changed by selection of the winding pattern used in the ferrite device. One and one half turns of additive choke windings on each firing lead was necessary for the EBC to pass MIL STD 1385B environments, but other winding patterns can be used for commercial applications where the RF exposure hazards are lower.

It was independently determined that the improved ferrite devices did not significantly attenuate the DC firing pulse, even when they were used to protect the semiconducting bridge (SCB) igniters that use microsecond DC firing pulses. One design of the Mk 66 Igniter, containing a single ATI high Curie Temperature

lossy ferrite choke, has been reported as passing MIL STD 1385B RF testing as well as the electrostatic testing.

**Production Status:** ATI is currently working with three USA ferrite device manufacturers to produce these lossy, high Curie Temperature, controlled DC resistance, ferrite devices using high volume, low cost production techniques. So far, the largest production lot has only been 25,000 bare ferrite chokes. This quantity, while very small by ferrite manufacturer's standards, was produced without significant production problems. ATI is also working with an overseas source for potential applications in Europe.

**Certification Approach:** Some of the ferrite manufacturers are offering their versions of high Curie Temperature, lossy ferrite devices that are purported to be as effective as our MN 68<sup>TM</sup> Ferrite Devices. We have been awarded the USA Trademark on MN 68<sup>TM</sup> to distinguish our ferrite devices, certified by ATI, from those produced with similar formulations but not tested as comprehensively. ATI has a Certification Mark pending at the US Patent and Trademark Office.

Since this technology niche has not been investigated before, ATI was forced to develop the techniques and measurement equipment on its own to measure the performance and certify the effectiveness of these ferrite devices. ATI has developed these to the point where, once a specific ferrite device has been qualified for a specific EED appli-

cation, subsequent production lots can be certified to the levels required.

ATI is maintaining certified ferrite device samples from each EED successfully qualified. These samples are maintained to assure that new lots of the ferrite devices produced in future years can be directly compared to the original and certified equivalent in performance to the baseline sample. If the project sponsor wants improved performance (based on how the technology has progressed in the meantime) or the projects safety requirements have increased in the interim, an improved version ferrite device can also be manufactured and made available. It now appears that it may be possible to produce the improved performance ferrite devices without any modifications to the production tooling.

**US Patents:** Since all of this work has been funded solely by ATI, patent protection is the main form of intellectual property rights protection. ATI's issued patents are:

1. US 5,036,768 Basic Patent on MN 68<sup>TM</sup> Applications
2. US 5,243,911 Near-by Lightning Protection for EED

The main, generic approach, patent application revealing the principles of EED protection regardless of the controlled property ferrite formulation used or the winding pattern employed is expected to be issued shortly. ATI has other patent applications pending in the areas of EED

protection and ferrite device certification areas.

During the EED protection technology evolution, ATI determined that the technology can be modified to protect other devices as well. The first medical protection device patent US 5,197,468 has been issued. Other patent applications are pending covering many classes of equipment.

**Conclusion:** Since this is a completely different approach to protecting EEDs from both RF and ES inadvertent ignition with a single device, ATI is prepared to discuss any potential applications of this new technology area with anyone interested. Each solution must be tailored for each application. The technology appears to have progressed sufficiently so that can be done. Please contact us if you are interested in considering this new approach.

512-28  
6992  
P. 12

Unclassified

Distribution Unlimited

SAND94-0246C

## UNIQUE PASSIVE DIAGNOSTIC FOR SLAPPER DETONATORS

William P. Brigham  
Explosive Projects and Diagnostics Department

John J. Schwartz  
Stockpile Evaluation Department

Sandia National Laboratory  
Albuquerque, New Mexico

### ABSTRACT

The objective of this study was to find a material and configuration that could reliably detect the proper functioning of a slapper (non-explosive) detonator. Because of the small size of the slapper geometry (on the order of a 15 mils), most diagnostic techniques are not suitable. This program has the additional requirement that the device would be used on a centrifuge so that it could not use any electrical power or output signals. This required that the diagnostic be completely passive.

The paper describes the three facets of the development effort: complete characterization of the slapper using VISAR measurements, selection of the diagnostic material and configuration, and testing of the prototype designs. The VISAR testing required the use of a special optical probe to allow the laser light to reach both bridges of the dual-slapper detonator. Results are given in the form of flyer velocity as a function of the initiating charge voltage level. The selected diagnostic design functions in a manner similar to a dent block except that the impact of the Kapton disk from a properly-functioning slapper causes a fracture pattern. A quick visual inspection is all that is needed to determine if the flyer velocity exceeded the threshold value. Sub-threshold velocities produce a substantially different appearance.

### Introduction

Slapper-detonators are used in current weapon systems because of their fast function time, small jitter, and relatively low energy requirements compared to other types of detonators. As part of the Sandia National Laboratories (SNL) evaluation program, detonators are typically tested in the

-----  
This work was supported by the United States Department of Energy under Contract DE-AC04-94AL85000.

laboratory under realistic physical and environmental conditions. The unique operation and design of the slapper requires sophisticated diagnostics like VISAR or closure switches to evaluate performance parameters. The complexity of these techniques makes their use difficult in the evaluation lab. This paper discusses a device developed to provide a simple evaluation of slapper function within the constraints

imposed by the laboratory environment. It consists of a small glass target that provides a unique visual record when impacted by the flyer from the slapper.

### Slapper Detonator

The SNL slapper detonator is shown in Figure 1. It consists of a central "bullseye" connector for attachment to the firing set with the flat copper cables extending in opposite directions to form a single loop. The upper layer of thin copper narrows at each end to form a "bridge" that causes the current density to increase significantly. The current through each bridge is strong enough to drive the copper into vapor. The pressure of the gas causes the Kapton to shear against the sapphire "barrel" forming a rapidly-accelerating flyer with a diameter of about 0.015".

Flyer velocity is a function of the initial firing set charge voltage and the resulting current. Typical terminal velocity is on the order of 3-4 mm/ $\mu$ s, although other designs are capable of nearly 6 mm/ $\mu$ s. It is assumed that the flyer begins to come apart soon after it leaves the barrel, but good data have been obtained for distances up to 1 mm. The most common practice is to place the explosive of the next assembly in contact with the barrel.

### Slapper Characterization

Prior to the development of the passive diagnostic, it was necessary to determine the performance (velocity-time history) of the slapper detonator over a range of initial firing set voltage. The best tool for this measurement is VISAR (Velocity Interferometer System for Any Reflector) that uses Doppler-shifted laser light from the slapper surface to infer the velocity. Because this

slapper is a dual-bridge functioned from a common firing set, it was desired to measure both flyers simultaneously. Most VISAR's are "dual-leg" to provide redundant measurement of a single device using two interferometers with different experimental constants. A unique optical probe was therefore developed to convert the existing equipment into a dual system to make the two separate measurements.

The probe allows the light from a single laser to be split into two equal beams that are then fiber-coupled to the target locations. A simplified schematic of the probe is shown in Figure 2 to demonstrate the path of the light. The input fiber connects to optics that allow the light to be focused onto the target surface. The target surface causes the light to be scattered diffusely where it is collected by other optics within the probe. The light is then collimated and focused onto the return fiber located at the rear of the probe. In this manner the image from each slapper can be routed to a different VISAR leg.

A unique feature of the optic probe is the incorporation of a small camera to give a TV image of the target surface. The selective coating on the angled mirror causes a portion of the returned light to be transmitted to the camera element. The TV image is then present on a monitor within the test area. This feature is essential when testing slappers with a small active area because it allows the operator to precisely align the input laser light onto the Kapton element in the center of the barrel. Placing each end of the slapper on a separate translation stage allows adjustment of the position just prior to the test.

Additional diagnostics include detection of the charge voltage and current waveforms from the firing set. Each of these along with the VISAR



data were recorded on Tektronix DSA 602 transient digitizers. Data reduction was performed following each test and stored on computer disk.

Figure 3 shows VISAR data from an experiment where the initial charge voltage was 2.6 kV. The data are in the form of flyer velocity and displacement versus time where the distance is obtained by numerical integration of the velocity-time record. The behavior is typical of slapper detonators in that the acceleration of the flyer is less abrupt than a conventional explosively-driven plate, although the final velocity at the exit of the barrel is over 3 mm/ $\mu$ s. Note that the record continues for a distance approaching 0.75 mm. At the higher initial charge voltage levels, breakup of the flyer is assumed as manifested by increasingly noisy signal quality.

The data of Figure 3 can be cross-plotted to give velocity as a function of displacement as shown in Figure 4. This is particularly useful in assessing the velocity as a given distance, such as the exit of the barrel or the location of the next assembly.

The firing set for all tests was a Hi-Voltage Components, Inc. model CDU2045 with a 0.2  $\mu$ fd, 5-kV capacitor. Initial charge voltage was varied from 1.6 kV to 3.0 kV. Two tests were done at each voltage level to provide redundant data.

Results for the characterization test matrix are given in Figure 5 in the form of flyer velocity as a function of firing-set charge voltage. The numerical results from the same tests are shown in Table 1. The velocity is obtained at a propagation distance of 0.5 mm, or just beyond the exit of the barrel. The four data points at each voltage represent the measurement of each side of the slapper, with two tests at each level. In all cases,

the designation "A" refers to the bridge that first receives the firing pulse, based on the direction of the current flow. The "B" suffix then denotes the opposite bridge.

The results given in Figure 5 indicate that the behavior of the detonator is significantly more erratic at voltage levels below 2 kV. It is thought that at the lower voltage, minor tolerance differences in the construction of the bridges have a more pronounced effect on the behavior. At the higher voltage levels, sufficient energy is available to overcome these differences and the velocity achieved by the two bridges is more consistent. For both tests at 1.6 kV, the "B" side of the unit failed to cause acceleration of the Kapton to a velocity sufficient to be measured by the VISAR, which has a lower detection limit of about 0.2 mm/ $\mu$ s. Inspection of the bridge following the shot indicated that the copper had failed in the region of the bridge.

Results in the voltage range above 2.0 kV show a correspondence between the applied voltage and the resulting velocity. The greatest velocity, on the order of 4 mm/ $\mu$ s, was achieved at the highest voltage level. Some scatter is present above 3.5 mm/ $\mu$ s that is probably caused by breakup of the Kapton flyer. There does not appear to be a discernible trend to establish that side "A" or "B" is consistently higher in velocity at a given voltage.

#### Passive Diagnostic

As mentioned previously, the purpose of this work was to develop a passive diagnostic for the slapper used during evaluation testing. The specific requirements were that the device would not require any external communication (input power or signal cables) and that the visual indication could be easily detectable. Previous

experience had shown that brittle-like fracture could be introduced into some plastic or ceramic materials using metallic flyers from hot-wire detonators. This observation suggested that a similar arrangement could be used for the Kapton flyer from the slapper.

Initial screening tests looked at a variety of material types, sizes, and thicknesses. The presumed 50% probability threshold velocity for detection corresponded to an initial voltage of about 2.1 kV, although tests were done at higher and lower levels to ascertain the sensitivity of each configuration. Table 2 contains the results from the initial screening tests. Some of the tests used a single-bridge and are shown as one configuration only, while the remainder are dual-bridge that may have a different device on each end.

The screening matrix demonstrated a number of viable candidates for selection based on the appearance of obvious cracks above the threshold voltage level. The best material was sapphire, but was rejected because of prohibitive expense. The 0.036" thick microscope slide also showed excellent performance, but a source for this material could not be located. The next alternative was to obtain standard fused silica material in thicknesses in the range of 0.020" to 0.030". Although this is thinner than typically produced, several vendors were found that could grind 1" diameter disks to virtually any value. Disks were purchased in 0.020" and 0.025" thicknesses of BK-7, a standard fused silica composition made for the optics industry. A total of 16 tests were conducted, six using the 0.020" thickness and the remainder with the 0.025" pieces. Table 3 shows the results of the BK-7 tests.

The 0.020" thick BK-7 samples from tests at 2.2 and 2.4 kV demonstrated a large number of cracks at both voltage

levels, while the 0.025" samples only showed cracks at the higher charge voltage. The behavior described above was relatively consistent throughout the remaining tests. One additional modification was made for the last nine tests of the shot series. A simple fixture of aluminum was made to hold the glass against the slapper, using a 1/16" thick O-ring to provide a mild compressive load. The other side of the slapper continued to use the glass glued to the sapphire barrel. This was done to determine if a fixture would have any effect on the crack initiation and propagation.

The results with the fixture suggest that it may have induce a slight increase in the crack sensitivity of the glass. This is not consistently true for all the shots, but in no case did the unfixtured end show greater damage than the corresponding fixtured side.

### Conclusion

As part of the development of a passive diagnostic for surveillance testing of a slapper detonator, a unique optical probe was constructed that allows simultaneous VISAR measurement of both flyers. The characterization of the slapper was done to establish the correlation between applied firing voltage and the resulting flyer velocity. At voltages below 2 kV, significant differences were seen between the two sides of the unit and from one unit to another. This was attributed to minor differences in the construction of each device.

A variety of materials were tested to determine which would provide a discernible crack pattern at flyer velocities above a predetermined threshold value. Standard fused silica was selected based on performance, availability, and cost. For this slapper, a thickness of

0.020" to 0.025" and a diameter of 1" provides acceptable performance. Efforts are continuing using an intermediate thickness and fixturing to improve the device's behavior for the intended application.

Table 1  
Slapper Flyer Velocity Results

| Firing Set<br>Voltage (kv) | Velocity at 0.5 mm  |                           |
|----------------------------|---------------------|---------------------------|
|                            | Bridge A<br>(mm/ms) | Bridge B<br>(mm/ $\mu$ s) |
| 1.6                        | 2.37                | -                         |
| "                          | 2.20                | -                         |
| 1.7                        | 2.90                | 1.72                      |
| "                          | 2.52                | 2.52                      |
| 1.8                        | 2.55                | 2.70                      |
| "                          | 3.06                | 2.50                      |
| 1.9                        | 3.15                | 2.66                      |
| "                          | 2.85                | 2.76                      |
| 2.0                        | 2.88                | 2.93                      |
| "                          | 3.05                | 3.08                      |
| 2.1                        | 3.12                | 3.15                      |
| "                          | 3.26                | 2.98                      |
| 2.2                        | 3.36                | 3.52                      |
| "                          | 3.27                | 3.33                      |
| 2.4                        | 3.58                | 3.52                      |
| "                          | 3.52                | 3.44                      |
| 2.6                        | 3.68                | 3.88                      |
| "                          | 3.50                | 3.60                      |
| 2.8                        | 3.78                | 3.96                      |
| "                          | 3.68                | 3.84                      |
| 3.0                        | 4.05                | 4.14                      |
| "                          | 4.10                | 3.85                      |

Table 3  
BK-7 Test Results

| Charge<br>Voltage<br>(kV) | Sample<br>Thickness<br>(in.) | Number of<br>Cracks |      |
|---------------------------|------------------------------|---------------------|------|
|                           |                              | (A)                 | (B)  |
| 2.2                       | 0.020                        | 0                   | 0    |
| 2.4                       | "                            | 4                   | 6    |
| 2.6                       | "                            | 5                   | 6    |
| 2.2                       | 0.020                        | 6                   | many |
| 2.0                       | "                            | 4                   | 2    |
| 1.9                       | "                            | 3                   | 5    |
| 1.8                       | "                            | 0                   | 0    |
| 2.2                       | 0.025                        | 6                   | 8*   |
| 2.0                       | "                            | 0                   | 0*   |
| 2.1                       | "                            | 0                   | 0*   |
| 2.2                       | "                            | 0                   | 0*   |
| 2.3                       | "                            | 0                   | 0*   |
| 2.4                       | "                            | 3                   | 9*   |
| 2.3                       | "                            | 2                   | 0*   |
| 2.0                       | 0.020                        | 5                   | 0*   |
| 2.2                       | "                            | 4                   | 0*   |

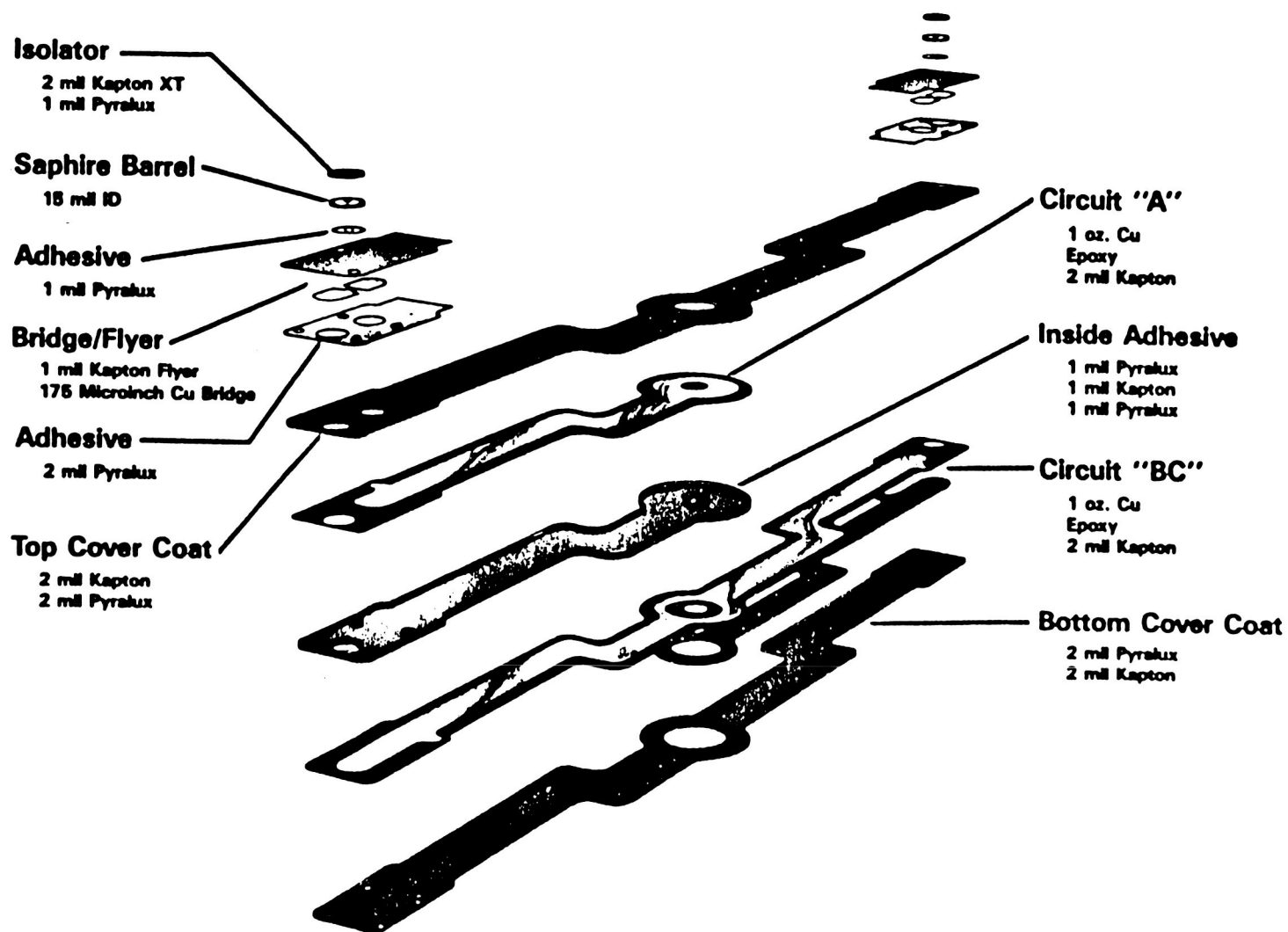
\* indicates fixture was used  
on Side B

Table 2  
Results From Initial Screening Tests

| Shot Number | Charge Voltage (kv) | Sample Configuration                 | Results                               |
|-------------|---------------------|--------------------------------------|---------------------------------------|
| 1           | 1.8                 | 0.03" thk PMMA                       | surface damage                        |
| 2           | 2.8                 | "                                    | surface damage                        |
| 3           | 2.8                 | 0.036" microscope slide 1/2" x 3/4"  | numerous cracks                       |
| 4           | 1.8                 | "                                    | 4 cracks from contact point           |
| 5           | 2.0                 | .006" cover glass 22 mm square       | 4 cracks                              |
|             |                     | .065" quartz glass 1" square         | no damage                             |
| 6           | 2.8                 | .006" cover glass 22 mm square       | >10 cracks                            |
|             |                     | .065" quartz glass 1" square         | 3 cracks                              |
| 7           | 2.0                 | .039" microscope slide 1" square     | damage in center<br>no cracks to edge |
|             |                     | silicon substrate .016" x ~1" square | 6 cracks                              |
| 8           | 2.8                 | .039" microscope slide 1" square     | damage in center<br>no cracks to edge |
|             |                     | silicon substrate .016" x ~1" square | many cracks,<br>center missing        |
| 9           | 2.8                 | plate glass 1/8"                     | no damage                             |
|             |                     | .036" microscope slide 1/2" x 3/4"   | 6 cracks                              |
| (continued) |                     |                                      |                                       |

Table 2 (Continued)

|    |      |                                     |  |
|----|------|-------------------------------------|--|
| 10 | 2.8  | .039" microscope<br>slide 1" square | minor damage                             |
|    |      | .036 microscope<br>slide 1" square  | 4 cracks                                 |
| 11 | 2.0  | .062" plain glass<br>~1" square     | no damage                                |
|    |      | .020" x 3/4" dia<br>sapphire disk   | no damage                                |
| 12 | 2.8  | .062" plain glass<br>~1" square     | no damage                                |
|    |      | .020" x 3/4" dia<br>sapphire disk   | 3 cracks, rear<br>spall                  |
| 13 | 2.4  | .065" quartz ~1"<br>square          | no damage                                |
|    |      | .020" x 3/4" dia<br>sapphire disk   | 1 diagonal crack<br>edge to edge         |
| 14 | 2.2  | .038" quartz ~1"<br>square          | 1 crack, edge to<br>edge                 |
|    |      | .020" x 3/4" dia<br>sapphire disk   | incipient fracture<br>no complete cracks |
| 15 | 2.2  | .018" quartz, ~1"<br>square         | several cracks,<br>not from center       |
|    |      | .038" quartz ~1"<br>square          | incipient cracks                         |
| 16 | 1.95 | .019" Dynasil, odd<br>shape         | 6 cracks                                 |
|    |      | .019" Dynasil, odd<br>shape         | 5 cracks                                 |
| 17 | 1.95 | .034" Dynasil, odd<br>shape         | no damage                                |
|    |      | .034" Dynasil, odd<br>shape         | no damage                                |

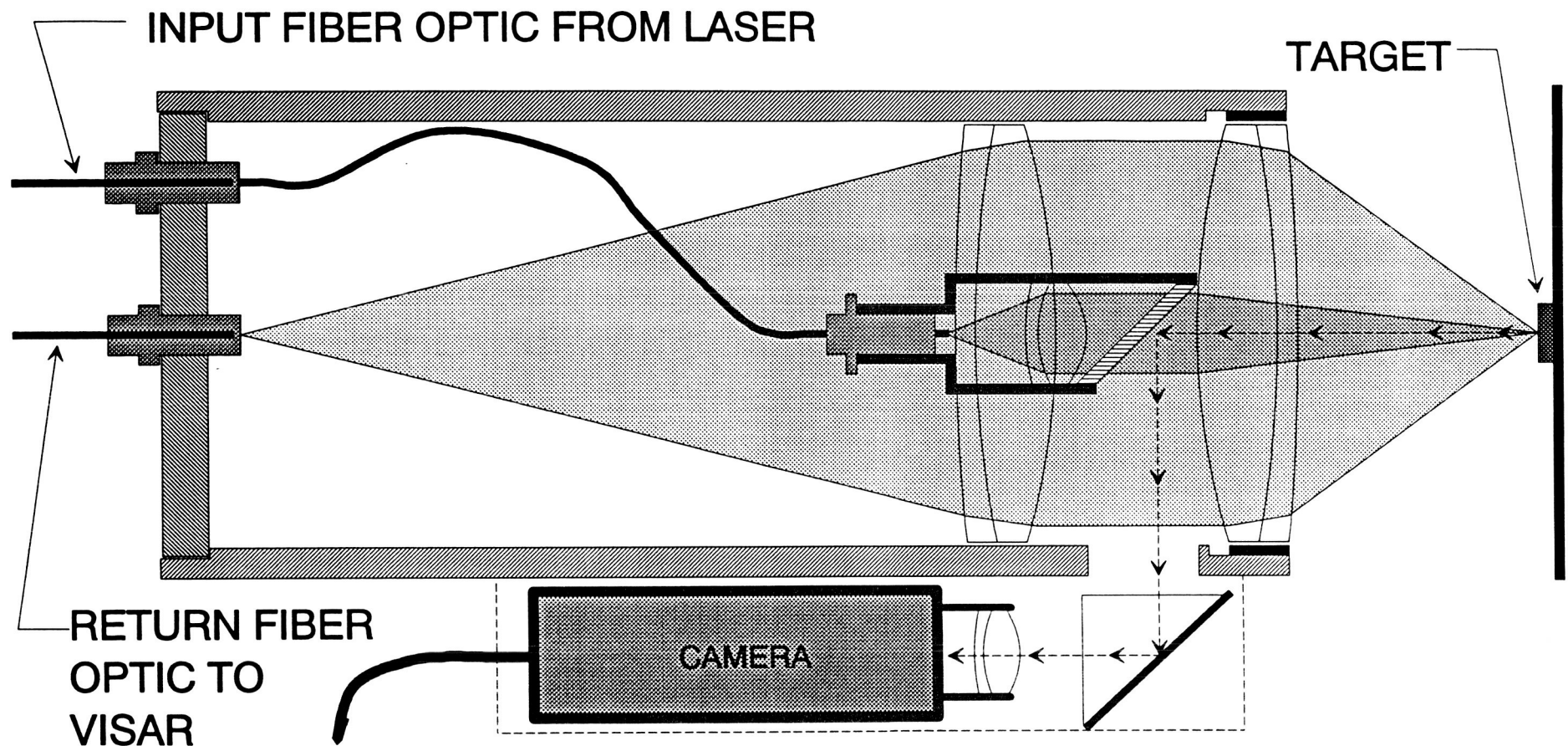


# SLAPPER DETONATOR



figure 1

## IMAGING FIBER OPTIC COUPLED SENSOR



SECTIONAL VIEW OF SENSOR. LASER LIGHT FROM SOURCE ILLUMINATES TARGET, REFLECTED LIGHT IS COLLECTED AND FOCUSED INTO RETURN FIBER OPTIC FOR ANALYSIS. PAT. PEND.

figure 2

VELOCITY/DISPLACEMENT VS TIME LEG "A" 2.6kV Date: 01/20/94

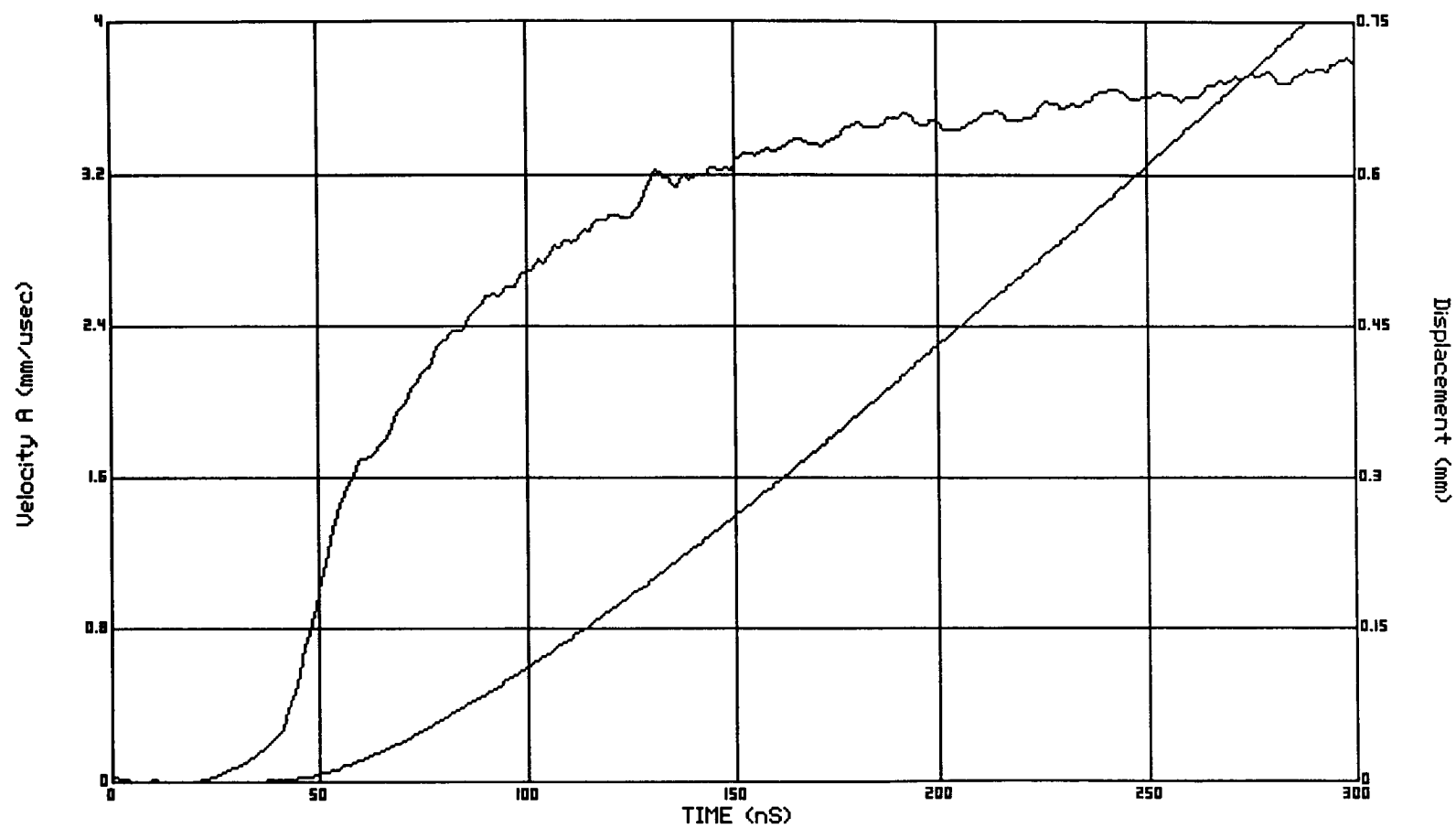


figure 3



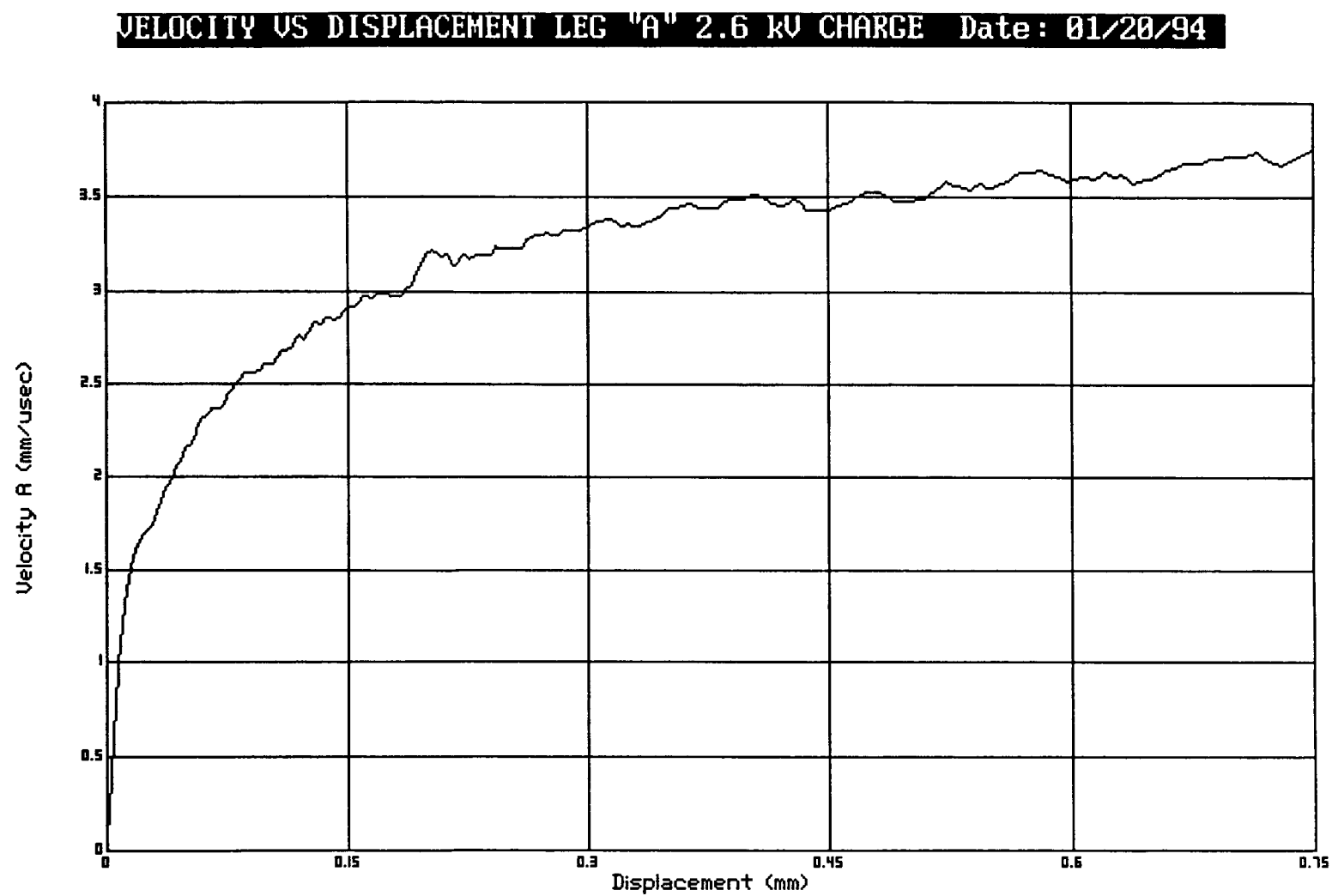


figure 4

# SLAPPER DETONATOR

VELOCITY @ .5mm

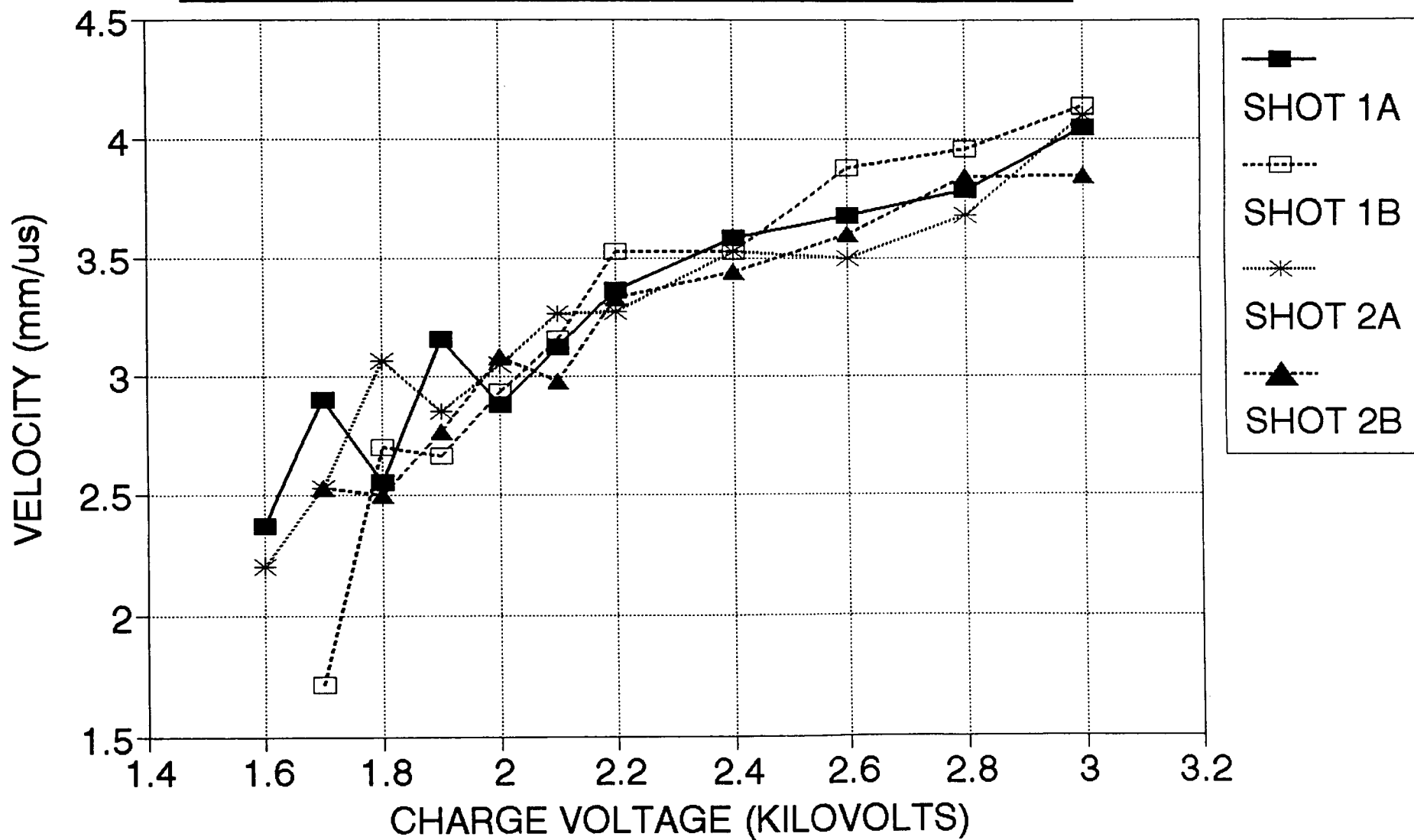


figure 5

513-33  
6493  
P. 6

## APPLYING ANALOG INTEGRATED CIRCUITS FOR HERO PROTECTION

By:

Kenneth E. Willis  
Quantic Industries, Inc.  
990 Commercial Street  
San Carlos, CA 94070  
(415) 637-3074

Thomas J. Blachowski  
Naval Surface Warfare Center  
Indian Head, MD  
(301) 743-4876

### INTRODUCTION

One of the most efficient methods for protecting electro-explosive devices (EEDs) from HERO and ESD is to shield the EED in a conducting shell (Faraday cage). Electrical energy is transferred to the bridge by means of a magnetic coupling which passes through a portion of the conducting shell that is made from a magnetically permeable but electrically conducting material. This technique was perfected by ML Aviation, a U.K. company, in the early 80's, and was called a Radio Frequency Attenuation Connector (RFAC). It is now in wide use in the U.K. Previously, the disadvantage of RFAC over more conventional methods was its relatively high cost, largely driven by a thick film hybrid circuit used to switch the primary of the transformer.

Recently, through a licensing agreement, this technology has been transferred to the U.S. and significant cost reductions and performance improvements have been achieved by the introduction of analog integrated circuits.

An integrated circuit performs the following functions: 1) Chops the DC input to a signal suitable for driving the primary of the transformer, 2) Verifies the input voltage is above a threshold, 3) Verifies the input voltage is valid for a preset time before enabling the device, 4) Provides thermal protection of the circuit, and 5) Provides an external input for independent logic level enabling of the power transfer mechanism. This paper describes the new RFAC product and its applications.

### BACKGROUND

Electro-explosive devices (EEDs) must, in many applications, be protected against unintended initiation by Electromagnetic Radiation (EMR) or Electrostatic Discharge (ESD).

A variety of methods are in use to mitigate these problems; they include:

- 1) Low resistance bridgewires which can dissipate some elec-

trical energy before heating to ignition temperature.

- 2) Filters consisting of capacitive or inductive elements which can absorb or reflect RF energy.
- 3) Shielding to create a Faraday cage around power source, conductors and the EED.
- 4) Voltage spike dissipation or "clamping" functions.
- 5) Switches or relays to disconnect/short the EED pins until ready for function.

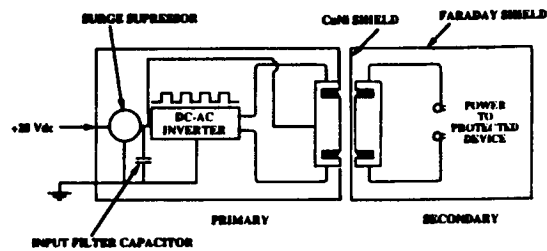
All of these solutions suffer from one or more of the following deficiencies:

- 1) Not completely effective.
- 2) Impose undesirable constraints on the system, e.g., weight, power, and envelope.
- 3) Adds cost.

Depending on the system requirements, these deficiencies can be more or less annoying.

The ideal solution is to simply surround the EED with a Faraday cage - cheap and 100% effective. This solution leaves only one problem: how do you get the firing energy into the bridgewire when it is supposed to function. A practical implementation of this concept is shown in Figure 1.

The Faraday closure surrounds the EED and the secondary of the trans



## PRACTICAL IMPLEMENTATION

Figure 1

former. The material between the transformer cores is a conducting, but magnetically permeable, alloy. The secondary of a narrow band-pass transformer inside the Faraday closure generates the firing current. The conducting copper-nickel alloy maintains the integrity of the Faraday cage. The primary of the transformer is driven with an AC signal at the mid-frequency of the pass band, generated by the DC-AC inverter.

This concept, of course, is not new. The physics has been around a long time. The application to EED protection, as near as I could trace its origins, was proposed by Wing Commander Reginald Gray of the Royal Air Force in 1957. In the mid to late 1970's, Mr. Raymond Sellwood of ML Aviation, a U.K. defense company, adapted this concept to a practical device called the Radio Frequency Attenuating Connector (RFAC). Mr. Sellwood was then granted several patents for these designs, including a U.S. Patent in 1979.

The RFAC has been successfully deployed on a number of U.K. weapon systems, and has per-

formed flawlessly. These systems include:

- Chevaline SLBM
- Airfield Attack Dispenser (Tornado)
- Torpedoes (Spearfish and Stingray)
- Stores Ejection Systems
- ASDIC (Cormorant)

In 1989, Mr. Tom Blachowski, this paper's co-author, completed testing of an RFAC equipped impulse cartridge for a Naval Surface Warfare Center (Indian Head) application.

### **EVALUATION TESTING**

The Indian Head Division, Naval Surface Warfare Center (NSWC) completed an evaluation of the inductive coupling technology for electrically actuated cartridges and cartridge actuated devices (CADs). This effort was performed as part of the Naval Air Systems Command Foreign Weapons Evaluation (FWE)/ NATO Comparative Test Program (CTP). The FWE Program is designed to assess the applicability for foreign-developed, off-the-shelf technology for procurement and implementation in the U.S. Fleet. The FWE goal is production procurement offering fleet users enhanced performance while lowering the per item cost to the program managers.

The FWE effort to analyze the inductive coupling initiation technology was structured as follows: A Navy standard electrically initiated cartridge, the Mark 23 Mod 0 impulse cartridge, was selected to be

modified to accept the inductive coupling initiation hardware. The MK23 Mod 0 cartridge was previously tested by the Navy in numerous configurations and rated as "susceptible" when subjected to Hazards of Electromagnetic Radiation to Ordnance (HERO) electrical field strengths. There have been several documented instances in which MK23 Mod 0 cartridges have inadvertently actuated when subjected to a HERO or electromagnetic interference environment. These inadvertent actuations resulted in mission aborts, loss of essential equipment, and an increased threat to crew members and ground personnel during an electrical event. ML Aviation Limited was contracted by NSWC to install the inductive coupling hardware into the existing MK23 Mod 0 cartridge envelope maintaining the same form, fit, and functions as the Navy standard device. ML Aviation packaged the existing RFAC secondary transformer into the MK23 Mod 0 impulse cartridge and designed a primary transformer into an electrical connector which must be installed in the cartridge firing circuit.

These primary electrical connectors and inductively coupled MK23 Mod 0 impulse cartridges were subjected to a specialized design verification test series at the Indian Head Division, NSWC. Two phases of design verification test were conducted: the first phase was electrical requirements and analysis (performed in accordance with MIL-I-23659C, "General Design Specification for Electrical Car-

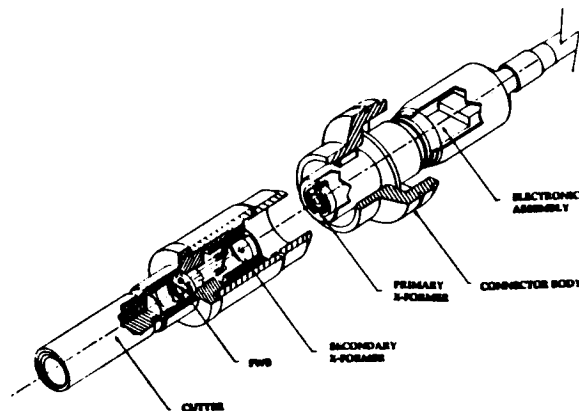
tridges"), and the second phase was the functional testing of the cartridges (performed in accordance with MIL-D-21625F, "Design and Evaluation of Cartridges and Cartridge Actuated Devices").

All of the inductively coupled MK23 Mod 0 impulse cartridge tests were successful and the results exhibited the potential to implement the inductive coupling technology in a wide range of electrically initiated cartridges and CADs. The Indian Head Division, NSWC published the results of this effort in Indian Head Technical Report (IHTR) 1314 dated 17 November 1989, "Evaluation of the Inductive Coupling Technology Installed in a Standard Impulse Cartridge Mark 23 Mod 0".

Based on the excellent test results, and the Navy's desire for a U.S. producer for the RFAC, Quantic Industries and ML Aviation entered into a license agreement for U.S. and Canadian production and sales of RFAC.

### **DESIGN**

A typical configuration of the RFAC, used in a connectorized version is shown here (Figure 2). The primary electronics module is housed in a 7mm diameter x 35mm long tube. The magnetics in this configuration will transfer a minimum of five watts to the sec-



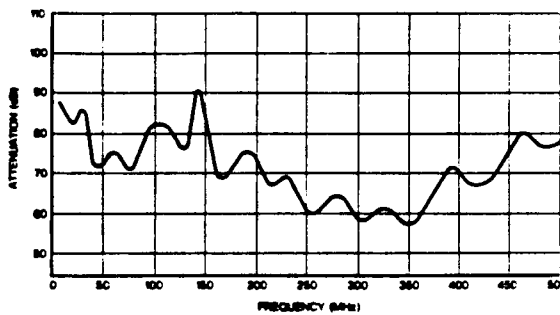
### **RFAC ASSEMBLY**

Figure 2

ondary bridgewire. The electronics can drive larger magnetics in a 9, 11, or 14mm outside diameter configuration, to provide more power.

In the original ML Aviation design, a self oscillating feedback circuit was implemented in a thick film hybrid. Quantic implemented substantial cost reductions and performance improvements by replacing the original thick film hybrid circuit with an analog application specific integration circuit (ASIC). Relatively new technology in high voltage analog array ASICs made this economically viable.

The electromagnetic attenuation performance of the RFAC is unchanged by the change in electronics. Sixty (60) to 80 dB attenuation is achieved. A typical attenuation performance is shown here in Figure 3.



### RFAC PERFORMANCE

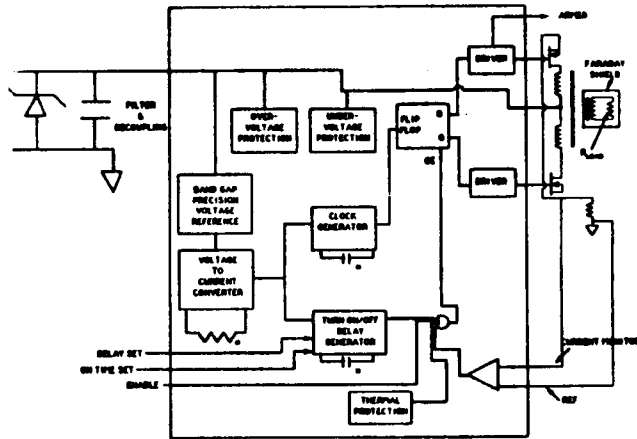
Figure 3

Some additional safety and performance features were added to the ASIC, which, incidentally, adds no cost to the product. These features include:

1. Self contained oscillator.
  - Stable over wide temperatures and voltages
  - Simpler magnetics: original design used - feedback loop to self oscillate
2. Programmable delay time - an additional guard against voltage transients.
3. Input voltage threshold test.
4. Output enable - separate logic level input needed to transfer power.
5. Thermal cut-off.
6. High current output - can be used for larger units.
7. ESD and over voltage protection (note that the ordnance section is intrinsically SAFE from ESD).
8. Programmable turn-off time (0-10 ms).

9. Designed to be nuclear hard.

A block diagram of the RFAC is shown in Figure 4:



### RFAC SIMPLIFIED ELECTRICAL BLOCK DIAGRAM

Figure 4

### CURRENT STATUS

At this time (November 1992) the development and engineering tests of the enhanced inductively coupled MK23 Mod 0 cartridge are complete. The Indian Head Division, NSWG is conducting a qualification program to allow for production procurement and implementation in a wide variety of fleet applications. The inductively coupled MK23 Mod 0 cartridge has been renamed the CCU-119/A Impulse Cartridge as part of this program. The functional test phase of the qualification program is again based upon MIL-I-23659C and MIL-D-21625. Successful completion of these tests will allow Indian Head to recommend approval for release to service. The tests that will be performed as part of the qualification effort are:

Visual inspection  
Radiographic Inspection  
Bridgewire integrity  
Electrostatic discharge  
Stray voltage  
Forty foot drop  
Six foot drop  
Temperature, humidity, and altitude cycling  
Salt fog  
Cook-off  
High temperature exposure  
High temperature storage  
Low temperature (-65°F) testing  
Ambient temperature (+70°F) testing  
High temperature (+200°F) testing

### **APPLICATIONS**

The potential applications of RFAC include essentially all EEDs which must operate in HERO and ESD environments. We expect the reduced cost, made possible by integrated circuit technology, will substantially expand these applications in both the U.S. and U.K. However, In closing, I would like to discuss one novel application that may be of interest to this audience.

The increasing availability of high power diode lasers has sparked the interest of the ordnance community. A fiber optic cable can conduct the optical energy into an initiator which is totally immune to RF and ESD hazards. Offering very lightweight and potentially low cost for safing and arming functions, the diode laser is nearly ideal for many applications. There is one catch; the diodes laser generates the optical energy with a low voltage (typically 3 volts) source. This creates a single point failure safety problem unless mechanical means are used to block the light. However, using an RFAC to isolate the

diode power supply makes this problem disappear. A system which protects the diode and its power supply inside a Faraday closure should meet all safety requirements for diverse applications such as crew escape systems, rocket motor arm fire devices and automotive air bag initiation.

### **BIOGRAPHIES**

Mr. Blachowski has held his present position as an Aerospace Engineer in the Cartridge Actuated Devices Research and Development Branch at the Indian Head Division, Naval Surface Warfare Center for 5 years. In that time, he has been involved in exploratory R&D, advanced development, product improvement, and program support for cartridges and cartridge actuated devices throughout the Navy. Mr. Blachowski received his Bachelor of Science degree in Aeronautical and Astronautical Engineering from Ohio State University in 1985.

As division vice president at *Quantic Industries, Inc.*, Mr. Willis is responsible for directing internal research and development activities, developing new products and new business activities. Product areas include electronic, electromechanical and ordnance devices used for safety and control of systems using energetic materials and processes.

Mr. Willis received his Master of Science Degree in Physics from Yale University in 1959 and a Bachelor of Arts Degree from Wabash College.



514-28  
6994  
16

## **Cable Discharge System for Fundamental Detonator Studies\***

Gregg R. Peevy and Steven G. Barnhart  
Explosives Components Department

William P. Bringham  
Explosives Projects and Diagnostics Department

Sandia National Laboratories  
Albuquerque, NM 87185

### **ABSTRACT**

Sandia National Laboratories has recently completed the modification and installation of a cable discharge system (CDS) which will be used to study the physics of exploding bridgewire (EBW) detonators and exploding foil initiators (EFI or slapper). Of primary interest are the burst characteristics of these devices when subjected to the constant current pulse delivered by this system. The burst process involves the heating of the bridge material to a conductive plasma and is essential in describing the electrical properties of the bridgewire foil for use in diagnostics or computer models. The CDS described herein is capable of delivering up to an 8000 A pulse of 3  $\mu$ s duration. Experiments conducted with the CDS to characterize the EBW and EFI burst behavior are also described. In addition, the CDS simultaneous VISAR capability permits updating the EFI electrical Gurney analysis parameters used in our computer simulation codes. Examples of CDS generated data for a typical EFI and EBW detonator are provided.

### **1.0 INTRODUCTION**

This paper describes the Cable Discharge System (CDS) and its use in fundamental detonator studies. The CDS is preferred over a conventional capacitor discharge unit (CDU) that delivers a decaying sinusoidal current pulse. The fast rising constant, "stiff", current, provided by the CDS charged cable(s) eliminated the uncertainty of a continuously changing current density that comes from a CDU. The CDS is actually two systems; the cable discharge system which provides a square wave current pulse to the detonator and the instrumentation system which measures the detonator parameters of interest. Fundamental detonator studies using the CDS generates information to be used in diagnostics or computer models. Computer modeling provides electrical/mechanical performance predictions and failure analysis of exploding foil initiator (EFI) and exploding bridgewire (EBW) detonators. This project is being performed in order to improve computer modeling predictive capabilities of EFI and EBW detonators. Previous computer simulations predicted a much higher voltage across the bridge than was measured experimentally. The data used in these simulations, for the most part, was collected two decades ago. Since this data does not adequately predict performance/failure, and instrumentation and measurement methods have improved over the years, the gathering of new data is warranted.

\*This work was supported by the United States Department of Energy under Contract DE-ACO4-94AL85000.

## 2.0 SYSTEM DESCRIPTION

The cable discharge system (CDS) resides at Sandia National Laboratories New Mexico in Technical Area II and consists of the following hardware:

- Four 1000 foot long rolls of RG218 coaxial cable
- A high-voltage power supply (100 kV, 5 mA)
- A gas pressurized, self-breaking switch
- A gas system for pressurizing and venting the switch
- Custom output couplings with integral current viewing resistor (CVR)
  - Flat cable coupling for testing of exploding foil initiators (EFI)
  - Coaxial coupling for testing of exploding bridgewires (EBW)
- Instrumentation for measuring:
  - System current - current viewing resistor (CVR)
  - Voltage across the EBW/EFI bridge elements - voltage probes
  - Free-surface velocity of flying plate and particle velocities at interfaces for determining device output pressure - velocity interferometer system for any reflector (VISAR)<sup>1</sup>
- Tektronix DSA602A digitizers
- 486DX33 PC

The CDS is operated by pressurizing the output switch with nitrogen, charging the cables up to a pre-determined voltage which will deliver the required current to the device being tested when the switch is operated. The switch is operated by venting the gas with a fast-acting solenoid valve. Current from the CVR is used as a trigger source for the data recording system. A photograph of the CDS is given in Fig. 1 and a schematic of the CDS is given in Fig. 2.

## 3.0 CAPABILITIES

The four 1000 foot long RG218 coaxial cables can be configured to provide a current pulse ranging in amplitude from 100 to 8000 A with a width of 3  $\mu$ s and a risetime of 25 - 35 ns, Fig. 3 and 4. This wide range of current is made possible by the parallel connection of one to four cables.

The system current is measured with a series 0.005  $\Omega$  CVR that is integral to the output of the CDS. A voltage probe is used to measure the voltage drop across the exploding element, either a bridgewire in the case of the EBW or the foil of an EFI (slapper).

The voltage probe is a 1000  $\Omega$  resistor placed in parallel with the bridge and a Tektronix CT-1 current viewing transformer which measures through it. This allows for decoupling the measurements from ground and minimizes the possibility of ground loop problems.

The VISAR is used to measure the free-surface velocity of the flyers of an EBW or EFI. It also can be used to measure particle velocity at a window interface which in turn, through the use of Hugoniot curves, can determine the explosive output pressure of an EBW. Two separate and independent VISAR modules can make these measurements simultaneously. They have different sensitivities therefore giving a high degree of confidence in these measurements.

All three of these measurements (current, voltage, and velocity) are recorded on Tektronix DSA602A digitizing signal analyzers. These instruments have high bandwidth (up to 1 GHz) and high sampling rates (1 GHz for 2 channels of data). They also can produce calculated waveforms from basic current and voltage measurements representing:

- Resistivity
- Specific action
- Energy

These calculated waveforms are produced from the measured data automatically as soon as they are recorded on the digitizer, see Fig. 5.

The 486DX33 PC can acquire up to 16 waveforms on any shot and store it on a 90 megabyte Bernoulli disk. Other custom software does VISAR data reduction/analysis to give profiles of:

- Flyer velocity vs. time
- Flyer displacement vs. time
- Flyer velocity vs. flyer displacement

Other commercial or custom software packages can then be used to create tables and/or graphs for presentation and report format.

## 4.0 FUNDAMENTAL DETONATOR STUDIES

This section briefly states the basic electrical/mechanical theory of EBW and EFI detonators. For a more detailed explanation see the referenced reports 2 through 6. The CDS can be used to observe both electrical and mechanical behavior of detonators. From these observations, models with their parameters can be generated. Tucker and Toth<sup>2</sup> demonstrated that exploding wire (and foil)

resistivity,  $\rho$ , at fixed current density,  $j$ , may be uniquely specified as a function of either of two parameters: energy,  $e$ , or specific action,  $g$ . These relationships and equations are summarized below.

$$\rho = f(e) \text{ or } f(g) \quad (1)$$

The resistivity of the bridge is the voltage gradient across the bridge divided by the current density through the bridge. The resistivity is characteristic of the bridge metallic material. Resistance of the metallic bridge can be determined by accounting for the bridge volume; cross sectional area,  $A$ , and length,  $L$

$$R = \rho L / A \quad (2)$$

The energy deposited to the bridge is the integral of the voltage,  $V$ , and the current,  $i$ , over time.

$$e = \int V i \, dt \quad (3)$$

The specific action deposited to the bridge is the integral of the current density squared over time.

$$g = \int j^2 \, dt \text{ or } (1/A^2) \int i^2 \, dt \quad (4)$$

The characteristic resistivity versus specific action curve shows the resistivity of the bridgewire (foil) as it passes through the material phase changes; solid, liquid, and vapor, Fig. 6. Bridge burst is the condition in which the bridge is vaporized and arc breakdown occurs through the vapor. This corresponds to the peak resistivity.

The characteristic resistivity as a function of energy or specific action curve is obtained from the instrumentation system by the measurement of the current through the bridge and the voltage drop across the bridge, Fig. 7. The voltage drop across the bridge divided by the current through the bridge gives the bridge resistance. Resistivity is calculated by multiplying the resistance by the bridge cross sectional area and dividing by the bridge length. Specific action is calculated by squaring the current and integrating over time while dividing by the square of the bridge cross sectional area. Energy is calculated by multiplying voltage and current and integrating over time.

Tucker and Stanton<sup>3</sup> extended the Gurney method of predicting the terminal velocity of explosively driven projectiles to flyers driven by exploding foils in an

EFI detonator. This couples input electrical parameters with EFI detonator mechanical output parameters; namely flyer velocity. The Gurney analysis of an explosive system is based on conservation of momentum and the assumption that the kinetic energy of the system is proportional to the total energy released by the exploding foil. The following is an approximate or simplified analysis (known as a modified Gurney analysis). The ratio of the system kinetic energy to the energy released is the Gurney efficiency,  $\eta$ , and the Gurney energy,  $E_g$  is given by

$$E_g = \eta e \quad (5)$$

where  $e$  is the energy deposited into the foil. The solution of the momentum and energy equation yields a prediction of the terminal flyer velocity,  $u_f$

$$u_f = (2 E_g)^{0.5} f(\text{geometry}) \quad (6)$$

where  $f(\text{geometry})$  is a known factor dependent upon the EFI geometry.

Tucker and Stanton<sup>3</sup> also showed that the Gurney energy could be empirically related to the burst current density of the foil.

$$E_g = k j_b^n \quad (7)$$

where  $k$  is the Gurney coefficient and  $n$  is the Gurney exponent. Measurement of the burst current density and knowledge of the Gurney energy allows the calculation of the Gurney coefficient and exponent. Once the Gurney coefficient and exponent are known, the terminal flyer velocity can be calculated for a determined burst current density.

From the measurement of the flyer velocity, the flyer pressure pulse magnitude,  $P$ , and duration,  $\tau$ , imparted to the explosive receptor can be calculated from Hugoniot pressure - particle velocity ( $P-u$ ) relationships.<sup>4</sup> Explosive initiation criteria can then be calculated to determine initiation margin. Some explosives are characterized by the relationship

$$P^n \tau \geq K \quad (8)$$

where  $K$  is a constant and  $n$  is an exponent specific to an explosive.<sup>5</sup> For explosive initiation (detonation), this criterion must equal or exceed the specified constant,  $K$ . Other explosives are characterized by initial shock pressure,  $P$ , versus run

distance to detonation,  $x$ , plots or "Pop plots".<sup>6</sup> These plots can be expressed empirically by the relationship

$$\log P = A - B \log X \quad \text{or} \quad (9)$$

$$P = C + D x^{-1} \quad (10)$$

where A, B, C, and D are constants for least squares data fit.

#### 4.1 SAMPLE DATA

A typical EBW and EFI detonator were selected and tested in order to present typical data output. The EBW is a 1.2 x 20 mil Au bridgewire in contact with a PETN explosive DDT column (18.5 mg 0.88 g/cm<sup>3</sup> initial pressing, 9.3 mg 1.62 g/cm<sup>3</sup> output pellet). The EFI is a 15 x 15 x 0.165 mil square Cu bridge with a 1 mil thick Kapton flyer. An investigation was conducted to observe the behavior of the detonators over a range of operating current density. The response of the EBW and EFI detonators to a similar CDU burst current level pulse was also investigated to verify that CDU and CDS generated data are comparable. The data is presented in a summary format at bridge burst condition. Bridge burst resistivity, specific action, and energy are plotted versus current density, Fig. 8 through 13.

Based upon these results, several observations could be made.

- Resistivity at bridge burst decreases with increasing current density for the EBW, Fig. 8.
- Specific action to bridge burst remains fairly constant over current density range for both the EBW and EFI, Fig. 9 and 12.
- Energy to bridge burst increases with increasing current density for both the EBW and EFI, Fig. 10 and 13.
- Resistivity at bridge burst remains fairly constant over current density range for the EFI, Fig. 11.
- CDU and CDS generated data are comparable, Fig. 11 through 13.

From these observations, in order to adequately model an EBW or EFI detonator, resistivity versus specific action or energy data needs to be taken at three current levels; slightly above threshold (50% fire/no-fire), 1.5 times threshold, and 2 times threshold (normal minimum operation).

Previous computer simulations always predicted a much higher voltage across the bridge than was

measured. The "old" resistivity versus specific action look-up table data for a gold EBW and a copper EFI are compared to recently, "new", generated data in Fig. 14 and 15. Since the peak resistivity is much lower, predicted voltages now closely match actual values.

The mechanical output of both the EBW and EFI detonators was also observed over the range of operating current density by using the VISAR. The flyer velocity of the EBW closure disk was measured at a PMMA window interface. Flyer velocity did not change over the current range. This was expected, Fig. 16. EFI flyer velocity increased with increasing current density as expected, Fig. 17. The EFI Gurney energy was calculated from the flyer velocity and current density, Fig. 18. A least squares data fit yielded a Gurney coefficient of 0.00125 and a Gurney exponent of 1.28.

#### 5.0 INTEGRATION OF DETONATOR STUDIES DATA INTO PREDICTIVE COMPUTER CODES

Detonator studies data are used in computer codes to predict the electrical and mechanical behavior of bridges as they burst. An electrical circuit solver computes current as a function of time and then "looks up" resistivity in a look-up table or calculates the resistivity with an empirical relationship as a function of computed energy or specific action to get the instantaneous bridge resistance. Once a burst current is known, for an EFI, a flyer velocity can be calculated. A list of some of the electrical circuit solvers available along with a brief description follows.

- AITRAC - complex circuit solver with bursting wire & foil look-up table<sup>7</sup>
- CAPRES - simple circuit solver with bursting foil look-up table and electrical Gurney routine
- PSpice© - complex circuit solver with bursting elements added by Furnberg (empirical function) and Peevy (look-up table) with electrical Gurney and  $P^{n\tau}$  initiation criterion<sup>8,9</sup>
- Fireset - code by Lee with empirical resistivity function<sup>10</sup>
- Slapper - code by R. J. Yactor, Los Alamos National Laboratories, with empirical resistivity function, electrical Gurney, and Pop plot explosive initiation criteria.

Electrical Gurney and  $P^{n\tau}$  initiation criterion are implemented into the PSpice electrical circuit

simulator as custom circuit elements using the Analog Behavioral Modeling capability.

### 5.1 COMPUTER PREDICTION VERSUS DATA

A computer simulation of a typical capacitor discharge unit (CDU) firing system with a single EFI detonator was performed using the latest CDS generated resistivity versus specific action data look-up table. The firing system lumped parameters are:

$$C = 0.2 \mu\text{F}$$

$$R = 100 \text{ m}\Omega$$

$$L = 17 \text{ nH.}$$

Simulation output versus test data is shown graphically in Fig. 19 and 20. As can be seen in Table 1, simulations compare well to experiment.

### 6.0 CONCLUSION

The CDS has been fully documented. Newly obtained data are more accurate and improves computer simulation, electrical/mechanical performance predictions and failure analysis of EBW and EFI detonators. Future plans are to model other EBW and EFI detonators of interest.

### 7.0 REFERENCES

1. O. B. Crump, Jr., P. L. Stanton, W. C. Sweatt The Fixed Cavity VISAR, Sandia National Laboratories, Report No. SAND-92-0162.
2. T. J. Tucker, R. P. Toth, EBW1: A Computer Code for the Prediction of the Behavior of Electrical Circuits Containing Exploding Wire Elements, Sandia National Laboratories, Report No. SAND-75-0041.
3. T. J. Tucker, P. L. Stanton, Electrical Gurney Energy: A New Concept in Modeling of Energy Transfer from Electrically Exploded Conductors, Sandia National Laboratories, Report No. SAND75-0244.
4. P. W. Cooper, "Explosives Technology Module D, Shock and Detonation," Sandia National Laboratories Continuing Education in Science and Engineering, INTEC Course No. ME717D.
5. A. C. Schwartz, Study of Factors Which Influence the Shock-Initiation Sensitivity of Hexanitrostilbene (HNS), Sandia National Laboratories, Report No. SAND80-2372.
6. B. M. Dobratz, P. C. Crawford, LLNL Explosives Handbook Properties of Chemical Explosives and Explosive Simulants, Lawrence Livermore National Laboratory, Report No. UCRL-52997, 1985.
7. Berne Electronics Inc., Sandia National Laboratories, Albuquerque, AITRAC Augmented Interactive Transient Radiation Analysis by Computer User's Information Manual, Sandia National Laboratories, Report No. SAND77-0939.
8. PSpice (a registered trademark of) Microsim Corporation, 20 Fairbanks, Irvine, California.
9. G. R. Peevy, S. G. Barnhart, C. M. Furnberg, Slapper Detonator Modeling Using the PSpice® Electrical Circuit Simulator, Sandia National Laboratories, Report No. SAND92-1944.
10. R. S. Lee, FIRESET, Lawrence Livermore National Laboratory, Report No. UCID-21322, 1988.

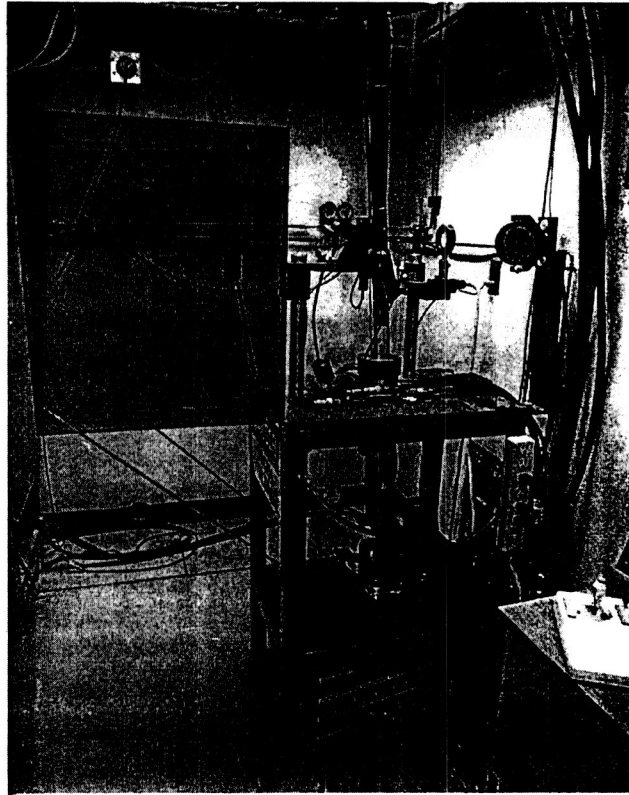


**Fig. 1** Photograph of Cable Discharge System

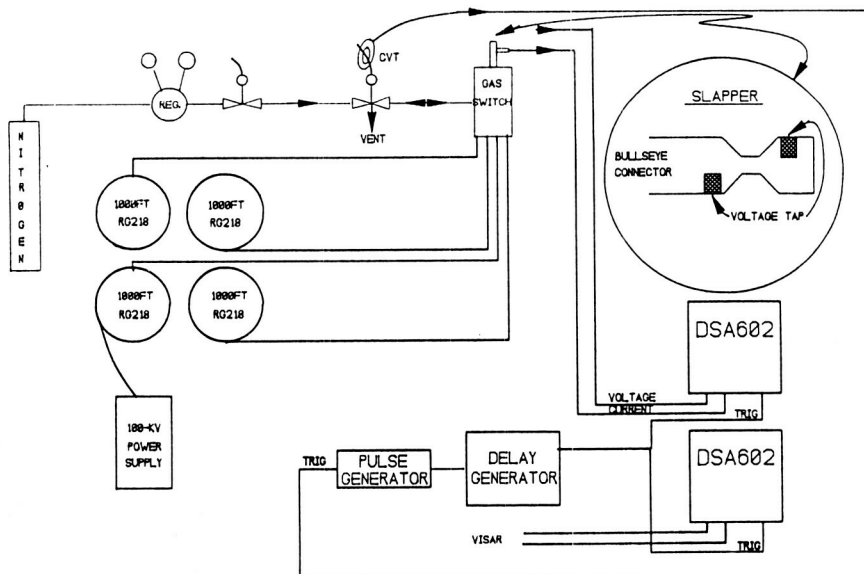


**Fig. 2** Schematic of Cable Discharge System

DSA 602A DIGITIZING SIGNAL ANALYZER  
date: 5-JAN-94 time: 10:52:01

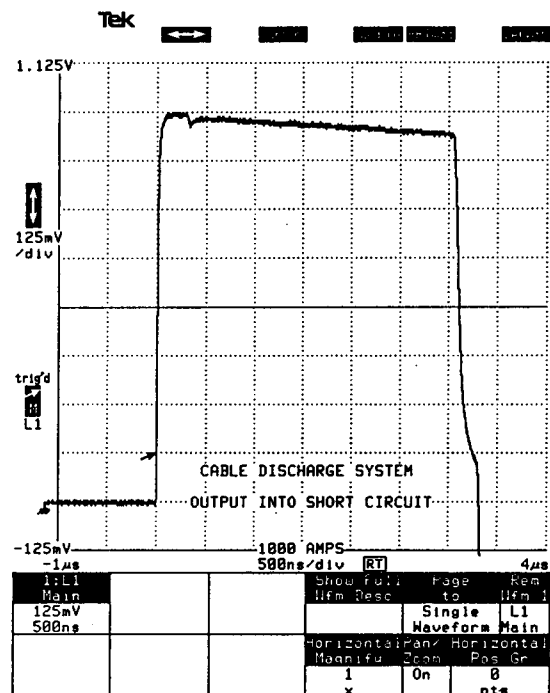


Fig. 3 Typical DSA Current Waveform

DSA 602A DIGITIZING SIGNAL ANALYZER  
date: 5-JAN-94 time: 10:55:13

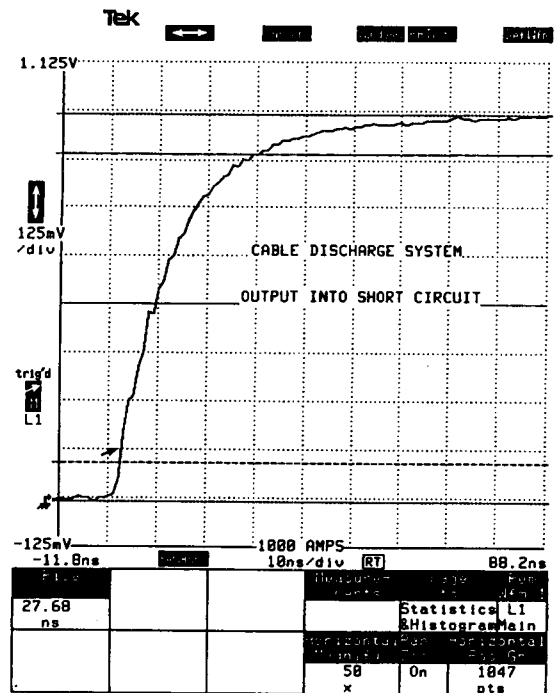


Fig. 4 Typical Current Leading Edge

DSA 602A DIGITIZING SIGNAL ANALYZER  
date: 6-AUG-93 time: 13:20:30

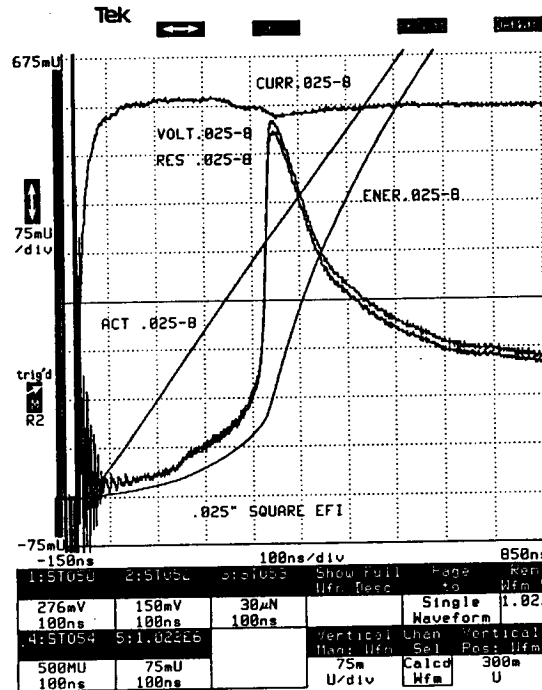


Fig. 5 Calculated Waveforms

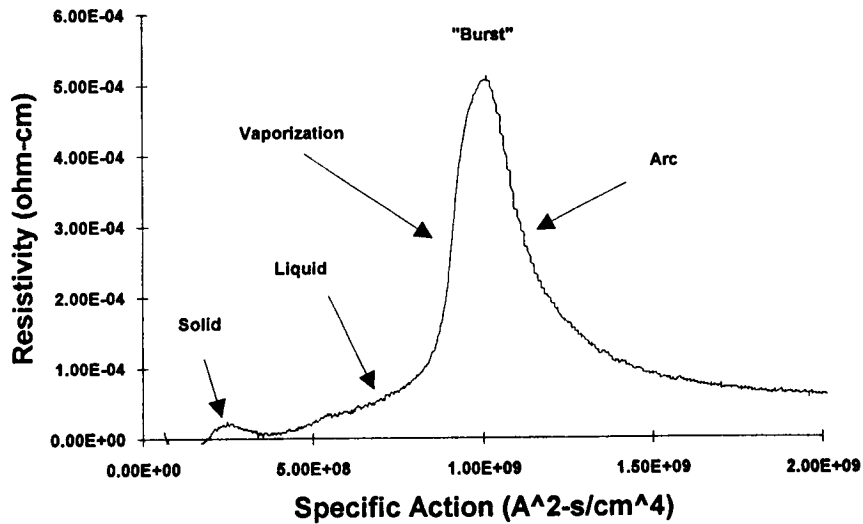
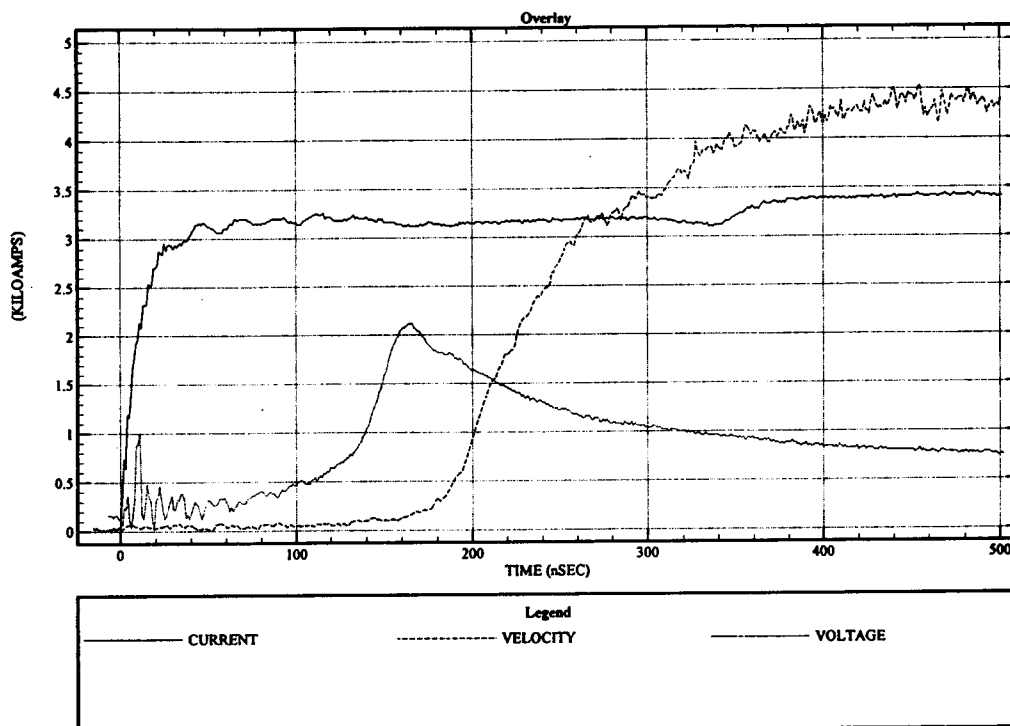
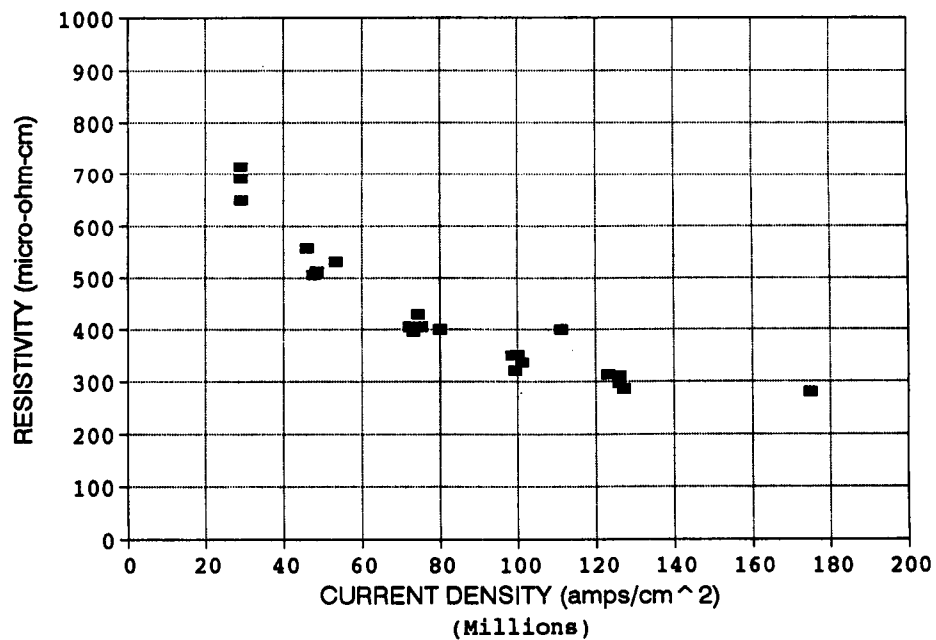


Fig. 6 Typical Resistivity vs. Specific Action Profile





**Fig. 7 Cable Discharge System Waveform for EFI**



**Fig. 8 EBW Burst Data Summary of Resistivity vs. Current Density**

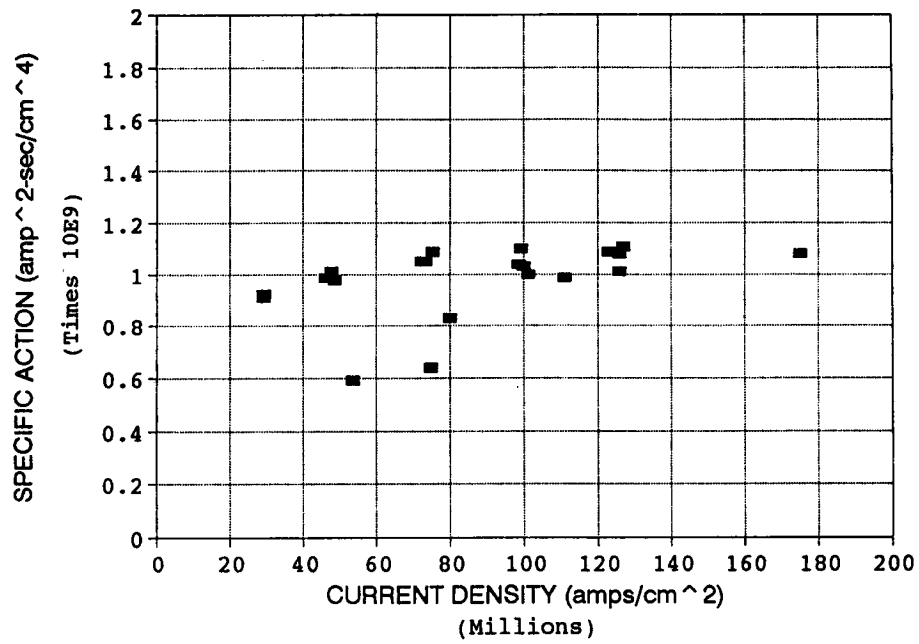


**Fig. 9 EBW Burst Data Summary of Specific Action vs. Current Density**

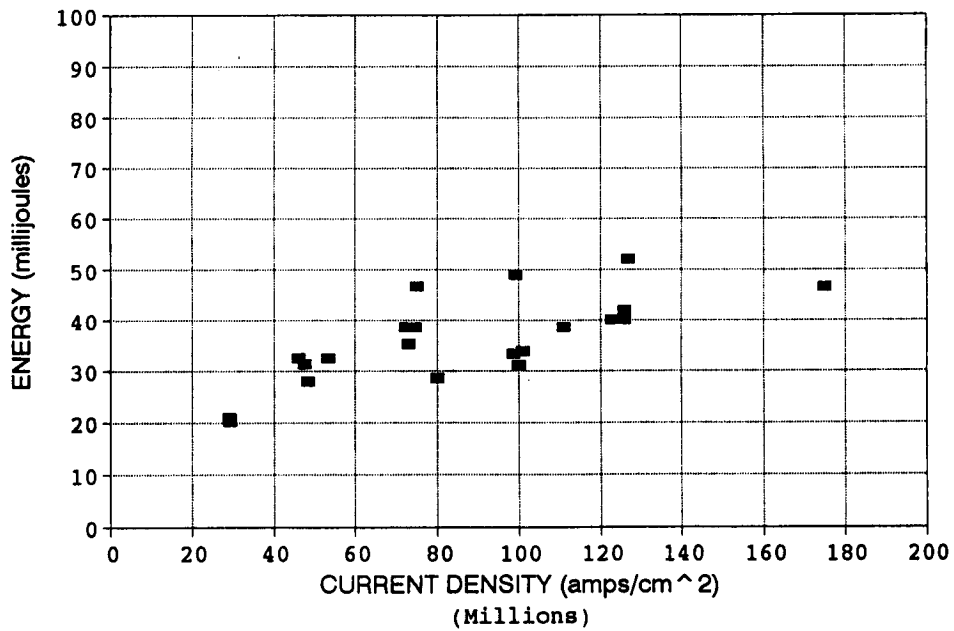


**Fig. 10 EBW Burst Data Summary of Energy vs. Current Density**

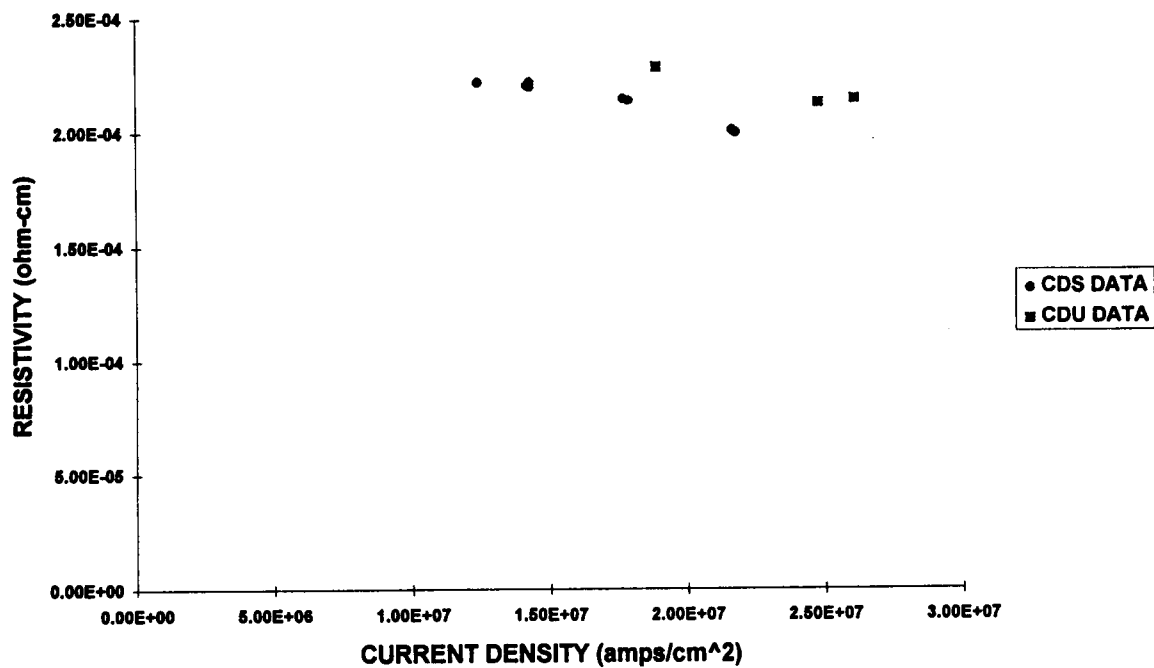


Fig. 11 EFI Burst Data Summary of Resistivity vs. Current Density

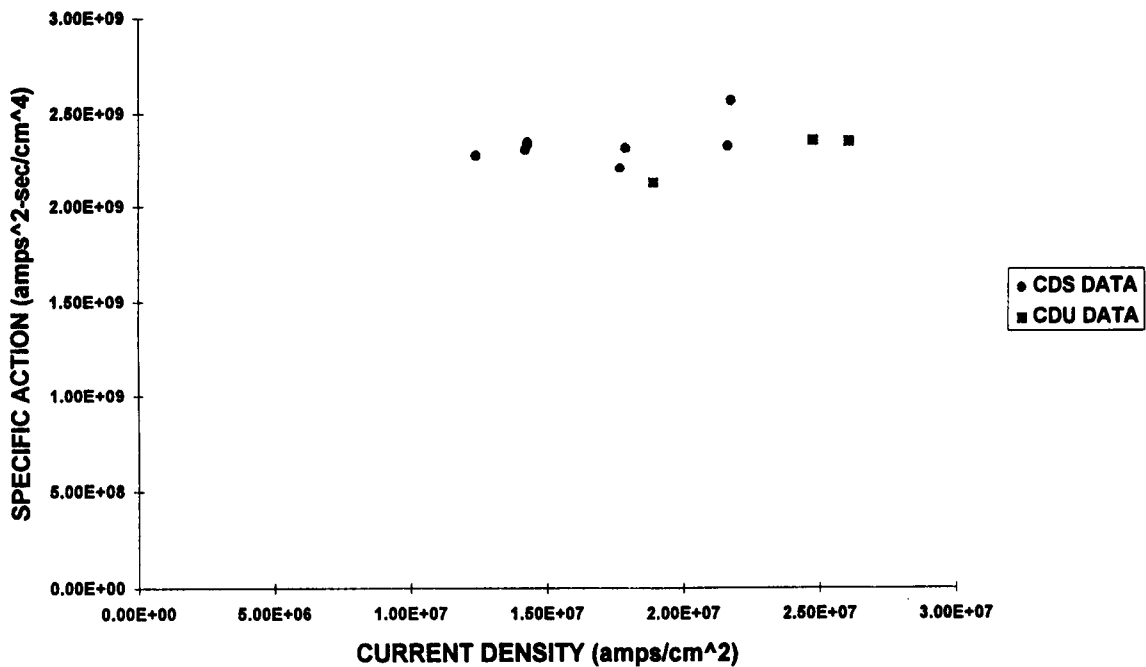


Fig. 12 EFI Burst Data Summary of Specific Action vs. Current Density

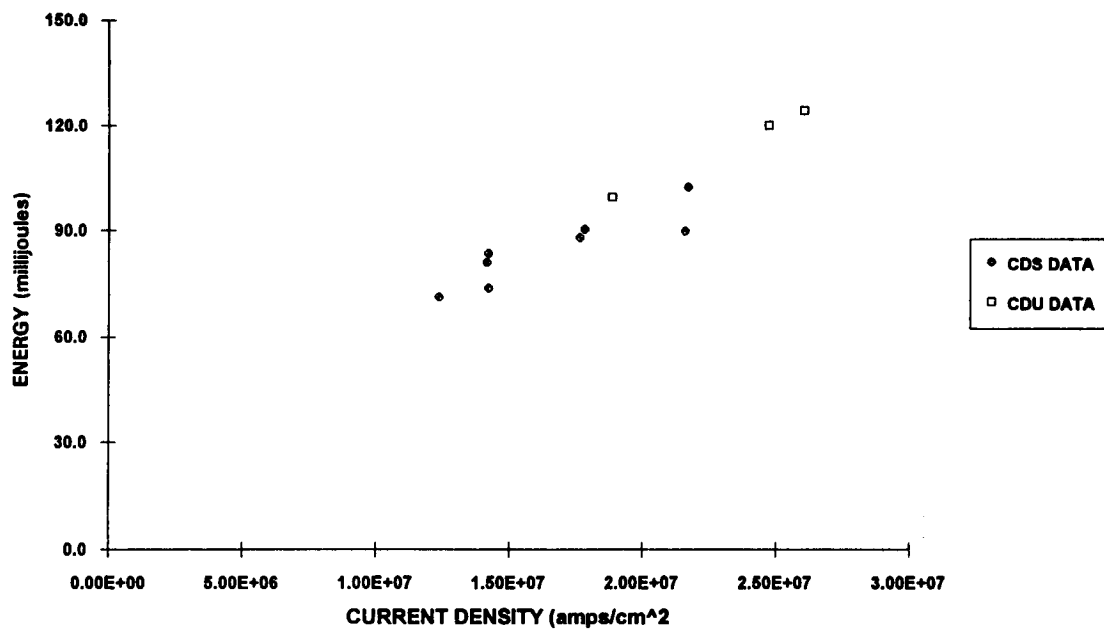


Fig. 13 EFI Burst Data Summary of Energy vs. Current Density

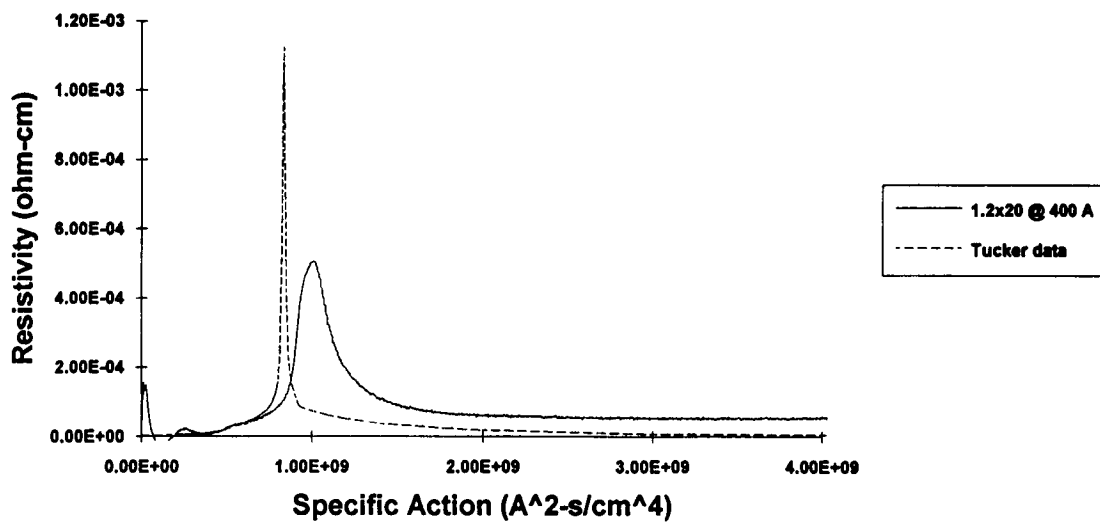


Fig. 14 New vs. Old EBW "Look-up" Table

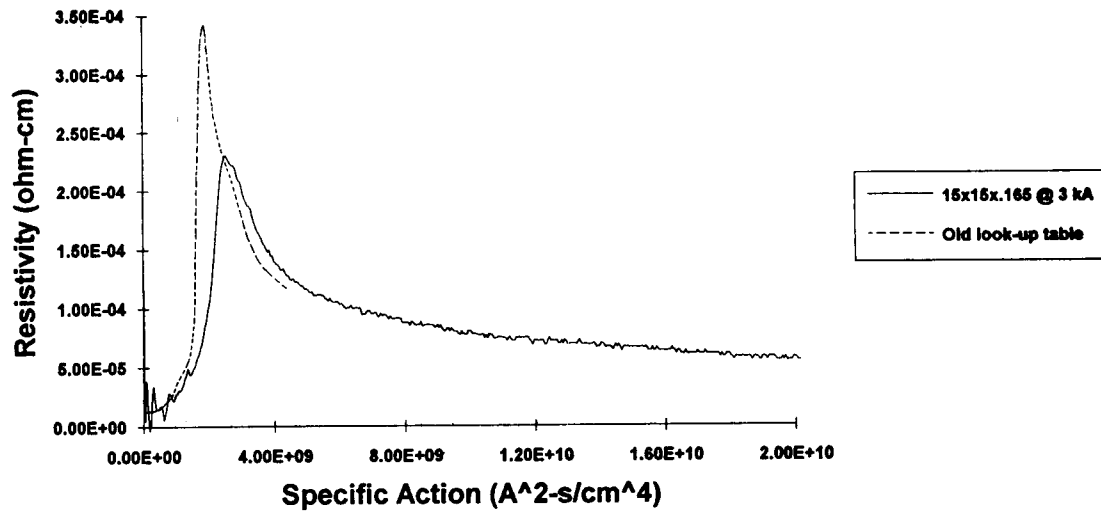


Fig. 15 New vs. Old EFI "Look-up" Table

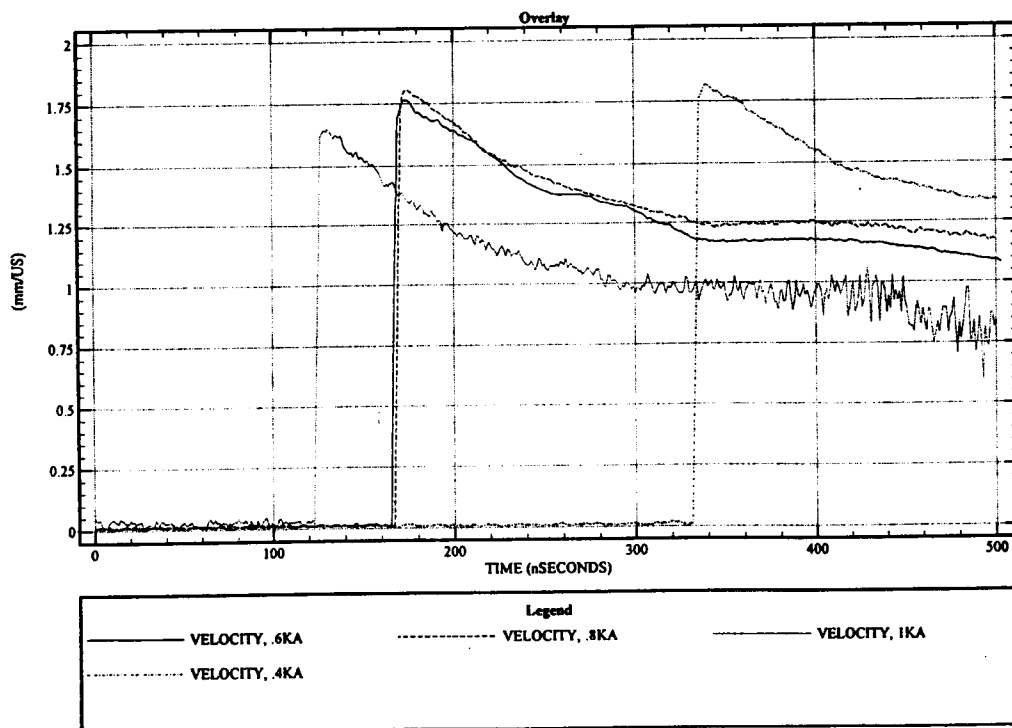


Fig. 16 EBW Output Flyer Velocity vs. Current Density

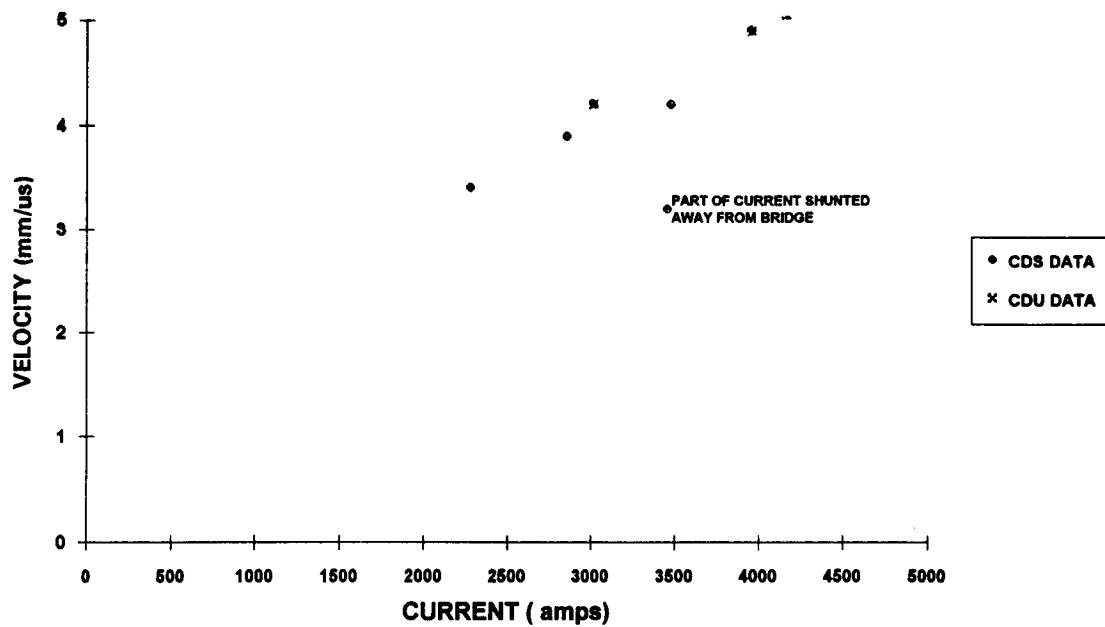


Fig. 17 EFI Flyer Velocity vs. Current Density

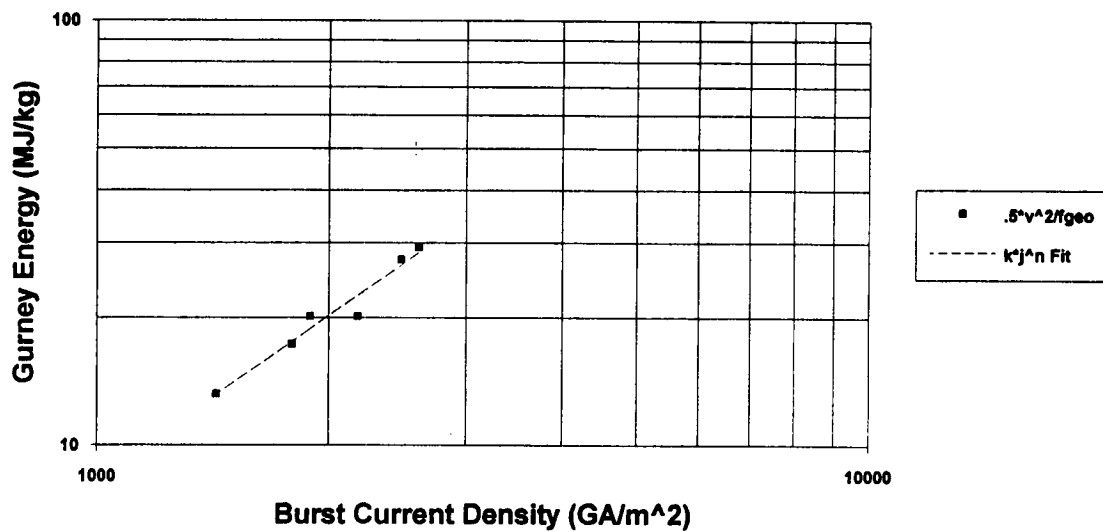
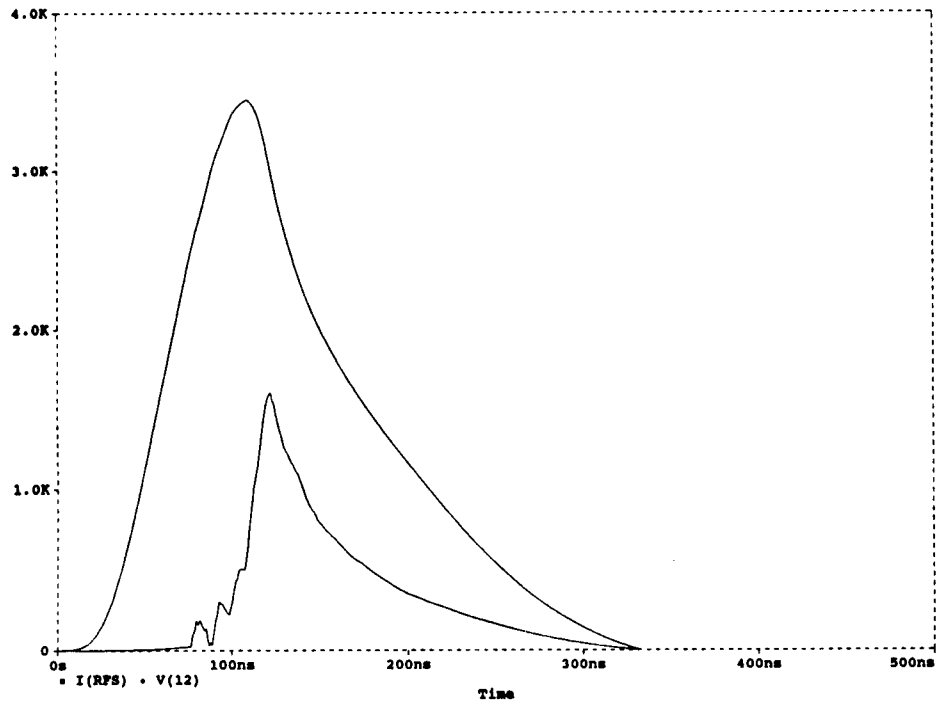
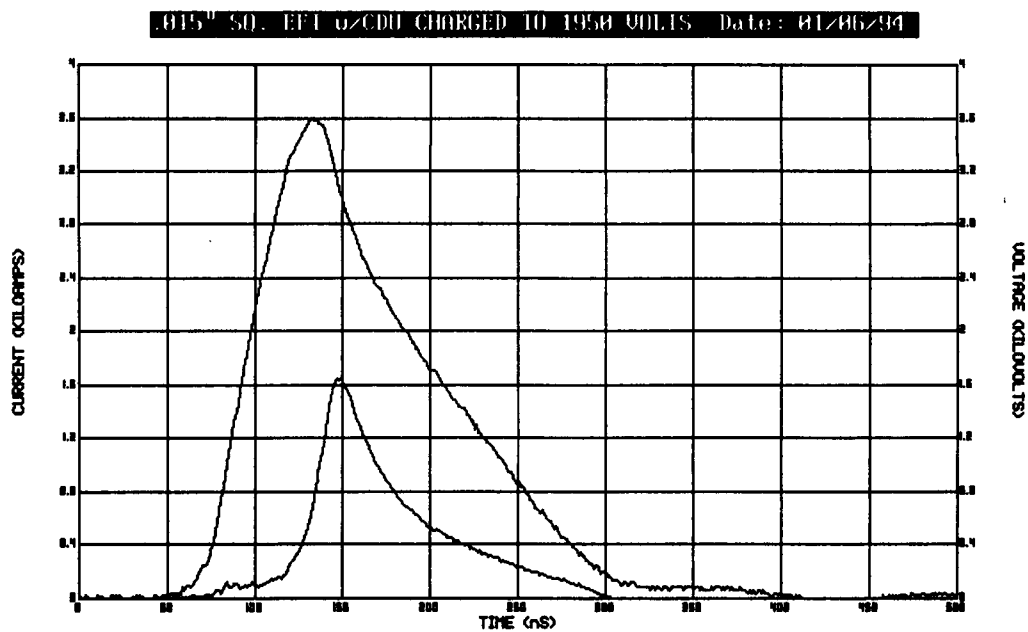


Fig. 18 EFI Gurney Energy vs. Burst Current Density



**Fig. 19 Simulation Using New Look-Up Table Voltage and Current Traces**



**Fig. 20 Test Data Voltage and Current Traces**

**Table 1**  
**EFI Simulation Output vs. Test Data**

| <b>CDU<br/>Charge<br/>Voltage<br/>(V)</b> | <b>Calculated<br/>Burst<br/>Current<br/>(A)</b> | <b>Calculated<br/>Flyer<br/>Velocity<br/>(mm/<math>\mu</math>s)</b> | <b>Burst<br/>Current<br/>(A)</b> | <b>Flyer<br/>Velocity<br/>(mm/<math>\mu</math>s)</b> |
|---|---|---|----------------------------------|--|
| 1950                                      | 3009  | 4.1   | 3020                             | 4.2  |
| 2600                                      | 4072  | 4.8   | 3960                             | 4.9  |
| 2800                                      | 4325  | 5.0   | 4170                             | 5.1  |



515-28  
6995  
P. 12

## INITIATION CURRENT MEASUREMENTS FOR HOT BRIDGEWIRE DEVICES

Gerald L. O'Barr (Retired, General Dynamics, 1 Oct 1993)

**ABSTRACT** One-shot type testing of hot bridgewire explosive cartridges provides the weakest possible firing characteristic data. One-shot type testing includes the Bruceton and the Probit methods, and all their off-shoots. One-shot testing is used for only one reason: the fear of "dudding." Modern programmable power supplies and oscilloscopes can now be used to obtain data with no fear of dudding. Any continued use of these old, one-shot type test methods is irresponsible behavior. Our society deserves better testing methods and will get them through the courts if we cannot make these changes on our own.

### 1.0 INTRODUCTION

Explosive cartridges often use a bridgewire initiation system. A bridgewire is a very small wire, approximately 0.005" in diameter and 0.2" long, through which electrical current can be forced to flow. Because of the electrical resistance of the wire, the current can cause the wire to become hot like the filament in a light bulb. Around the bridgewire is a sensitive ignition mix that will ignite with temperature. As the bridgewire gets hot, it ignites the ignition mix, which then sets off the main charge of the cartridge, often through intermediate mixes between the ignition mix and the main charge.

The reliability of operation of an explosive device is critical. Being a destructive event, one would not want an explosive cartridge to go off

before it is needed (for safety) and yet, when its function is required, since explosive devices are usually used for critical operations, it must work quickly and reliably. Since the primary initiation is by the flow of current, the following questions must be asked:

- A. What is the maximum current that can flow through the bridgewire and not have it ignite or explode?
- B. What is the minimum current that can be used and still be sure that it will ignite or explode?

The answer to A provides what is called the "no-fire" current. It tells one the degree of safety that might exist in using this device. If the current for A is so low that random stray voltages might induce sufficient

current to set it off, then it would be unacceptable. Often, a one-ampere current is specified as being the minimum acceptable no-fire current. If the bridgewire resistance could be less than one ohm, a power minimum of one watt is also sometimes specified.

The answer to B provides the "all-fire" current. This value must obviously be more than A, and hopefully low enough that the power supply being used to set it off can provide the current that is required. Values of 3.5 to 5 amperes are often specified. In statistical terminology, the all-fire and no-fire current requirements are often stated as follows:

- A. The cartridges shall have a 1 ampere/1 watt or greater no-fire current with a reliability of 99.9%, at a confidence level of 95%.
- B. The cartridges shall have a 3.5 ampere or less all-fire current with a reliability of 99.9%, at a confidence level of 95%.

These statistical requirements can be determined if the firing currents are normally distributed and the mean and the standard deviation of the lot's firing current can be determined. Basically, this report will discuss a new test method for measuring the mean and the standard deviation of the firing current for a lot of

explosive cartridges.

## 2.0 DIFFICULTIES IN MEASURING THE INITIATION CURRENT

The phrase "firing current" has many different meanings. This results in certain difficulties that we will take care of now. The firing current is often used to mean the current being applied to the bridge-wire. It is also used for the minimum current required to ignite a cartridge. It is this minimum current, along with its distribution, that allows us to determine the all-fire and the no-fire. Therefore, when we mean this minimum current, we shall use the words, "initiation current."

To measure the initiation current, it would seem easy to connect a cartridge up to a variable power source and manually turn up the current until it ignites. Another method would be to use a series of ever increasing steps or pulses of current. The current at which it ignites could then be the desired data.

When cartridges were originally made (over 30 years ago), such efforts often proved to be impossible. The "sensitive" ignition mix, when exposed to heat, could degrade. If one raised the current too slowly, or exposed a cartridge to several firing currents below that required for ignition, the cartridge could actually become impossible to ignite. When the chemicals making up the

ignition mix become sufficiently degraded, the cartridge becomes a dud. Thus, the initiation current was often dependent on the rate at which the current was applied, and could become infinite. The industry quickly learned that only "virgin" cartridges could be tested in a one-time-only test.

For this reason, all tests for explosive cartridges (Bruceton testing, Probit testing, and a multitude of testing based upon these approaches) use a one-shot approach. A cartridge is exposed to one pre-selected current value, and a fire or no-fire result is recorded.

The data obtained by this approach is not good. If a cartridge is tested at 2.30 amperes and it fires, no one can say that this was the initiation current for this cartridge. The Bruceton and Probit test methods would use this data as a firing point, but all one knows for sure is that the true initiation current for this cartridge was this value or less. It could have been much less. It could have been so much less that it could have skewed all the rest of the data. But in the one-shot method, one will never know the true initiation current for that particular cartridge.

The same things are true if the cartridge did not fire. Again, the Bruceton and the Probit test methods assume

that it is the no-fire point. The actual no-fire point might be much greater. It could even be a dud, with an infinite firing current value. Neither the Bruceton nor the Probit methods will be sensitive to these situations.

Because the data that comes from a one-shot test is not normally the initiation current for that cartridge (if it fires), nor the real no-fire current for that cartridge (if it does not fire), then the data is extremely poor data. It has almost no meaning except as limits to the values being sought, and these limits have no value unless they are repeated a great number of times in a well controlled lot. If you are making tests on a lot that is not well controlled, the limit data will be entirely useless. Worst of all, one can seldom tell by looking at the Bruceton or Probit data if the data is from an adequately controlled lot, or when the number of limit tests are really adequate.

### 3.0 NEW METHODS

Today, one does not need to manually turn up the current to fire a cartridge. One does not need to follow a moving indicator to read what might have been the initiation current. Today, with programmable current generators, and oscilloscopes, very controlled current profiles and measurement devices can measure the actual initiation current of a

device. It can be done at a rate where no significant degrading will occur.

Thus, today, in any modern laboratory, there is no need to work with the out-of-date, and very poor data generating methods such as the Bruceton or Probit one-shot methods. A "dynamic ramp" test method can supply reliable and specific initiation data for all cartridges tested.

It is also a fact that over these many years, much more stable ignition mixes are now being used. For most modern explosive cartridges, one could probably even use a manual method and obtain better data than what a Bruceton or Probit method might provide.

**4.0 THE DYNAMIC RAMP TEST METHOD** The dynamic ramp test used a programmable power supply that puts out a controlled current ramp from zero to five amperes. The rate of the ramp, as used in these tests, was approximately 3.5 amperes per second. The current circuit included a standard one-ohm resistor in series with the explosive cartridge. The voltage across the one-ohm resistor was recorded on an oscilloscope with memory trace recording. The scope was calibrated so that within the expected firing levels, currents could be read to the nearest 0.01 amperes, with an overall accuracy estimated to be better than  $\pm 0.02$  amperes.

The firing point of the cartridges being tested appeared to be a clean break in the circuit, with the voltage returning to zero when the bridgewire initiated the cartridge. If the programmable power supply has too high of a voltage capability, current can continue to flow even when the bridgewire is "broken" by flowing the current through the ionized gas that is created in an explosion. This would indicate a higher firing current than that actually required. When ionization flow is present, the trace is usually very uneven without a clean break.

#### 5.0 RESULTS

The results for a series of ten consecutive firings are shown in Table I. The results from a small Bruceton test of 17 firings is shown in Appendix A.

The means determined from these two tests were almost identical, 2.43 amperes in the dynamic ramp test and 2.44 amperes in the Bruceton. The standard deviations, however, are much different, 0.234 amperes for the dynamic ramp test and only 0.070 amperes for the Bruceton test. This difference in the standard deviation is over three to one.

Table 2 shows the results after 20 firings. The data continues to confirm the statistics that had been obtained in Table 1. Figure 1 shows the distribution for

# TABLE 1. DYNAMIC RAMP TEST

PART NO. :55-06018-2 LOT 13-37700 DATE: 1 FEB 1993

|    | CARTRIDGE<br>NO. | PEAK<br>CURRENT (Xi) | (Xi-X)^2 |
|----|------------------|----------------------|----------|
| 1  | 86845            | 2.50                 | 0.0045   |
| 2  | 86811            | 2.14                 | 0.0858   |
| 3  | 86881            | 2.39                 | 0.0018   |
| 4  | 86850            | 2.32                 | 0.0128   |
| 5  | 86854            | 2.71                 | 0.0767   |
| 6  | 86864            | 1.97                 | 0.2144   |
| 7  | 86991            | 2.66                 | 0.0515   |
| 8  | 86883            | 2.55                 | 0.0137   |
| 9  | 86866            | 2.60                 | 0.0279   |
| 10 | 86816            | 2.49                 | 0.0032   |

SUM Xi = 24.33 SUM(Xi-X)^2 = 0.4924

N = 10  
t (for 90%,n= 9) = 1.83

MEAN = X = SUM Xi / N = 2.433

STANDARD DEVIATION = S.D. =  
(SUM(Xi-X)^2 / (N-1))^.5 = 0.234

STANDARD ERROR  
OF THE MEAN (S.D.)/(N^.5) = 0.074

STANDARD ERROR  
OF THE S.D. = (S.D.)/(2N^.5) = 0.052

ALL FIRE =  
X + t (S.D./N^.5) + 3.09 ( S.D. + t S.D./(2N)^.5) = 3.587

NO FIRE =  
X - t (S.D./N^.5) - 3.09 ( S.D. + t S.D./(2N)^.5) = 1.279

## TABLE 2. DYNAMIC RAMP TEST

PART NO. :55-06018-2      LOT 13-37700      DATE: 1 FEB 1993

|    | CARTRIDGE<br>NO. | PEAK<br>CURRENT (Xi) | (Xi-X)^2 |
|----|------------------|----------------------|----------|
| 1  | 86845            | 2.50                 | 0.0057   |
| 2  | 86811            | 2.14                 | 0.0809   |
| 3  | 86881            | 2.39                 | 0.0012   |
| 4  | 86850            | 2.32                 | 0.0109   |
| 5  | 86854            | 2.71                 | 0.0815   |
| 6  | 86864            | 1.97                 | 0.2066   |
| 7  | 86991            | 2.66                 | 0.0555   |
| 8  | 86883            | 2.55                 | 0.0158   |
| 9  | 86866            | 2.60                 | 0.0308   |
| 10 | 86816            | 2.49                 | 0.0043   |
| 11 | 86826            | 2.50                 | 0.0057   |
| 12 | 86907            | 2.50                 | 0.0057   |
| 13 | 86815            | 2.35                 | 0.0056   |
| 14 | 86863            | 2.54                 | 0.0133   |
| 15 | 86888            | 2.02                 | 0.1636   |
| 16 | 86885            | 2.58                 | 0.0242   |
| 17 | 86814            | 2.05                 | 0.1403   |
| 18 | 86829            | 2.47                 | 0.0021   |
| 19 | 86956            | 2.65                 | 0.0509   |
| 20 | 86926            | 2.50                 | 0.0057   |

SUM Xi = 48.49      SUM(Xi-X)^2 = 0.9101

N = 20  
t (for 90%,n=19) = 1.725

MEAN =  $\bar{X} = \text{SUM Xi} / N = 2.425$

STANDARD DEVIATION = S.D. =  $(\text{SUM}(Xi-X)^2 / (N-1))^{.5} = 0.219$

STANDARD ERROR  
OF THE MEAN  $(S.D.)/(N^{.5}) = 0.049$

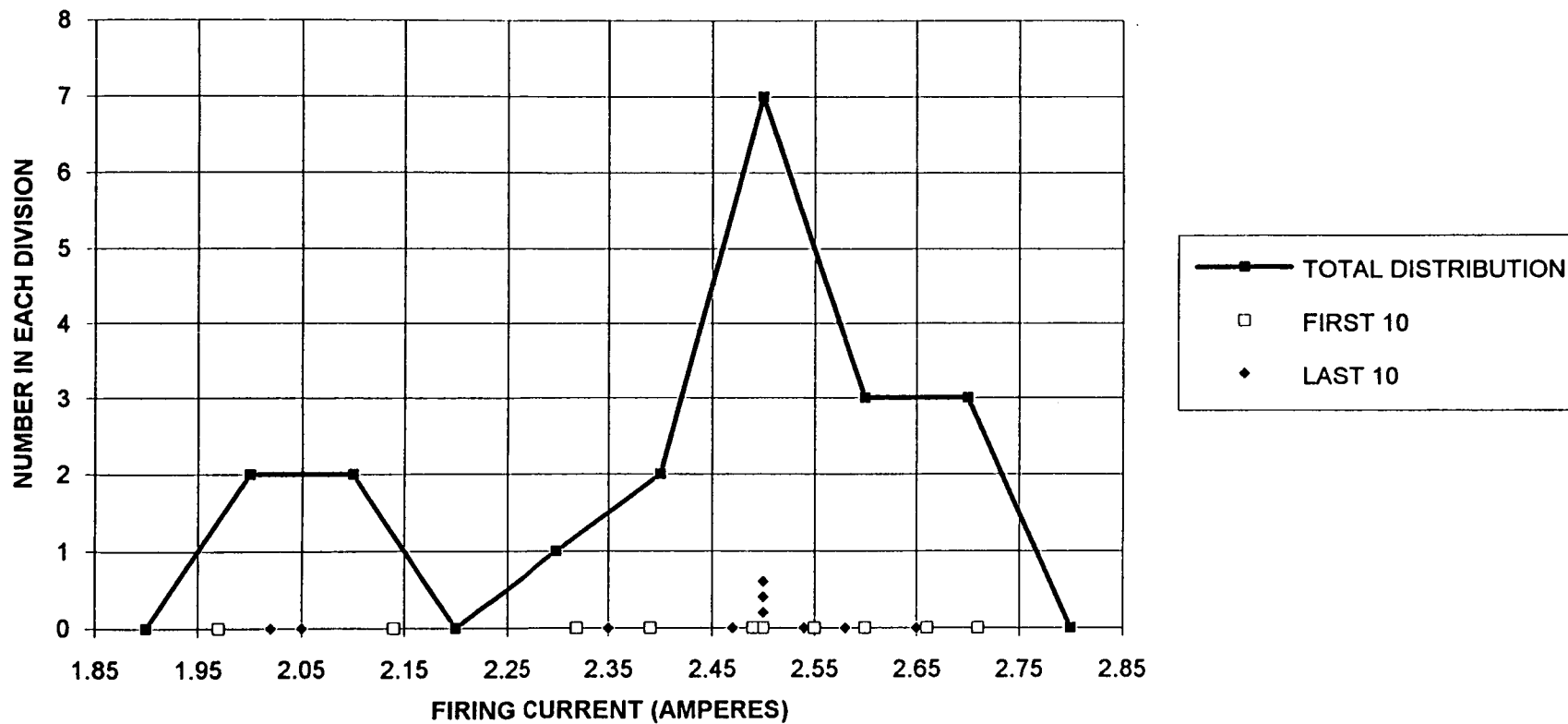
STANDARD ERROR  
OF THE S.D. =  $(S.D.)/(2N^{.5}) = 0.035$

ALL FIRE =  $\bar{X} + t (S.D./N^{.5}) + 3.09 (S.D. + t S.D. / (2N)^{.5}) = 3.370$

NO FIRE =  $\bar{X} - t (S.D./N^{.5}) - 3.09 (S.D. + t S.D. / (2N)^{.5}) = 1.479$

**FIGURE 1.    FIRING DISTRIBUTION**

55-06018-2   LOT 13-37700   1 FEB 1993



these firings. A deviation from a normal distribution does exist, but a larger set of data would be desirable before too much should be made of these details. The important point is made, the distribution function is obtainable by this test method.

#### **6.0 LIMITATIONS OF THE NEW METHOD**

There are only two limitations in using the dynamic ramp test method. The current ramp can be too slow or too fast.

If one were to use a very fast current ramp (possibly over 30 amperes per second), a thermal diffusivity effect might be observed. This effect is due to the amount of time it takes the heat energy generated in a bridgewire to distribute itself out to the ignition mix to ignite it. If during this time, the current in the bridgewire changes, the initiation current will appear to be slightly greater than that actually required. Because bridgewires are so small, and are made of metals that have relatively high thermal conductivity values, this time is very small.

This time can be estimated in other ways. The cartridges which we were testing normally fire in one millisecond when using twice their mean initiation current. Therefore, their time constant is about 3.5 milliseconds. Using a ramp rate of only 3.5 amperes per second, an error of about .01 amperes would

occur due to these diffusivity effects.

The other limit is being too slow. The slower the ramp rate, the greater could be the degradation of the ignition mix. With a ramp rate of 3.5 amperes per second, and all firings being at a value of less than 3.5 amperes, this means that all the units fired within one second of time. Very little degradation could be expected in conditioning times as short as one second.

#### **7.0 ADVANTAGES OF THE NEW METHOD**

Explosive cartridges are usually very expensive. In order to obtain reliability they must be made in large lots under controlled conditions, and a large percentage of the lot tested. The dynamic ramp test will directly reduce the number of cartridges required for testing. Even better than this, however, is a great increase in reliability. The dynamic ramp test will catch all cartridges that might be outside of the normal distribution. Bruceton and Probit type testing cannot produce data specific to a single cartridge, and therefore abnormal cartridges tested with these methods cannot make much, if any, change in the final results.

The real power of the dynamic ramp test is providing, for the very first time, the specific initiation current for individual cartridges. This data will now make it possible to actually confirm



the true current distribution of a lot.

## 8.0 CONCLUSION

If one has modern test equipment, there are no known reasons why one would not want to use the dynamic ramp test method. It brings the testing of explosive cartridges back to standard statistics.

Books have been written on the questionable assumptions and misuse of data from the Bruceton and Probit methods. All those questions disappear with the use of the dynamic ramp test. The applications of the Bruceton and Probit methods require special charts and calculations. The dynamic ramp test uses the same statistics that would be used in any other normal approach.

It is true that the dynamic ramp test is still a statistical test. The meaningfulness of the results will, as always, depend upon how well the test units reflect the distribution of the lot. If non-random or incomplete selections are made from a lot, the dynamic ramp test data will be faulty to the extent that this occurs. But, this is true for all statistics, and can be guarded against in the same way that all other statistical tests are handled.

This new method actually allows additional research. If at any time a set of cartridges are identified as being "out-of-family," having seen some unexpected exposure

or has some other observed anomaly, the dynamic ramp test, with very few test units, can quickly tell if those anomalies are causing any effect in their firing characteristics. For Bruceton or Probit testing, you might need 30 or 40 units before you could feel good as to whether a difference exists between two different groups.

Research into thermal diffusivity effects and into degradation effects could also be easily accomplished. These reasons make the dynamic ramp test an exciting approach to a problem that has existed for over thirty years. It will be a powerful and necessary approach if we are to remain competitive.

## 9.0 RECOMMENDATIONS

Government regulations requiring Bruceton or Probit testing of bridgewire type explosive cartridges should be modified to include, as a preference, the dynamic ramp testing approach. The dynamic ramp testing is a major improvement. It provides stronger, more direct statistical data for determining the mean and the deviation of the initiation current for bridgewire type explosive cartridges. In addition, the true distribution of the data is observable. For all previous testing methods, assumptions of the distributions were required and could never be actually confirmed. Therefore, all previous testing was always with some

uncertainty, especially where projections of several standard deviations were required.

The dynamic ramp test method allows the initiation current of individual cartridges to be measured. This greatly increases the research that can be done with explosive cartridges. The effects of any manufacturing variable or any environmental exposures can readily be assessed. Also, by taking the ramp rate to great extremes, the diffusivity effects and the degrading effects (if any) of any particular design can be quickly determined.

# APPENDIX A

CALCULATIONS (55-06018-2, Lot 13-37700)

| <u>Applied I</u> | <u>i</u> | <u>Fires</u> | <u>No-Fires</u> (N <sub>i</sub> ) | <u>i x N<sub>i</sub></u> | <u>i<sup>2</sup> x N<sub>i</sub></u> |
|------------------|----------|--------------|-----------------------------------|--------------------------|--------------------------------------|
| 2.6              | 3        | 1            | 0                                 | 0                        | 0                                    |
| 2.5              | 2        | 5            | 1                                 | 2                        | 4                                    |
| 2.4              | 1        | 3            | 4                                 | 4                        | 4                                    |
| 2.3              | 0        | 1            | 2                                 | 0                        | 0                                    |
|                  |          | <u>10</u>    | <u>N = 7</u>                      | <u>A = 6</u>             | <u>B = 8</u>                         |

Mean (X<sub>R</sub>)

$$\begin{aligned}
 X_R &= I_0 + \Delta I (A/N + 1/2) \\
 &= 2.3 + 0.1 (6/7 + 1/2) \\
 &= 2.44 \text{ amperes}
 \end{aligned}$$

Standard Deviation (σ<sub>R</sub>)

$$\begin{aligned}
 M &= \frac{N \times B - A^2}{N^2} \\
 &= \frac{7 \times 8 - 6^2}{7^2} \\
 &= 0.4082
 \end{aligned}$$

Therefore,

$$\begin{aligned}
 S &= 0.70 \text{ (from table)} \\
 \sigma_R &= S(\Delta I) \\
 &= (0.70) (0.1) \\
 &= 0.070
 \end{aligned}$$

Sampling Error (σ<sub>σ</sub>)

$$\begin{aligned}
 \sigma_\sigma &= \sigma_R H/N^{1/2} \text{ (H from table)} \\
 &= 0.07 (1.7)/7^{1/2} \\
 &= .045
 \end{aligned}$$

Sampling Error (σ<sub>X</sub>)

$$\begin{aligned}
 \sigma_X &= \sigma_R G/N^{1/2} \text{ (G from table)} \\
 &= 0.07 (1.3)/7^{1/2} \\
 &= 0.0344
 \end{aligned}$$

Confidence Intervals (single tail statistics)

$$Y \pm t\sigma_Y \text{ (t = 1.94 from table at 95\% level of confidence)}$$

1. For the mean:  $X_R \pm t\sigma_X$
2. For the standard deviation:  $\sigma_R \pm t\sigma_\sigma$

## APPENDIX A - Continued

No-Fire (0.999 reliability at 95% confidence)

$$(X_R - t\sigma_X) - 3.09 (\sigma_R + t\sigma_\sigma) \geq 1 \text{ ampere}$$

$$2.44 - 1.94 (0.0344) - 3.09 [0.07 + 1.94 (0.045)] \geq 1 \text{ ampere}$$

$$1.88 \geq 1 \text{ ampere}$$

All-Fire (0.999 reliability at 95% confidence)

$$(X_R + t\sigma_X) + 3.09 (\sigma_R + t\sigma_\sigma) \leq 3.5 \text{ amperes}$$

$$2.44 + 1.94 (0.0344) + 3.09 [0.07 + 1.94 (0.045)] \leq 3.5 \text{ amperes}$$

$$2.99 \leq 3.5 \text{ ampere}$$

516-28  
6996  
p. 14

DEVELOPMENT AND DEMONSTRATION  
OF AN  
NSI-DERIVED GAS GENERATING CARTRIDGE (NGGC)

by

Laurence J. Bement  
NASA Langley Research Center  
Hampton, Virginia

Morry L. Schimmel  
Schimmel Company  
St. Louis, Missouri

Harold Karp  
Hi-Shear Technology  
Torrance, California

Michael C. Magenot  
Universal Propulsion Co.  
Phoenix, Arizona

Presented at the 1994 NASA Pyrotechnic Systems Workshop  
February 8 and 9, 1994  
Sandia National Laboratories  
Albuquerque, New Mexico

# DEVELOPMENT AND DEMONSTRATION OF AN NSI-DERIVED GAS GENERATING CARTRIDGE (NGGC)

Laurence J. Bement  
NASA Langley Research Center  
Hampton, Virginia

Morry L. Schimmel  
Schimmel Company  
St. Louis, Missouri

Harold Karp  
Hi-Shear Technology  
Torrance, California

Michael C. Magenot  
Universal Propulsion Co.  
Phoenix, Arizona

## Abstract

*Following functional failures of a number of small pyrotechnically actuated devices, a need was recognized for an improved-output gas generating cartridge, as well as test methods to define performance. No cartridge was discovered within the space arena that had a larger output than the NASA Standard Initiator (NSI) with the same important features, such as electrical initiation reliability, safety designs, structural capabilities and size. Therefore, this program was initiated to develop and demonstrate an NSI-derived Gas Generating Cartridge (NGGC). The objectives of maintaining the important features of the NSI, while providing considerably more energy, were achieved. In addition, the test methods employed in this effort measured and quantified the energy delivered by the NGGC. This information will be useful in the application of the NGGC and the design of future pyrotechnically actuated mechanisms.*

## Introduction

Failures have occurred in several small pyrotechnically actuated devices, which attempted to use the NASA Standard Initiator (NSI) as the sole energy source. "Small pyrotechnically actuated devices" are defined here as those mechanisms that require 500 to 1000 inch-pounds input energy from a cartridge for reliable functioning. The NSI has been used extensively within the space community as both an initiator and a gas generating cartridge. The NSI, shown in figure 1 and described in reference 1, is an electrically initiated cartridge that contains a quantity of pyrotechnic material. The output produced by this material is heat, light, gas and burning particles, which can be used to ignite other materials and do work. An assessment was made of the problems encountered in the use of the NSI within the NASA. A survey was conducted to determine if a cartridge existed or needed to be developed to prevent these problems. A problem that was immediately recognized in this survey

was the lack of test methods to define performance of gas generating cartridges. Upon finding no cartridge that met the requirements set by this effort, an NSI-derived Gas Generating Cartridge (NGGC) was then developed. The approach for this development was to modify the NSI to produce more gas energy, to demonstrate its performance through baseline firing tests, and to demonstrate that it could meet the NSI environmental qualification requirements. This section has been divided into subsections to describe: (1) the failures that occurred with the NSI, and the lack of test methods, (2) the survey that was conducted to find candidate cartridges, (3) the objectives to develop and demonstrate an NGGC, and (4) the approach that was used to develop and demonstrate the NGGC.

## Failures and Lack of Test Methods

The failures that have occurred in critical cartridge-actuated mechanisms, such as pin pullers (ref. 2), separation nuts and explosive bolts, can be attributed not only to insuffi-

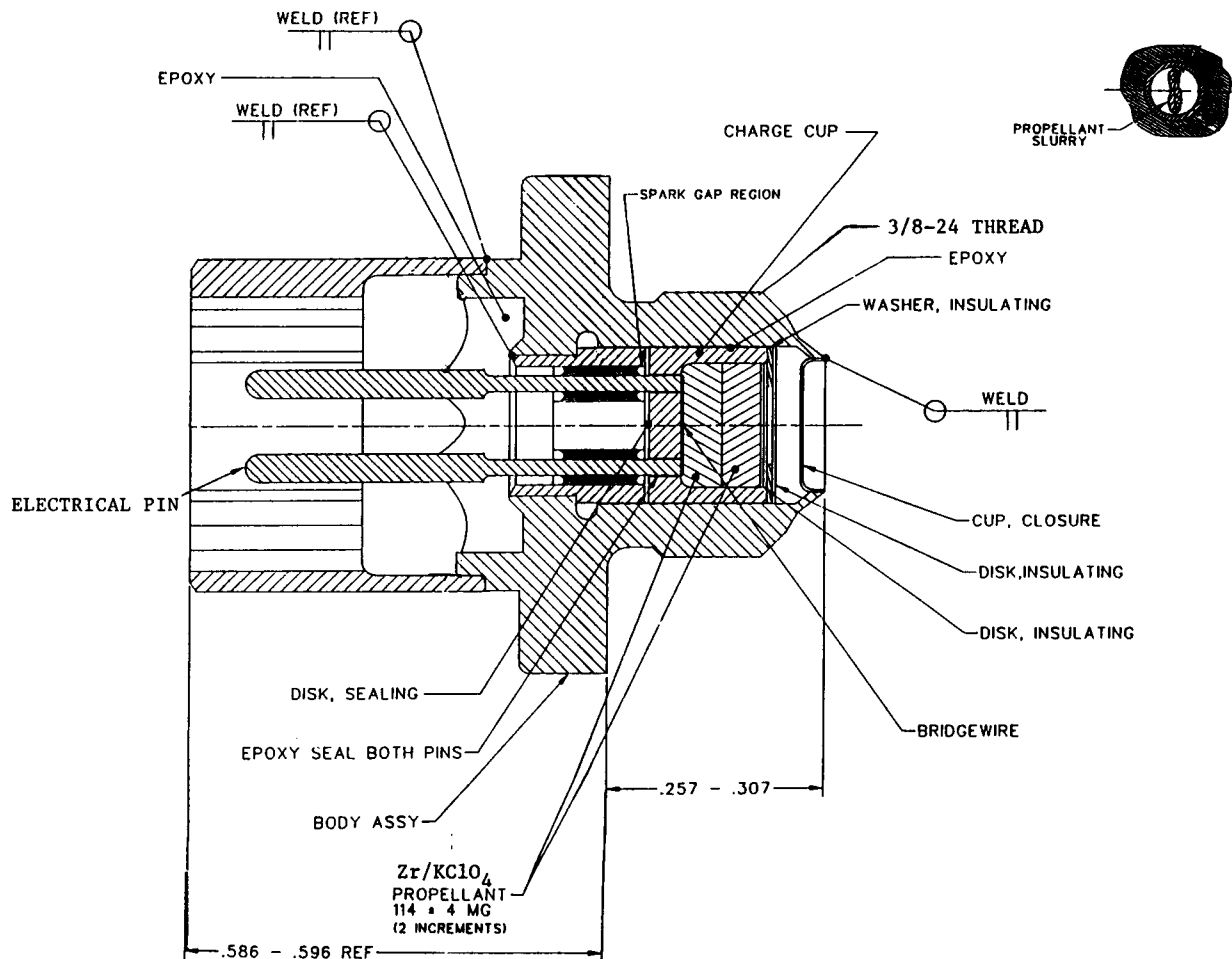


Figure 1. Cross sectional view of NASA Standard Initiator (NSI).

cient input energy, but also to a lack of understanding of pyrotechnic mechanisms and testing methods (ref. 3). The energy output of pyrotechnic gas generating cartridges is influenced by the conditions into which they are fired. For typical piston/cylinder configurations, these conditions are volume (shape and size), mass moved, resistance to motion (friction), and thermal absorptivity/reflectivity of the structure.

The only existing standard for measuring cartridge output performance in the field of pyrotechnics is the closed bomb, reference 4, which is inadequate for measuring energy delivered by cartridges. The closed bomb is a fixed volume into which the cartridge is fired. The pressure produced in the volume is monitored with pressure transducers and the data (pressure

versus time) are recorded. As described in reference 5, the closed bomb provides no quantitative information that can be related to work performed in an actual device.

The use of the NSI as a gas generating cartridge has both advantages and limitations. The advantages are: (1) it is accepted in the community with no additional environmental qualification required, (2) it has excellent safety features, 1-amp/1-watt no-fire, and electrostatic protection, (3) it has a demonstrated structural integrity and (4) it has a demonstrated reliability of electrical initiation and output as an igniter. The limitations are: (1) it was not designed for use as a gas generator, (2) the gas output produced is inconsistent in different manufacturing groups (ref. 2), and (3) it does not

provide sufficient work output for many small mechanisms. To overcome these problems, the NSI has been used with booster modules. These modules are sealed assemblies that contain additional pyrotechnic gas generating material and are installed into the structure of the mechanical device. This requires additional volume, mass and seals, as well as additional costs for development, demonstration, and qualification.

### **Survey of Gas Generating Cartridges**

A survey of literature and personnel within NASA and Air Force space centers was conducted, using the following criteria:

1. Provide the following important features that are the same as those in the NSI:
  - \* safety
  - \* reliability of electrical initiation
  - \* high-strength construction
  - \* small size
2. Output performance greater than that of the NSI
3. Long-term thermal/vacuum stability for space applications.

The survey revealed the following information. Some cartridges do not have the NSI safety features. None have the NSI demonstrated reliability. Several use the same pyrotechnic materials as the NSI. Several use gas generating materials that are not stable under thermal/vacuum conditions. None offer sufficient advantages for further evaluation.

Based on this information, a decision was made to develop a new, NSI-derived, Gas Generating Cartridge (NGGC).

### **Objectives for Development and Demonstration of the NGGC**

The objectives of this effort were to demonstrate the feasibility of designing/developing an NSI-derived Gas Generating Cartridge (NGGC) by:

1. Maintaining the important electrical initiation and structural reliability of the NSI
2. Providing significantly more energy than is provided by the NSI
3. Characterizing the work performance of the NSI and NGGC to assist in the design of pyrotechnically actuated devices, and

4. Maintaining the same environmental survivability as the NSI.

### **Approach Used for Development and Demonstration of the NGGC**

The approach for this effort was divided into designing/developing, demonstrating/characterizing and environmental survivability.

Figure 2 shows the design for the NGGC, which utilizes the NSI body and electrical interface. The electrical interface is defined as the electrical pins, bridgewire, bridgewire slurry mix and the initial load of 40 milligrams of NSI mix. The remaining volume within the NSI was filled with a thermal/vacuum-stable gas-generating mix, including the additional second load above the ceramic cup. A joint development was conducted with the two certified NSI manufacturers, Hi-Shear Technology and Universal Propulsion Company (UPCO).

The performance of the NGGC was established by measuring and recording input and output characteristics for comparison to the same measurements in other cartridges. That is, for input electrical ignition performance tests, a direct-current electrical circuit was used to apply input electrical currents in discrete steps, measuring the times from current application to bridgewire break and to first indication of pressure. The output performance of the NGGC was characterized with four test methods, the industry standard and three work-measuring devices: (1) The Closed Bomb is the industry standard, which involves firing the cartridge into a closed, fixed volume, measuring the pressure versus time in the volume, (2) The Energy Sensor, which involves firing the cartridge against a constant force, measuring energy as the distance stroked times the resistive force, (3) The Dynamic Test Device, which involves firing the cartridge to jettison a mass, determining energy by measuring velocity of the mass to calculate  $1/2mv^2$  and (4) The Pin Puller, which involves firing the cartridge to withdraw a pin for release of an interface, determining energy by measuring velocity of the pin to calculate  $1/2mv^2$ .

To demonstrate the environmental survivability of the NGGC, the input and output performances of as-received (untested) units were used as performance baselines for comparison to the performances achieved by units that were environmentally tested. Changes in functional performance would indicate a sensitivity to environments.



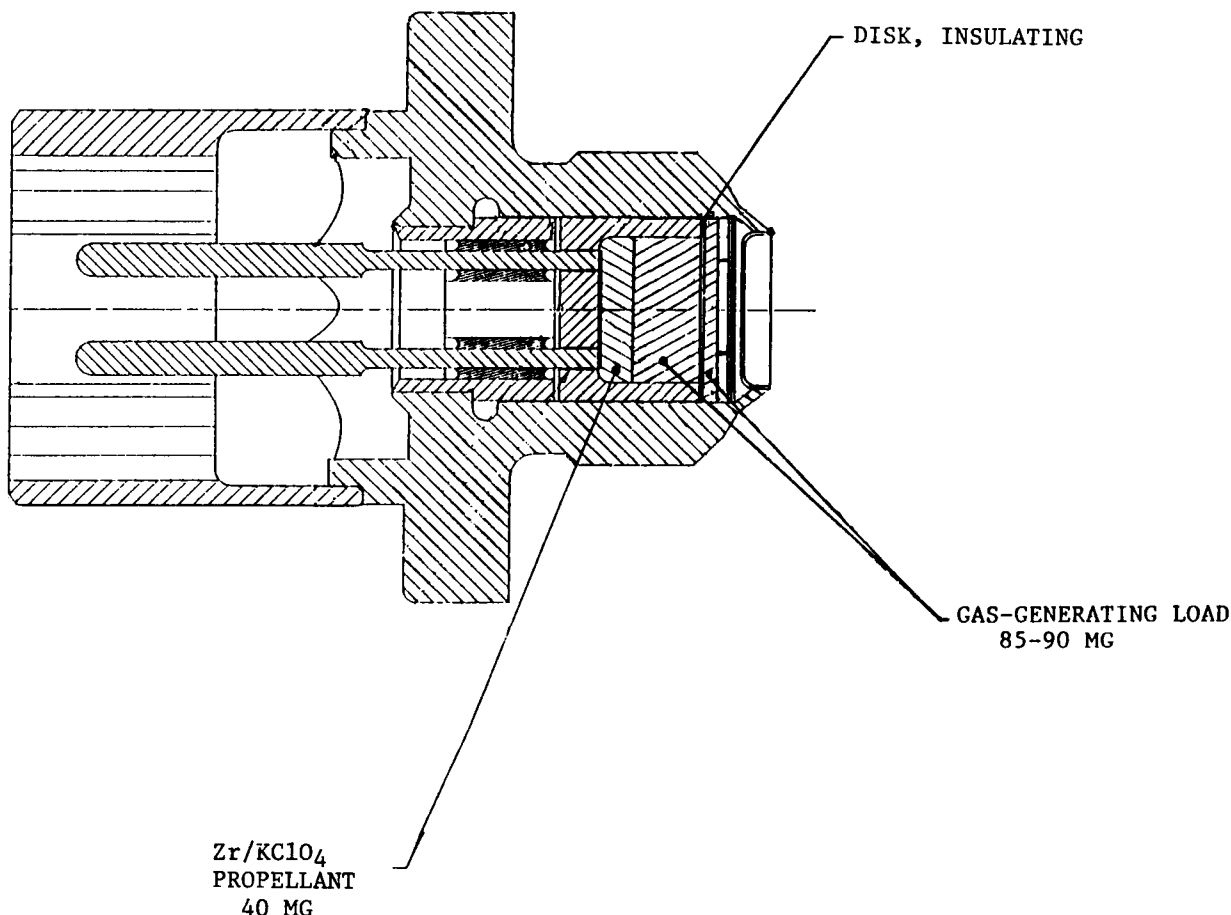


Figure 2. Cross sectional view of NASA Standard Gas Generator (NSGG), showing changes to NSI configuration.

### Cartridges Tested

Four cartridges were evaluated in this program, the NSI the Viking Standard Initiator (VSI), and two NGGC models, which were produced by different manufacturers.

#### NASA Standard Initiator (NSI)

The NSI units evaluated in this program were manufactured by Hi-Shear Technology. Hi-Shear Technology utilized the same  $\text{Zr/KClO}_4$  in both the NSI and their NGGC.

#### Viking Standard Initiator (VSI)

The VSI is functionally identical to the NSI and was manufactured by Hi-Shear Technology in 1972 for the Viking Program's lander on the surface of Mars. Since very few NSI units were available, the VSI functional performances were used to represent that produced by the NSI.

#### NSI-derived Gas Generating Cartridge (NGGC)

The NGGC units, manufactured by Hi-Shear Technology and UPCO, are the same as the NSI, except for the major changes shown in figure 2. The electrical interface from the bridgewire remained the same with the slurry mix, but the first press was 40 mg of  $\text{Zr/KClO}_4$  at 10,000 psi, instead of the 57 mg for the NSI. The gas generating materials were selected by each manufacturer, based on a demonstrated stability against elevated temperature and long-term vacuum environments. This material was pressed into and completely filled the charge cavity of the ceramic cup. An isomica insulating disc was bonded across the face of the cup to prevent an electrical path from the bridgewire through the pyrotechnic material to the cartridge case. A second increment of gas-generating material was pressed on top of the insulating disc to fill as much of the free volume as possible. The

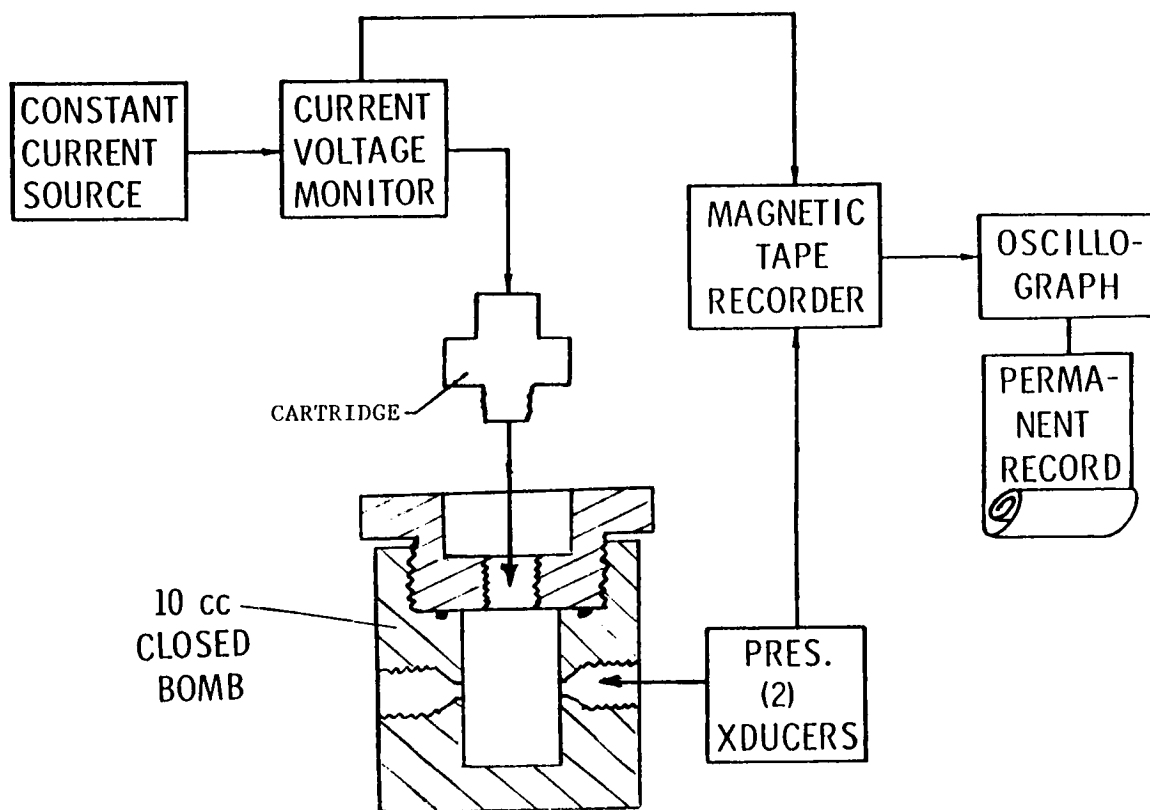


Figure 3. Cross sectional view of closed bomb and schematic of firing and monitoring system.

materials selected and the loading procedures used were the suppliers' choice and are considered proprietary. Hi-Shear Technology loaded 90 mg of gas generating material, while UPCO loaded 85, yielding a total pyrotechnic load of 130 and 125 mg respectively, as compared to the 114-mg load for the NSI. The same electrical and thermal insulation discs used at the output end of the NSI load were also installed on the NGGC.

### Test Apparatus and Methods

To characterize the input/output performance of the test cartridges, an Electrical Firing Circuit was used for input measurements, and four different test methods were used for output measurements. These output test methods were: the Closed Bomb, the Energy Sensor, the Dynamic Test Device, and the Pin Puller. All output test hardware was made of steel and was reusable.

#### Electrical Firing Circuit

A direct current firing circuit, shown schematically in figure 3 and described in reference 4,

was employed to measure the electrical ignition characteristics (function times) of cartridges tested. Long-duration, square-wave electrical pulses were applied at levels of 20, 15, 10, 5 and 3 amperes. The input current and the pressure produced by the cartridges in the various output test methods were recorded on an FM magnetic tape recorder with a frequency response that was flat to 80 KHz. Electrical initiation function times were measured from application of current to bridgewire break and from application of current to first indication of pressure from the cartridge.

#### Closed Bomb

The closed bomb, shown in figure 3 and described in references 3 and 4, is the industry standard for measuring the output of cartridges. The cartridge is fired into a fixed, 10-cc cylindrical volume, and the pressure produced is measured with the pressure transducers, recorded on the FM tape recorder. The data collected are the peak pressure and the time to peak pressure. This approach has limitations, as described

in reference 5, in trying to relate the pressure produced to a mechanical or ignition function. For example, the NSI performance requirement in reference 1 is 650 +/- 125 psi peak pressure, achieved within 5 milliseconds at direct-current inputs of five amperes or greater. These data provide no quantitative information that can be related to work performed in an actual device.

### Energy Sensor

The Energy Sensor, shown in figure 4 and described in references 4 and 5, represents an application where the cartridge output works against a constant resistive force. This resistive force is provided by precalibrated, crushable aluminum honeycomb. The strength of the honeycomb selected for this study was 500 pounds force. The cartridge is fired on the axis of a piston/cylinder as shown. The amount of work accomplished is obtained by multiplying the length of honeycomb crushed during the firing by the honeycomb's crush strength to yield an energy value in inch-pounds.

### Dynamic Test Device

The Dynamic Test Device, shown in figure 5 and described in references 4 and 5, represents the jettisoning of a mass. A one-inch diameter, one-pound, cylindrical mass is jettisoned through a one-inch stroke, when the o-ring clears the cylinder. The velocity of the mass is measured electronically by a grounded needle on the mass successively contacting spaced, charged foils to trigger electronic pulses. These pulses were recorded on a magnetic tape recorder to measure the time interval between contact of the needle with the foils. Velocity was calculated by dividing the spacing distance (0.250 inch) by the time interval. The energy of the mass was calculated as  $1/2 mv^2$ , where  $m$  is the total mass of the 1-pound mass and the needle. The pressure in the working volume was measured by a pressure transducer installed in the port as shown, and was recorded on the same magnetic tape recorder. The data collected were the energies delivered in inch-pounds and the peak pressures achieved.

### Pin Puller

The Pin Puller, shown in figure 6 and described in reference 3, represents a pyrotechnic function with a low-mass retractor. It also presents a tortuous flow path of gases from the cartridge to

the working piston. The cartridge's output gas, generated 90° from the working axis of the piston/pin, must vent through a 0.1-inch diameter orifice into the working volume. Energy was obtained and calculated by measuring the velocity of the piston/pin, as described for the Dynamic Test Device. Pressure in the working volume was measured by a transducer installed in the second port, as shown. The data collected were the energies delivered in inch-pounds and the peak pressures achieved.

### Test Procedure

The testing effort was divided into three major areas, as summarized in table I. This table shows the number of units fired in each test, as well as

Table I. Allocation of Cartridge Test Units  
Performance Baseline Firings

| Test condition      | VSI | NSI | NGGC     |      |
|---------------------|-----|-----|----------|------|
|                     |     |     | Hi-Shear | UPCO |
| Closed bomb         | 13  | 3   | 6        | 5    |
| Energy sensor       | 5   |     | 5        | 5    |
| Dynamic test device | 8   | 3   | 7        | 5    |
| Pin puller          | 5   |     | 7        | 5    |
| Total               | 31  | 6   | 25       | 20   |

### Environmental Testing

|         | Temp. cycling | Mech. vibr. | Mech. shock | Thermal shock | NGGC     |      |
|---------|---------------|-------------|-------------|---------------|----------|------|
|         |               |             |             |               | Hi-Shear | UPCO |
| Group 1 |               |             |             |               | 16       | 12   |
| Group 2 |               | 2           |             |               | 16       | 12   |
| Group 3 |               | 3           | 3           |               | 16       | 12   |
| Group 4 |               | 4           | 4           | 4             | 16       | 13   |
|         |               |             |             | Total         | 64       | 49   |

The units were visually, electrically and x-ray inspected before and after exposure to each environment.

### Post-Environment Firings

| Test condition      | NGGC     |      |
|---------------------|----------|------|
|                     | Hi-Shear | UPCO |
| Closed bomb         | 16       | 12   |
| Energy sensor       | 16       | 12   |
| Dynamic test device | 16       | 12   |
| Pin puller          | 16       | 13   |
| Total               | 64       | 49   |

Units from the environmentally exposed groups were equally subdivided into each functional test group.

|                        |    |    |
|------------------------|----|----|
| Total NGGC test units: | 89 | 69 |
|------------------------|----|----|

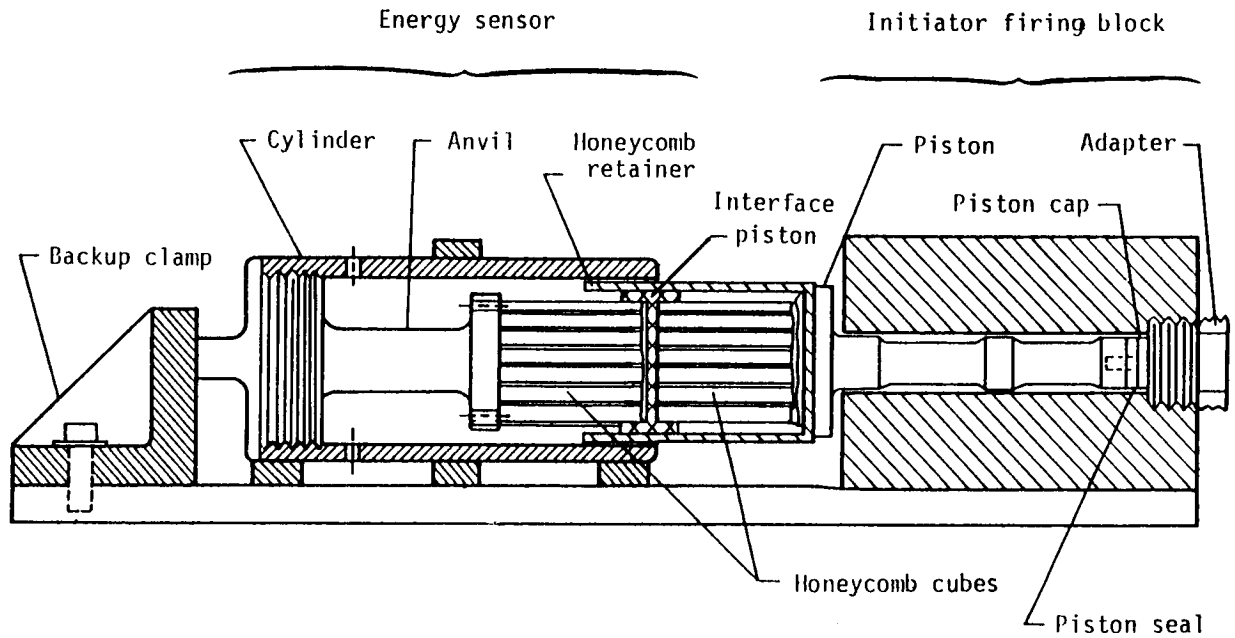


Figure 4. Cross sectional view of McDonnell Energy Sensor.

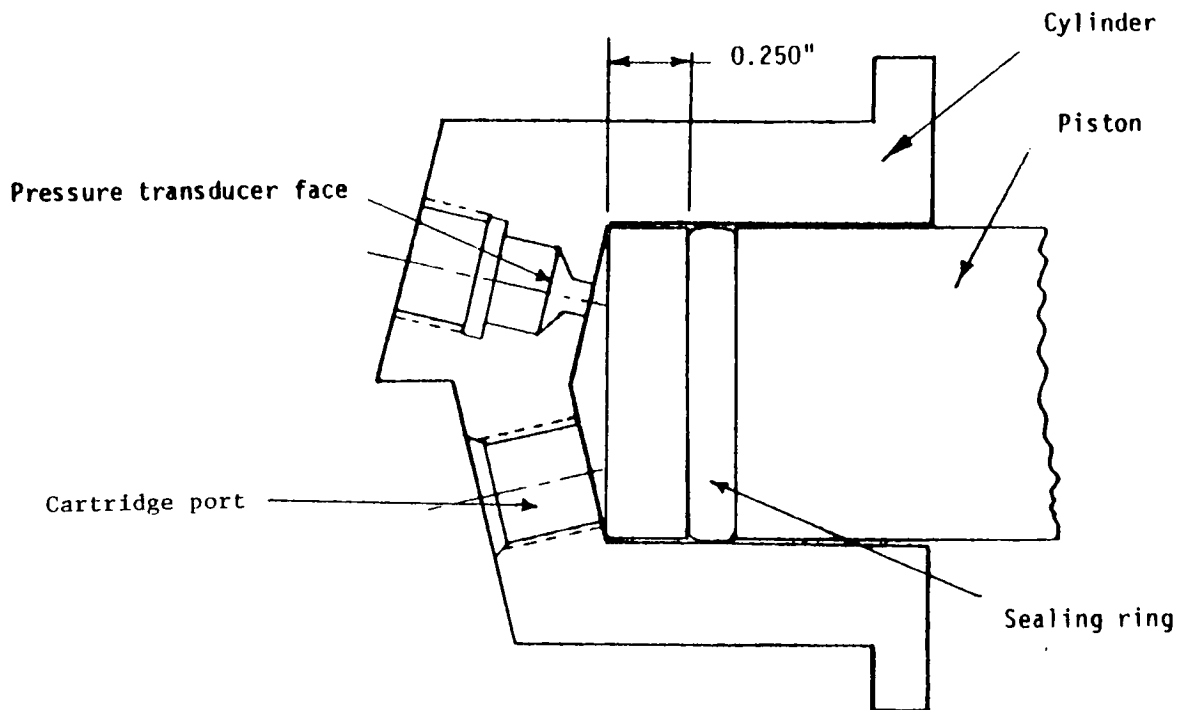


Figure 5. Cross sectional view of Dynamic Test Device.

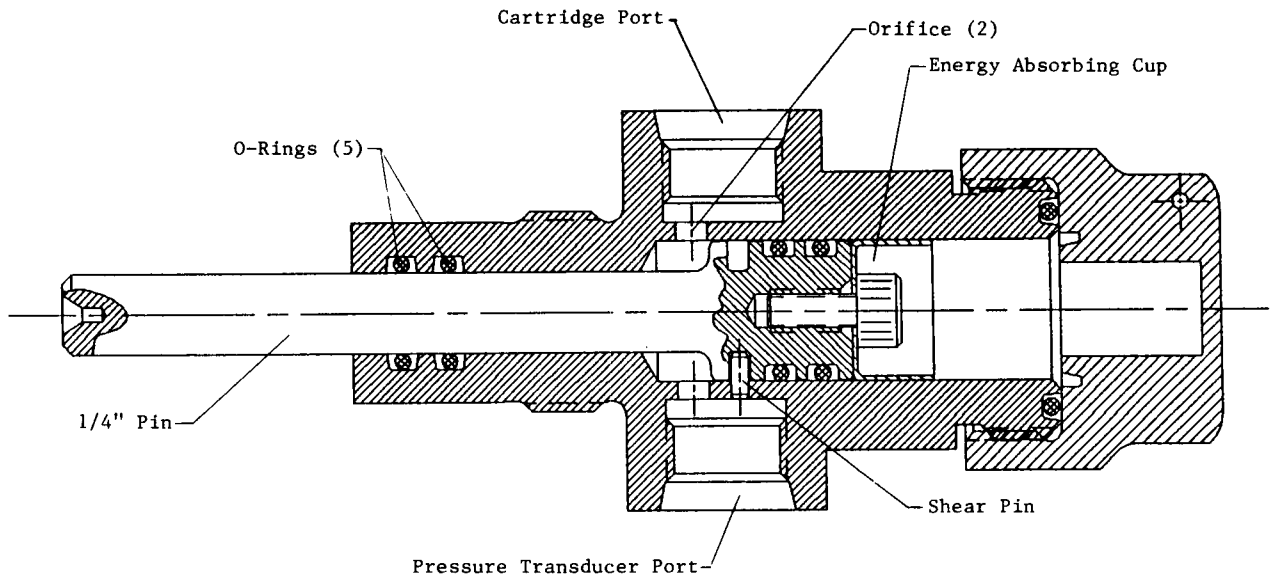


Figure 6. Cross sectional view of NASA Pin Puller.

the number of units subjected to the various environments. The Electrical Firing Circuit was used to collect input electrical ignition characteristics (function time) data for all units (except the NSI) that were fired in the Performance Baseline and in the Post-Environment tests. Electrical inspections were accomplished on all units at the start of the program with 50-volt bridge-to-case and 10 milliamperes bridgewire resistance measurements.

### Performance Baseline Firings

The performance baseline firings were conducted with as-received cartridges to provide a functional reference for comparisons among all cartridge types and to compare with post-environmental performance of the NGGC. Performance data included input electrical ignition and the four output measurements. The Electrical Firing System was used as the input firing source for all cartridges, except the NSI. (NSI firings were conducted prior to the use of the Electrical Firing System). The cartridges were subdivided as equally as possible for firings at current levels of 20, 15, 10, 5 and 3 amperes. As an example of output test firings described in table I, the Closed Bomb was used for 13 VSI, 3 NSI, 6 Hi-Shear Technology NGGC, and 5 UPCO NGGC units. Due to their scarcity, no NSI units were functioned in the Energy Sensor or Pin Puller. VSI units were used to supplement the data collected on the NSI, since

their design and performance were essentially the same.

### Environmental Testing

Environmental tests, duplicating the qualification levels and test order required for the NSI, were conducted on the NGGC. The NGGC units from each source were divided into four groups for testing as shown in table I. Thermal stabilization in these tests was established by thermocouples attached to several cartridges; once the desired temperature level was indicated by the thermocouples, the units were soaked for at least 15 minutes before the environmental tests began. The units were visually, electrically and x-ray inspected before and after each environment. Electrical inspection was accomplished with 50-volt bridge-to-case and 10 milliamperes bridgewire resistance measurements.

The definition of each environmental test follows:

**Temperature cycling.** The units were placed in a wire basket for transfer between chambers that were stabilized at  $-260$  and  $+300^{\circ}\text{F}$ . The following describes one of twenty cycles conducted:

1. Insert units into  $-260^{\circ}\text{F}$  chamber, and once stabilized, maintain that temperature for one hour
2. Transfer units to  $+300^{\circ}\text{F}$ , and once stabilized, maintain that temperature for one-half hour

2. Transfer units to +300°F, and once stabilized, maintain that temperature for one-half hour

**Mechanical vibration.** The units were mounted into test blocks in a thermal chamber for vibration tests on all three axes. Two series of tests were conducted at +300 and -260°F. The units were conditioned at each temperature and the following spectrum, which produced an overall G rms value of 27.5, was applied for 7.5 minutes in each axis:

| Frequency (Hz) | Level (G/Hz)                    |
|----------------|---------------------------------|
| 10 - 100       | 0.01 to 0.8 (6 db/oct increase) |
| 100 - 400      | 0.8 constant                    |
| 400 - 2000     | 0.8 to 0.16 (3 db/oct decrease) |

**Mechanical shock.** The units were mounted in the same test blocks used for the vibration tests. The units were subjected to +/− pulses on each axis to the following trailing edge sawtooth pulse: 100 G peak with an 11 ms rise and a 1 ms decay. Tests were conducted at laboratory ambient conditions.

**Thermal shock.** The units were placed in a wire basket and immersed in a container of liquid nitrogen and allowed to stabilize (no bubbles). The units were then removed from the nitrogen and allowed to stabilize at room temperature with no protection from water condensate. The units were subjected to this process for five cycles, except during the fifth cycle, following stabilization, the units were held in the liquid nitrogen for 11 hours.

### Post-Environment Firings

Following the environmental exposures, the NGGC units were subdivided equally and fired with the electrical firing circuit using the four test methods. That is, four units of the 16 environmentally tested in Group 1 were fired in each test method. The data collected were compared to the performance baseline.

### Results

The results of the tests are presented in the same format as the Test Procedure section.

### Performance Baseline Firings

The data collected for the functional performance baselines (input electrical function time and output tests) for each cartridge are summarized in

the top portions of tables II through VI and figures 7 through 10.

Table II. Electrical Ignition Performance Data on Cartridges

(Average/Standard Deviation)

| Cartridge                              | Current applied amperes | No. fired | Time to BW break, ms | Time to first press, ms |
|--|-------------------------|-----------|----------------------|-------------------------|
| Performance baseline (no environments) |                         |           |                      |                         |
| VSI                                    | 20                      | 6         | .124/.005            | .158/.014               |
|  | 15                      | 3         | .182/.007            | .215/.013               |
|  | 10                      | 2         | .354                 | .389                    |
|  | 5                       | 1         | 1.431                | 1.480                   |
|  | 3                       | 1         | 121.020              | 121.060                 |
| Hi-Shear NGGC                          | 20                      | 1         | .120                 | .175                    |
|  | 15                      | 1         | .190                 | -                       |
|  | 10                      | 1         | .335                 | .362                    |
|  | 5                       | 1         | 1.350                | 1.370                   |
|  | 3                       | 1         | 12.400               | 12.425                  |
| UPCO NGGC                              | 20                      | 3         | .130/.030            | -                       |
|  | 15                      | 1         | .160                 | .225                    |
|  | 10                      | 2         | .324                 | .373                    |
|  | 5                       | 3         | 1.295/.018           | 1.298/.020              |
|  | 3                       | 2         | 8.355                | 8.373                   |
| Post environments                      |                         |           |                      |                         |
| Hi-Shear NGGC                          | 20                      | 16        | .135/.012            | .187/.025               |
|  | 15                      | 12        | .184/.020            | .224/.029               |
|  | 10                      | 12        | .329/.044            | .443/.199               |
|  | 5                       | 12        | 1.245/.050           | 1.274/.063              |
|  | 3                       | 12        | 10.653/5.452         | 11.315/5.789            |
| UPCO NGGC                              | 20                      | 12        | .121/.013            | .792/.663               |
|  | 15                      | 12        | .176/.012            | .639/.481               |
|  | 10                      | 10        | .348/.045            | .739/.441               |
|  | 5                       | 8         | 1.238/.100           | 1.327/.145              |
|  | 3                       | 8         | 7.641/4.015          | 7.353/3.746             |

Table III. Closed Bomb Performance Data on Test Cartridges

(Average/Standard Deviation)

| Cartridge                              | No. fired | Time to peak pressure, ms | Peak pressure, psi |
|--|-----------|---------------------------|--------------------|
| Performance baseline (no environments) |           |                           |                    |
| VSI                                    | 13        | .09/.05                   | 675/81             |
| NSI                                    | 3         | .23/.06                   | 660/53             |
| Hi-Shear NGGC                          | 6         | 1.15/.34                  | 1083/41            |
| UPCO NGGC                              | 5         | .48/.13                   | 1120/58            |
| Post environments                      |           |                           |                    |
| Hi-Shear NGGC                          | 16        | 1.11/.30                  | 1076/25            |
| UPCO NGGC                              | 12        | .28/.07                   | 1250/47            |

Table IV. Energy Sensor Performance Data on Test Cartridges  
(Average/Standard Deviation)

| Cartridge                             | No. fired | Energy delivered, inch-pounds |
|---------------------------------------|-----------|-------------------------------|
| Performance baseline (no environment) |           |                               |
| VSI                                   | 5         | 466/21                        |
| Hi-Shear NGGC                         | 5         | 815/99                        |
| UPCO NGGC                             | 5         | 812/90                        |
| Post environments                     |           |                               |
| Hi-Shear NGGC                         | 16        | 869/80                        |
| UPCO NGGC                             | 12        | 927/58                        |

Table V. Dynamic Test Device Performance Data on Test Cartridges  
(Average/Standard Deviation)

| Cartridge                             | No. fired | Energy delivered, inch-pounds | Peak pressure, psi |
|---------------------------------------|-----------|-------------------------------|--------------------|
| Performance baseline (no environment) |           |                               |                    |
| VSI                                   | 8         | 337/64                        | 5580/940           |
| NSI                                   | 3         | 351/15                        | 5540/755           |
| Hi-Shear NGGC                         | 7         | 785/66                        | 4983/993           |
| UPCO NGGC                             | 5         | 756/74                        | 9408/2002          |
| Post environments                     |           |                               |                    |
| Hi-Shear NGGC                         | 16        | 667/45                        | 6953/1866          |
| UPCO NGGC                             | 12        | 777/50                        | 8337/1980          |

Table VI. Pin Puller Performance Data on Test Cartridges  
(Average/Standard Deviation)

| Cartridge                             | No. fired | Energy delivered, inch-pounds | Peak pressure, psi |
|---------------------------------------|-----------|-------------------------------|--------------------|
| Performance baseline (no environment) |           |                               |                    |
| VSI                                   | 5         | 154/20                        | 7056/143           |
| Hi-Shear NGGC                         | 7         | 450/36                        | 12313/797          |
| UPCO NGGC                             | 5         | 526/39                        | 16392/1514         |
| Post environments                     |           |                               |                    |
| Hi-Shear NGGC                         | 16        | 462/21                        | 11720/440          |
| UPCO NGGC                             | 13        | 514/17                        | 15532/680          |

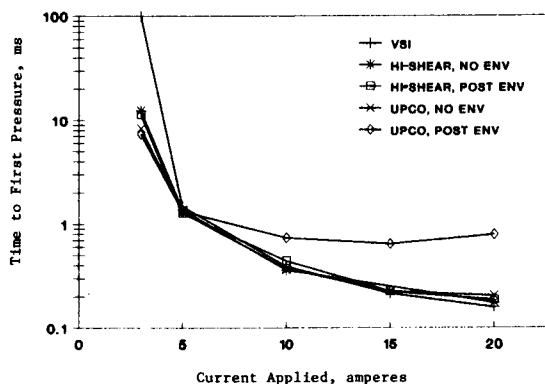
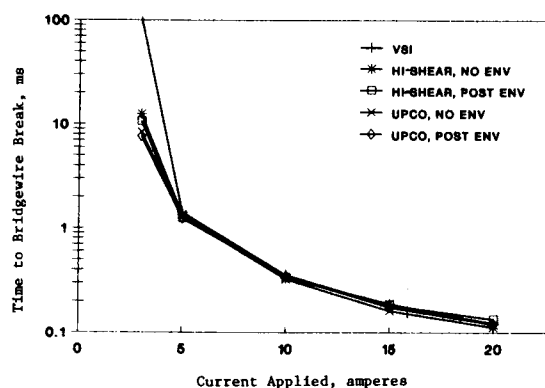


Figure 7. Plots of current applied versus time to bridge-wire break (top) and to first pressure (bottom).

**Electrical ignition performance.** The electrical ignition performance baselines (no environments) for the VSI and NGGC are shown in table II and figure 7. As mentioned earlier, no NSI data were collected. Each of the data points on the plots is the averaged value of the function times for each cartridge type at each current level. Very little difference in performance could be detected among any of the cartridge groups.

**Closed bomb.** The closed bomb performance baseline data are shown in table III. Typical traces for each cartridge type are shown in figure 8. The times to peak pressure for the VSI and NSI are smallest. The average time to peak pressure for the Hi-Shear Technology NGGC is considerably longer than for the UPCO units (1.15 versus 0.48 ms). The NGGC peak pressures achieved are comparable (1083 and 1120 psi).

**Energy sensor.** The Energy Sensor performance baseline data are shown in table IV. The

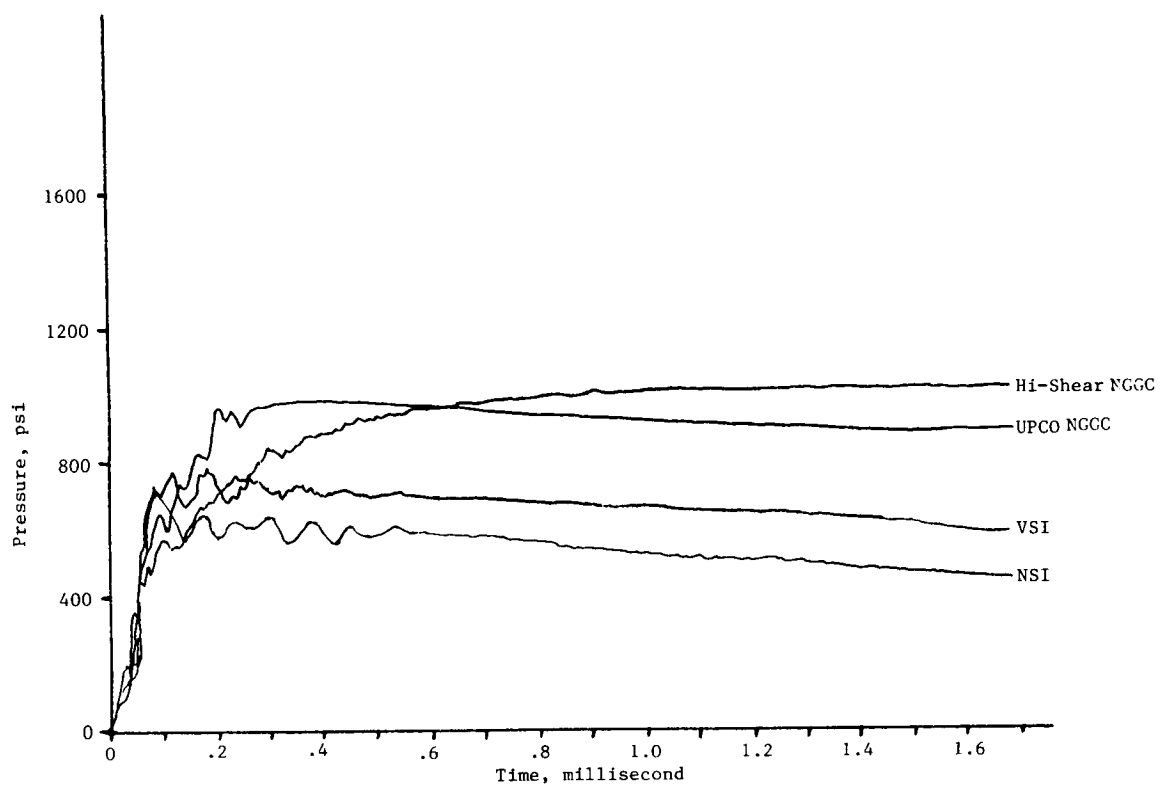


Figure 8. Typical pressure traces produced by the NSI, VSI and UPCO, and Hi-Shear NGGC in the closed bomb.

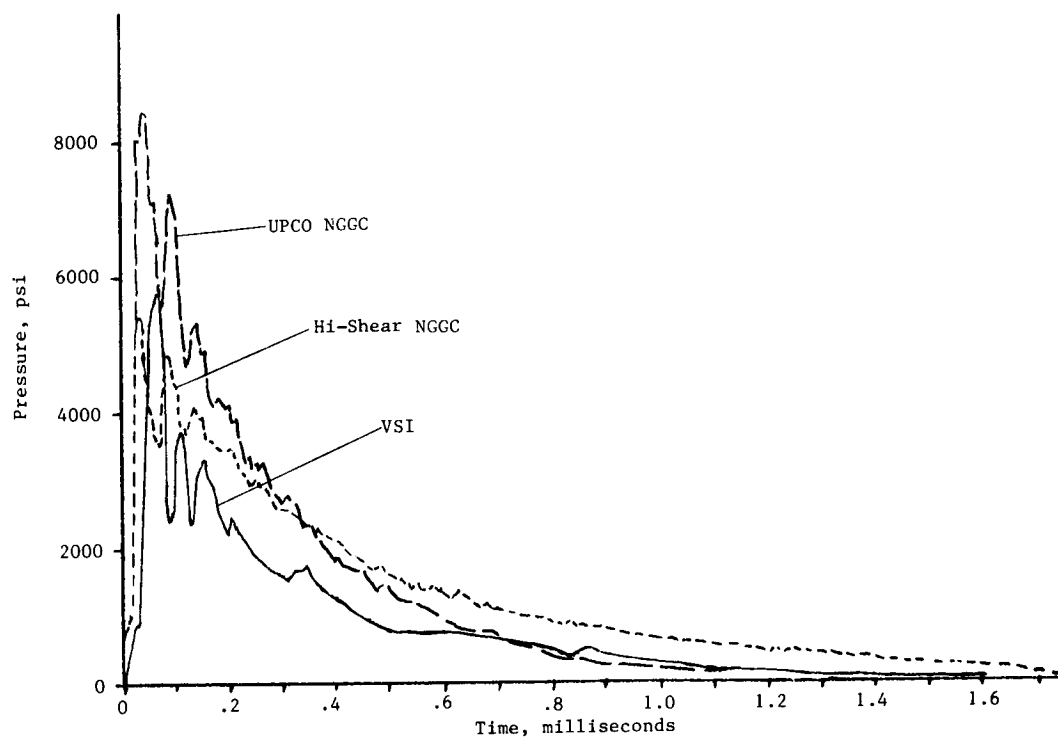


Figure 9. Typical pressure traces produced by the VSI and Hi-Shear and UPCO NGGC in the dynamic test device.



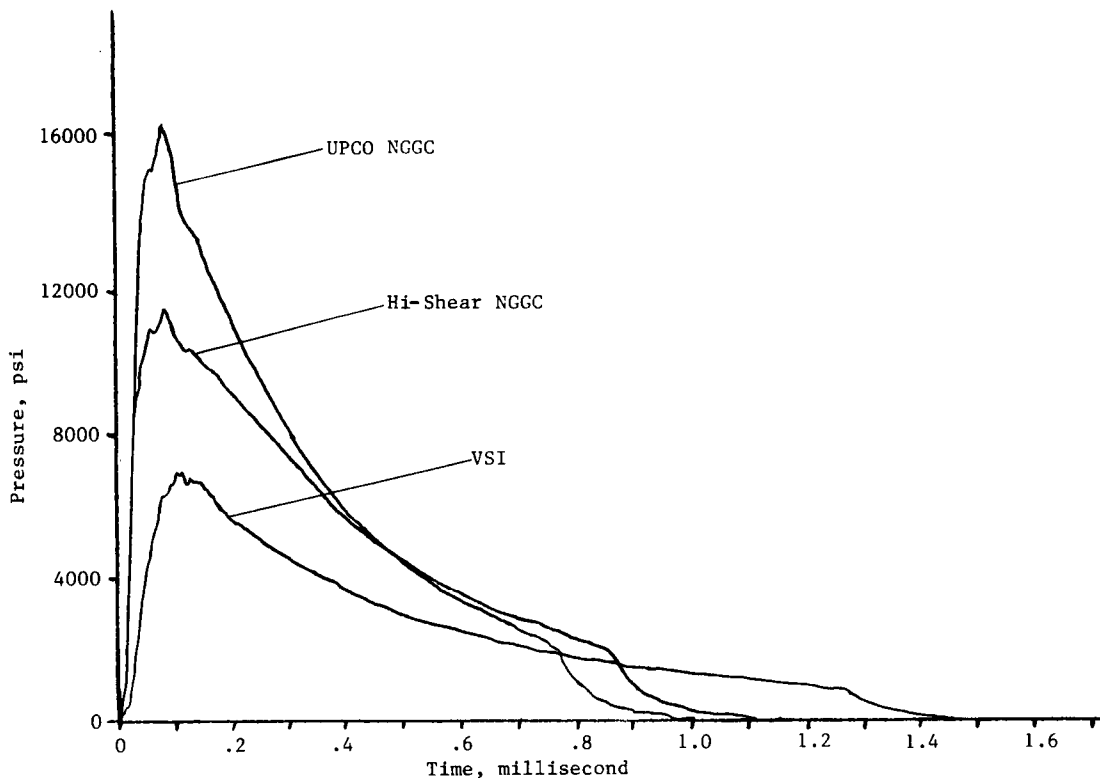


Figure 10. Typical pressure traces produced by the VSI and Hi-Shear and UPCO NGGC in the pin puller.

NGGC performances are comparable (815 and 812 inch-pounds) and nearly twice that of the VSI (466 inch-pounds).

**Dynamic test device.** The Dynamic Test Device performance baseline data are shown in table V. The performance of the VSI and NSI are comparable (337 and 351 inch-pounds), as are the two NGGC models to each other (785 and 756 inch-pounds). The NGGC performance is over twice that of the VSI and NSI. Figure 9 shows typical pressure traces from each cartridge type. The peak pressure for the UPCO NGGC is appreciably higher and more dynamic than the Hi-Shear Technology units.

**Pin puller.** The Pin Puller baseline data are shown in table VI. The performance of the NGGC models (450 and 526 inch-pounds) are three times that produced by the VSI (154 inch-pounds). Figure 10 shows distinctively different pressure traces from each cartridge type.

### Environmental Testing

The environmental testing was completed with no evidence of physical damage through visual, x-ray and electrical inspections.

### Post-Environment Firings

The data collected for the post-environment functional performance tests (input electrical function time and output tests) for each cartridge are summarized in the lower portions of tables II through VI.

**Electrical ignition performance.** The electrical ignition data are shown in table II and figure 7. The only change between pre- and post-environment performance was a small increase in times to first indication of pressure in the UPCO NGGC units. All values were within the 5 millisecond delay times at 5 amperes or greater, allowed by the NSI specification, reference 3.

**Closed bomb performance.** The data following environmental exposure are shown in table III. No appreciable change in performance was observed.

**Energy sensor.** The Energy Sensor baseline data are shown in table IV. The apparent increase in energy delivered (54 and 115 inch-pounds) by the NGGC models following environmental exposures is insignificant, considering

the standard deviations of the pre- and post-environments data. These standard deviations total 179 and 148 inch-pounds for the respective NGGC models, which could include this range of data.

**Dynamic test device.** The Dynamic Test Device data are shown in table V. No significant change in performance was observed following environments, again considering the standard deviations.

**Pin puller.** The Pin Puller data are shown in table VI. No change was detected following environments.

## Conclusions

All objectives of this effort were met, which should allow for immediate consideration for the application of the NGGC. The NGGC was manufactured using the same body and electrical interface as the NSI. The electrical initiation characteristics are the same as the NSI. A slight delay was observed in the time to first pressure for the UPCO NGGC following environmental exposures. This delay, caused by a decrease in thermal transfer from the bridgewire, is acceptable, since it is well within the NSI performance specification. The cartridge functional evaluations used in this effort clearly show that output working energy is affected by the configuration in which it is used. The Energy Sensor and Dynamic Test Device measured the most energy delivered by the NGGC, about 800 inch-pounds, while the Pin Puller was much less efficient, delivering only about 500 inch-pounds. Although the two NGGC manufacturers selected different thermal/vacuum-stable gas generating materials, as evidenced by the different pressure traces observed, the output performance of the two models was essentially the same in each of the four test methods. Under the assumption that the NSI produces the same output performance as the VSI, the NGGC produces approximately twice the output of the NSI/VSI in the Energy Sensor and the Dynamic Test Device, and three times that of the NSI/VSI in the Pin Puller. No significant change in output performance was observed following exposure of the NGGC to the rigorous thermal/mechanical environmental requirements for the NSI.

A work-producing cartridge has been developed with the key attributes of the NSI. Designers

of pyrotechnic mechanisms now have a cartridge that is defined in terms of work, and they can relate the test configurations and energy deliveries documented in this report to their design requirements. This cartridge performance can meet the requirements of a substantial portion of small aerospace pyrotechnic devices (including many applications where the NSI with booster modules are now employed), such as pin pullers, nuts, valves and cutters.

A word of caution is warranted. The successful completion of this developmental effort does not "qualify" the NGGC for any application. Users must conduct a developmental effort, including demonstrating functional margins, environmental qualification, and system integration/operation demonstrations for devices in which the NGGC is to be used.

The acquisition of the NGGC should be based on performance, as measured by at least one of the energy measuring devices described in this report, the Energy Sensor, the Dynamic Test Device or the Pin Puller.

## References

1. Design and Performance Specification for NSI-1 (NASA Standard Initiator-1), SKB26100066, January 3, 1990.
2. Bement, Laurence J. and Schimmel, Morry L.: "Determination of Pyrotechnic Functional Margin." Presented at the 1991 SAFE Symposium, November 11-14, 1991, Las Vegas, Nevada. Also presented at the First NASA Aerospace Pyrotechnic Systems Workshop, June 9-10, 1992, NASA Lyndon B. Johnson Space Center, Houston, TX.
3. Bement, Laurence J.: "Pyrotechnic System Failures: Causes and Prevention." NASA TM 100633, June 1988.
4. Bement, Laurence J.: "Monitoring of Explosive/Pyrotechnic Performance." Presented at the Seventh Symposium on Explosives and Pyrotechnics, Philadelphia, Pennsylvania, September 8-9, 1971.
5. Bement, Laurence J. and Schimmel, Morry L.: "Cartridge Output Testing: Methods to Overcome Closed-Bomb Shortcomings." Presented at the 1990 SAFE Symposium, San Antonio, Texas, December 11-13, 1990.

517-18  
6997  
P- 2

## DEVELOPMENT OF THE TOGGLE DEPLOYMENT MECHANISM

Christopher W. Brown  
NASA Lyndon B. Johnson Space Center, Houston, Tx

### Abstract

The Toggle Deployment Mechanism (TDM) is a two fault tolerant, single point, low shock pyro/mechanical releasing device. Many forms of releasing are single fault tolerant and involve breaking of primary structure. Other releasing mechanisms, that do not break primary structure, are only pyrotechnically redundant and not mechanically redundant. The TDM contains 3 independent pyro actuators, and only one of the 3 is required for release.

The 2 separating members in the TDM are held together by a toggle that is a cylindrical stem with a larger diameter spherical shape on the top and flares out in a conical shape on the bottom. The spherical end of the toggle sits in a socket with the top assembly and the bottom is held down by 3 pins or hooks equally spaced around the conical shaped end.

Each of the TDM's 3 independent actuators shares a third of the separating load and does not require as much pyrotechnic energy as many single fault tolerant actuators. Other single separating actuators, i.e., separating nuts or pin pullers, have the pyrotechnic energy releasing the entire preload holding the separating members together.

Two types of TDM's, described in this paper, release the toggle with pin pullers, and the third TDM releases the toggle with hooks. Each design has different advantages and disadvantages. This paper describes

the TDM's construction and testing up to the summer of 1993.

### Introduction

Numerous aerospace programs have been a need for low shock, single point separators that are multi-fault tolerant and can separate without breaking primary structure. In late 1987, such requirements were applied on an Orbiter Disconnect Assembly that is part of the Stabilized Payload Deployment System (SPDS). Two different types of TDM's were developed. They differed by way of solving an initial design problem. Both TDM's had 3 pin pullers each and were vulnerable to unexpected tensile load spikes creating plastic deformation. If the pins were bent, they could not retract which would lead to a separation failure with little to no preload holding the 2 structures together.

In late 1988 a request for a TDM in a different envelope shape was considered, and a third concept, the TDM20KS, was designed. This TDM was met the envelope constraints and was designed to function with the inner parts deformed from tensile load spikes. The TDM20KS application dissolved, but the development tests continued.

Most of the tests performed considered the 2 fault tolerant case by using only one of the 3 separation members.

### The First Toggle Deployment Mechanisms

The original SPDS requirements were translated into the first pin-puller configured TDM and resulted in the United States Patent 4,836,081.<sup>1</sup> The original concept, shown in figure 1, had a problem with the preload forcing the pins back and causing the shear pins to function as primary structure. The less the angle "a" from the horizontal on the toggle, the less load there is pushing the pins back. However, the less angle "a", the harder it is for the toggle to swing away from the unretracted pins. If angle "a" was zero, there would be no moment on the toggle, created by the 2 unretracted pins, for the toggle to swing away from.

The first NASA-JSC pin-puller configured TDM, seen in figure 2, has the axis of the pins parallel to the conical surface of the toggle. The tension of the toggle pushes the conical surface perpendicular to the pin's axis and does not act on the shear pins.

Preloading the toggle was completed by unscrewing the preload collar that pulls the toggle up. To prevent twisting of the toggle while preloading, a tool was placed in the socket holes to hold the toggle and socket from turning. This TDM was designed to hold and release a preload of 1000 pounds.

Testing was performed with pneumatics and NASA Standard Initiators (NSI). With pneumatics, a static pressure of about 500 psi was needed to release the 1000 pound preload. Dynamic pressure releasing was performed by opening a solenoid valve into the NSI port. Plumbing orifices and other dynamics required a higher static pressure behind the solenoid valve for separation. Figure 3 shows pressure versus preload with two types of piston/pin coatings.

Friction coefficients of the TDM parts play an important role in releasing energy. Figure 3 also shows a difference between the original piston finish and a Teflon impregnated nickel plate finish called NEDOX from General Magniplate Corp.. The NEDOX finish shows a consistent improvement in releasing energy.

The second TDM concept had a different design to avoid transferring the preload into the axis of the pins. This resulted in development of the double swivel toggle and lead to United States Patent 4,864,910.<sup>2</sup> As seen in Figure 4, this TDM had the axis of the pins running perpendicular the axis of the toggle. When one pin was retracted, the bottom of the toggle could swivel down and clear itself from the 2 unretracted pins. This TDM was successfully developed and qualified to meet SPDS requirements.

#### Toggle/Hook Deployment Mechanism TDM20KS

The TDM20KS was designed to release a preload up to 20,000 pounds even if some internal parts were plastically deformed. Figures 5 and 6 show the fastened and released configurations of the internal parts. In figure 5, the toggle is held down with 3 hooks that pivot in the body. Each hook is held from pivoting by a piston. As seen in figure 6, the piston has moved up and the toggle is released when a hook is free to swing back into the void of the piston.<sup>3</sup>

Two TDM20KS's were made with differences in the angle of toggle/hook contact. One TDM20KS had a 45 degree angle of contact, and the other assembly had a 30 degree angle contact from the

horizontal. Both toggle stems had full strain gauge bridges applied inside holes going through their axes. Each piston port had 2 NSI ports. Most parts of the TDM20KS were plated or coated with low friction surfaces.

#### TDM20KS Development Test

Three sets of development tests were completed. After initial testing, the next 2 development tests were performed with design changes that were needed during the initial testing. The initial development tests were performed with hydraulics and with NSI's, but the first goal was applying the preload.<sup>4</sup> With 2 NSI ports per cylinder, pressure monitoring was easily accomplished.

#### TDM20KS Initial Development Testing

Preloading was similar to the original TDM by way of pulling the socket up when unscrewing the preload collar (otherwise known as a preload bolt). Figure 7 shows the setup used to get the maximum preload. A tension machine would pull the socket up by stretching the toggle, and the preload bolt was unscrewed until it was snug with the socket. The bolts connecting the tension machine to the socket had a 17,000 pound maximum limit, and the TDM20KS assembly would settle down to about 12,000 pounds preload. A future design was able to obtain a 20,000 pound preload.

Releasing the preload with hydraulic pressure in one cylinder showed the difference between the 45 degree TDM and the 30 degree TDM. Figure 8 shows 3 different releasings at 3 different preloads for the 45 degree TDM, and figure 9 shows the same tests with the 30 degree TDM. As expected, there was

less pressure needed to release the 30 degree TDM due to less force between the hooks and pistons. What was unexpected is the inconsistency of releasing pressure as a function of preload.

NSI firing showed similar pressure/preload results after the TDM's were exposed to vibration, shock, and thermal environments. Ambient firings revealed a design problem in the piston stops. The pistons traveled too far and leaving the bottom of the piston voids pushing the hook back up which prevented toggle releasing. All toggle releases, with the original piston stops, were performed with one NSI per piston. The second phase of development testing, with 2 NSI's per piston, showed some success in an improved design.

Figures 10 and 11 show pressure and preload curves in the 30 and 45 degree TDM chambers during 275 degree F. firings. The TDM's were successfully fired in -90 degree F. environment. Figure 12 shows the data on the 45 degree TDM cold firing.

Both hydraulic and NSI tests showed a preload increase when separating. This is believed to be caused by the piston bending in toward the hook while traveling up.

A plastic deformation test was performed with the 45 degree TDM while the 30 degree TDM was saved for testing improved piston stops and preloading mechanisms.

The 45 degree TDM was first preloaded, and the separating members were tensioned to 29,000 pounds. There was a .040 inch gap in the separation plane, but no separation was noticed while the tension was within the preload. The 29,000 pound load was released, and the remaining preload in the TDM

was unknown due to strain gauge damage in the toggle stem. Figure 13 shows the average permanent change in the deformed parts. The 45 degree TDM was preloaded and put back into tension. The toggle stem finally broke at 34,000 pounds tension. Besides the toggle, the internal parts were deformed a little more and were still able to function in the TDM body.

#### TDM20KS Post Development Tests

The 2 post development tests evaluated a redesigned piston stop and a new type of preloading mechanism.

#### Piston Stop Redesign

The initial NSI firing tests revealed that the piston stops were not stopping the piston with the actuation of one NSI. The existing stops, made of AL7075-T6, were set to start taper locking the piston tops at a position too high for the piston to settle in the correct position. In addition, the original piston stops were cracking at the sides where the bolts held them down. The original piston stops were lowered and extra side supports were bolted down, but these created assembly problems that led to the new piston stop.

Besides making the new piston stops out of 15-5 CRES, the design was beefed-up on the outside, and the interior dimensions had tighter tolerances. Figure 14 shows the difference in the piston stops.

Six firings of the TDM were conducted at various temperatures, preloads, and number of NSI's.<sup>5</sup> Most tests were performed with 2 NSI's per piston unlike the initial development tests. Tests proved the piston stops did not deform, but the original 1/4-20UNC-3A bolts,

holding the stops, elongated and were bent. Figure 15 shows how the deformed bolts allowed the piston to travel too far, pushing the hook back up, and wedging the piston between the hook and cylinder. Testing with bolts made of carbon steel, instead of 300 series SST, also resulted in stretched bolts but not as deformed as the older ones. The bottom surface of the piston void was lowered 0.15 inches to give room for successful releasing with 2 NSI's per piston.

#### Top Member Redesign

The last of the TDM20KS development solved the preloading problem by completely redesigning the top preloading members. As noticed in earlier TDM preloading, one set of threads could apply a certain tension regardless to the diameter. Also, the tension machine would have to load the toggle about 1.4 times the desired preload to get what the TDM would settle down to. The theory behind the new top TDM section is to design in as many sets of threads as possible, and the tensions from all threads would sum up to a desired preload.

Figure 16 shows the major parts used in the new top members designed to get up to 20,000 pounds preload without using a tensile machine. The only existing part used is the socket. It sits in a tensioner that contains 18 sets of 3/8"-24 threaded holes surrounding the socket. Eighteen hex cap screws were threaded into the tensioner and sit in the base plate. This base plate has 18 counter bores with the same bolt circle as the tensioner threads. Each base plate counter bore has 2 SST washers with a brass washer between. These washers act as thrust bearings for the bolts. Tightening the bolts in a star

pattern would separate the tensioner from the base plate and create tension on the toggle.

Testing of the new top member and releasing over 20,000 pound preload with one NSI was successful.<sup>6</sup> Each bolt was torqued at 20 in. lb. increments, in a star pattern, until the toggle's strain gauge failed at 18,000 pounds. Preload, as a function of torque, was continued until 20,000 pounds was estimated. The maximum torque/preload tested was 200 in.lb. on each bolt and 24,000 pounds preload. At ambient conditions, one NSI was still able to release the 24,000 pound preload.

### Conclusions

Each of the three toggle deployment mechanism concepts tested successfully. Other designs were considered which had different hook shapes and pivot locations. Besides pivoting hooks, sliding members can also apply to fit envelope constraints.

### References

1. Patent Number 4,836,081 Jun. 6, 1989 "TOGGLE RELEASE". Inventors: Thomas J. Graves; Robert A. Yang; Christopher W. Brown. Assignee: The United States of America as represented by the Administrator of the National Aeronautics and Space Administration, Washington, D.C.
2. Patent Number 4,864,910 "DOUBLE SWIVEL TOGGLE RELEASE". Inventors: Guy L. King; William C. Schneider. Assignee: The United States of America as represented by the Administrator of the National Aeronautics and Space Administration, Washington, D.C.
3. NASA Tech Briefs Vol. 15 No. 11 P. 71 "Redundant Toggle/Hook Release Mechanism" Nov. 1991.
4. NASA JSC Thermochemical Test Area No. JSC 26486 "Internal Note For the Toggle Deployment Mechanism (TDM)" April 1993.
5. NASA JSC Thermochemical Test Area No. JSC 25964 "Internal Note For Toggle Deployment Mechanism Piston Stop Test" July 1992.
6. NASA JSC Thermochemical Test Area Task History 2P809 " August 1993.

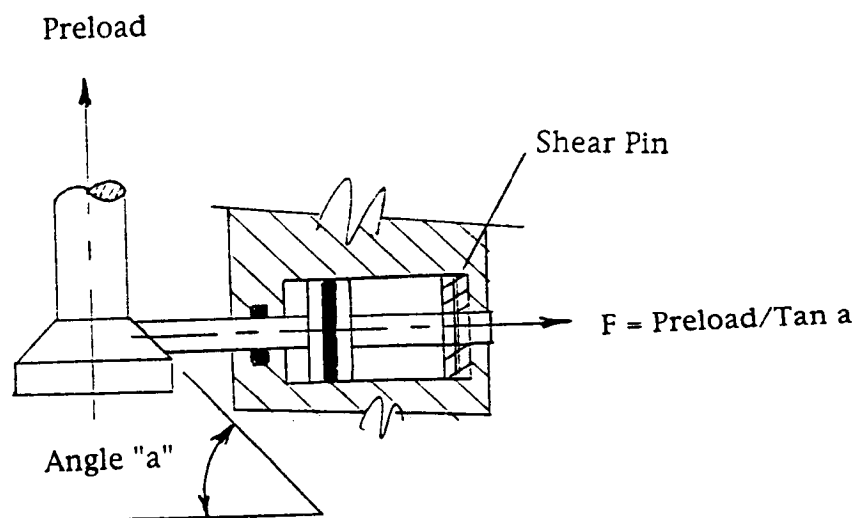


**Figure 1**  
Original Toggle Deployment Mechanism Concept.



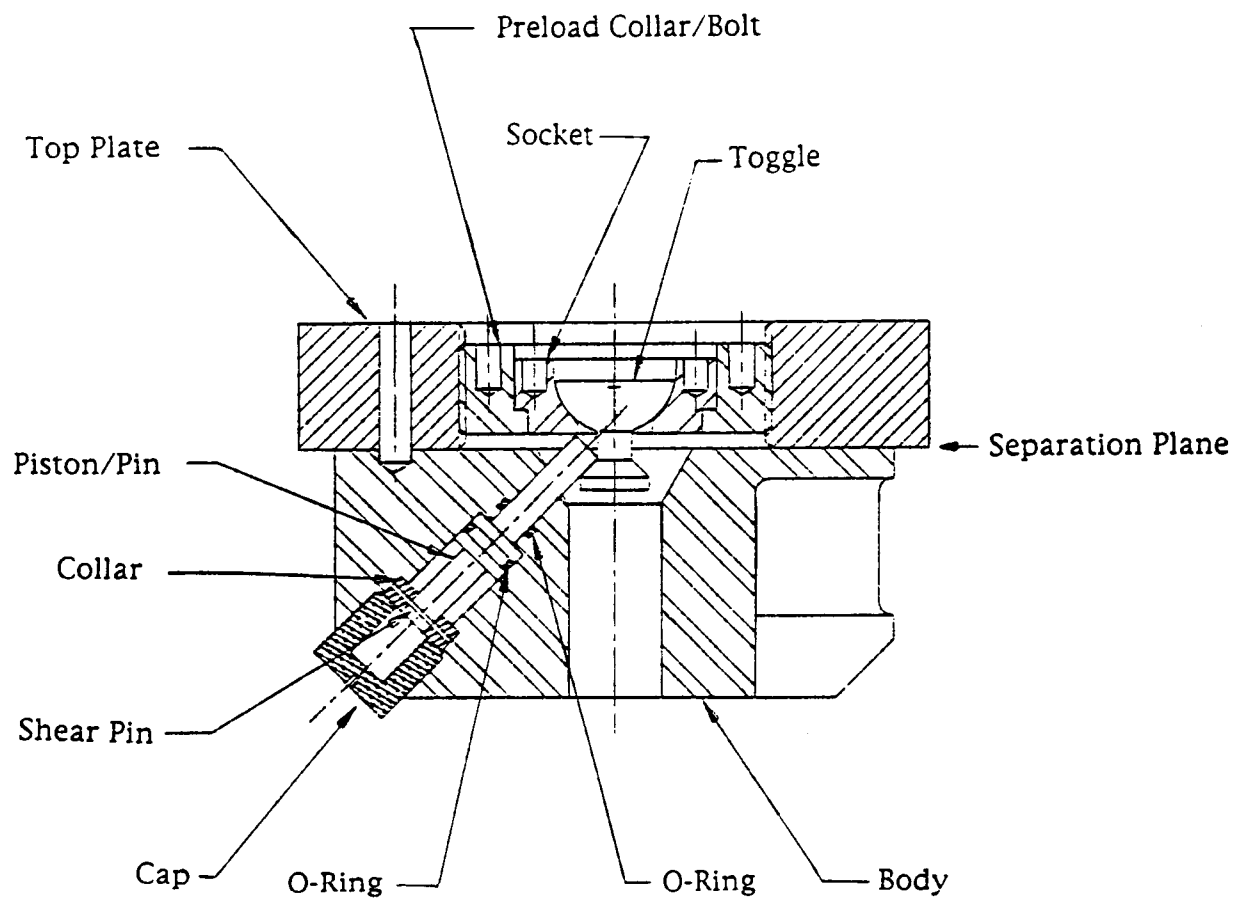


**Figure 2**  
Toggle Deployment Mechanism, Pin-Puller Configuration.

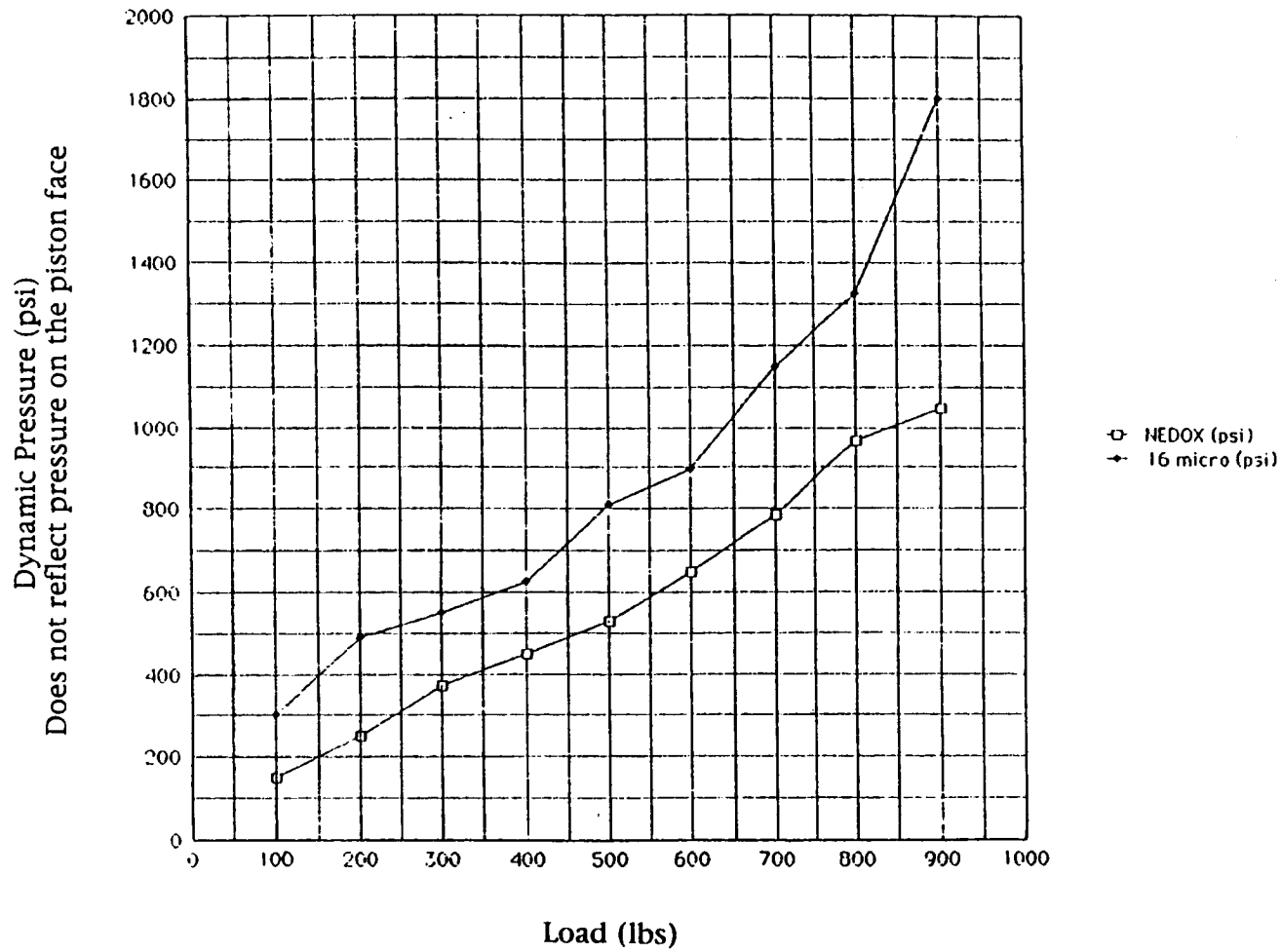


**Figure 3**  
Pressure pulse v.s. preload for releasing the TDM.

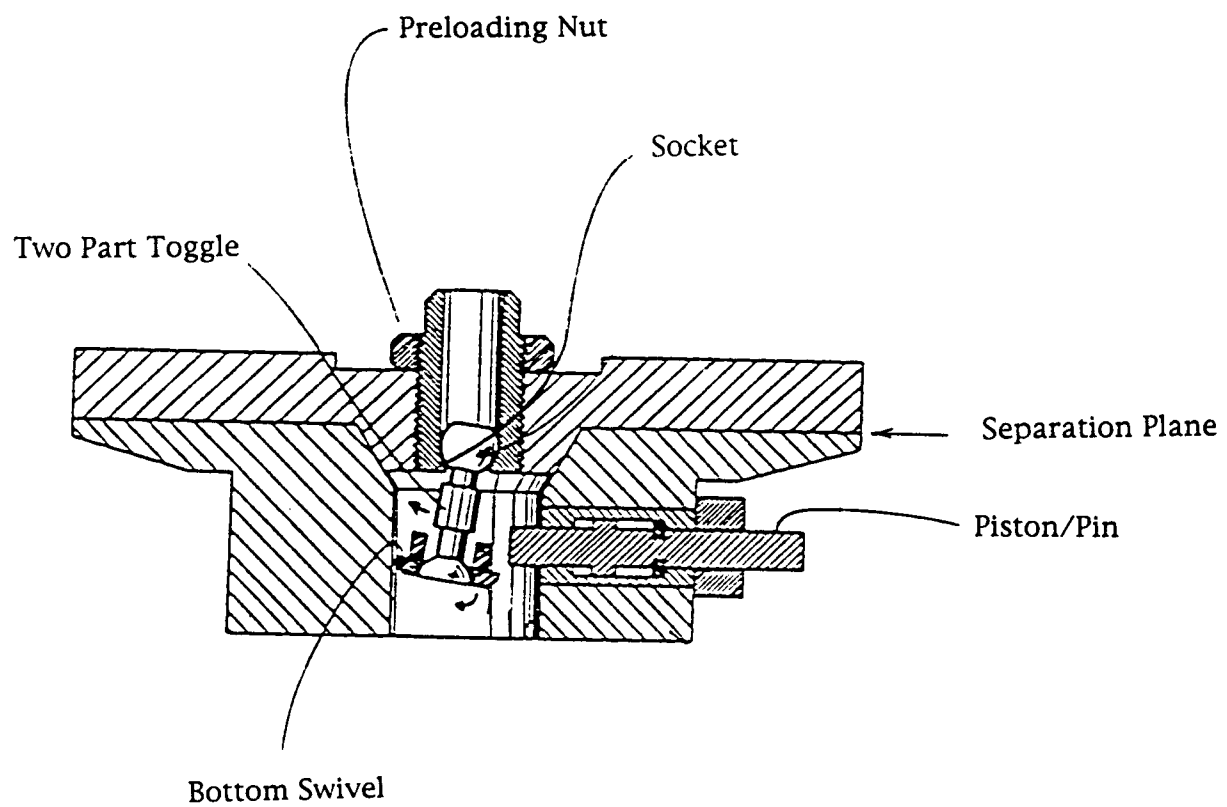


**Figure 4**  
Double Swivel Toggle Release.

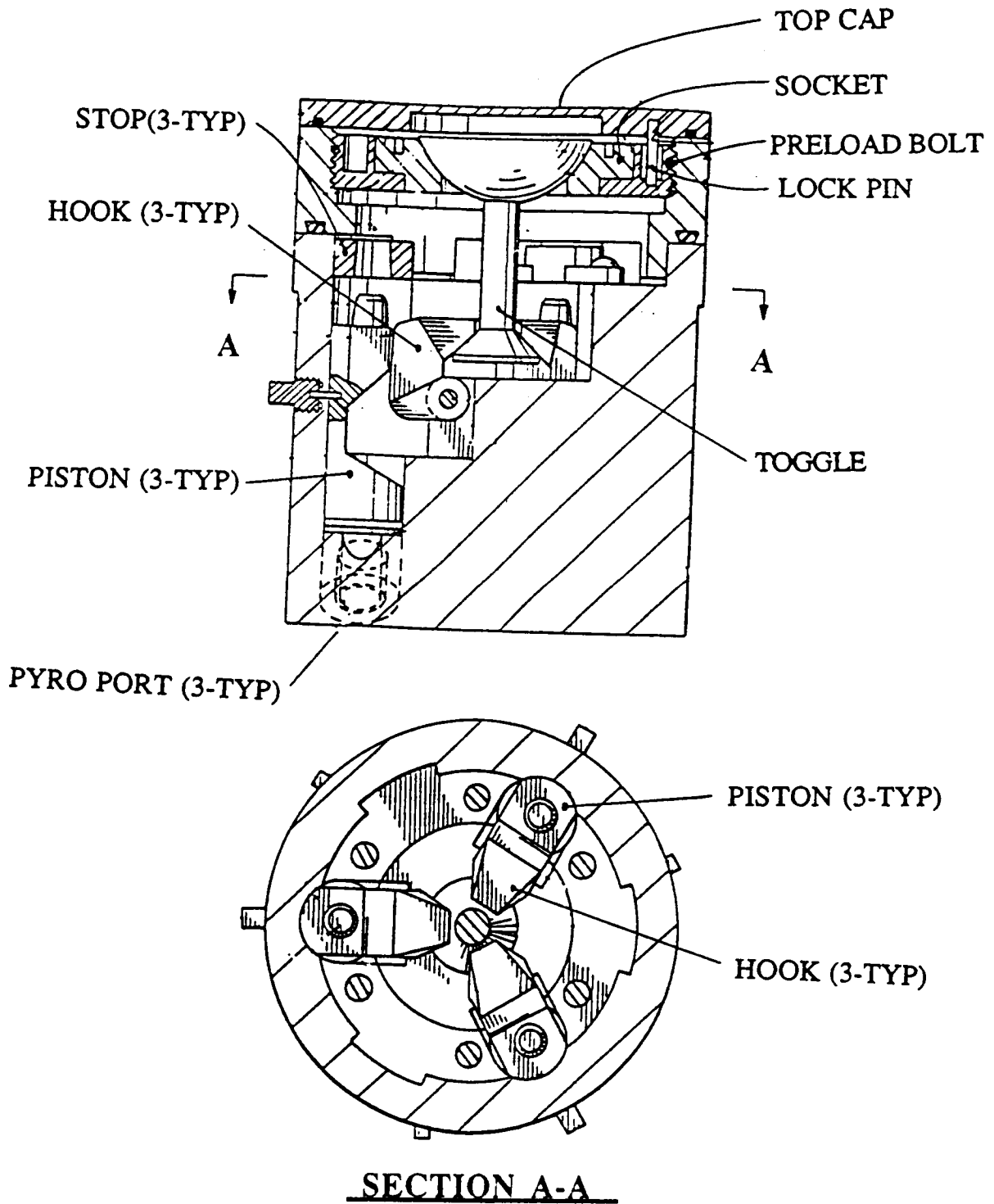


**Figure 5**  
 Toggle/Hook Deployment Mechanism TDM20KS before separation.

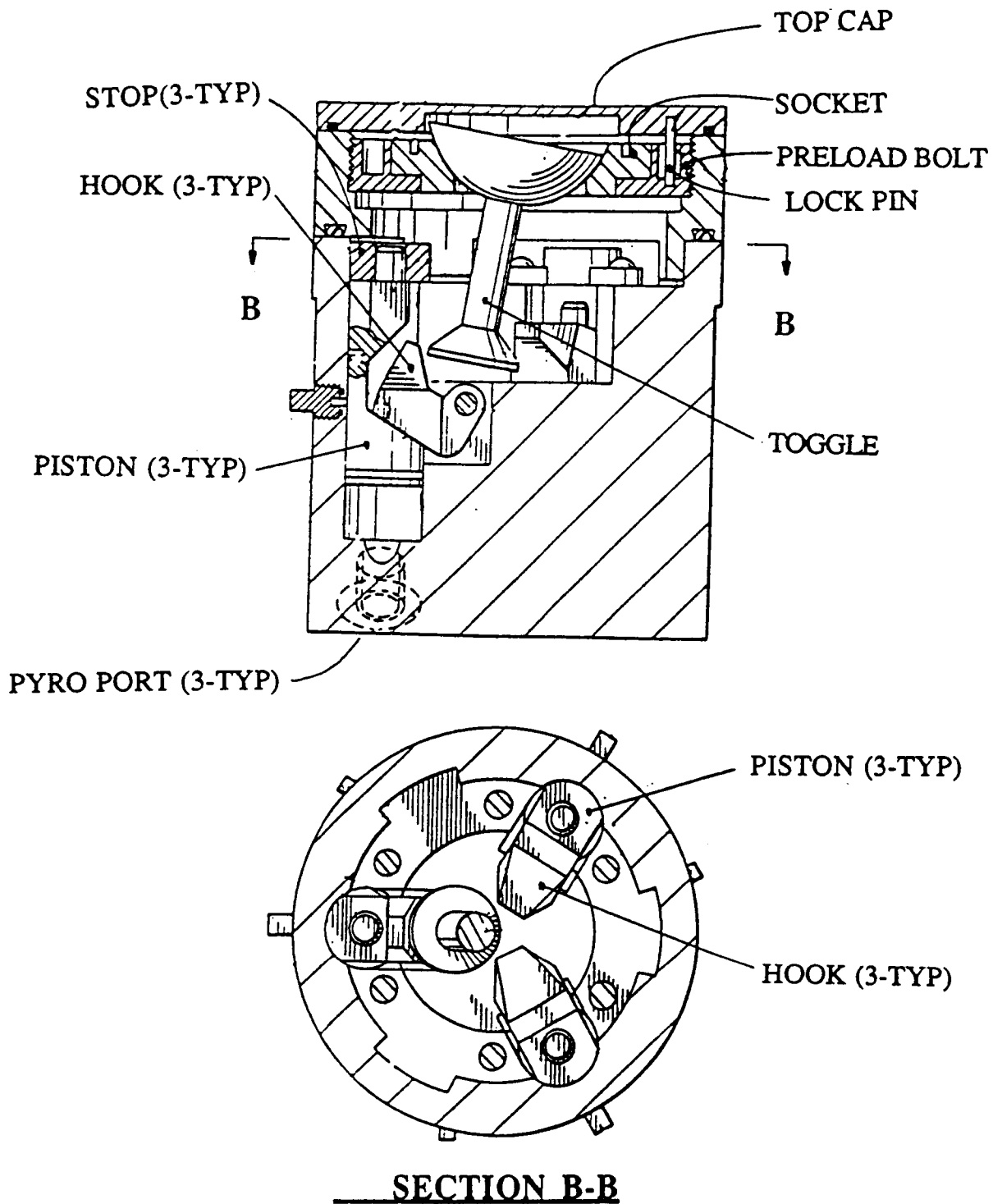


**Figure 6**  
 Toggle/Hook Deployment Mechanism TDM20KS during deployment.  
 Separation plane is at section B-B.

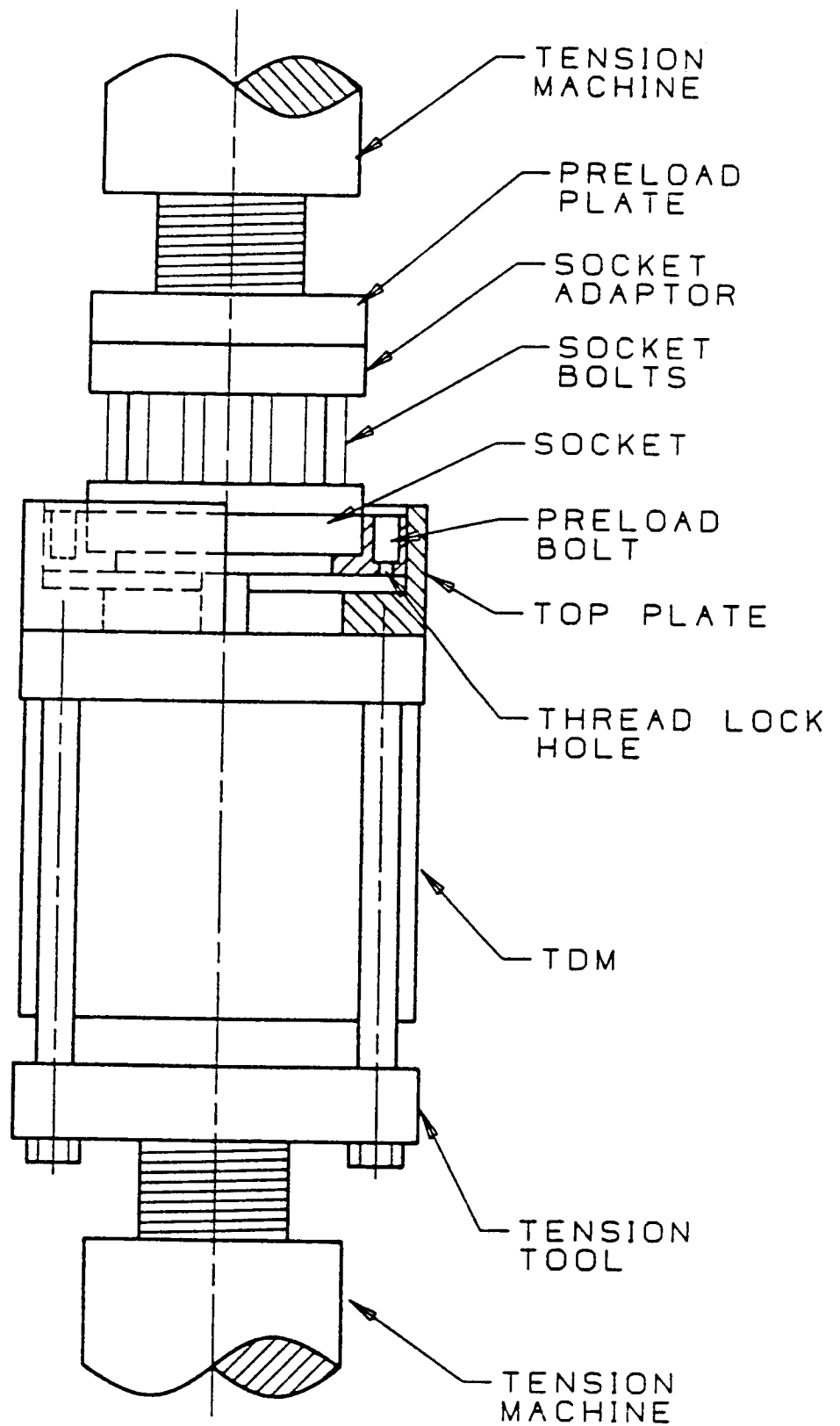


**Figure 7**  
Preloading the TDM20KS.

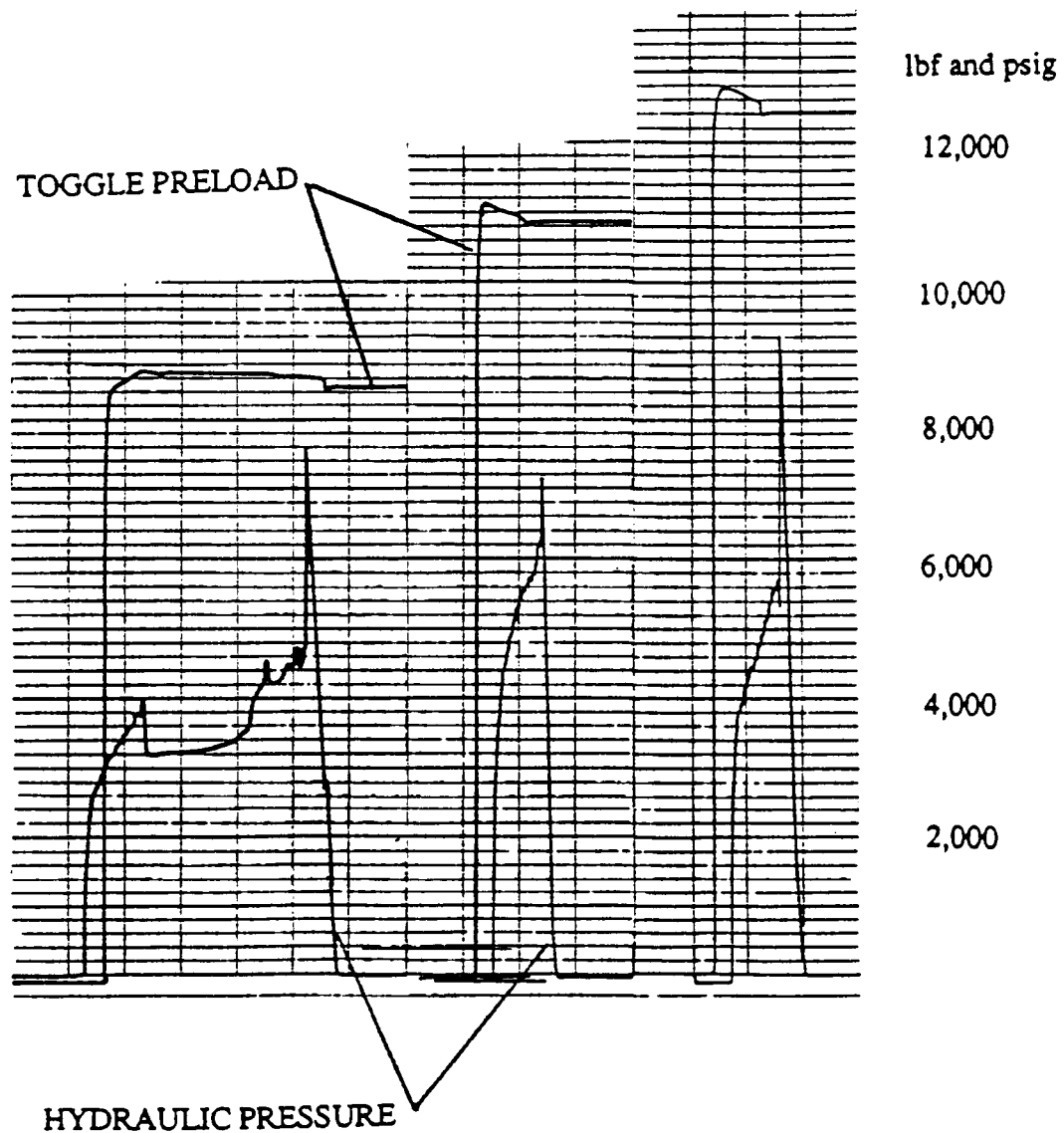


**Figure 8**

Hydraulic release tests for the 45 degree TDM. Load cell and toggle gauge lines were staggered due to pen locations on the strip chart recorder.

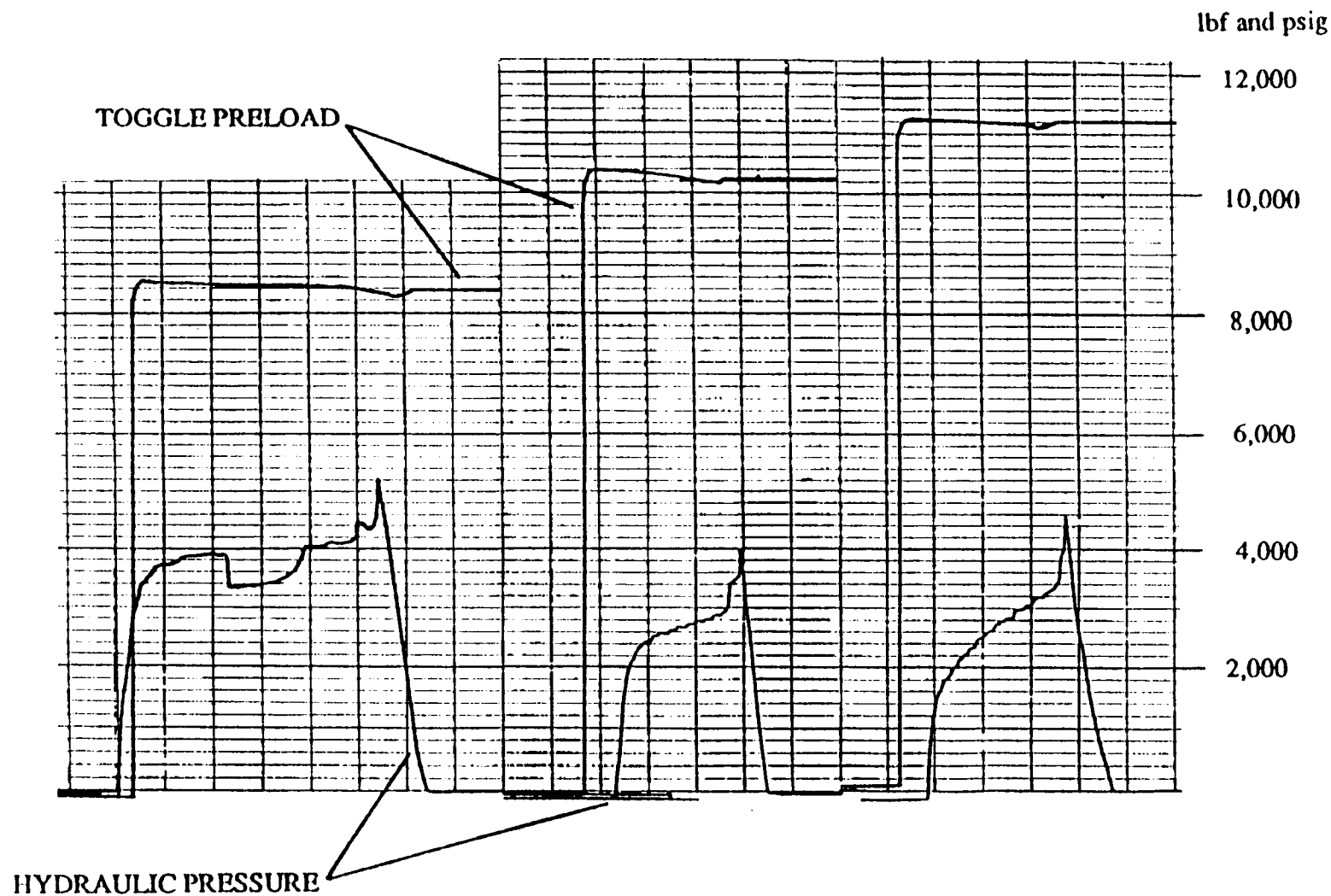


**Figure 9**

Hydraulic release tests for the 30 degree TDM. Load cell and toggle gauge lines were staggered due to pen locations on the strip chart recorder.



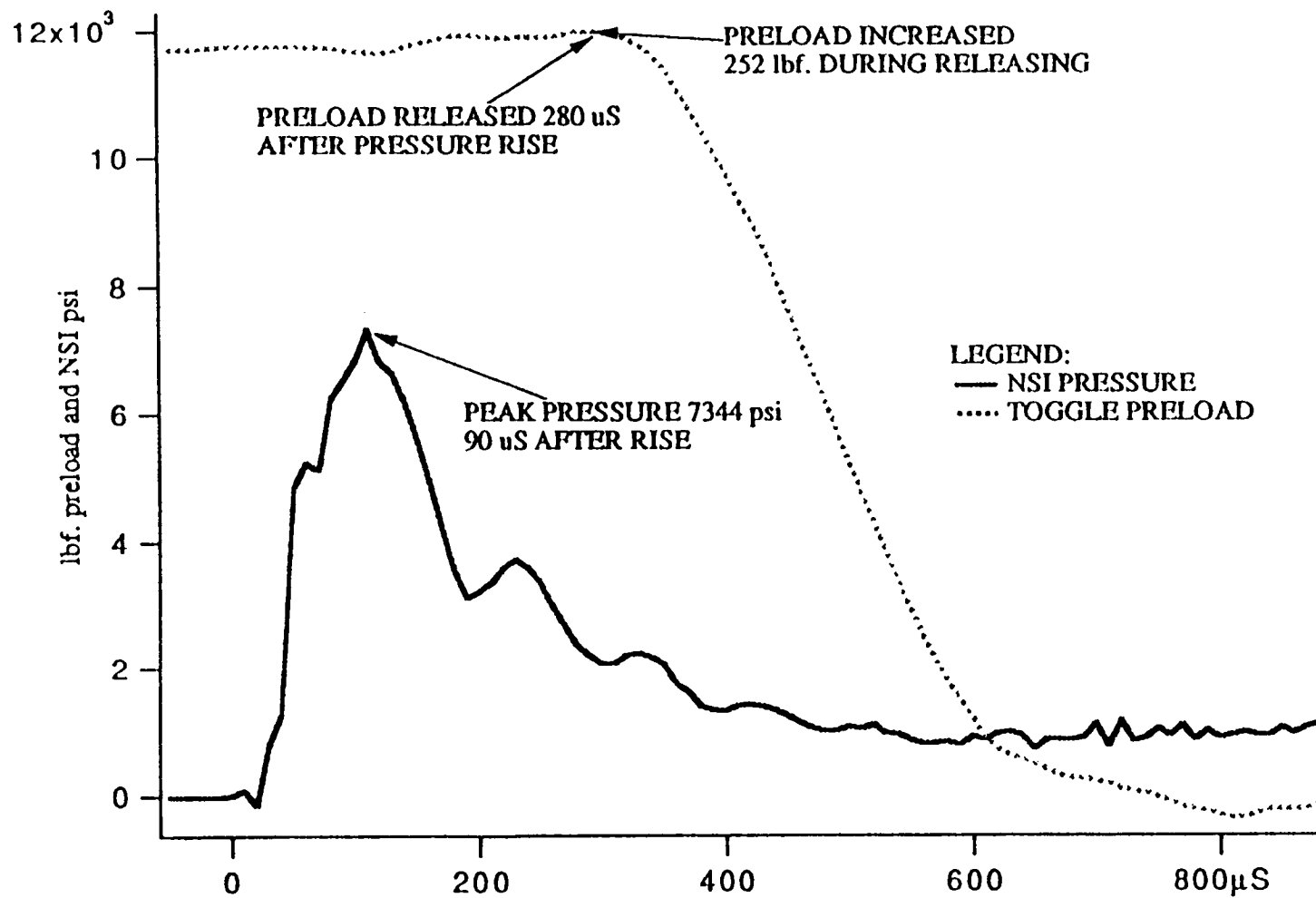


**Figure 10**

Forty-five degree TDM pyrotechnic release at 275 degrees F. Toggle preload values are not compensated for thermal effects on toggle gauges.

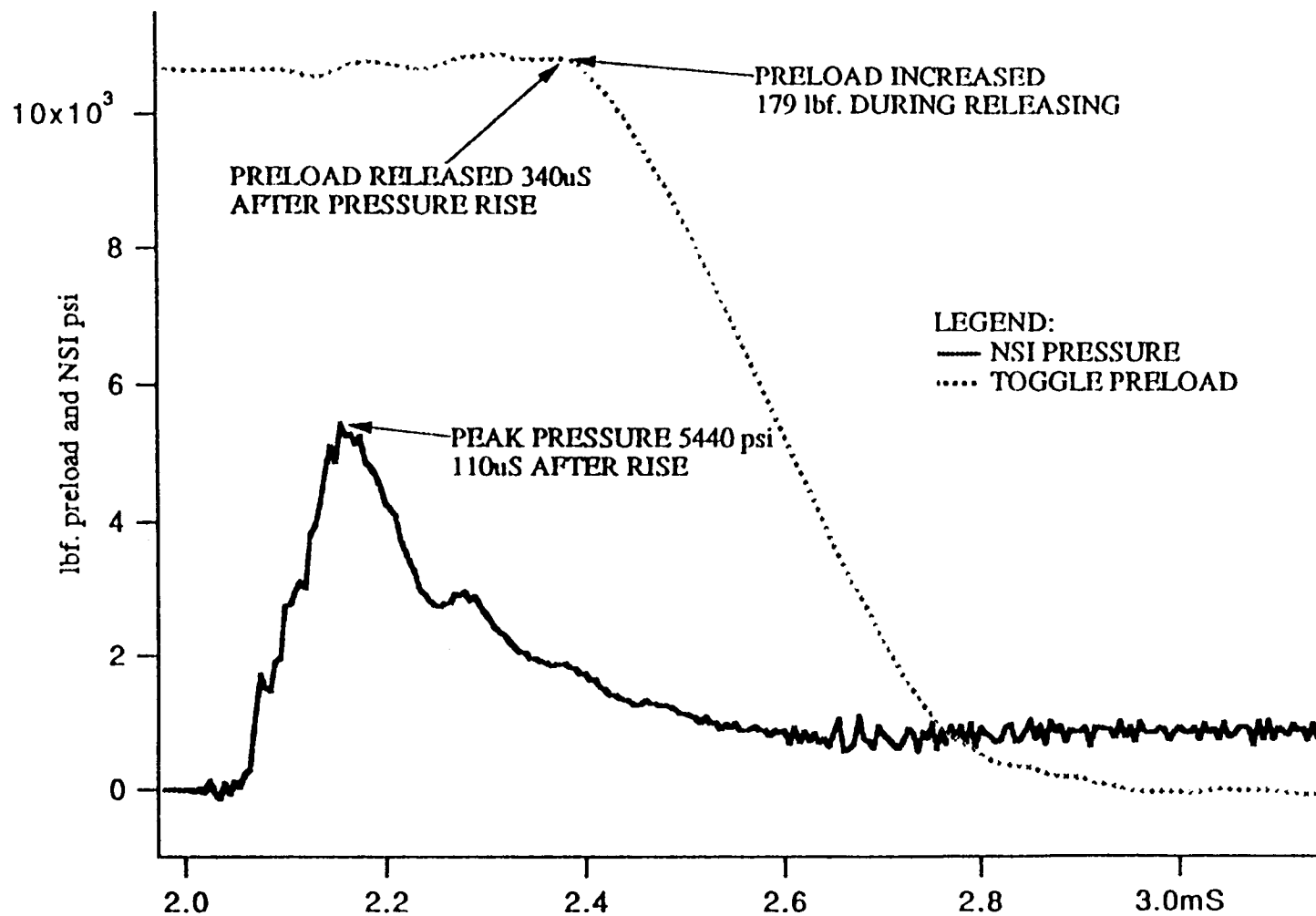


**Figure 11**

Thirty degree TDM pyrotechnic release at 275 degrees F. Toggle preload values are not compensated for thermal effects on toggle gauges.

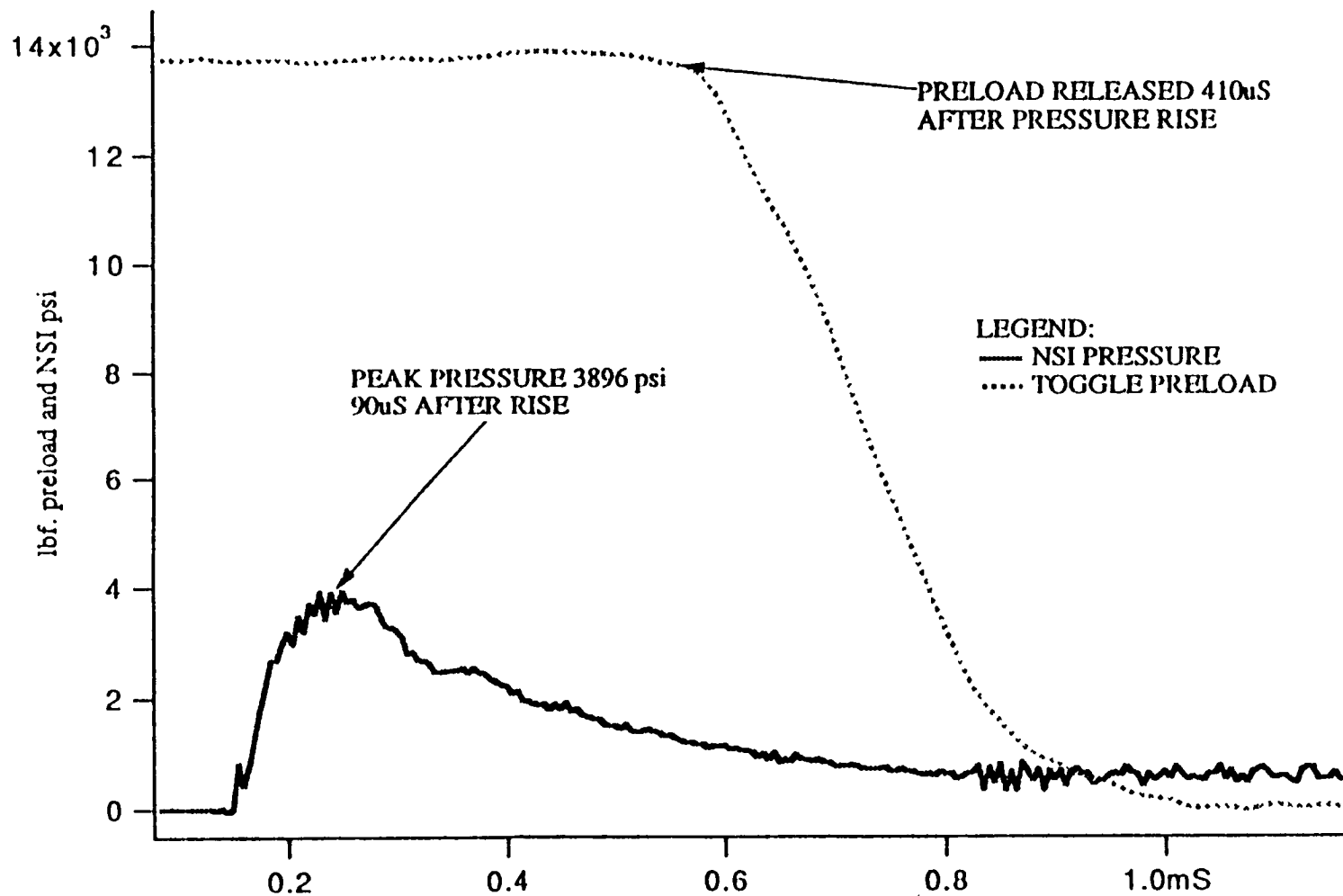


**Figure 12**  
Forty-five degree TDM pyrotechnic release at -90 degrees F. Toggle preload values are not compensated for thermal effects on toggle gauges.

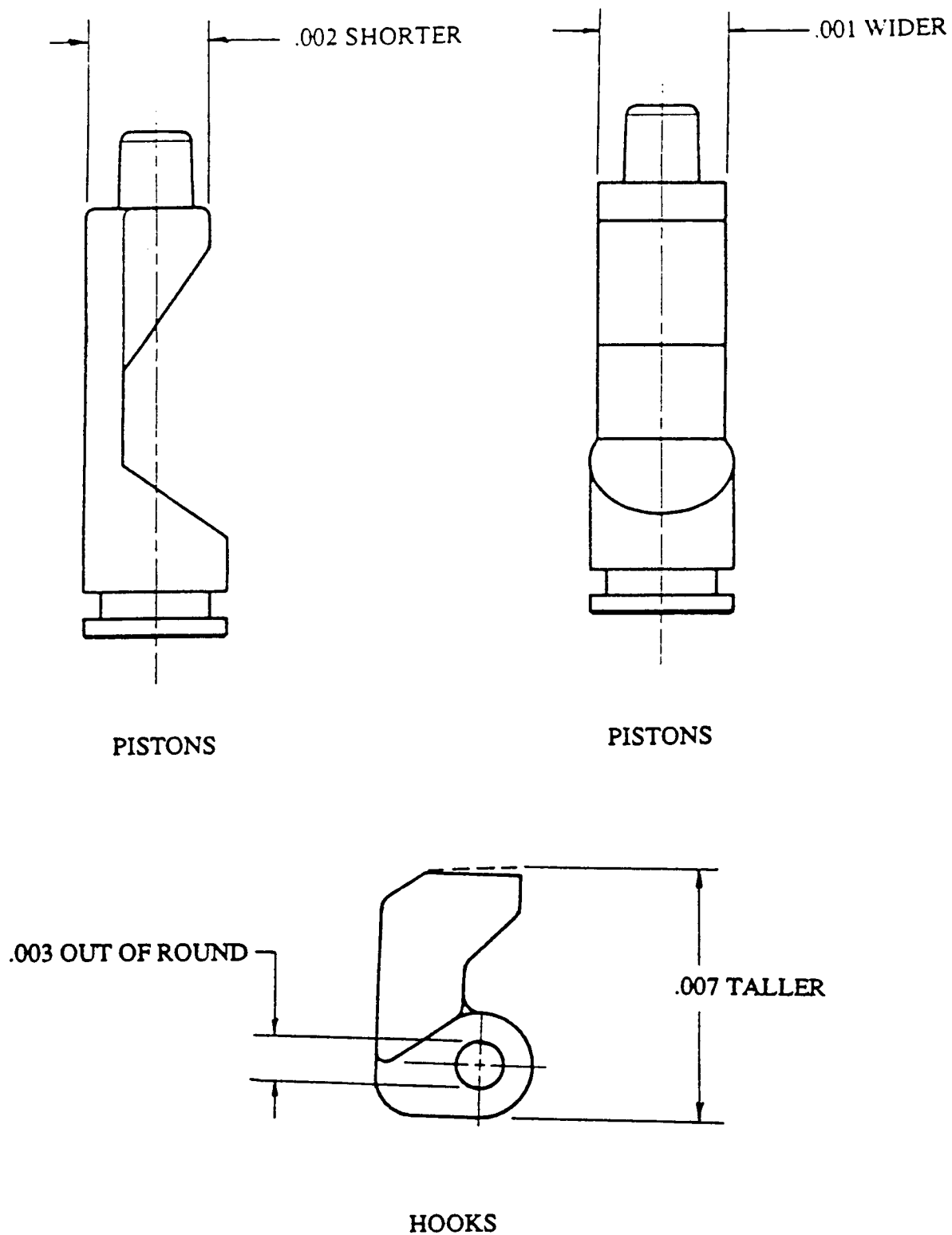
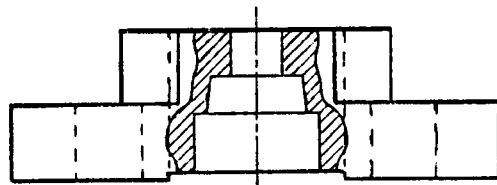
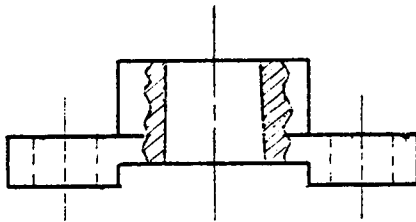
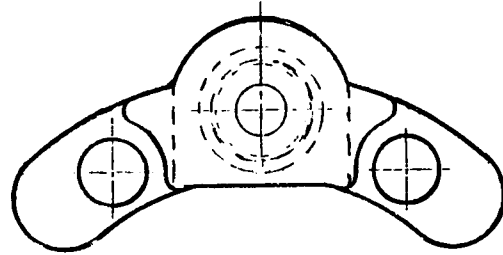
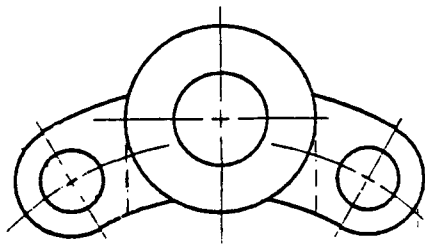


**Figure 13**

Dimensional analysis of the deformed 45 degree TDM parts after a 29,000 lbf structural load test. Dimensions are averages of all parts and in inches.



Original Piston Stop  
AL 7075-T6

Redesigned Piston Stop  
15-5 PH CRES

**Figure 14**  
TDM20KS Piston Stops.

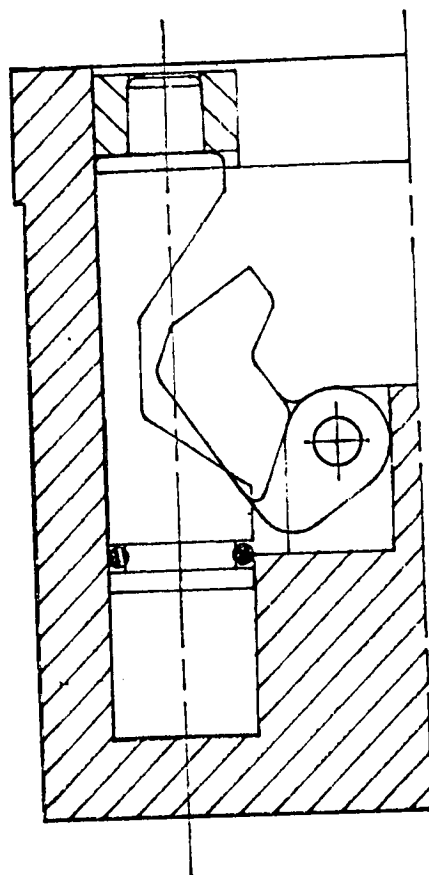


**Figure 15**  
TDM20KS Piston/Hook interference after excessive piston travel.

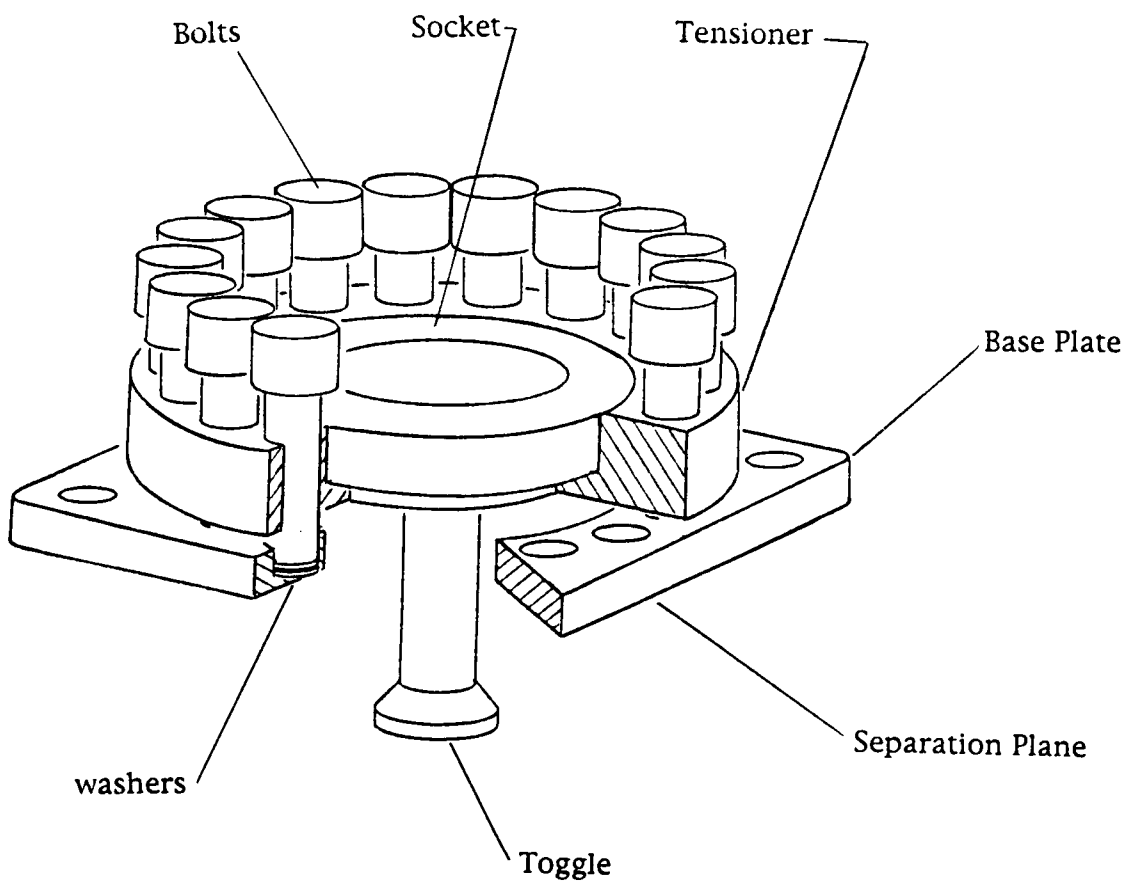


**Figure 16**  
TDM20KS Redesigned Top Assembly

518-28  
0998  
1-10

## **THE ORDNANCE TRANSFER INTERRUPTER, A NEW TYPE OF S&A DEVICE**

John T. Greenslade, Senior Staff Engineer  
Pacific Scientific Company, Energy Dynamics Division

### **ABSTRACT**

A discussion is given in this paper of a new approach to the Safing and Arming of aerospace ordnance systems interconnected by detonation transfer lines, in which the conventional type of S&A device normally used for this purpose is replaced by a relatively simple electro-mechanical switching device, referred to as an "Interrupter." In this approach the Interrupter, which is interposed in the transfer line between the system initiator and output device, is completely passive in that it contains no pyrotechnic devices or materials. Being passive (therefore, non-initiating), the Interrupter is much less hazardous to handle and install, as well as being significantly less complex and costly than conventional S&A devices containing EEDs and explosive leads.

Details are presented relative to the design, development and qualification, by PS/EDD, of an ordnance transfer Interrupter intended for use on a commercial launch missile. This device, which is capable of simultaneously "switching" multiple detonation transfer lines, incorporates a rod-type rotary barrier with independent transverse apertures for each transfer line. Barrier actuation is bi-modal, i.e., the barrier can be driven from safe-to-arm or from arm-to-safe positions by independent electro-mechanical actuators. The Interrupter described also features visual and remote status monitoring provisions and, in common with range-approved conventional S&A devices, a pre-flight safety locking mechanism functioned by a removable safing key.

Successful development of the Interrupter required the resolution of such problems as ensuring reliable detonation propagation (between opposed booster tips in the transfer lines) across unusually large airgaps within the barrier apertures, and the damping of the barrier drive train to prevent inadvertent actuation during vibration and shock extremes. The latter problem was solved by the incorporation of in-line pneumatic dampers in each of the barrier drive-trains.

### **INTRODUCTION**

For safety reasons, all ordnance systems, regardless of their level of complexity, must be capable of being maintained in an inoperative "Safe" state, prior to when they are required to function. At the simplest level, the Safing function could be exemplified by the switching of a firing circuit of a single electro-explosive device (EED). In most missile and spacecraft ordnance systems, the Safing function, and its converse, the Arming function are effected by a specifically designed, and often complex, Safe/Arm Device, or SAD. A brief discussion relative to the conventional usage and technology of these devices will provide an appropriate introduction to the subject of this paper.

The SADs employed in missile ordnance systems have generally been classifiable in either of two broad categories, namely, the "Command" type and the "Inertial" type. SADs of the former type are "commanded" to change their state from Safe to Arm (and reverse, in some cases) by the input of electrical signals generated by a remote controller. On the other hand, the Safe to Arm transition is achieved automatically



with the "Inertial" type SAD, when it is subjected to a specific level of vehicle acceleration for a specific minimum duration. The arming mechanisms in the Command type SADs have most commonly been electro-mechanical, although electronic devices have become competitive, and laser based Command type SADs have started to make an appearance. The Inertial SADs are armed by inertia forces, resulting from the missile acceleration, acting on a spring-loaded "set-back" weight. With these devices, the movement of the set-back weight is controlled by an escapement mechanism, similar in principle to the escapements used in clocks.

Figure 1 tabulates some of the more common types of SAD which have been used in missile applications.

Conventional SADs, Command and Inertial, are more than just a system safing and arming mechanism; they are also the ordnance system initiator. For that purpose, they incorporate electro-explosive devices, usually detonators, and very often explosive transfer components such as "leads," or confined detonating cords. This, of course, increases the hazard potential associated with pre-flight testing and installation of

conventional SADs. As such, it is one of the factors which led to the concept of the Interrupter, which contains no pyrotechnic or explosive components, as a replacement for conventional Command SADs in systems employing linear ordnance transfer lines such as shielded Mild Detonating Cord (SMDC), or Confined Detonating Fuze (CDF).

In the Safe mode, conventional Command type SADs must either physically hold their internal detonators out of alignment with their output ports, or, interpose a barrier between the detonators and ports. They must also disable the firing circuits to the electro-explosive detonators, and impose a safety shunt across those circuits. Conversely, when in the Armed mode, the Command SADs must align their detonators with the output ports (or remove the barrier), and they must complete the firing circuits to the detonators. In comparison, the Interrupter, having no internal EEDs, is not involved in disabling or enabling the firing circuits to the system initiators. This considerably simplifies its internal circuitry and switching requirements. The Interrupter would, as the name implies, have to interrupt the system firing train, in this case by a removable barrier. The functional requirements for a typical conventional Command SAD are compared, in Figure 2 with those for the Interrupter.

| TYPE     | COMBINATIONS OF:                       |  |  |
|----------|--|--|--|
|          | ENABLE                                 | ARM  | INTERRUPT  |
| COMMAND  | LANYARD<br>SOLENOID<br>GAS<br>PRESSURE | ROTARY<br>SOLENOID<br>LINEAR<br>SOLENOID<br>SPRING<br>GAS PRESSURE | ROTARY<br>SOLENOID<br>LINEAR<br>BARRIER<br>MOVABLE EDD |
| INERTIAL | AS ABOVE                               | INERTIA  | AS ABOVE   |
| OTHER    | ELECTRONIC                             | ELECTRONIC   | RELAY  |

**Figure 1:**  
**SADs Used in Missile Applications**

A number of the design requirements for SADs have been dictated by the Government's Missile Test Ranges, predicated primarily on safety considerations. Such requirements relate, for instance, to the minimum amount of firing train misalignment needed, the integrity of status monitoring provisions, and the "hand-safe" capability of the device, i.e., its ability to remain intact in the event of an inadvertent detonation of its EEDs.

| MODE    | FUNCTION                               | CONVENTIONAL SAD | INTERRUPTER |
|---------|--|------------------|-------------|
| SAFE    | PHYSICALLY BLOCK FIRING TRAIN          | X                | X           |
|         | DISRUPT FIRING CIRCUIT                 | X                | -           |
|         | SHUNT FIRING CIRCUIT INDICATOR         | X                | -           |
| ARM     | PHYSICALLY ALIGN FIRING TRAIN          | X                | X           |
|         | COMPLETE FIRING CIRCUIT                | X                | -           |
|         | REMOVE INITIATOR SHUNT                 | X                | -           |
| MONITOR | PROVIDE INDICATION OF "SAFE"           | X                | X           |
|         | PROVIDE INDICATION OF "ARMED"          | X                | X           |
| SAFING  | MANUAL SAFING FROM ANY POSITION        | X                | X           |
|         | PREVENT MANUAL ARMING                  | X                | X           |
|         | LOCK IN SAFE PRIOR TO FLIGHT           | X                | X           |
|         | PREVENT INADVERTENT SAFETY PIN REMOVAL | X                | X           |
|         |  |                  |             |
| FIRE    | INITIATE INTERNAL EED                  | X                | -           |

**Figure 2: Functional Requirements: Conventional Command SADs Vs. Interrupter**

One important aspect of the design criteria influenced by the Test Ranges relates to manual safing and the Safing Key. The SADs must be capable of being manually transferred to the Safe condition from the Armed state (or any intermediate state), but not vice-versa. The Safing Key used for manually safing, normally doubles as the Safety Pin used to lock the unit in the Safe mode, prior to flight. Current range requirements dictate that the installed safety pin must not be removable if arming is inadvertently attempted.

The Interrupter, shown in Figure 3, has been designed to satisfy all Test Range requirements relative to firing train misalignment, status monitoring, manual safing, and the "interlocking" of the Safing Key to prevent its removal during inadvertent arming attempts. Since the device contains no EEDs, the "hand-safe" requirement does not apply.

## DESIGN CONSIDERATIONS

Before undertaking the design of any new conventional SAD, certain issues must be addressed relative to the functional elements of the device. Several of these will be defined in the product specification, the others will involve trade-off studies to

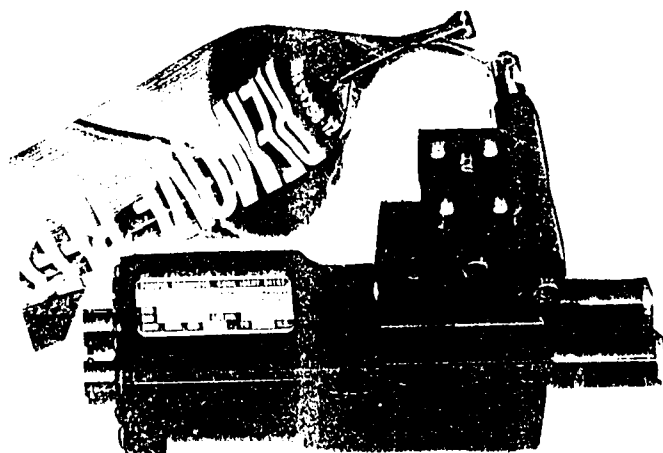


**Figure 3:  
The Ordnance Transfer Interrupter**

optimize the selection of functional approaches. Examples of the specified criteria might be as follows:

- The general type of SAD (Command or Inertial)
- Single or dual firing trains?
- Hermeticity?
- Reversibility of the drive train?
- Detonation or deflagration output?...etc.

Choices that can be made by the designer, based on such factors as cost and reliability, include the type of prime-mover in the

drive-train (e.g., solenoids, or springs, or ..), movable EEDs versus a movable barrier, and the type of electrical switching components to be used (e.g., rotary or snap-action, or ...).

When generating the design of the Interrupter, the ground rules had changed slightly, and different choices were to be made. This unit was to contain no EEDs, therefore, questions regarding firing trains only related to the external ordnance transfer lines. The issue of SMDC versus CDF lines arose, and the propagation characteristics were found to be somewhat different for the two types. Hermeticity was not specified, which simplified the design of the interlocking Safing Key, since a welded metal bellows "pass-through" was not required. It should be noted that the Interrupter is environmentally sealed, with and without the Safing Key installed.

Because the unit interrupts fixed transfer lines, the interruption must be done by a movable barrier. Design choices for the barrier included a linear displacement type and two rotary displacement types, one a disc the other a shaft. Workable designs could have been generated based on any of these approaches, but the rotating shaft option was selected because it was believed that it would facilitate the interfacing of the barrier with the drive train and the required manual safing mechanism.

A linear solenoid/bellcrank solution was chosen for the drive train, rather than a more conventional rotary solenoid. The selection was based on lower cost, and the ability to readily obtain a reversible 90 degree rotation of the barrier without resorting to a gear reduction train.

## INTERRUPTER DESIGN

As shown in Figure 4, the Interrupter housing is a complex rectilinear structure with overall dimensions of 5 1/4 L x 3 5/8 W x 2 7/8 H inches. The lower LH view in Figure 4 shows two of the four input/output detonator ports (the other two oppose the ones shown) in the aft section of the housing, and two electrical connectors. One of these interconnects with the drive train power circuits, the other connector interfaces with the remote monitoring circuits. The two lower views depict the Safing Key, which is located in a cylindrical projection on top of the unit. The two cylindrical projections at one end of the Interrupter house the pneumatic damper components.

Figure 5 shows the drive train components. The prime movers are two identical pull type solenoids, installed in parallel, one for driving the mechanism from the Safe to the Armed state, the other for reversing the procedure. The plunger in each solenoid is pinned to a rod extension on which a roller is mounted. A low-inertia rotor is mounted on a shaft aligned on an axis normal to the solenoid axes and half way between them. As shown in Figure 5, the rod-mounted rollers contact opposite faces on the Rotor. A retraction of the Arm solenoid causes its coupled roller to cam-drive the Rotor in the clockwise direction (viewed from the rotor side of the unit). Conversely, the Safe solenoid will drive the Rotor in the CCW direction. An overcenter spring, pinned to the Rotor and housing, completes the Rotor's full 90 degree rotation after it is driven past top-dead-center by either solenoid. The overcenter spring is also designed to detent the Rotor in either the Safe or Armed position.

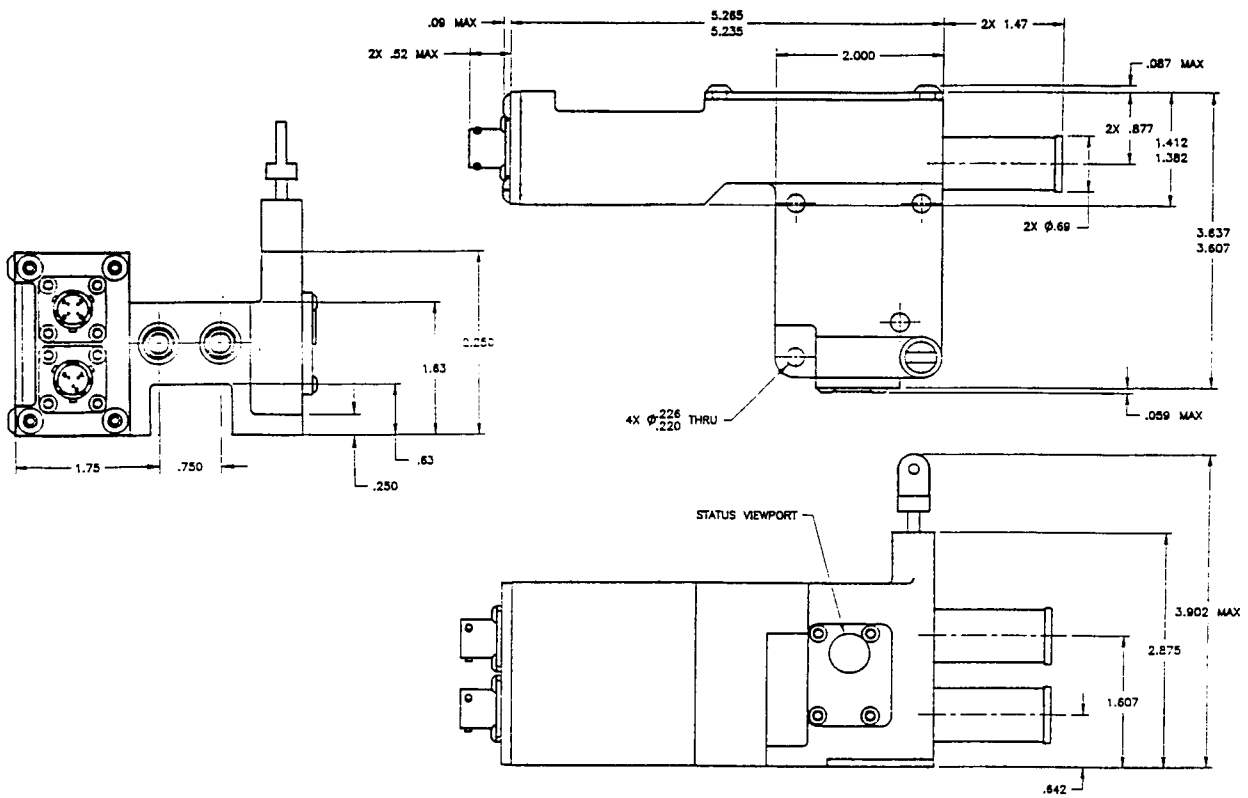


**Figure 4: The Interrupter Configuration and Envelope**

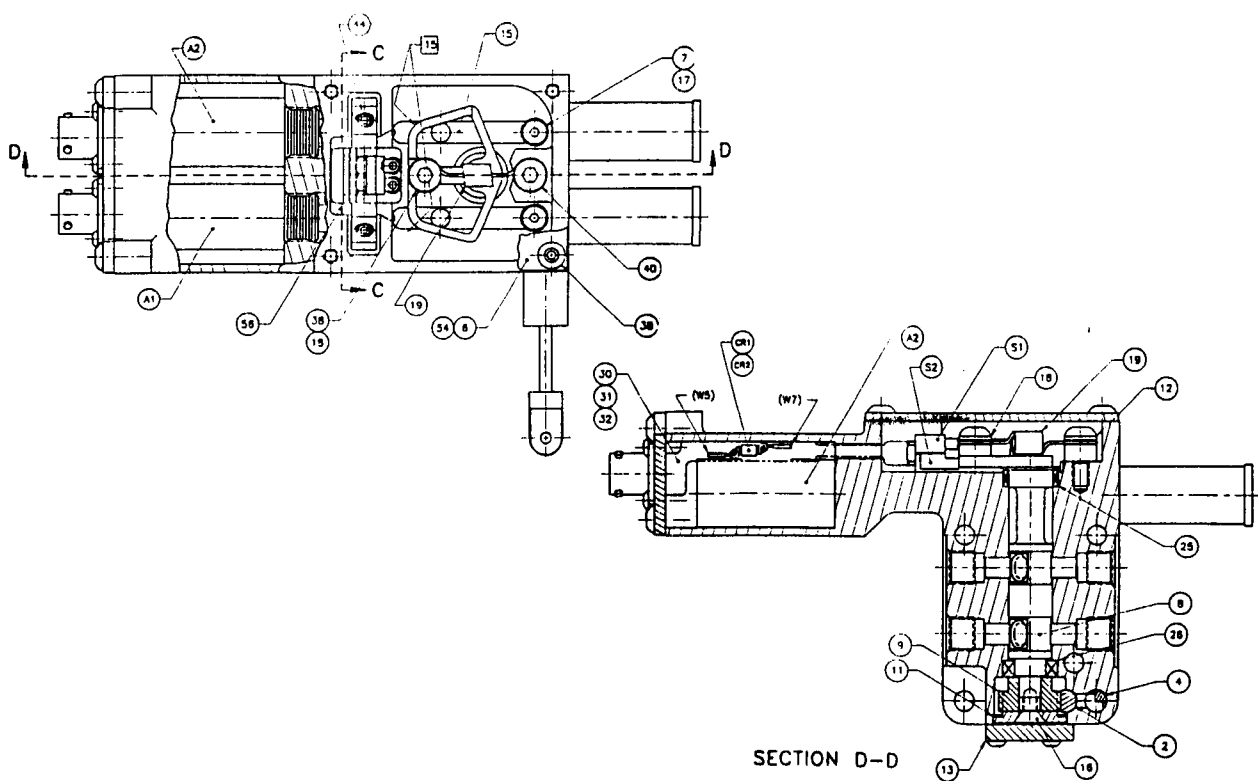


**Figure 5: Cross-Sectional Views of the Interrupter**

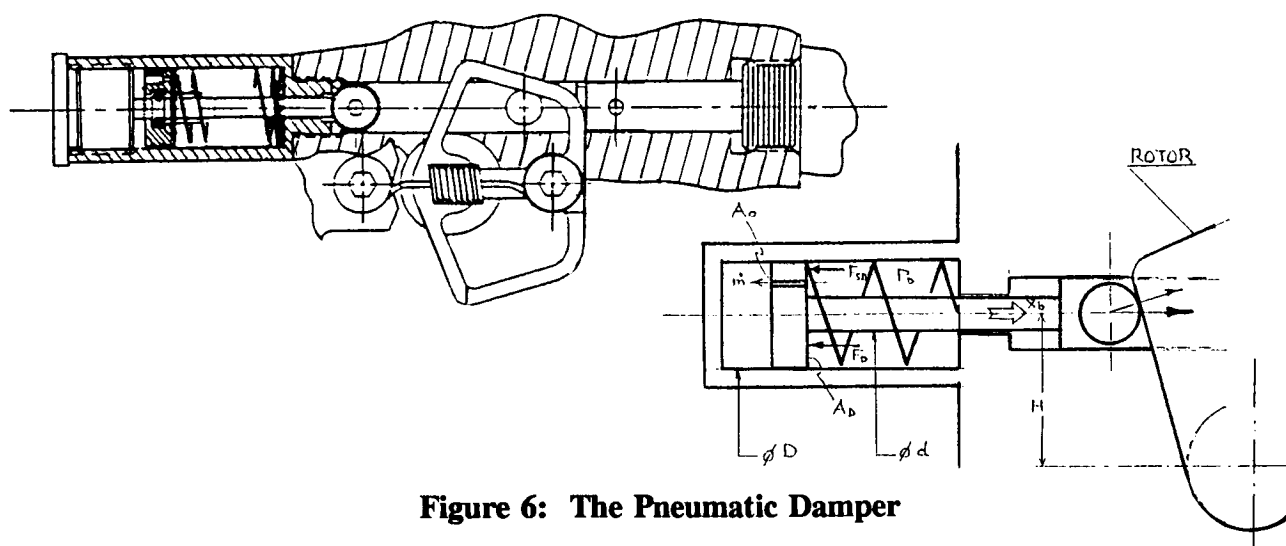


**Figure 6: The Pneumatic Damper**

An unusual feature of the Interrupter drive train is the incorporation of pneumatic dampers, which are coupled in-line with each of the solenoid actuated pull rods. The purpose of these dampers is to prevent the rollers from hammering on the rotor, during shock and vibration exposure. Each damper, as shown in Figure 6, consists of a spring-loaded piston riding in the bore of a tubular extension on the housing. The damper-piston head and rod are sealed by dynamic "labyrinth" glands designed to minimize friction drag. The damping force is controlled by an orifice through the head of the piston. Figure 7 shows the calculated effect of one of these dampers on the rotational velocity of the rotor. The rotor shaft, which is mounted in plain bearings at each end, is the barrier which blocks (or permits) detonation propagation between the input (donor) and output (receptor) tips on the ordnance transfer lines which are coupled to the Interrupter. Two transverse apertures in the shaft are aligned with the ports to provide propagation paths when the rotor is in the Armed state. When Safe, the apertures are maintained at 90 degrees to the propagation paths. The apertures, which are carefully configured slots rather than cylindrical bores, are shown in Figure 8.

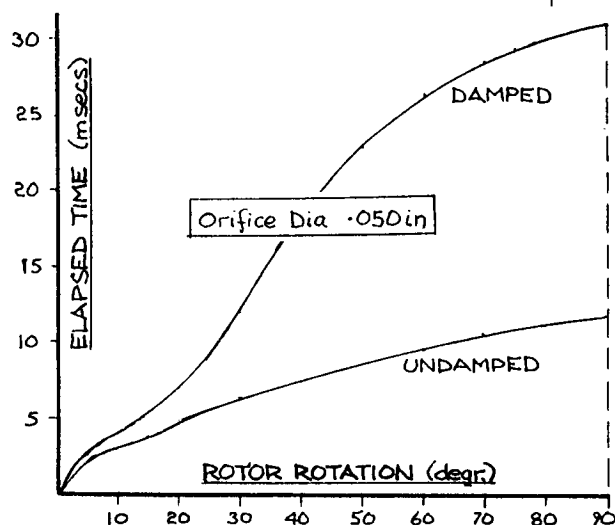


**Figure 7:  
Damper Effect on Rotor**

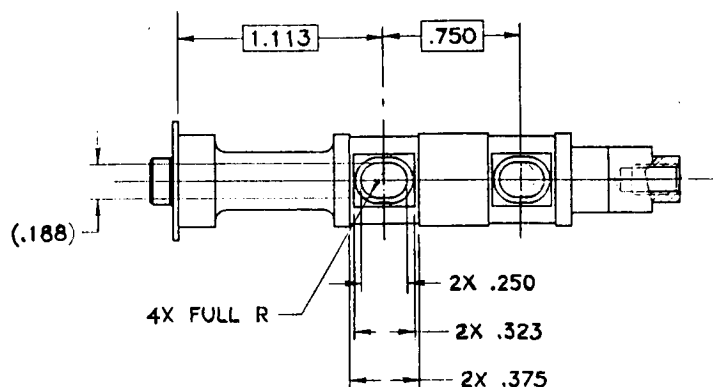


**Figure 8:  
Propagation Apertures in Rotor Shaft**

The dimensions and configuration of these slots evolved during development testing, to provide reliable detonation propagation across an airgap of almost 1/2 inch. To put this simple fact in perspective, the airgaps between donor and receptor tips in ordnance transfer lines are usually of the order of 40 to 60 thousandths of an inch.

As shown in Figure 9 a spur gear is mounted on the outboard end of the rotor shaft. This gear meshes with a floating gear-rack, which is coupled, by means of a pin projecting from its back-face, with a spring-loaded push rod. Depressing the push rod against its spring, by the insertion of a Safing key, will thus activate the rack, thereby causing the spur gear, and hence the rotor shaft, to rotate. This is the mechanism for manually driving the interrupter from the Arm to the Safe state. A partially slotted section in the push rod ensures that it can only drive the rack in the Safing direction. In other words, the unit cannot be manually driven from the Safe to the Arm position. The Safing Key that is used with this device is a simple bayonet-type pin featuring a radial button and integral blade at one end. When the key is inserted into the housing, its radial button engages a slot which guides the blade on the key into engagement with a clevis on the end of the push rod. As insertion continues, the key depresses the push rod, which is also guided by a pin-in-slot feature, thereby safing the unit. After the key is fully inserted, it is rotated 90 degrees, where its button meets a stop. From this position, the spring-loaded push rod forces the key back, until its button is captured in a detent slot. At this point, with the Safing Key detented while holding the push rod in a depressed (and rotated) state, the Interrupter is locked in the Safe condition.

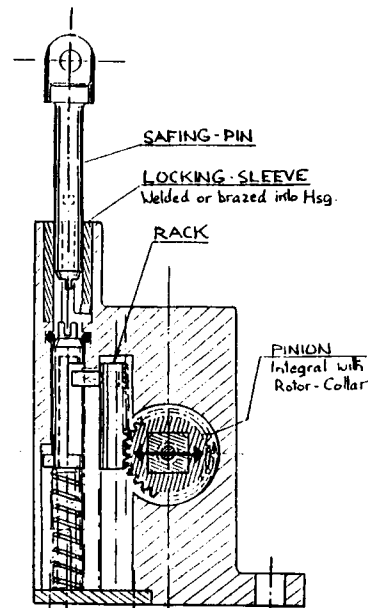


**Figure 9:**  
**Manual Safing Mechanism**

One simple feature on the push-rod permits the Interrupter to satisfy a current test range requirement which stipulates that, when installed, SAD safing keys must not be removable when an inadvertent attempt is made to arm the device. A notch in the push rod is aligned with the pin on the rack when the detented Safing Key has rotated the engaged push rod through 90 degrees. This notch permits a small amount of rack movement if an attempt is made to drive the rotor from Safe to Arm. The amount of rack travel, which corresponds to approximately 10 degrees of rotor rotation, is sufficient to drive the rack pin into the push-rod notch. When trapped in the notch, the pin prevents rotation of the push-rod, which, in turn, prevents rotation of the Safing Key, and hence its removal from the unit.

As well as providing the detonation transfer barrier and an important part of the manual safing mechanism, the rotor shaft serves one more purpose, namely that of a flag bearer. A two-color disc is mounted on the end of the shaft, and viewed through an offset window in the housing, for visual status monitoring. When the shaft is in the Safe position, only the green side of the "Flag" disc is observable, when in the Armed

position, only the red side is seen.

A pair of passive electrical circuits are incorporated in the Interrupter, for remote interrogation and monitoring of the unit's Safe/Arm status. These circuits, which are shown schematically in Figure 10, are alternately closed by sub-miniature snap-action electrical switches, actuated by the rotor. This design approach was selected primarily because of its simplicity, hence potential reliability and cost effectiveness, compared with the PCB/brush-contact type of rotary switches commonly used in SADs. The approach was rendered viable by the fact that no EED firing circuits require switching within the Interrupter.

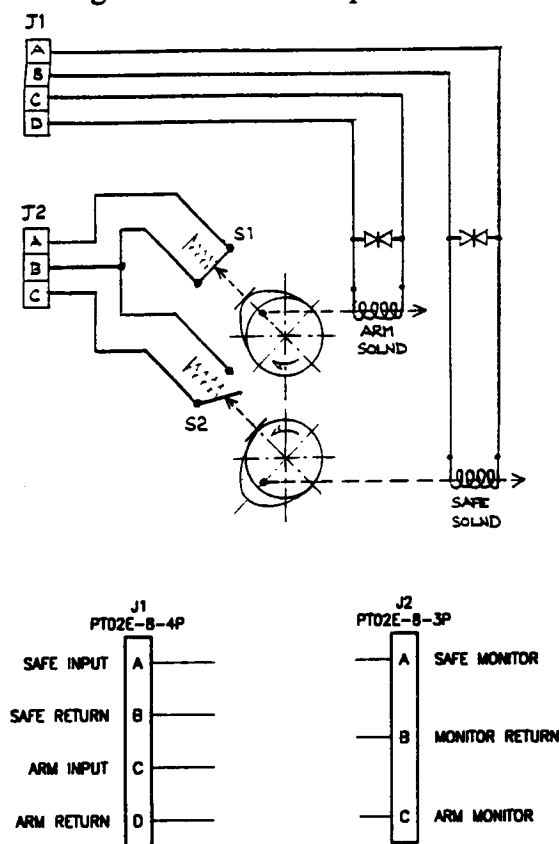


**Figure 10:**  
**Interrupter Electrical Schematic**

## DEVELOPMENT

A comprehensive development test program was undertaken, directed towards the design characterization and refinement of the barrier, relative to its effectiveness, both as a block, and as a propagation path in the ordnance transfer line. The blocking tests were conducted using special fixtures capable of precision settings of a range of angular misalignments. Short lengths of CDF line, with standard detonation end-tips, were used to accurately represent the transfer lines in these tests. Effective and reliable blocking was found with the barrier apertures less than 40 degrees out of alignment with the output ports. In the Safe position, the apertures are misaligned a full 90 degrees.

During the transfer tests, several changes were made to the barrier aperture configuration before reliable propagation across the 1/2 inch airgap could be achieved. When the optimum aperture size and shape appeared to have been derived, it was proven by means of a Bruceton series of tests.

A commercially available linear solenoid was selected as the drive-train prime mover, because of its compact size and advertised high pull-in force. During development testing, the solenoid proved to be marginal in performance at the specified lowest input voltage level. This was partly because the switch actuator drag forces, on the rotor, were higher than expected. Changes were made to the switch actuators, and eventually the switches themselves were changed, resulting in a solution to the problem. In a recent design refinement of the Interrupter, the solenoids were increased in size to substantially enhance the pull-in force margin.

**EXPLOSIVE GAP PROPAGATION:** Tests per DOD-E-83578

**VIBRATION:**

| <u>Frequency</u> | <u>X and Y Axis</u>     | <u>Z Axis</u>           |
|------------------|-------------------------|-------------------------|
| 20 Hz            | .026 G <sup>2</sup> /Hz | .041 G <sup>2</sup> /Hz |
| 20 to 70 Hz      | +6 dB per Octave        | +6 dB per Octave        |
| 70 to 800 Hz     | 0.32 G <sup>2</sup> /Hz | 0.50 G <sup>2</sup> /Hz |
| 800 to 20000 Hz  | -6 dB per Octave        | -6 dB per Octave        |
| 2000 Hz          | .051 G <sup>2</sup> /Hz | .080 G <sup>2</sup> /Hz |
| Overall          | 19.8 GRMS               | 25.0 GRMS               |

**SHOCK:**

| <u>Frequency</u> | <u>Peak Acceleration</u> |
|------------------|--------------------------|
| 100              | 45                       |
| 100 to 1500      | +5 dB per Octave         |
| 1500             | 4100                     |
| 3000             | 4100                     |

**BENCH TEST:** 25 cycle test at vacuum (26.8V input)

**TEMPERATURE CYCLING:** 8 cycles -85°F and +180°F

**CYCLE LIFE TEST:** 1000 cycles

**STALL TEST:** 32V input for 5 minutes and for 1 hour

**Figure 11: The Qualification Test Program**

One area of concern, going into the development program, was the possibility of the linear drive trains dislodging and displacing the detented rotor, when subjected to the full range of shock and vibration environments specified by the customer. No such problems were experienced when the units were subjected to the dynamic tests, thus indicating the effectiveness of the pneumatic dampers.

## **QUALIFICATION**

In September of 1993, a group of Interrupters successfully completed a qualification test program, as defined by the customer. Figure 11 shows the tests that were conducted, which included temperature cycling and a 1,000 cycle life test, as well as the dynamic environments. This program has qualified the Interrupter for flight at the Wallops Island Test Range.

## **FUTURE REFINEMENTS**

The Interrupter is a new product, and as such, we would be very naive to think that it cannot be improved. As already noted, the solenoids in the first units were smaller than optimum, and the next larger standard frame size solenoid is planned for future units.

Already, studies have been made on a cost effective installation of a rotary switch, as shown in Figure 12. This will reduce frictional drag on the rotor, as well as provide for the switching of additional circuitry. In a current new application for the Interrupter, EEDs will replace the input transfer lines. The firing circuits for these EEDs will be routed from the power input connector to the rotary switch, and back outside the housing through an additional connector. The EEDs would be cabled to the additional connector, which will be



mounted on the aft face of the housing.

Another possible design refinement would be full integration of the pneumatic dampers within the main housing, rather than in the tubular extensions. This would have the advantage of reducing the overall length of the unit, although it might make the assembly of the device slightly more difficult, therefore, more expensive.

## CONCLUSION

The Interrupter described in this paper is a "patent pending" device which offers a significantly lower cost alternative to conventional Safe and Arm devices, for some applications. The original design was limited to applications involving ordnance transfer lines interconnecting system initiators with independent output devices. A recent refinement to the Interrupter, in which a rotary switch replaces the original microswitches and an additional connector is added, permits electrically initiated detonators to be installed in the unit's input ports. This would allow the Interrupter to be used in many more SAD applications. The refinements will not eliminate the basic advantage that prompted the generation of the Interrupter concept in the first place. That is, the Interrupter will remain a completely passive device, with no internal ordnance components, hence it will be completely safe to handle.

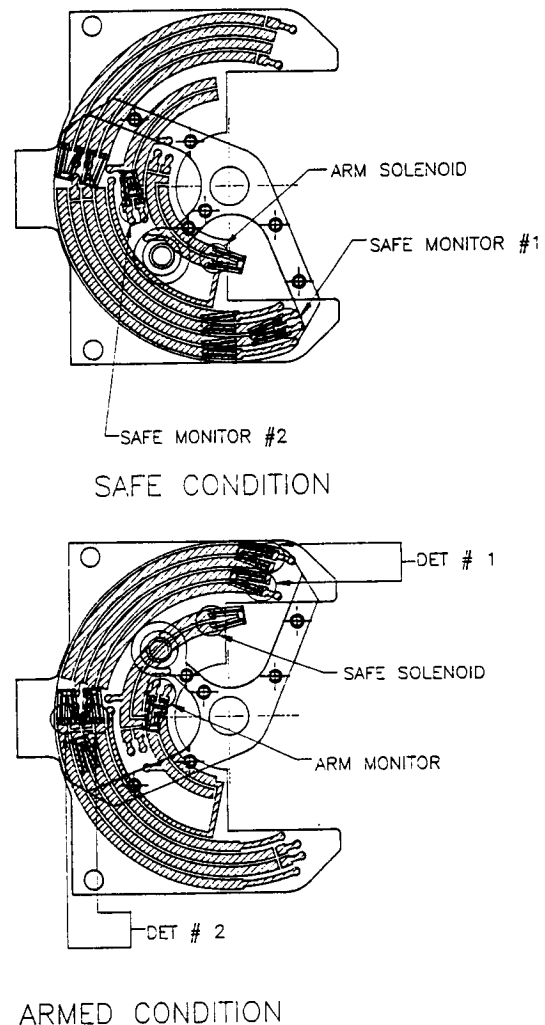


**Figure 12:**  
**The Rotary Switch Refinement**

## A VERY LOW SHOCK ALTERNATIVE TO CONVENTIONAL PYROTECHNICALLY OPERATED RELEASE DEVICES

Mr. Steven P. Robinson  
Senior Mechanical Design Engineer - Research & Technology  
Boeing Defense & Space Group  
Seattle, Washington

### ABSTRACT

NiTiNOL is best known for its ability to remember a preset shape, even after being "plastically" deformed. This is accomplished by heating the material to an elevated temperature up to 120 degrees C. However, NiTiNOL has other material and mechanical properties that provide a novel method of structural release. This combination of properties allows NiTiNOL to be used as a mechanical fuse between structural components. When electrical power is applied to the NiTiNOL fuse(s), the material is annealed reducing the mechanical strength to a small fraction of the as-wrought material. The preload then fractures the weakened NiTiNOL fuse(s) and releases the structure.

This paper describes the mechanical characteristics of the NiTiNOL alloy used in this invention, structural separation design concepts using the NiTiNOL material, and initial test data. Elimination of the safety hazard, high shock levels, and non-reusability inherent with pyrotechnic separation devices allows NiTiNOL actuated release devices to become a viable alternative for aerospace components and systems.

### INTRODUCTION

Explosive bolts and separation nuts have been successfully applied for structural release operations for over 40 years. These devices were simple, cost effective and very reliable. However, the increased sophistication, and susceptibility, of electrical and electronic systems in aircraft, missiles and spacecraft has increased the effect of pyrotechnically actuated release devices from being a mere nuisance to a critical path situation that must be accounted for in assuring successful system performance. This has elevated the status of structural separation testing, via

explosive bolts, to a very time consuming and costly endeavour.

Within the last five years, emphasis has been placed on finding alternatives to explosive bolts and separation nuts. The reason for this change of direction is based primarily with the explosive nature of these devices. The safety issues, when dealing with explosives, add additional costs to assembly, testing and storage of aerospace components. The shock generated by these devices is becoming a critical design consideration because of the sophisticated electronics being implemented to lower cost and improve system performance. EMI susceptibility, potential contamination from explosive byproducts and limited shelf life are other factors that demonstrate explosive structural separation is no longer as cost effective and simple to use as in the past.

Historically, non-explosive structural separation involved electro-magnetic solenoids or wax actuators pulling pins to release the structural elements. These are capable of performing the release functions but operate at a distinct disadvantage because of the slower actuation speed and greater volume and weight compared to pyrotechnic devices.

Since 1986, Boeing Defense & Space Group has been actively researching a class of materials known as Shape Memory Effect (SME) alloys to provide a simple actuation mechanism that will combine the best features of both non-pyrotechnic and pyrotechnic release technologies. Through this work, Boeing has developed proof-of-concept structural release concepts based on the shape memory effect characteristic of NiTiNOL. These early concepts demonstrated that NiTiNOL is capable of achieving most of the design goals of eliminating explosives, providing reliable performance, and demonstrating multiple operation capability. However, these devices were volume

inefficient and slow compared to existing pyrotechnic equivalents.

To improve the performance of our release design concepts, a review of the basic characteristics of NiTiNOL was initiated to determine if any properties were overlooked that would help reduce the size and/or increase speed of operation. This review uncovered the fact that "as-wrought" NiTiNOL, prior to annealing, is very strong. The ultimate tensile strength can be as high as 270 KSI. When the NiTiNOL is annealed, restoring the crystalline phase structure necessary for shape recovery, the ultimate tensile strength is reduced by a factor of 2 or more. This fact along with other characteristics such as high electrical resistance, excellent corrosion and fatigue capabilities led us to believe that a simple, effective, and fast NiTiNOL mechanical "fuse" separation concept is feasible.

Using NiTiNOL as a mechanical "fuse" appeared to be a simple structural separation concept with few of the problems associated with pyrotechnic devices.

#### INITIAL CONCEPT DEVELOPMENT

The first test to demonstrate the NiTiNOL mechanical fuse concept was relatively simple. This is shown in Figure 1. One end of a NiTiNOL wire was mounted

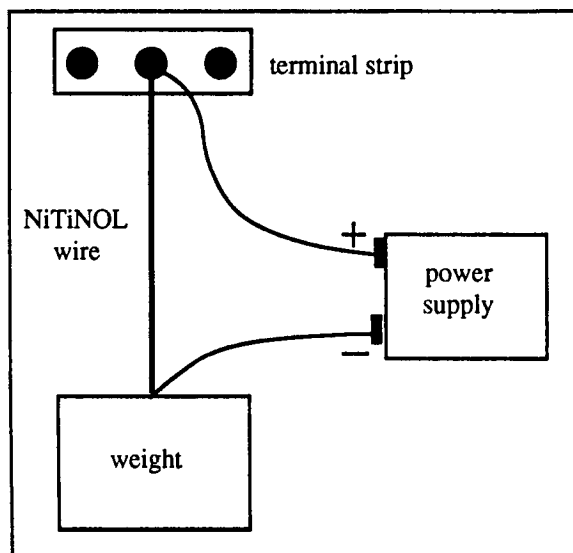


Figure 1 NiTiNOL Structural "Fuse" Test Set-up

to a terminal strip. This was also the positive terminal of a power supply. A weight was suspended from the wire. The other end of the NiTiNOL wire was tied to the negative terminal of the power supply. When power is applied, the NiTiNOL is heated well into its annealing temperature zone. The strength of the NiTiNOL falls to near zero allowing the dead weight to fracture the wire releasing the weight.

This demonstrated that using NiTiNOL as a mechanical fuse as a means of holding and releasing a given preload was feasible. However, any structural alloy should be capable of accomplishing the same task. A comparison chart showing the requirements of a mechanical fuse compared to the characteristics of NiTiNOL, nichrome, beryllium-copper, and steel is given in Figure 2. As shown, NiTiNOL has the best combination of properties necessary for a mechanical fuse release concept.

The most significant factor is the dramatic change in strength capability at elevated temperature. This reduction in the tensile strength of NiTiNOL is crucial to the preload breaking the structural tie and releasing the load. None of the other materials show as large a strength reduction at elevated temperature.

The demonstration of fusing a single NiTiNOL element does not automatically demonstrate the idea can be scaled up to practical sizes and applications. Since conventional separation nuts are capable of loads up to 25,000 lbf, the NiTiNOL separation idea would also have to be capable of achieving these load levels. In order to accomplish this, a relatively large number of NiTiNOL fuses would have to be incorporated in parallel fashion to increase the load carrying capability to levels equivalent to explosive bolts and nuts. Multiple NiTiNOL fuse element arrangements appear to be the only way to maintain large load carrying capability and still have the resistance of the elements high enough for efficient electrical heating

However, the large number of elements, if they were all heated at the same time, would require a prohibitive amount of electrical power. This is not possible with existing power system ratings on today's aerospace systems. A NiTiNOL fusible element requires a low voltage, high current electrical pulse to efficiently heat the element in the shortest amount of time.

A review of separation time requirements showed a large percentage of release operations do not require separation times less than 10 milliseconds as is typical of pyrotechnically operated separation nuts and bolts. The near instantaneous release time is just a consequence of utilizing explosives in the separation device. This fact allows us to reduce the number of elements being heated at any one time to a minimum because separation time is not always critical.

By applying this fact to the NiTiNOL fuse concept, we can reduce the instantaneous power requirement to manageable levels. This is shown in figure 3. The 5 element group is mechanically attached in parallel to

distribute the load and increase the overall load carrying capability. The element lengths are all

Material Property Comparison Chart

| Properties                          | fuse req'm'ts | NiTiNOL | 17-4PH Steel | 304 Steel | Beryllium Copper | Nichrome Ni 70, Cr 25, other s |
|-------------------------------------|---------------|---------|--------------|-----------|------------------|--------------------------------|
| electrical resistivity (microhm-cm) | High          | 100     | 100          | 72        | 20               | 134                            |
| tensile strength (KSI) (room temp.) | High          | 250     | 210          | 110       | 115              | 150                            |
| tensile strength (KSI) (1000 deg F) | Low           | >25     | 150          | 50        | 85               | 100                            |
| corrosion resistance                | High          | High    | High         | High      | Med.             | High                           |
| fatigue resistance                  | High          | High    | High         | Med.      | High             | -                              |
| thermal conductivity (BTU/hr-ft-F)  | Low           | 10.4    | 10.4         | 9.4       | 120              | 5.4                            |

Comparison of NiTiNOL to other structural alloys

Figure 2

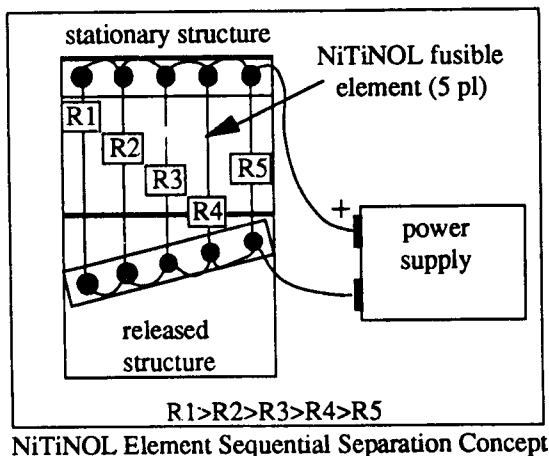
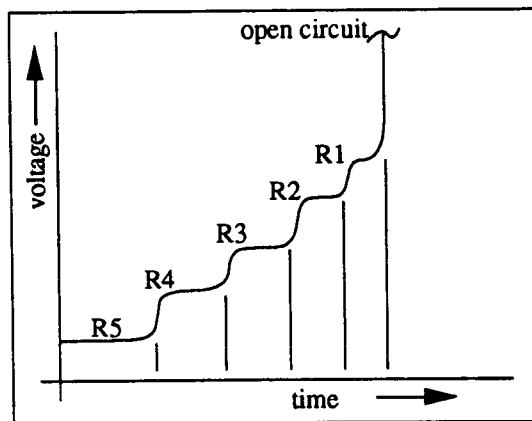


Figure 3

different to produce a uniformly increasing resistance value range. The elements are wired in parallel. When current flows through the elements, the shortest NiTiNOL fuse draws the most current, heats the fastest and fractures first. Now the load is carried among fewer elements. This increases the stress levels in each element. The power is also shared among fewer elements causing the elements to heat even faster. This cascading effect fractures each higher resistance element until the last one in the group separates. Figure 4 shows an idealized trace of the cascading separation effect. The increasing resistance of each successive element causes a distinctive zipping effect.

To further increase the load carrying capability, multiple groups of these subsets of NiTiNOL fusible elements can be arranged to be released in series. As soon as the last element in the first group separates, power is transferred to the next group of elements, thereby continuing the separation sequence.



NiTiNOL Fusible Element Release Sequence

Figure 4

The number of element groups can be increased to accommodate a wide range of loading conditions. The time-to-separate requirement must be addressed to assure there is no impact to the overall separation operation.

However, the increase in the separation time may not be critical if a two step separation approach is taken. An "arming" operation could take place which would release the majority of NiTiNOL fuse elements. This would leave a minimum number of elements to maintain the structural attachment. When actual separation occurs, the power required and separation time will be kept to a minimum due to the minimum number of elements left to fuse open. This concept allows a large number of structural elements to be maintained across the joint satisfying a wide range of available power, time-to-separate, and structural load cases.

This concept is postulated for large separation joints such as payload fairings and other large linear structural interfaces. In fact, the majority of this work was performed in anticipation of the next generation heavy lift launch vehicles (HLLVs).

As a result of this initial work, a patent (#5,046,426) has been awarded to The Boeing Company.

#### NASA/JSC SEQUENTIAL SEPARATION TEST

Using the concept described in the previous section, Boeing Defense & Space Group was contracted by

NASA/JSC to perform a feasibility experiment demonstrating that a NiTiNOL sequential structural separation system is capable of loads in the range needed for commercial applications. Since this was a small experiment, a candidate separation load was assumed to be 5000 lbf. This would provide a reasonable loading condition without imposing extra costs.

The basic design concept is shown in figure 5. To expedite the experimental hardware fabrication, we utilized NiTiNOL strip, 1.4" w x 0.004" t, that was available in-house, as part of our ongoing IR&D effort. Although the dimensions of the strip was not optimized for this experiment, we felt valuable information on laser cutting of NiTiNOL and operation of this patented NiTiNOL non-pyrotechnic release concept could be achieved.

The structural members were fabricated from 4.0" dia. molybdenum disulfide impregnated nylon. This provided an inexpensive, electrically isolating material capable of handling the 5000 lbf projected load. Mounting studs were attached to the center of the nylon parts to provide sufficient grip length for installation onto an Instron tensile test machine. The NiTiNOL fusible element strip was installed across the interface between nylon members. The NiTiNOL fusible element member was attached by two(2) rows of 32 each 6-32 fasteners. These were installed into tapped holes in the nylon parts. The load across each fastener was 125 lbf max. The one concern was whether the attachment holes, in the NiTiNOL strip, were strong enough to react the tensile load without tearing out.

The cutout pattern and slots, defined the five (5) NiTiNOL fusing elements per each of the eight (8) groups. The cutouts were produced by a high powered laser cutting system located in the Boeing Materials Technology Laboratory located in Renton, Wa. Utilizing computer controlled laser cutting provided several benefits. Unique patterns can be cut into the strip with great accuracy. This also provides a high degree of dimensional repeatability, critical for some operations. Laser cutting also provides a way to minimize the area of the heat affected zone which would compromise the large differential strength characteristic of NiTiNOL from its unannealed state to its annealed state.

The structural separation operation uses an electrical circuit that applies battery power to opposite pairs of fusing elements. This assures a symmetrical release of the load minimizing any off-axis unloading situations resulting in excessive tip-off rates. As the last elements of the first two groups are fused opened, battery power is switched to the next pair of fusing

element groups. This continues until all fusing pairs of element groups have been severed. The circuit diagram is shown in figure 6. To expedite the circuit design, automobile starter solenoids were utilized in the circuit design to transfer battery power between NiTiNOL fusing element groups.

When switch S1 is engaged, 28 V is applied to the first starter solenoid closing the circuit and applying 12 V battery power across opposite groups of NiTiNOL elements. The 4 ohm resistor prevents the second solenoid from engaging until the last NiTiNOL element, from the first 2 groups, has fused open. Battery power is then switched to engage the second solenoid, which in turn applies battery power to the next pair of opposite NiTiNOL element groups. This continues until the last NiTiNOL elements are fractured releasing the structural load.

#### EXPERIMENTAL TEST RESULTS

Using 0.004" thick foil for this test generated concern that the foil might fail in the attachment holes at the required load of 5000 lbf. A load test was performed to determine the maximum load capability. As predicted, the failure occurred in the mounting holes at approximately 3200 lbf. It was obvious that a goal of 5000 lb was not possible with the current material. However, no alternative was available to support testing. Therefore, it was recommended that the test load be reduced to 2000 lbf. This would still demonstrate the feasibility of this technology with the current experimental hardware at a realistic load value.

One test was performed to demonstrate feasibility. The test article was mounted on an Instron tensile test machine with full scale readout of 5000 lbf. The load was uniformly increased to 2000 lb indicated. As the load reached the test level, switch S1 was closed applying power to the first solenoid. The first pair of NiTiNOL element groups fused opened in 156 milliseconds, the second pair in 182 msec, the third pair in 164 msec, and the last pair in 194 msec. The total time to release was 0.838 seconds. The trace of the release operation is shown in figure 7. As the oscilloscope trace shows there was some bounce of the solenoid contacts generating some delay of power to the NiTiNOL elements, increasing the apparent separation time.

The circuit performed as designed. Once the switch was engaged, the application of battery power was autonomous and continuous. This resulted in a very simple circuit capable of transferring high current pulses as many times as needed.

# NITINOL RELEASE TEST FIXTURE(FULLY ASSEMBLED)

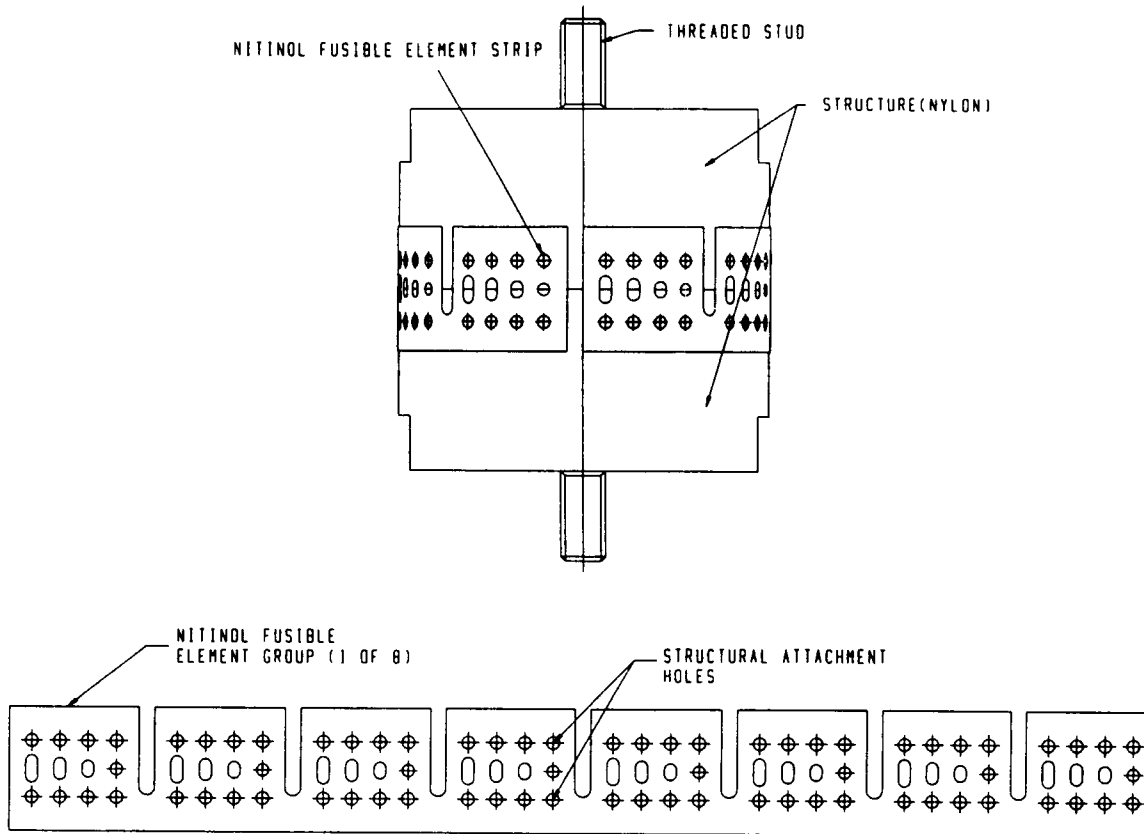


Figure 5 NASA/JSC Sequential Structural Separation Demonstration Experiment

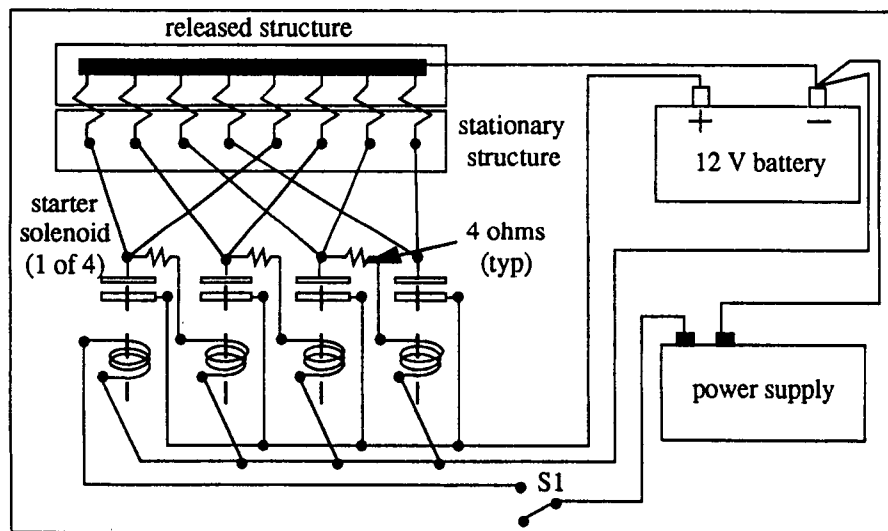


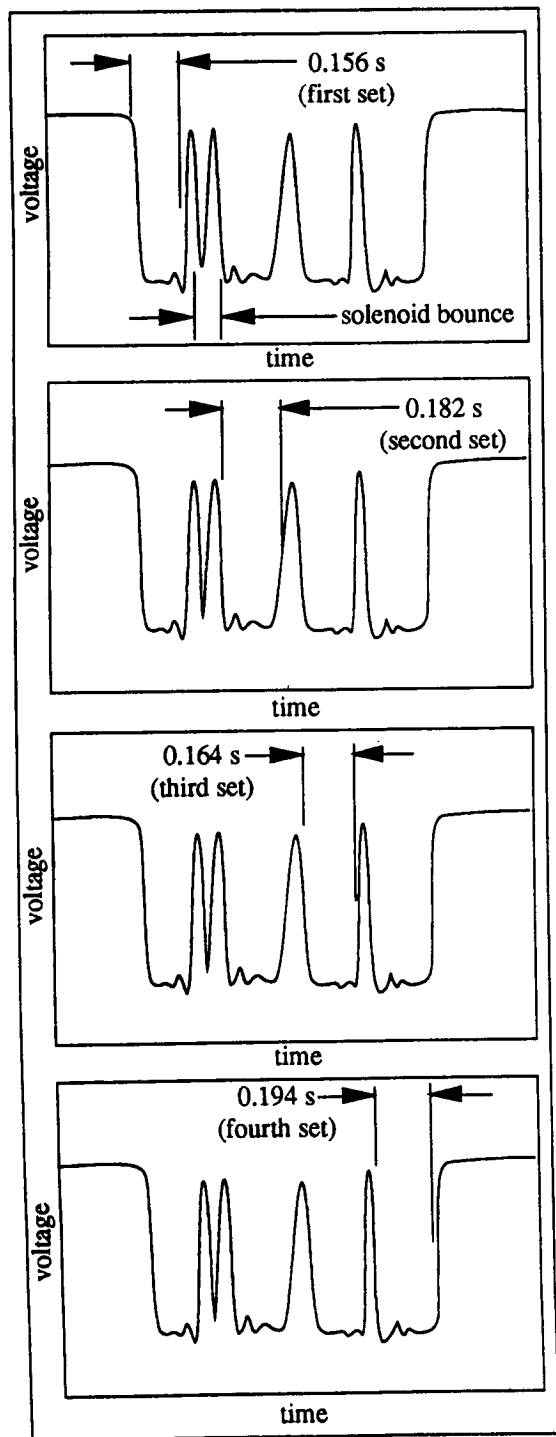
Figure 6 NASA/JSC NiTiNOL Fusing Element Electrical Circuit

## SUMMARY

Boeing Defense & Space Group believes this technology could provide a viable alternative to explosive separation systems utilizing linear shaped charges to weaken and fracture a structural joint, such

as those on large payload shrouds. Further research into the possibility of gradually releasing the preload, prior to full separation, offers design possibilities that could reduce the shock of separation, power usage, and separation time even further.

Although this type of release concept may require a unique electrical system, such as dedicated on-board batteries, the changes appear to be minimal and simple to implement.



Time-to-Release Separation Test - Oscilloscope Traces (2000 lbf preload)

Figure 7

If an existing electrical system, capable of operating pyrotechnic devices with 5A DC max. current output is the only source of power, work was accomplished, under contract with the Naval Research Laboratory, to develop such a release device, for spacecraft use, based on this invention. This work is described in the following section.

#### NiTiNOL FUSIBLE LINK RELEASE DEVICE (NAVAL RESEARCH LABORATORY)

The Naval Research Laboratory contracted with Boeing to develop a NiTiNOL based mechanism to be included as part of the Advanced Release Technologies (ARTs) program. The requirement of being able to interface with an existing 28V/5A spacecraft power bus system needed a different design approach than the NASA/JSC concept. In order to accomplish separation of a 2000 lbf preload within 0.250 second using a limited power budget, we used a single NiTiNOL fusible element, in conjunction with a large mechanical advantage, as the active member to accommodate a 2000 lbf preload. The basic concept is shown in figure 8.

The overall size of the device is 3.50" x 3.50" x 1.5". Although larger than conventional separation nut designs, the size envelope is small enough to be useful in many separation operations. Future design iterations can conceivably reduce the size even further.

The most significant change between the NASA/JSC concept and this concept is the use of a 9:1 step-down transformer. The transformer, along with the DC/AC converter electronics, allows the device to operate with an existing 28V/5A max electrical power bus system. This system is typical of current spacecraft designs. The electronics converts 28V DC to 28V AC at 100 KHz. The step-down transformer converts the chopped 28 V/5A AC to approx. 3.1 V/45 A AC power. The high frequency of the chopper electronics allows us to use the smallest transformer possible. The total power usage has not changed. However, it has been converted to a more useable form for efficient heating of the NiTiNOL fusible element.

The design concept provides a mechanical advantage of approximately 24:1. This enables a NiTiNOL fusible link, sized for 150 lbf, to be able to withstand a 2000 lbf preload. In fact, the fusible link is sized for 3600 lbf. This corresponds to a positive margin of safety of approximately +1.75. The NiTiNOL fusible link design is also shown in figure 8. In order to minimize the transformer lead lengths, the design of the fusible link is a U-shape configuration allowing both transformer leads to be on the same side of the release device. This also provided the added benefit of

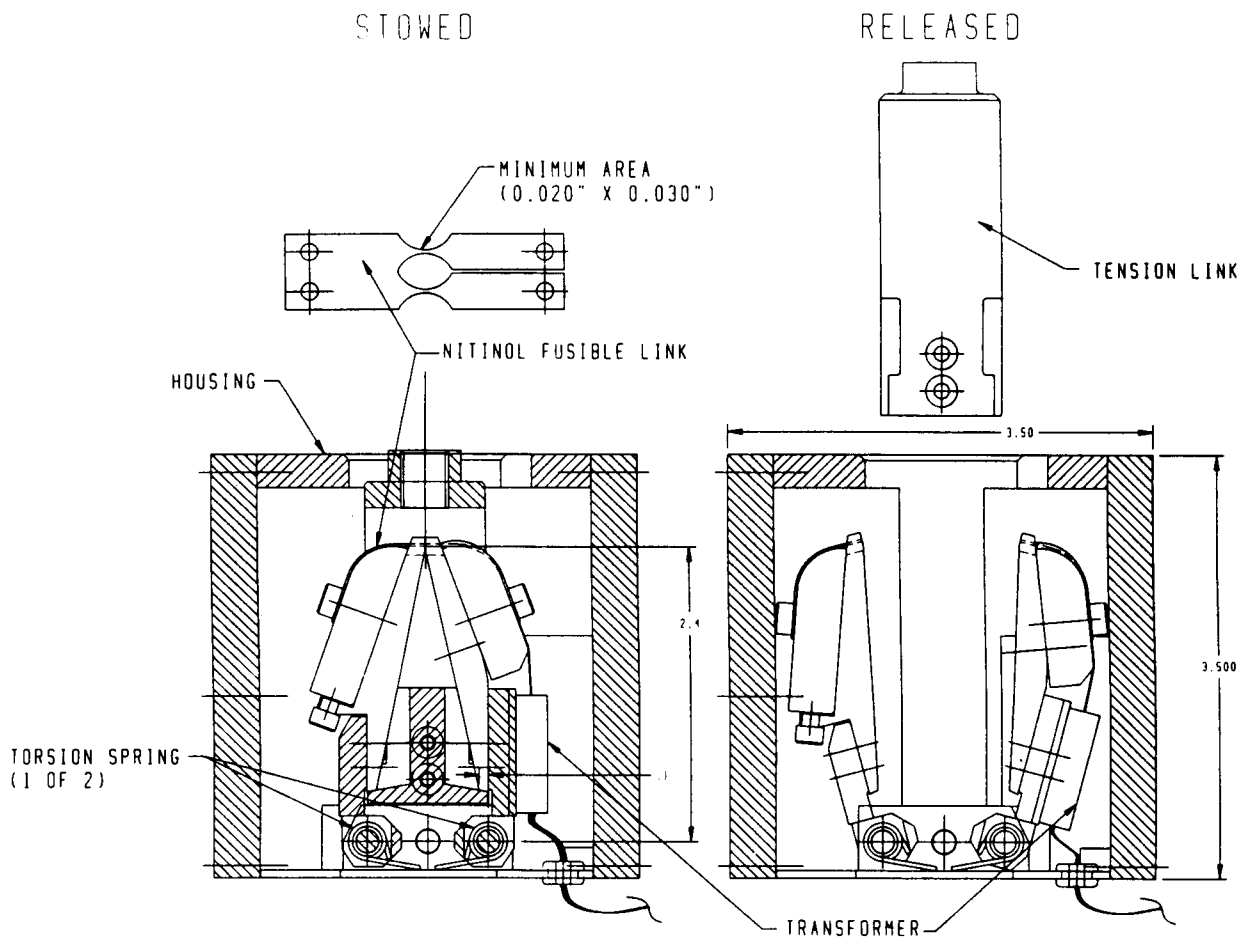


Figure 8 NiTiNOL Fusible Link Release Device (NRL)

doubling the strength of the NiTiNOL mechanical fuse without increasing the overall size of the release device.

The release device configuration is straightforward. Two (2) spring loaded jaws are closed to capture the tension link. The NiTiNOL fusible link is installed on two phenolic blocks at the ends of the jaws. The jaws have a step at the bottom where the tension link engages the jaws. When the preload is applied through the tension link, the step creates a 0.10" moment arm. The NiTiNOL fusible link has a moment arm of 2.4". This creates a 24:1 mechanical advantage. This allows a relatively small fusible link to be employed against a substantial preload. Figure 9 describes the geometry in greater detail.

In order to keep the device weight and volume to a minimum, the transformer, designed to operate at a frequency of 100 KHz, was used. The transformer size

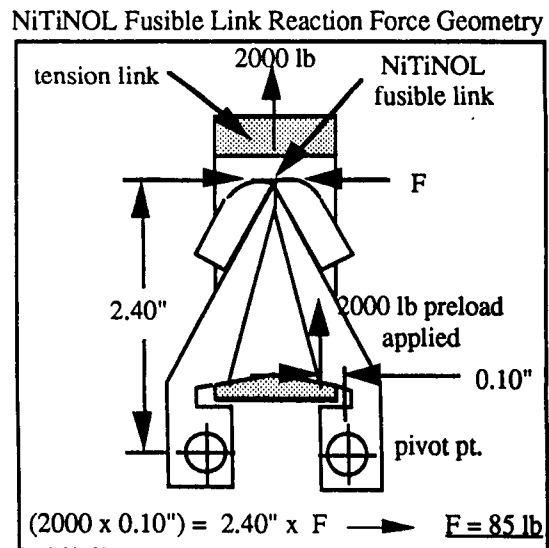


Figure 9



was 1.3" L x 1.0" W x 0.25" t. Mounting the transformer to one of the jaws kept wire lengths to a minimum. This prevented inductance from becoming a problem. Too much inductance would reduce the amount of power through the NiTiNOL fusible link compromising the heating of the NiTiNOL and the performance of the device.

The preload is applied by threading a bolt into the top of the tension link assembly. As the bolt was torqued, the tension link would be pulled up and engage the jaws. The moment generated by the tension link against the jaw tries to force the jaws apart. The NiTiNOL fusible element reacts this torque until the NiTiNOL is electrically heated. When this occurs, the link becomes structurally weak and fractures, allowing the jaws to spring out and the tension link to be extracted.

The DC to AC chopping circuit is on a separate board and can be installed in any convenient place. It can also be installed on the release device housing itself.

#### TEST RESULTS

The release device was proofloaded to 2000 lbf without separation. When power was applied, the release device demonstrated release time less than 200 msec. Several tests were also conducted at lower preloads. The effect of the preload variation on release time was apparent. It showed that lower preload values yielded higher release times. At no preload, the release time was approximately 50% greater. This required the NiTiNOL to be heated to near the melting temperature. Under actual conditions, this zero preload situation would be very remote.

A longterm loading effects test was also performed on a NiTiNOL fusible element. This was to determine if any stress relaxation or creep phenomenon was present using NiTiNOL. The link was mounted in a fixture with a simulated preload. This was stored for approximately six (6) months. Measurements were taken on a daily basis. No significant increase in length was observed for the entire 6 month period.

Separation tests confirmed the ability of a NiTiNOL fusible link release device to maintain and release a 2000 lbf preload reliably. Testing at NRL is ongoing. Initial testing shows separation times are consistently within 50 msec. However, this is dependent on the same power and preload being applied during each separation test.

#### SUMMARY

This non-pyrotechnic release concept demonstrated that a single NiTiNOL fusible element can reliably

hold and release a given preload using a typical 28V, 5A electrical bus system. Even with the apparent dependency of release time to preload, this can be attributed to the limited power available. The effect can be minimized by proper sizing of the NiTiNOL fusible link and optimizing the heating to the power availability. In addition, the shock of separation was insignificant. There is no contamination or safety issues associated with this device.

The release device is completely reusable except for the NiTiNOL fusible link. This feature allows the same device to be operated many times during ground testing, and still be available as the flight unit. The benefits of this device are shown in figure 10.

| Benefits                         |
|----------------------------------|
| 1) Non-pyrotechnic               |
| 2) Fly-as-tested capability      |
| 3) Little or no separation shock |
| 4) No shelf life limitations     |
| 5) No safety hazards             |
| 6) No EMI susceptibility         |
| 7) Fast separation time          |
| 8) No contamination potential    |

Figure 10 NiTiNOL Benefits Chart

These features can provide a very cost effective product especially if extensive ground testing is contemplated. The cost of the NiTiNOL material does not appear to be a limiting factor because commercial usage continues to increase as more applications are realized. As usage increases, the material price will decline accordingly.

#### CONCLUSION

Load capability and separation times demonstrated by these concepts show that NiTiNOL fusible element based devices, using this Boeing patent, have the potential to achieve the same performance as pyrotechnic devices. This can be accomplished without the detrimental effects attributed to the use of explosives.

Boeing Defense & Space Group feels this technology will provide a much needed reduction in safety related and shock environment issues involving aerospace vehicles. Reducing shock environmental requirements imposed on vehicle sub-systems and components will play a major role in reducing vehicle development costs. The costs associated with handling, storage and

assembly of pyrotechnic devices can be practically eliminated if this technology can be developed to its fullest capability.

Both of the concepts, described previously, offer both ends of the design spectrum that is possible using this simple technology. Many design alternatives can be created if the drawbacks, associated with pyrotechnic devices, can be eliminated. We understand this and are continuing to improve the basic concepts described here.

One of the most intriguing design possibilities is the two-step arming/separation function described previously. This idea offers unique advantages and

design flexibility that provides the designer with options not possible with conventional pyrotechnic systems. This ability to slowly release large preloads all but eliminates the heavy shock environment imposed on the surrounding structure. This can be accomplished without jeopardizing the actual release function.

The future of non-pyrotechnic structural separation, based on this patent, will be expanding. The capabilities offer so many advantages that this technology will become a major part of structural separation for the next generation of aerospace vehicles.

# INVESTIGATION OF FAILURE TO SEPARATE AN INCONEL 718 FRANGIBLE NUT

William C. Hoffman, III  
Carl Hohmann  
NASA Lyndon B. Johnson Space Center, Houston, TX

## Abstract

The 2.5-inch frangible nut is used in two places to attach the Space Shuttle Orbiter to the External Tank. It must be capable of sustaining structural loads and must also separate into two pieces upon command. Structural load capability is verified by proof loading each flight nut, while ability to separate is verified on a sample of a production lot. Production lots of frangible nuts beginning in 1987 experienced an inability to reliably separate using one of two redundant explosive boosters. The problems were identified in lot acceptance tests, and the cause of failure has been attributed to differences in the response of the Inconel 718. Subsequent tests performed on the frangible nuts resulted in design modifications to the nuts along with redesign of the explosive booster to reliably separate the frangible nut. The problem history along with the design modifications to both the explosive booster and frangible nut are discussed in this paper. Implications of this failure experience impact any pyrotechnic separation system involving fracture of materials with respect to design margin control and lot acceptance testing.

## Introduction

The 2.5-inch frangible nut is used in the Space Shuttle Program to attach the Orbiter to the External Tank at two aft attach points as shown in figure 1. Structural loads illustrated in table 1 are carried by each frangible nut. Upon completion of Space Shuttle Main Engine cutoff, at approximately 8 minutes, 31 seconds after Shuttle launch, the Orbiter is separated from the External Tank by initiation of pyrotechnics at the forward and aft attach points. Aft structural separation is accomplished by fracturing each of four webs on the two frangible nuts, as illustrated on figure 2. Separation is accomplished by initiating one or both of the -401 configuration booster cartridges shown in figure 3. The Orbiter frangible nuts are safety critical devices which are required to reliably operate for Shuttle crew safety. Production lots beginning in 1987 experienced an inability to operate reliably with the performance margins demonstrated in the original qualification. An intensive failure investigation followed which has identified the Inconel 718 used in the frangible

nuts as the cause of the failures. The manufacturer of Inconel 718 forgings used in the qualification and initial lots of frangible nuts for the Shuttle Program went out of business, and NASA was forced to solicit new sources for the frangible nuts. The change in Inconel 718 suppliers and the differences in the characteristics of the material led to a performance degradation.

The first section of this paper discusses the original qualification program and the original Inconel 718 material and chemical properties. The second section of the paper discusses the failure analysis performed by NASA and the resultant design solution arrived at through iterative testing.

## Design and Qualification History of 2.5-inch Frangible Nut

The 2.5-inch frangible nut is designed with two primary requirements. The first requirement is that the nut have the capability to carry structural loads with specified margins against material yield and rupture. The second requirement is that the frangible nut reliably separate into two pieces when either one or both booster cartridges are initiated. Inconel 718 was selected for the frangible nut due to the combined high material strengths, and to its resistance to creep and corrosion. The qualification matrix shown in table 2 illustrates the type and number of tests performed to demonstrate reliable operation in the presence of flight and ground environmental conditions. The performance margin was demonstrated using nominal booster cartridges in frangible nuts whose web thicknesses were increased above the maximum allowable by 20% as shown on the -101 margin nut in figure 4. Shuttle Program requirements dictate a margin demonstration of 15%, but the additional 5% margin was chosen to gain confidence in the frangible nut design. All margin tests were successful. Design, development, and test of the 2.5-inch frangible nut were conducted under NASA contract NAS 9-14000 and results of the qualification were reported in document CAR 01-45-114-0018-0007B<sup>1</sup>.

## Material Configuration of the Original Manufacturer's 2.5-inch Frangible Nut

The supplier of the qualification nuts and boosters procured Inconel 718 which was manufactured to meet AMS 5662<sup>2</sup>. A compilation of chemical data, material properties, and typical microstructure grain size for a representative Inconel 718 heat lot used in the original

manufacturer's frangible nuts is shown in table 3. No additional restrictions were placed on the Inconel 718 other than requiring compliance with AMS 5662. Figure 5 is a representative micrograph of the original manufacturer's Inconel 718 shown at a magnification of 100X.

Based upon the successful qualification program, the design was considered complete and production contracts were issued to support Shuttle flights.

#### Frangible Nut Production Failures

NASA solicited new manufacturers of the 2.5-inch frangible nut in 1987 in order to develop additional sources of supply for the Shuttle Program. Two qualification contracts were issued with the intent of demonstrating the new manufacturer's processes. The second manufacturer was awarded NASA contract NAS 9-17496 and the third manufacturer was awarded NASA contract NAS 9-17674. During qualification testing performed under NAS 9-17496<sup>3</sup>, in accordance with table 4, failures were encountered during frangible nut margin tests. The frangible nut failed to sever the outer web, web number 4 as shown in figure 6, when fired using a single booster cartridge. Further testing resulted in a successful separation using a margin nut with webs 15% over the maximum allowable thickness. In an effort to establish performance margin for the frangible nuts and booster cartridges, the weight of RDX in the booster cartridges used in margin tests was reduced by 15%, and nominal frangible nuts were used instead of nuts with 120% webs. Three margin tests successfully separated using 85% charge weight booster cartridges and nominal frangible nuts as shown in table 4.

Material properties, chemical data, and microstructure grain size for the Inconel 718 are shown in table 3. The Inconel 718 heat lot number for the NAS 9-17496 qualification lot is 9-11446. Figure 7 illustrates a 100 X micrograph taken for heat lot 9-11446. There is a dramatic difference in the precipitate distribution for heat lot 9-11446 as compared with the original manufacturer's Inconel 718 micrograph shown in figure 5.

The second manufacturer was authorized to produce additional frangible nuts based upon successful completion of the qualification program. The second lot of frangible nuts, Inconel 718 heat lot 9-10298, experienced an inability to separate under zero preload using a single booster cartridge. The gap developed from the single booster cartridge firing, illustrated in figure 6, was measured to be less than 0.100" for the failed unit. Web numbers 1 and 2 were fractured while web numbers 3 and 4 did not experience any cracking. Table 5 shows the chronology of tests performed to understand the failure cause and develop a means of overcoming the problem. A design solution was arrived at through the test series which consisted of modifications to both the frangible nut and booster cartridge.

NASA's first response to the failure was to redesign the booster cartridge to provide additional charge to overcome the resistance to separate. Booster cartridge internal cross sectional area was increased in increments

of 5% until successful separation was achieved. In the course of performing the above tests, the nut was observed to "clamshell" open until the outer ledge gap, shown in figure 6, was reduced to 0.00". The frangible nut outer ledge was machined to provide additional rotational motion for web number 4 (the outer web) and the modification to the frangible nut is illustrated in figure 8. The modified frangible nut was identified as a -302 configuration. An additional change was made by loading the nominal charge weight into the bore of a booster cartridge body which had been increased in cross sectional area by 20%. An example of this booster cartridge is shown by the -402 configuration in figure 3. By combining the two modifications, the frangible nut, which was unable to separate under zero preload using a single booster cartridge with 1950 mg of RDX, successfully separated with no increase in the explosive weight of RDX or no reduction in the web thickness<sup>4</sup>.

Material properties, chemical data, and microstructure grain size for Inconel 718 heat lot 9-10298 are shown in table 3. A 100X micrograph for heat lot 9-10298 is shown in figure 9. Heat lot 9-10298 is markedly more resistant to separation than the qualification heat lot 9-11446.

The third manufacturer of 2.5-inch frangible nuts operating under NAS 9-17674 used Inconel 718 from heat lot 9-11446 in its qualification test program. Heat lot 9-11446 is common to the heat lot used in the qualification program performed by the second manufacturer under NAS 9-17496. The third manufacturer began qualification testing in accordance with the test matrix shown in table 6. Testing began with a margin nut which, at NASA's request, had a web thicknesses 20% over the maximum allowable thickness. The 120% margin nut is represented in figure 4 by the -101 configuration. The 120% margin nut failed to separate. The margin test was selected due to experience with failures in margin tests during the second manufacturer's qualification test program.

The failure to separate the frangible nuts using single booster cartridges under zero preload or to demonstrate margin using frangible nuts with overthick webs raised concern at NASA over the new manufacturers' booster cartridge performance. Potential causes in degradation of the RDX detonation output were investigated by chemical and physical analysis of each lot of RDX used by each manufacturer. No evidence of degradation was found. NASA then initiated a test program to investigate whether the original manufacturer's booster cartridges performed differently from new production lots. The first test consisted of firing a frangible nut from the original manufacturer under zero preload conditions using a booster cartridge from recent production. The second test involved firing a frangible nut from the second manufacturer under zero preload conditions using a booster cartridge from the original supplier. The original supplier's frangible nut separated using a new manufacturer's booster cartridge, and the new manufacturer's frangible nut did not separate using the original supplier's booster cartridge. These tests indicated

that the booster cartridge was not the cause of the frangible nut failure to separate.

Further qualification testing under NAS 9-17674, illustrated in table 6, resulted in failures to separate under zero preload conditions even though three frangible nut margin tests were conducted under preload conditions using booster cartridges loaded with 85% of the nominal charge weight. The failure of the zero preload, single booster cartridge frangible nut test resulted in the frangible nut opening until the outer ledges contacted and the outer ledge gap, illustrated in figure 6, was reduced to 0.00". All of the third manufacturer's nuts were modified to remove the outer ledges, illustrated in figure 8, thus providing more rotational freedom for the outer web during a single booster cartridge firing. The third manufacturer resumed the sequence of tests described in table 6 without failure following the frangible nut modification<sup>5</sup>. The modifications to the frangible nut were a result of tests performed during the failure investigation matrix shown in table 5. Material properties, chemical data, and microstructure grain size data for the Inconel 718 used in the third manufacturer's qualification lot are shown in table 3, and the 100X micrograph of the material heat lot is shown in figure 10.

#### Discussion

In each of the above qualification and production heat lots, the Inconel 718 was produced in accordance with AMS 5662. The material properties, yield strength, tensile strength, elongation and reduction in area are illustrated in table 3. Although a significant difference is exhibited in Charpy impact strength<sup>6</sup> between recent production lots and the original Inconel 718, reference table 3, no correlation between Charpy impact strength and frangible nut performance has been made. A NASA test<sup>7</sup> using material having impact strength of 15 and ultimate tensile strength 191.1 ksi, 0.2% offset yield strength of 168.2 ksi, elongation of 16.0%, and reduction of area of 27.0% resulted in failure when fired using a single booster cartridge and under zero preload. The exact combination of chemical, microstructural, and physical data required to assure successful separation of a heat lot of Inconel 718 under zero preload conditions using a single booster cartridge has not been defined. Additional test programs are underway at NASA to further understand the cause of failures for the frangible nuts produced under NAS 9-17496 and NAS 9-17674 and to define what characteristics in the Inconel 718 are critical for successful operation of the frangible nuts. The investigations focus on material property variations in Inconel 718 and on efficiency of coupling explosive potential energy into the fracture of the four webs.

Future production of frangible nuts will be assessed using additional destructive lot acceptance tests to assure reliable operation of the flight hardware. At this time, no quantitative test exists to differentiate Inconel 718 as acceptable or unacceptable for use in flight nuts short of a full scale destructive performance test. If failure occurs at that point in production, the products are in final delivery status and no rework is possible.

#### Conclusions

The most significant conclusions from the failure investigations which NASA has performed on the 2.5-inch frangible nuts are as follows:

A. Specification of Inconel 718 per AMS 5662 is not adequate to guarantee successful separation of the frangible nut using the original design booster cartridge.

B. No single chemical or material property currently measured is an adequate gage of whether the Inconel 718 used in a frangible nut will result in failure or success during performance tests.

C. The critical nature of the 2.5-inch frangible nut mandates extensive testing be performed on each production lot to demonstrate operational response and performance margin.

#### References

1. Contract NAS 9-14000, Document Number CAR 01-45-114-0018-0007B, "Qualification Test Report for Frangible Nut, 2-1/2 Inch and Booster Cartridge," Released May 29, 1980.
2. AMS 5662 Revision F, "Alloy Bars, Forgings, and Rings, Corrosion and Heat Resistant, 52.2Ni - 19 Cr - 3.0Mo - 5.1(Cb + Ta) - 0.90Ti - 0.50Al - 18Fe, Consumable Electrode or Vacuum Induction Melted 1775°F (968°C) Solution Heat Treated," Issued September 1, 1965, Revised January 1, 1989.
3. Contract NAS 9-17496, Document Number 3936-10-301-401, Revision A, "Qualification Test Report for 2.5-inch Frangible Nut, NASA PN SKD26100099-301 and Booster Cartridge, NASA PN SKD26100099-401," January 15, 1991.
4. Contract NAS 9-17496, Document Number RA-468T-B, "Acceptance Data Package for 2.5-inch Frangible Nut, NASA PN SKD26100099-302," June 5, 1992.
5. Contract NAS 9-17674, Document Number 0718(03)QTR, "Qualification Test Report 2.5-inch Frangible Nut with Booster Cartridge, Used on the Space Shuttle Aft Separation System," June 19, 1992.
6. American Society for Testing and Materials Standard E23-88, "Standard Methods for Notched Bar Impact Testing of Metallic Materials, Type A Specimen."
7. NASA Test Report 2P333, "Frangible Nut Test Program."

#### Acknowledgements

The authors wish to acknowledge the work of Ms. Julie Henkener, materials engineer for Lockheed Engineering and Sciences Company, Houston, Texas, in preparing, reviewing, and interpreting the Inconel 718 metallurgical data throughout the frangible nut failure investigation.

**TABLE 1**  
**2.5 INCH FRANGIBLE NUT STRUCTURAL LOAD REQUIREMENTS**

|                     | Limit Load | Ultimate Load | Proof Load |
|---------------------|------------|---------------|------------|
| Axial Load<br>(Lbs) | 415,270    | 581,400       | 456,800    |
| Moment<br>(in-Lbs)  | 53,275     | 75,215        | 59,097     |

**TABLE 2**  
**ORIGINAL MANUFACTURER QUALIFICATION TEST MATRIX FOR**  
**2.5 INCH FRANGIBLE NUT AND BOOSTER CARTRIDGE**

| Test   | Nut<br>Group<br>NO | Functional<br>Temp<br>(-F) | Preload Booster<br>Tension Mount<br>(lbs) (in-lb) |        | Cartridges<br>Dual/Single | Functional<br>(pass/fail) |
|--|--------------------|----------------------------|---|--------|---------------------------|---------------------------|
| Room Temp.<br>Firing                         | A                  | 70-F                       | 240,000   | 0      | Single                    | Passed                    |
|  | A                  | 70-F                       | 240,000   | 0      | Single                    | Passed                    |
|  | A                  | 70-F                       | 240,000   | 0      | Single                    | Passed                    |
|  | A                  | 70-F                       | 240,000   | 0      | Dual                      | Passed                    |
| High Temp.<br>Firing                         | B                  | 200-F                      | 240,000   | 0      | Single                    | Passed                    |
|  | B                  | 200-F                      | 240,000   | 0      | Single                    | Passed                    |
|  | B                  | 200-F                      | 240,000   | 0      | Single                    | Passed                    |
|  | B                  | 200-F                      | 240,000   | 0      | Dual                      | Passed                    |
| Low Temp.<br>Firing                          | C                  | -65-F                      | 240,000   | 0      | Single                    | Passed                    |
|  | C                  | -65-F                      | 240,000   | 0      | Single                    | Passed                    |
|  | C                  | -65-F                      | 240,000   | 0      | Single                    | Passed                    |
|  | C                  | -65-F                      | 240,000   | 0      | Dual                      | Passed                    |
| Low Temp.<br>Firing with<br>Limit Axial Load | E                  | -65-F                      | 378,000   | 65,200 | Single                    | Passed                    |
|  | E                  | -65-F                      | 378,000   | 65,200 | Single                    | Passed                    |
|  | E                  | -65-F                      | 378,000   | 65,200 | Single                    | Passed                    |
|  | E                  | -65-F                      | 378,000   | 65,200 | Dual                      | Passed                    |
| Room Temp.<br>Firing with<br>Zero Preload    | F                  | 70-F                       | 0   | 0      | Single                    | Passed                    |
|  | F                  | 70-F                       | 0   | 0      | Single                    | Passed                    |
|  | F                  | 70-F                       | 0   | 0      | Single                    | Passed                    |
| Margin Demo.<br>Firing                       | G *                | 70-F                       | 240,000   | 0      | Single                    | Passed                    |
|  | G *                | 70-F                       | 240,000   | 0      | Single                    | Passed                    |
|  | G *                | 70-F                       | 240,000   | 0      | Single                    | Passed                    |

\* Group G nuts had web thicknesses 120% the nominal maximum allowable

**TABLE 3**  
**MATERIAL PROPERTIES, CHEMICAL DATA, AND MICROSTRUCTURE GRAIN SIZE FOR INCONEL 718 USED**  
**IN FRANGIBLE NUTS BY MANUFACTURERS**

|                                | ORIGINAL<br>MANUFACTURER<br>HEAT LOT | NAS9-17496<br>QUALIFICATION<br>HEAT LOT<br>9-11446 | NAS9-17674<br>QUALIFICATION<br>HEAT LOT<br>9-11446 | NAS9-17496<br>PRODUCTION<br>HEAT LOT<br>9-10298 |
|--------------------------------|--------------------------------------|--|--|---|
| <b>0.2% Yield</b>              |                                      |  |  |   |
| Avg (ksi)                      | 148.4                                | 165.8  | 160.3  | 152.6   |
| Std. Dev. (ksi)                | 6.5                                  | 0.2  | 2.3  | 0.6   |
| <b>Ultimate Tensile</b>        |                                      |  |  |   |
| Avg (ksi)                      | 188.5                                | 194.2  | 192.0  | 190.7   |
| Std. Dev. (ksi)                | 4.1                                  | 1.2  | 2.4  | 0.8   |
| <b>Elongation</b>              |                                      |  |  |   |
| Avg. (%)                       | 18.6                                 | 18.7   | 20.2   | 13.0  |
| Std. Dev.                      | 1.6                                  | 0.5  | 0.6  | 0   |
| <b>Reduction of Area</b>       |                                      |  |  |   |
| Avg. (%)                       | 28.2                                 | 30.3   | 33.2   | 38.0  |
| Std. Dev.                      | 2.5                                  | 1.2  | 1.5  | 0   |
| <b>Charpy Impact Strength:</b> |                                      |  |  |   |
| Avg. (Ft-Lbs)                  | 19.8                                 | 28.8   | 29.3   | 39.7  |
| Std. Dev.                      | 2.3                                  | 1.0  | 0.8  | 2.9   |
| <b>Grain Size (ASTM)</b>       |                                      |  |  |   |
|                                | 5                                    | 5-8  | 5-8  | 6-8   |
| <b>Chemical Data:</b>          |                                      |  |  |   |
| C                              | 0.034                                | 0.027  | 0.027  | 0.023   |
| Ti                             | 0.98                                 | 0.98   | 0.98   | 0.910   |
| S                              | 0.001                                | 0.002  | 0.002  | 0.002   |
| B                              | <.0001                               | <.001  | <.001  | <0.00001  |
| Fe                             | 17.672                               | 17.78  | 17.78  | 18.55   |
| Al                             | .5                                   | 0.510  | 0.51   | 0.52  |
| Cu                             | .1                                   | 0.06   | 0.06   | 0.050   |
| Ni                             | 53.5                                 | 53.75  | 53.75  | 53.05   |
| Co                             | 0.18                                 | 0.34   | 0.34   | 0.41  |
| B                              | 0.003                                | 0.003  | 0.003  | 0.003   |
| P                              | 0.01                                 | 0.013  | 0.013  | 0.010   |
| Si                             | 0.14                                 | 0.13   | 0.13   | 0.100   |
| Mn                             | .1                                   | 0.08   | 0.08   | 0.120   |
| Mo                             | 2.99                                 | 2.98   | 2.98   | 2.940   |
| Cr                             | 18.4                                 | 18.0   | 18.0   | 17.950  |
| Se                             | <.0003                               | <.0003   | <.0003   | <0.0003   |
| Pb                             | <.0001                               | <.0001   | <.0001   | <0.0001   |
| Cb+Ta                          | 5.29                                 | 5.34   | 5.34   | 5.360   |

**TABLE 4**  
**NAS 9-17496 FRANGIBLE NUT AND BOOSTER CARTRIDGE**  
**QUALIFICATION TEST MATRIX**

| Test                                      | Nut Group NO | Functional Temp (-F) | Preload Tension Mount (lbs) (in-lb) |        | Booster Cartridges Dual/Single | Functional (pass/fail) |
|---|--------------|----------------------|-------------------------------------|--------|--------------------------------|------------------------|
| Room Temp. Firing                         | V            | 70-F                 | 350,000                             | 0      | Single                         | Passed                 |
|   | I            | 70-F                 | 270,000                             | 0      | Single                         | Passed                 |
| High Temp. Firing                         | II           | +200-F               | 270,000                             | 0      | Single                         | Passed                 |
|   | II           | +200-F               | 270,000                             | 0      | Dual                           | Passed                 |
| Low Temp. Firing                          | III          | -65-F                | 270,000                             | 0      | Single                         | Passed                 |
|   | III          | -65-F                | 270,000                             | 0      | Single                         | Passed                 |
|   | III          | -65-F                | 270,000                             | 0      | Dual                           | Passed                 |
| Low Temp. Firing with Limit Axial Load    | V            | -65-F                | 415,270                             | 53,725 | Single                         | Passed                 |
|   | I            | -65-F                | 415,270                             | 53,725 | Dual                           | Passed                 |
|   | V            | -65-F                | 415,270                             | 53,725 | Dual                           | Passed                 |
| Room Temp. Firing with Zero Preload       | VI           | 70-F                 | No Load                             | 0      | Single                         | Passed                 |
| Margin Demo. Firings                      | VII          | 70-F                 | 270,000                             | 0      | Single                         | Passed (115% Web)      |
|   | VII          | 70-F                 | 270,000                             | 0      | Single                         | Failed (126% Web)      |
|   | VII          | 70-F                 | 270,000                             | 0      | Single                         | Failed (120% Web)      |
| 85% Booster Cartridge Margin Demo. Firing | IV           | 70-F                 | 270,000                             | 0      | Single                         | Passed                 |
|   | IV           | 70-F                 | 270,000                             | 0      | Single                         | Passed                 |
|   | VIII         | 70-F                 | 270,000                             | 0      | Single                         | Passed                 |



**TABLE 5**  
**FAILURE INVESTIGATION TEST MATRIX**

| Test | Preload<br>(Klbs) | Nut Web<br>Thicknesses<br>(%) | Chamfered<br>Outer Ledge<br>(Y/N) | Booster<br>Load<br>(%) | Booster<br>Bore Area<br>(%) | Results<br>(Pass/Fail) |
|------|-------------------|-------------------------------|-----------------------------------|------------------------|-----------------------------|------------------------|
| 1    | 0                 | 100                           | N                                 | 110                    | 110                         | Fail                   |
| 2    | 0                 | 100                           | N                                 | 115                    | 115                         | Fail                   |
| 3    | 0                 | 100                           | N                                 | 120                    | 120                         | Pass                   |
| 4    | 0                 | 80                            | N                                 | 100                    | 100                         | Fail                   |
| 5    | 0                 | 100                           | Y                                 | 110                    | 110                         | Pass                   |
| 6    | 270               | 100                           | Y                                 | 100                    | 100                         | Fail                   |
| 7    | 0                 | 100                           | N                                 | 100                    | 120                         | Fail                   |
| 8    | 0                 | 100                           | Y                                 | 100                    | 120                         | Pass                   |
| 9    | 0                 | 100                           | Y                                 | 105                    | 105                         | Fail                   |
| 10   | 270               | 115                           | Y                                 | 100                    | 120                         | Pass                   |

**TABLE 6**  
**NAS 9-17674 FRANGIBLE NUT AND BOOSTER CARTRIDGE QUALIFICATION TEST MATRIX**

| Test   | Nut<br>Group<br>NO | Functional<br>Temp<br>(-F) | Pre-Load<br>tension Mount<br>(lbs) (in-lb) | Booster<br>Cartridges<br>Dual/Single | Functional<br>(pass/fail) |
|--|--------------------|----------------------------|--|--------------------------------------|---------------------------|
| Low Temp.<br>Firing                          | C                  | -65-F                      | 270,000 0                                  | Single                               | Passed                    |
| Low Temp.<br>Firing with<br>Limit Axial Load | E                  | -65-F                      | 415,270 53,725                             | Single                               | Passed                    |
|  | E                  | -65-F                      | 415,270 53,725                             | Single                               | Passed                    |
|  | E                  | -65-F                      | 415,270 53,725                             | Dual                                 | Passed                    |
| Room Temp.<br>Firing with<br>Zero Preload    | D                  | 70-F                       | No Load 0                                  | Single                               | Failed                    |
|  | D                  | 70-F                       | No Load 0                                  | Single                               | Failed                    |
|  | D                  | 70-F                       | No Load 0                                  | Single                               | Passed (-302 Nut)*        |
|  | D                  | 70-F                       | No Load 0                                  | Single                               | Passed (-302 Nut)*        |
|  | D                  | 70-F                       | No Load 0                                  | Single                               | Passed (-302 Nut)*        |
| Margin Demo.<br>Firings                      | G                  | 70-F                       | 270,000 0                                  | Single                               | Failed (120% Web)         |
|  | G                  | 70-F                       | 270,000 0                                  | Single                               | Passed (-102 Nut)**       |
|  | G                  | 70-F                       | 270,000 0                                  | Single                               | Passed (-102 Nut)**       |
| 85% Booster<br>Cartridge                     | G                  | 70-F                       | 270,000 0                                  | Single                               | Passed                    |
|  | G                  | 70-F                       | 270,000 0                                  | Single                               | Passed                    |
| Margin Demo.<br>Firing                       | G                  | 70-F                       | 270,000 0                                  | Single                               | Passed                    |

\* -302 Nut represents nominal web thickness and chamfered outer ledges.

\*\* -102 Nut represents 115% nominal web thickness with chamfered outer ledges.

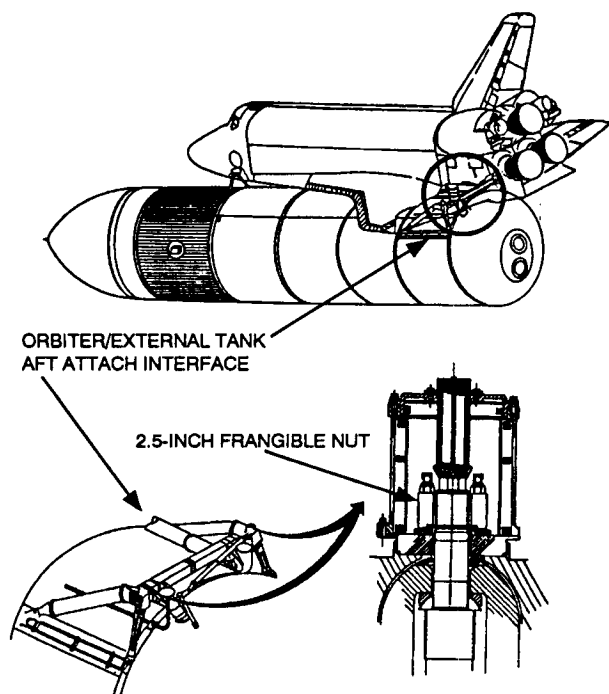


Figure 1. Illustration of orbiter/external tank aft attach interface and cross section of 2.5 inch frangible nut installation.

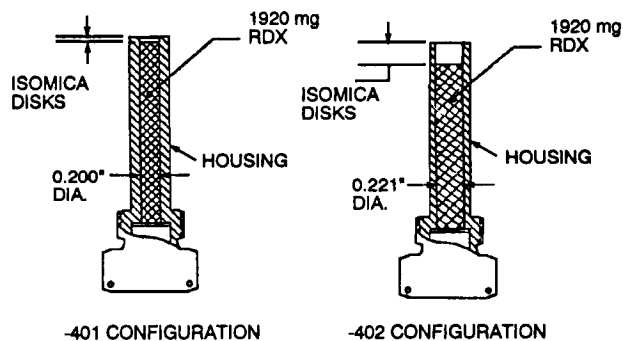


Figure 3. Illustration of 2.5-inch booster cartridge -401 configuration and modified design, -402 configuration.

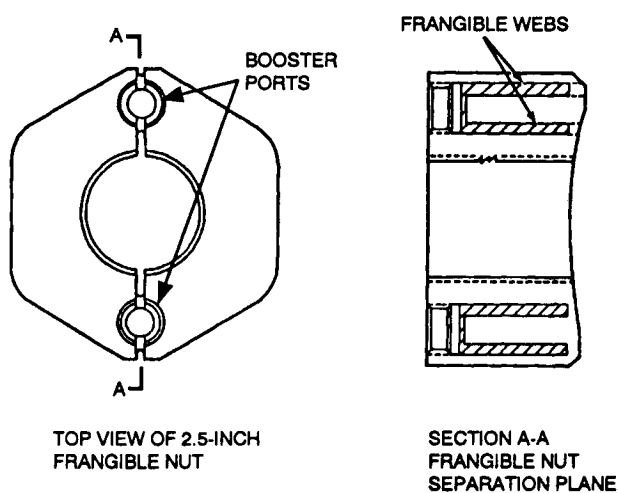


Figure 2. 2.5-inch frangible nut separation plane and frangible webs.

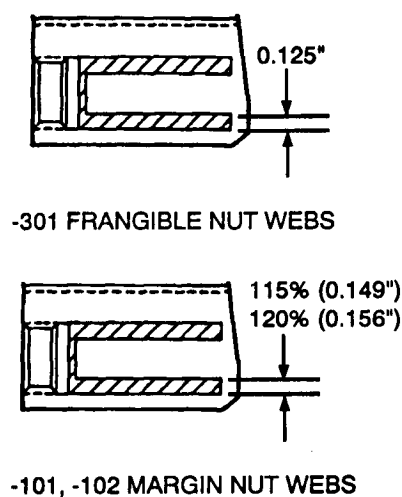


Figure 4. 2.5-inch frangible nut nominal web thickness, (-301 configuration), 120% nominal web thickness, (-101 configuration) and 115% nominal web thickness (-102 configuration).

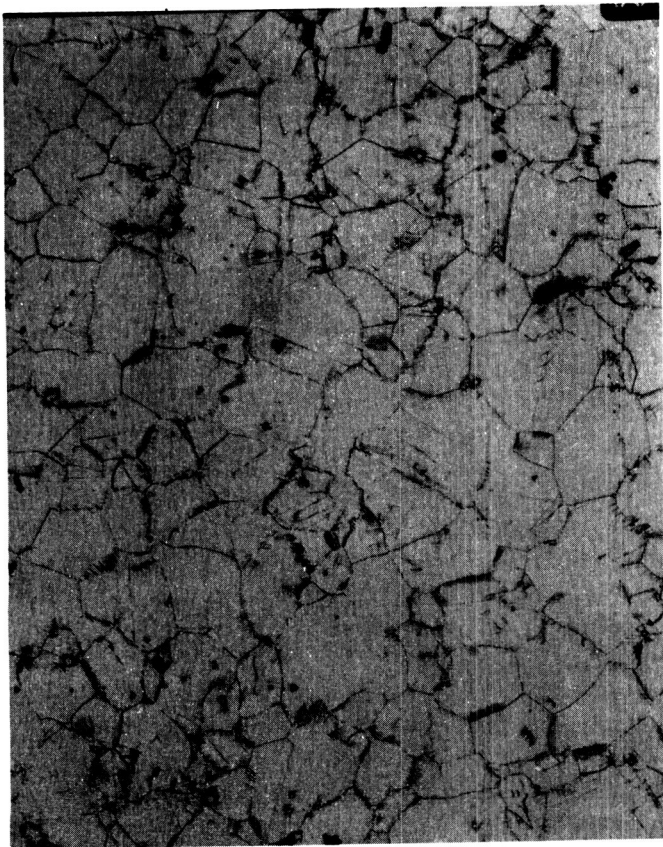


Figure 5. 100 X micrograph of original frangible nut supplier's Inconel 718.

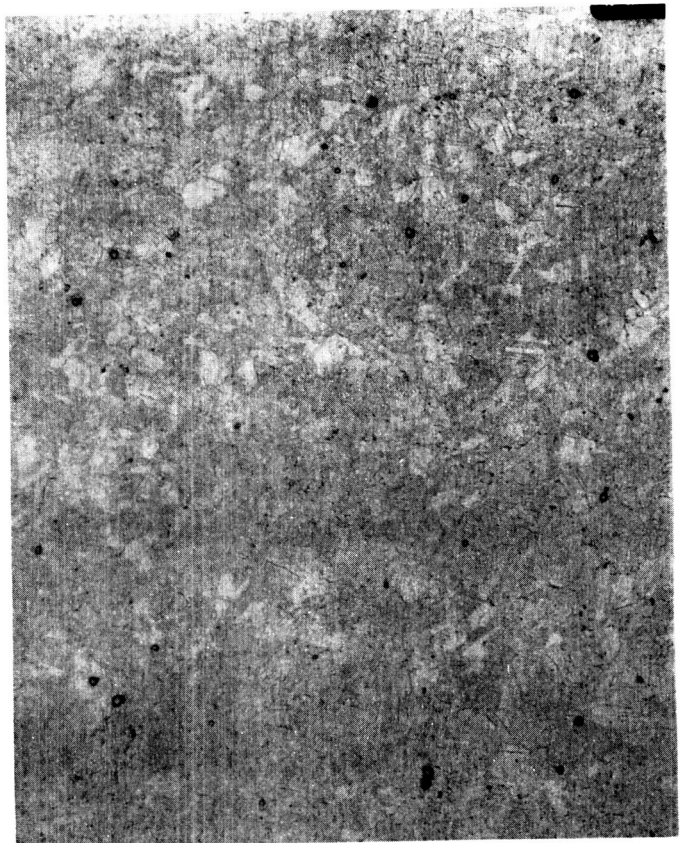


Figure 7. 100X micrograph of Inconel 718 used in qualification test program under NASA contract NAS 9-17496.

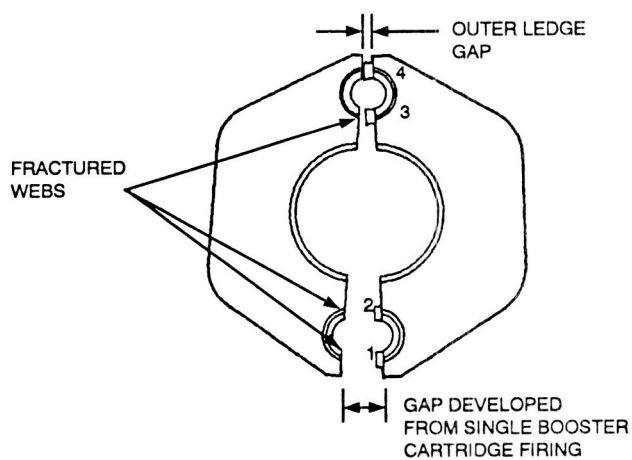


Figure 6. Illustration of clamshell motion experienced by 2.5-inch frangible nut during single booster cartridge firing.

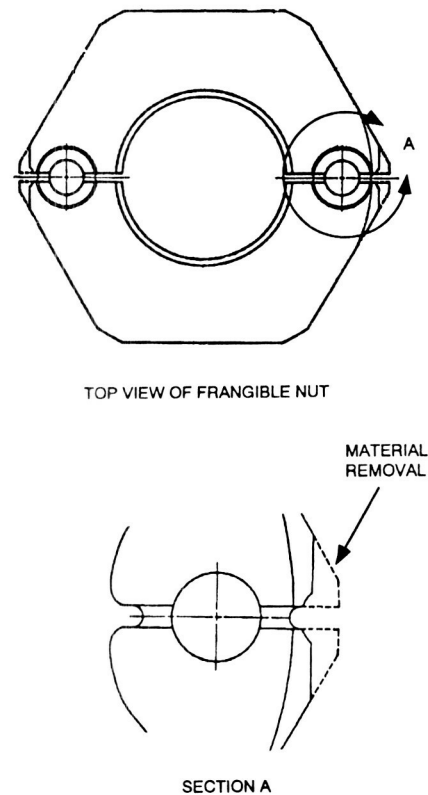


Figure 8. Illustration of material removal from outer ledge of 2.5-inch frangible nut.



Figure 9. 100X Micrograph of Inconel 718 Used in  
Production Lot under NASA Contract  
NAS 9-17496.



Figure 10. 100X Micrograph of Inconel 718 Used in  
Qualification Lot under NASA Contract  
NAS 9-17674.

S21-18  
7001  
P-16

## BOLT CUTTER FUNCTIONAL EVALUATION

S. Goldstein, T. E. Wong, S. W. Frost, J. V. Gageby, and R. B. Pan  
The Aerospace Corporation  
2350 E. El Segundo Blvd., El Segundo CA 90245

### ABSTRACT

The Aerospace Corporation has been implementing finite difference and finite element codes for the analysis of a variety of explosive ordnance devices. Both MESA-2D and DYNA3D have been used to evaluate the role of several design parameters on the performance of a satellite separation system bolt cutter. Due to a lack of high strain rate response data for the materials involved, the properties for the bolt cutter and the bolt were selected to achieve agreement between computer simulation and observed characteristics of the recovered test hardware. The calculations provided insight into design parameters such as the cutter blade kinetic energy, the preload on the bolt, the relative position of the anvil, and the anvil shape. Modeling of the cutting process clarifies metallographic observation of both cut and uncut bolts obtained from several tests. Understanding the physical processes involved in bolt cutter operation may suggest certain design modifications that could improve performance margin without increasing environmental shock response levels.

### BACKGROUND

The Aerospace Corporation Explosive Ordnance Office (EOO) was given hardware from a series of satellite separation system ground tests wherein several bolt cutters successfully severed the interfacing bolts and others did not. EOO also obtained a severed bolt from a lot acceptance test of the cutter. The EOO was asked to assess causes of the anomalous performance and to determine corrective actions. A multi-disciplinary team was assembled and a review initiated.

The bolt cutter used in this application was developed in 1972 by Quantic (*a.k.a.* Whittaker or Halex) for McDonnell Douglas, Huntington Beach. A family of cutters known by part number R13200 has since evolved. The Quantic outline drawing for R13200 states that its severance capacity is a 5/16 inch diameter-A286 CRES bolt having a tensile strength from 180 to 210 ksi and tensioned between zero and 6000 lbs. A photograph of the hardware is shown in *Figure 1*.

A finite element model, to be discussed further

in a later section, is shown in *Figure 2* and illustrates the configuration of the installed bolt and cutter before functioning. The bolt cutter consists of an explosive initiator, a chisel shaped cutter blade, a blade positioning shear pin, and an anvil in a cylindrical housing. The bolt to be cut fits through a clearance hole in the housing that places it against the anvil. When the initiator is functioned, the blade is accelerated and impacts the bolt. In both system separation and lot acceptance testing of the bolt cutter, it is seen that the cutter blade penetrates only part way through the bolt diameter. The cutting process is completed by fracture of the bolt.

The initial finding of the team was that the ductility of the bolt used in the anomalous system separation tests was not compatible with the specification in the bolt cutter outline drawing. That is, a more ductile bolt than the R13200 bolt cutter requires had been used. The bolts used in the tests were solution annealed and aged to AMS 5737. This specification only requires a minimum ultimate tensile strength (UTS) of 140 ksi.

Presented to the Second NASA/DOD/DOE Pyrotechnic Workshop, February 8-9, 1994

To obtain the 180-210 ksi UTS, the A286 material requires cold working per AMS 5731. The bolts used in the system separation tests had not been cold worked. It was found that the Quantic target bolts, part number F12496, used in bolt cutter lot acceptance tests are cold worked. The F12496 drawing states that the target bolt material comply with AMS 5731 and be cold worked to obtain 180-210 ksi UTS following heat treat per Mil-H-6875. Since 1972, a large number of bolt cutters from many production lots have successfully severed the F12496 target bolts. No data base was found to assess cutter performance with A286 bolts which had not been cold worked.

The team also found that the mass of the bolts used in the system separation tests was at least six times greater than the Quantic test target bolt. The greater mass is due to greater length and end diameter, which is required for installation. The concern then was the lack of information on the effect of bolt inertia on bolt cutter performance.

The team directed efforts toward analyzing the cut and uncut test bolts and in attempting to duplicate the cutter performance analytically. A F12496 target bolt, used in a bolt cutter lot acceptance test, was obtained from Quantic and also analyzed. In addition to assessing bolt inertia effects, the team attempted to determine the effect of bolt tension on the bolt cutter performance. The parameters assumed to affect the ability of the bolt cutter to sever the bolts are:

- bolt configuration
- ductility of the bolt material
- preload in the bolt

Other parameters such as gapping between the bolt and anvil and the anvil configuration were also considered.

The following are the results of the material analysis from metallographic evaluation of the test bolts, descriptions of the analytic modeling techniques, a comparison of model attributes and the team conclusions.

## METALLURGICAL ASSESSMENT OF A286 BOLTS

Metallurgical analyses were performed to infer the role of each parameter in the cutting process. The analyses were performed on fractured segments of a short bolt obtained from a Quantic lot acceptance test and on both fractured and unfractured long bolts from the system separation tests. The analyses included a microscopic examination of the fracture surfaces, metallurgical studies of the regions of deformation and fragmentation at the beginning of the cutting process, and measurements of material hardness and microstructure.

These studies, and an examination of the photographs in *Figures 3 through 9* lead to the following observations:

- Grain size and hardness differences exist between the long and short bolts. The short bolt had a fine grain size and high hardness (Rc 42), and was consistently severed. The long bolt was larger grained and softer (Rc 35), and was not consistently severed. See *Figures 10a and 10b*.
- The long and short bolts which had been successfully severed exhibited adiabatic shear bands in the deformed material regions adjacent to both the cutter blade and the anvil. Adiabatic shear bands are regions of highly localized plastic deformation resulting from the high material temperatures that are caused by high strain rate loading.
- No evidence of adiabatic shear bands were seen in the deformed material regions adjacent to the anvil on the long bolt which had failed to separate.

## MODELING WITH MESA-2D

MESA-2D is a finite difference code that was used to analyze the behavior of the bolt cutter and bolt during the early time portion of its functioning. MESA is a reactive hydrodynamic

code that assumes, to a first approximation, that material behavior can be described by fluid dynamics when strong shocks are present. The equations of motion to be solved are then the time dependent nonlinear equations of motion for compressible fluids.

Throughout a calculation, MESA-2D computes and records all relevant dynamic and thermodynamic properties for each cell (mass element) in the model. These variables could include position, velocity, pressure, internal energy, temperature, density, intrinsic sound speed, elastic and plastic work, plastic strain, strain rate, and deviator stress. All of these quantities output in graphical form or in tabular form for further analysis. By integrating over very small time steps, typically less than 1 nanosec, the MESA calculation can handle impulsive loading of materials and allows their dynamics to be resolved with sufficient accuracy to elucidate the physical processes involved [1].

The numerical integrations required by the calculations were performed with coordinate meshes of between 40,000 and 60,000 cells. This gives better than 0.1 mm resolution, which is required to understand small systems such as the bolt cutter.

#### Finite Difference Models

*Figure 11* shows the cutter blade, the anvil, and the bolt to be cut that were included in the MESA finite difference model. It also shows the particle velocity distribution after 20  $\mu$ sec. An alternative configuration was also developed in which the massive ends of the flight bolt were eliminated. The models were analyzed using slab geometry and transmissive boundary conditions for the hydrodynamic equations. Bolt preload was not included.

In the computer simulations, the available material properties of 304 stainless steel were used as the basis for the properties of all metallic components. The yield strength and shear modulus were adjusted by using 4340 steel for the blade and A286 for the bolt. Strain rate effects were accounted for by allowing these constants to vary [2, 3, 4].

The simulations were assumed to start when the cutter blade begins to move, and neglects the functioning of the initiator and the transfer of energy to the cutter blade.

The initiator consists of 70% by weight ammonium perchlorate (AP), 27% polybutadiene acrylic acid (PBAA), and 3% combined zirconium barium peroxide (ZBP), ferric oxide (FO), and epoxy resin. The ZBP and FO as oxidizers will enhance the performance of the main constituent, AP. The remaining materials are inert binders. The material properties of all these materials are not known. An upper and lower bound estimate of kinetic energy output was made from the available chemical energy of the AP assuming instantaneous energy release via detonation. Since the exact energy partition is unknown, trial computer models were run using several candidate velocities within these limits. The cutter velocity was determined by trial and error, matching the resulting penetration into the bolt to the experimental data. This velocity was 332 m/sec.

#### Computational Results

The calculations began at time zero with the bolt cutter blade poised to impact the surface of the bolt and with the initial constant velocity of 332 m/sec. The proper penetration of the cutter blade into the material to agree with the test data from *Figures 5, 6 and 7* is achieved in approximately 20  $\mu$ sec. The material interfaces show that both light and heavy bolts have responded identically to this point. The time elapsed to this point in the cutting process is one order of magnitude smaller than the time it had previously been assumed by the community for bolt cutter function.

Compression and tension waves propagating through the bolt show that there is no net motion of the bolt ends since the particle velocities of the end cells go to zero. The velocity of the cutter blade also changes direction several times after it penetrates the bolt. This is evidence of an oscillation that is set up which will cause the blade to bounce back.

The model shows, as does the test hardware, that all material deformation occurs within a 1 cm radius of the impact point of the cutter blade. No rigid body motion of the bolt is required for penetration, and indeed the coordinates of the bolt ends do not change throughout the cutting process in the calculation.

Shear deformation can be discerned from inflections in the particle velocity distributions as early as 10  $\mu$ sec. These patterns are apparent in *Figure 11*. This result agrees with the evidence of the same behavior in the photomicrographs of the cut surfaces. Ejection of particles from the top surface of the bolt can be seen. There is also a small crack that appears near the tip of the cutter blade. All of these features were seen in the hardware, especially *Figures 5 and 6*. The indentation from the anvil on the underside of the bolt can also be seen beginning to form although it is not obvious until some time later.

The material deformation is due almost entirely to plastic work. The elastic contribution is between two and three orders of magnitude smaller than the plastic, and the penetration process is completed before the effects of any elastic waves can be seen. Therefore, the ends of the bolt, and whether or not they are massive, may have no effect on cutter performance.

Blunting of the cutter blade edge occurs as well. *Figures 12 and 13* show this in the hardware. The assumption had been that this blunting resulted from the impact of the blade against the anvil after the bolt had separated. While there is undoubtedly some effect from this, the blade edge is also blunted by erosion during the bolt penetration process.

As configured, the MESA calculations do not show that the cutter completely severs the bolt. This may be partly attributed to insufficient brittleness in the material description. However, the highest shear locations match those in the photomicrographs of the test bolt that failed to cut. The shear deformation regions that originate at the anvil side of the bolt are not as clear with the

resolution available in the calculation.

Additional calculations were performed using both smaller and larger velocities for the cutter blade. When the velocity is 133 m/sec, the blade does not penetrate far enough to match the data. When it is increased to 431 m/sec, it is possible to separate the bolt by penetration alone, independent of the formation of a shear fracture. These calculations indicated that depth of penetration of the blade into the bolt is dependent on this variable alone. This is consistent with the results of various empirical penetration analyses for projectiles [5], which show that penetration depth is a function of the velocity of the penetrator and the ratio of densities of the materials of penetrator and target. Since both blade and bolt have the same density, the only other determining factor is penetrator velocity.

### MODELING WITH DYNA3D

Due to analytical considerations of nonlinear dynamics and stress wave propagation effects in bolt cutter structural response, transient dynamic analyses were performed using the DYNA3D code. The DYNA3D code is an explicit, nonlinear, finite element analysis code developed by Lawrence Livermore National Laboratory [8]. It has a sophisticated simulation capability for handling frictional and sliding interactions between independent bodies.

A built-in feature in the DYNA3D code was selected for modeling the sliding surface failure behavior. A failure criterion based on the total cumulative effective plastic strain is defined for the elements adjacent to the contact surface. When the rate-dependent plastic strain value within an element satisfies this failure criteria, the element is removed from further calculation and a new sliding surface boundary is defined.

Parameters compared in this study include the approaching speed of the cutter blade, the applied bolt preload, the gap clearance between the bolt and the anvil, and the contact surface area of the anvil. TABLE I lists the four parameters and their variations considered in



the finite element analysis matrix. In this table, the 3,270 lbs bolt preload and a maximum gap allowable of 0.065 inch between the bolt and anvil were based on drawing specifications. The loss of preload and a 50% reduction in anvil's contact area were chosen to study their impact in cutter performance.

The speed for the blade was determined using system separation test data. In these tests, six A286 bolts were preloaded to 3,270 lbs. Two of the bolts had a cutting depth of 40% of the bolt diameter and did not fracture. The other four bolts had a slightly deeper blade penetration, were totally severed and the cutter blades also indented the anvil. The transient dynamic analysis duplicated these conditions by using a 6,000 in/sec (152 m/sec) speed.

#### Finite Element Analysis Matrix

The Taguchi experimental design technique [6, 7] was then adopted for establishing the analysis matrix. This technique was also used to analyze the finite element calculation results to identify the optimum bolt cutter configuration, especially in relation to preload or applied tension on the bolt.

A Taguchi analysis matrix with 8 study cases (a  $L_8$  orthogonal array [6, 7]), shown in TABLE II, was established to evaluate the criticality of the four chosen parameters mentioned above. Interaction effects between these parameters were assumed to be negligible. Based on the analysis matrix and the chosen parameter listed in TABLE II, 8 different finite element models were constructed. A baseline finite element model of the bolt cutter configuration (case 1 in TABLE II) as shown in *Figure 2*. Due to symmetry of the bolt cutter geometry, only one half of the bolt cutter configuration was modeled. This model consists of 618 solid elements and 1027 nodes to simulate the 60 degree cutter blade, the 5/16 inch diameter bolt, and the anvil.

#### Transient Dynamic Analysis

TABLE III lists the mechanical properties used in the analysis. The values chosen for S7 tool steel and A286 stainless steel were obtained

from references [9] and [10], respectively.

In the finite element analysis model, nonreflecting boundaries were assumed at the two ends of the bolt and the anvil to prevent artificial stress wave reflections re-entering the model and contaminating the results. A fixed end boundary condition was assumed at the lower end of the anvil. The bolt preload was first generated by applying pressure loading on the bolt with a built in dynamic relaxation option. The cutter blade with the appropriate approaching speed was then applied. A transient dynamic analysis was performed to estimate the damage in the bolt. The analysis results for the eight study cases are listed in the last column of TABLE II. The 0's and 1's are corresponding to a partial or a complete cutting of the bolt, respectively. *Figure 14* shows the simulation results at 0.4 ms for the baseline model in TABLE II. In *Figure 15*, with a finer mesh model, it can be seen that the bolt is completely severed by the cutter. It can be seen that the failure configuration matches fairly well with the test data in *Figure 3*.

#### Bolt-Cutter Performance Assessment

From finite element analysis results listed in the last column of TABLE II, the bolt cutter performance, based on variation levels for each parameter, can be summarized. For example, the cutter performed well with a bolt preload (parameter A) of 3,270 lbs (level 1). It resulted in three successful cuts and one failure. The cutter performed poorly with parameter A at level 2 (zero preload), with only one success and three failures. Therefore, the analysis results of level sum  $A_1$  and  $A_2$  are:

$$\begin{aligned} A_1 &= 1 + 1 + 1 + 0 = 3 \text{ cuts} \\ A_2 &= 1 + 0 + 0 + 0 = 1 \text{ failure} \\ \hline \text{Total} &= 4 \text{ cases} \end{aligned}$$

Other parameter sums are similarly calculated and summarized in TABLE IV. These results are also plotted in *Figure 16* in bar chart format in terms of the percentage of success. It can be seen that the bolt cutter performance can be improved with the design parameter setting of  $A_1$ ,  $B_1$ ,  $C_1$ ,  $D_2$ . That is, it is desirable to

improve the cutter performance by applying a bolt preload of 3,270 lb, providing sufficient energy for the cutter blade to reach a speed of 6,000 in/sec, ensuring that no gap exists between the bolt and the anvil before firing, and by reducing the anvil and the bolt contact surface area by half.

### Omega Transformation

In order to verify the assumption that interaction effects between these four parameters are negligible and to estimate the response of the optimum condition of the bolt cutter system, the omega transformation technique [7] can be used. The omega transformation is defined as follows:

$$\Omega(P) \equiv -10 \log (1/P - 1) \text{ dB}$$

where P is the percentage of success. For the cases of cutter failure (0%) and cutter success (100%), they are treated as follows:

0% case - Consider this as 1/(number of cases) and perform the omega transformation. For the current study, the number of cases is 8; thus,  $(1/8) \times 100 = 12.5\%$  or  $\Omega(12.5\%) = -8.45 \text{ dB}$ .

100% case - Consider this as (number of cases - 1)/(number of cases) and perform the omega transformation. For the current study,  $[(8-1)/8] \times 100 = 87.5\%$  or  $\Omega(87.5\%) = 8.45 \text{ dB}$ .

Based on the approach as shown in [7], the optimum response, m, can be estimated by an additive model.

$$\begin{aligned} m(A_1, B_1, C_1, D_2) &= T_{A_1} + T_{B_1} + T_{C_1} + T_{D_2} - 3 \times T \\ &= \Omega(75\%) + \Omega(75\%) + \Omega(75\%) \\ &\quad + \Omega(75\%) - 3 \times \Omega(50\%) \\ &= 4.77 + 4.77 + 4.77 + 4.77 - \\ &\quad 3 \times 0 \\ &= 19.08 \text{ dB } ( > 8.45 \text{ dB } ) \\ &= 98.8\% \quad ( > 87.5\% ). \end{aligned}$$

Here T is the overall mean percentage of success for all cases analyzed in Table IV and  $T_{xy}$  is the average for parameter X at level y. Thus, under the optimum conditions, the bolt could be totally severed by the design of  $A_1, B_1, C_1, D_2$ . This was later confirmed by the

finite element analysis prediction. This result indicates that the additive model is adequate for describing the dependence of the structural response on various parameters, and also confirms that the assumption of negligible interaction effects between various governing parameters was valid.

### CONCLUSIONS

The evidence obtained from the metallurgical examination of test hardware suggests that bolt severance from the impact of the bolt cutter blade occurs as a result of a combination of processes. These include:

- reduction of the bolt diameter by penetration of the blade;
- reduction of the bolt diameter by penetration of the anvil;
- wedge opening forces generated by the cutter blade as it penetrates;
- applied preload on the bolt; and
- adiabatic shear band formation under the combined effects of shock heating and the applied stresses on the bolt.

The two analysis techniques that were employed proved to be complementary to each other in that they each were able to elucidate different features of the ductile bolt behavior and of the governing design parameters of the system. In addition to the above conclusions, which they confirm, are the following.

The MESA-2D analysis indicates:

- The bolt cutting process is completed in less than 60  $\mu\text{sec}$ .
- Neither the length nor mass of the bolt has any effect on the ability of the cutter blade to penetrate the bolt.
- The depth of penetration of the cutter blade into the bolt is a function of the cutter blade velocity.

- The bolt fractures due to shear in the second part of the separation process.

The DYNA3D analysis also indicates:

- With the available explosive energy, a preload in the bolt is necessary for the fracture to occur and complete the bolt separation.
- For effective severing, there should be contact between the bottom surface of the bolt and the anvil.
- The bolt cutter is more effective if the surface area of the anvil in contact with the bolt is decreased.

This last conclusion presents a possible design modification that is an alternative to increasing the kinetic energy of the cutter blade with additional explosive. Increasing the amount of explosive could increase the shock from functioning the device, whereas a change in anvil configuration would not.

Further work is still needed on the bolt cutter system to analyze the performance under conditions where the cutter blade has a non-parallel impact to the cross section of the bolt.

#### ACKNOWLEDGMENTS

The authors would like to thank the following individuals for their contributions to this work:

G. Wade of Quantic Industries, for providing drawings, hardware, and other information on the design and materials in the 13200 bolt cutter; A. M. Boyajian, The Aerospace Corporation program office, for his support of this work; R. W. Postma, L. Gurevich, G. T. Ikeda and R. M. Macheske, The Aerospace Corporation, and J. Yokum of Defense Systems, Inc. for their interest and participation in many valuable technical discussions.

#### REFERENCES

- [1] S. T. Bennion and S. P. Clancy, "MESA-2D (Version 4)", Los Alamos National Laboratory, LANL Report LA-CP-91-173, 1991.
- [2] E. L. Lee, H. C. Hornig, and J. W. Kury, "Adiabatic Expansion of High Explosive Detonation Products", Lawrence Livermore National Laboratory, LLNL Report UCRL-50422, 1968.
- [3] D. J. Steinberg, S. G. Cochran, and M. W. Guinan, "A Constitutive Model for Metals Applicable to High Strain Rate", J. Appl. Phys. 51 (3), 1498 (1980).
- [4] G. R. Johnson and W. H. Cook, "Fracture Characteristics of Three Metals Subjected to Various Strains, Strain Rates, Temperatures and Pressures", Eng. Frac. Mech. 21 (1), 31 (1985).
- [5] Joint Technical Coordinating Group for Munitions Effectiveness (Anti-Air), Aerial Target Vulnerability Subgroup, Penetration Equations Handbook for Kinetic Energy Penetrators (U), 61 JTCG/ME-77-16 Rev. 1, 15 Oct. 1985.
- [6] Phadke, M. S., Quality Engineering Using Robust Design, Prentice Hall, Englewood Cliffs, NJ, 1989.
- [7] Mori, T., The New Experimental Design, ASI Press, 1990.
- [8] Whirley, R. G. and Hallquist, J. O., "DYNA3D Users Manual," Lawrence Livermore Laboratory, Rept. UCRL-MA-107254, May 1991.
- [9] American Society for Metals, Metals Handbook, Vol. 3, 9th Edition, 1980.
- [10] Frost, S. W., "Metallurgical Evaluation of Separation Bolt," Aerospace Corporation Interoffice Correspondence, 9 Nov. 1992.

**Table I. Parameters for Bolt Cutter Study**

| Parameter | Description                     | Variation Level |       |
|-----------|---------------------------------|-----------------|-------|
|           |                                 | 1               | 2     |
| A         | Bolt Preload, lbs.              | 3270            | 0     |
| B         | Cutler Blade Speed in./sec.     | 6000            | 5000  |
| C         | Gap between bolt and Anvil, in. | 0               | 0.065 |
| D         | Anvil Surface Reduction, %      | 0               | 50    |

**Table II. Finite Element Analysis Matrix  
(Taguchi L<sub>8</sub> Orthogonal Array)**

| Analysis Run | Parameters |   |   |   | Results * |
|--------------|------------|---|---|---|-----------|
|              | A          | B | C | D |           |
| 1            | 1          | 1 | 1 | 1 | 1         |
| 2            | 1          | 1 | 2 | 2 | 1         |
| 3            | 1          | 2 | 1 | 2 | 1         |
| 4            | 1          | 2 | 2 | 1 | 0         |
| 5            | 2          | 1 | 1 | 2 | 1         |
| 6            | 2          | 1 | 2 | 1 | 0         |
| 7            | 2          | 2 | 1 | 1 | 0         |
| 8            | 2          | 2 | 2 | 2 | 0         |

\* 1 represents bolt totally fractured, 0 represents bolt partially fractured

**Table III. Mechanical Properties Used for DYNA3D Analysis**

| Structure    | Material Type        | Poisson's Ratio | Yield Strength (ksi) | Tensile Strength (ksi) | Elongation (%) |
|--------------|----------------------|-----------------|----------------------|------------------------|----------------|
| Cutter Blade | S7 Tool Steel        | 0.31            | 210                  | 315                    | 7              |
| Bolt         | A286 Stainless Steel | 0.31            | 139                  | 172                    | 20             |
| Anvil        | A286 Stainless Steel | 0.31            | 139                  | 172                    | 20             |

**Table IV. Cutting Efficiency**

| Parameter | Variation Level |        |
|-----------|-----------------|--------|
|           | 1               | 2      |
| A         | 3 (75)          | 1 (25) |
| B         | 3 (75)          | 1 (25) |
| C         | 3 (75)          | 1 (25) |
| D         | 1 (25)          | 3 (75) |

Numbers in parentheses are percentage (%).

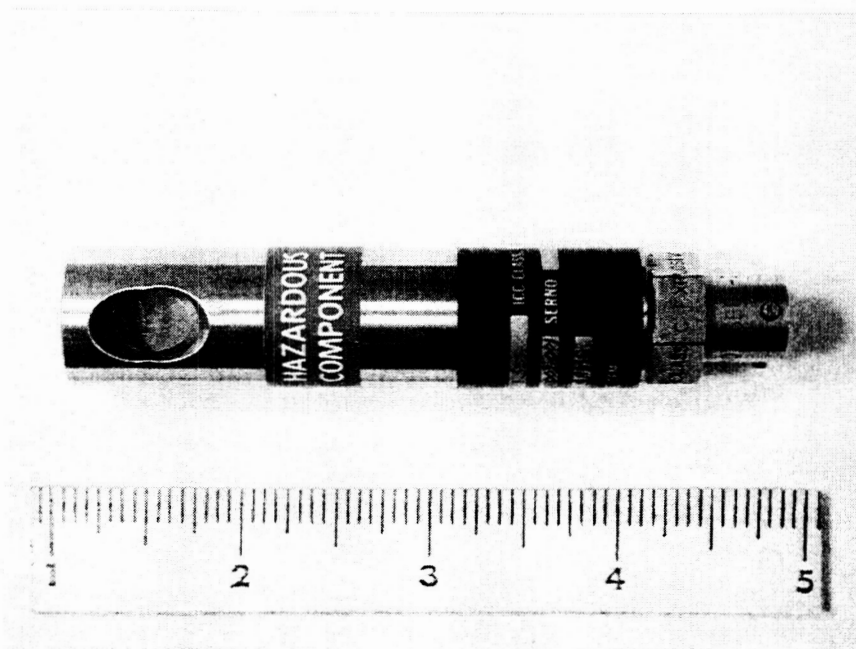
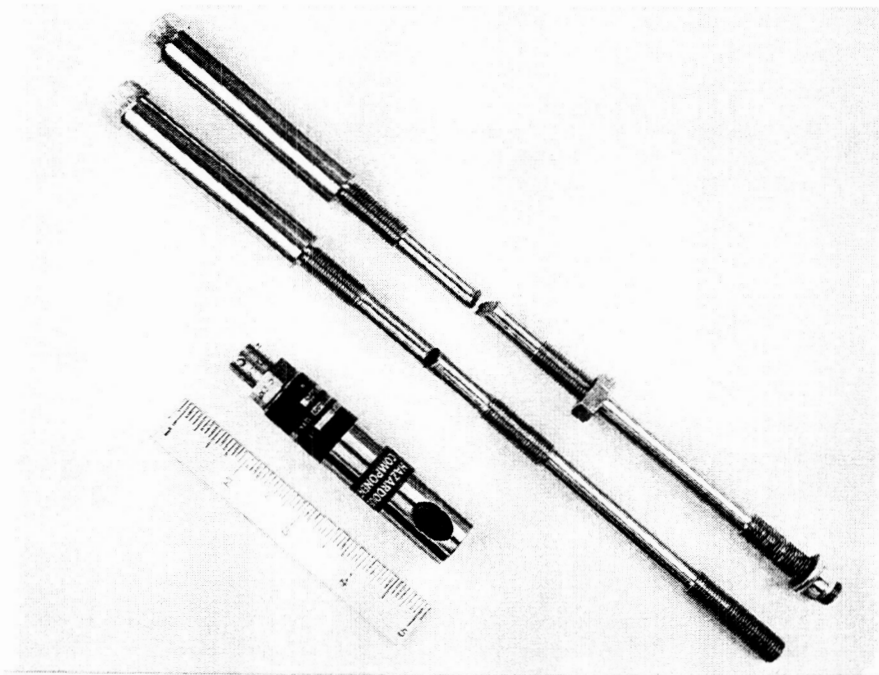


Figure 1: Top photo is the configuration of the long bolt used in system separation tests. One bolt is fully separated, the other is not. Bottom photo shows the bolt cutter with the internal blade visible through the hole at the anvil end of the cutter.

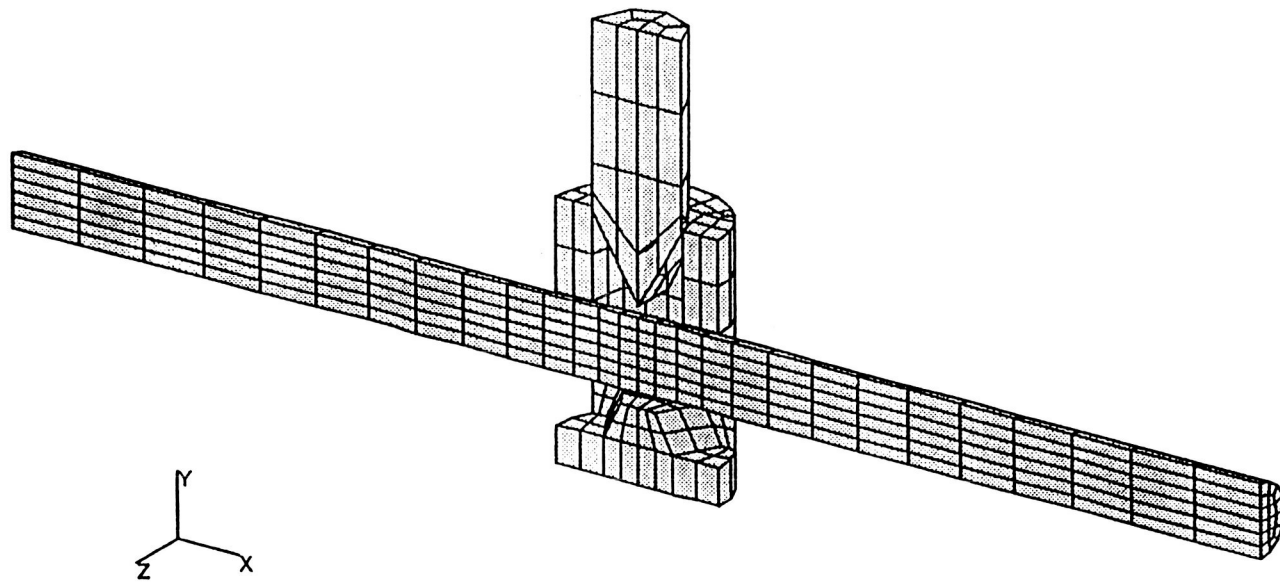


Figure 2: Bolt cutter and bolt finite element model showing 1/2 the configuration before functioning.

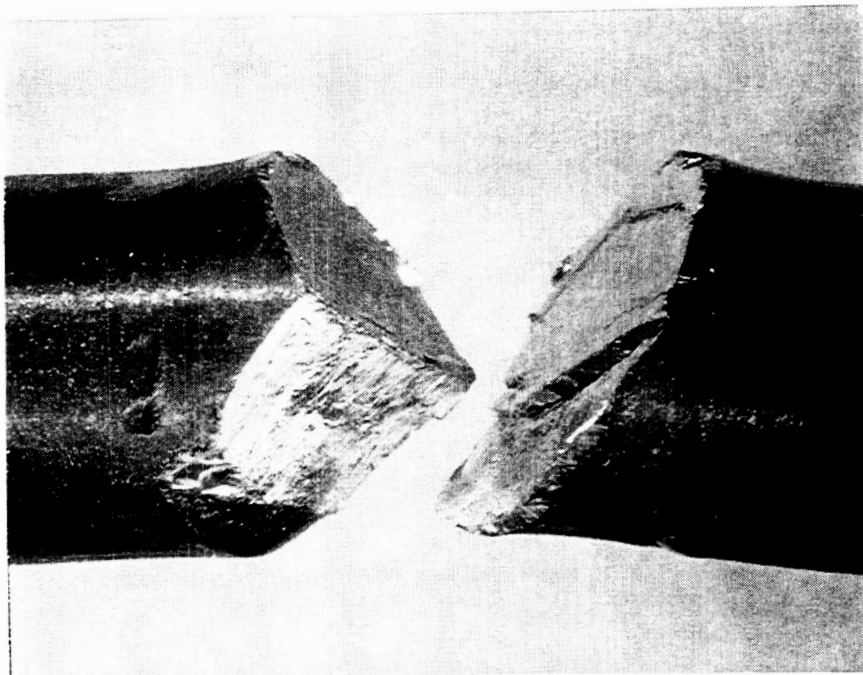


Figure 3:

Top photo shows separation area on the short bolt. Bottom photo is an SEM micrograph providing a face-on view of the fracture on the top right. Note secondary cracks on the blade cut area and complex fracture surface in lower quadrants.



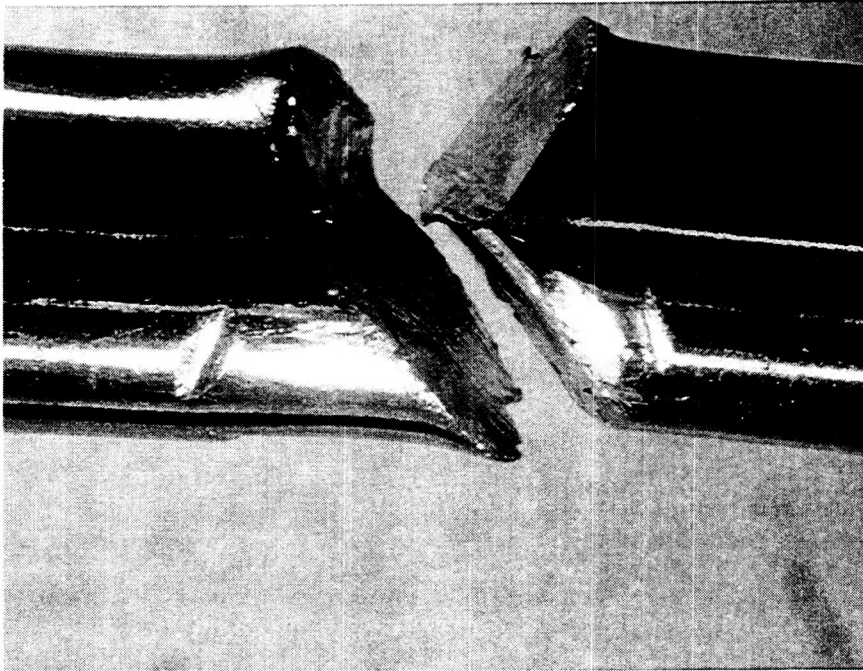


Figure 4:

Top photo shows separation area on the long bolt. Bottom photo is an oblique view of the fracture seen on the top left. Note the limited extent of the blade cut surface remaining on this segment.



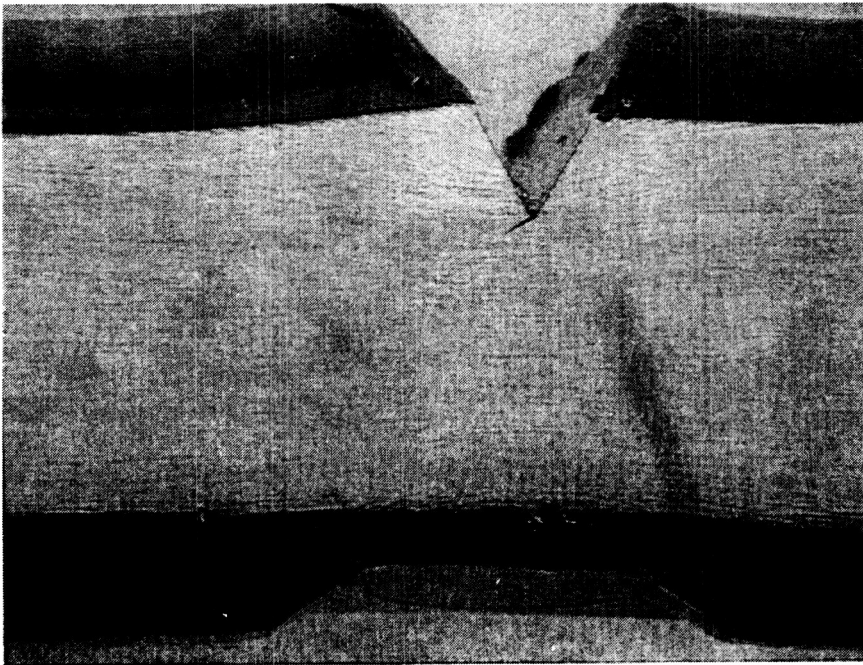
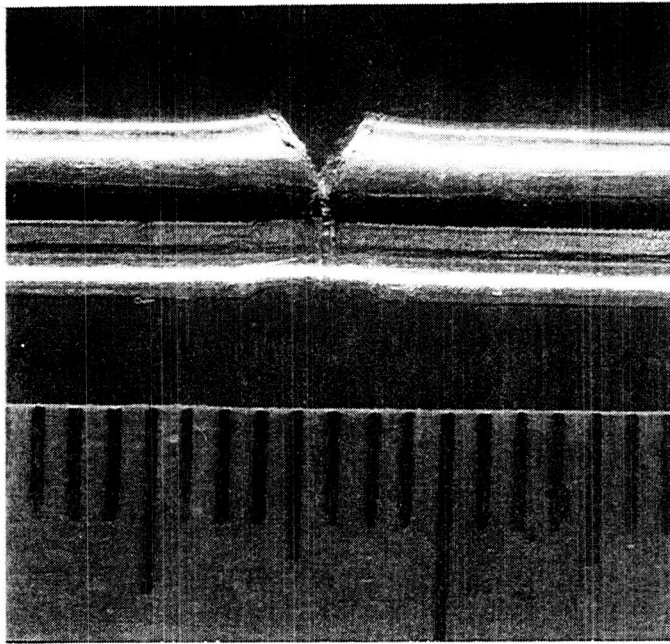


Figure 5: Top photo shows impact area of the long bolt which failed to separate. Bottom photo shows impact area after polishing away 1/4 of the bolt diameter from the side of the bolt. Note the small 45° crack at the tip of the notch produced by the blade impact.

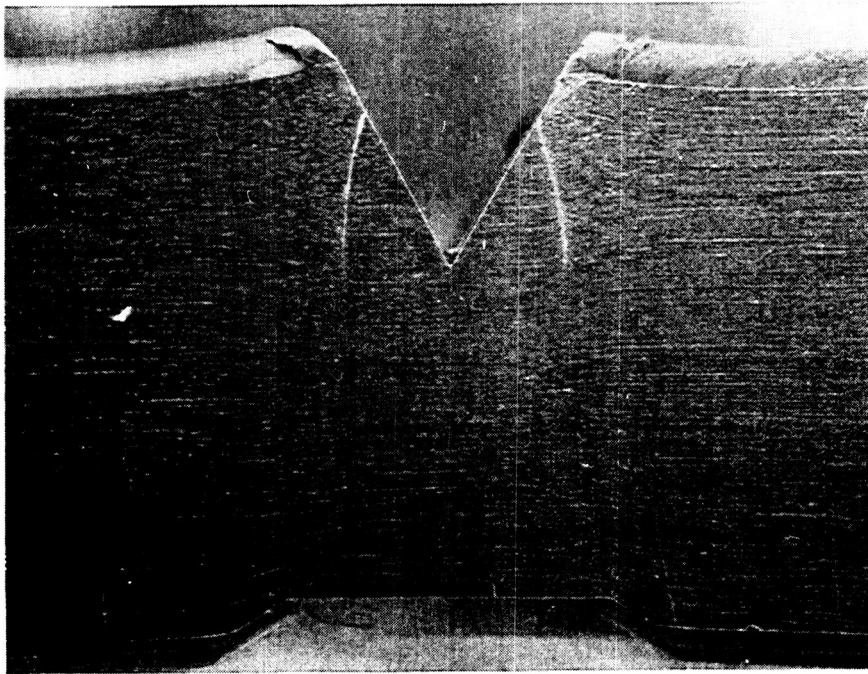
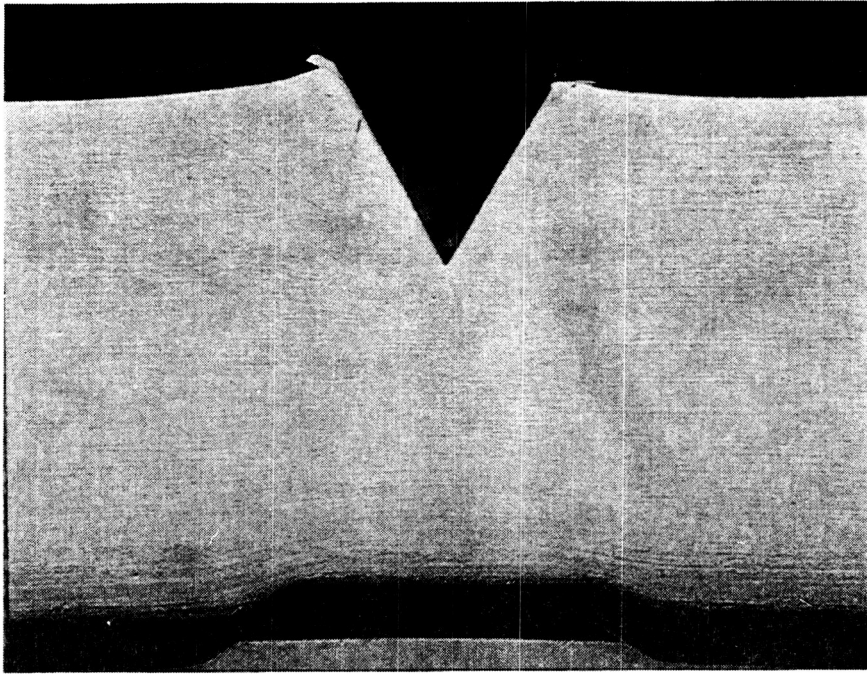


Figure 6: Top photo shows impact area of the long bolt after polishing away 1/3 of the bolt diameter. Bottom photo shows same area after etching (with dilute hydrochloric and nitric acid mixture). Note in this section there is no crack at the tip of the notch. Adiabatic shear bands of localized deformation are seen on both sides of the notch.

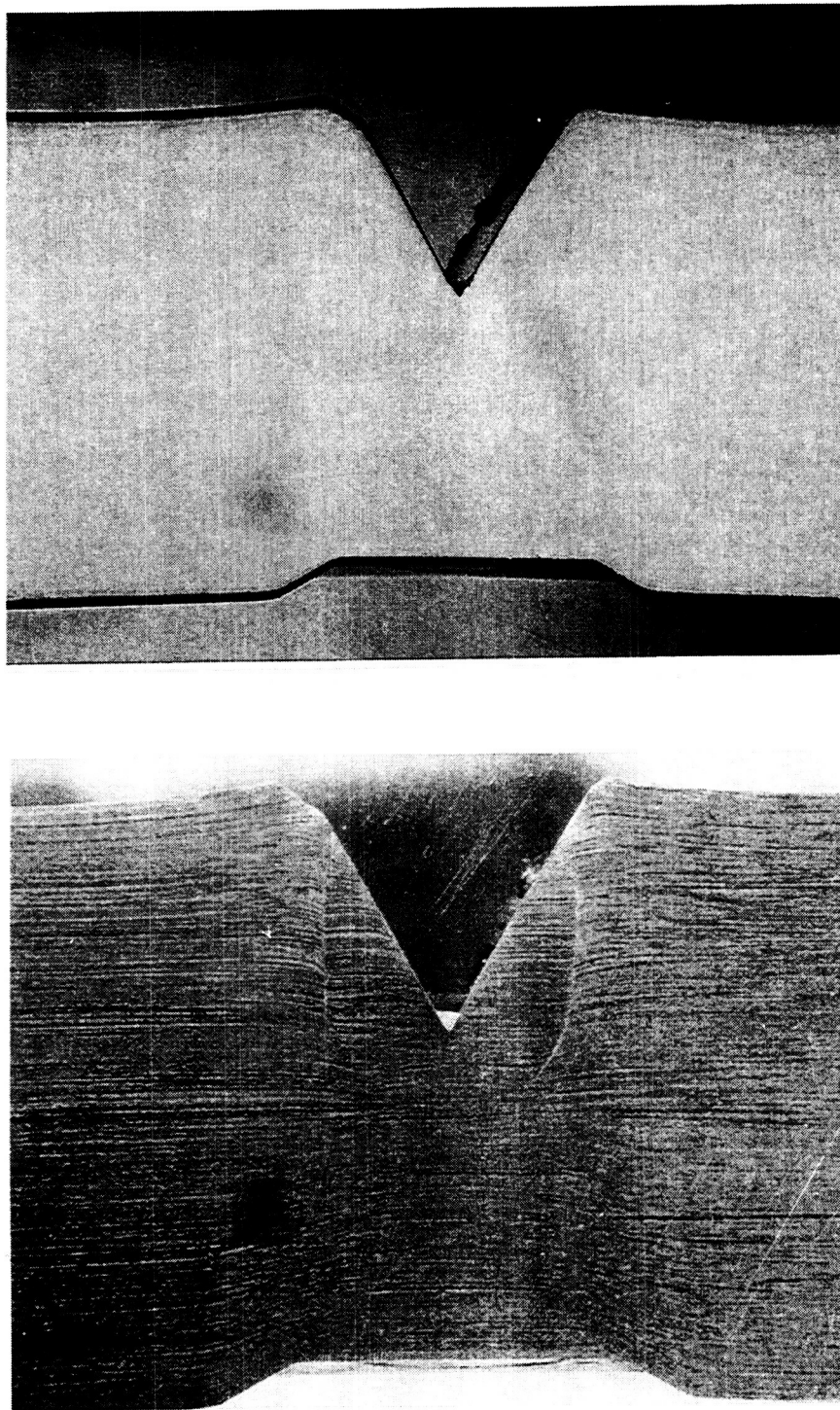


Figure 7: Top photo shows impact area of the long bolt after polishing away 1/2 of the bolt diameter. Bottom photo shows same area after etching. Adiabatic shear bands emerge from the sides of the notch. There is no evidence of similar bands adjacent to the anvil.



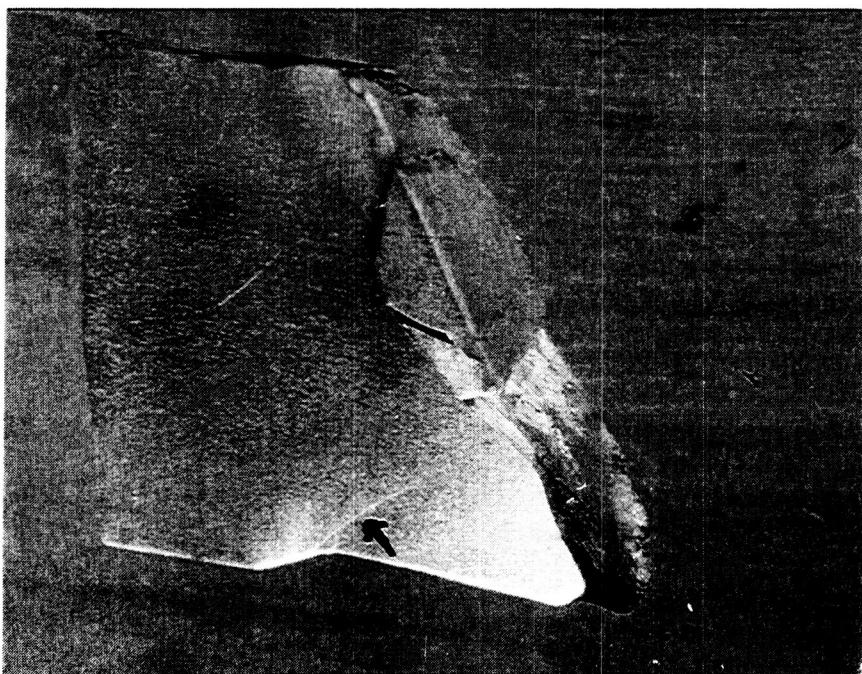
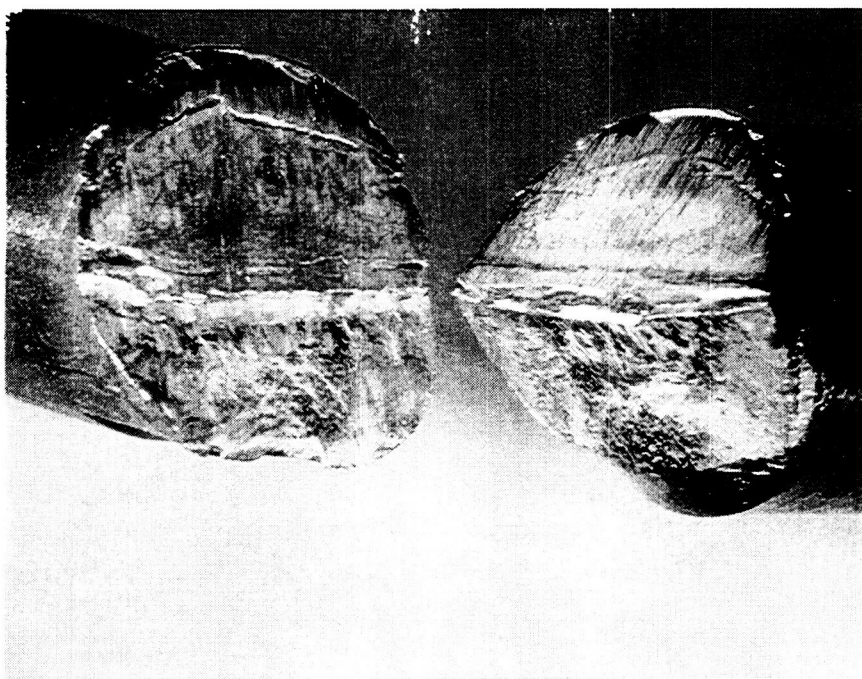


Figure 8: Top photo shows separation area of the short bolt. Bottom photo is a view of the midplane of the bolt segment shown on the top left. Note that a band of localized deformation (adiabatic shear band) has formed in the deformed material above the anvil (see arrow).

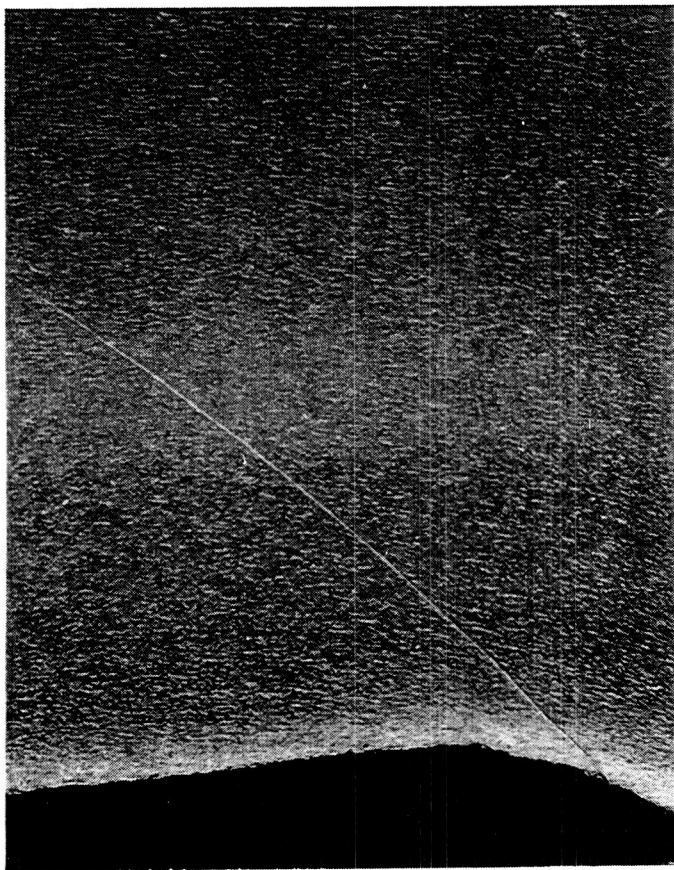
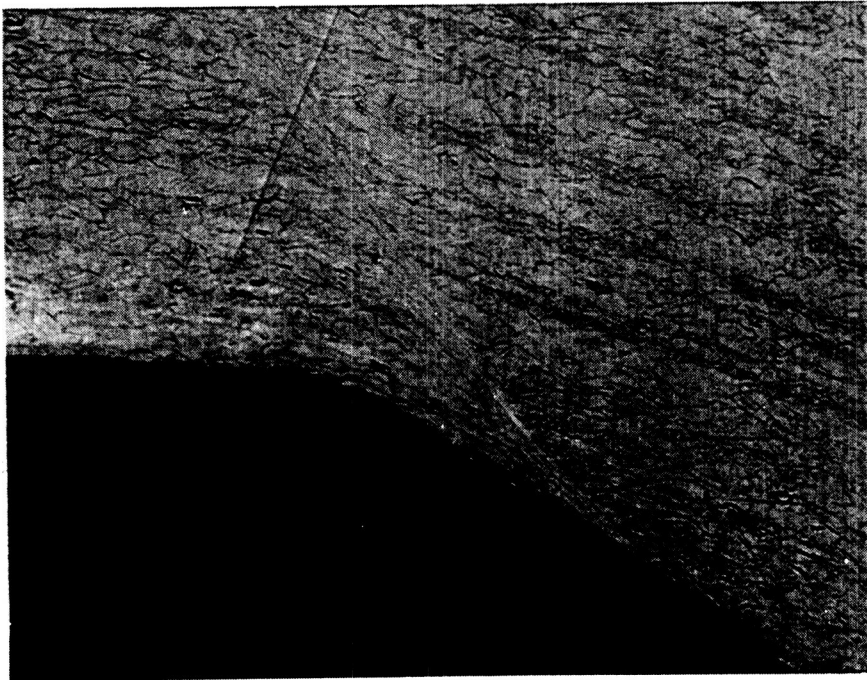


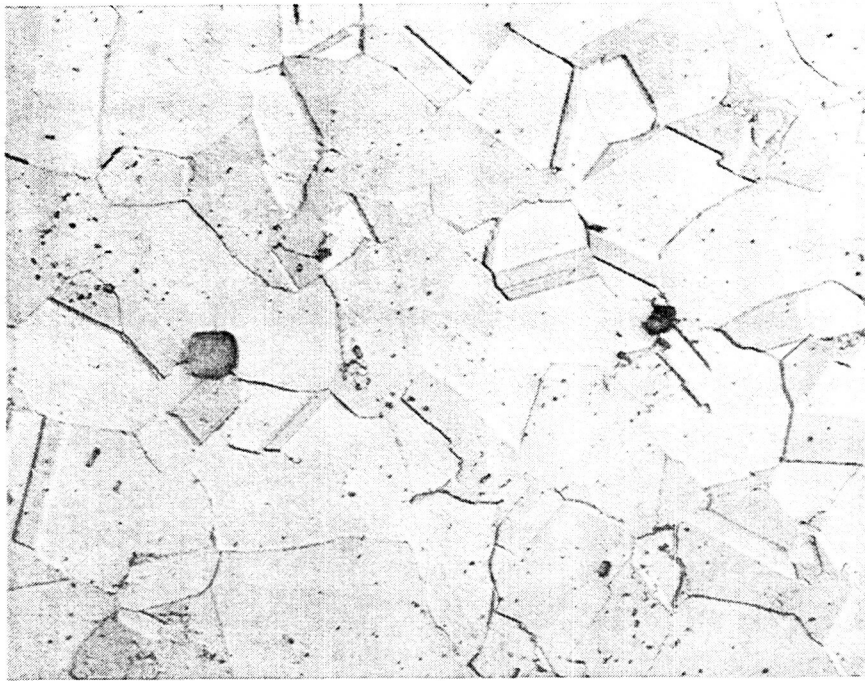
Figure 9:

Top photo shows polished and etched section through the deformed area above the anvil on the short bolt. Bottom photo shows polished and etched section through the deformed area above the anvil on the fractured long bolt. Adiabatic shear bands of localized deformation are emerging in the area of the bolt near the corner of the anvil.

50x



200x



1000X

Figure 10a: Optical micrographs showing typical microstructure in the center of a transverse section through the long bolt (etched with Glyceregia). Microhardness measurements indicate Rockwell "C" of 35-36. This corresponds to a tensile strength of 160 ksi.



1000X

Figure 10b: Optical micrographs showing typical microstructure in the center of a transverse section through the short bolt (etched with Glyceregia). Microhardness measurements indicate Rockwell "C" of 41-43. This corresponds to a tensile strength of 192 ksi.

# VECTOR VELOCITIES

TIME 20.0084

LOCAL MAX 2.857E-02

GLOBAL MAX 2.857E-02



SCALED VEC 2.857E-02

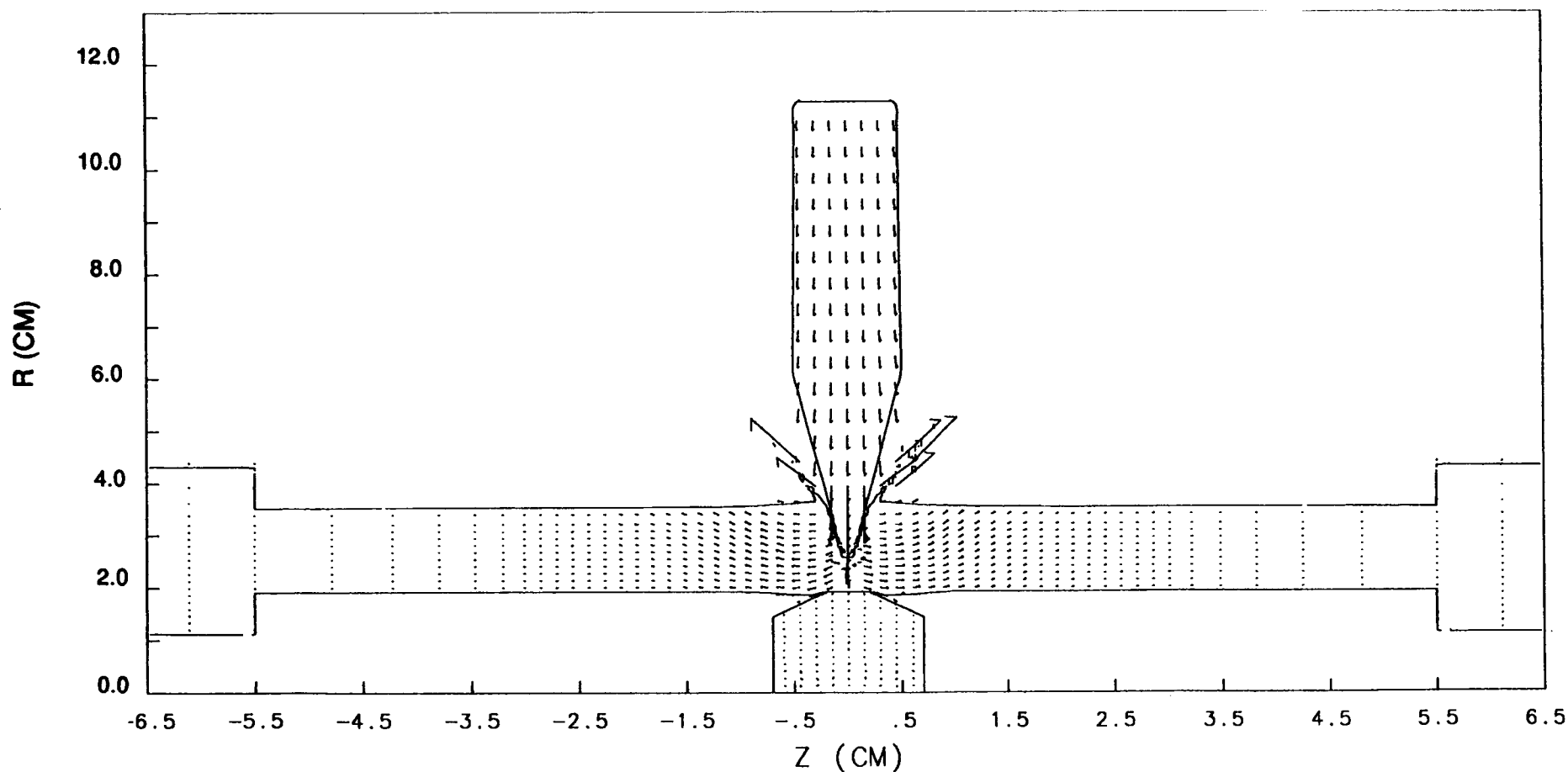


Figure 11. MESA-2D model of cutter blade and bolt 20  $\mu$ sec after impact.



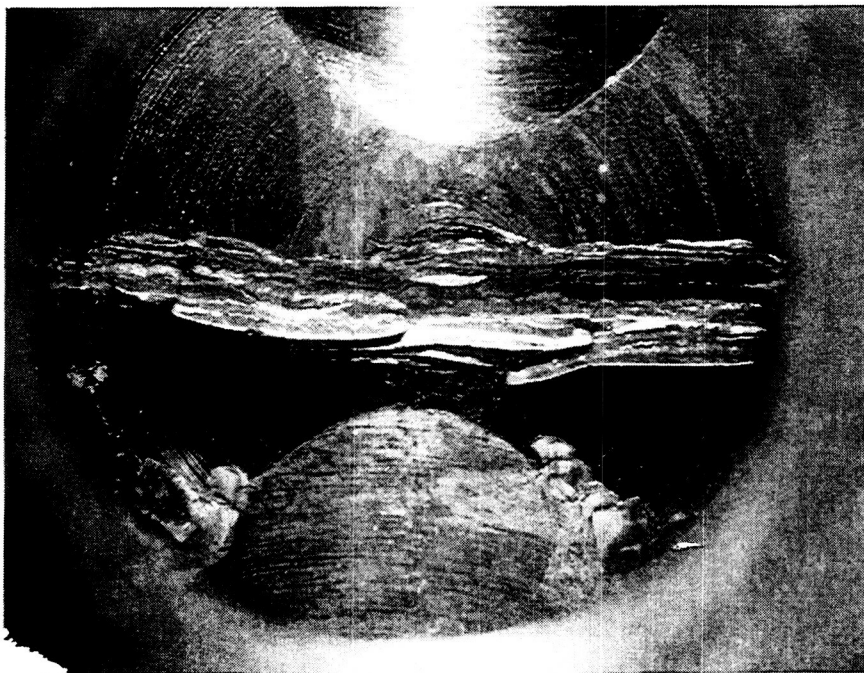
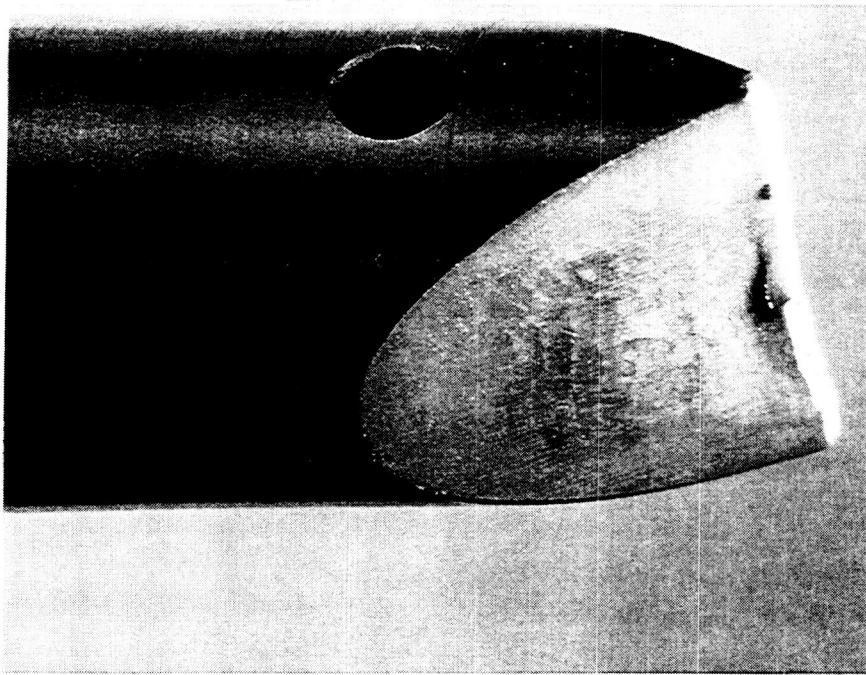


Figure 12: Top photo shows the cutting edge of the blade used in separating the long bolt. Bottom photo shows damage to the anvil resulting from impact of the blade after bolt separation.

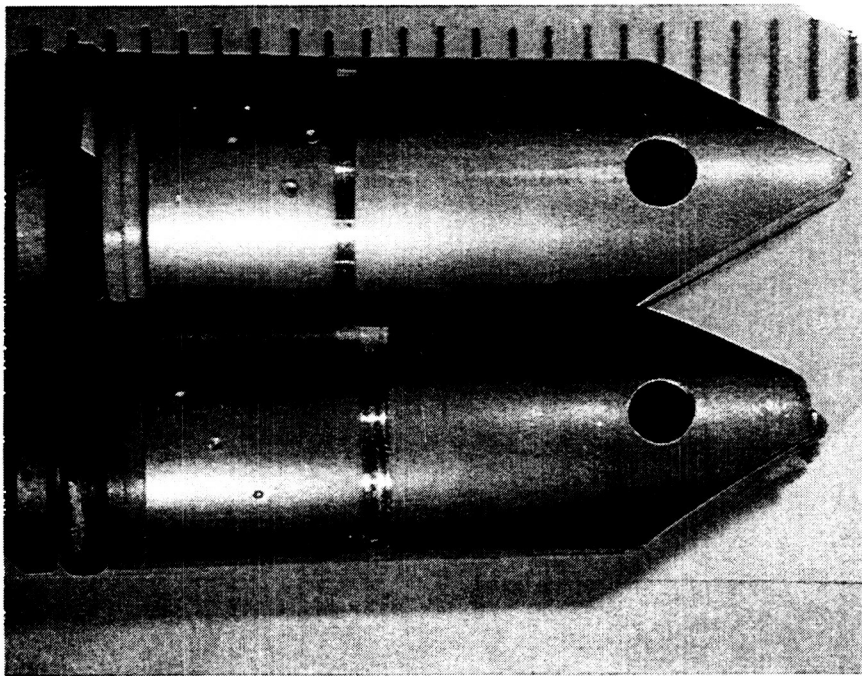
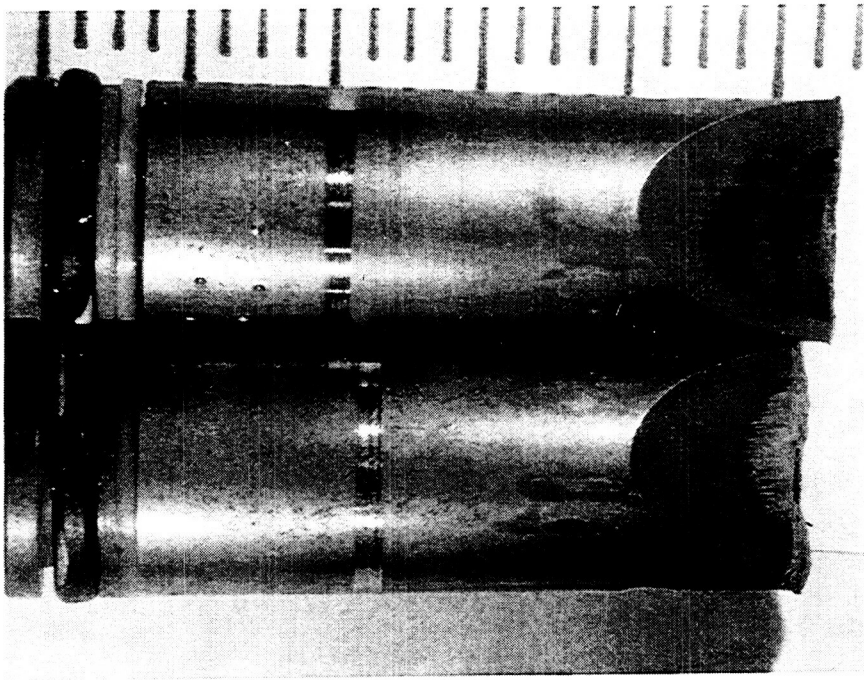


Figure 13: Comparison of damage to the cutter blades used in separating the long and short bolts. Blade used for the short bolt is missing more material (bottom of each photo).

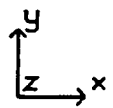
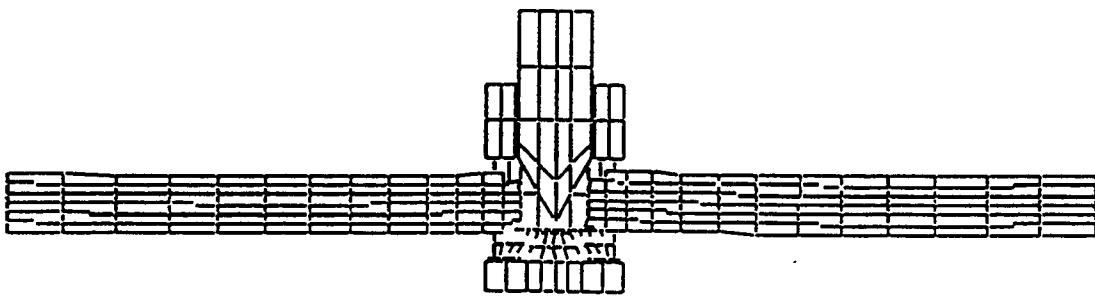


Figure 14: Bolt during impact of cutter blade at 0.4 msec in DYNA3D.

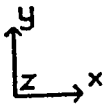
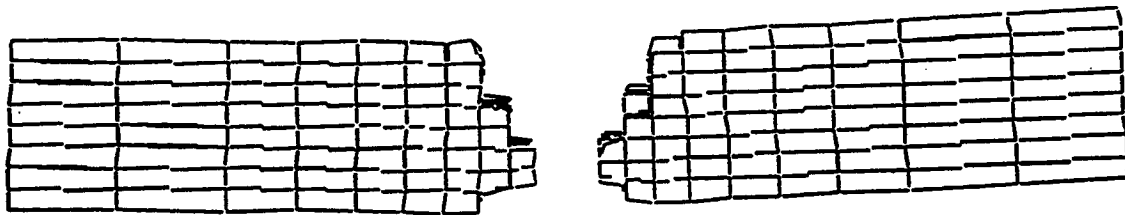


Figure 15: Fractured bolt configuration for finite element analysis.

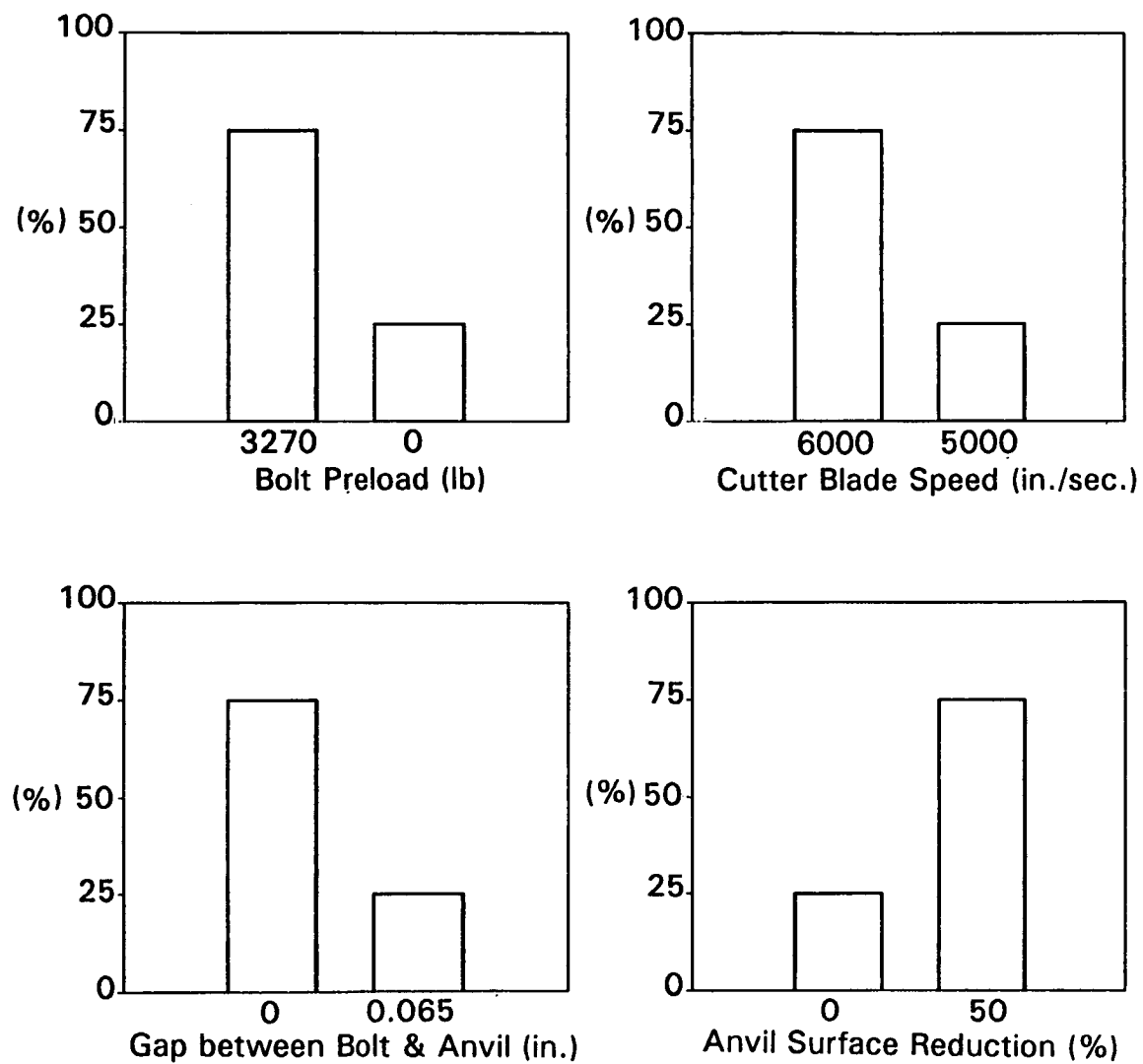


Figure 16: Parameter effects in bolt fracture study.

## Choked Flow Effects in the NSI Driven Pin Puller\*

Keith A. Gonthier<sup>†</sup> and Joseph M. Powers<sup>‡</sup>

Department of Aerospace and Mechanical Engineering  
University of Notre Dame  
Notre Dame, Indiana 46556-5637

### Abstract

This paper presents an analysis for pyrotechnic combustion and pin motion in the NASA Standard Initiator (NSI) actuated pin puller. The conservation principles and constitutive relations for a multi-phase system are posed and reduced to a set of eight ordinary differential equations which are solved to predict the system performance. The model tracks the interactions of the unreacted, incompressible solid pyrotechnic, incompressible condensed phase combustion products, and gas phase combustion products. The model accounts for multiple pyrotechnic grains, variable burn surface area, and combustion product mass flow rates through an orifice located within the device. Pressure-time predictions compare favorably with experimental data. Results showing model sensitivity to changes in the cross-sectional area of the orifice are presented.

### Introduction

Pyrotechnically actuated devices are widely used for aerospace applications. Examples of such devices are pin pullers, exploding bolts, and cable cutters. Full-scale modeling efforts of pyrotechnically driven systems are hindered by many complexities: three dimensionality, time-dependency, complex reaction kinetics, *etc.* Consequently, simple models have been the preferred choice of many researchers.<sup>1,2,3,4</sup> These models require that a number of assumptions be made; typically, a well stirred reactor is simulated; also, the combustion product composition is typically predicted using principles of equilibrium thermochemistry, and the combustion rate is modeled by a simple empirical expression.

Recently, Gonthier and Powers<sup>5</sup> described a methodology for modeling pyrotechnic combustion driven systems which is based upon principles of mixture theory. Though this approach still requires that simplifying assumptions be made, it offers a rational framework for 1) accounting for systems in which unreacted solids and condensed phase products form a large fraction of the mass and volume of the total system, and 2) accounting for the transfer of mass, momentum, and energy both within and between phases. The methodology was illustrated by applying it to a device which is well characterized by experiments: the NSI driven pin puller.

---

\*Presented at the Second NASA Aerospace Pyrotechnic Systems Workshop, February 8-9, 1994, Sandia National Laboratories, Albuquerque, New Mexico. This study is supported by the NASA Lewis Research Center under Contract Number NAG-1335. Dr. Robert M. Stubbs is the contract monitor.

<sup>†</sup>Graduate Research Assistant.

<sup>‡</sup>Assistant Professor, corresponding author.

The focus of this paper is on using the methodology presented in Ref. 5 to formulate a pin puller model which additionally accounts for the flow of combustion products through an orifice located within the device; the model is then used to determine the influence of product mass flow rates on the performance of the device. The present model also accounts for multiple pyrotechnic grains and variable burn surface area. The model presented in this paper is an extension of the model presented in Ref. 5 which did not account for product flow through the orifice, multiple grains, or variable burn surface area.

Figure 1 depicts a cross-section of the NSI driven pin puller in its unretracted state.<sup>6</sup> The primary pin, which will be referred to as the pin for the remainder of the paper, is driven by gases generated by the combustion of a pyrotechnic which is contained within the NSI assembly. Two NSI's are tightly threaded into the device's main body. Only one NSI need operate for the proper functioning of the pin puller; the second is a safety precaution in the event of failure of the first. The pyrotechnic consists of a 114 *mg* mixture of zirconium fuel (54.7 *mg* *Zr*) and potassium perchlorate oxidizer (59.3 *mg* *KClO<sub>4</sub>*). Initially a thin diaphragm tightly encloses the pyrotechnic. Combustion is initiated by the transfer of heat from an electric bridgewire to the pyrotechnic. Upon ignition, the pyrotechnic undergoes rapid chemical reaction producing both condensed phase and gas phase products. The high pressure products accelerate the combustion rate, burst the confining diaphragm, vent through the NSI port (labeled "port" in Fig. 1), and enter into the gas expansion chamber. Once in the chamber, the high pressure gas first causes a set of shear pins to fail, then pushes the pin. After the pin is stopped by crushing an energy absorbing cup, the operation of the device is complete. Peak pressures within the expansion chamber are typically around 50.0 *MPa*; completion of the stroke requires approximately 0.5 *ms*.<sup>6</sup>

For sufficiently high NSI assembly/gas expansion chamber pressure ratios ( $\sim 2.0$ ), and for a fixed cross-sectional area of the NSI port, there exists a maximum flow rate of combustion product mass through the port. The occurrence of this maximum flow rate is referred to as a choked flow condition. Such a condition results in the maximum flux of energy into the expansion chamber; the energy contained within the chamber can then be used to perform work in moving the pin and can be lost to the surroundings in the form of heat. However, if the time scales associated with the flux of energy into the expansion chamber and the rate of heat lost from the products within the chamber to the surroundings are of the same magnitude, there may be insufficient energy available to move the pin; functional failure of the device would result. Therefore, it is possible that variations in the flow rate of product mass through the port may significantly affect the performance of the device.

Included in this report are 1) a description of the model including both the formulation of the model in terms of the mass, momentum, and energy principles supplemented by geometrical and constitutive relations and the mathematical reductions used to refine the model into a form suitable for numerical computations, 2) model predictions and comparisons with experimental results, and 3) results showing the sensitivity of the model to changes in the cross-sectional area of the NSI port.

## Model Description

Assumptions for the model are as follows. As depicted in Fig. 2, the total system is taken to consist of three subsystems: incompressible solid pyrotechnic reactants (*s*), incompressible condensed phase products (*cp*), and gas phase products (*g*). The solid pyrotechnic is assumed to consist of *N* spherical grains having uniform instantaneous radii. The surroundings are taken to consist of the walls of the NSI assembly, the NSI port, and

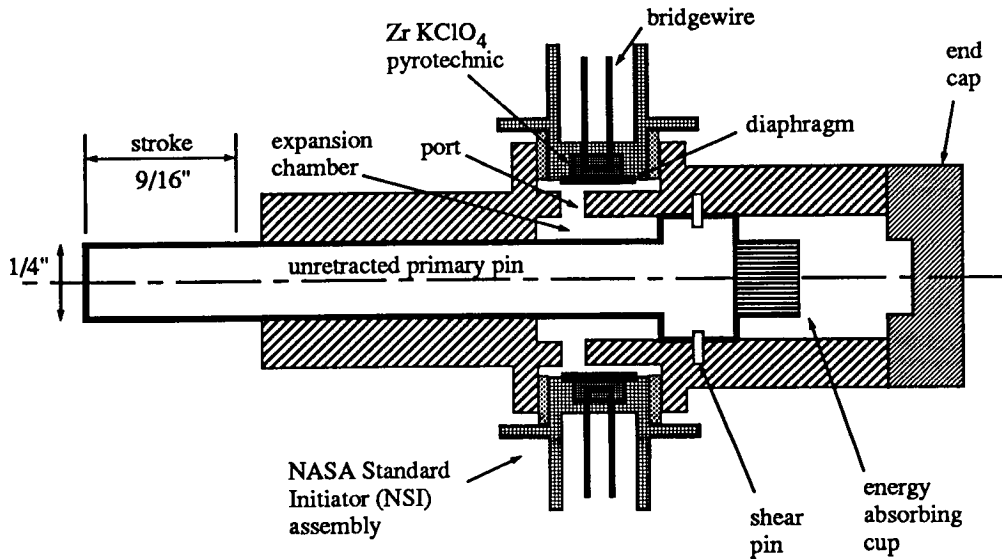


Figure 1: Cross-sectional view of the NSI driven pin puller.

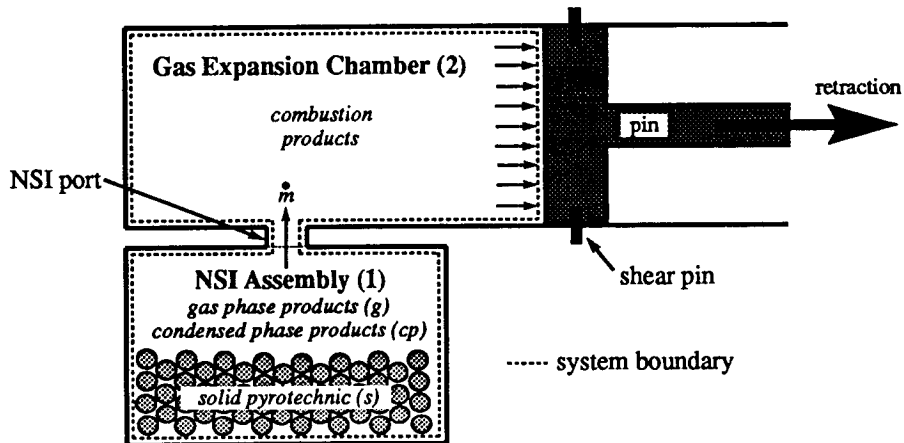


Figure 2: Schematic of the two component system for modeling choked flow effects.

the gas expansion chamber. Both the NSI assembly and the gas expansion chamber are modeled as isothermal cylindrical vessels. The gas expansion chamber is bounded at one end by a movable, frictionless, adiabatic pin while the volume of the NSI assembly remains constant for all time. The NSI port is assumed to have zero volume and is characterized by its cross-sectional area.

Mass and heat exchange between subsystems is allowed such that 1) mass can be transferred from the solid pyrotechnic to both the condensed phase and gas phase products, and 2) heat can be transferred from the condensed phase to the gas phase products. The condensed phase - gas phase heat transfer rate is assumed to be sufficiently large such that thermal equilibrium between the product subsystems exists. There is no mass exchange between the system and the surroundings. Both product subsystems are allowed to interact across the system boundary in the form of heat exchanges. The gas phase products are allowed to do expansion work on the surroundings. No work exchange between subsystems is



allowed. Spatial variations within subsystems are neglected; consequently, all variables are only time-dependent and the total system is modeled as a well-stirred reactor. The kinetic energy of the subsystems is ignored, while an accounting is made of the kinetic energy of the bounding pin. Body forces are neglected.

The rate of mass exchange from the reactant subsystem to the product subsystems is taken to be related to the gas phase pressure within the NSI assembly, namely  $dr/dt = -bP_{g1}^n$ , where  $r$  is the instantaneous radii of the pyrotechnic grains,  $t$  is time,  $P_{g1}$  is the gas phase pressure within the NSI assembly, and  $b$  and  $n$  are experimentally determined constants. All combustion is restricted to the burn surface of the pyrotechnic grains. In the absence of burn rate data for  $Zr/KClO_4$ , we have chosen values for  $b$  and  $n$  so that pressure-time predictions of our model agree with experimental data. The equilibrium thermochemistry code CET89<sup>7</sup> calculated for the constant volume complete combustion of the  $Zr/KClO_4$  mixture is used to predict the product composition; the initial total volume of the pin puller ( $0.95 \text{ cm}^3$ ) was used in this calculation since a significant portion of the system mass is contained within the gas expansion chamber at the time of complete combustion. The component gases are taken to be ideal with temperature-dependent specific heats. The specific heats are in the form of fourth-order polynomial curve fits given by the CET89 code and are not repeated here.

The rate of gas phase product mass flowing from the NSI assembly, through the NSI port, and into the gas expansion chamber is modeled using standard principles of gas dynamics. The flow of condensed phase product mass through the port is assumed to be proportional to the gas phase mass flow rate. The only energy interaction between the NSI assembly and the gas expansion chamber is due to the energy flux associated with the exchange of mass between these two components.

Using principles of mixture theory, a set of mass and energy evolution equations can be written for each subsystem contained within the NSI assembly and gas expansion chamber. These equations, coupled with an equation of motion for the pin, form a set of ordinary differential equations (ODE's) given by the following:

$$\frac{d}{dt}(\rho_{s1} V_{s1}) = -\rho_{s1} A_b r_b, \quad (1)$$

$$\frac{d}{dt}(\rho_{cp1} V_{cp1}) = \eta_{cp} \rho_{s1} A_b r_b - \dot{m}_{cp}, \quad (2)$$

$$\frac{d}{dt}(\rho_{g1} V_{g1}) = (1 - \eta_{cp}) \rho_{s1} A_b r_b - \dot{m}_g, \quad (3)$$

$$\frac{d}{dt}(\rho_{s1} V_{s1} e_{s1}) = -\rho_{s1} e_{s1} A_b r_b, \quad (4)$$

$$\frac{d}{dt}(\rho_{cp1} V_{cp1} e_{cp1}) = \eta_{cp} \rho_{s1} e_{s1} A_b r_b - h_{cp1} \dot{m}_{cp} - \dot{Q}_{cp,g1} + \dot{Q}_{cp1}, \quad (5)$$

$$\frac{d}{dt}(\rho_{g1} V_{g1} e_{g1}) = (1 - \eta_{cp}) \rho_{s1} e_{s1} A_b r_b - h_{g1} \dot{m}_g + \dot{Q}_{cp,g1} + \dot{Q}_{g1}, \quad (6)$$

$$\frac{d}{dt}(\rho_{cp2} V_{cp2}) = \dot{m}_{cp}, \quad (7)$$

$$\frac{d}{dt}(\rho_{g2} V_{g2}) = \dot{m}_g, \quad (8)$$

$$\frac{d}{dt}(\rho_{cp2} V_{cp2} e_{cp2}) = h_{cp1} \dot{m}_{cp} - \dot{Q}_{cp,g2} + \dot{Q}_{cp2}, \quad (9)$$

$$\frac{d}{dt}(\rho_{g2} V_{g2} e_{g2}) = h_{g1} \dot{m}_g + \dot{Q}_{cp,g2} + \dot{Q}_{g2} - \dot{W}_{out2}, \quad (10)$$

$$m_p \frac{d^2}{dt^2}(z_p) = F_p. \quad (11)$$

In these equations, the notation subscript “1” and subscript “2” are used to label quantities associated with the NSI and the gas expansion chamber, respectively. Subscripts “s”, “cp”, and “g” are used to label quantities associated with the solid pyrotechnic, condensed phase products, and gas phase products, respectively. The independent variable in Eqs. (1-11) is time  $t$ . Dependent variables are as follows: the density  $\rho_{gi}$  (here, and for the remainder of this report, the index  $i = 1, 2$  will be used to denote quantities associated with the NSI and the gas expansion chamber, respectively); the volumes  $V_{s1}$ ,  $V_{cp1}$ ,  $V_{g1}$ ; the specific internal energies  $e_{s1}$ ,  $e_{cp1}$ ,  $e_{g1}$ ; the specific enthalpies  $h_{cp1}$ ,  $h_{g1}$ ; the pin position  $z_p$ ; the pyrotechnic burn rate  $r_b$ ; the area of the burn surface  $A_b$ ; the rates of product mass flowing through the NSI port  $\dot{m}_{cp}$ ,  $\dot{m}_g$ ; the rates of heat transfer from the surroundings to the gas phase products  $\dot{Q}_{in1}$ ; the rates of heat transfer from the condensed phase products to the gas phase products  $\dot{Q}_{cp,g1}$ ; the rate of work done by product gases contained within the expansion chamber in moving the pin  $\dot{W}_{out2}$ ; and the net force on the pin  $F_p$ .

Constant parameters contained in Eqs. (1-11) are the mass of the pin  $m_p$ , the density of the unreacted solid pyrotechnic  $\rho_{s1}$ , the density of the condensed phase products  $\rho_{cp1}$  and  $\rho_{cp2}$ , and the mass fraction of the products which are in the condensed phase  $\eta_{cp}$ . As it is understood that the pyrotechnic is contained entirely within the NSI, the notation subscript “1” will be dropped when referring to quantities associated with the solid pyrotechnic. Also, since  $\rho_{cp1} = \rho_{cp2} = \text{constant}$ , these two quantities will be referred to as  $\rho_{cp}$ .

Equations (1-3) govern the evolution of mass and Eqs. (4-6) govern the evolution of energy for the solid pyrotechnic, the condensed phase products, and the gas phase products contained within the NSI, respectively. Equations (7) and (8) govern the evolution of mass and Eqs. (9) and (10) govern the evolution of energy for the condensed phase products and gas phase products contained within the gas expansion chamber, respectively. Equation (11) is Newton’s Second Law which governs the motion of the pin.

Geometric and constitutive relations used to close Eqs. (1-11) are as follows:

$$V_1 = V_s + V_{cp1} + V_{g1}, \quad (12)$$

$$V_2 = V_{cp2} + V_{g2}, \quad (13)$$

$$z_p = \frac{V_2}{A_p}, \quad (14)$$

$$r[V_s] = \left( \frac{3V_s}{4\pi N} \right)^{1/3}, \quad (15)$$

$$A_b[V_s] = \left( 36\pi N V_s^2 \right)^{1/3}, \quad (16)$$

$$P_{gi} = \rho_{gi} R T_{gi}, \quad (17)$$

$$r_b[P_{g1}] = -\frac{dr}{dt} = b P_{g1}^n, \quad (18)$$

$$e_s[T_s] = \sum_{j=1}^{N_s} Y_s^j e_s^j[T_s], \quad (19)$$

$$e_{cp_i} [T_{cp_i}] = \sum_{j=1}^{N_{cp}} Y_{cp}^j e_{cp}^j [T_{cp_i}], \quad (20)$$

$$e_{g_i} [T_{g_i}] = \sum_{j=1}^{N_g} Y_g^j e_g^j [T_{g_i}], \quad (21)$$

$$c_{vs} [T_s] = \sum_{j=1}^{N_s} Y_s^j \frac{d}{dT_s} (e_s^j [T_s]), \quad (22)$$

$$c_{vcp_i} [T_{cp_i}] = \sum_{j=1}^{N_{cp}} Y_{cp}^j \frac{d}{dT_{cp_i}} (e_{cp}^j [T_{cp_i}]), \quad (23)$$

$$c_{vg_i} [T_{g_i}] = \sum_{j=1}^{N_g} Y_g^j \frac{d}{dT_{g_i}} (e_g^j [T_{g_i}]), \quad (24)$$

$$h_{cp_1} [T_{cp_1}] = \sum_{j=1}^{N_{cp}} Y_{cp}^j h_{cp}^j [T_{cp_1}], \quad (25)$$

$$h_{g_1} [T_{g_1}] = \sum_{j=1}^{N_g} Y_g^j h_g^j [T_{g_1}], \quad (26)$$

$$c_{pcp_1} [T_{cp_1}] = \sum_{j=1}^{N_{cp}} Y_{cp}^j \frac{d}{dT_{cp_1}} (h_{cp}^j [T_{cp_1}]), \quad (27)$$

$$c_{pg_1} [T_{g_1}] = \sum_{j=1}^{N_g} Y_g^j \frac{d}{dT_{g_1}} (h_g^j [T_{g_1}]), \quad (28)$$

$$\dot{Q}_{cp,g_i} [T_{cp_i}, T_{g_i}] = h_{cp,g} A_{cp_i} (T_{cp_i} - T_{g_i}), \quad (29)$$

$$\dot{Q}_{cp_i} = \dot{Q}_{cp_i} [T_{cp_i}], \quad (30)$$

$$\dot{Q}_{g_i} = \dot{Q}_{g_i} [T_{g_i}], \quad (31)$$

$$\dot{W}_{out_2} = P_{g_2} \frac{dV_2}{dt}, \quad (32)$$

$$F_p = \begin{cases} 0 & \text{if } P_{g_2} A_p < F_{crit} \\ P_{g_2} A_p & \text{if } P_{g_2} A_p \geq F_{crit}, \end{cases} \quad (33)$$

$$\dot{m}_g = \begin{cases} \rho_{g_1} A_e \sqrt{\gamma R T_{g_1}} \sqrt{\frac{2}{\gamma-1} \left( \frac{P_{g_1}}{P_{g_2}} \right)^{-\frac{\gamma+1}{\gamma}} \left( \left( \frac{P_{g_1}}{P_{g_2}} \right)^{\frac{\gamma-1}{\gamma}} - 1 \right)} & \text{if } \left( \frac{P_{g_1}}{P_{g_2}} \right) < \left( \frac{\gamma+1}{2} \right)^{\frac{\gamma}{\gamma-1}} \\ \rho_{g_1} A_e \sqrt{\gamma R T_{g_1}} \left( \frac{2}{\gamma+1} \right)^{\frac{\gamma+1}{2(\gamma-1)}} & \text{if } \left( \frac{P_{g_1}}{P_{g_2}} \right) \geq \left( \frac{\gamma+1}{2} \right)^{\frac{\gamma}{\gamma-1}}, \end{cases} \quad (34)$$

$$\dot{m}_{cp} = \left( \frac{\eta_{cp}}{1 - \eta_{cp}} \right) \dot{m}_g. \quad (35)$$

Here, and throughout the paper, braces [ ] are used to denote a functional dependence on the enclosed variable. Equations (12-14) are geometrical constraints; in Eq. (14),  $A_p$  is the cross-sectional area of the pin. Equation (15) is an expression for the radius  $r$  of each

spherical pyrotechnic grain;  $N$  is the total number of pyrotechnic grains. The area of the burn surface is given by Eq. (16); it is assumed here that the area of the burning surface is the total surface area of the  $N$  pyrotechnic grains. Equation (17) is a thermal equation of state for the gas phase products. Occurring in this expression are the gas phase pressure  $P_{gi}$ , the gas phase temperature  $T_{gi}$ , and the ideal gas constant for the gas phase products  $R$  (the quotient of the universal gas constant and the mean molecular weight of the product gases). The pyrotechnic burn rate  $r_b$  is given by Eq. (18).

Equations (19-21) are caloric equations of state for the solid pyrotechnic, condensed phase products, and gas phase products, respectively. Here,  $T_s$  is the temperature of the solid pyrotechnic, and  $T_{cp_i}$  is the temperature of the condensed phase products. Also,  $Y_s^j$ ,  $Y_{cp_i}^j$ ,  $Y_{gi}^j$ ,  $N_s$ ,  $N_{cp}$ , and  $N_g$  are the constant mass fractions and number of component species of solid pyrotechnic, condensed phase product, and gas phase product species, respectively. Here, and throughout the paper, the notation superscript "j" is used to label quantities associated with individual chemical species. Since for both ideal gases and condensed phase species, the internal energy is only a function of temperature, the specific heat at constant volume for the solid pyrotechnic,  $c_{vs}$ , the condensed phase products,  $c_{vcp_i}$ , and the gas phase products,  $c_{vgi}$ , can be obtained by differentiation of Eqs. (19-21) with respect to their temperature. Expressions for the specific heats at constant volume are given by Eqs. (22-24). The specific enthalpies for the condensed phase products and the gas phase products contained within the NSI assembly are given by Eqs. (25) and (26), respectively. These expressions can be differentiated with respect to their temperature to obtain the specific heats at constant pressure  $c_{pcp_i}$  and  $c_{pgi}$ , Eqs. (27) and (28).

Equation (29) gives an expression for the rate of heat transfer from the condensed phase products to the gas phase products. In this expression,  $h_{cp,g}$  is a constant heat transfer parameter, and  $A_{cp_i}$  is the surface area of the condensed phase products. The term  $h_{cp,g}A_{cp_i}$  is assumed large for this study. The functional dependencies of the heat transfer rates between the surroundings and the product subsystems are given by Eqs. (30) and (31). The functional form of these models will be given below.

Equation (32) models pressure-volume work done by the gas contained within the expansion chamber in moving the pin. Equation (33) models the force on the pin due to the gas phase pressure and a restraining force due to the shear pins which are used to initially hold the pin in place. Here,  $F_{crit}$  is the critical force necessary to cause shear pin failure. The work associated with shearing the pin is not considered.

The flow rate of gas phase product mass through the NSI port is given by Eq. (34).<sup>8</sup> Occurring in this expression are the cross-sectional area of the port,  $A_e$ , and the specific heat ratio for the product gases contained within the NSI assembly,  $\gamma$  ( $= c_{pg1}/c_{vg1}$ ). This expression accounts for mass choking at elevated NSI assembly/gas expansion chamber pressure ratios. The condensed phase product mass flow rate through the port is given by Eq. (35).

With the assumption of large heat transfer rates between the condensed phase and gas phase product subsystems (*i.e.*,  $h_{cp,g}A_{cp_i} \rightarrow \infty$ ), the product subsystems remain in thermal equilibrium for all time. Therefore, we take  $T_{p1} \equiv T_{cp1} = T_{g1}$  and  $T_{p2} \equiv T_{cp2} = T_{g2}$ , with  $T_{p1}$  defined as the temperature of the combined product subsystem contained within the NSI assembly and  $T_{p2}$  the temperature of the combined product subsystem contained within the gas expansion chamber. With this assumption, one can define the net heat transfer rates  $\dot{Q}_{p1}$  and  $\dot{Q}_{p2}$  governing the transfer of heat from the surroundings to the combined product

subsystems:

$$\dot{Q}_{p1}[T_{p1}] \equiv \dot{Q}_{cp1} + \dot{Q}_{g1} = hA_{w1}(T_w - T_{p1}) + \sigma A_{w1}(\alpha T_w^4 - \epsilon T_{p1}^4), \quad (36)$$

$$\dot{Q}_{p2}[T_{p2}] \equiv \dot{Q}_{cp2} + \dot{Q}_{g2} = hA_{w2}[V_s](T_w - T_{p2}) + \sigma A_{w2}[V_2](\alpha T_w^4 - \epsilon T_{p2}^4), \quad (37)$$

where

$$A_{w1} = 2\sqrt{\frac{\pi}{A_1}}V_1 + 2A_1 - A_e, \quad A_{w2}[V_2] = 2\sqrt{\frac{\pi}{A_p}}V_2 + A_p - A_e. \quad (38)$$

Equations (38) are expressions for the surface area of the NSI assembly and the gas expansion chamber, respectively, through which heat transfer with the surroundings can occur; the parameter  $A_1$  in the first of these relations is the constant cross-sectional area of the NSI assembly.

### Mathematical Reductions

In this section, intermediate operations are described that reduce the governing equations to a final autonomous system of first order ODE's which can be numerically solved to predict the pin puller performance. To this end, it is necessary to define a new variable  $\dot{V}_2$  representing the time derivative of the gas expansion chamber volume:

$$\dot{V}_2 \equiv \frac{dV_2}{dt}. \quad (39)$$

The final system consists of eight first order ODE's of the form

$$\frac{d\mathbf{u}}{dt} = \mathbf{f}(\mathbf{u}), \quad (40)$$

where  $\mathbf{u} = (V_2, V_s, V_{cp1}, \rho_{g1}, T_{p1}, V_{cp2}, T_{p2}, \dot{V}_2)^T$  is a vector of dependent variables and  $\mathbf{f}$  is a non-linear vector function. These eight dependent variables will be referred to as primary variables. It will now be shown how to express all remaining variables as functions of the primary variables.

Quantities already expressed in terms of the primary variables are the gas phase pressure inside the NSI  $P_{g1}[\rho_{g1}, T_{p1}]$ , the heat transfer rates  $\dot{Q}_{p1}[T_{p1}]$  and  $\dot{Q}_{p2}[V_2, T_{p2}]$ , the specific internal energies  $e_{cp1}[T_{p1}]$  and  $e_{g1}[T_{p1}]$ , the specific heats at constant volume  $c_{vcp1}[T_{p1}]$  and  $c_{vg1}[T_{p1}]$ , the specific enthalpies  $h_{cp1}[T_{p1}]$  and  $h_{g1}[T_{p1}]$ , and the specific heats at constant pressure  $c_{pcp1}[T_{p1}]$  and  $c_{pg1}[T_{p1}]$ . Also, with a knowledge of  $P_{g1}$ , Eq. (18) can be used to express  $r_b$  as functions of  $\rho_{g1}$  and  $T_{p1}$ :

$$r_b[\rho_{g1}, T_{p1}] = bP_{g1}^n[\rho_{g1}, T_{p1}]. \quad (41)$$

Addition of Eqs. (1), (2), (3), (7), and (8) results in a homogeneous differential equation expressing the conservation of the total system's mass:

$$\frac{d}{dt}(\rho_s V_s + \rho_{cp} V_{cp1} + \rho_{g1} V_{g1} + \rho_{cp} V_{cp2} + \rho_{g2} V_{g2}) = 0. \quad (42)$$

Integrating this expression, applying initial conditions, denoted by the subscript "o", using Eq. (12) to eliminate  $V_{g1}$  in favor of  $V_1$ ,  $V_s$ , and  $V_{cp1}$ , using Eq. (13) to eliminate  $V_{g2}$  in favor of  $V_2$  and  $V_{cp2}$ , and solving for  $\rho_{g2}$  results in the following:

$$\rho_{g2}[V_2, V_s, V_{cp1}, \rho_{g1}, V_{cp2}] = \frac{m_o - \rho_s V_s - \rho_{cp} V_{cp1} - \rho_{g1}(V_1 - V_s - V_{cp1}) - \rho_{cp} V_{cp2}}{V_2 - V_{cp2}}, \quad (43)$$

where

$$m_o = \rho_s V_{s_o} + \rho_{cp} V_{cp1_o} + \rho_{g1_o} V_{g1_o} + \rho_{cp} V_{cp2_o} + \rho_{g2_o} V_{g2_o}.$$

Here,  $m_o$  represents the initial mass of the system. Substituting Eq. (43) into Eq. (17) determines  $P_{g2}$  as a function of the primary variables:

$$P_{g2} [V_2, V_s, V_{cp1}, \rho_{g1}, V_{cp2}, T_{p2}] = \rho_{g2} [V_2, V_s, V_{cp1}, \rho_{g1}, V_{cp2}] RT_{p2}. \quad (44)$$

With a knowledge of  $P_{g2}$ , Eqs. (32), (33), (34), and (35) can be expressed in the following forms, respectively:

$$\dot{W}_{out2} = \dot{W}_{out2}[V_2, V_s, V_{cp1}, \rho_{g1}, V_{cp2}, T_{p2}, \dot{V}_2], \quad (45)$$

$$F_p = F_p [V_2, V_s, V_{cp1}, \rho_{g1}, V_{cp2}, T_{p2}], \quad (46)$$

$$\dot{m}_g = \dot{m}_g [V_2, V_s, V_{cp1}, \rho_{g1}, T_{p1}, V_{cp2}, T_{p2}], \quad (47)$$

$$\dot{m}_{cp} = \dot{m}_{cp} [V_2, V_s, V_{cp1}, \rho_{g1}, T_{p1}, V_{cp2}, T_{p2}]. \quad (48)$$

We next simplify the remaining mass evolution equations. Since both  $\rho_s$  and  $\rho_{cp}$  are constant, Eqs. (1), (2), and (7) can be rewritten as

$$\frac{dV_s}{dt} = -A_b r_b, \quad (49)$$

$$\frac{dV_{cp1}}{dt} = \frac{\eta_{cp} \rho_s A_b r_b - \dot{m}_{cp}}{\rho_{cp}}, \quad (50)$$

$$\frac{dV_{cp2}}{dt} = \frac{\dot{m}_{cp}}{\rho_{cp}}. \quad (51)$$

To simplify Eq. (3), we use Eq. (12) to replace  $V_{g1}$  in favor of  $V_s$  and  $V_{cp1}$ , use Eqs. (49) and (50) to eliminate the resulting volume derivatives, and solve for the time derivative of  $\rho_{g1}$ :

$$\frac{d\rho_{g1}}{dt} = \frac{\left(1 - \frac{\rho_{g1}}{\rho_s} - \left(1 - \frac{\rho_{g1}}{\rho_{cp}}\right) \eta_{cp}\right) \rho_s A_b r_b - \dot{m}_g - \frac{\rho_{g1}}{\rho_{cp}} \dot{m}_{cp}}{V_1 - V_s - V_{cp1}}. \quad (52)$$

The energy evolution equations will now be simplified. We first multiply Eq. (1) by  $e_s$  and subtract the result from Eq. (4) to obtain

$$\frac{de_s}{dt} = 0.$$

Thus, in accordance with our assumption of no heat transfer to the solid pyrotechnic, its specific internal energy remains constant for all time. Integrating this result, we obtain

$$e_s = e_{s_o}. \quad (53)$$

Addition of Eqs. (5) and (6), and addition of Eqs. (9) and (10) result in expressions governing the evolution of energy for the combined product subsystems contained within the NSI assembly and gas expansion chamber, respectively:

$$\frac{d}{dt} [\rho_{cp} V_{cp1} e_{cp1} + \rho_{g1} V_{g1} e_{g1}] = \rho_s e_s A_b r_b - h_{cp1} \dot{m}_{cp} - h_{g1} \dot{m}_g + \dot{Q}_{p1}, \quad (54)$$

$$\frac{d}{dt} [\rho_{cp} V_{cp2} e_{cp2} + \rho_{g2} V_{g2} e_{g2}] = h_{cp1} \dot{m}_{cp} + h_{g1} \dot{m}_g + \dot{Q}_{p2} - \dot{W}_{out2}. \quad (55)$$

The net heat transfer rates given by Eqs. (36) and (37) have been incorporated into these expressions. Multiplying Eq. (2) by  $e_{cp1}$ , multiplying Eq. (3) by  $e_{g1}$ , subtracting these results from Eq. (54), using Eqs. (20) and (21) to re-express the derivatives in terms of  $T_{p1}$ , and solving for the derivative of  $T_{p1}$  yields:

$$\frac{dT_{p1}}{dt} = \frac{\rho_s (e_s - \eta_{cp} e_{cp1} - (1 - \eta_{cp}) e_{g1}) A_b \tau_b - (h_{cp1} - e_{cp1}) \dot{m}_{cp} - (h_{g1} - e_{g1}) \dot{m}_g + \dot{Q}_{p1}}{\rho_{cp} V_{cp1} c_{vcp1} + \rho_{g1} V_{g1} c_{vg1}}. \quad (56)$$

Similarly, multiplying Eq. (7) by  $e_{cp2}$ , multiplying Eq. (8) by  $e_{g2}$ , subtracting these results from Eq. (55), using Eqs. (20) and (21) to re-express the derivatives in terms of  $T_{p2}$ , and solving for the derivative of  $T_{p2}$  yields:

$$\frac{dT_{p2}}{dt} = \frac{(h_{cp1} - e_{cp2}) \dot{m}_{cp} + (h_{g1} - e_{g2}) \dot{m}_g + \dot{Q}_{p2} - \dot{W}_{out2}}{\rho_{cp} V_{cp2} e_{cp2} c_{vcp2} + \rho_{g2} V_{g2} c_{vg2}}. \quad (57)$$

Lastly, Eq. (11) can be split into two first order ODE's. The first of these equations is given by the definition presented in Eq. (39). The second equation, obtained by using Eq. (39) and the geometrical relation given by Eq. (14), is expressed by the following:

$$\frac{d\dot{V}_2}{dt} = \frac{A_p F_p}{m_p}. \quad (58)$$

Equation (39), (49), (50), (52), (56), (51), (57), and (58) for a coupled set of eight non-linear first order ODE's in eight unknowns. Initial conditions for these equations are

$$\begin{aligned} V_2(t=0) &= V_{2o}, & V_s(t=0) &= V_{so}, & V_{cp1}(t=0) &= V_{cp1o}, \\ \rho_{g1}(t=0) &= \rho_{g1o}, & T_{p1}(t=0) &= T_o, & V_{cp2}(t=0) &= V_{cp2o}, \\ T_{p2}(t=0) &= T_o, & \dot{V}_2(t=0) &= 0. \end{aligned} \quad (59)$$

All other quantities of interest can be obtained once these equations are solved.

## Results

Numerical solutions were obtained for the simulated firing of an NSI into the pin puller device. The numerical algorithm used to perform the integrations was a stiff ODE solver given in the standard code LSODE. The combustion process predicted by the CET89 chemical equilibrium code followed the chemical equation given in Table 1. Parameters used in the simulations are given in Table 2.

Predictions for the pressure history inside the NSI and the gas expansion chamber are shown in Fig. 3. Also shown in this figure are experimental values obtained by pressure transducers located inside the gas expansion chamber.<sup>9</sup> A rapid increase in pressure is predicted within the NSI assembly immediately following combustion initiation ( $t = 0$  ms); the pressure continually rises to a maximum value near 195 MPa occurring near the time of complete combustion ( $t = 0.023$  ms). The pressure within the expansion chamber increases more slowly due to mass choking at the NSI port. Following completion of the combustion process, the pressure within the NSI assembly decreases to 53.9 MPa occurring near  $t = 0.06$  ms; during this same time, the pressure within the gas expansion chamber uniformly increases to a maximum value of 53.4 MPa. There is a subsequent decrease in

both pressures to values near  $22.5 \text{ MPa}$  at completion of the pin's stroke ( $t_{st} = 0.466 \text{ ms}$ ). These decreases in pressure result from work done by the product gases in moving the pin and heat transfer from the combined product subsystems to the surroundings.

Figure 4 shows the predicted temperature history for the combustion products contained within the NSI assembly and the gas expansion chamber. Since the only energy exchange between subsystems contained within these two components is due to the flux of product mass through the NSI port, the resulting temperatures of the combined product subsystems do not thermally equilibrate. Figure 5 shows the predicted density history for the gas phase products inside the NSI and the gas expansion chamber. As a consequence of the product temperature difference, a significant difference in gas phase density is also predicted.

The predicted velocity history of the combustion products flowing through the NSI port is given in Fig. 6. Here, a rapid rise in velocity to a maximum value near  $928 \text{ m/s}$  is predicted immediately following combustion initiation; during this time, the flow through the port becomes choked. The flow remains choked as the velocity slowly decreases to  $830.3 \text{ m/s}$ . Subsequently, there is a rapid decrease in velocity to a minimum value of approximately  $7 \text{ m/s}$  occurring at  $t = 0.63 \text{ ms}$ . This rapid decrease in velocity occurs as the pressures within the NSI assembly and the gas expansion chamber equilibrate following completion of the combustion process. As the pin retracts, gases within the expansion chamber expand creating a slight pressure imbalance across the NSI port; consequently, the velocity of the flow begins to slowly increase to a value of  $23 \text{ m/s}$  at completion of the stroke.

Figure 7 shows the time history of the predicted pin kinetic energy. A continual increase in kinetic energy to a maximum value of approximately  $31.4 \text{ J}$  at completion of the stroke is predicted. This value compares to an experimentally measured value of approximately  $22.6 \text{ J}$ . The larger value for the predicted kinetic energy is consistent with the fact that frictional effects, which would tend to retard the motion of the pin, have not been accounted for in the model.

Figure 8 gives results showing the sensitivity of the model to changes in the NSI port cross-sectional area,  $A_e$ . For this study, we use the predicted pin puller solution as the baseline solution (baseline parameters given in Table 2). The sensitivity of the model is determined by solving the pin puller problem and finding the parametric dependency of three predicted quantities: the pin kinetic energy at completion of the stroke, the stroke time, and the maximum pressure attained within the NSI assembly. Quantities presented in this figure have been scaled by values obtained from the pin puller simulation presented above. For decreasing values of  $A_e$ , pin kinetic energy decreases while both the stroke time and maximum pressure within the NSI increase. These results are primarily due to smaller mass flow rates through the port resulting from decreasing port cross-sectional areas. For slightly larger values of  $A_e$ , both the stroke time and the pin kinetic energy approach a nearly constant value while the peak pressure within the NSI decreases.

## Conclusions

The model presented in this paper is successful in predicting the dynamic events associated with the operation of an NSI driven pin puller. In addition to tracking the interactions between the reactant and product subsystems, the model also accounts for multiple pyrotechnic grains, variable burn surface area, and combustion product mass flow rates through the NSI port. Results of a sensitivity analysis reveal that variations in the cross-sectional area of the port may significantly effect the performance of the device. Specifically, significant decreases in the pin kinetic energy result from decreases in port cross-sectional



area. In the presence of friction, the smaller kinetic energy of the pin may be insufficient to overcome frictional effects resulting in functional failure. Decreases in cross-sectional area may arise from the partial blockage of the NSI port by foreign matter or by the accumulation of condensed phase combustion products. Moreover, it is possible that the very high predicted pressures within the NSI assembly resulting from decreasing port cross-sectional areas may be sufficient to cause structural failure of the NSI's webbing, thereby jamming the pin and preventing it from retracting. Such structural failures have been reported in the past.<sup>6</sup>

## References

- <sup>1</sup>Razani, A., Shahinpoor, M., and Hingorani-Norenberg, S. L., "A Semi-Analytical Model for the Pressure-Time History of Granular Pyrotechnic Materials in a Closed System," *Proceedings of the Fifteenth International Pyrotechnics Seminar*, Chicago, IL, 1990, pp. 799-813.
- <sup>2</sup>Farren, R. E., Shortridge, R. G., and Webster, H. A., III, "Use of Chemical Equilibrium Calculations to Simulate the Combustion of Various Pyrotechnic Compositions," *Proceedings of the Eleventh International Pyrotechnics Seminar*, Vail, CO, 1986, pp. 13-40.
- <sup>3</sup>Butler, P. B., Kang, J., and Krier, H., "Modeling of Pyrotechnic Combustion in an Automotive Airbag Inflator," *Proceedings - Europyro 93, 5<sup>e</sup> Congrès International de Pyrotechnie du Groupe de Travail de Pyrotechnie*, Strasbourg, France, 1993, pp. 61-70.
- <sup>4</sup>Kuo, J. H., and Goldstein, S., "Dynamic Analysis of NASA Standard Initiator Driven Pin Puller," AIAA 93-2066, June 1993.
- <sup>5</sup>Gonthier, K. A., and Powers, J. M., "Formulation, Predictions, and Sensitivity Analysis of a Pyrotechnically Actuated Pin Puller Model," *Journal of Propulsion and Power*, accepted for publication, 1993.
- <sup>6</sup>Bement, L. J., Multhaup, H. A., and Schimmel, M. L., "HALOE Gimbal Pyrotechnic Pin Puller Failure Investigation, Redesign, and Qualification," NASA Langley Research Center, Report, Hampton, VA, 1991.
- <sup>7</sup>Gordon, S., and McBride, B. J., "Computer Program for Calculation of Complex Chemical Equilibrium Compositions, Rocket Performance, Incident and Reflected Shocks, and Chapman-Jouguet Detonations," NASA Lewis Research Center, SP-273, Cleveland, OH, 1976.
- <sup>8</sup>Fox, R. W., and McDonald, A. T., *Fundamentals of Heat and Mass Transfer*, 3<sup>rd</sup> ed. John Wiley and Sons, Inc. 1985, pp. 599-617.
- <sup>9</sup>Bement, L. J., private communication, NASA Langley Research Center, Hampton, VA, 1992.

Table 1: Stoichiometric equation used in pin puller simulations.

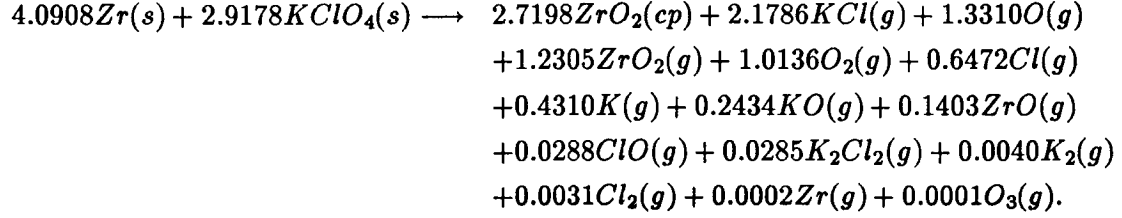


Table 2: Parameters used in pin puller simulation.

| <i>parameter</i> | <i>value</i>                                    |
|------------------|---|
| $\eta_{cp}$      | 0.43  |
| $N$              | 100   |
| $A_e$            | $0.100 \text{ cm}^2$                            |
| $A_p$            | $0.634 \text{ cm}^2$                            |
| $A_1$            | $0.634 \text{ cm}^2$                            |
| $V_1$            | $0.125 \text{ cm}^3$                            |
| $\rho_s$         | $3.57 \text{ g/cm}^3$                           |
| $\rho_{cp}$      | $5.89 \text{ g/cm}^3$                           |
| $T_s$            | $288.0 \text{ K}$                               |
| $T_w$            | $288.0 \text{ K}$                               |
| $h$              | $1.25 \times 10^6 \text{ g/s}^3/\text{K}$       |
| $\epsilon$       | 0.60  |
| $\alpha$         | 0.60  |
| $F_{crit}$       | $3.56 \times 10^7 \text{ dyne}$                 |
| $b$              | $0.003 (\text{dyne/cm}^2)^{-0.60} \text{ cm/s}$ |
| $n$              | 0.60  |
| $V_{2o}$         | $0.824 \text{ cm}^3$                            |
| $V_{so}$         | $0.038 \text{ cm}^3$                            |
| $V_{cp1o}$       | $7.425 \times 10^{-8} \text{ cm}^3$             |
| $\rho_{g1o}$     | $6.202 \times 10^{-6} \text{ g/cm}^3$           |
| $T_o$            | $288.0 \text{ K}$                               |
| $V_{cp2o}$       | $6.576 \times 10^{-7} \text{ cm}^3$             |
| $V_2$            | $0.0 \text{ cm}^3/\text{s}$                     |

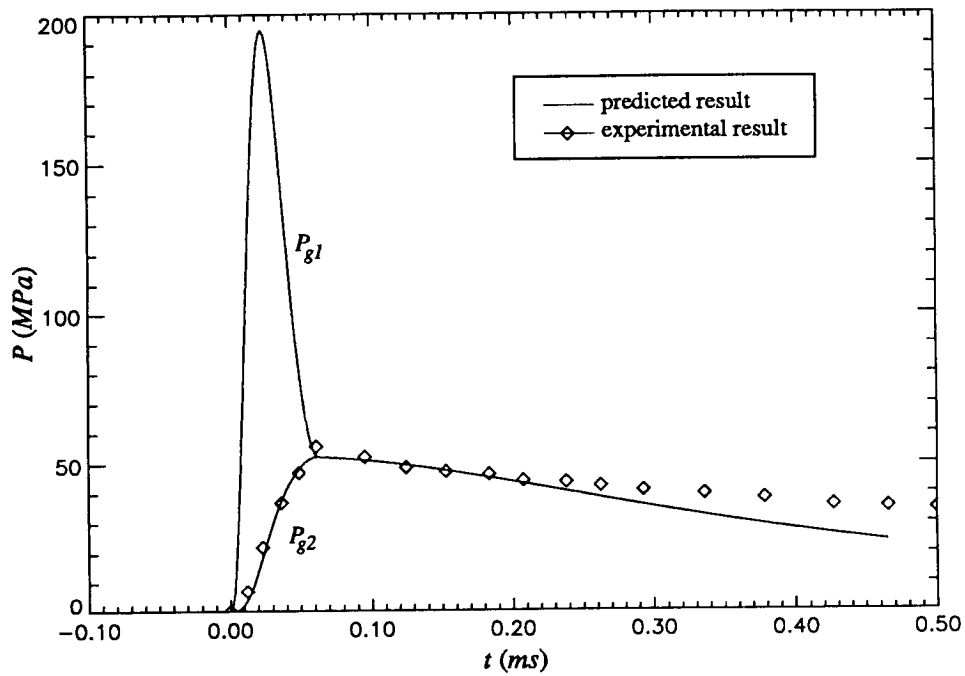


Figure 3: Predicted and experimental pressure histories for the pin puller simulation.

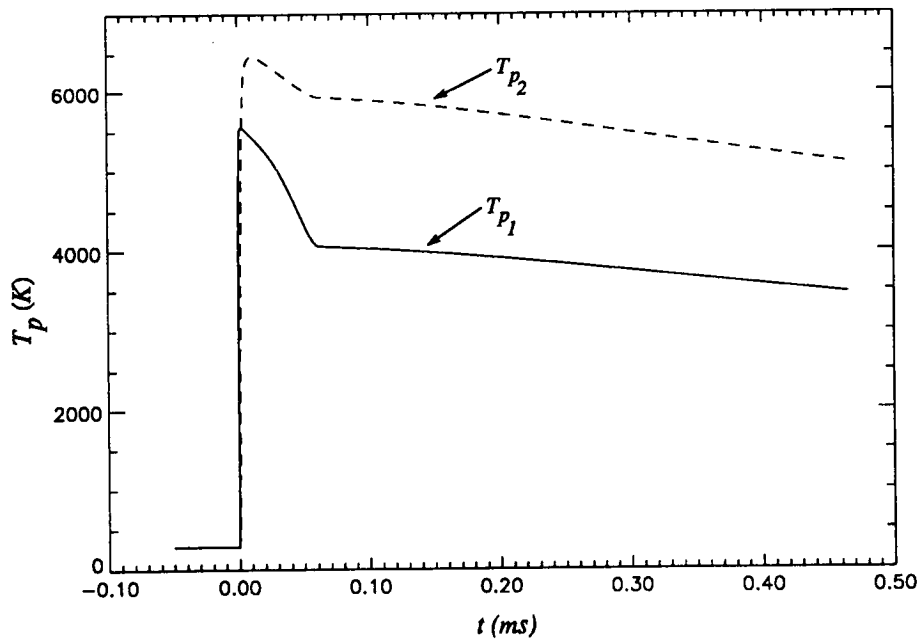


Figure 4: Predicted temperature histories for the pin puller simulation.

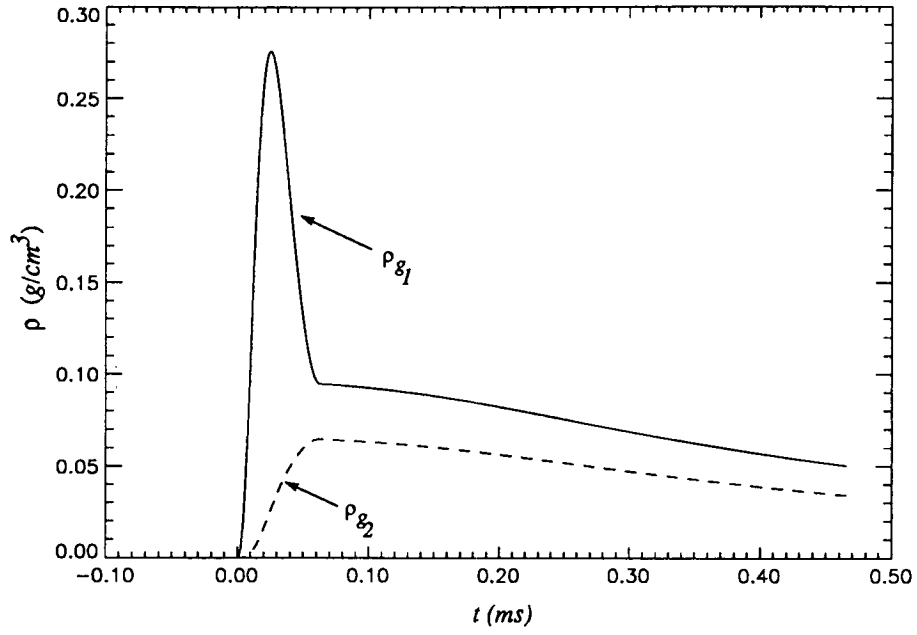


Figure 5: Predicted temperature histories for the pin puller simulation.

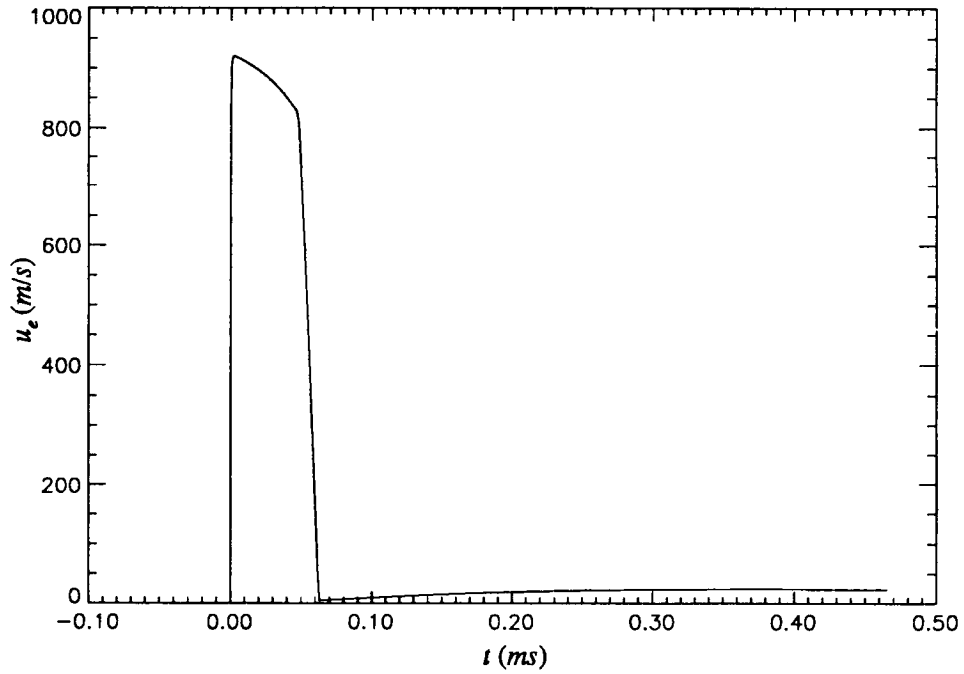


Figure 6: Predicted velocity of the flow through the NSI port for the pin puller simulation.

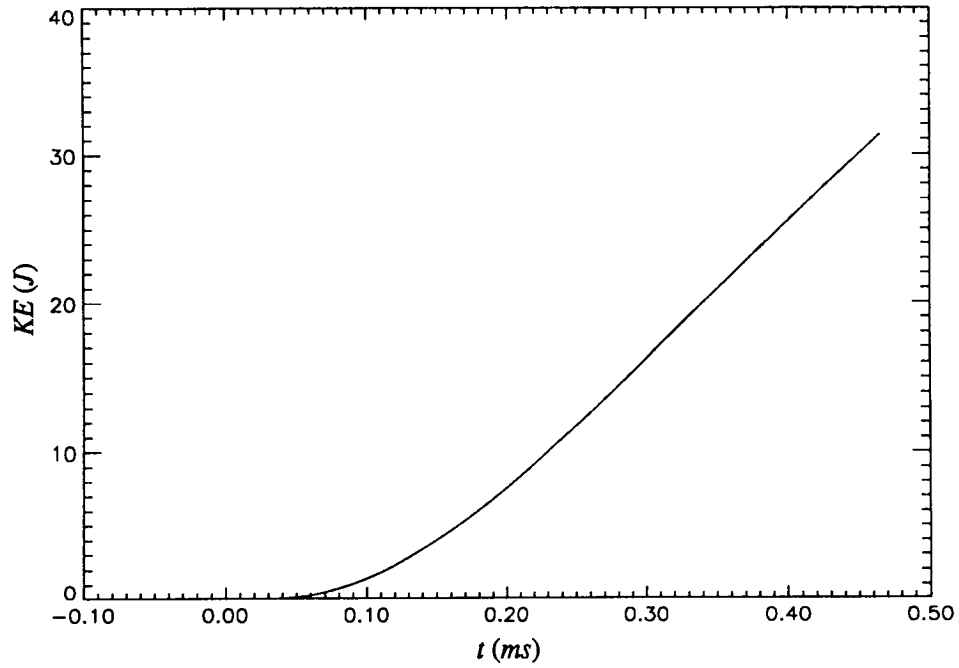


Figure 7: Predicted kinetic energy of the pin for the pin puller simulation.

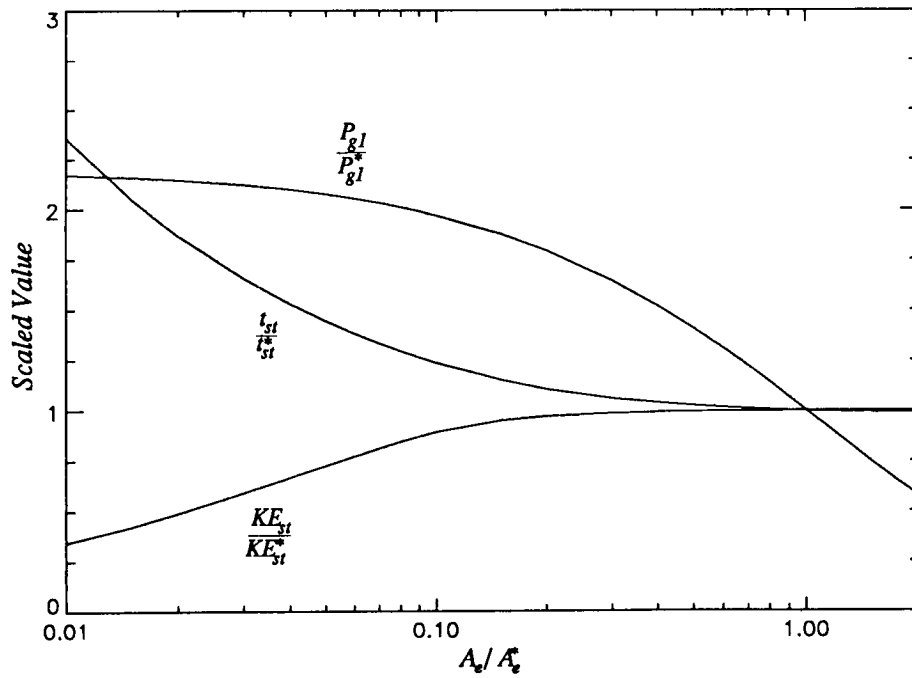


Figure 8: Sensitivity of the model to changes in the NSI port cross-sectional area. The values presented in this figure have been scaled by the gasline values  $A_e^* = 0.10 \text{ cm}^2$ ,  $KE^* = 31.4 \text{ J}$ ,  $t_s^* = 0.466 \text{ ms}$ , and  $P_{g1}^* = 195.2 \text{ MPa}$ .

523-15  
7003  
P- 12

FINITE ELEMENT ANALYSIS OF THE SPACE SHUTTLE  
2.5-INCH FRANGIBLE NUT

Darin N. McKinnis  
NASA Lyndon B. Johnson Space Center, Houston, TX

Abstract

Finite element analysis of the Space Shuttle 2.5-inch frangible nut was conducted to improve understanding of the current design and proposed design changes to this explosively-actuated nut. The 2.5-inch frangible nut is used in two places to attach the aft end of the Space Shuttle Orbiter to the External Tank. Both 2.5-inch frangible nuts must function to complete safe separation. The 2.5-inch frangible nut contains two explosive boosters containing RDX explosive each capable of splitting the nut in half, on command from the Orbiter computers. To ensure separation, the boosters are designed to be redundant. The detonation of one booster is sufficient to split the nut in half. However, beginning in 1987 some production lots of 2.5-inch frangible nuts have demonstrated an inability to separate using only a single booster. The cause of the failure has been attributed to differences in the material properties and response of the Inconel 718 from which the 2.5-inch frangible nut is manufactured. Subsequent tests have resulted in design modifications of the boosters and frangible nut. Model development and initial analysis was conducted by Sandia National Laboratories (SNL) under funding from NASA Lyndon B. Johnson Space Center (NASA-JSC) starting in 1992. Modeling codes previously developed by SNL were transferred to NASA-JSC for further analysis on this and other devices. An explosive bolt with NASA Standard Detonator (NSD) charge, a 3/4-inch frangible nut, and the Super\*Zip linear separation system are being modeled by NASA-JSC.

Introduction

The 2.5-inch frangible nut is used in two places to attach the aft end of the Space Shuttle Orbiter to the External Tank, as shown in figure 1. Each 2.5-inch frangible nut must function to complete safe separation

of the Orbiter from the External Tank. Separation of each nut requires fracturing of four webs as shown in figure 2. The 2.5-inch frangible nut contains two explosive boosters containing 100% RDX each capable of splitting the nut in half. To ensure separation, the boosters are designed to be redundant. The detonation of one -401 configuration booster, figure 3, is sufficient to split the nut in half. However, beginning in 1987 some production lots of 2.5-inch frangible nuts demonstrated an inability to separate using only a single -401 booster. The cause of the failure has been attributed to differences in the material properties and response of the Inconel 718 from which the 2.5-inch frangible nut is manufactured. Details of the failure investigation were reported by Hoffman and Hohmann<sup>1</sup>. Subsequent tests have resulted in design modifications of the boosters and frangible nut.

Finite element analysis of the Space Shuttle 2.5-inch frangible nut was conducted in cooperation with Sandia National Laboratories (SNL), Albuquerque, New Mexico using two finite element analysis computer programs developed at SNL: JAC and PRONTO. JAC is a quasistatic finite element solver. JAC was used to simulate tensile pulls of Inconel 718 in order to generate material characterizations of the Inconel 718. The output of JAC can be used to qualitatively determine the advantage of one sample of Inconel 718 over the other. JAC's output however can also be provided as input to PRONTO to improve the accuracy of booster and nut simulations. PRONTO is a dynamic, large deformation, finite element solver. PRONTO was used to conduct simulations of booster detonation and the response of the nut. These codes were primarily run at SNL, on a Cray Y-MP supercomputer. At NASA-JSC the codes were installed and run on a Sun workstation.

The first part of this paper discusses the material characterization process necessary for an accurate analysis. The second part of this paper discusses the structural analysis and design changes to the nut which were analyzed with comparison to test results. The third part of this paper briefly describes other devices which are being analyzed with this process.

#### Inconel Material Characterization Process

To conduct a structural analysis of the 2.5-frangible nut, material characterization of Inconel 718 is necessary. Material characterization requires a tensile test and a tensile test simulation using the JAC2D program. The procedure used is:

1) Perform a tensile test. The tensile test must be carried out through failure, if at all possible, or at a minimum into necking. This is because reduction in area is a significant factor in the characterization process.

2) Convert the tensile test engineering stress/strain data to true stress/strain over the range from yield to necking. Conversion of the data to true stress/strain is straight forward but necessary as the finite element programs use true stress/strain. True stress is found from engineering data according to the equation:

$$\sigma_{\text{true}} = \sigma_{\text{eng}} (\epsilon_{\text{eng}} + 1)$$

True strain can be calculated according to the following equation.

$$\epsilon_{\text{true}} = \ln(\epsilon_{\text{eng}} + 1)$$

Both equations are valid until necking begins, when the cross sectional area is no longer constant.

3) Curve fit the true stress/strain data to a power-law hardening relationship, of the form

$$\sigma = \sigma_{ys} + A(\epsilon_p - \epsilon_L)^n$$

to determine the hardening constant,  $A$ , and hardening exponent,  $n$ .  $\sigma$  is the effective stress,  $\sigma_{ys}$  is the yield strength,  $\epsilon_p$  is the equivalent plastic strain, and  $\epsilon_L$  is the Luders strain. Inconel displays no Luders strain so this term can be considered zero.  $\epsilon_p$  should be evaluated according the Heavyside function, designated by the brackets, i.e. zero if its value is negative.

4) Conduct a simulation of the tensile test using the JAC2D program. The finite element mesh for this simulation is shown in figure 4. The left hand side is the initial mesh. The right hand side is the mesh near failure. Note that only the upper quadrant of the test is simulated due to two symmetry planes. A 2 mil reduction in diameter, which was measured from the test samples, and included in the mesh geometry assures localization at the symmetry plane on  $Z=0$ .

5) Convert and review the results of the JAC2D analysis to obtain the tearing parameter. The results of the JAC2D analysis are converted in post-processing to the selected form of the tearing parameter, in this analysis it is

$$TP = \int_0^{\epsilon_f} \frac{\langle 2\sigma_T \rangle}{3(\sigma_T - \sigma_m)} d\epsilon$$

where  $\sigma_T$  is the maximum principal stress,  $\sigma_m$  is the mean stress, and  $\epsilon$  is the equivalent plastic strain. This is evaluated from zero to  $\epsilon_f$ , the strain at fracture. Knowledge of the final reduction in area from the tensile test is used here. The time step,  $t_f$ , in the simulation is noted when the radius of the  $Z=0$  symmetry plane equals the radius of the failed test sample.

The tearing parameter can then be plotted versus time for the node at the center of the sample, where the tearing parameter is at a maximum in this model. The tearing parameter is then the value of the curve at  $t_f$ . Using this method, tearing parameter sensitivity to time and/or reduction in area is displayed.

The yield stress and elastic modulus from the tensile test, and the calculated values of tearing parameter, hardening constant (A) and hardening exponent (n) are necessary to define Inconel 718 for the structural analysis to follow. The only other data required is the Poisson's ratio and density. These are all the parameters required by PRONTO's constitutive model for this analysis.

To confirm the results of the curve fit and JAC2D analysis, the JAC2D results can be plotted against the original tensile test data. If necessary, adjustments in A and n can then be made and another JAC2D analysis can be run until the analysis and tensile test agree. The tearing parameter can then be reevaluated. When the analysis and test agree, the material characterization process is complete and the structural analysis can be conducted on the 2.5-inch nut with the PRONTO program.

#### Selection of the Tearing Parameter Failure Definition

Chapter 16 of Numerically Modelling of Material Deformation Processes<sup>2</sup> describes some of the prominent models that have been developed for ductile failure. However, in finite element analysis, most empirical models share the common approach of conducting an experiment or test on the material in question to determine the critical value, or tearing parameter, of the material. For example, the original model used a tensile test on a notched specimen to determine a tearing parameter. There are then different theories for which stress and strain components should contribute to the accumulation of the tearing parameter and in what empirical formulation. Apparently the correct formulation is strongly dependent on the material, geometry, and other factors for a specific problem, as well as the experience of the analyst.

Using JAC, the calculation for tearing parameter is done in post-processing, providing complete flexibility to change the formulation of the tearing parameter calculation. The tensile test simulation does not even have to be

rerun. New post processing commands are all that is required. PRONTO's designers also anticipated the need for alternative constitutive models and tearing parameter formulations to meet the needs of the specific problem. And PRONTO supports post processing to permit reformulation of the tearing parameter if desired.

However, NASA-JSC sought the ability to visualize in real-time the death, or failure, of material based on the tearing parameter. PRONTO supported adaptive or real-time death for energy, Vonmises stress, pressure, and other variables but not the tearing parameter. Therefore, the tearing parameter selected to describe failure of the Inconel 718 in the 2.5-inch frangible nut was added to the elastic/plastic power law hardening material model of PRONTO specifically for this application. This new constitutive model, the power law hardening strength model, was based on the elastic/plastic power law hardening material model. The elastic/plastic power law hardening material model used by PRONTO was documented by Stone, Wellman, and Krieg<sup>3</sup>.

#### RDX Material Characterization

Using PRONTO, explosives are modeled using Jones-Wilkins-Lee (JWL) parameters which were obtained from the Lawrence Livermore National Laboratories (LLNL) Explosives Handbook Properties of Chemical Explosives and Explosive Simulants<sup>4</sup>. The LLNL handbook also describes the formulation of the JWL parameters and their use to predict the "pressure-volume-energy behaviour of the detonation products of explosives in applications involving metal acceleration". However, JWL parameters were not available from the handbook for 100% RDX, the explosive used by the booster. JWL parameters for 95% HMX were used instead. HMX is known to be slightly more energetic than RDX.

#### Structural Analysis - Phase I Nut and Booster Geometry

Initial structural analysis of the 2.5-inch nut began in the spring of 1992. At that time, tensile test data from yield through necking was not available for the Inconel 718. However, structural analysis was conducted to evaluate the



sensitivity of the nut to various geometrical factors. The finite element mesh currently being used is shown in figure 5. The slight differences between this mesh and the mesh used in phase I of the analysis are described later in this paper. Figure 6 shows in detail the side of the nut with a booster included where detonation will be modeled. The following changes in the nut geometry were analyzed to determine the effect on nut separation: radial gap between the booster cartridge material and the nut, outer notch depth of the nut, as shown in figure 7, and the booster aspect ratio. The results were reported by K. E. Metzinger<sup>5</sup>.

Radial gap between the booster and the nut is limited to 7 mil maximum by the tolerances on the nut and booster. The analysis and tests agree that minimizing the gap as much as possible, including the use of grease, is beneficial. Analysis shows the benefit is greatest in reducing gap from 7 mil to 4 mil, 5 times greater than from 4 mil to 2 mil. The advantage of reducing gap from 4 mil to 2 mil is the same as from 2 mil to 0.5 mil. This suggests that tightening tolerances on the part to reduce gap probably would not be cost effective beyond 4 mil. Reduction of gap from 2 mil to 0.5 mil through the addition of grease, epoxy, or other agents would probably not justify the added complexity and cost of such a change.

The outer notch depth of the nut has also been shown to be a factor in nut separation. The original flight configuration of the 2.5-inch frangible nut had an outer notch depth of 0.303 inches. Reducing the depth from 0.303 to 0.018 allows the nut halves to rotate further about the fourth web, from approximately 25 degrees to over 60 degrees. Without a reduction, the corners of the nut at the outer notch pinch together, resulting in energy lost to compressive plastic strain. Rotation of the halves places the elements of the fourth web, the last web to fail, under increasing tension. Increased tension means increased tearing values in those elements and improved likelihood of failure. This change was first

demonstrated in test and repeated by the analysis. The outer notch depth was reduced to 0.075 in the -302 configuration of the nut which is the current flight configuration.

Although testing preceded analysis, the analysis showed two disadvantages to decreasing the outer notch depth: reduction in delivered energy to the nut from the booster and increased time until separation. Reducing the outer notch depth the nut causes web 1, the first web to fail, to fail earlier in time, before all the energy of the booster can be imparted to the nut. The analysis showed this loss to be small but significant if the outer notch depth is not properly sized. An outer notch depth of 0.153 inches was actually shown to be less likely to separate than either a larger notch, 0.303 inches, or a smaller notch, 0.018 inches. The nut has not yet been designed to the optimum notch size. Further analysis will be required to determine the optimum size of the outer notch depth to ensure separation. Furthermore, the increased rotation permitted by the smaller notch depth causes the nut to fail later in time, in general. Although this is not a concern in the current design, this factor may be important in applications with smaller tolerances in separation time.

Booster aspect ratio is defined as the diameter of the charge over the length of the charge. It was proposed that increasing the aspect ratio would increase the effect impulse delivered by the booster to the nut, with no additional RDX. Considerable energy was being lost or underutilized because it was located at or below the bottom of the webs of the nut and the separation was thought to be progressing in zipper fashion, from the top of the web toward the bottom. The advantage of increased aspect ratio was demonstrated in tests and analysis. As a result, NASA-JSC has modified the booster from the -401 configuration to the -402 configuration as shown in figure 3 for all future production of the booster.

## Structural Analysis - Phase II

### A Copper Booster

A second phase of analysis was conducted in September 1992 to study the effect of changing the booster cartridge material from stainless steel to copper. This study is briefly documented by K. E. Metzinger in a memo to D. S. Preece<sup>6</sup>. This study showed that a copper booster would absorb less energy in expanding within the booster port of the nut, making more energy available for nut separation. A nut would thus be more likely to fracture with a copper booster than with a stainless steel booster, as shown in figure 8.

The analysis also showed that the NASA Standard Detonator (NSD), the initiating charge of the booster, is capable of blowing the top of the booster off and allowing the booster pressures to vent. This is confirmed by tests in which the booster top consistently separates from the assembly. Analysis showed that a copper booster would vent earlier than a stainless steel booster and the existing design does not permit strengthening in the area of fracture to prevent venting. However, venting is not considered to be a major concern as the analysis showed that the impulse delivered from the booster to the nut precedes the loss of the booster top.

Unfortunately, copper has known compatibility problems with RDX. So a copper booster is not feasible. Testing has confirmed the analysis results by using modified stainless steel boosters, outer diameters machined down and copper sleeves inserted over the stainless steel, shown in figure 9. These boosters were successful in every test. Although these modified boosters have not been accepted for use in flight at this time, they have an advantage over a pure copper booster in that they would not increase the generation of shrapnel or increase venting because the top of the booster is unchanged from the flight boosters, solid stainless steel.

## Structural Analysis - Phase III

### Refining the Model

In 1993 the goal of the analysis was to improve the accuracy of the model

so that design changes or variability between production lots of Inconel 718 could be compared quantitatively. Qualitative accuracy had already been demonstrated in the earlier analyses. To provide quantitative accuracy in the analysis it would be necessary to perform material characterization, as previously described, for different lots of Inconel 718 and correlate test performance with the analysis.

The selected lots were HSX and HBT. It had been shown in earlier actual tests that these two lots of Inconel 718 had significantly different characteristics based on their performance. No HBT nut has ever separated completely using the -401 booster, while no HSX nut has ever failed to separate with a -401 booster. The analysis had to show that HBT would not separate and HSX would not.

The first step was to conduct a material characterization of HSX and HBT, then a structural analysis with the calculated material properties. The tensile test data for HSX and HBT is shown on figure 10.

The model accurately predicted that HSX nuts would be much easier to fracture than HBT nuts. Significantly different tearing parameters, 0.345 for HSX and 0.675 for HBT, indicated this trend. However, structural analysis conducted on HSX nuts failed to simulate a nut which completely separated. Clearly the model was not yet quantitatively accurate. Since the material characterization process with JAC analysis appeared sound, geometry and other characteristics were evaluated to increase the accuracy of the model and simulate a separating HSX nut. Three factors were found to increase accuracy of the model: the addition of a simulated bolt, increasing the granularity of the mesh in the webs, and increasing the number of points used to initiate detonation of the explosive.

One of the refinements was that the number of elements in the webs was increased slightly. This is done by remeshing the nut's geometry. This reduces the size of the average

element in the web area of the nut. In PRONTO, the tearing parameter must be exceeded for the entire element for failure of that element to occur. A smaller element is thus more likely to fail due to localized increases in tearing parameter. Reducing average element size increases the number of elements which increases output file sizes and run times. Smaller elements also require smaller time steps, further slowing model processing. Thus this step, while increasing accuracy, increases run times, a common problem in finite element analysis.

To increase accuracy of the model, the explosive material was provided with more initial detonation points. The original model had a single detonation point at time = 0. From this point the detonation wave was calculated to spread throughout the RDX. Ten detonation points were added to the model, each simulating detonation at time=0. Thus the detonation of all the RDX occurs in a more even distribution and shorter time period. This produces slightly more output from the explosive and simulates a mature detonation wave as opposed to an initiating charge. This change did not require remeshing and was very easy to implement.

A bolt was inserted into the hole of the nut. The addition of the bolt is significant to the separation of the nut, critical in some borderline cases, according to the analysis. Figure 11 shows the nut opening for 2.5 mil radial gap and 4.5 mil radial gap HSX nuts. The 4.5 mil nut is opening similarly to the 2.5 mil nut until about 2 milliseconds. At that point opening has stopped and the nut is beginning to close down. However, at 3.5 milliseconds the nut which is moving to the left impacts the stationary bolt. The impact provided the necessary energy to complete the failure of web 4 and separation. At this time there is no experimental data to confirm this effect. However, testing is typically conducted with a bolt and no pre-load and should be included in the analysis. The effect of threads is not considered in the analysis. This change requires remeshing, the addition of a new material elastic Inconel 718, and

the addition of contact surfaces. The number of elements added was kept to a minimum by treating the bolt as a perfectly elastic pipe.

The simulation of an HSX nut with these changes resulted in a separating nut, failure of all four webs. Even with the changes which resulted in more energy to the nut and easier fracture, HBT nuts did not separate, still in agreement with tests. This study was documented in an SNL report<sup>7</sup>.

#### Future Studies of the 2.5-inch Nut

A tearing parameter is used to determine when the Inconel 718 material would fail. It has been proposed that the stainless steel of the booster should also be allowed to fail using a tearing parameter calculated by a JAC analysis. Even if the stainless steel is not permitted to fail, performing a JAC analysis, including a tensile test, should enhance the model's accuracy. Modeling conducted to date has not included material characterization of stainless steel as was done for the Inconel 718. NASA-JSC is currently conducting tensile testing of stainless steel samples from booster lots to perform this analysis.

One geometrical design consideration which has not been modeled is the application of a backing plate or washer to the nut. During testing this was shown to have significant effect on the separation of the nut, overshadowing most other variables. Nuts without the backing plate, were not as likely to separate. However, to include the backing plate the model must be converted into three dimensions. NASA-JSC plans to conduct these analyses in 1994. NASA-JSC will probably run this analysis on their Cray to handle the significant increase in the number of elements necessary to conduct this analysis.

#### Structural Analysis and Material Characterization Conclusions

The most significant conclusions from the analysis performed on the 2.5-inch frangible nuts are as follows:

A. Radial gap between the booster and the frangible nut is an

important dimension. This gap should be minimized if complete separation is desired.

B. The energy absorbed by the stainless steel booster is significant. Switching from an all stainless steel cartridge to a cartridge of reduced diameter and the addition of a copper sleeve should increase the impulse delivered to a nut. An all copper booster housing is not recommended due to compatibility issues between copper and RDX. However, a hybrid booster made of stainless steel with a copper sleeve has been shown in test to be effective.

C. Reduction in area obtained from a tensile test of an Inconel 718 sample is significant. Reduction in area is a significant factor of the tearing parameter. Inconel with a relatively small reduction in area will be easier to break.

#### Other Applications

NASA-JSC is currently pursuing analysis models of the Space Shuttle 3/4-inch frangible nut, the Super\*Zip linear separation system, and a JSC-designed explosive bolt utilizing the NASA Standard Detonator (NSD) as the actuating charge. These models can use the same process as was used for the 2.5-inch frangible nut with slight variations.

The mesh for the explosive bolt model is shown in figure 12. Six prototype explosive bolts have been fired to date. Agreement with the analysis has been excellent. The analysis has provided design modifications which will be used to slightly change the separation plane and ensure positive retention of the bolt in its confining washer.

The mesh for the Super\*Zip linear separation system model is shown in figure 13.

#### Conclusions

The test and finite element analysis methodology developed by SNL and NASA-JSC has been successfully demonstrated. This methodology requires the use of SNL developed software which has been successfully transferred, with substantial assistance from SNL, to NASA-JSC.

Training in the use of these codes has been provided. This methodology can now be used by NASA-JSC in several ways.

Analysis can be conducted on new production lots of Inconel 718. Inconel 718 lots which possess material properties and tearing parameters outside of acceptable limits can be rejected before expensive machining and acceptance testing is conducted.

Analysis can be conducted on sample lots of Inconel 718 to determine the effect of various heat treatment procedures on the microstructure. This approach will suggest measures to further control the forging process.

Analysis can be conducted to quantify the effects of proposed design changes before manufacturing and testing is initiated. Analysis could also be used to establish the design margin of the current configuration or select a more meaningful design margin criteria. Currently design margin is determined by increasing the web thickness to 120% of the maximum allowable, as shown in figure 14. This choice for margin demonstration is not ideal. It is unlikely that the web thickness will be incorrectly manufactured and that this error will be overlooked in acceptance inspections. Furthermore, no additional information beyond separation versus failure to separate is obtained. It has been suggested that velocity of the nut halves as the nut separates would be a better demonstration of margin where failure to separate provides a velocity of zero. At this point, test methods including breakwires and high-speed photography are being used to determine the velocity of nut halves for comparison with the analysis.

The test and analysis methodology is general enough that it can be successfully applied to other mechanical devices and design problems. NASA-JSC is currently pursuing analysis models of the 3/4-inch frangible nut, the Super\*Zip linear separation system, and a NASA-JSC designed explosive bolt

utilizing the NSD as the actuating charge.

#### References

1. Investigation of Failure to Separate an Inconel 718 Frangible Nut, William C. Hoffman, III, and Carl Hohmann, NASA Lyndon B. Johnson Space Center, Houston, TX.
2. Numerical Modelling of Material Deformation Processes, Edited by Peter Hartley, Ian Pillinger, and Clive Sturgess, Springer-Verlag, Germany, 1992.
3. A Vectorized Elastic/Plastic Power Law Hardening Material Model Including Luders Strain, Charles M. Stone, Gerald W. Wellman, Raymond D. Krieg, Sandia National Laboratories, Albuquerque, New Mexico, SAND90-0153, March 1990.
4. LLNL Explosives Handbook Properties of Chemical Explosives and Explosive Simulants, B. M. Dobrantz and P. C. Crawford, UCRL-52997. Lawrence Livermore National Laboratory, Livermore, California, January 1985.
5. NASA Frangible Nut Preliminary Findings, Memo from K. E. Metzinger to D.S. Preece, Sandia National Laboratories, Albuquerque, New Mexico, August 25, 1992.
6. NASA Booster Cartridge Material, Memo from K. E. Metzinger to D.S. Preece, Sandia National Laboratories, Albuquerque, New Mexico, October 5, 1992.
7. Structural Analysis of a Frangible Nut Used on the NASA Space Shuttle, Kurt E. Metzinger, Sandia National Laboratories, SAND93-1720, November 1993.

#### Acknowledgments

The author wishes to acknowledge the work of D.S. Preece and Kurt E. Metzinger, Sandia National Laboratories, Albuquerque, New Mexico, in model generation, initial modeling and analysis, and in technical support for NASA-JSC

modeling. The author also wishes to thank Carl Hohmann, NASA-JSC, who recommended many of the design modifications and variables which were studied and supported the interpretation of the analysis.

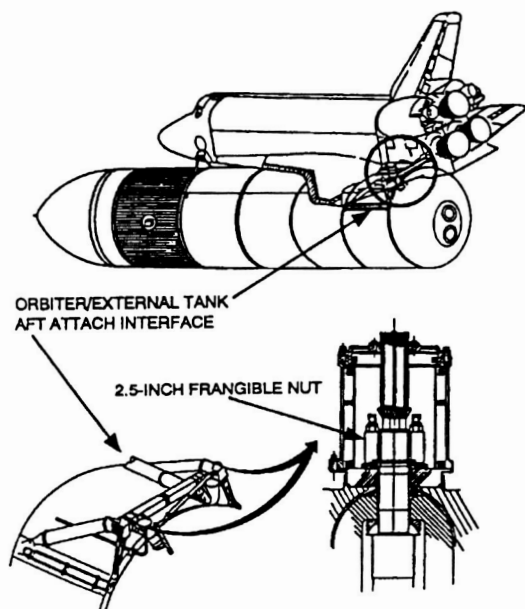


Figure 1. Location of the 2.5-inch frangible nut between the Space Shuttle Orbiter and External Tank.

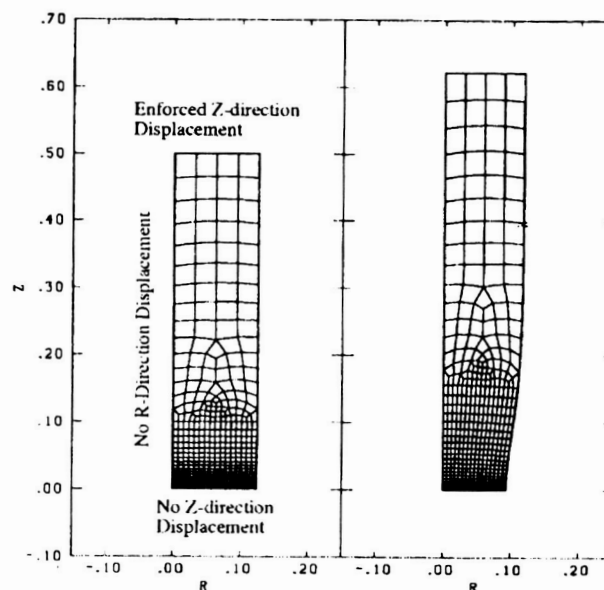


Figure 4. Tensile test mesh for simulation by JAC2D.

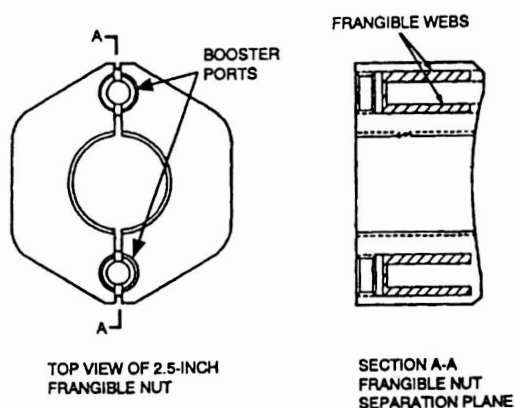


Figure 2. Top view and side view of the 2.5-inch frangible nut.

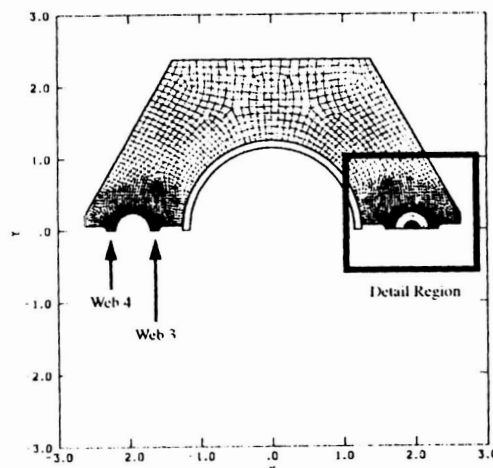


Figure 5. 2.5-inch frangible nut mesh.

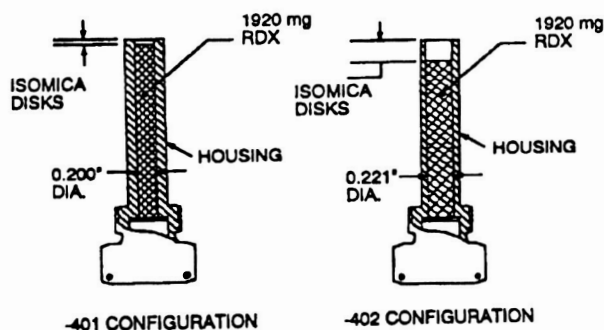


Figure 3. Side view of the 2.5-inch frangible nutbooster, -401 and -402 configurations.

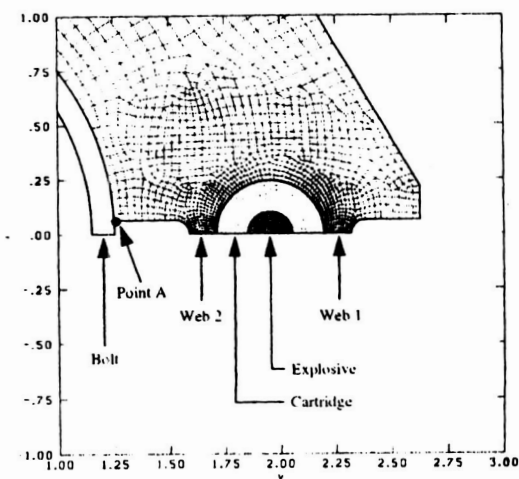
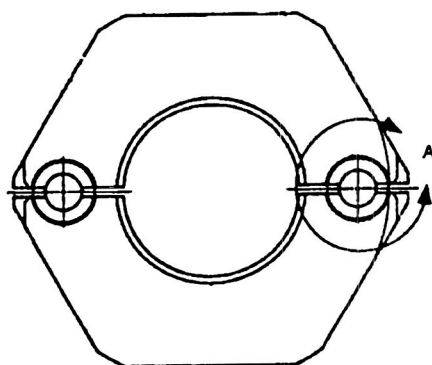
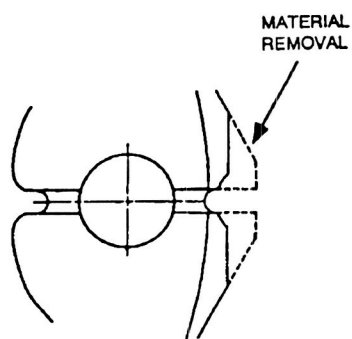


Figure 6. 2.5-inch frangible nut mesh, detailed view.



TOP VIEW OF FRANGIBLE NUT



SECTION A

Figure 7. Outer notch depth of the nut.

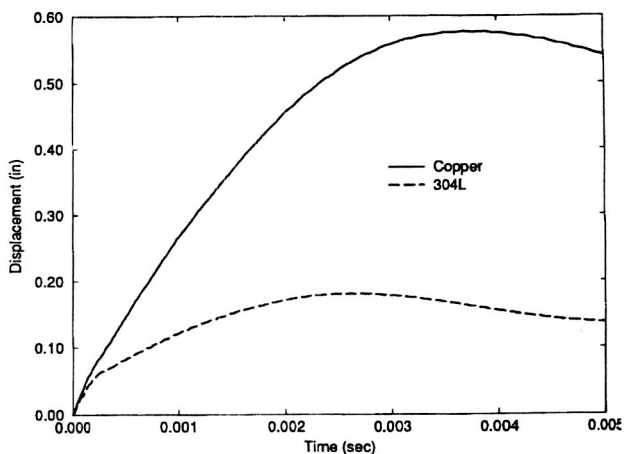


Figure 8. Nut opening as a function of booster material, copper versus stainless steel.

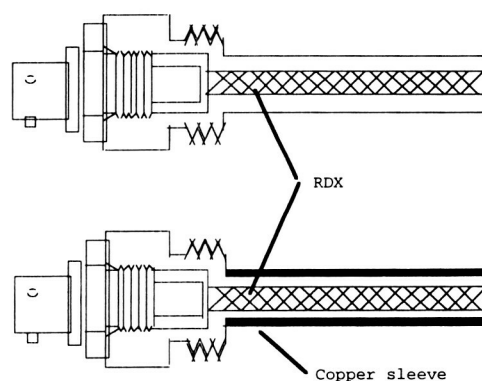


Figure 9. Stainless steel booster and stainless steel booster with copper sleeve.

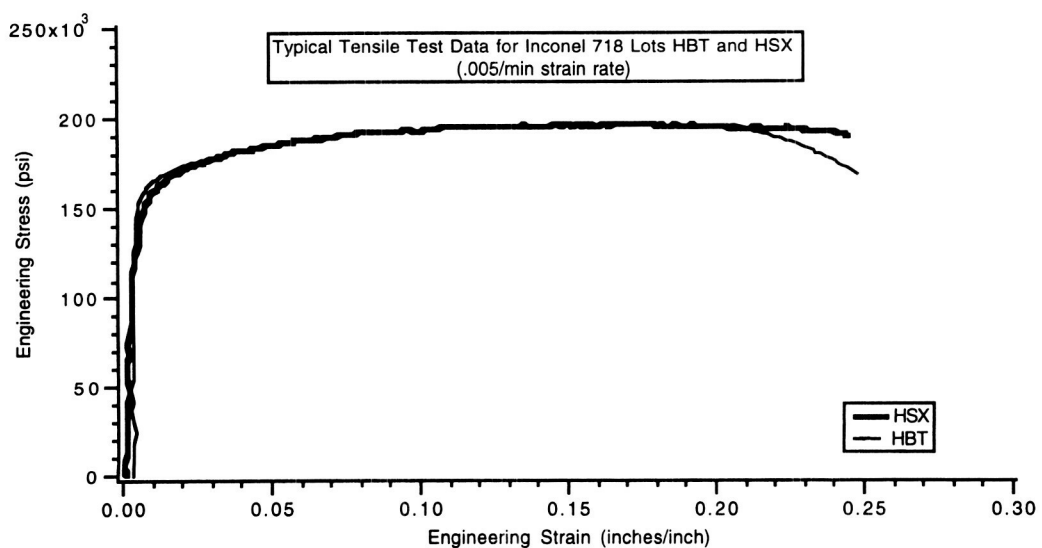


Figure 10. Tensile test data for Inconel 718 lots HBT and HSX.

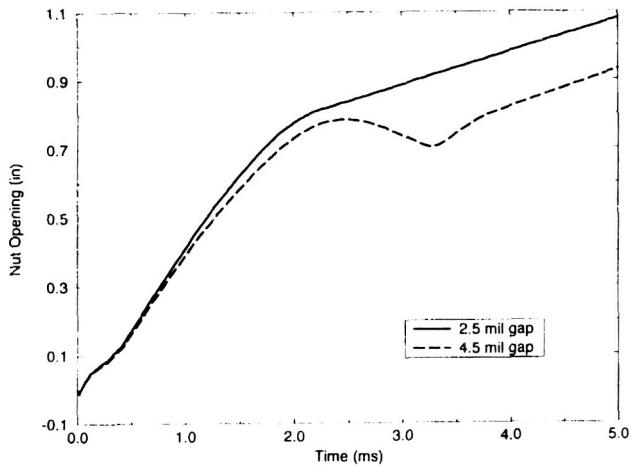


Figure 11. Nut opening as a function of gap.

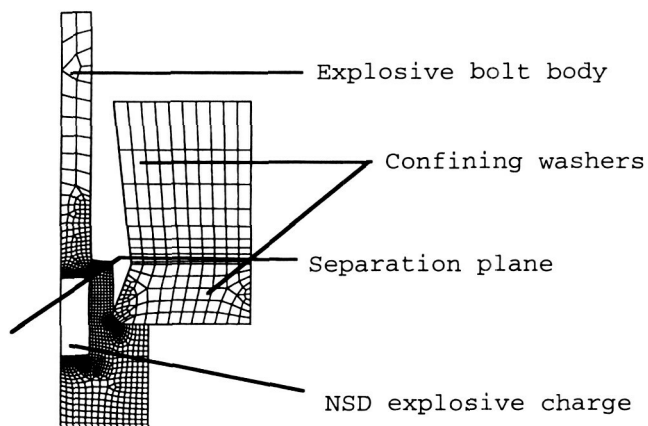


Figure 12. Finite element mesh for the explosive bolt with NSD charge.

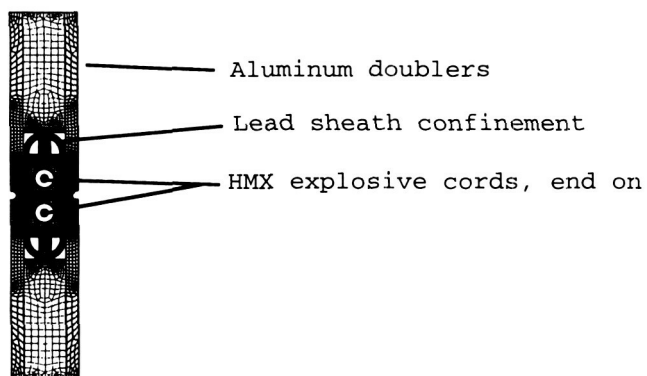
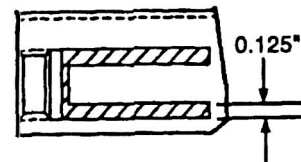
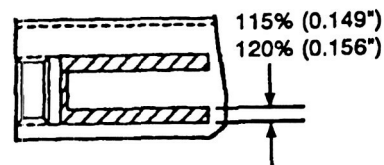


Figure 13. Super\*Zip linear separation system finite element mesh.



-301 FRANGIBLE NUT WEBS



-101, -102 MARGIN NUT WEBS

Figure 14. Web dimensions for 2.5-inch frangible nuts, -301 flight configuration, and -101 and -102 margin configurations.



524-15  
7004  
1-12

## ANALYSIS OF A SIMPLIFIED FRANGIBLE JOINT SYSTEM

Steven L. Renfro  
The Ensign-Bickford Company  
Simsbury, CT

James E. Fritz  
The Ensign-Bickford Company  
Simsbury, CT

### Abstract

A frangible joint for clean spacecraft, fairing, and stage separation has been developed, qualified and flown successfully. This unique system uses a one piece aluminum extrusion driven by an expanding stainless steel tube. A simple parametric model of this system is desired to efficiently make design modifications required for possible future applications. Margin of joint severance, debris control of the system, and correlation of the model have been successfully demonstrated.

To enhance the understanding of the function of the joint, a dynamic model has been developed. This model uses a controlled burn rate equation to produce a gas pressure wave in order to drive a finite element structural model. The relationship of the core load of HNS-IIA MDF as well as structural characteristics of the joint are demonstrated analytically. The data produced by the unique modeling combination is compared to margin testing data acquired during the development and qualification of the joint for the Pegasus<sup>®</sup> vehicle.

### Introduction

Frangible joints have been demonstrated as robust and contamination free separation systems for various spacecraft and launch vehicle stage and fairing separation. Typical frangible joint systems are initiated using mild detonating fuse (MDF) detonation products to expand an elastomeric bladder which then compresses dynamically against a formed stainless steel tube. The high pressure developed at the tube forces it to a more round shape in order to fracture an aluminum

plate along a stress concentration groove. This fracture provides separation without fragmentation or contamination because the products are contained within the steel tube. A typical joint cross section is depicted in Figure 1.

Integrating this technology into new systems, with more challenging environmental conditions, could benefit from analytical modeling to properly configure each system. Understanding the mechanism required to sever the aluminum extrusion is crucial to meet new system requirements with full confidence.

The purpose of this report is to document The Ensign-Bickford Company's efforts to develop a simple analytical tool using widely available hydrodynamic and finite element computer codes.

### Background

The ANSYS 5.0<sup>®</sup> finite element software allows for transient input to structures in the frequencies expected during a small damped detonation event. The frangible joint geometry is believed suitable for this type of analysis. To generate transient pulses for input into the finite element

<sup>®</sup> Pegasus is a Registered Trademark of Orbital Sciences Corporation

<sup>®</sup> ANSYS is a Registered Trademark of Swanson Analysis Systems, Inc.

model, simple one-dimensional hydrodynamic analysis is used.

For a one-dimensional Lagrangian model, a cylindrical geometry was assumed. The SIN' hydrodynamic code was used to solve conservation equations of momentum, mass, and energy. In order to use this information as input for the finite element model, individual or groups of cells were monitored to develop input equations for the finite element calculations.

Since the hydrodynamic analysis is one dimensional, it limits the amount of understanding developed regarding the specific stress state existing in the aluminum. Peak stress locations and probable points of secondary failure cannot be determined, and assumptions must be made for the stiffness and response characteristics. A two dimensional hydrodynamic analysis would assist in understanding these effects, but such analysis is time consuming, and requires access to sufficient hardware and software resources. Also, the hydrodynamic model is unable to account for a wide range of thermal loads and structural preloads in the parts, and cannot be used to evaluate stresses in the part due to events other than the explosive loading (i.e., flight loads, thermal response, assembly loading).

To understand the dynamic response of the frangible joint, an ANSYS 5.0 finite element model was created for use in a non-linear transient analysis. This analysis was used to determine the dynamic response of the aluminum when subject to transient loads driving the material above its yield strength. This methodology had been successfully used

by The Ensign-Bickford Company to solve problems involving explosively and pyrotechnically loaded structures. This paper represents the first time this technique used input developed by a one dimensional hydrodynamic analysis code.

### Model Development

Using the SIN analysis, the critical areas were determined for input into the ANSYS 5.0 model. The timing and reaction of the shock waves incident and reflected from the interior steel wall result in two distinct types of relationships, both of which are decaying sinusoidal functions.

The area of the stress riser has extremely high initial amplitude which rapidly decays. This is consistent with the geometry present at this location. A thin layer of elastomeric material and a thin aluminum section bounding the steel do not support reflected pressure waves as well as the thicker off axis areas. Basically, the initial detonation front experiences a rapid ring down within the wall of the steel tube. The inside surface of the steel responds approximately as illustrated in Figure 2.

The second input function used is from a cross section at 45° from the stress riser. This relationship was similar in frequency to Figure 2 with a much lower initial amplitude. Figure 3 shows this relationship.

A logical choice for a third function is 90° to the separation plane. Most frangible joint designs use air gaps combined with thin silastic sections to control position of the MDF and to allow easy installation. If no air gaps are assumed, the resulting function resembles the data in Figure 3

with lower amplitude. Introducing the air gaps increases the difficulty of the hydrodynamic analysis without any real benefit. This third function was therefore not used for this simplified approach.

The source explosive used for this particular design is HNS-IIA. The equation of state for HNS is not currently available as part of the SIN database. Alternate explosive materials were used to bracket the response of HNS. The density, chemistry, detonation velocity, and Chapman-Jouget pressure were matched as closely as possible with candidate materials from the SIN database. Table 1 lists the explosives used and their properties compared to HNS.

To simplify the ANSYS model geometry, symmetric constraints are used along the notch edge and one half of the joint mounting flange. The length of the flange was shortened to reduce the number of degrees of freedom which needed to be incorporated into the model. This model is shown in Figure 4.

The transient loads are applied as pressure pulses along the interior of the aluminum. These loads have the same time profile as that predicted by the one dimensional hydrodynamic analysis, however input pressure amplitudes are reduced to achieve numerical stability. Unfortunately, this assumption is required, although it is expected that the results still allow development of an understanding of the aluminum response. The aluminum material (6061-T6) was assumed to act in an elastic-perfectly plastic manner. That is, once the yield strength of the material is exceeded, no additional load can be supported by that material. Plastic convergence is

achieved using the Modified Newton-Raphson method, based on a Von-Mises yield criterion. For the transient portion of the analysis, the Newmark time integration scheme is utilized, using Rayleigh damping with only mass matrix contributions (Beta damping). This applied damping is necessary in order to provide stability of the solution. However, a Beta term is chosen which ensures a low level of damping (0.05% or less) above 10,000 Hz.

For the initial time steps, the symmetry constraints are applied to both the top notch and the flange edges of the model. When sufficient stress levels are determined in the notch to induce section failure, this symmetry constraint on the notch is removed and the leg of the section is allowed to bend up and away from its initial position. This is done to simulate proper function of the joint during the explosive event.

### Results of Finite Element Model

As part of the preliminary work performed using this model, simple static stress analysis (linear and non-linear) as well as modal analysis were performed to verify model integrity and to learn about the basic structural characteristics of the model. Some important data was gleaned from these runs, including the presence of a potential plastic hinge near the flange region of the aluminum structure. Additionally, the modal runs showed that the aluminum had its second, third, and fourth normal modes between 50 and 200 kHz. This was important information, since it showed that the aluminum is capable of dynamic elastic structural response near the input frequency of the shock pulse. The 2<sup>nd</sup>, 3<sup>rd</sup>, and 4<sup>th</sup>, mode shapes are shown in

Figure 5.

Once the simpler analysis had been run and verified with hand calculations, the more complex non-linear transient analysis was run. The input pulse was characterized as a shock pulse with a 1.5  $\mu$ sec rise and a 1.5  $\mu$ sec decay at the notch location. The magnitude of this pressure pulse was chosen to remain slightly below the yield point of the material (approximately 36 ksi) to avoid model stability problems. As noted above, this assumption needed to be made, however; much information about the dynamic response of the structure was still learned.

The final results are illustrated in Figure 6. During the rise time of the initial pressure pulse, the structure cannot significantly respond to the high frequency input. The structure simply transmits the shock wave through the material thickness. By the time the pulse is damped, the structure begins to significantly respond, and peak stresses in the notch exceed the allowable material strength. A plastic condition through the wall is reached. It is at this time that separation occurs, and the symmetric boundary condition along the notch edge is removed. After this time, the load is no longer applied and the inertial loads of the aluminum leg are all that is left driving the deflection. Obviously, the loading assumption is somewhat non-realistic; the shock wave applied to the aluminum will continue along the inner wall even after separation has occurred.

After this, the frangible joint is behaving as a cantilever beam with a fixed edge along the mounting flange. A plastic zone develops along much of the length

of the flange wall. It is interesting to note that a plastic hinge develops in the bend region of the aluminum leg. This hinge location corresponds well to explosive over tests where a section of the aluminum became a flyer.

Finally, at 24  $\mu$ sec, the leg has plastically deformed over its entire length. a plastic hinge occurs near the top of the extrusion, and model convergence is no longer possible using the elastic-perfectly plastic static strength allowable. The predicted deflection at this time is 0.103 inches. For the actual hardware, it would be expected that energy would be expended by bending at the plastic hinge until the impulse had been dissipated.

#### Discussion

The aluminum is capable of responding to the input shock pulse in the 2 to 3  $\mu$ sec regime, suggested by the modal analysis and supported by the transient analysis. At approximately 3  $\mu$ sec after the shock pulse has arrived at the interior of the aluminum stress riser, failure at the groove is expected to occur. There remains sufficient energy to severely deform the legs once the failure at the stress riser has occurred. A secondary plastic hinge forms at the bend joint near the mounting flange for this particular design.

The aluminum cross section is very efficiently dissipating the applied impulse once the stress riser failure occurs. In other words, plastic stresses do not localize and exist over much of the inner and outer surfaces of the aluminum.

All of these discussion items show good agreement with test specimen articles. No failures of this particular joint have

occurred which would disagree with the conclusions of this analysis.

The hydrodynamic analysis would provide much better resolution if a two dimensional model were used. Digital resolution of individual cell results could be used as forcing function for the finite element techniques.

Although not specifically addressed by this paper, the one dimensional hydrodynamic analysis combined with the two dimensional ANSYS analysis shows good promise for evaluation of the effects of thermally induced strains and launch load induced stresses. A two dimensional hydrodynamic input would further enhance the ability of this technique to simulate flight functional conditions.

#### References:

- 1) Charles L. Mader; Numerical Modeling of Detonations; University of California Press; 1979; pp. 310 - 332.
- 2) B.M. Dobratz; LLNL Explosives Handbook; UCRL-52997,

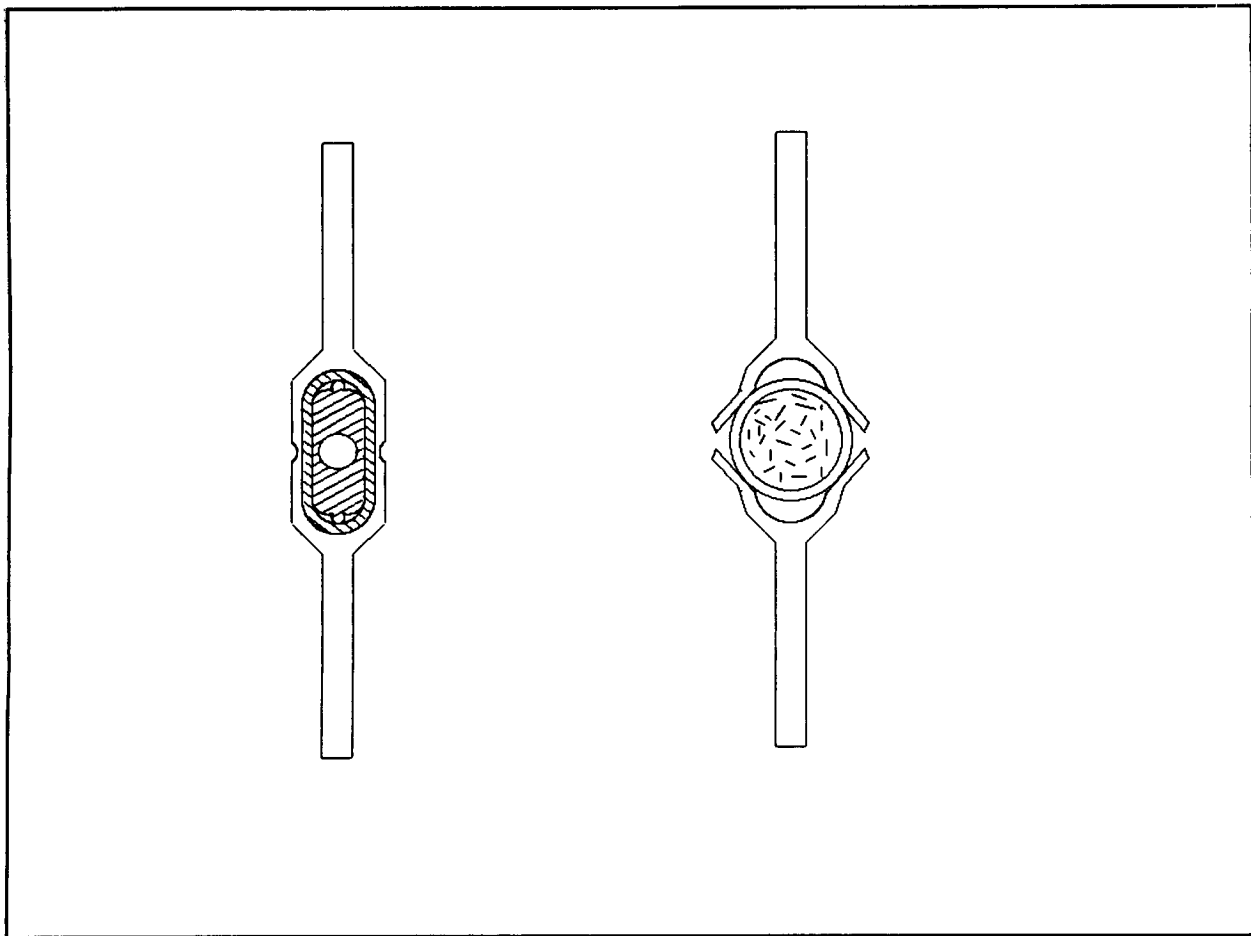


**Figure 1** Frangible Joint Before and After Function

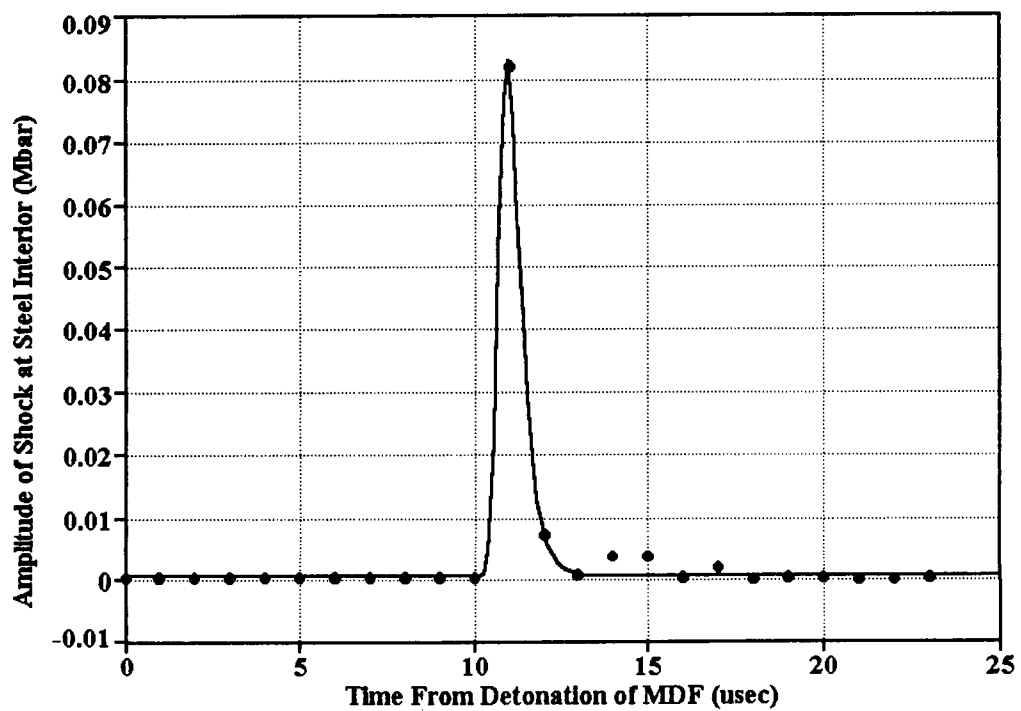


**Figure 2** Pressure Time History at Interior of Steel Tube at Stress Riser

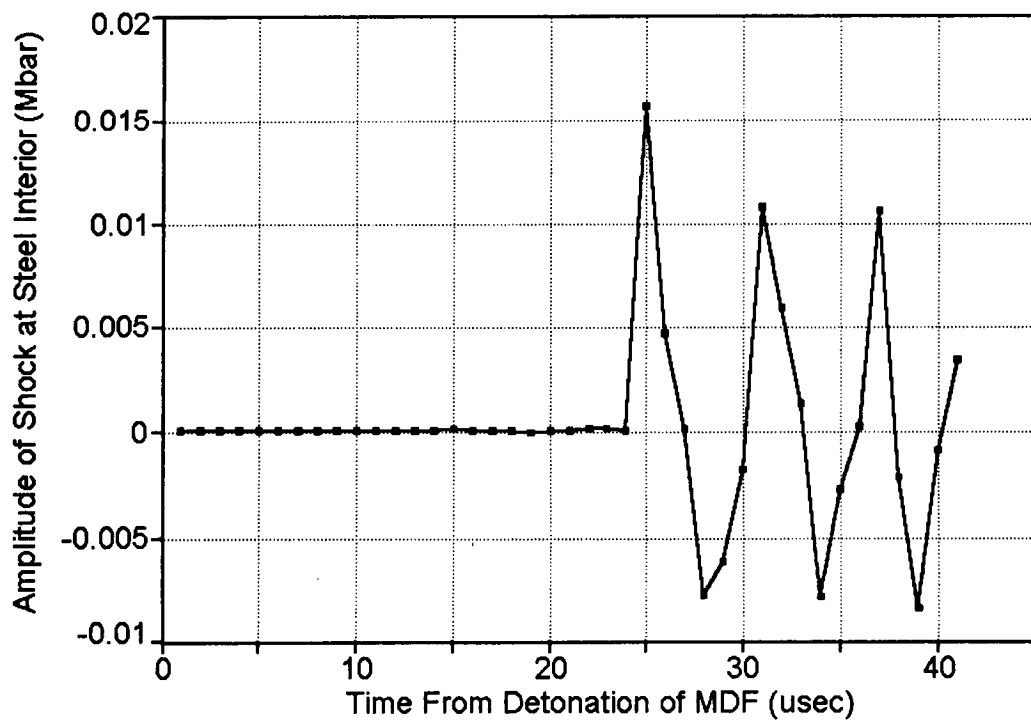


**Figure 3** Pressure Time History at 45° From Stress Riser



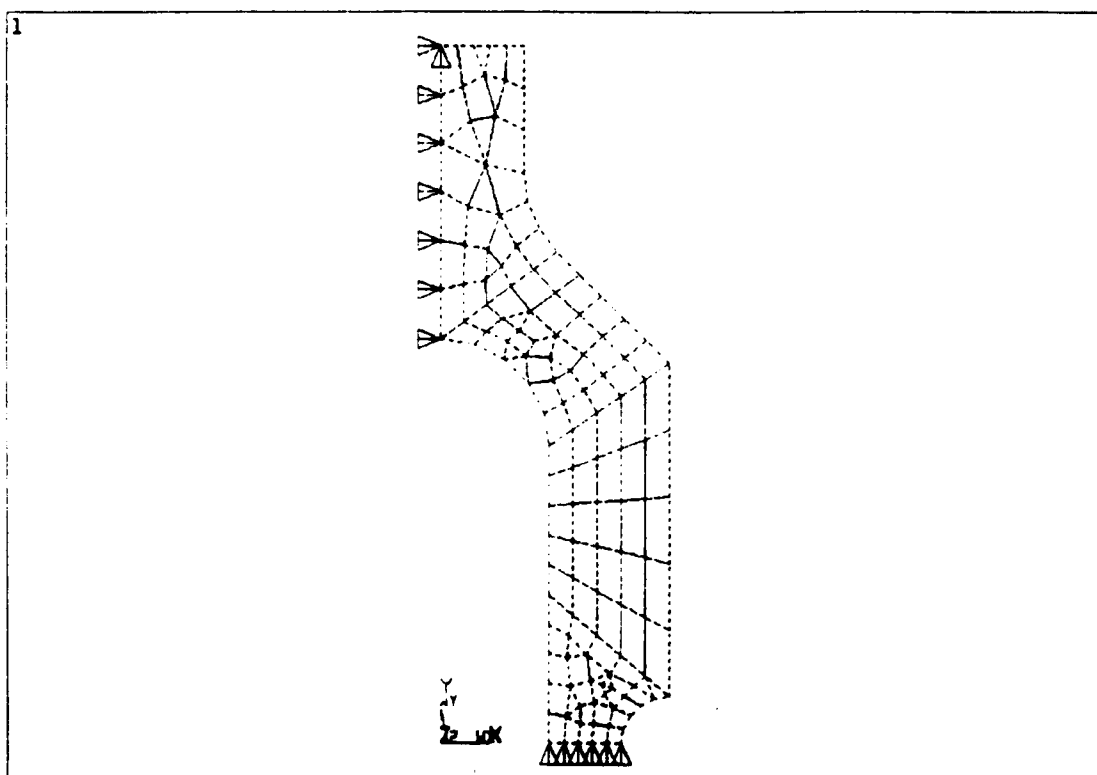
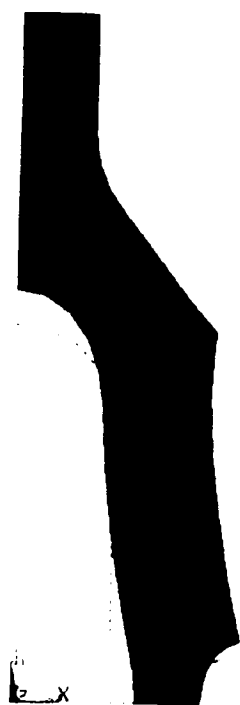
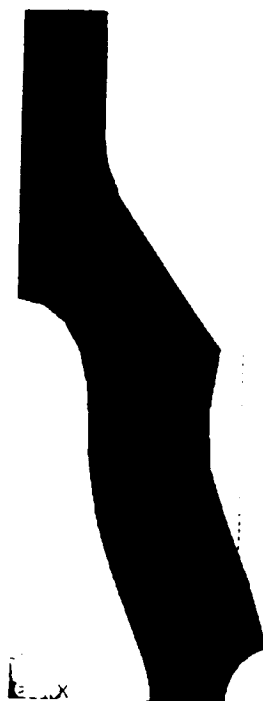


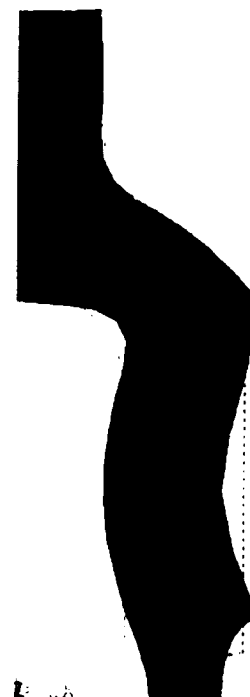
**Figure 4** ANSYS Finite Element Model



MODE 2  
52.827 HZ



MODE3  
102.348 HZ



MODE 4  
154.759 HZ

**Figure 5** ANSYS Finite Element Model Elastic Normal Modes

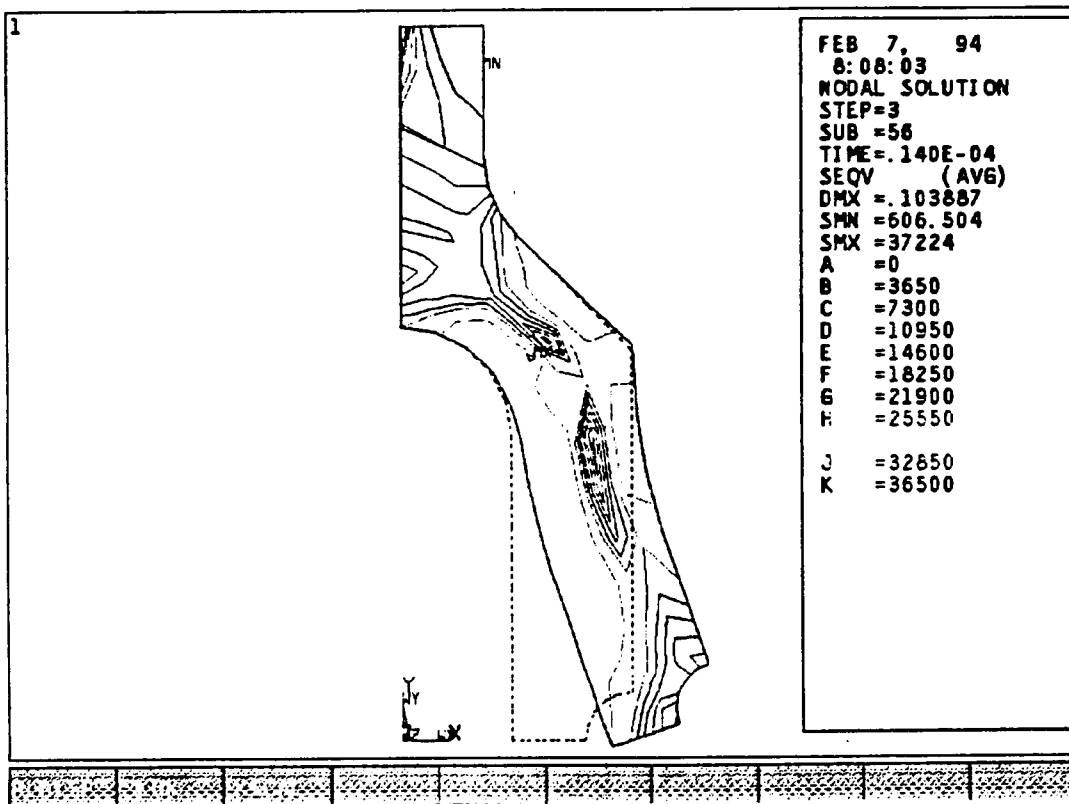


**Figure 6** Results of Hydrodynamic and FEA Combined Model

**Table 1. Explosive Properties Used to Bracket HNS Performance<sup>2</sup>**

| Material | Chemical Formula  | Density (g/cm <sup>3</sup> ) | Detonation Pressure (kbar) | Detonation Velocity (mm/ $\mu$ sec) |
|----------|---|------------------------------|----------------------------|-------------------------------------|
| HNS      | C <sub>14</sub> H <sub>8</sub> N <sub>8</sub> O <sub>12</sub> | 1.60                         | 200                        | 6.80                                |
| TATB     | C <sub>6</sub> H <sub>6</sub> N <sub>6</sub> O <sub>6</sub>   | 1.88                         | 291                        | 7.76                                |
| TNT      | C <sub>7</sub> H <sub>5</sub> N <sub>3</sub> O <sub>6</sub>   | 1.63                         | 210                        | 6.93                                |

525-35  
7005  
P-8

## UNLIMITED DISTRIBUTION

### PORTABLE, SOLID STATE, FIBER OPTIC COUPLED DOPPLER INTERFEROMETER SYSTEM FOR DETONATION AND SHOCK DIAGNOSTICS

K. J. Fleming, O.B. Crump  
Sandia National Laboratories  
Albuquerque, New Mexico, 87123

VISAR (Velocity Interferometer System for Any Reflector) is a specialized Doppler interferometer system that is gaining world-wide acceptance as the standard for shock phenomena analysis. The VISAR's large power and cooling requirements, and the sensitive and complex nature of the interferometer cavity have restricted the traditional system to the laboratory. This paper describes the new portable VISAR, its peripheral sensors, and the role it played in optically measuring ground shock of an underground nuclear detonation. The Solid State VISAR uses a prototype diode pumped Nd:YAG laser and solid state detectors that provide a suitcase-size system with low power requirements. A special window and sensors were developed for fiber optic coupling (1 kilometer long) to the VISAR. The system has proven itself as a reliable, easy to use instrument that is capable of field test use and rapid data reduction using only a notebook personal computer (PC).

## INTRODUCTION

Detailed analysis and accurate models of shock phenomena and high speed motion require an instrument that is capable of measuring the high acceleration of surfaces accurately and non-intrusively. Dent blocks and stress gauges can only infer the final velocity of detonations while critical information pertaining to the acceleration is unknown. A versatile instrument that optically measures acceleration, displacement and velocity is VISAR. VISAR (Velocity Interferometer System for Any Reflector) uses coherent, single frequency laser light to illuminate a target that has some reflectivity. The reflected light is collected and routed through a modified, unequal leg, Michelson interferometer. As the target moves, the resulting Doppler information is detected and electronically analyzed, then the data are converted to velocity and displacement time histories using software operating

on a personal computer (PC). The sensitivity, accuracy, and high bandwidth of VISAR is attributed to the optical method of measurement and its 400 MHz bandwidth is primarily limited only by the electronics in the system.

Although the VISAR technique is excellent for measuring shock phenomena, there are some limitations with the conventional VISAR, such as; inherent sensitivity to adverse environments found outside the laboratory, hazardous unenclosed laser beam, high current, voltage and cooling requirements, and an inability to measure devices not in the "line of sight" of the laser beam, e.g. through smoke, tunnels and inside chambers. In an attempt to improve on the versatility of VISAR, a solid state system with fiber optic coupling and rugged components has been developed and rigorously tested in harsh environments. The fiber optic coupled sensor used to send and collect the light at

the target is unique from previous techniques and, in recent tests, has performed flawlessly even after four months encapsulation in curing concrete. The solid state VISAR described in this paper was used to measure ground shock generated by a nuclear detonation at the Nevada Test Site (NTS).

## BACKGROUND

The VISAR was developed by Barker and Hollenbach<sup>1</sup> primarily for measuring free surface velocities of materials in gas gun experiments. An improved version of VISAR, developed by Hemsing<sup>2</sup>, electronically inverts and adds the 180° out-of-phase optical signals that were previously wasted, which effectively cancels target self-light and doubles the signal intensity. During fast shock jumps, the system may miss Doppler information which can cause discrepancies in measured velocity. For this reason, Kennedy and Crump<sup>3</sup> developed the double-delay-leg system. The double-delay-VISAR takes the return light, splits the optical signal and routes it through two interferometer cavities with different sensitivities. The data can then be more accurately reduced by comparing the results of the two systems. The conventional VISAR has many sensitive components mounted on an optical table. The Fixed-Cavity VISAR, developed by Stanton, Crump and Sweatt<sup>4</sup>, simplifies the interferometer cavity by cementing the movable components together. The result is a rugged, small, easy to use system with a minimal amount of adjustment.

A low cost, portable VISAR using a diode laser and a fiber optic coupled sensor has been developed by Fleming, and Crump<sup>5</sup> with successful velocity measurements taken on electrically initiated slappers. The diode's invisible laser light makes alignment to the target difficult and the aberrated, high divergence beam profile of the laser is difficult to propagate through space for any extended length. Both problems are solved by the development of an imaging fiber optic coupled sensor<sup>6</sup> that has intra-optic video capabilities. The sensor allows for

remote target measurements and verification of the correct area of target illumination. (figure 1).

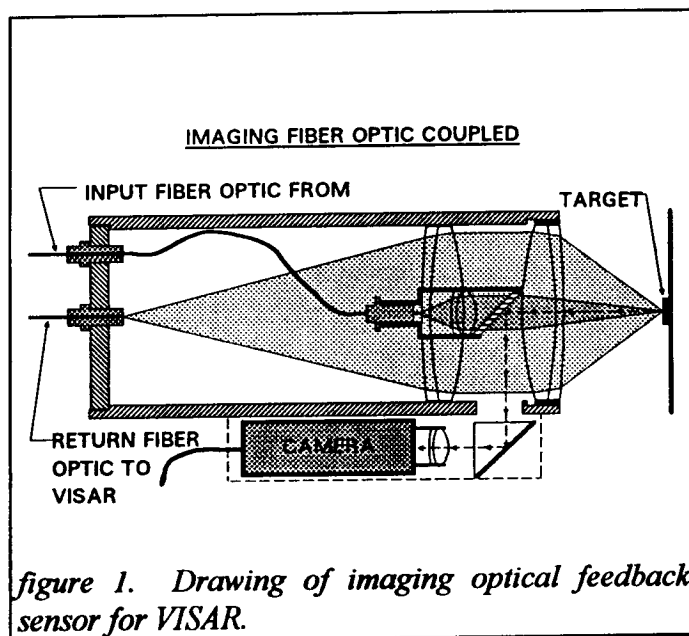


figure 1. Drawing of imaging optical feedback sensor for VISAR.

## THEORY OF OPERATION

In a typical experiment, a laser beam is focused to a small spot onto a target of interest. The reflected light is collected and routed to the interferometer cavity (figure 2). A dichroic mirror is inserted into the light collecting assembly to transmit the laser light and reflect the other wavelengths (This technique is valuable for viewing the target, allowing for precise alignment of the laser beam.).

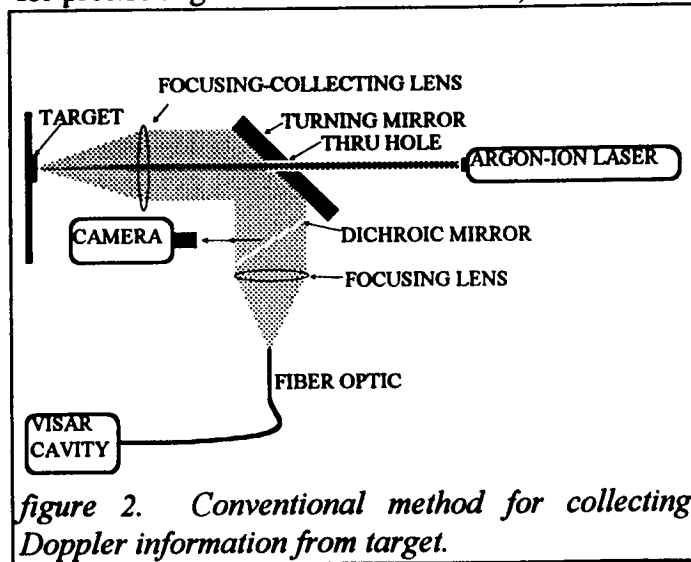
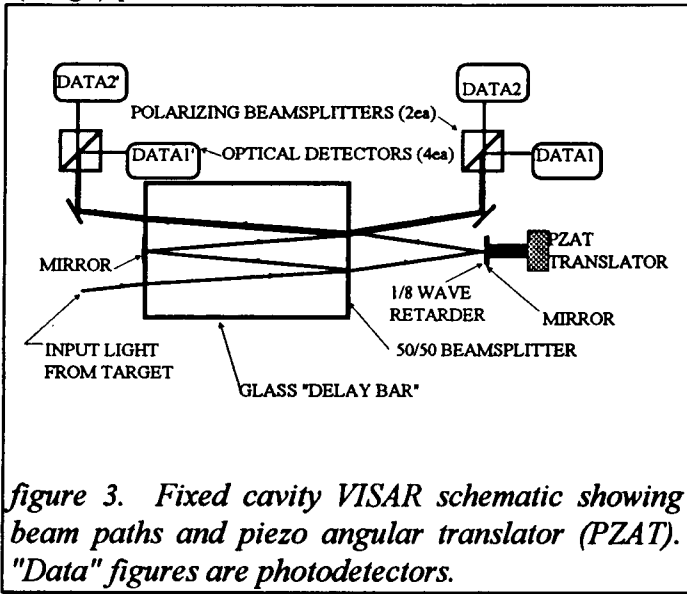


figure 2. Conventional method for collecting Doppler information from target.

The return light, containing equally distributed *S* and *P* polarization components, is collimated and sent through the interferometer cavity (*figure 3*). A 50/50 beamsplitter separates the light so that one beam travels through the glass "delay bar" and the other travels through air and an 1/8 wave retarder before recombining and producing an interference (fringe) pattern .



*figure 3. Fixed cavity VISAR schematic showing beam paths and piezo angular translator (PZAT). "Data" figures are photodetectors.*

In order to obtain quality fringe patterns, the **image** distances in both legs of the interferometer must be equal to within a few thousandths of an inch. If both legs of the interferometer are air, the measured distance would be equal. However, the refractive properties of glass make the image distance in the glass **delay** leg farther away than the image distance in the air **reference** leg. This relationship is defined by:

$$x=h(1-1/n)$$

where *h* is the delay leg length and *n* is the index of refraction. The distance the light has to travel in the delay leg is farther than the reference leg **and** the velocity of light is slower in glass than in air. Using

the relationship from equation (1), the delay time  $\tau$  is given by:

$$\tau=(2h/c)(n-1/n)$$

where *c* is the speed of light in a vacuum. Using these relationships, the fringe count *F(t)* relates to target velocity *u(t- $\tau$ /2)* as<sup>7</sup>:

$$u(t-\tau/2)=\frac{\lambda F(t)}{2\pi(1+\Delta v/v)}\cdot\frac{1}{1+\delta}$$

in which  $\lambda$  is the wavelength of the laser light,  $\Delta v/v$  is an index of refraction correction factor if a window is used,  $\delta$  is a correction factor with respect to wavelength for dispersion in the delay bar. Equation (3) may be manipulated to obtain the *velocity-per-fringe* (VPF)\* constant for the interferometer. The VPF equation is:

$$VPF=\frac{\lambda}{2\pi(1+\Delta v/v)}\cdot\frac{1}{1+\delta}$$

With these relationships, VISAR cavities with different sensitivities can be designed for optimal performance with regard to anticipated velocity versus Doppler resolution parameters. In any experiment, it is helpful to know that everything is operating correctly. Active feedback from the measuring instrument is a good method of assuring proper operation. The piezoelectric angular translator (PZAT) performs one such function by electrically moving a mirror in the cavity, effectively changing the cavity dimensions. When the cavity dimension changes by  $\lambda/2$ , a 180° phase change occurs which effectively simulates the fringe record for a velocity change equivalent to one-half the VPF value. The return interference signal is monitored and the experimenter is now able to verify that the system is functioning correctly.

\* The VPF is a numerical constant unique to an interferometer cavity, typically given as mm/us or km/s. For instance, a cavity with a VPF of 1 would have an interference pattern of a 360° sine wave for a target accelerating to 1 mm/us.

In *figure 3*, one component of light passes through the 1/8 wave retarder twice, which makes it 90° out of phase with the other component. The polarizing-beam splitting cubes then separate the *S* from the *P* light and each beam is sent to a photo detector coupled to a digitizer. Recording two 90° out of phase signals produces an interference pattern that is a sinusoidal plot. Phase resolution of the signal is poor when the intensity of the sine wave is at a maxima or minima. Making the two sinusoidal traces 90° out of phase insures that at any point in time one of the signals will be in a region of good resolution. Also, target acceleration or deceleration can be discriminated. During target acceleration, one signal pattern will lead the other by 90° and a deceleration will cause the opposite to occur.

#### SOLID STATE VISAR DEVELOPMENT

The original intent for the development of the Solid State VISAR was for a portable "in house" tool that could be shared by several experimenters and used in the laboratory or in the field. At the same time the Defense Nuclear Agency (DNA) was interested in optical based instrumentation for use at (NTS). One particular experiment required an "up close" measurement of ground shock generated by the detonation. Since the nuclear event yields radiation and electro-magnetic fields, optical sensors are preferred because of their relative insensitivity to these phenomenon. Also, the sensors require no electricity which adds a greater margin of safety to personnel. The following are some of the requirements for the system to function:

- Doppler measurement over kilometer-length fiber optics
- Rugged system, operating on 120VAC
- Must run several days with no adjustments
- Sensors must withstand mechanical and chemical abuse
- Window and sensors must survive concrete encapsulation and measure ground shock a few meters from the detonation
- Data acquisition bandwidth limited to 20 MHz

#### EXPERIMENT DESCRIPTION

Measurement of ground shock produced by the detonation is important because it contains valuable information used for analysis and modeling of the test. This ground shock measurement method uses a window, with sensors coupled by fiber optics to a VISAR cavity. The window is oriented towards the device and the entire area is filled with concrete. When the device detonates, a shock wave is transmitted through the concrete and into the window where the shock wave imparts a particle velocity in the window. The Doppler shift, which corresponds to the particle velocity in the window, is transmitted through the fiber optic to the VISAR cavity. The fringe data are converted to electronic signals and stored on digitizing oscilloscopes (digitizers). The mechanism for triggering the digitizers is a time of arrival (TOA) gauge. The TOA gauge is simply a fiber optic loop protruding in front of the window with a laser connected to one end and a photodetector attached to the other. When the shock wave breaks the fiber optic, laser light no longer enters the detector, it's output voltage drops, triggering the digitizers in VISAR.

The characteristics of the window and the material transmitting the shock wave into the window **must** be known for accurate particle velocity measurements. The simplest way to use a window is to choose a material that has already been characterized. Unfortunately, the unusual laser wavelength and the large window thickness required for adequate recording time (40μs) did not allow previously characterized windows to be used. The material chosen for the window used in this experiment is Schott BK-7 glass, which has good broadband optical transmittance and is available in the 8" thick x 14" diameter required for the test. Several specimens of BK-7 as well as cored samples of the concrete were analyzed for their shock properties by impacting them into other known window materials, then into themselves using a gas gun as the target accelerator. The results from the analysis, commonly called a Shock Hugoniot,



determine whether the material is suitable for the shock pressure predicted for the event. The data also correlate the impedance mismatch at the grout/glass interface. The anticipated shock pressure for the NTS test, a few meters from the device, is  $\approx 70$  kBar in the grout. **Figure 4** is a display of the type of plots for the shock pressure tests obtained using BK-7 as the impacted material. The BK-7 behaves like fused silica up to 90 kBar. Although BK-7 does not turn opaque at pressures above 90 kBar as fused silica does, the non-linear "shock-up" makes particle velocity correlations more difficult.

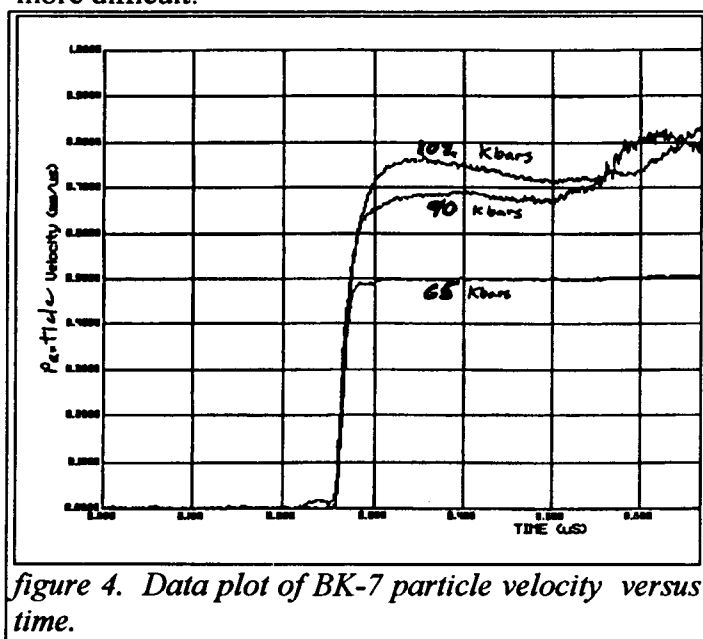


figure 4. Data plot of BK-7 particle velocity versus time.

The VISAR designed for the underground test contains a diode pumped Nd:YAG laser operating at 1319 nm wavelength, with a CW output of 160 mW, and a 5 kHz, single frequency linewidth. This laser is a good choice for this system because it is stable, has low sensitivity to optical feedback, and the wavelength exhibits very low attenuation and high bandwidth in silica fiber optics. This high performance is due, in part, to the self cancellation of different wavelength-dependent dispersion effects that occur in fiber. The photodetectors in the system are comprised of indium-gallium-arsenide (InGaAs) photodiodes coupled to low noise/high gain operational amplifier circuitry. The peak

sensitivity for these detectors happens to be at 1320 nm wavelength, which not only affords greater sensitivity, but also increases the signal to noise ratio. The linear response range for the detector/amplifiers is DC to 125MHz with a linear response better than 3% and an output voltage of 40mV/ $\mu$ W of light at 1320 nm wavelength (The flat linear response is critical for accurate data collection).

One of the most critical parts of the system design was the fiber optic coupled sensors. Laser radiation is injected into a 50 micron graded index, multimode fiber optic connected to sensors which image the fiber optic onto the rear surface of the window. The return light reflected from the window's rear surface is collected and injected into a 100  $\mu$ m step index, multimode fiber optic connected to the VISAR cavity. A redundant sensor is linked to the VISAR cavity in the event of damage to one of the sensors (**figure 5**). Correctly designing the optical train is paramount to attaining good signal strength that won't degrade under harsh environmental conditions (Obviously, after the sensors are encapsulated in 100 foot thick concrete, re-aligning is impossible.). There was some concern about stress induced polarization after observing wildly fluctuating *S* and *P* ratios when the fiber optic was bent. These fluctuations in polarization will change the sine-cosine relationship critical to accurate data analysis. In most cases, this polarization problem occurs when highly polarized laser beams are injected in short lengths of fibers. The root cause is the mode structure is not fully mixed in the fiber optic and stressing the fiber optic redistributes these modes causing a change in the polarization (The laser output is single mode-single frequency and should not be confused with fiber optic propagation modes.). Since there is no room for error on the real test, three solutions are incorporated to remedy the problem: installing a mode scrambler that pinches the fiber optic into a serpentine shape, using a long fiber optic to mix the modes, installing a rotatable linear polarizer at the entry into the

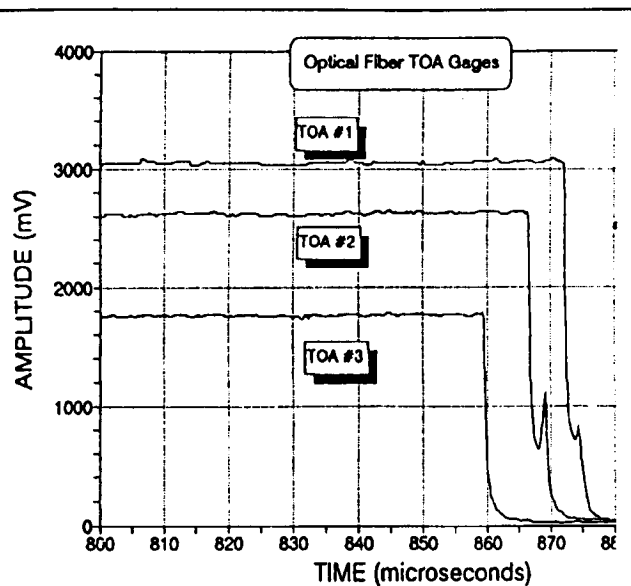


figure 6. Three of several TOA gauges

interferometer cavity. The new modifications solved the problem.

The sensors perform three functions; collimating and

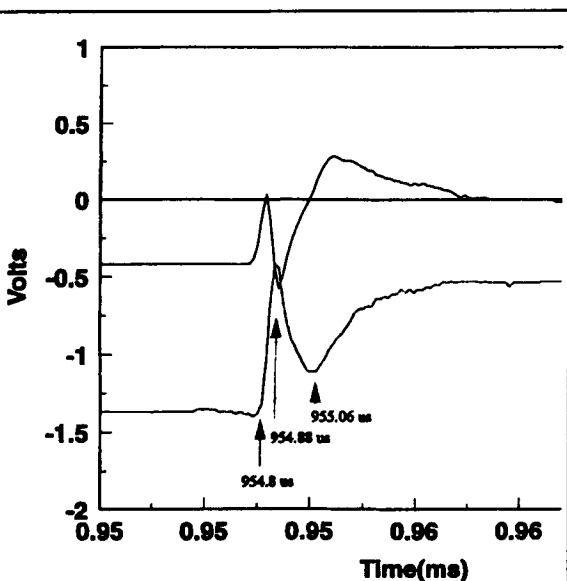


figure 7. Raw, unreduced data. Notice the 90° out-of-phase signals.

focusing the laser radiation onto the rear surface of the window, collecting the return light, and injecting the light into the return fiber optic. The sensor configuration is similar to figure 1 except that the

camera is omitted, since there is no need to see the rear window surface.

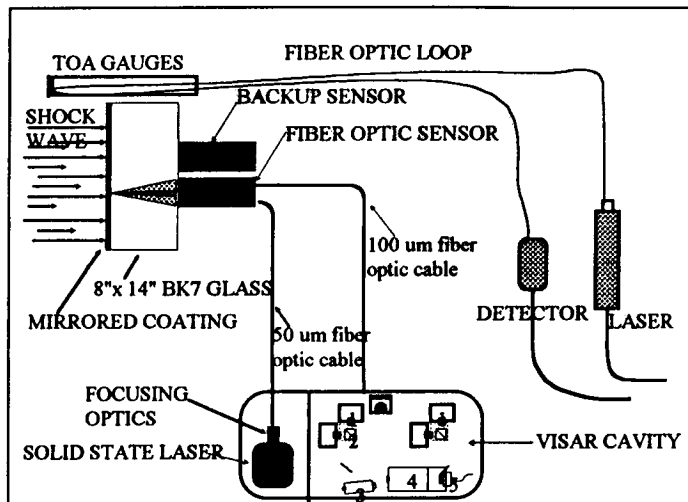


figure 5. Diagrammatic layout of the window, sensors, time of arrival (TOA) gauges, VISAR cavity, and laser.

Although the primary function of the TOA gauge is to trigger the digitizers, utilizing a TOA array provided additional shock data. Several gauges were placed around the window with the tips of the TOAs staggered to intercept the shock wave front at different points in time (figure 6). As the shock front breaks the TOAs, the digitizers record the time-of-break that is then correlated to shocks arrival time and velocity.

## EXPERIMENTAL RESULTS

The VISAR and TOA gauges performed with strong, clean signals recorded on all instrumentation channels. The Doppler information, in unreduced form, is shown in figure 7. The signal strength is 1Volt peak to peak which is well above the noise floor that has, in the past, caused difficulty in accurate data reduction. The 90° phase relationship between the two traces indicates the stress induced polarization problem has been cured.

Figure 8 shows the reduced data. There is an impedance mismatch between the BK-7 and the grout but the shock Hugoniot for these materials is

known and was used in calculating the final particle velocity. The peak recorded particle velocity was on the order of 0.6 mm/ $\mu$ s, which corresponds to a pressure at the interface of 85 kBar.

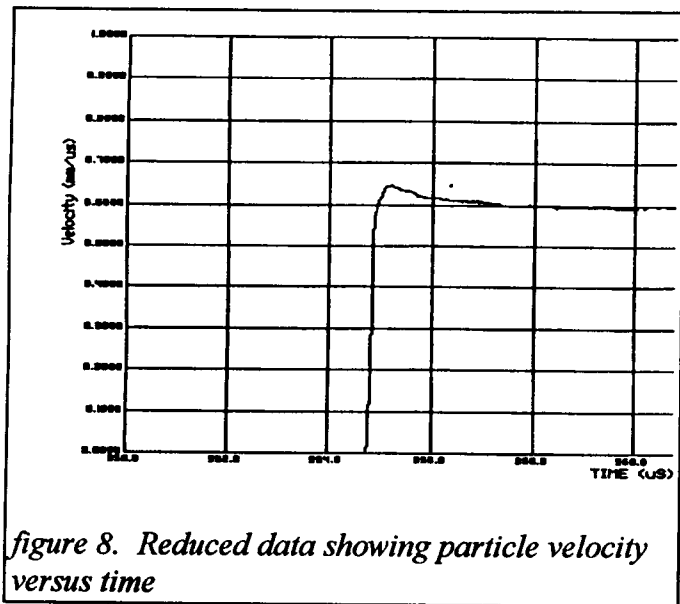


figure 8. Reduced data showing particle velocity versus time

The results indicate that the yield of the device was greater than expected (60 kBar). The choice of BK-7 was fortunate because if fused silica was available and used, the data would have been lost. (Fused silica is known to become opaque at pressures above  $\approx$  82 kBar.) The BK-7 is apparently able to withstand slightly greater shock pressures before going opaque and at 1/3 the cost, it is significantly less expensive.

## ACKNOWLEDGMENTS

This work was performed at Sandia National Laboratories, Albuquerque, NM for the United States Department of Energy under Contract DE-AC04-76DP0089. This project was truly a team effort and the authors gratefully thank the following people for their participation:

*Leonard Duda-* financial and technical design support, *John Matthews* and *Richard Wickstrom-* software support, *Larry Weirick*, *Mike Navarro*,

*Heidi Anderson-* BK-7 characterization & gas gun support, *Bill Brigham*, *Theresa Broyles*, *Dan Sanchez-* Electronic design & fabrication, *Dan Dow-* mechanical fabrication, *Terry Steinfort*, *Robert Vasquez-* mechanical design & installation, and *William Tarbell-* shock analysis. A special thanks to *Lloyd Bonzon* for supporting the concept in its infancy.

## REFERENCES

1. L.M. Barker and R. E. Hollenbach, Laser Interferometer for Measuring High Velocities of Any Reflecting Surface, *Journal of Applied Physics* 43:11 (Nov 1972)
2. W.F. Hemsing, Velocity Sensing Interferometer (VISAR) Modification, "Review of Scientific Instruments 50:1 (Jan 1979).
3. J.E. Kennedy, Org 7130, private communication.
4. K.J. Fleming, O.B. Crump Jr., Portable, Solid State VISAR, *SAND92-1361*. April, 1992
5. O.B. Crump Jr., P.L. Stanton, W.C. Sweatt, The Fixed Cavity VISAR, *SAND92-0162* (March 1992). Sandia National Laboratories, Albuquerque, NM.
6. K.J. Fleming, Fiber Optic Coupled Probe for Versatile Interferometry, *Department of Energy Patent Disclosure* SD-5034, S-74-181
7. L.M. Barker and K.W. Schuler, Velocity Interferometry System. *Journal of Applied Physics*. 45,3692 (1974).

526-28

7006

P-14

**DEVELOPMENT AND QUALIFICATION TESTING OF A  
LASER-IGNITED, ALL-SECONDARY (DDT) DETONATOR**

Mr. Thomas J. Blachowski  
CAD R&D/PIP Branch  
Indian Head Division  
Naval Surface Warfare Center  
Indian Head, MD 20640

Mr. Darrin Z. Krivitsky  
CAD Weapons/Aircraft Systems Branch  
Indian Head Division  
Naval Surface Warfare Center  
Indian Head, MD 20640

Mr. Stephen Tipton  
B-1B Systems Engineering Branch  
Oklahoma City  
Air Logistics Center  
Tinker AFB, OK 73145

**Abstract:**

The Indian Head Division, Naval Surface Warfare Center (IHDI, NSWC) is conducting a qualification program for a laser-ignited, all-secondary (DDT) explosive detonator. This detonator was developed jointly by IHDI, NSWC and the Department of Energy's EG&G Mound Applied Technologies facility in Miamisburg, Ohio to accept a laser initiation signal and produce a fully developed shock wave output. The detonator performance requirements were established by the on-going IHDI, NSWC Laser Initiated Transfer Energy Subsystem (LITES) advanced development program. Qualification of the detonator as a component utilizing existing military specifications is the selected approach for this program. The detonator is a deflagration-to-detonator transfer (DDT) device using a secondary explosive, HMX, to generate the required shock wave output. The prototype development and initial system integration tests for the LITES and for the detonator were reported at the 1992 International Pyrotechnics Society Symposium and at the 1992 Survival and Flight Equipment National Symposium. Recent results are presented for the all-fire sensitivity and qualification tests conducted at two different laser initiation pulses.

### Introduction:

The INDIV, NSWC is the lead service for cartridges, Cartridge Actuated Devices (CADs), and Aircrew Escape Propulsion Systems (AEPS) for all services. The CAD Engineering Division at IHDIV, NSWC manages and implements the development and engineering functions in the fields of ballistic power sources, energy transmission systems, and control devices such as cartridges, CADs, and their associated signal or energy transmission subsystems for the three services. The CAD Engineering Division also recommends and establishes policy and conducts service qualification for cartridges, CADs, and related power signal transmission systems for aircrew escape and survival and stores/weapons delivery and deployment for the Department of Defense (DoD). In addition, administration of research, design, development, and Product Improvement Programs (PIP) for ignition devices and electro-explosive devices for CADs is performed by the Division. Development of design specifications for cartridges, CADs, and related ballistic systems is maintained under this authority.

### Background:

The IHDIV, NSWC has pursued development of LITES for these applications. LITES utilizes chemical flashlamps to generate light which is amplified by a laser rod, focused into fiber optic transfer lines, and delivered to optically initiated pyrotechnic output devices. Proof-of-Principle tests and the exploratory development program (13th International Pyrotechnics Society Proceedings - 1988) were completed. An advanced development program was conducted to miniaturize the laser housing while maintaining the proven neodymium doped phosphate glass rod and commercially available flashlamp concept. The miniaturized laser (Figure 1) is a mechanically actuated device which generates sufficient energy, when delivered through a bundle of fiber optic lines, to initiate an optical output device. The LITES advanced development program has designed optical output devices which produce ballistic pressure or a shock wave output (detonator) as required for a specific aircrew escape system application (18th International Pyrotechnics Society Symposium - 1992).

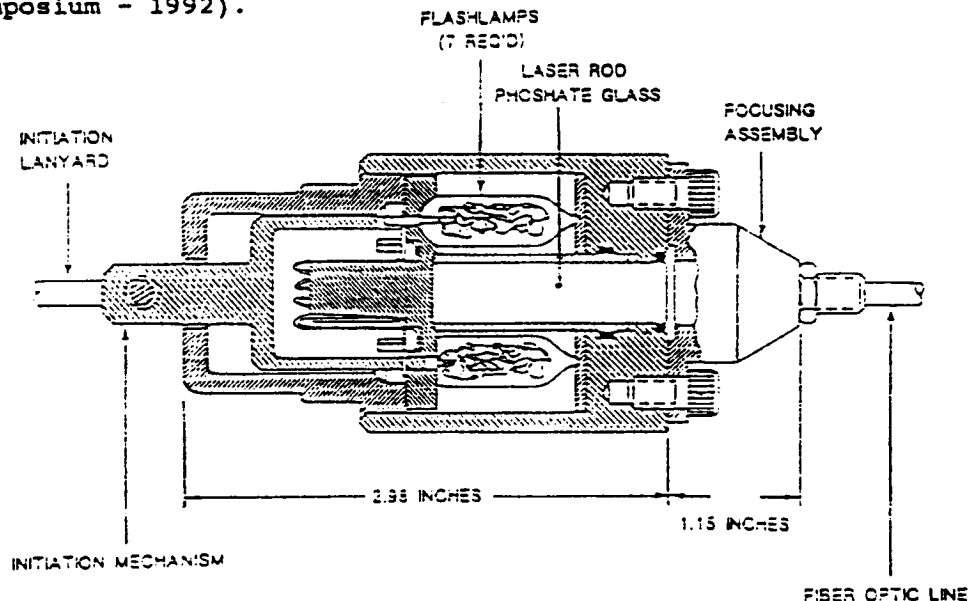


Figure 1: LITES Mechanically Actuated Laser Assembly

As part of the LITES program, through a series of discussions with EG&G Mound Applied Technologies, INC., NSWC established the following requirements (Table 1) for the laser-ignited detonator. Specifically, this deflagration-to-detonation transfer (DDT) device (Figure 2) would accept a 1.06  $\mu\text{m}$  laser wavelength input and could only contain secondary explosives that are commercially available from several sources in the United States. These requirements, along with the window and generation of an output equivalent to a Shielded Mild Detonating Cord (SMDC) tip, allows the optical detonator to be independent of the fiber optic signal transmission system. Although developed specifically for use with LITES, efforts were taken to permit this optical detonator to be used by a variety of energy pulse duration and fiber optic line configuration laser ignition systems. In addition, transition of the technology required to manufacture the detonator to industry was held as a design goal throughout this development program (18th International Pyrotechnics Society Symposium - 1992).

| Detonator Requirements   |
|--|
| • All secondary explosive device   |
| • Flat window configuration  |
| • Shielded Mild Detonating Cord (SMDC) tip output                                    |
| • Hermetically sealed  |
| • Structurally sound, all Reactants contained  |
| • No proprietary components  |
| • Transition government developed technology to industry for competitive procurement |

Table 1: Laser-Ignited Detonator Design Requirements

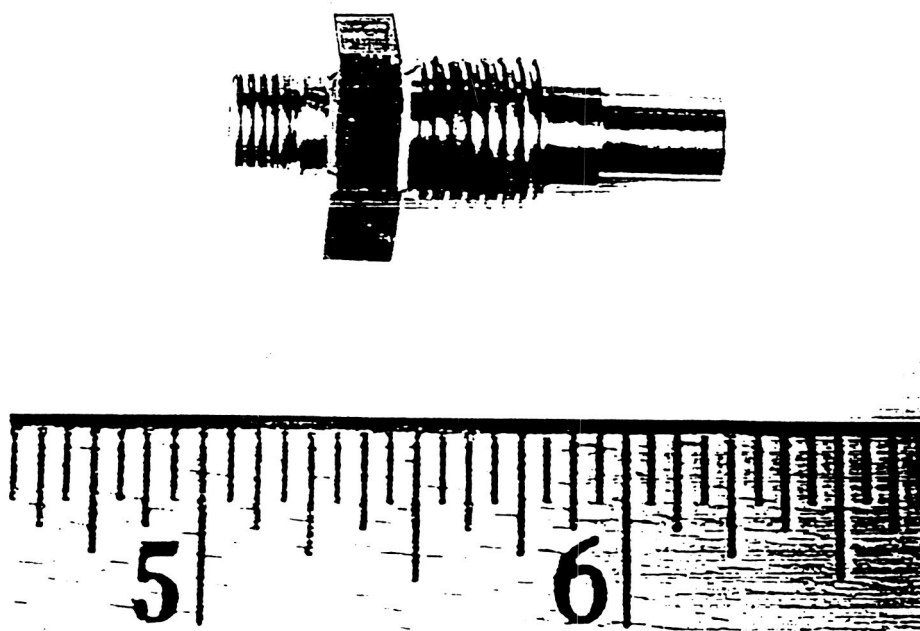


Figure 2: Laser-Ignited, All Secondary (DDT) Detonator

### Test Program Preparation:

### Definitions:

Prior to establishing the qualification test matrix and performance requirements for the laser-ignited detonator itself, it was necessary to define the components and the parameters involved in the overall aircrew escape system. For this paper, an Ordnance Initiation System is defined as a system consisting of three distinct components: (1) a signal generator and controller which is capable of establishing an initiation pulse of sufficient intensity at the required time interval, (2) a signal transmission system capable of transferring the pulse to all output devices within the envelope of the application, and (3) output devices (initiators or detonators) which either perform the required work function directly or initiate a second in-line device which performs the function. As previously described, these output devices include items such as initiators, squibs, gas generators, electro-explosive devices, thermal batteries, cutters, and detonators. An example of an aircrew escape system ordnance initiation system is shown in Figure 3.

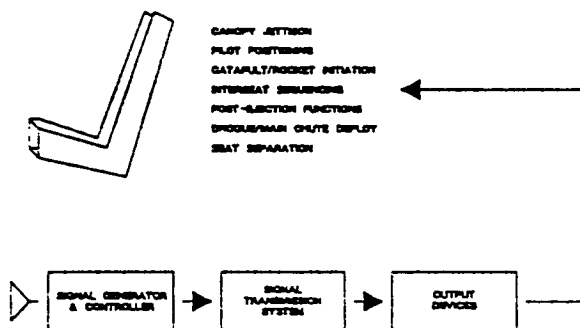


Figure 3: Generic Aircrew Escape System

During the evaluation of an ordnance initiation system, the parameters of the output devices must be clearly identified. Several existing government specifications clearly define the "all fire" energy of an output device and the "no fire" energy of an output device. The "all fire" energy level of an output device is defined as the minimum amount of energy or power required to initiate that output device in its final configuration with a reliability of 0.99 at a 0.95 confidence level. The "all fire" energy level will be determined by any suitable test method consisting of a sample size of not less than 20 output devices. This quantity is not defined in the existing specifications; however, a statistically significant sample size must be tested to verify the stated energy levels.

Threshold energy levels, a 50% initiation energy level, or a reliability of 0.9999 at a 0.98 confidence level are technically very useful values and may be required for a specific application. Any of these values; however, cannot be identified as the "all fire" energy level of an output device.

Conversely, the "no fire" energy level of an output device is the maximum amount of energy or power which does not initiate the output device in its final configuration within five minutes of application. At this initiation level, less than 1.0 per cent of all output devices at a level of confidence of 0.95 can actuate. Again, the "no fire" energy level will be determined by any suitable test method consisting of a sample size of not less than 20 output devices.

### Current Specifications:

There are no general specifications in place to specifically address qualification and ultimately implementation of laser initiation system technology in the U. S. Department of Defense, the Department of Energy, and the National Aeronautics and Space Agency (NASA). Much discussion has taken place over the past years as to which existing specification or series of specifications are most applicable to this new technology. A partial list has been compiled of the specifications most often mentioned in these discussions (Table 2).

| Specification | Title  |
|---------------|--|
| MIL-STD-1316  | • Safety Criteria for Fuze Design  |
| MIL-STD-1512  | • Design Requirements and Test Methods for Electrically Initiated Electroexplosive Subsystems    |
| MIL-STD-1576  | • Safety Requirements and Test Methods for Space Systems Electroexplosive Subsystems             |
| MIL-E-83578   | • General Specification for Explosive Ordnance for Space Vehicles                                |
| MIL-C-83125   | • General Design Specification for Cartridges and Cartridge Actuated/Propellant Actuated Devices |
| MIL-C-83124   | • General Design Specification for Cartridge Actuated Devices/Propellant Actuated Devices        |
| MIL-D-81980   | • General Design Specification for Design and Evaluation of Signal Transmission Subsystems       |
| MIL-I-23659   | • General Design Specification for Electric Initiators   |
| MIL-D-21625   | • Design and Evaluation of Cartridges for Cartridge Actuated Devices                             |
| MIL-D-23615   | • Design and Evaluation of Cartridge Actuated Devices  |

Table 2: Current Specifications for Laser Technology Implementation

### Specification Selection Process:

To successfully conduct and complete development and qualification testing on the laser-ignited detonator and to ultimately implement this device and other laser initiation system technology into next generation aircrew escape systems, three different approaches have been identified (Table 3, next page).



| APPROACH                 | ADVANTAGES   | DISADVANTAGES   |
|--------------------------|--|---|
| NEW SPECIFICATION        | <ul style="list-style-type: none"> <li>• GENERAL FORMAT</li> <li>• TECHNOLOGY SPECIFIC</li> </ul>  | <ul style="list-style-type: none"> <li>• LENGTHY APPROVAL PROCESS</li> <li>• NEW REQUIREMENTS</li> <li>• TECHNOLOGY NOT MATURE</li> </ul> |
| SYSTEM SPECIFIC DOCUMENT | <ul style="list-style-type: none"> <li>• SPECIFIC REQUIREMENTS MET</li> <li>• WRITTEN TO SCHEDULE</li> <li>• RFI/RFQ DOCUMENTS PREPARED</li> </ul> | <ul style="list-style-type: none"> <li>• NOT GENERAL</li> <li>• VERY DETAILED</li> </ul>  |
| EXISTING SPECIFICATION   | <ul style="list-style-type: none"> <li>• GENERAL FORMAT</li> <li>• NO NEW REQUIREMENTS</li> <li>• PRECEDENCE</li> </ul>                            | <ul style="list-style-type: none"> <li>• DATED REQUIREMENTS</li> <li>• MUST BE AMENDED</li> </ul>   |

Table 3: Specification Approach Advantages/Disadvantages

The first approach is to generate a new specification for laser initiation system components. The general format of this type of specification will allow implementation of the technology on a wide variety of platforms. The technology definitions included in this specification will allow Program Managers and design engineers the ability to better compare alternatives during the preparation of Trade Studies, program plans, etc. The required testing and reporting will better establish this technology baseline that will serve all users.

The disadvantages of this approach are severe. Laser initiation technology is rapidly advancing to new levels. What was thought to be a technical barrier a few years ago has changed. As these continued advancements occur, there has not been sufficient time for the "off-the-shelf" components to mature. The baseline has been moving. Writing a specification without fully identifying this baseline is very difficult. Once an agency has officially undertaken the specification writing task, there is a well defined and lengthy approval process through any Department of the Government. With the constantly changing baseline of the technology and the lengthy approval process, this approach is unattractive.

The second approach is to allow Program Managers to prepare specifications for a single system. The advantages of this approach are numerous. The Program Managers have a "hands on" feel of the requirements for their platform. Specialized needs, power requirements, safety margins, output performance among other parameters would be contained in this single document. Potential suppliers then have a defined goal to design an individual technology alternative as a solution and all the pre-selection testing and reporting needs are highlighted. Competing solutions, trade studies, and the overall program technical risk are clearly outlined to the Program Managers. This overall approach will be conducted for every system; however, the amount of assets allocated (management time, engineering assets) is great.

This leads directly into the disadvantages of this approach. The very detailed system specific document requires an investment of Program Management time and resources. The amount of technical detail in these documents will depend on the individual program office or on the contractor assigned with their preparation. Issues such as competitive procurement of the selected technology or sole sourcing the procurement to a particular vendor for the life of the platform must be addressed at this step. If the system specific document becomes too detailed, sole source procurement or its variations, are very likely. Upon completion of these documents, they may not be applicable to other platforms. Some requirements may transition to a general system very well; however, most will not.

The third approach is to utilize existing specifications to implement laser initiation technology into current and planned platforms. There are several advantages to this approach. Existing specifications are written to a general format thus allowing all alternative technologies to design engineering solutions. The previous test requirements for each platform are well defined and established. Potential vendors for a specific platform have a defined baseline of past knowledge to build upon. Precedence has been established by the Program Managers utilizing these specifications. There are no new technical limitations for implementing laser initiation technology onto any platforms.

The disadvantages of this approach include the time dated nature of all the listed specifications (Table 1), and they must be amended somewhat to address new technical concerns. The listed specifications were written to address the general design issues of that time and, even including amendments and re-issuances, do not address some of the attributes of laser initiation technology. Minor modifications to these specifications to address these special attributes allow these documents to govern implementation of a new technology onto current and future DoD platforms.

#### Existing Specifications Selected:

Following this process, the third approach of selecting existing specifications was chosen to allow for implementation of laser initiation system technology into DoD applications. The specifications selected by IHDIIV, NSWC are as follows:

- (1) the signal generator and controller (Laser Assembly) will be governed by MIL-C-83124,
- (2) the signal transmission system (STS) will be governed by MIL-D-81980, and
- (3) the optical output devices (Initiators and detonators) will be governed by MIL-C-83125.

These documents were selected because MIL-C-83124 and MIL-C-83125 apply to energy sources and ballistic devices (cartridges and CADs) for all three services. This tri-service approval is very attractive in making the specification requirements as general as possible while still meeting a DoD baseline. For the STS, MIL-D-81980 was selected. This document is a Department of the Navy specification but has precedence in testing energy transfer systems for the other services.

The laser-ignited detonator is an optical output device and the Qualification Test Procedure (QTP) to allow for qualification and implementation of this device was written against the requirements specified in MIL-C-83125.

#### Qualification Test Procedure:

A QTP was prepared by IHDIIV, NSWC to detail all environmental test conditions and output performance requirements for the laser-ignited detonator. As previously described, this procedure governs only the laser-ignited detonator; the laser signal generator (Laser Assembly) and the fiber optic signal transmission system will not be subjected to these environmental tests. All of the environmental tests and required number of detonators are shown in Table 4 (next page). The test matrix requires 161 detonators to successfully demonstrate this technical concept.

| Environmental Test / Quantity    | 4 | 6 | 6 | 9 | 9 | 9 | 9 | 12 | 12 | 6 | 9 | 30 | 10 | 30 |
|----------------------------------|---|---|---|---|---|---|---|----|----|---|---|----|----|----|
| Visual Inspection                | 4 | 6 | 6 | 9 | 9 | 9 | 9 | 12 | 12 | 6 | 9 | 30 | 10 | 30 |
| X-Ray & n-Ray Inspection         | 4 | 6 | 6 | 9 | 9 | 9 | 9 | 12 | 12 | 6 | 9 | 30 | 10 | 30 |
| Dry Gas Leakage                  | 4 | 6 | 6 | 9 | 9 | 9 | 9 | 12 | 12 | 6 | 9 | 30 | 10 | 30 |
| Non-Electric Initiation (-90° F) | 4 |   |   |   |   |   |   |    |    |   |   |    |    |    |
| 40' Drop Test                    |   | 6 |   |   |   |   |   |    |    |   |   |    |    |    |
| 6' Drop Test (70° F)             |   |   | 6 |   |   |   |   |    |    |   |   |    |    |    |
| • Shock                          |   |   |   | 9 | 9 | 9 | 9 |    |    |   |   |    |    |    |
| • TSH&A                          |   |   |   |   | 9 | 9 | 9 |    |    |   |   |    |    |    |
| • Low Temp. Conditioning         |   |   |   |   |   | 9 | 9 |    |    |   |   |    |    |    |
| • Vibration                      |   |   |   |   |   |   | 9 |    |    |   |   |    |    |    |
| Cook-Off                         |   |   |   |   |   |   |   | 12 |    |   |   |    |    |    |
| High Temp. Exposure (70° F)      |   |   |   |   |   |   |   |    | 12 |   |   |    |    |    |
| Salt Fog (70° F)                 |   |   |   |   |   |   |   |    |    | 6 |   |    |    |    |
| High Temp. Storage (200° F)      |   |   |   |   |   |   |   |    |    |   | 9 |    |    |    |
| Functional Low Temp. (-65° F)    |   |   |   |   |   |   |   |    |    |   |   | 30 |    |    |
| Functional Ambient Temp. (70° F) |   |   |   |   |   |   |   |    |    |   |   |    | 10 |    |
| Functional High Temp. (225° F)   |   |   |   |   |   |   |   |    |    |   |   |    |    | 30 |

Table 4: Qualification Test Matrix for Laser-Ignited Detonator

- Table 4 Notes:**
- (1) TSH&A is defined as Temperature, Shock, Humidity, and Altitude Cycling.
  - (2) The temperature in parentheses is the functional firing temperature of the detonators.
  - (3) The "•" denotes **SEQUENTIAL TESTING** which means the nine vibration detonators were subjected to all four environments and functionally tested; three detonators at -65° F, three detonators at 70° F, and three detonators at 200°F. The Low Temp. Conditioned detonators were also subjected to TSH&A cycling and Shock prior to functional tests as described above.
  - (4) For the 40' Drop and Cook-Off Tests, no functional test firings are required. The detonators must survive these environments and be safe to handle and discard.

Successful completion of this QTP demonstrates the laser-ignited detonator concept. Additional testing will be required prior to release of this device to service use. The application specific locking connectors (both from the fiber optic transmission system to the detonator and from the detonator to its work performing device) must be demonstrated through a similar environmental test series prior to aircrew escape system implementation.

#### Short Pulse Qualification Test Results:

Defining the specific laser energy pulse, its duration, and the configuration of the energy delivery system was performed at this time. Driven by a specific aircrew escape system application, the viability of a microsecond(s) long pulse duration was considered. Based on the recommendations from EG&G Mound and by this Activity's research, the laser-ignited detonator was capable of being successfully initiated with a pulse of this duration. A 150-microsecond pulse duration delivered through a hard clad silica (numerical aperture of 0.37) fiber optic line was established as the initiation condition. A 20 unit Neyer threshold test<sup>1</sup> was conducted to determine the all-fire energy of the laser-ignited detonator. Based on these test results, the 0.99 reliable at a 0.95 confidence interval energy value was determined to be 131.3 millijoules in this configuration. The diagnostic equipment was verified for this configuration (Figure 4). To further insure initiation of the detonator in this configuration, the following values were used to begin the qualification testing:

- 150 millijoules of laser energy
- 150 microsecond pulse duration
- 200 micron fiber (NA = 0.37)

#### Nd:YAG Laser Pulse

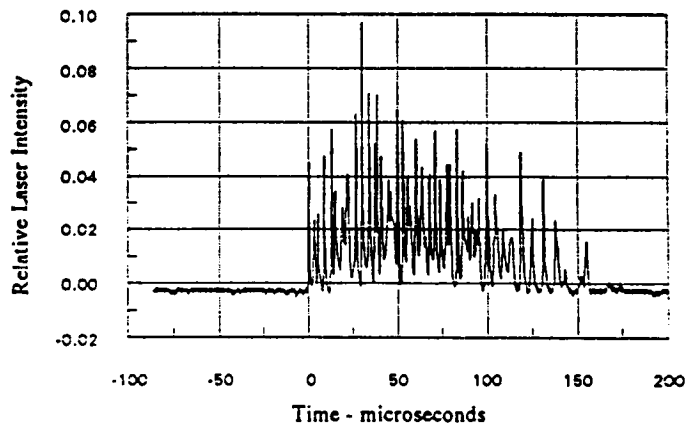


Figure 4: 150 Millijoule Laser Energy Pulse from Quantaray DCR-2A Laser

Ten detonators were selected from the Functional Ambient Temperature group of the QTP to begin the testing (Table 5, next page). The first six detonators successfully initiated and met all the performance requirements. The seventh detonator did not initiate. After a series of discussions, IHDIIV, NSWC and EG&G Mound representatives agreed to continue the testing. The eighth and ninth detonators functioned as designed. The tenth detonator did not initiate. At this point, the qualification testing was halted.

<sup>1</sup> - "More Efficient Sensitivity Testing" Barry T. Neyer, MLM-3609 EG&G Mound Applied Technologies - October 20, 1989.

| Test # | Function Temperature | Pre-Shot Tests (mJ) | Function? | Pulse Duration ( $\mu$ sec) | Function Time ( $\mu$ sec) | Indent (in.) |
|--------|----------------------|---------------------|-----------|-----------------------------|----------------------------|--------------|
| 1      | 70° F                | 151.9 $\pm$ 1.3     | YES       | 150                         | 55.5                       | 0.058        |
| 2      | 70° F                | 151.2 $\pm$ 0.4     | YES       | 150                         | 77.5                       | 0.052        |
| 3      | 70° F                | 149.5 $\pm$ 0.3     | YES       | 150                         | 58.0                       | 0.051        |
| 4      | 70° F                | 150.3 $\pm$ 0.6     | YES       | 153                         | 50.5                       | 0.055        |
| 5      | 70° F                | 149.7 $\pm$ 2.2     | YES       | 150                         | 63.5                       | 0.055        |
| 6      | 70° F                | 149.7 $\pm$ 1.7     | YES       | 153                         | 71.5                       | 0.053        |
| 7      | 70° F                | 149.6 $\pm$ 1.4     | NO        | 150                         | -                          | -            |
| 8      | 70° F                | 152.3 $\pm$ 0.4     | YES       | 150                         | 60.0                       | 0.051        |
| 9      | 70° F                | 148.7 $\pm$ 0.6     | YES       | 149                         | 73.0                       | 0.051        |
| 10     | 70° F                | 150.9 $\pm$ 2.6     | NO        | 156                         | -                          | -            |

Table 5: Short Pulse Laser-Ignited Detonator Test Results

Short Pulse Failure Investigation:

A complete failure investigation was undertaken to determine the cause of the non-initiation of these detonators and to establish engineering solutions to eliminate these non-initiation causes from the design concept. This was a wide ranging investigation which included a re-assessment of the window design and status during the testing, the energetic material post-test condition, and the diagnostic test equipment itself.

The fiber optic line delivering the required energy pulse was examined. A standard SMA-905 connector was used to link the line to the detonator. This connector centers the fiber optic line in a stainless steel sleeve with epoxy filling the surrounding gap. One potential failure cause was that if this epoxy slightly covered the face of the fiber or at the tip of the fiber, the epoxy was vaporized as the energy pulse exits the fiber. This phenomena would block the laser energy from the window and result in a greatly decreased amount reaching the energetic material, inducing non-initiation of the detonator.

A second cause involving damage to the window was also investigated. During detonator manufacture, optical transmission of the window was tested prior to loading of the energetic material. This detonator design requires a contact between the fiber optic line and the window. Due to this design and the optical transmission testing, surface damage occurred to the window. These damage patterns were identified for all detonators and these patterns were grouped into eight categories: flawless windows, small pits in the center of the window, small pits in the center and damage outside the center of the window, very light scratches and small dots on the window, deep scratches, film coating on the window, a deep inclusion in the window, and small center dots in the window with extra debris. Either or both of these investigated causes could result in non-initiation of the detonator.

Based on this completed failure investigation and the assets available to continue this development and qualification program, the overall system initiation configuration was re-addressed. A question was posed to the aircrew escape system and aircraft system designers, "Could a system be designed, within existing aircraft parameters, to generate and support a laser pulse duration of 12 milliseconds?" The response from these designers was that a 12 millisecond long pulse could be implemented to resolve the demonstrated failure pattern.

#### Long Pulse Qualification Test Results:

Re-establishing the detonator conceptual design initiation pulse duration was the primary solution to the non-initiation experienced during the short pulse qualification testing. This longer duration lowers the power density of the pulse and greatly lessens the potential for laser induced damage in the window and/or the fiber optic line. In addition, lowering this power density and increasing the pulse duration renders slight imperfections in the window less critical to successful initiation of the detonator. This pulse duration allows the laboratory designed and developed detonator to be demonstrated as rugged enough for field applications. No enhancements, such as re-polishing the windows to reduce surface damage, were performed on any of the environmentally stressed detonators.

As for the transmission system itself and the diagnostic test equipment, to further reduce the possibility of inducing a non-initiation, a glass/glass fiber optic line was selected (with a numerical aperture of 0.22). The SMA-905 end connector was assembled into this line utilizing a minimum of epoxy that was held away from the fiber tip itself. A 20 unit Neyer threshold test was conducted in this configuration to determine the 0.99 reliable at a 0.95 confidence interval all fire energy of the detonator. Based on this test series, the following values were used for the long pulse qualification testing:

- 132.8 millijoules of laser energy
- 12 millisecond pulse duration
- 200 micron fiber (NA = 0.22)

The 132.8 millijoule, 12 millisecond laser energy pulse was confirmed through the diagnostic test equipment as before. The Function Time (defined as the time from laser pulse initiation to the output shock wave impacting a detector at the back of the test fixture) of the detonators was recorded and a minimum of 0.040 inch indent was established as the detonator output requirement. A total of 131 detonators were functionally tested using the initiation configuration and the results are grouped by environmental test condition (Table 6, next page). An additional 18 detonators successfully completed the QTP requirements without undergoing functional testing (the 40' Foot Drop Test and the Cook-off detonators). Also, 12 detonators that had undergone environmental conditioning were functionally tested for information only (Table 7, second page). Using the long pulse configuration, the laser-ignited detonator did not achieve all of its design goals for this QTP.

| Environmental Tests                | Function Temp. (°F) | # Required | # Successful | Function Time (msec.) | Indent (in.)  | Other Results   |
|------------------------------------|---------------------|------------|--------------|-----------------------|---------------|---|
| NON-ELECTRIC INITIATION            | -90° F              | 4          | 4            | 3.59 ± 0.89           | 0.053 ± 0.003 | NONE  |
| 6 FOOT DROP                        | 70° F               | 6          | 6            | 4.54 ± 2.23           | 0.053 ± 0.002 | NONE  |
| SHOCK                              | -65° F              | 3          | 3            | 5.55 ± 0.68           | 0.054 ± 0.002 | NONE  |
|                                    | 70° F               | 3          | 3            | 3.21 ± 0.77           | 0.054 ± 0.001 | NONE  |
|                                    | 200° F              | 3          | 3            | 6.33 ± 0.42           | 0.050 ± 0.002 | NONE  |
| SHOCK, TSH&A                       | -65° F              | 3          | 2            | 7.57 ± 1.42           | 0.048 ± 0.001 | (0.027)   |
|                                    | 70° F               | 3          | 2            | 6.36 ± 0.23           | 0.048 ± 0.004 | (0.025)   |
|                                    | 200° F              | 3          | 2            | 6.99 ± 1.18           | 0.043 ± 0.002 | (0.026) {0.041}                                       |
| SHOCK, TSH&A, LOW TEMP.            | -65° F              | 3          | 3            | 6.16 ± 0.21           | 0.050 ± 0.004 | NONE  |
|                                    | 70° F               | 3          | 1            | 6.85 ± 0.84           | 0.046         | (0.016) (0.031)                                       |
|                                    | 200° F              | 3          | 2            | 6.41 ± 0.48           | 0.045 ± 0.001 | (0.025)   |
| SHOCK, TSH&A, LOW TEMP., VIBRATION | -65° F              | 3          | 1            | 6.18 ± 1.00           | 0.042         | (0.031) (0.033)                                       |
|                                    | 70° F               | 3          | 2            | 3.30 ± 1.02           | 0.055 ± 0.000 | 1   |
|                                    | 200° F              | 3          | 3            | 7.59 ± 1.23           | 0.048 ± 0.004 | NONE  |
| SALT FOG                           | 70° F               | 6          | 6            | 3.65 ± 1.06           | 0.051 ± 0.004 | NONE  |
| HIGH TEMP. STORAGE                 | 200° F              | 9          | 8            | 6.60 ± 1.78           | 0.050 ± 0.003 | (0.031)   |
| LOW TEMPERATURE                    | -65° F              | 30         | 30           | 3.62 ± 1.12           | 0.051 ± 0.003 | NONE  |
| AMBIENT TEMPERATURE                | 70° F               | 10         | 10           | 2.83 ± 0.43           | 0.053 ± 0.002 | NONE  |
| HIGH TEMPERATURE                   | 225° F              | 30         | 25           | 7.71 ± 1.50           | 0.051 ± 0.003 | (0.025) (0.025)<br>(0.033) (0.025)<br>(0.024) {0.042} |

Table 6: Long Pulse Laser Ignited Detonator QTP Results

- Table 6 Notes:**
- (1) The Other Results indicated in "( )" are unacceptable indents. They are below the QTP mandated 0.040 inch indent.
  - (2) The Other Results indicated in "{ }" are marginal indents. These very closely achieve the 0.040 inch indent.
  - (3) The "1" indicates an initiation failure.

| Environmental Tests    | Function Temp. (°F) | # Required | # Successful | Function Time (msec.) | Indent (in.)  | Other Results   |
|------------------------|---------------------|------------|--------------|-----------------------|---------------|-----------------|
| COOK-OFF<br>SURVIVORS  | 375 °F / 70° F      | 3          | 2            | 11.85 ± 3.21          | 0.049 ± 0.001 | (0.016)         |
|                        | 400° F / 70° F      | 1          | 0            | 5.36                  |               | (0.011)         |
| HIGH TEMP.<br>EXPOSURE | 325° F / 70° F      | 3          | 0            | 12.32 ± 2.66          | -             | ALL ≤ (0.015)   |
|                        | 300° F / 70° F      | 2          | 0            | 8.76 ± 1.36           | -             | (0.025) (0.022) |
|                        | 275° F / 70° F      | 3          | 0            | 13.18 ± 0.54          | 2             | (0.021) (0.023) |

Table 7: Long Pulse Laser Ignited Detonator Non-QTP Results

Table 7 Notes: (1) The Other Results indicated in "( )" are unacceptable indents. They are below the QTP mandated 0.040 inch indent.  
(2) The "2" indicates an initiation failure.

#### Long Pulse Failure Investigation:

At this writing, the long pulse failure investigations are underway. There are two separate investigations being conducted by IHDIV, NSWC and EG&G Mound personnel: the first is to determine the cause of the two non-initiations, and the second is to determine the apparent temperature and/or temperature cycling effect on the detonator and its not consistently achieving the minimum 0.040 inch indent into an aluminum dent block.

Determining the cause of the non-initiations is the first priority. Of the 143 functional detonator tests completed, there were 2 non-initiations. Both of these detonators had been subjected to elevated temperature environments (one during the TSH&A cycling had seen 160° F and the other during High Temperature Exposure had seen 275° F for a period of 12 hours). The detonators that had passed the indent requirement exhibited longer function times after being subjected to elevated temperatures. Some of the detonators in the non-QTP test series had even functioned after the 12 millisecond laser pulse was completed. For the detonators subjected to cold environments, the function times are somewhat faster and all of these indents are acceptable. The diagnostic test set-up and operator handling procedures are also under review as part of this failure investigation. All of this information is being evaluated to determine the cause of these two non-initiations.

The second investigation to determine the lack of sufficient indent into the dent block is also of great importance. Obtaining the 0.040 inch indent demonstrates this HMX, laser-ignited detonator is a one-for-one replacement candidate for the widely used SMDC lines and output tips which use HNS (Hexanitostilbene) as their energetic material. Demonstrating an identical indent for this laser-ignited detonator will greatly reduce the number of future tests required to assure this one-for-one replacement in all fielded applications. To begin this investigation, a record of the post-test detonator column condition is being compiled. For tests that achieved the 0.040 inch indent, the column had fragmented or blossomed outward. In some cases, this expansion had not fragmented the metal column, just widened it slightly. And, in some other cases, the output column of the detonator remained the same size. Several theories are being explored to explain these test results. Once these theories are proven through additional testing, engineering solutions can be implemented to the detonator design concept to eliminate the potential of low indents.

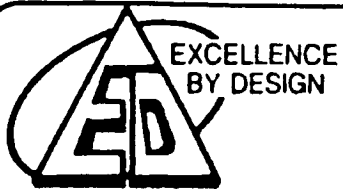


### Conclusions:

This paper has presented a new laser-ignited detonator concept developed jointly by IHDIV, NSWC and EG&G Mound. Development and qualification methods for this new technology and new device have been presented using existing military specifications to establish the acceptance requirements. Diagnostic test equipment development, set-up, and specialized operating procedures were designed to demonstrate the performance of the detonator. Two Neyer sensitivity test series were conducted to establish the "all fire" energy level. Two different initiation systems (different pulse durations, all fire energy levels, and connector interfaces) were investigated during this program. The laser-ignited detonator design was demonstrated as feasible within the system constraints. The concept is not completed. The reasons for non-initiation and the low indent results must be identified and resolved before this device is subjected to further system tests. Through the on-going failure investigations, solutions to these shortfalls are seemingly attainable. Upon implementation of these solutions, this detonator will be subjected to a final test series. Successful completion of this delta qualification test series will allow the detonator to be released for field applications including aircrew escape systems.

### Biography:

Mr. Thomas J. Blachowski has held his present position as an Aerospace Engineer in the CAD Research and Development/Product Improvement Program Branch at IHDIV, NSWC for the past 8 years. He has been directly involved in LITES, laser initiation, and laser detonator development efforts since 1988. In addition, he has managed the Cartridge Actuated Device (CAD) Exploratory Development and Advanced Development programs since 1989. Mr. Blachowski received his Bachelor of Science degree from The Ohio State University in 1985.



**ENGINEERING DIRECTORATE**



Lewis Research Center

# **Pyrotechnically Actuated Systems Database and Catalog**

## **Second NASA Aerospace Pyrotechnic Systems Workshop**

**February 8-9, 1994  
Sandia National Laboratories  
Albuquerque, NM**

**NASA Lewis Research Center  
Cleveland, OH**

**Prepared by:  
Analex Corporation**

- 351 -

OMIT TO  
END

## Presentation Agenda

- ◆ Purpose of Database/Catalog
- ◆ Database Ground Rules
- ◆ Format for Database
- ◆ Schedule
- ◆ Database/Catalog availability

1

## Purpose of Database/Catalog

### Pyrotechnically Actuated Systems Database

The purpose of the Database is to store all pertinent design, test and certification data for all existing aerospace pyro devices into a standardized Database accessible to all NASA/DOD/DOE agencies.

### Applications Catalog

The purpose of the Applications Catalog is to identify and provide a quick reference for the pyrotechnic devices available, including basic performance and environmental parameters.

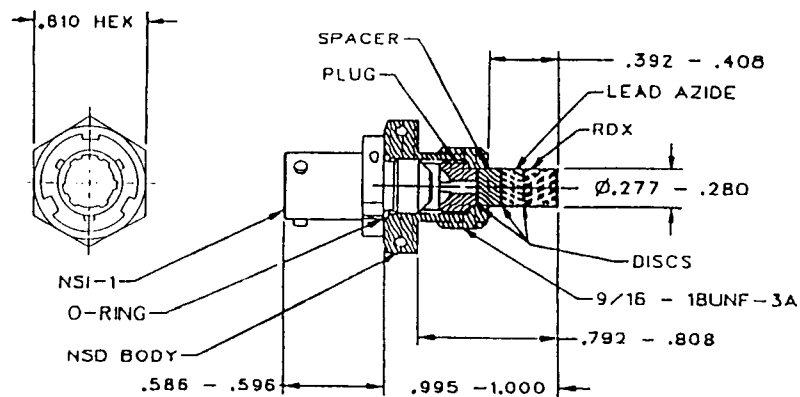
## Database and Catalog Ground Rules

- ◆ Develop database on the Macintosh computer system using OMNIS 7 software.
- ◆ Include current and past (non-obsolete) pyro devices used on launch vehicles, spacecraft, and support systems. Compile information from all NASA/DOD/DOE Centers.
- ◆ Include pertinent design and specification data.
- ◆ Include sketches for each device and system.
- ◆ Provide cross reference indexes in Catalog.
- ◆ Catalog to be extracted from the database.
- ◆ Provide for updating capability.

3

## Format

**Example:** TITLE: Detonator - NASA Standard  
AGENCY/CENTER: NASA Johnson Space Center (JSC)  
PHYSICAL DATA:



NASA STANDARD DETONATOR (NSD) SCHEMATIC

CONTRACTOR: n/a  
SUBCONTRACTOR: HI Shear Tech. Corp., Explosive Technology Co., and Universal Propulsion Co.  
DEVICE IDENTIFICATION NUMBER: NASA SEB26100094  
PURPOSE: To provide a high leveled detonating shockwave for initiating an explosive train or separating frangible devices.

### Format (Cont.)

**Example:** PREVIOUS USAGE: Apollo, Skylab, Apollo-Soyuz, and Space Shuttle.

**OPERATIONAL DESCRIPTION:** The NSD is the standard detonator for the Space Shuttle and is provided as GFE to all shuttle users by the Johnson Space Center. The NSD consists of the NASA Standard Initiator (NSI) threaded into an A-286 stainless steel body containing a column of Lead Azide progressing into a column of RDX. When the NSI is fired with the Pyrotechnic Initiator Controller (PIC) 38 vcs capacitor (680 microfarads) discharge, the NSD produces a 0.040 inch minimum dent into a mild steel block at ambient temperature.

**ENERGY SOURCE:**

TYPE OF INITIATION: NSI.

CHARGE MATERIAL: Dextrinated Lead Azide (376 mg) and RDX (400 mg).

ELECTRICAL CHARACTERISTICS: n/a.

OPERATING TEMPERATURE/PRESSURE:

TEMPERATURE RANGE: Low -420°F, High +200°F.

PRESSURE: n/a.

**DYNAMICS:**

SHOCK: 30g, 11 msec sawtooth.

VIBRATION: Random (-65°F to +200°F) at 2000cps.

**QUALIFICATION:**

DOCUMENTATION: SKD-26100097 Design & Performance Spec, Qualification Documentation provided by each contractor and on file at JSC.

**SERVICE LIFE:**

SHELF: 4 years minimum from Lot Acceptance test date, 10 years maximum based upon successful passing Age Life Testing per NSTS 08060.

OPERATIONAL: See Shelf Life above.

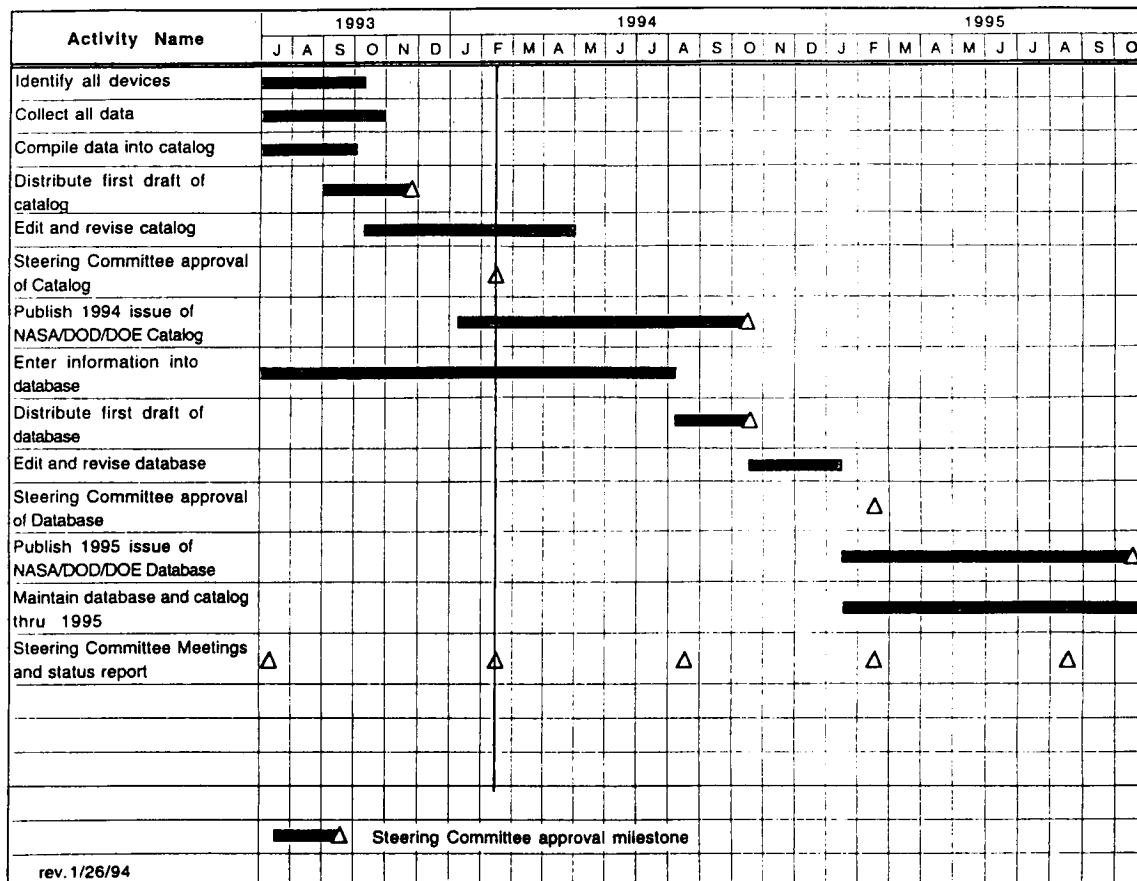
**ADDITIONAL REFERENCES:** n/a.

ADDITIONAL COMMENTS: DOT Class-C explosive.

**SPECIAL FEATURES:** n/a.

5

## Schedule for Pyrotechnically Actuated Systems Database and Reference Catalog





## Database and Catalog Availability

- ◆ Database and Catalog will be released as government issue.
- ◆ Catalog will be available in October 1994.
- ◆ Database will be available in October 1995.

**Page intentionally left blank**

# FIRE, AS I HAVE SEEN IT

Dick Stresau  
Stresau Laboratory, Inc.  
Spooner, WE 54801

## ABSTRACT

Fire (and much else) is described as I have seen it (in the sense that "to see" is "to understand") from a succession of perspectives (which seems, like that of most moderns, to parallel the sequence of perspectives had been assumed by scholars in the past) since childhood. Origin and originators of some of these perspectives (e.g., that of the "Bohr atom" and the Chapman-Jouguet theory of detonation) are mentioned in passing. For the most part, I believe my views to be quite similar to those of others who have concerned themselves with fire in its various forms. However, data, which may not have considered by others, have led me to see explosion and the shock to detonation transition from apparently new perspectives, which are discussed.

## INTRODUCTION

Like, I suppose, most people I first saw fire from an "on scene, eyewitness" perspective, Explanations, by adults, of fire and other things we sensed (saw, heard, felt, tasted, or smelled) helped me to see things in the sense that "to see" is "to understand", from a "common sense" perspective. The explanations, however, were in words which may not have been understood as they were intended. As punsters often remind us, each of many words and phrases of English, and other living languages, has a number of meanings. For example, the 1967 edition of the "Random House Dictionary of the English Language" (1) gives fifty-four definitions of "fire".

## PYROTECHNICS

"Pyrotechnics" the subject of this workshop, is given as a synonym of "pyrotechny" - "The science of the management of fire and its application to various operations" (2). So defined, it is among the oldest of technologies (2½). The survival of the human race (adapted as it was and is, to the climate of equatorial Africa) in the "temperate" zones, during the "ice ages" depended upon the establishment of (indoor) environments similar to that to which it is adapted, for which pyrotechny, "The management of fire" is essential. Its most prevalent application is still to this purpose. More fires are used to heat buildings than for any other purpose. It is an essential part of such other prehistoric technologies as pottery, glass making,

metal smelting, casting and forging, as well as the arts of cooking, baking, etc. Remains of fireplaces are accepted by archaeologists, as evidence of the presence of early man at a site. It could be said that pyrotechnics, as defined above, played an essential role in "the ascent of the mind" (3) and the rise of civilization. Pyrotechny or pyrotechnics (also referred to, by some who practice it, as "combustion engineering") is also part of modern practices of these ancient technologies and arts and of currently practiced technologies and arts including those of "firemen" (members of both fire departments and steam locomotive crews), heat-power, automotive, and jet aircraft engineers, (torch) welders, and heating contractors.

As defined in most dictionaries and to most people who use the term, "pyrotechnics" are "fireworks", especially those used in public parks on Fourth of July evenings. Of these, the most spectacular are the skyrockets, which explode at their apogees in luminous "sprays". Such displays were made, in China, several hundred years B.C.(4).

"The rockets' red glare,-" of our national anthem was that of military rockets, used by the British in the 1814 bombardment of Fort McHenry, which, by the way, utilized and verified the capability of rockets of carrying substantial payloads.

In the late 1920s and early 1930s, science fiction often about outer space travel, was popular (notably, with preteen and teen aged boys, which included me at that



time). We read that this interest had been shared, since their boyhood, by some scientists, including Goddard, in U.S.A., and Ley and von Braun, in Germany, all of whom made and tested rockets.

During World War II, when most combatants developed rocket propelled weapons (including the U.S. "bazooka" ammunition), von Braun led the group at Peenemunde, where the German ballistic missiles, including the V-2, were developed. After the war, many of the group were recruited by D.O.D. agencies. Von Braun came to Redstone Arsenal to participate in the U. S. Army's guided missile program, and, when interest in "outer space" was intensified by the success of the Russian "Sputnik" he realized part of his boyhood dream as the leader of the group that put "Explorer I" into orbit (5).

The events mentioned, parts of the sequence which led to the establishment of NASA, have led me to speculate as to whether von Braun or any of his associates or their successors in the space effort thought of the design and development of space vehicle propulsion systems as applications of "pyrotechny" or "pyrotechnics". They do refer to explosives and propellants (which Picatinny Arsenal and the American Defense Preparedness Association include among "energetic materials") as "pyrotechnics".

#### LANGUAGES AND PERSPECTIVES

As the years passed, having participated in conversations, committee meetings, workshops, seminars, symposia, etc., I have come to recognize that each art, profession, specialty, and often working group or family, communicates in its own language, each, in U.K., Canada, U.S., etc, a variant of English, using many of the same words often with different meanings. In recognition of the possibility of having been misunderstood, explanations are apt to conclude with, "See what I mean?", and include efforts to illustrate the meanings of the words by means of metaphors and models, such as working and scale models, sketches, "layout" and "detail" drawings, graphs, chemical formulas and equations, mathematical equations and sets of them, and, in recent years, computer manipulated numerical models, each of which shows the subject, from a different perspective. "Model" as used here indicates "a description or analogy used to help visualize something (as an atom) which cannot" (literally) "be seen" (2). It can serve this purpose if the analogy is to something which can be seen (literally or in the sense that "to see" is "to

understand"). What some refer to as "models" are referred to as "theories" by others.

Each of us sees things from a constantly changing perspective. In each encounter, and when we are reading, or writing, we try to consider each subject from the perspective of the speaker, writer, listener, or reader. Pursuant to this effort, each of us has assumed a succession of perspectives, those of parents, playmates, teachers, professors, lecturers, bosses, commentators, the authors of books and articles we have read and those of the people whose views are conveyed. Thus we have viewed our vicinities, the world, the universe, and much within them from a variety of perspectives, including those which can be categorized as "eyewitness", "common sense", "reasonable", "intuitive", "practical", "rational", "theoretical", references to those credited with proposing them, as "Aristotelian", "Newtonian", "Cartesian", etc., and those of several trades, sports, sciences, etc.

Consideration of any subject begins with the choice of a perspective from which details which we wish to consider are visible and others are obscured. Such choices are called "simplifying assumptions (or approximations)", in which numbers which seem too small to consider are dropped as "infinitesimals of the second order" and numbers too large to think about are equated to infinity (6). Sometimes such simplifying assumptions (or approximations) must be reassessed on the basis of more recent experience or data, which result in the consideration of a subject from another perspective. Such changes of perspective have been essential to the advance of science, and to the education of each individual.

To reiterate, the perspective from which each of us sees things is and has been constantly changing. The "steam" from a teakettle and the melting of ice showed us that water exists in more than one state. (Other observations and experiences showed us that other substances also freeze, melt, boil and condense.). Steam emerging from the teakettle spout was invisible as air, (or, at least transparent), forming a visible cloud a few inches from the end of the spout. Someone may have explained that steam is a gas, like air (and thus, invisible) which, mixing with the cooler air, condensed to liquid water, in droplets too small to settle out, which we saw as a cloud. If they thought we could understand, they may have gone on to say that such suspensions of droplets of liquids or particles of solids, which are too small to settle out of fluids (liquids or gases) in which they are insoluble, are

called "colloidal suspensions" and that, when the fluid is air, they are called "aerosols" and are the "stuff" of clouds, fog, and mist, and (of other compositions) of smoke and smog

#### FIRE, FROM "KID'S" PERSPECTIVES

The earliest impressions of fire, which I can remember, were the sights of the yellow flames of candles on a birthday cake and of trash and wood fires. Fire had been the source of most artificial light until a bit over a century ago. As we (including the earliest human observers) saw the flames spread over the surface of the fuel, it was apparent that the light, which seemed to be the essential property of fire, is "catching", like a cold or the flu. This impression is perpetuated in the usage of "light" for "ignite" and "catch fire" for what the fuel does when lit.

Our perspective changed with the passage of time and the accumulation of experience, and we came to see fire, from a more "practical" perspective, as a source of heat, and it became clear that firelight is a manifestation of the heat of combustion. Some of us had noted that "firelight" is similar, in color to the light emitted by glowing coals or metal or ceramic which was a bit hotter than "red hot". With a little thought, it became apparent that black smoke, is air borne soot which, when hot enough, emits black body radiation, so the yellow flames of candles, oil lamps, and wood and trash fires can be seen as "yellow hot black smoke". Flames of other colors are effects of atomic and molecular emission (whereby elements and compounds are identified in spectroscopic analysis) which occur at elevated temperatures. Although the usage of "light" for ignite persisted in our conversation, we came to recognize that ignition occurred when a fuel element was "hot enough". By this time we had learned to think of heat in the quantitative terms of temperature and it became generally accepted that the temperature at which each fuel started and continued to burn was its "kindling point" or "ignition temperature". The propagation of fire (combustion) is seen by many as the progressive heating of unburned fuel to its "kindling point" by the heat of combustion of the burning fuel. (The title "Fahrenheit 451" (6½) of the novel by Ray Bradbury, and the movie made from it, is derived from the supposition that 451°F is the "kindling point" of paper). However, the episode described below has left me skeptical of this view.

When five or six years old, at a friend's invitation, I joined him in watching his father paint their dining

room wall. He (the father) having painted the wall a light beige, let it dry, was applying a darker brown paint, a few square feet at a time, and, while each patch was "fresh", "blotting" it with crumpled newspaper to expose the lighter paint in a "stippled" pattern. He tossed the paint soaked clumps of paper into a bushel basket. After about an hour, the pile of paint soaked paper in the basket began to smoke and the man grabbed the basket and ran out in the yard before it burst into flame. He managed to drop it so quickly that the only damage to him was some slightly singed hair. A few years later, when a fireman, visiting our school to talk about fire and its prevention, warned of the danger of "spontaneous combustion", I knew, from on scene, eyewitness observation, what he was talking about, from the "practical" perspective of the fire fighter, but didn't see why "spontaneous combustion" could happen if the "ignition temperature" of the paper was as high as it seemed to be.

At the time of the above episode, our family lived in a suburb of Milwaukee. Sunday drives (in the "Model T") often carried us to deserted stretches of Lake Michigan beach, on which there were, often "fireplaces", made by arranging rocks in a circle. My Dad often built fires of driftwood, which was usually available. If suitable vegetation grew nearby, he'd sharpen "green" branches or "shoots" to make "spits" for toasting marshmallows or broiling hot dogs. As we sat around the fire I saw it as the focal point of the family's togetherness".

A few years later, I went with my parents on an automobile trip around Lake Michigan. Most memories of the trip, particularly that of the ferry boat crossing of the Straits of Mackinac, are pleasant, but one, less pleasant but more vivid, is that of mile after mile of "burnt over country" left by the "Peshtigo fire", which, fifty years earlier (on the date, Oct. 20, 1871, of the more notorious though less disastrous Chicago fire.) had devastated 1,280,000 acres, including three-quarters of the shores of Green Bay (7). Even after fifty years, the effects of the fire were quite apparent. I suppose that my parents thought that I had been sufficiently persuaded of the importance of keeping fire under control to trust me, as they did, with the responsibility of burning trash (in a woven wire trash burner) and leaves (in the gutter, as was the practice in our oak shaded neighborhood).

My household duties, as subteen, besides trash burning, raking and burning leaves, and lawn mowing, included tending the coal furnace, which involved shaking out ashes, adjusting the damper when neces-

sary, and shoveling coal, in the course of which I had plenty of opportunity to observe the fire, which was mostly glowing coals, with a few flickering flames. When the fuel was coke, there were no flames nor smoke.

After a few years, as a Boy Scout, I became involved in a discussion of the concept of "kindling points" or "ignition points". In the course of the discussion, I recalled the "spontaneous combustion" episode I'd seen. By that time, of course, I'd forgotten, if I ever knew, the temperature on the day when I'd witnessed spontaneous combustion but guessed that it must have been between 60°F and 90°F and wondered, out loud, whether paint soaked newspaper had a kindling point in that range. The answer was that it didn't but that "self heating" had raised the temperature of the stuff in the bushel basket to its kindling point. It would be more years before I could sort out the distinctions between "self heating", "burning", "fire", and "combustion". (Perhaps I haven't yet, but consideration from various perspectives has helped me to understand those who use these words.).

Based on our earliest impressions of such matters, the aphorism that, "Where there's smoke. there's fire.", seemed to be a "matter of common sense". However, when we saw smoke, but no flames, coming from an overloaded extension cord or from toasting bread or frying bacon that was getting black and said to be "burning", with no flame evident, and that, as fire spread across burning wood, smoke often appeared ahead of the flame, we pondered the questions as to what was meant by such words as "smoke" and "fire" and, specifically, what is the composition of smoke (including the liquid "hickory smoke" and "mesquite smoke" in bottles on grocery store shelves). We'd find answers in considering these questions from an "intermolecular" perspective of fire and fuels.

We may have noticed that, if metal ceramic or anything else that can stand the heat, is heated sufficiently, it gets "red hot" and, if heated more, the red brightens to orange, yellow, and, with further heating, the object becomes "white hot". Although I don't remember hearing the phrase, "yellow hot", it seems an appropriate designation of a condition between "red hot" and "white hot". We may have heard or read that such glow is called "black body radiation", although a red hot poker doesn't look black.

Some of us noticed that, the flames of candles and kerosene or alcohol lamps are yellow, those of a gas

stove are blue (if the burner is "properly" adjusted, but yellow if the air intake is restricted to make a "rich" mixture.

We learned, when quite young, that, although candles and matches could be "blown out", fire, in general, was energized by blowing or "fanning" ("red hot" glowing coals brightened and became "yellow hot"), controlled by "damping the draft" and "smothered" by depriving it of air. It is apparent that the foregoing was known by prehistoric humans. Smelters, foundries, and forges in archeological sites had flues, dampers, and other means of forcing and limiting the supply of air to fires.

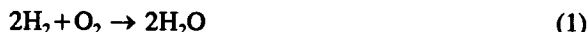
Those of us who are old enough to have had spending money in the 1920s (before the passage of "safe and sane Fourth" ordinances) celebrated the Fourth of July with firecrackers and other fireworks (some, apparently, still do), in the course of which, we learned that gunpowder and other pyrotechnics burn without air (and, in fact, burn faster when confined - "smothered"), which had been known by some alchemists as long ago as the ninth century (4).

"Educational toys" included chemistry sets, which provided amusement, seeing the color changes and foaming resulting from chemical reactions, and, perhaps, the beginning of a "chemical" perspective. While, since "playing with fire" was discouraged, ingredients of gunpowder and similar mixtures were not included in chemistry sets, some of us learned (by reading) what they were and found ways to get some, and set out to make our own fireworks. I joined a fourth grade classmate in the "Universal Research Laboratories" as he called his basement in the preparation of some black gunpowder which we loaded into a home made skyrocket (which flew straight up to about six feet from the ground before it lost stability and tumbled). In the course of these efforts, we viewed chemistry from the "practical" perspective from which it seemed that what had worked for others should work for us (a perspective shared with the Middle Ages alchemists who had practiced pyrotechny since antiquity).

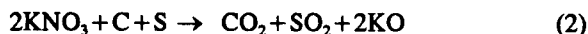
#### A "CHEMICAL" PERSPECTIVE

When, in high school, we were shown a "chemical" perspective, we saw that (as Lavoisier had shown in 1779 (5)) the fire we had seen (from an "eyewitness" perspective) was "oxidation" (combining with the oxygen of air) and that gunpowder and other pyrotechnics burn without air because they are mixtures of

fuels with nitrates, chlorates, or other compounds which decompose when heated releasing oxygen which reacts with the fuels. All of which is expressed in stoichiometric equations, such as:



for the reaction of hydrogen and oxygen, and:



for the burning of black powder of stoichiometric composition.

In stoichiometric equations, as equations (1) and (2), the symbols (H, O, C, K, N, and S) stand for elements (hydrogen, oxygen, carbon, potassium, nitrogen, and sulfur) and the formulas, which are essentially inventories of the proportions of the elements of which each compound (water ( $\text{H}_2\text{O}$ ), carbon dioxide ( $\text{CO}_2$ ), potassium nitrate ( $\text{KNO}_3$ )) are referred to as "empirical" formulas, since they are based on empirical (experimental) data as are valences (upon which predictions are made, of formulas of compounds which have yet to be made) assigned each element. The small integers, which express these proportions, suggested to Proust (in 1799) and corroborate the "law of definite proportions", which suggested (in turn, in 1801, to Dalton) the basis of modern atomic and molecular theories. Atomic theories were proposed, some hundreds of years B.C., by Pythagoras, Democritus, and Lucretius (5,8). The modern theories are based on and supported by empirical data. Some see atoms as portrayed by models. The structural formulas, which are used to represent organic compounds are models (diagrams) of their molecules. Some organic chemists, before trying to make a compound, try to build a scale model of its molecule, in which the atoms are represented by plastic spheres of various sizes and colors. As I understand it, the colors are only for identification of the elements represented but the sizes are scaled (typically 2 or 3 centimeters per angstrom) from the effective sizes of the atoms represented. Similar models (typically, styrofoam balls, joined by tooth-picks (Figure 1) are used for educational purposes.

Figure 1. Educational Models of Molecules (enlarged, from Edmund Scientific Co. catalog)

The perspective induced by such models can be referred to as an "intermolecular" perspective. Fire can be seen from this perspective, in the sense that "to see" is "to understand", only with reference to other perspectives, views from some of which have been mentioned in the foregoing discussion. Consideration from "practical", "empirical", "scholarly", and "theoretical" (including laws of gravity, magnetism, fluid mechanics, thermodynamics, heat transfer, and reaction kinetics is necessary to "see" fire clearly.

## "PRACTICAL" PERSPECTIVES

Based on some of our earliest experiences, such as falling down and dropping things, and observations, such as those of falling objects and the flight of balls, led us to accept the aphorism that "what goes up, must come down.", which I've heard cited (on television) as "the law of gravity". Rubber band (referred to, by some, as "elastic bands" showed us that some things are elastic, that is, when deformed, they tended to recover their previous shape. These and similar experiences and observations gave us, when we were very young, a practical, through rudimentary perspective of gravity and mechanics.

Most of us played with magnets, usually horseshoe shaped steel items, painted red, except at the ends, which picked up nails, pins, etc, to which they came close. If we had two magnets, we found, after a few tries, that they attracted or repelled one another, depending upon which end of one was close to which end of the other. Someone older, probably told us that the ends were called "poles", one "north" and the other "south" and that opposite poles attract, and like poles repel one another. They may have gone on to say that the earth is a giant magnet and the needle of a compass a tiny one, which aligns itself with the earth's magnetic field.

Our earliest impressions of electricity were related to its practical applications. Lights could be turned off and on from across a room or upstairs from downstairs or vice versa, by "closing" or "opening" a switch. Vacuum cleaners, electric fans, and washing machines ran if "plugged in" and "turned on". When we first learned of such possibilities, electricity seemed akin to magic. Play, with electric trains, the small motors which came with Erector sets, and the lighting fixtures associated with them improved our "practical" perspective of electricity. The electricity involved in such play came from transformers, which were "plugged in". We learned, quite early that a direct connection of the - terminals of a transformer made it hum

quite loudly and get warm. We were told to "break" the "short circuit" before it "burned out" the transformer.

Some of us learned that batteries could be used instead of transformers to run electric trains, etc. We all became aware of batteries as parts of flashlights and/or battery operated toys. We found that batteries differed from transformers in three ways;

1. They have "positive" and "negative" terminals, marked "+" and "-".
2. They discharge as they are used and in a short time, when "shorted".
3. They don't hum, even when "shorted" (but do warm).

We were told that the reason for these differences was that the "electrical current" from a battery is "direct current" - "D.C.", which flows, without variation, in the same single direction, while the current from a transformer, and "house current" are "alternating current" - "A.C." which flows, alternately, in opposite directions. Since the direction changes and changes back again sixty times per second, it is called "sixty cycle", or, in recent years, "sixty hertz", current. The reason most "house current" is A.C. is that its voltage can be changed by means of transformers. Most of us had learned, when quite young, that one could get a "shock" from 110 volt "house current", but not from the 5 to 10 volt output of a transformer. Later we learned that the compelling motive for the use of A.C. by utilities was the greater efficiency of transmission at thousands of volts, which would be unsafe as "house current", so the high voltage of the transmission lines is transformed to 110 volts by a transformer near each point of use.

With the passage of time, we acquired some "practical" perspectives of household and automotive electrical systems and the magneto powered ignition systems of outboard motors, chain saws, and lawnmowers, all of which are powered by "internal combustion engines" in which a fuel-air mixture is ignited by "spark plugs" which emit sparks when actuated by electrical pulses from their "ignition systems". To many "spark" became synonymous with "ignition" (a matter to be discussed when we get to "ignition").

In the late 1920s, as a result of the interaction of advancing technology, patent law, and business competition the best radios were home made, so lots of people made their own (which were battery

powered). By the early '30s, the "art" had advanced and "store bought", "plug in" radios replaced the home made battery sets the parts of which became available to teenagers for basement experimentation, from which we gained "practical" perspectives of electronics. One misconception, which was corrected, by the view from the "electronic" perspective was that electrical current flows from positive to negative. We became aware that electrical current is the movement of negatively charged electrons, from negative to positive. We had previously learned, from demonstrations of electrostatic effects (with combs and bits of paper), that like charges (as like magnetic poles) repel one another, and opposite charges attract. We were to learn, later, that these principles apply to chemical reactions, including fire as well as electrolysis.

"Practical" perspectives are acquired, along with "know how", skills, or "arts", by imitation, instruction, and experience. Experience is gained by "trial and error" (referred to, by old time machinists as "cut and try" and, by those who would dignify it, as "Edisonian research"), followed by practice of techniques which were found to be successful. "Practical" perspectives are those from which we (including everyone who has ever lived) consider the application of things and materials to immediate or anticipated purposes. The "practical" motorist is aware that the high compression engine of a "Corvette" will run best on "high octane" gas (which may cause a "Model T" to overheat) but may not have considered, from a "scientific" perspective, the reasons for a high compression engine, nor why "high octane" gasoline does what it does. My impressions of such matters go back to the late twenties, when "Ethyl" and "Benzol" pumps began to appear at gasoline stations and we heard that it was needed for the newer cars (like the recently introduced Chrysler) with "high compression" engines (7 to 1 was considered "high") which would "knock" on "regular" gas". I saw and heard it tried and the "knocks sounded as if something was trying, with a hammer, to beat its way out of the engine. I was told that knock was the result of the "regular" "burning too fast" at high pressures and that the burning could be slowed by adding tetraethyl lead or benzine to make "Ethyls" or "Benzol". Still later, I learned that gasoline was rated for its resistance to "knocking" by means of the "Research Method", which involves the use of an internal combustion engine of adjustable compression ratio, which has been calibrated using mixtures of isooctane (100 octane) and normal heptane (zero octane) (10), I have never had occasion for further consideration of such tests. I have, somehow, gained the impression that "knocking"

of an internal combustion engine has been ascribed to "detonation" of the fuel-air mixture. In this respect, I don't know don't know which of the several meanings of "detonation" was intended, but would guess the definition of Chapman(12) and Jouguet(13), which is reviewed in the later section hereof headed - EXPLOSION AND DETONATION.

Also, in the late 1920s (I was in my early 'teens), I was on a seagull banding expedition (for the National Bird Survey) in northern Lake Michigan aboard a Diesel powered Coast Guard tug (similar to the fishing tugs which were common in the upper lakes at that time). The Diesel engine, as I recall, was about six feet high and ten feet long. Preparatory to starting it, the engineer lit a blow torch over each of the four cylinders. When they were hot enough, he ran the engine as a compressed air motor to "crank it", after which he quickly reset hand operated valves and the engine ran as a Diesel engine. I was told that, in a Diesel engine, the fuel (kerosene - or "coal oil", as some called it then) was ignited by "compression ignition" rather than a spark". My dad and the organizer of the expedition (to whom bird banding was a combination hobby and public service activity) were engineers by profession. One of them explained the "Diesel cycle" to me, about (as remembered after sixty-some years) as follows;

Air, which had been drawn into the cylinder in the intake stroke, is compressed "adiabatically" (my introduction to this word, and to the subject of thermodynamics) which raises its temperature above the ignition temperature of the fuel, which burns as it is injected. (the engine can't "knock" because the fuel can't burn any faster than it is injected into the hot air). The heat of combustion of the fuel raises the temperature and hence the pressure of the air and product gases, which expand adiabatically, imparting more mechanical energy to the system than was used in the compression stroke.

The above explanation, in combination with the rationale that Diesel engines, which have higher compression ratios than gasoline engines, should be more powerful and efficient, besides which, they used cheaper fuel. All of which persuaded me that automobiles should have Diesel engines. Based on this conviction, I enrolled, a few years later (in 1934), - at M.I.T. in Course IXB, "General Engineering" (in which each student could choose courses appropriate for his intended specialty) to specialize in automotive

Diesel engines. After a year or so, recognizing that I was taking the same courses as those in Course II "Mechanical Engineering" whose schedules had been prearranged, so I switched course to avoid the hassle of trying to arrange my own, while others in my classes were doing the same. These moves were motivated by the recognition that practical objectives are most attained by those who understand the principles involved.

This transition, of my perspective, from "practical" to the "scholarly" is one of many I, and, seemingly many others, have made since humans became human.

### "SCHOLARLY" PERSPECTIVES

As the word implies, a "scholarly" perspective was gained in school. That acquired in the lower grades is scholarly" in the sense that, like that of the Medieval "Scholastics", it presented the perspective from which the world was seen a few millennia ago, when the classics, which, often, explained phenomena with reference to such models as anthropomorphic animals (e.g. the tortoise and the hare) and objects (the mountain which talked with the squirrel), supernatural entities such as, fairies, brownies, trolls, gods, and the heroes of Greek, Norse, etc. mythology, were written. From a modern perspective, it is, sometimes, hard to tell where the line was drawn between the metaphorical and the literal. Even in modern discourse, the location of this line is sometimes indefinite. As we progressed in school, the, "scholarly" perspective melded into "classical", "historical", "mathematical" and "scientific" perspectives, which were narrowed to those of specific subjects" or, "academic disciplines", such arithmetic, science, algebra, geometry, chemistry, and physics, and further, to trigonometry, calculus, organic and physical chemistry, applied mechanics, thermodynamics, electrostatics, and vector analysis. As a result we saw fire and other phenomena and things from a succession of perspectives, between which we shifted, often after a few seconds.

"Classical" perspectives included those mentioned above based on mythology and those of Greek philosophers, including Plato, Euclid, Pythagoras, and Aristotle. Euclid's geometry in which the subject is considered from a "logical" perspective, is, in English, still taught. Aristotle viewed physical science from a "logical" perspective in which phenomena are explained in terms of relationships derived from "first principles", which, like the axioms of geometry were considered (on the basis of what some modern

scientists view as "intuition" when they refer to a phenomenon as "counter-intuitive") to be "self evident truths". While the axioms of geometry have stood the test of time, some of Aristotle's "first principles", such as that "heavy objects fall more rapidly than light ones" were discredited by empirical data. Consideration of phenomena from the "empirical" perspective, followed by views from "graphical", "analytical", and "theoretical" perspectives has advanced science since the renaissance. Empirical data are quantitative data, the product of measurements of physical quantities, including time, dimensions, position, force, mass, etc, and functions thereof, such as velocity, acceleration, pressure, energy, and power. Some such measurements (for example, those of astronomers, microscopists, etc.) are made, using instruments, of natural phenomena which are beyond the control of the observers. Others are made in the course of experiments, including the establishment of preconditions and determination of results. By "plotting" such data a "graphical" perspective is gained, the view from which may suggest relationships, which can be expressed in algebraic equations, manipulation of which can yield an "analytical" perspective. Consideration of an object, material, system, or phenomenon from "empirical", "graphical" and/or "analytical" perspectives may lead to the conception of a model or theory, usually, at first "heuristic" but, for purposes of discussion and analytical verification, represented by a diagram, mathematical or chemical formula, equation or set of equations, graph or scale model, which provides another perspective, which can serve as the basis for verification, or at least support, of the theory by prediction of observed or experimental data. Such a sequence has resulted in the advance of each science. However, since the sciences differ with respect to the phenomena and quantities with which they are concerned, each has evolved an unique perspective (each of which is the result of such a sequence).

From "hydraulic" perspectives, water and other liquids are seen as "incompressible fluids" which behave in accordance with Pascal's law, that "Pressure (force per unit area) exerted at any point on confined liquid is transmitted, undiminished, in all directions" (10). The "hydrostatics" perspective is that from which systems in which the effect of flow upon pressure is negligible. so that Pascal's law can be applied without reservation.

Systems and phenomena in which the effect of movement upon pressure is significant are considered from the "hydrodynamic" perspective, from which this

effect is seen to be determined by Bernoulli's principle (which is the law of the conservation of energy stated in terms of pressure, density, and velocity (5,11).

Although, for liquids, the assumption of incompressibility is a reasonable approximation (in fact, when the empirical data, upon which the principles of hydraulics and hydrodynamics were based, were obtained, the available instruments were sufficiently precise to determine the compressibility of liquids, the compressibility of gases was apparent to Hero in the first century (5) and must be taken into account in considering their behavior. The behavior of gases is considered from a "thermodynamic" perspective in terms of the "gas laws", which relate pressure, specific volume, and temperature.

Liquids and gases are seen, from "hydraulic", "hydrodynamic", and "thermodynamic" perspectives (as they are from "eyewitness", "common sense", "intuitive" "practical" and "empirical" perspectives) as continuous media (thus legitimizing the application of algebra, calculus, and differential equations in the generation of theory from empirical data. In contrast, from the "intermolecular" perspective, which is mentioned a few pages back, a gas is seen as a "swarm" of atoms and molecules, moving in random directions at random velocities, and bouncing, elastically, from one another ("like tiny billiard balls" as Mach, scornfully, put it) when they collided. as envisioned by Maxwell and Boltzmann, who considered this motion in terms of statistical mechanics, assuming what has become known as the "Boltzmann factor",  $\exp(-E/RT)$ , for the statistical distribution of kinetic energy,  $E$ , among the molecules and atoms of a volume of gas, at absolute temperature,  $T$ , where  $R$  is the "gas constant" for the mechanical equivalent of heat. The result of their consideration (in 1871) from this "intermolecular perspective has become known as "The Maxwell-Boltzmann kinetic theory of gases", that heat is molecular motion and pressure is the aggregate effect of impacts of many (if the order of Avogadro's number ( $6.026 \times 10^{23}$ ) times the "Boltzmann factor") molecules on a surface. That the "gas laws", which had been established in the previous century, on the basis of experimental data, by Boyle and Charles, can be derived from the kinetic theory of gases has validated the theory.

As Mach's remark, alluded to in the preceding paragraph, implies, heat is viewed from more than one perspective. Some, apparently including Mach, view it as a fluid (as it seem to be from casual observation as well as carefully controlled "heat flow" experi-

ments). Even today, though heat is generally seen as "molecular motion", the phrase "heat flow" is common. Although the Maxwell-Boltzmann kinetic theory of gases, when generally accepted, established the view that heat is molecular motion, I'm not sure that Maxwell or Boltzmann considered the motion to include rotation and/or vibration.

Watt's invention of the steam engine (in 1769) and its widespread application motivated the development of the thermodynamics of steam, in the course of which it became evident that, although the "gas laws" apply to "superheated steam", they don't to "wet steam", so that "steam tables" and "Mollier charts" were needed for quantitative prediction of operating characteristics of steam engines. Van der Waals considering such "two phase" systems from the "intermolecular" perspective of Maxwell and Boltzmann, assuming finite sizes of (and attractions between) molecules derived the "equation of state", which is known by his name, in 1873.

Chemistry, considered from the "empirical" perspective, had suggested and corroborated the "law of definite proportions" which, in turn, suggested the atomic and molecular theories. Faraday, viewing electrolysis from an "empirical" perspective, established his "laws of electrolysis", which introduced the concepts of "equivalent weight" and valence. in 1832 (5). (He also favored the proposition that electric current is composed of particles (something that Franklin had suggested nearly a century earlier (incorrectly assuming the particles to have what he designated, and is still referred to as a "positive" charge) and would be verified, in the 1890s, by Arrhenius and Thomson, who corrected Franklin's error) (5).

"Equivalent weights" as measured by Faraday's methods, are ratios of atomic weights or valences. By 1860, the lack of consensus regarding the means of separating atomic weight from valence had chemistry in a state of controversy and confusion which motivated the convening of the First International Chemical Congress, in which these matters were resolved. By the late 1860s, atomic weights and valences of all elements known at the time had been determined. When Mendeleev tabulated the elements in order of atomic weights, and entered valences in the table, he noted a periodicity of the valences. and in 1871, he published the, now ubiquitous, Periodic Table of the Elements.

As pointed out and illustrated herein, perhaps too often, each of us sees things, substances, systems, and phenomena from a sequence of constantly changing perspectives, and the sequences are individual. In my case, the perspectives alluded to in the foregoing were gained by observation, experience, study in school, and recreational reading. I don't remember the exact sequence, but it seems that before I acquired an "intermolecular" perspective (in fact, before the styrofoam used to make the models shown in Figure (1) was invented) I had read a book (9) which induced an "intra-atomic" perspective, from which I saw an atom as a "nucleus" of closely packed protons and neutrons, surrounded (as the sun is by planets) by electrons.

#### AN "INTRA-ATOMIC" PERSPECTIVE

Each electrostatically positive proton attracts an electrostatically negative electron, so the electrons, which don't fall into the nucleus (as the planets don't fall into the sun) because they are moving too fast. Thus, the electrons orbit about the nucleus as the planets do about the sun. The analogy of an atom to the solar system is flawed by the difference between gravity, which attracts all heavenly bodies to one another and the electrostatic forces, which attract electrons to protons but repel them from one another. The orbital patterns of electrons are determined by the interaction of these forces and the laws of motion established by Newton's demonstration that they can be invoked as the basis of the derivation of Kepler's (empirical) laws of planetary motion (as well as the principles of relativity, and wave and quantum mechanics postulated, formulated and demonstrated in the early 20th century, by Einstein, Planck, Bohr, Pauli, Heisenberg, and others (8)), of which my understanding was (and still is) too vague to include in the model upon which my "intra-atomic" perspective was based). In this model, the equilibrium positions of the electrons, as determined by their attraction to the nucleus and their repulsion of each other is attained when they are spaced in an orbit where the attraction of the electrons to the nucleus is balanced by their repulsion of each other (plus the centrifugal force due to their motion in that spherical surface). Two electrons can occupy such an orbit, from which additional electrons are excluded in accordance with the Pauli exclusion principle. (that only two electrons (with opposite "spins") can occupy any given "quantum state") (8). It seemed that, in the language of atomic physics, the term "orbit" meant the spherical surface (referred to, by some (5)(8) as a "shell") where these forces are in equilibrium such that the



attraction of the electrons to the nucleus balanced their repulsion of one another plus the centrifugal force due to their motion in this spherical surface and the effect of the Pauli exclusion principle etc. Electrons which are excluded from this inner orbit locate in surrounding orbits, which are larger because the net attractive force of the nucleus has been diminished by the repulsive force of the electrons in the inner orbit, so there is room for eight electrons to attain equilibrium positions in compliance with the Pauli exclusion principle. A third orbit has room for eight electrons, while the fourth and fifth orbits contain eighteen electrons each and the sixth has room for thirty-two. A seventh orbit, presumably could contain thirty-two, if and when elements that heavy are discovered.

The foregoing is a description of the heuristic model of an atom, which I remember, after sixty years as the basis of the intra-atomic perspective got from reading "Inside the Atom", by Langdon-Davies (9), as well as high school courses I had completed in chemistry, physics, and solid geometry. In my reconstruction of the model, I was helped by the copy of the book (9), which I got for Christmas in 1933 and still have, as well as more recent publications, including periodicals and references (5), (8), and (10), by university courses in chemistry, physics, mechanics, thermodynamics, physical chemistry, fluid mechanics, etc and from conversations with and lectures by scientists, including Gamow, Eyring, and Kistiakowski, all of which may have "edited" my memory of some details. It is apparent, from "browsing" through references (5) and (8), that the model described above is an approximation of that which is sometimes referred to as "the Bohr Atom", which is the result of the work, guided by Niels Bohr at the Bohr Institute, by an international group of physicists, including Heisenberg, Pauli, Gamow, Fermi, and Oppenheimer who considered their work in progress, from perspectives of earlier contributors to science, including Pythagoras, Dalton, Avogadro, Mendeleev, Thomson, Maxwell, Boltzmann, Van der Waals, Rutherford, Planck, and Einstein, to mention a few (8). As a high school senior, I saw the model, as one sees a ship on a foggy night (only by its running lights), befogged as it is by relativity (which equates matter to energy) and wave and quantum mechanics (which consider light and electrons, seemingly alternately, as waves, particles, vibrations, and/or orbits(8)) and my present view is still quite misty. The model described above, however, has clarified, somewhat, my view of chemistry, electronics, and thermodynamics.

## AN "INTERATOMIC" PERSPECTIVE

The electrostatically negative field of a "saturated" (filled) electron orbit or "shell", in combination with the Pauli principle, results in a repulsion of electrons or other electron "shells" which increases with proximity so abruptly that (for atoms of so called "monatomic", "noble", or "inert" gases (helium, neon, argon, krypton, xenon, and radon) all of whose electron orbits are saturated), Mach's reference to the molecules (which include atoms of monatomic gases) in accordance with the Maxwell-Boltzmann kinetic theory of gases as that of "tiny billiard balls" can be considered an accurate analogy.

Of the hundred plus known elements, only the six inert gases mentioned above have saturated outer electron orbits. Atoms with unsaturated outer orbits join in groups in which the electrons of the unsaturated outer shells (orbits) are shared. The most familiar grouping (from a "chemicals" perspective) is in molecules, where atoms with relatively few electrons in their outer shells (metals, such as sodium, which has one) combine with those with nearly saturated outer orbits (nonmetals, like halogens, including chlorine, whose outer orbits lack one electron each of saturation, in which all orbits are saturated, such as that of sodium chloride (NaCl table salt).

The electrons of the unsaturated outer electron orbits are referred to as "valence electrons" because their numbers correspond with the valences of the elements to which they apply.

As mentioned a few pages back, Faraday had introduced the concept of valence in 1832, and Mendeleev had published his Periodic Table in 1871. The "Bohr atomic model", roughly described above, was conceived, in part, as an explanation of the empirical evidence of the periodicity indicated in Mendeleev's table.

The "valence electrons" of two or more atoms are drawn into saturated orbits by some of the forces whose equilibrium determines the numbers of electrons in the saturated orbits (or "shells") while the electrostatic equilibrium between the protons and electrons of each atom hold it together. Thus molecules are formed in which atoms are so grouped that they can share electrons to saturate all orbits while the electrostatic equilibrium of each atom is maintained. Such combinations of forces, which hold molecules together, are called molecular bonds. Figure 1 shows models of such molecules, of which the

"billiard balls" are a less accurate analogy than they are of the on atomic molecules of "inert" gases in that they are assemblies of spheres rather than separate balls, so that their movement, involving significant fractions of their kinetic energy ("heat") includes that of rotation and vibration. While models, such as those shown in Figure 1, are usually scale models they cannot be viewed as "working" models, because the "atoms" are rigidly joined, while the real atoms of real molecules assume equilibrium relative positions (determined electrostatic, electromagnetic, and other forces involved in the for saturation of atomic electron orbits) about which they vibrate or orbit (orbiting is, essentially, vibration in two or three dimensions.) Consideration of heat as molecular motion, from this perspective has led to the distinction between "rotational", "vibrational", and "translational" heat, which accounts for the differences between gases with respect to ratios ( $k = C_p/C_v$ ) of specific heat at constant pressure ( $C_p$ ) to that at constant volume ( $C_v$ ).

Molecules are groups of atoms held together by the combination of the quantum mechanical forces which establish conditions for saturation of atomic electron orbits end the electrostatic equilibrium which results in the equality, in each atom, between the number of positive protons in the nucleus and the total number of electrons which orbit about it. The repulsion of "saturated" orbits for additional electrons (including those in other "saturated" orbits) increases so sharply with proximity that the comparison to "tiny billiard balls (or golf, tennis, ping-pong, or basket balls) is an accurate analogy of the bounce of colliding molecules, atoms, or groups of atoms, including "ions" (atoms or groups of atoms of which all electron orbits are saturated). The forces which hold the electrons in orbit, and thus maintain saturation, combine with the electrostatic force which maintains the equality between the nuclear protons and orbiting electrons of each atom to result in attraction which, like gravity, is relatively constant close in and, varies inversely as a function of greater separation so that that which is referred to as "vibrational heat" is alternate collision and separation of atoms and groups of atoms, including "ions" (atoms with outer orbits saturated by the transfer of electrons, which leaves each ion with an electrical charge). Those with more electrons in orbit than protons in their nuclei have negative charges and those with less have positive charges. The attraction between the atoms and groups of atoms (including ions) of a molecule (in the gaseous state), like the gravitational field of a planet, varies so little "close in" that it can be viewed as constant and varies as an inverse function of greater distances, while their

repulsion of one another increases with proximity, as sharply as that of elastic solid objects. Thus, the motion of those components of molecules associated with "vibrational heat" is more analogous to that of bouncing balls than to that of vibrating piano strings.

## AN "INTERMOLECULAR" PERSPECTIVE

The specific heat of a gas is the quantity of energy associated with a one degree increase in the temperature, of a unit quantity of the gas. Considered from the Maxwell-Boltzmann intermolecular perspective, heat is the kinetic energy of molecular motion. At constant volume, the energy required to heat a given quantity of gas one degree is only the sum of the corresponding "translational", "vibrational", and "rotational" motion of the molecules, while, at constant pressure, the energy involved in the expansion is added. Since only translational heat is involved in expansion, where vibrational and rotational heat are significant fractions of specific heat, ratios of specific heat at constant pressure to specific heat at constant volume are reduced.

From the perspective of the Maxwell-Boltzmann kinetic theory of gases, only the mutual repulsion of molecules, atoms, and ions (at very close proximity), (which result in effectively elastic rebound from collisions, like those of "tiny billiard balls") are discernible. As mentioned, the empirically established gas laws of Boyle and Charles can be derived from the theory. However, from the "interatomic" perspective discussed in the previous section hereof, molecules, except for those of inert gases, are more complex than balls. A more accurate analogy would be an assemblages of balls as represented by the models shown in Figure 1, except that they are not rigidly connected, but vibrate about equilibrium relative positions, since molecules, atoms, and ions are attracted to and repelled from one another by forces (mostly electrostatic and magnetic) which vary with their degrees of proximity, relative positions, and orientations. From this perspective, it is apparent that the kinetic theory of gases, including the "Boltzmann factor", applies to "vibrational" and "rotational" as well as "translational" heat.

## NOTES ON THERMODYNAMICS

Carnot "founded" (5) the science of thermodynamics with his book, a partial title of which is "On the Motive Power of Fire", in which he cited empirical data showing that, in expansion of a gas, heat is transformed into "work" and conversely, in

compression, "work" is transformed into heat, a half century before Maxwell and Boltzmann presented their kinetic theory of gases (which includes the postulate that that which is sensed and measured as pressure of a gas is the integrated effect of impact of molecules upon the surface). If, as implied by the "tiny billiard ball" analogy, the molecular motion, which the kinetic theory of gases equates to heat, was only translational, thermodynamics would be much simpler since the interchange between heat and work would be complete and direct in all adiabatic processes.

Carnot "founded" the science of thermodynamics to provide a rational approach to the design of steam engines for maximum efficiency (conversion of as much of available heat as possible into work). He and such successors as Rankine and Joule developed and verified thermodynamic theory which is still in use, with reference to empirical data, and included the "gas laws" of Boyle and Charles, which were also based on empirical data, before Maxwell and Boltzmann proposed the kinetic theory of gases and, of course, before that theory had been elaborated to include consideration of vibration and rotation of molecules.

#### "STATES" OF MATTER (THE VAN DER WAALS' EQUATION OF STATE)

Thermodynamics, as noted above, is concerned, from a practical perspective, with transitions of "heat" to "work" and vice versa. In its rudimentary form, such consideration involves the "gas laws", which, though originally based on empirical data, can be derived from the "kinetic theory of gases". However, as each of us has "always known", the gaseous state is only one of several in which matter exists. The first application of thermodynamics was to steam, which is the gaseous phase of water, which, when cold enough, freezes into ice.

The "gas laws" of Boyle and Charles, for purposes of "engineering thermodynamics" are usually combined in the "ideal gas equation":

$$PV = nRT \quad (3)$$

where:

P is pressure,  
V is specific volume,  
n is the quantity (gram moles) of gas,  
R is the "gas constant", and  
T is the absolute temperature.

Although "live" or "dry" steam behaves as an "ideal gas", at lower temperatures and higher pressures,

steam condenses to liquid water and the "gas laws" cease to apply.

Van der Waals accounted for this changed behavior with the change from the gaseous to the liquid state in terms of the Maxwell-Boltzmann "kinetic theory of gases" by assuming an attraction (a) between, and a finite volume (b) of molecules, to derive (in 1873 (5)) his "equation of state":

$$(P + a/V^3)(V - b) = nRT \quad (4)$$

as given in Ref. (11).

Considered from the intermolecular perspective, the van der Waals equation of state implies that, as two molecules approach one another they are mutually attracted by a force which varies inversely with their separation until they collide and bounce apart "like tiny billiard balls". After bouncing apart, each molecule flies until it bounces off another. If the temperature T, is above the "boiling point", the molecules behave in accordance with Maxwell-Boltzmann "kinetic theory of gases" and, of course, as an "ideal gas" in accordance with the "gas laws". At lower temperatures, their kinetic energy is insufficient for each molecule to escape the attraction of its neighbors before it is bounced back by collision with a molecule of the gas. This effect, at liquid gas interfaces, is known as "surface tension".

As it seems from casual observation and all but the most precise empirical data, water (as well as other liquids) is considered in hydraulics and hydrodynamics to be of constant density. Although more precise data have shown water and other liquids to have finite compressibilities and thermal expansion coefficients, the fact that they are considered to be negligible in most practical applications is evidence that the amplitude of the molecular motion, apparent as "heat", is small compared with the gross linear dimensions of the molecules, so that it can be considered "vibrational heat" like that of the relative movement of atoms, ions, and other groups of atoms within molecules as discussed above.

Considered from a closer perspective, the analogy of molecules to "billiard balls" is seen to be a simplifying approximation which applies to gases and liquids at temperatures high enough that the amplitudes of the vibrations of "vibrational heat" are large compared with the deviations from spherical symmetry of the molecules. At lower temperatures, the weaker vibrations (which are still random) result in repeated

"trials" (reorientations) until adjacent molecules "fit together" and move closer, with a resulting increase in their mutual attraction (the "van der Waals force"), which, along with their asymmetry, maintains their relative positions and orientations. This is the process we observe as "freezing", "solidification", or "crystallization".

Each of us has been aware since early childhood that water boils and freezes, and as our vocabularies increased we learned that "water", "ice", and "steam" are three "phases" or "states" of the same substance. With the passage of time, we found out that most other substances also can exist in "gaseous", "liquid" and "solid" states.

Our earliest memories (not quite earliest for those in my age group) include the sight of "neon signs" glowing on store fronts, billboards, etc. Later, we heard or read that the neon lights were tubes filled with rarified gases, (neon, in the originals, which glow red). Other gases glow in other colors, but they are all called "neon signs" which glowed when "ionized" by the flow through them of electric current. In this context, we learned, as we became more sophisticated, that "ionization" meant the separation of electrons from atoms (or the ions of molecules from one another), after which, in an electrical field, the electrons (and negative ions) are attracted to the "anode" (positive electrode), and the positive ions (atoms or groups of atoms with electrons missing) are propelled toward the cathode (negative electrode). If the electrical field is sufficiently strong, and the free paths are long enough, the ionization is maintained by collisions, which "knock" more electrons free as others enter atomic orbits with resulting luminosity. Gases are also ionized by temperatures high enough that the "vibrational heat" is sufficient to overcome the attraction between their ions and collisions between molecules "knock them apart". Ionized gas is referred to as "plasma", and as a "fourth state of matter"(9).

Plasma glows. Its light emission can be seen, from the "intra-atomic" perspective, to result from the falling of electrons into orbit. The color, wave length, or spectral characteristics of the light are unique for each element, and are used in spectroscopic analysis, to identify them. The familiar blue flame of a gas stove results from such luminosity of plasma of which carbon and oxygen are principal constituents, and the red light of a railroad "fuzee" is the spectral emission of strontium,

Van der Waals (in 1873) considered the relationship between temperature, pressure, and specific volume of substances close to their "boiling points" from the perspective of the recently (1871) presented Maxwell-Boltzmann "kinetic theory of gases", assuming a finite size of each molecule and an attraction between similar atoms and molecules which became known as the "van der Waals force". A half century or more later, from the intra-atomic perspective of the "Bohr atom", the "van der Waals force" was seen to be "caused by a temporary change in dipole moment arising from a brief shift of orbital electrons from one side to another of adjacent atoms or molecules" (16).

The van der Waals equation of state was derived as a basis for thermodynamic analysis of systems involving "wet steam" in which water is present in both gaseous and liquid states. The "van der Waals force" is also, as discussed a few paragraphs back a factor in crystallization, the transition from the liquid to the solid state. However although it plays a role, the "van der Waals force" is not all that holds crystals together. Other forces, visible from the "interatomic" and similarly close perspectives, contribute. Thus though, as would be expected (based on the description of crystallization a page back, in which the "van der Waals force" was invoked), most substances "shrink" when they solidify, water does not. My impressions, from "intra-atomic", "inter-atomic" and "intermolecular" perspectives are too "fuzzy" to include as a logically cohesive part of this paper, but a few seem sufficiently relevant to mention. Some molecules, particularly those of a number of "organic" compounds, are so large and/or complex that they exist only in the solid state. They "decompose" (break into smaller molecules) at rates dependent on temperature and the "reaction kinetic" properties of the substance. Conversely some compounds which are liquid at "room temperature", "polymerize" (their molecules join to form larger ones, which exist only in the solid state) when heated or "catalyzed" and they solidify.

Crystalline and chemical bonds are similar in that they are effects of and governed by forces and principles discernible from "intra-atomic", "inter-atomic", and "inter-molecular" view-points and that, from the empirical perspective, they are "exothermal" (evolve heat) (because solidification prevents translational and rotational movement of atoms and molecules so that all thermal energy becomes "vibrational heat", which is "sensible").

Purity is a relative term. The word "pure" is often (in some contexts, usually) preceded by a percentage. "100% pure" is not quite credible. So, all substances are mixtures. Each solid and liquid has a finite vapor pressure (or gaseous decomposition product) and thus an odor, which may not be apparent to most humans, but is to many animals and can be detected by means of spectroscopy. Similarly, gases and solids are soluble in liquids and gases and liquids are absorbed or adsorbed by solids. The distinction between the states of matter is, thus, based on practical and empirical considerations.

Many familiar substances, including wood, whipped cream, mud, smoke, mashed potatoes, glue, wet-cement, and shaving cream are composed of matter in more than one state and owe their characteristic properties to interactions of their components in two or more states. The properties of such mixtures depend, to some extent, upon the "state of aggregation" (the size, shape (often fibrous), hardness, frictional properties, and distribution of solid components, and the sizes and distribution of droplets, bubbles, and pores, and, where such mixtures seem solid, from the "empirical" perspective, upon the structure of the substance, including the bonds (molecular, crystalline, and other) between the components, as well as their distribution.

Matter, in its various states, has been viewed from "practical" and "empirical" perspectives. With a view to prediction of the behavior of systems, empirical data are plotted, and the indicated relationships are expressed in algebraic equations, which, when used in analysis with calculus or differential equations, are assumed to apply to infinitesimal intervals, an assumption whose validity, is questionable when considered from the "intermolecular" or other theoretical perspectives which have been discussed herein, but have been essential to the advance in the states of the arts to which they apply, and, where the principles of logic and mathematics have been applied to the satisfaction of the scientific community, have come to be accepted as "rigorous theory".

Although the van der Waals equation of state (equation (4)) relates pressure (P), specific volume (V), and absolute temperature (T) for substances under conditions where both gaseous and liquid states exist, the phrase "equation of state" seems to have acquired the more general meaning of any equation relating specific volume to pressure, such as that for adiabatic compression or expansion of an gas";

$$PV^\gamma = \text{a constant} \quad (5)$$

which has been referred to as the "gamma ( $\gamma$ ) law equation of state", which is considered to be one of the "ideal gas laws" derived from the empirically established laws of Boyle and Charles, which can be derived from the Maxwell-Boltzmann "kinetic theory of gases"(17) The "wet steam", to which the van der Waals equation of state was first applied, is a "colloidal suspension" of liquid water in gaseous steam. As has been mentioned, "colloidal suspensions" consist of droplets or particles of liquids or solids which are too tiny to settle out from the fluid in which they are suspended. Qualitatively, their failure to settle out can be ascribed to their bombardment from all directions by molecules close to their size and (in the case of "wet steam") of a similar density. A quantitative explanation is beyond the scope of this paper. However, the observation, in 1827, by Brown, of what came to be known as "Brownian motion" of colloiddally suspended cells and particles, was explained on these bases (in 1871) by the Maxwell-Boltzmann "kinetic theory of gases" and elucidated by the concept of "Maxwell's demons" (5).

It is my impression that the phrase "equation of state" was first used to identify the relations between pressure (P), temperature (T), and specific volume (V) of "wet steam", a colloidal suspension of liquid water in gaseous steam. In the "gamma equation of state" in its original application, to "ideal gases", the effect of temperature is taken into account by the use of "gamma" the ratio of specific heat at constant pressure to that at constant volume ( $= C_p/C_v$ ).

For hydrodynamic consideration of the behavior of substances in other states or "states of aggregation", experimentally determined relationships of specific volume (V) to pressure (P), referred to as "equations of state" (often "gamma law" equations of state" with empirically determined values of gamma) are used.

From the practical perspective of the designer of hydraulic systems, water and other liquids are seen as incompressible fluids. However, in consideration of large or sudden changes of pressure (particularly, those of detonation and the strong shock waves it induces), their compressibility must be taken into account (11).

To some, the mention of detonation in the above paragraph may seem to be a change of subject from that of "fire" indicated in the title hereof. It's not, because detonation is a form of combustion as will be pointed out in the section hereof headed - EXPLOSION AND DETONATION. However, it may

be somewhat premature at this point, so further discussion is postponed until we get to it there.

The subject of detonation came up at this point because consideration of detonation from a theoretical perspective involves relationships between pressure and specific volume which, as mentioned above, have come to be known as "equations of state", even for porous solids, where materials in more than one state are present. For such materials, a more appropriate term for the pressure/volume relationship might be "equation of state of aggregation" (which doesn't "roll off the tongue like "equation of state")

Fire, usually, involves changes of state. Yellow flames of candles and wood and trash fires are glowing black smoke (a colloidal suspension of carbon particles (soot), the result of evaporation and condensation of the fuel or volatile components or decomposition products thereof and the subsequent decomposition of this colloiddally suspended condensate to carbon and gaseous products whose oxidation provides the heat which sustains the process. Such fires involve transitions from solid to liquid to gaseous states, followed by reversals to the liquid state (in a colloidal state of aggregation), and finally back to the gaseous state before the oxidation takes place.. The familiar blue flame light of a gas stove flame is spectral emission of the plasma to which the gaseous products of combustion have changed. Glowing coals glow due to the oxidation of solid carbon to gaseous carbon dioxide.

That changes of state occur at specific temperatures was common knowledge long before quantitative scales of temperature were proposed. Both Fahrenheit and Celsius established their "degrees" as fractions (1/180th by Fahrenheit, and 1/100th by Celsius) of the difference between the freezing and boiling points of water. The scales having been established, and instruments for measuring temperature having become available, determinations were made of freezing and melting points of other substances. Since it was known that fuels started to burn when heated sufficiently, it seemed reasonable to determine the "ignition point" or "kindling point" (the lowest temperature at which a substance will continue to burn without addition of external heat (16)) of each of various substances. For most fuels, which require air, oxygen, or some other oxidant for combustion, such determinations present experimental difficulties. Pressure had been found to affect freezing and boiling points and, it was suspected, might affect kindling points. Where the fuel was solid and the oxidant gaseous, the temperature and

fiber stress of the fuel and the temperature and pressure of the oxidant could interact to affect ignition. These experimental difficulties seem to have resulted in such skepticism on the part of their editors regarding "ignition points" that none of the standard handbooks (10,11,17) at hand as I write this, includes such data. These difficulties are alleviated for substances or mixtures which contain or include oxygen or another oxidant or which react "exothermally", (with the evolution of heat). Thus the Smithsonian Physical Tables (18) include tables of ignition temperatures of gaseous and dust mixtures with atmospheric air of several fuels and several publications (4, 19, 20, 21) include "ignition points" or "explosion temperatures" of pyrotechnics and explosives.

Although my doubts regarding the concept of an "ignition point" as a physical property of each fuel dated from my childhood observation of "spontaneous combustion", the general concept by those with whom I discussed such matters, (and apparently others (6½)) combined with my practical experience with "lighting" fires persuaded me of its general validity. I visualized, the propagation of fire as the progressive heating of the fuel, by the heat of combustion, to its "ignition point".

"Fire", the subject of this paper, has been defined (2) as "The visible heat and light emanating from any body during the process of its combustion or burning." As has been pointed out, or at least implied, in the foregoing, heat and light are forms of energy, of which my changing perspectives are discussed in the following.

## CHANGING PERSPECTIVES OF ENERGY

As mentioned before, herein, each of us sees things from a constantly changing series of perspectives. The following account of the succession of my perspectives of energy is included in the belief that it roughly parallels that of most who may read this, as well as those who have considered such matters in the past and whose views have been alluded to.

My earliest impression of energy was that of a busy person who could stay busy all day. This perspective, which seems to be that of the fitness program participant who reported "having more energy" as a result of a low calory diet and an exercise program (which seems contradictory from perspectives I have gained more recently.)

As seen from this earliest perspective, play required energy. The experiences which came with play, coasting down hill, bouncing balls, etc., lent reality to views of energy from perspectives to be gained in school and elsewhere.

Work, like lawn mowing, also took energy, and after such work, I had less energy left for other activities. After school work, on the other hand, I had more energy for play.

In ninth grade "General Science", I began to acquire "physical" perspectives of energy. "Work" was defined as a form of energy equal to force times distance, which was transformed to other forms of energy as it was accomplished. For example, the work of lifting a pound weight a foot was transformed to one "foot-pound" of "potential energy". If the weight is dropped, the potential energy is transformed to "kinetic energy".

My science teach, aware that we were also taking algebra, taught us equations for work (W):

$$W = Fx$$

where F is force and x is distance,

potential energy (PE):

$$PE = mhg = wh \quad (6)$$

where m is mass, w = mg is weight, h is height, and g is the acceleration of gravity,

and kinetic energy (KE):

$$KE = mv^2 \quad (7)$$

where v is velocity.

Since we were familiar with the English system of units, he told us that work (w) was measured in foot-pounds, force (F) in pounds, distance (x) in feet, mass (m) in "slugs" (a mass of one slug weighs 32 pounds) and velocity (v) in feet per second. Thus, I began to see things, including energy, from "analytical" and "mechanical" perspectives.

He told us that, as a weight falls, the sum of its potential energy and kinetic energy remains constant in accordance with the "law of the conservation of energy". He demonstrated the conservation of energy with a pendulum, which continued to swing, alternately transforming potential energy to kinetic energy and kinetic energy to potential energy. He explained the reduction of the swing as the result of

friction, which, he said, transformed the kinetic energy to heat, which, he said, is another form of energy.

As its name implies, "General Science" includes many subjects, including those mentioned above and heat, chemistry, electricity, waves, (gravity (on water surfaces), elastic (including sound), and electromagnetic - radio, light, etc.), radiation (usually electromagnetic waves, but sometimes streams of such particles as electrons, protons, etc.). Each of these subjects deals with one or another form of energy and/or transformations of one form of energy to another. The conservation of energy was shown (from perspectives assumed to be familiar to ninth graders) to apply to all transformations from one form to another.

Play, experience, conversation, observation, and recreational reading extended the range of my perspectives, some of which have been discussed herein before. Some early impressions, like that (from an Aristotelian perspective) that heavy objects fall faster than light ones, were corrected in the above mentioned "General Science" course. It was explained that air friction slows light objects more than it does heavy ones. Similarly a sled, coaster wagon, or bicycle is slowed less by friction on a steep hill than on a gentle slope, so it goes faster. If it weren't for friction, the speed, after a given change in elevation would be unaffected by the slope, since all of the potential energy would have been transformed to kinetic energy.

As I advanced through high school, geometry (both plane and solid), trigonometry, and advanced algebra provided "graphical" and "analytical" perspectives, and chemistry and physics provided "scientific" perspectives, from which I could reexamine impressions gained, since early childhood, from such previously mentioned perspectives as "eyewitness", "common sense", "intuitive", and "practical".

The combination and interaction of experience, observation, and education persuaded me that work, heat, light, and sound are forms of energy and such forces as those of gravity, and magnetic and electrostatic "attractions of opposites" are factors of energy, as are time and distance, and that, in any isolated system, the total energy remains constant (which is "the law of the conservation of energy")

The freshman physics course, which was required for all M.I.T. students, in which the notation of calculus (also required) was used to express Newton's laws of

motion and gravity, and to derive from them equations of motion of falling bodies, basic principles of ballistics, and the equations of orbital motion of the planets, as Newton had nearly 300 years before, showing that Kepler's Laws, which were generalizations of Brahe's observations, were empirical verification of his laws of motion and gravity.

The lecturer of the course Nathaniel H. Frank, who was also the author of the textbook "Introduction to Mechanics and Heat" (22), used in the course, which included consideration of the language of physics and unit systems (metric and English), kinematics (both linear and plane - introducing the concept of vectors), kinetics, and statics of mass points and particles (including Newton's laws of motion and gravity - planetary motion is considered from Copernicus' and Kepler's extra orbital perspective, from which the planets are seen as mass points), linear and plane dynamics, work and energy, potential energy, hydrostatics, elasticity, acoustics, heat conduction, thermodynamics, the first law of which is the conservation of energy, which it shows to be applicable in gases to adiabatic systems (from which no heat is lost), as well as to reversible mechanical processes (as distinguished from irreversible processes such as frictional heating). The text discusses "entropy" (S), a term coined by Clausius (5) for the ratio ( $S=Q/T$ ) of the heat content (Q) of a system to its absolute temperature (T), which was shown to be a measure of the unavailability of the heat for transformation to work, and quotes Clausius statement of the first and second laws of thermodynamics in closing, - "The energy of the universe remains constant. The entropy is always increasing." Recently, in retrospect, I have wondered how I reconciled this statement with my impression, from the "cosmic" perspective gained in recreational reading, that the sun and other stars had been radiating energy for billions of years. Perhaps Frank had cited Einstein's "Special Theory of Relativity", which holds that mass (M) is a form of energy (E) which is expressed in:

$$E = Mc^2 \quad (8)$$

where c is the speed of light.

I do remember having read, a few years earlier, that the energy radiated by stars was the product of reactions of atomic nuclei and that there was enough energy in a glass of water to propel an ocean liner across the Atlantic, which had led me to envision a device capable of transforming nuclear energy into work, which would fit into the rear hub of a bicycle

(like a coaster brake). I had no idea as to how this might be accomplished, but thought it would be nice to have one installed in my bike. My freshman year was 1934-'35. A decade later, the conversion of nuclear to other forms of energy (on a much larger scale) was an important factor in the conclusion of World War II. I still have no idea as to how it might be applied to bicycle (or even automobile) propulsion, but it is now used to propel submarines and generate electric power, some of which has been used to charge the batteries of electrically propelled cars. However, in the 1930s, nuclear energy was considered to be the "stuff of science fiction" (like space travel) and engineering courses were concerned with more "practical" matters.

Another freshman course was Synthetic Inorganic Chemistry.

Sophomore courses included physics (optics, electrostatics, electrodynamics, and magnetism) differential equations, machine drawing, physical chemistry, graphic analysis, and industrial stoichiometry.

As a mechanical engineering major, I took courses in applied mechanics (including stress analysis, kinematics, and kinetics), metallurgy, fluid mechanics, materials testing, manufacturing and construction processes, as well as such "general" subjects as English, history, descriptive astronomy, and economics.

Each course considered its subject from a unique perspective, each of which was somewhat familiar to me from earlier education, experience, and reading, and some of which have been mentioned herein. From one perspective it is apparent that each form of energy is either potential or kinetic energy or a combination thereof, and that other forms of energy, such as heat, sound, electromagnetic radiation (including light), etc. are manifestations of these. Each classification is the result of the perspectives from which it has been considered. From the "intermolecular" perspective of the Maxwell-Boltzmann kinetic theory of gasses, for example, heat is seen as kinetic energy of molecules, ions, and atoms. From the "interatomic" perspective, which has been discussed, it becomes apparent that, while this view is applicable to "translational" heat, "rotational" and "vibrational" heat are combinations of kinetic and potential energy as are sound and vibration as well as gravity waves on water surfaces. An electrical charge is potential energy while "direct current" is kinetic energy of electrons and "alternating



current" alternates between kinetic and potential energy. The "heat of combustion" of fuels, in general, is the potential energy of the attraction of the atoms and ions of the carbon, hydrogen, and other elements with positive valences, which they may contain, to those of oxygen.

Consideration from the several perspectives discussed herein has left me with the conviction that physical and chemical phenomena and processes are, in general, transformations of energy between forms, often involving changes of state of the matter involved. Although views from several perspectives, which have led me to this conviction, have been discussed previously herein, the following account of my progress toward it (as recalled decades later) may tend to substantiate the conviction in the minds of readers:

My earliest quantitative impressions related to energy were in terms of power (which, I was to learn, means, in general, the rate at which energy is transformed from one form to another). Light bulbs were (and are) graded in watts, a unit of power. Then, as now, illumination of a room or other space was quantified, by many, in terms of "watts of light". I'm still not sure that those who refer to light in these terms are aware that the watt is a unit of power and I doubt that many recognize (as I have come to with the passage of years) that the rating of a light bulb in watts is a statement of the rate at which it is expected to transform electrical energy, by "ohmic heating" into heat, which is, in turn transformed, as "black body radiation" into electromagnetic radiation, mainly in the visible range of the spectrum. My earliest impressions of the relative power of automobiles and outboard motors came from advertisements of their "horsepower". I heard (or read) that James Watt had coined the term "horsepower" for use in advertisements of the steam engine he had invented in terms which, he hoped, would appeal to his intended customers. In 1783, based on experiments with a strong horse, he established the value of a horsepower as 550 foot pounds per second. By 1800, the metric system, which included the watt, so named in honor of Watt, who had defined "power" as a physical quantity (a horsepower is 746 watts), had been accepted by an international commission and has since been adopted internationally by scientists. Although most ratings of devices which are activated by electricity seemed to be in terms of power, it was paid for by the "kilowatt hour", a unit of energy. Of course, a kilowatt hour is more than 2½ million foot-pounds (the foot pound was the first quantitative unit of energy I learned about in school).

A difficulty in the consideration of transformations of energy in quantitative terms is the variety of units in which physical quantities (including energy) are expressed. The above discussion of transformation of energy between mechanical forms is a repetition of the explanations, (as I remember after sixty-some years) by my science teacher, who used the English system, with which we were familiar. It seemed reasonable that it took a foot-pound of work to lift a pound a foot.

I learned, in ninth grade "General Science", that the work of lifting an object weighing a pound a foot was transformed into a foot-pound of potential energy and that, if the object was dropped, the potential energy would be transformed into kinetic energy. All of which seemed to confirm my previous experience and the aphorism that: "What goes up, must come down.", which has been applied, with varying degrees of pertinence, to prices, temperatures, unemployment, voltages, and the popularity of entertainers. I had also noticed that some things, when lifted and dropped on to same surfaces, bounced, and/or made a noise when they hit. With the passage of time, I learned to explain the bounce as the result of the transformation of kinetic energy to elastic potential energy followed by its transformation back to kinetic energy, and the noise as the result of the transformation of some of the energy to sound (which is alternately kinetic and potential energy). Nothing seems to bounce forever, because, I learned, at each bounce, some of the kinetic energy is transformed into sound and some is transformed into heat. The foregoing seemed a satisfactory qualitative explanation, but a demonstration in quantitative terms was difficult, not only because of the problems of measuring the quantities of sound and heat evolved during a bounce, but also because of the problems of conversion between the units in which the results of such measurements would be expected and those in which kinetic energy is expressed. (Energy has been expressed, by specialists in various fields, in foot-pounds, inch-ounces, foot-tons, BTUs, ergs, joules (watt-seconds), watt-hours, kilowatt-hours, calories (cal.,(gm)), and Calories (cal.,(kg) or kilocalories). Some scientists express the view that confusion can be eliminated by the use of the "universal" metric system, Perhaps, but a Ph. D. chemist once told me of an instance when he and a colleague allowed the ice cubes in their drinks to melt in their mouths, assuming that this would absorb the calories in the alcohol, forgetting that some nutritionists refer to Calories as "calories" (so they'd have had to melt two kilograms, rather than two grams of ice to absorb the 150 nutritionists "calories" in each

drink). In view of these difficulties, I satisfied myself with consideration of this matter in terms of the "coefficient of restitution" the ratio ( $e = v_2/v_1$ ) of the (upward) velocity ( $v_2$ ) of an object after it bounced to its (downward) velocity ( $v_1$ ) before it hit.

The transformations of energy, mainly mechanical forms (work, kinetic, and potential energy are considered above, from "eyewitness", "common sense", and "empirical" perspectives). As a student of mechanical engineering, I acquired a thermodynamic perspective, from which transformations heat and work are considered and that of applied mechanics (which considers relationships of stress and strain, the integral of which is elastic potential energy). Other courses, which are mentioned a page or two back, presented hydraulic, hydrodynamic, aerodynamic, graphical, analytical, kinematic, dynamic, and stoichiometric, and other chemical (including organic) perspectives.

Recreational reading had, from early childhood, provided a succession of perspectives, including those of nursery rhymes, Bible stories, Aesop's fables, fairy tales, Indian legends, Greek and Norse mythology, history, geology (24), astronomy (22), cosmology (23), and atomic and intra-atomic physics (9). Considered from those perspectives which seemed "scientific" to me, in about 1940, I saw (and still see, with a few revisions based on what I've learned since then) energy transformations in the universe and the world about as follows:

Technical discussions should follow logical or chronological sequences, preferably both. The sequence of my perspectives, as remembered after fifty years, is neither. If I have failed in the following effort to put them in "proper" order, I hope that readers will be tolerant.

In 1940, I was unaware of the "big bang" theory of the origin of the universe, which had been proposed (by Le Maitre (5)) in 1927. (I was to learn, from Gamow, of the theory, a few years later.). However, I had been aware and accepting of the Chamberlin-Moulton theory that the planets, (including the earth) of the solar system were the "drops" formed in the "breaking" of a tidal wave raised from the surface of the sun to a connecting arm by a passing star, each of which was drawn together by gravity. In the contraction, gravitational potential energy was transformed into kinetic energy, which was, in turn, transformed into work, and then, to heat, some of which was radiated as black body radiation, cooling the planets until solid surfaces were formed, the

surface temperature of each planet continued to drop until equilibrium was reached between the radiant energy received from the sun and that lost by radiation from the planet. As each planet acquired an atmosphere by diffusion and volcanic eruption from its interior and by gravitational attraction of interplanetary gases and "solar wind", the temperature, in each case, was affected by absorption of radiation by atmospheric gases (referred to, in recent years, by "environmentalists", as the "greenhouse effect"), by the point to point variation of the "albedo" (reflectivity) of planetary surfaces, in combination with the rotational and orbital movement of each planet about non-parallel axes, has resulted in variations of surface and atmospheric temperatures with time and location, which result in the phenomena referred to as "weather" and "climate". The water vapor which has been a significant fraction of the earth's atmosphere has contributed to the complexity of these phenomena since the range of temperatures which include the mean equilibrium temperature of the earth's surface and atmosphere is conducive to the existence, of significant fractions of this water in each of all three (gaseous, liquid, and solid) states or phases, transitions between which are accompanied by mutations between translational, vibrational and rotational heat, which are seen from the "empirical" and "thermodynamic" perspective as "latent heats of fusion and vaporization", and changes of specific volume in which heat is transformed into work and consequent convection which transforms work into the kinetic energy of wind.

The liquid water, which covered most of the earth's surface, dissolved some of the gases and solids with which it came into contact to become a "primordial soup" in which many chemical reactions were bound to take place, producing a wide variety of chemical compounds of varying complexity. It has been postulated that, given "enough time", a molecule would form which would be capable of reproduction and have the other characteristics of a living cell, and that such cells would further organize themselves and adapt to their environments to evolve to the many organisms which have existed on the earth. Statistical calculations (in the 1950s), which are cited by "creationists", indicate that there hasn't been "enough time". More recently, numerical models of "coevolution", have reduced estimates of "enough time" (26).

I have yet to acquire mathematical or computational techniques or perspectives from which I can consider with confidence the relative validity of the views of

"evolutionists" and "creationists", but, based on paleontological evidence, I am persuaded that living organisms have existed on the earth for billions of years, which implies the presence of liquid water, and that the equilibrium between radiant energy received (less than 0.05 % of the sun's radiation) and lost during this period, would require radiation by the sun of a quantity of energy which is credible only on the basis of the consideration that (as stipulated in Einstein's "Special Theory of Relativity") that mass (M) is a form of energy (E) as related by:

$$E = Mc^2 \quad (8)$$

where  $c$  is the speed of light.

My view of energy transformations, past, present, and anticipated, which seem relevant to the subject of this paper, is outlined below:

Mass is transformed, in the interior of the sun and other stars, by thermonuclear reaction, to heat, which is transformed, at or near the surfaces of the sun and stars to "black body (electromagnetic) radiation". A fraction (referred to as the "albedo" of the planet) of the electromagnetic radiation which is intercepted by each planet is reflected. Most of the rest is transformed into heat, and, eventually, reradiated as "black body radiation" (maintaining its surface temperature equilibrium). Some of the radiation intercepted by the earth. is transformed, by photochemical reactions (including photosynthesis) into (chemical) potential energy, which, for the organic compounds synthesized in photosynthesis which are used as fuels, is referred to as their "heat of combustion", and when they are used as foods as their (nutritionist's) "calory content". In animals (including humans) the potential energy in foods referred to as "nutritionist's calories" is transformed into work and heat by movement and metabolic processes. Fire transforms the "heat of combustion" of a fuel into the kinetic energy of molecules referred to by some as "sensible heat".

Although neither prehistoric man nor I (as a kid) considered such matters from these perspectives. Transformations of energy, by fire from chemical potential energy ("heat of combustion") to heat, and from heat to light, sound, work, and kinetic energy have been applied to form the basis of most "know how", trades, technologies, crafts, arts, and sciences, and provided a series of perspectives, to and by mankind through prehistory and history, and to (by) me in the course of growing up, education, recreational reading, and research, both literature and

experimental, of the world and everything in it, and of all that has happened.

The word "efficient" seems to have originally, meant "effective". With the development of systems for the transformation of energy from one form to another, when preceded by a percentage, it has come to mean the percentage of available energy which has been transformed as intended.

#### MY PRE-'41 PERSPECTIVES OF FIRE

As mentioned earlier in the section headed: "A KID'S PERSPECTIVE OF FIRE", my earliest impression of fire was that of a yellow flame, which I generalized to the view that fire and light are aspects of the same thing. Grown ups talked about "lighting" fires and about "firelight", usages which I adopted.

Anyone who has tried will recognize the difficulties of recalling how the world looked and what each word meant in early childhood, without having one's memories distorted by more recent learning and experience. In view of these difficulties, I'm sure that this account is not completely accurate (for example, in the final paragraph of the previous section headed "LANGUAGES AND PERSPECTIVES" I quoted, adults, explaining that the visible "steam" from a teakettle was not steam, but a suspension of droplets of liquid water, I included the words "colloidal" and "aerosol", neither of which are defined in terms applicable to the explanation in a 1939 dictionary (2), so they couldn't have been included in an explanation to me in the 1920s), but it is the best that I can do.

I could see the light and feel the heat of a fire and of the sun, and got the idea that light and heat are related, but not the same. If the fire was in a stove, I couldn't see its light, but could feel its heat and, though I could see sunlight reflected from snowbank, I didn't feel much heat.

In time, I began to see that heat is needed to start a fire and that fire is a source of heat. The heating elements of other sources of heat, like electric stoves, toasters, and space heaters, glowed when they were hot enough, and I began to recognize that the light of a flame was an effect of its heat. After seventy some years, I can't remember my introduction to the concept of an "ignition" or "kindling point" as a property of each fuel, but I do remember my observation (which is described in that earlier section) of "spontaneous combustion", which was the source of my reservations regarding that concept. Practical experience induced

me to accept the concept, with the reservations alluded to. Paper was easy to light with a match, apparently because its thickness was small compared with the dimensions of a match flame so that some of it could be heated to its 'kindling point'. As a Boy Scout, learning to build a fire without paper, as required to pass the second class firemaking test, I was taught to use twigs or shavings of dimensions similar to those of a match stick to pick up the flame from the match. It took a few seconds, apparently, to heat the twigs to their kindling point. Once the twigs were burning, larger pieces of wood were placed in the flame. The larger sticks took longer to "catch fire", as I saw it, because there was more wood to heat to its "kindling point". It became apparent that the ignition and spread of fire depends upon the heating of the fuel to its kindling point by an external source of heat or the established fire.

I was told, when building a fire, to place the new sticks or logs, above those which were already burning, because "Heat rises.". As I grew older, I learned that the effective rise of "heat" was, more accurately, stated as "Hot air rises." due to convection, which occurs because fluids, including air, expand when heated, and become buoyant with respect to fluids of similar composition (but cooler.) I learned that other heat transfer mechanisms were conduction and radiation.

Like, I suppose, most people, both living and dead (some for long times), I had experienced heat transfer by all three mechanisms since early childhood. My early experiences with light and "radiant heat" (which, I learned, after a few years, is called "infrared radiation" in the language of physics), are recalled a page back. We have all felt the heat conducted from warm and hot objects. In the kitchen, heat is conducted by a frying pan, from the burner to the food, in toasting and broiling, heat is transferred by radiation. Boiling and baking involve convection.

Convection is utilized in a hot air heating system, to transfer the heat, from the furnace in the basement, through a duct system to living quarters on the floors above, and, for fireplaces, and coal and wood furnaces and stoves to provide the "draft" of air needed to keep the fire burning.

My memories of youthful impressions of heat transfer and, more specifically, convection are outlined above. In the course of the recall, it occurred to me to check recent references regarding the current meanings of the words. Dictionaries, both 1939 (2) and 1976 (16)

define "convection" essentially as described above. The Random House Dictionary (1) defines it as "The transfer of heat by the circulation of the heated parts of a liquid or gas", with no mention of cause of the circulation. The term seems to be sometimes used in this latter sense.

I had been aware, since early childhood, that fire required air. I'd watched while people "smothered" fire, or blown or fanned fires to make them burn faster or hotter, and had been shown how to regulate a fire by adjusting a "damper". All of which prepared me for the "chemical" perspective which is discussed in the earlier section under that heading, and the recognition that the fire with which I was familiar was oxidation.

As my perspectives changed between the several which have been mentioned in the foregoing, my views of fire and the changes of state and composition of matter, and transformations and transfers of energy between forms and locations involved, changed as if I was "channel surfing" on a television set with a "zapper" (to use a metaphor which would have been meaningless in the 1930s). On rainy days, I'd seen water flow down hill, faster down steeper slopes. When I acquired a graphical perspective, and saw it applied to hydrodynamics, electricity, and heat transfer, pressure, voltage, and temperature seemed, almost always, to be plotted as vertical displacements from the origins of graphical representations of the spatial distribution of these quantities. By analogy to water "seeking its level" I saw fluids, electricity, and heat flowing downward, from points or regions of high pressure, voltage or temperature at rates proportional to (and in the direction of) the gradients (or "slopes") of these quantities. I have recently learned that this view of heat transfer (as seen from the "empirical" perspective) led Lavoisier and, later Mach, to see heat as a fluid (5).

As I remember at the time of this writing, the perspectives I gained from play with a chemistry set was more accurately characterized as an "alchemic" than as a "chemical" perspective. Like the ancient and medieval alchemists, I followed recipes and observed reactions. The operations of the "Universal Research Laboratories", which are also mentioned in that section were, like Roger Bacon's thirteenth century experiments with gunpowder (4), more alchemy than chemistry.

Although I may have acquired a (somewhat indistinct) chemical perspective from the activities mentioned

above and recreational reading, my high school chemistry course clarified my chemical perspective and presented a few glimpses from the "intermolecular" perspective mentioned under that heading.

From the "intermolecular" perspective, it became apparent that even so simple a reaction as that depicted in equation (1):



is not the single step reaction implied by the stoichiometric equation (1). Each oxygen molecule must be dissociated to provide the single oxygen atom for each water molecule. Based on models of water molecules, such as those shown in Figure 1, in which the hydrogen atoms are on opposite sides of the much larger oxygen atoms, it seemed that the hydrogen molecules also must be dissociated to be oxidized.

I don't remember how or when, but at some time before I graduated from high school I became convinced that heat is molecular motion, the nature of which has been discussed herein. In the solid state, where crystalline bonds hold the molecules in their relative positions, only vibration about its equilibrium position is possible for each molecule (or atom). With increasing temperature, the amplitude of the vibration is sufficient to move each molecule so far from its equilibrium position that the crystalline bonding force can no longer restore it, and the solid melts. In the liquid state, molecules are free to move relative to one another, but are drawn together by the "van der Waals force", further increase in temperature results in movement beyond the effective range of this force and the liquid was said to "boil" or "vaporize". In the vapor or gaseous state, molecules are separated sufficiently that they move independently until they collide, as can be seen from the perspective of the Maxwell-Boltzmann kinetic theory of gases.

Considered from the perspectives outlined in the foregoing paragraphs, I saw heat conduction to be the result of essentially mechanical interactions of molecules and atoms. In a solid, the vibration of each molecule about its equilibrium position is communicated to its neighbors by the same crystalline binding forces that establish their equilibrium relative positions. In a liquid, the molecular motion is communicated mostly by the van der Waals intermolecular attraction force and the intermolecular repulsion which determines the effective volume of each molecule and hence the specific volume of the liquid. In a gas, viewed from the perspective of the Maxwell-Boltzmann kinetic theory of gases, the

movement is communicated by effectively elastic collisions between molecules,

Although the view of heat transfer as seen from the "intermolecular" perspective, as described above, was more consistent with the structure of matter in its various states, as seen from this perspective, quantitative consideration would involve too much complex computation (since it would have to take into account the variation with relative directions of the intermolecular, interionic, and interatomic attraction and repulsion forces) for practical purposes.

Like most students, I learned to consider heat transfer from the empirical perspective (from which Lavoisier and Mach had seen heat as a fluid), which is a more practical approach to heat transfer calculations. Such consideration, for engineering purposes (11), yields:

$$q = k A (T_1 - T_2) / x \quad (9)$$

where:  $q$  is the rate of heat transfer through a panel of area  $A$  and thickness,  $x$ , and  $T_1$  and  $T_2$  are temperatures on either side of the panel, while  $k$  is the thermal conductivity of the substance of the panel.

The value of  $k$  can be determined experimentally by measurements of  $q$  when values of other variables are preestablished.

For purposes of theoretical consideration of systems in which heat transfer is a factor, equation (9) can be generalized as a partial differential equation:

$$q = -k A \left[ \partial T / \partial x \right] \quad (10)$$

and in vector notation as:

$$q = -k A \nabla T \quad (11)$$

I gained this perspective of heat transfer, by conduction, several years after I had learned to build fires as a Boy Scout. From this perspective, in combination with the concept that each fuel has a "kindling point" and heat capacity, I began to see why the techniques I had learned as a Boy Scout were effective and necessary.

A log or large piece of wood can't be "lit" with a match because, although the temperature of the flame is well above the "kindling point" of the wood, its thermal conductivity is much lower so that the temperature at the surface attains an equilibrium such that the rate at which heat is conducted into the wood is equal to that at which it is conducted from the flame. Paper, twigs and shavings can be lit because the

heat transferred from the flame is conducted through the fuel only a short distance until it reaches another surface from which it is conducted by air, whose thermal conductivity is equal to or less than that of the flame, so the heat accumulates in the paper, twigs, or shavings until the "ignition" or "kindling point" is reached.

While the view of ignition, from the perspective of thermal conduction, outlined above, explained some of my experiences as a Boy Scout, they left some observations unexplained. From the perspective of "states" of matter, which are discussed earlier herein, it is apparent that, although most of the fuels discussed above are solid, the flames, like the visible "steam" from a teakettle, the clouds in the sky and most of the white "smoke" which rose from a burning pile of damp leaves, seemed to be lighter than air. As mentioned in the earlier section headed "LANGUAGES AND PERSPECTIVES" I was told that the visible "steam", white "smoke" and clouds, as well as fog and mist, were droplets of liquid water too small to settle out, and referred to as "colloidal suspensions" as were similarly suspended droplets and particles of other substances. Grey, brown and black smoke are such suspensions of other substances as is evidenced by their odor, while flames are suspensions of carbon which is so hot it glows. The droplets and particles are too widely scattered to have as much effect on the density of the air as the heat (from the fire?), so the "steam", "smoke" and clouds floated upward. This upward movement of flames, often referred to, by poets, novelists, and journalists, as "leaping", and in technical discussion as "convection", plays a role in the propagation of fire, as mentioned, a page or so back, in the account of my recollections of Boy Scout firemaking.

I don't remember when I first heard the aphorism, "Where there's smoke there's fire.", but I'm sure that it was before my twelfth birthday that I began to question its (absolute) truth. I'd seen smoke coming from overloaded extension cords, and stop after the appliances which had overloaded them were disconnected. I'd seen pictures of smoke (identified as such) coming from volcanoes although I hadn't been told of any underground source of the air which would have been needed to sustain a fire. I wondered what smoke was. The white smoke, from burning damp leaves was obviously, like visible "steam", fog, mist, and clouds, a colloidal suspension of liquid water, but the grey, brown, and black smoke were something else. I was a few years younger, when an aunt, who lived in an in-town apartment, reached out of her

window and showed me a blackened finger tip. She identified the black stuff on her finger as "soot" which, she explained, had settled out from the black smoke, which came from chimneys of building in which, she said, "soft coal" was burned. It seemed to me that grey smoke must be a mixture of black smoke and white smoke, but, from its odor, I was sure that all smoke contained something else.

Consideration of the observations, experiences and hearsay mentioned in the foregoing paragraph from my developing chemical perspective resulted in views of fire and smoke which I found satisfying. Although I questioned that "where there's smoke there's fire.", it was apparent that, where there was smoke, fire could be expected. If the overload which caused an extension cord to overheat wasn't removed, the cord would soon "burst into flame". By analogy to the formation of the aerosol referred to as visible "steam" beyond the spout of a teakettle, I reasoned that something in the insulation of the extension cord (bare wires, when heated by electric current, don't emit smoke) must have evaporated and condensed, after mixing with cooler air, to form the droplets of the colloid referred to as "smoke". Reflecting on earlier experiences and observations, some of which have been mentioned hereinbefore, I recalled that, when organic substances are heated, smoke often appears before flame.

The word "organic", like many others, has a number of meanings, the most general of which is "Arising from an organism." (2). Organic chemistry is essentially the chemistry of carbon, which owes its complexity to four "covalent" bonds whereby carbon atoms bond with one another, and those of other elements to form a wide variety of molecules (aver 15000 of which are listed in the Handbook of Chemistry and Physics (10)). Because carbon atoms combine in several ways, it is possible for different molecules (of compounds with different properties) to have the same composition in terms of the numbers of atoms of carbon and other elements. For this reason, organic compounds are usually identified by structural formulas which are, essentially, diagrams or models of their structure. It is quite apparent, from consideration of such structural formulas, that many organic molecules are too large and irregular in shape to bounce around like "tiny billiard balls" (as Mach characterized the picture presented by the Maxwell-Boltzmann kinetic theory of gases) but are more likely to break into smaller molecules. In other words, some organic compounds tend to decompose rather than evaporate when heated. (I became

somewhat dimly aware of such matters at an early age because of my father's involvement in the development and construction of "cracking stills" in which large molecules of crude oil were "cracked" into the smaller molecules needed in gasoline.)

The familiar fuels are organic materials (in the sense of "Arising from an organism." (2)). As such they are composites of a number of substances (Mostly organic compounds of carbon, hydrogen, and nitrogen, in solid, liquid, and gaseous states. Wood, for example is a mixture of cellulose, which is "made up of long-chain molecules (fibers) in which the complex unit  $C_6H_{10}O_5$  is repeated as many as 2000 times" (17), lignin ( $C_{41}H_{32}O_6$ ) sugars, resin, acetic acid, water, air, and other substances.

When a campfire had subsided to glowing coals and, for one reason or another, a hotter fire was desired, a few sticks of kindling were laid over the glowing coals. In few minutes (particularly if the glow was brightened by blowing or fanning the coals, the "kindling" began to emit smoke, which, a minute or two later, burst into flame. I had noticed that the smoke appeared before the flame.

Consideration from perspectives hereinbefore discussed, particularly the "chemical" perspective and that form which "states" of matter are viewed, led me to see the sequence of observable phenomena outlined above as resulting from the following sequence of chemical and physical events:

The "kindling" was heated by radiation and convection from the glowing coals. When it reached temperatures conducive to such processes, volatile components of the "kindling" began to evaporate and nonvolatile components decomposed to volatile compounds which evaporated. The vapor, mixing with cooler air condensed to form the droplets of the colloidal suspension (or "aerosol") referred to as "smoke". Further heating brought the smoke to its "ignition point" so it "burst into flame" .

The above description satisfied me in 1940, and it still does except for my continuing reservation regarding the concept of "ignition points" and the colloquialism of the phrase "burst into flame" and its implication of an "eyewitness" rather than a "chemical" or "physical" perspective.

These misgivings were alleviated by replacing the final sentence (which included the dubious phrases) with the following continuing description:

If and when the smoke was further heated, the gaseous decomposition products of the wood, such as methane ( $CH_4$ ), ethane ( $C_2H_6$ ), propane ( $C_3H_8$ ), carbon, hydrogen, etc. oxidize, raising the temperature still higher, decomposing and oxidizing the compounds which had condensed to form the droplets of the colloidal suspension referred to as "smoke".

Most decomposition products of the organic substances commonly used as fuels are in gaseous or plasma states at temperatures associated with combustion. The most notable exception is carbon, which is solid at much higher temperature. The charcoal, which is the most familiar decomposition product of wood is mostly carbon. The glowing coals which remain after the flames have subsided are mostly carbon, which continues to burn while oxygen is available. Enough of the heat of combustion is transferred from the carbon dioxide, which is the reaction product, to the oxygen of ambient air and unburned carbon to maintain the reaction and the glow, which is black body radiation. Similarly, the organic substance of the droplets of the colloidal suspension referred to as smoke decompose to the gaseous products mentioned above, and the small particles of carbon, referred to as "soot", whose colloidal suspension in air is called "flame", when it glows, and "black smoke" after it cools enough to stop glowing.

As mentioned a few paragraphs above, the "smoke" emitted by heated wood is a colloidal suspension of volatile components of the wood. Their composition varies from one species of wood to another. Many have proven useful. Perhaps the best application of wood smoke is to the preservation of food, such as ham, bacon, and fish.

The flavor of smoked meat has been sufficiently popular to inspire the invention of the "pit barbecue" on which meat is smoked while it is broiled and roasted, although preservation is not a consideration because the food is eaten while it is still hot. Hickory and mesquite smoke seem to be most popular for these purposes, as well as (in condensate form) as flavoring for barbecue sauce, etc.

Other volatile components of wood, which are undoubtedly seen as wood smoke but may not condense to "smoke" before they are condensed to liquids in stills, are turpentine, which is used as a paint thinner and brush cleaner, and creosote, which is used as a wood preservative and harsh disinfectant (17).

The last couple of pages contain descriptions of fires with which I was most familiar before 1941, in which wood or paper were the fuels, as I saw them from several perspectives. I was also aware of combustion of other fuels to which some parts of these descriptions are not applicable.

I was aware that although most of the other fuels I had seen burning were of organic origin, they tended to have properties more similar to the intermediates of wood burning than to the wood itself. Most were gaseous, volatile, or colloidal suspensions, like components of wood smoke, or mostly carbon and ash (like charcoal), when visibly burning.

I had heard coal, petroleum, and natural gas referred to as "fossil fuels", meaning that they were the remains of prehistoric organisms which had decomposed and been buried by such geological processes as volcanic eruption and sedimentation. I had seen the beginning of the formation of coal in the peat bogs of the upper midwest, many acres of spongy moss, where a misstep could result in a foot coated, almost to the knee, with dark brown rotted moss, referred to as "peat", which, in the United States, is used as fertilizer and (dried) as thermal insulation, packing, and "potting soil" for plants, but in countries where other fuels are expensive, dried peat is used, in large quantities, as fuel. The top layers in a peat bog are of relatively low density, but, at greater depths the older peat, which has been rotting longer and consolidated by the combination of increasing pressure and the upward diffusion of water and other low density (compared with that of carbon [3.51]) liquids and gases (most of which are products of the continuing decomposition (rotting) of the peat). Gases diffuse to the air above as "marsh gas" (which sometimes catches fire and is referred to as "will o' the wisp" or "ignis fatuus"). With the passage of time, the growth of the moss continues, piling up more peat, so that at the bottom continues to consolidate while decomposing, and its density, carbon content, and hardness increase with time and depth and the peat is changed, progressively, to lignite, bituminous and, finally, anthracite coal.

Petroleum, like coal, is a product of decomposition (decay) of organic matter, in this case, marine animals and plants, which, because of their much lower oxygen/hydrogen ratio than the peat moss, which is mainly cellulose (a carbohydrate (or hydrate of carbon, which can decompose to carbon and water)) tends to decay to hydrocarbons. As in the formation of coal,

the process includes the "piling up" of the matter for long periods of time.

In the course of the millions of years during which coal and petroleum have been forming, various geological events and processes, including volcanic eruptions, earthquakes, and continental drift, have occurred, resulting in deformation of the earth's crust and the formation of mountain ranges and displacement of continents, in the course of which some of the forming coal and petroleum were covered by layers of rock, which sealed pockets of the gaseous products of the decomposition of organic matter whereby the coal and petroleum are formed. These trapped gases are known as "natural gas".

Some fossil fuels are used as recovered. Coal is burned in furnaces to heat buildings, and in boilers of locomotives, ships, and power plants to generate steam. Natural gas is distributed through pipes to residences and other buildings where it is the fuel for furnaces, space heaters, cook stoves, fireplaces, and refrigerators.

Some coal, generally bituminous coal, is heated in kilns, to continue the process of decomposition to gaseous hydrocarbons (methane, ethane, etc.), which are referred to as "manufactured gas" and distributed through pipes in communities beyond the range of natural gas distribution pipelines, and carbon and ash, known as "coke", which is sold as household fuel, and used in blast furnaces in which iron ore is reduced to "pig iron", some of which is remelted and cast, to make the wide variety of cast iron items with which we are all familiar, but most of which is converted to steel by oxidization of most of its carbon content in Bessemer converters or open hearth furnaces. Much of the gas from coke ovens of iron works is used as the fuel of large (at the Engine and Condenser Department of Allis-Chalmers, where I had a summer job in 1937, there was an eight foot bore by twelve foot stroke engine, for this purpose, on the drawing boards) internal combustion engines, which drive the blowers for the blast furnaces, etc.

Petroleum is a mixture of hydrocarbons, which are separated, by distillation, into gases, including methane, butane, propane, and pentane, liquids, including naphtha, gasoline, kerosene, and fuel and lubricating oils, waxes, and asphalt. Asphalt, wax, and the "heavy" (viscous) oils owe their properties to the large size and complexity of their molecules, which, since the 1920s have been "cracked", at high temperature and pressure (which can be reduced by



using catalysts) to the smaller molecules of the more volatile compounds needed for internal combustion engines.

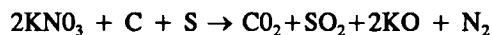
Not long after I'd learned to read, I discovered "car cards", - advertising posters mounted in a row over the windows of a street car. One of these (advertising "Carbona", a dry cleaner) included a picture of a woman, with an article of clothing in one hand, flying through clouds, with the caption, "You can go twenty miles on a gallon of gasoline" as at least one automobile maker claimed at that time. My mother explained the point of the ad - that gasoline vapor could form an "explosive mixture" with air, but Carbona doesn't. That night, my father explained that Carbona is carbon tetrachloride which, though volatile, like gasoline (so it is useful for dry cleaning) but, unlike gasoline, it was not enflammable (gasoline forms explosive mixtures with air because it is highly enflammable).

I accepted these explanations because they came from my parents, but didn't fully understand them at that age (between six and ten). The distinction between "enflammable" and "volatile" was unclear (as it still seems to be to some television news reporters). My father, sensing my perplexity, pointed out that "enflammable" meant "easily ignited to burst into flame" while "volatile" meant "easily evaporated". My view of the subject was obfuscated by the frequent spelling of "enflammable" as "inflammable", and the apparent interchangeability of the prefixes "in-", "un-", and "non-". (It would be fifteen years before I saw less ambiguous word "flammable" on a tank truck.) The meanings of such words as "explode", "explosion" "explosive", "detonate", and "detonation" and "detonable" were unclear to me then as they still seem to be to many. I am often, still, unsure what others mean by them, although I now think I know what I mean.

Consideration of such matters from the various perspectives, acquired in the course of education, reading, conversations, and basement and backyard activities, clarified my views of fire, while presenting new perspectives, consideration from which led to other pictures, some of which were somewhat "fuzzy", leading to further research (literary, experimental, or analytical), a sequence which continues to this day.

Following is an effort to summarize my picture of fire, as I now remember seeing it, in 1940 (which was two years after my graduation as a mechanical engineer):

Most of the fires which I'd seen consisted of flames, which behaved as gases or colloidal suspensions (like smoke), and/or glowing coals. Clearly, most solid and liquid filets volatilize as part of the combustion process which showed me that more than the single step, implied by stoichiometric equations, such as Equations (1) and (2), are involved in the process. In the burning of gunpowder, expressed in equation (2):



the potassium nitrate ( $\text{KNO}_3$ ) molecules must dissociate to provide the oxygen atoms to oxidize the carbon and sulfur. Considered from the "interatomic" perspective, which has been discussed herein before, it seemed that the oxidation of hydrogen must follow the dissociation of the oxygen molecules, and probably those of hydrogen. I began to see fire, except where elemental carbon, as coal, coke, or charcoal, or in a similar form, is the fuel, is a multistage process. The decomposition, melting or sublimation, and/or evaporation, and condensation to the aerosol referred to as "smoke", precedes its further decomposition, dissociation, oxidation, and ionization, the effects of which are seen as the flames of familiar fuels (except carbon in its various forms).

By 1940, I had acquired enough of the vocabulary of chemistry to understand that chemical processes and changes of state were either "exothermal" (characterized by the evolution of heat) or "endothermal" (characterized by the absorption of heat) and was aware that freezing, condensation, and the formation of most molecules by joining atoms, ions, or "free radicals" are exothermal, while melting, sublimation, boiling and other evaporation or vaporization, decomposition, ionization, and dissociation are endothermal. I came to recognize that "ignition" or "kindling", considered from the perspective outlined above, from which fire is seen as a multistage phenomenon, occurred only after sufficient heat had been transferred to a fuel element to result in the necessary succession of endothermal processes (which is unique for each fuel), and maintain the exothermal oxidation until the evolution of heat from the latter is sufficient to heat the "soot" (the particles of carbon which are products of the decomposition of the colloiddally suspended droplets of hydrocarbons called "smoke") to the incandescence visible as "flame". Fire, in general, stabilizes when heat losses reach equilibrium with evolution of heat. When losses exceed evolution of heat, a fire "dies out". When the evolution of heat exceeds losses and continues to do so, the fire is self accelerating. A few

years later, the course of "literature research at the Naval Ordnance Laboratory, I was to read of such a self accelerating fire referred to as a "thermal explosion" (which will be discussed in more detail a few pages hence), but, in 1940, "explosion still meant to me, as it had since I learned the word, a "bang" and a flash and an impulse which could throw things around (As a kid, I had seen tin cans, propelled by firecrackers, fly higher than a house.), and some times broke them. Dictionaries (1,2) gave "detonation" as a synonym of "explosion", and an encyclopedia (15) stated that "detonation is a distinct phenomenon in which the chemical transformation is induced in every particle at the same instant". Even then, I didn't believe that. I already saw fire as the Multistage phenomenon described above, of which each stage takes time. I had heard the combustion of an internal combustion engine referred to as "an explosion" (at the beginning of each power stroke), and the anti-knock property of Ethyl and other high octane gasoline ascribed to the fact that it was "slower burning" than regular. However, having considered the Otto cycle (which is employed in most automobiles), I was aware that even high octane gasoline burned fast enough that the reaction was complete before the piston moved enough that the volume change had to be considered in thermodynamic calculations, but "regular" , in a high compression engine, burned so fast that the resulting rapid pressure increase is propagated through the cylinder head to the air as a sound or "shock" wave. Waves had been familiar to since early childhood, when I saw them on water. My dad built a radio before I was ten and I soon learned to estimate where to set the dials from the wavelength of each station, published in the paper. I heard that radio waves were waves in "ether" but, before I found out what "ether" was, I read about the Michelson-Morley experiment, which showed that there was no such thing. As a teenager, I had built audio equipment, including amplifiers and recording equipment, in the course of which I acquired practical, empirical, and graphical perspectives of sound, which prepared me for acoustical and analytical perspectives of sound I was to learn in physics courses. In 1940, I was aware that both "explosion" and "detonation" are derived from Latin words describing sounds (those of clapping and thunder respectively), and that both referred to sudden fire (sudden enough that the pressure rise, due to the heat evolved, was propagated as a sound wave, from which I inferred that the reaction was completed) in a small fraction of a second (the maximum period of a sound wave), but my mental pictures of the processes were rather indistinct until, as a participant, at the Naval Ordnance Laboratory (N.O.L.), in the research

and development of systems of which pyrotechnics and explosives are components.

Although, in 1940, my impressions of explosion and detonation were not very clear, I could see, from a heuristic perspective of the Maxwell-Boltzmann kinetic theory of gases (as I understood it) that the combustion of an "explosive mixture" of gaseous fuel and air is the effect of random intermolecular collisions of sufficient magnitude to break (dissociate) molecules in into atoms, ions, free radicals. I saw that, in this state, hydrogen and carbon atoms and/or ions can bond to those of oxygen to form carbon dioxide and water, processes which are exothermal (evolving heat) - the kinetic energy of molecular motion) thus increasing the frequency of collisions of sufficient magnitude to initiate the sequence outlined above in the previously unreacted fuel/air mixture. I saw that this sequence should be expected to propagate at a velocity close to the average of those of the molecules (which is about that of sound).

Consideration of the heuristic model, described above from a quantitative perspective, would have required statistical analysis beyond my abilities. Perhaps I could have clarified my view by consideration from acoustical, hydrodynamic, and/or fluid mechanical perspectives, to each of which I had been introduced, but I didn't make such an effort until, at N.O.L., I was engaged in explosive research, the course of which I learned that others, including Rankine (whose steam engine cycle I had learned of in thermodynamics courses) had done so in the nineteenth century.

My earliest impressions of fire were effects of observations of and experience with such familiar fuels as paper wood, coal, charcoal, candle wax, and gasoline. I had become convinced that air is essential to fire. It didn't take long for experience with fireworks (which available, in late June and the first three days of July, in the 1920s, at grocery and drug stores, to any kid with a dime). to cast doubt on this conviction. My experience, at the "Universal Research Laboratory" (as a fourth grade classmate referred to his basement) in the preparation of black gunpowder, which burned quite vigorously in a rocket (which was lacking in aerodynamic stability and tumbled a few feet off the ground). I can't say, at this time (1995) whether, at that time (1926), I understood why gunpowder could burn without air, although other fuels couldn't. However, by 1940, I had learned that the burning of familiar fuels is oxidation, requiring the oxygen of air, but that gunpowder, as well as other explosives and pyrotechnics, burned without air

because they contained oxygen as a component of relatively unstable compounds, such as potassium nitrate. Thus, I saw, the burning of gunpowder is a multistage reaction (one stage of which is the decomposition of the nitrate) which, in fuses, is too slow to be called "an explosion".

In 1940, World War II had become the "Battle of Britain", Japan was rearming the invading Asiatic neighbors, and the U.S. armed services were engaged in an effort to regain and surpass the preparedness lost as the result of the pacifism and disarmament following World War I. Pursuant to this effort, the U.S. Naval Ordnance Laboratory (NOL) recruited over 1700 scientists and engineers, of which I was one.

#### FIRE, AS I SAW IT AT NOL (EAU)

Arriving at NOL, in early 1941, I was given new perspectives, particularly of fire, too frequently to retrace after fifty-odd years. My first assignment, at NOL, was to the Propellant and Pyrotechnics Group of the Experimental Ammunition Unit (EAU), where I worked with an "ordnance man", directed by the pyrotechnics specialist on the adaptation of display fireworks for use as signals (such as "Submarine Emergency Identification Signals"). My principal assignment, in that group was design and drafting, but I spent some time in the laboratory, where we did some preparation, fabrication, and testing of pyrotechnic mixtures, systems, subsystems, components, etc. Our approach, in such adaptation, was generally that of "trial and error" or, to dignify it, "Edisonian research". Based on the view, from the "practical" or "common sense" perspective, that mixtures and practices which had been used, with success, by others, were most likely to serve our similar purposes, we usually followed recipes, some dating back to those of medieval alchemists and ancient Chinese artisans. On occasion, we tried to improve mixtures by application of stoichiometry, but experience tended to confirm the above mentioned view, from the "practical" perspective. It was apparent that more than stoichiometry was involved. We noted that the behavior and properties of pyrotechnic mixtures were affected by the granulation of their ingredients as well as the densities to which they were loaded. Of the properties so affected, sensitivity, which includes their susceptibility to initiation by the stimuli available for this purpose when intended, as well as that to initiation by accidentally applied stimuli (and resulting hazards), is of primary

concern to all involved in the manufacture and application of pyrotechnics and explosives.

Although, from instruction, conversation, and "hands on" experience, I had acquired some "eyewitness", "common sense", "practical", and "empirical" perspectives of such matters, I felt a lack of applicable "chemical", and "scholarly" perspectives. The EAU had no official library, but I had noticed a number of books on ordnance, explosives, and pyrotechnics on desks and shelves, which I borrowed and read. One, which caught my eye was *The Chemistry of Powder and Explosives* (4), by Tenney L. Davis (who had been the lecturer of my second semester freshman chemistry course). The book was intended to be a textbook for a graduate course on the subject. the book includes ( in the 1941 edition) chapters on PROPERTIES OF EXPLOSIVES, BLACK POWDER, PYROTECHNICS, AND AROMATIC NITRO COMPOUNDS. It starts by defining an "explosive as:

"a material, either a pure of single substance or a mixture of substances which is capable of producing an explosion by its own energy".

"It seems unnecessary to define an explosion, for everyone knows what it is. -- a loud noise and the sudden going away of things from where they had been --".

As I read it, I accepted it, but soon began to recognize that, as with many words, although everyone knows what "explosion" means, it doesn't necessarily mean the same to everyone. Recently, a steam automobile enthusiast told me that "Explosion is the most inefficient form of combustion", implying, I support that a steam automobile should be more efficient than one with an internal combustion engine. Do those who talk about "the population explosion" mean "a loud noise - etc." or "the most inefficient form of combustion"?

Davis, in the first chapter on PROPERTIES OF EXPLOSIVES, points out that, although an explosive can produce an explosion by its own energy, it can liberate this energy without exploding (as black powder does in a fuse). Here, he injected an explanation of the difference between a "fuse" which is a device for communicating fire" and a "fuze", which is a device for initiating explosion (usually "detonation") of the "bursting charges" of shells, bombs, mines, grenades, etc.". A section of the first chapter on PROPERTIES OF EXPLOSIVES headed, *Classification of explosives* includes paragraphs (condensed below) on:

I. **Propellants**, or "low explosives" which (in their usual application) burn but do not explode, and function by producing gas which produces an explosion (by busting its container, such as the paper tube of a Chinese firecracker or the metal case of a bomb). Examples: black powder, smokeless powder.

II. **Primary Explosives** or "initiators", which explode or detonate when heated or subjected to shock. Examples: mercury fulminate, lead azide, lead salts of picric acid, etc.

III. **High Explosives**, which detonate under the influence of the shock of the explosion of a suitable primary. Examples: dynamite, TNT, tetryl, picric acid, etc.

It is pointed out that these classes overlap because the behavior of explosives is determined by the nature of the stimuli to which they are subjected and by the manner in which they are used. Nitrocellulose, "colloided" such smokeless powder, is a propellant, as compressed guncotton, is a powerful high explosive, and, as lower density guncotton, has been used as the "flash charge" of electric detonators, TNT, nitroglycerine, and other high explosives have been ingredients of smokeless powder. Mercury fulminate can be "dead pressed" so that it loses its power to detonate from flame.

A review of the foregoing two pages has led me to recognize the need for an explanation. Although the discussion FIRE AS I SAW IT AT NOL (EAU) is, as implied based on my memories after fifty-some years, the review of Davis's book (4), is a reflection of current "browsing" through a copy at hand. The quotations enclosed in quotation marks, including the following, are direct copies.

#### **"Propagation of Explosion"**

"When black powder burns the first portion to receive the fire undergoes a chemical reaction which results in the production of hot gas. The gas, tending to expand in all directions from the place where it was produced, warms the next portion of black powder to the kindling temperature. This then takes fire and burns with the production of more hot gas which raises the temperature of the next adjacent material. If the black powder is confined, the pressure rises, and the heat, since it cannot escape, is communicated more rapidly through the mass. Further, the gas- and heat-producing reaction, like any other chemical reaction, doubles its rate for every 10° (approximate) rise of

temperature. In a confined space the combustion becomes extremely rapid, but it is believed to be combustion in the sense that it is a phenomenon dependent upon the transmission of heat."

"The explosion of a primary explosive or of a high explosive, on the other hand, is believed to be a phenomenon which is dependent upon the transmission of pressure or, perhaps more properly, upon the transmission of shock. Fire, friction or shock, acting upon, say, fulminate, in the first instance cause it to undergo a rapid chemical transformation which produces hot gas and the transformation is so rapid that the advancing front of the mass of hot gas amounts to a wave of pressure capable of initiating by its shock the explosion of the next portion of fulminate, and so on, the explosion advancing through the mass with incredible quickness. In a standard No. 6 blasting cap, the explosion proceeds with a velocity of about 3500 meters per second."

"If a sufficient quantity of fulminate is exploded in contact with trinitrotoluene, the shock induces the trinitrotoluene to explode, producing a shock adequate to initiate the explosion of a further portion. The explosive wave traverses the trinitrotoluene with a velocity which is actually greater than the velocity of the initiating wave in the fulminate. Because this sort of thing happens, the application of the principle of the booster is possible. If the quantity of fulminate is not sufficient, the trinitrotoluene either does not detonate at all or detonates incompletely and only part way into its mass. For every high explosive there is a minimum quantity of each primary explosive which is needed to secure its certain and complete detonation. The best initiator for one high explosive is not necessarily best initiator for another. A high explosive is generally its own best initiator unless it happens to be used under conditions in which it is exploding with its maximum "velocity of detonation".

The section of Davis's book quoted above presents views of explosion and detonation from "common sense" and "empirical" perspectives. I am sure Davis was aware of "theoretical", "analytical" "hydrodynamic", etc. views which had been expressed in the previous century or more, but confined his description to views from perspectives with which, he felt confident, his students and other readers of his book would be familiar. References to the "kindling temperature" and the "doubling of reaction rate for every 10° rise of temperature" are evidence of an "empirical" perspective based on standardized tests

similar to those described a few pages on in the first chapter of the book (4).

The section of **Propagation of Explosion** is followed by a section on **Detonating Cord** which is also referred to as "cordeau" (after the French "cordeau detonant") and "Primacord" (a trademark of the Ensign Bickford Company), a narrow tube filled with high explosives whose principal use in blasting is the simultaneous (or in close sequence) initiation of detonation of two or more explosive charges. It can also be used to fell small trees as had been demonstrated in an ROTC class I had attended a few years before.

The first chapter of "The Chemistry of Powder and Explosives" (4), entitled **PROPERTIES OF EXPLOSIVES** also includes descriptions of experiments, which can be performed in a college chemistry laboratory to demonstrate some of these properties, as well as standardized tests for them, and cites U.S. War Department Technical Manual TM 2900 "Military Explosives" (25) and a number of Bulletins and Technical Papers of the U.S. Bureau of Mines in which such standardized tests are described in more detail. Properties for which tests are described in this chapter include **Velocity of Detonation Sensitivity** (including "explosion", "ignition", or "kindling" temperature and impact sensitivity) and **Tests of Power and Brisance**.

The section on **Velocity of Detonation** begins with a paragraph in which the subject is considered from the "empirical" perspective of the time (ca 1940), which no longer seems relevant. It mentions detonation velocity measurements by Berthelot and Vielle, who used a "Boulenger" chronograph" which is not described, except for the mention that its (lack of) precision was such that they were obliged to employ long columns of explosives". It goes on to say, "The Mettengang recorder, now commonly used, is an instrument of much greater precision and makes it possible to work with much shorter charges". The Mettengang recorder is described as an instrument whereby time is determined as proportional to the distance (measured with a micrometer microscope) between marks made on a rapidly moving smoked metal surface.

Also mentioned is the "Dautriche method" in which the detonation velocity of an explosive being investigated is compared with that of detonating cord, which can be determined using relatively imprecise timers with long lengths of the cord.

The use of high speed photography and cathode ray oscillographs, in measurement of detonation velocity, are mentioned as recent developments.

The section on **Sensitivity Tests** includes descriptions of "impact" or "drop" tests in which (typically) the height is determined which will result in the explosion of a sample of the explosive being investigated contained in a hole in a block of steel, when a two kilogram weight is dropped on a plunger in contact with the explosive sample.

Also described in a test of "temperature of ignition" or "explosion temperature" in which a blasting cap cup containing a sample of an explosive is thrust into Woods metal which has been heated to a known temperature. The procedure is repeated, with varying temperatures, until the temperature is determined at which the sample explodes or is ignited within five seconds. In another test which is also described, the blasting cap cup containing the explosive being tested is dunked in Wood's metal at 100°C and the temperature is raised at a steady rate until the sample ignites or explodes. The temperature at which this occurs is considered to be the "ignition" or "explosion temperature". When the temperature is raised more rapidly, the inflammation occurs at a higher temperature". (As is illustrated in an accompanying table).

In the section on **Tests of Power and Brisance** a definition of neither "power" nor "brisance" is included. It seems that, as with "explosion", Davis assumed that it was unnecessary to define "power" because everyone knew what it meant, while, in my view, as with "explosion", although everyone knew what "power" meant, it didn't mean the same to everyone. (Dictionaries I've consulted (1,2,16) include from eight to seventeen definitions). "Brisance" on the other hand, is not listed in a 1939 unabridged dictionary (2). More recent dictionaries (1,16) define it as "The sudden release of energy by a explosion", or something similar. Although "brisance" wasn't defined in Davis (4) or the dictionaries I consulted (2), it didn't take long for me to grasp its meaning, whether from conversation, recognition (having studied French in high school) that it was derived from "briser"-to break, or from descriptions, in Davis (4) and references cited therein, of tests of power and brisance (each of which rated an explosive in terms of the measurement of the deformation or other change of a solid specimen which had been exposed to its action.

The opening paragraph of the section on Tests of Power and Brisance mentions a "manometric bomb" as a means of measuring the energy liberated in an explosion, but goes on to point out that the effectiveness of an explosion depends upon the rate at which the energy is liberated ("Power" as understood by physicists and engineers). The high pressures developed by explosions (which reflect this rate) were first measured by the Rodman gauge, in which, according to Davis (4), the pressure caused a hardened steel knife to penetrate into a disc of soft copper. The depth of the penetration was taken as a measure of this pressure. Davis also mentions "crusher Gauges" in which copper cylinders are crushed between steel pistons, piezoelectric gauges, the "Trauzl lead block test", in which the enlargement of a hole is taken as a measure of "power" or "brisance", the "small lead block test" of the Bureau of Mines, in which the compression of the block is used as such a measure, the "lead plate test of detonators" in which the diameter of the hole punched through the plate by a detonator is a measure of its output. Similar tests with aluminum plates are also mentioned.

Explosive research was not, in 1941, among the missions of the NOL, but tests similar to those of PROPERTIES OF EXPLOSIVES mentioned and described by Davis (4) in the chapter so titled, which is reviewed above, were performed by ordnance men assigned to those Fuze Group of the EAU (whose laboratory, we of the Propellant and Pyrotechnics Group shared, so I could watch now and then) pursuant to the development of fuze explosive trains (an activity in which I was to become engaged in a few months, so that I acquired "hands on" experience with such tests). Meanwhile, however, my job was to help develop pyrotechnic signals as a member of the Propellants and Pyrotechnics Group.

The adaptations of display fireworks, which were the objects of our efforts, were, for the most part, charges of mixtures of fuels such as charcoal, sulfur, magnesium, sugar, aluminum, iron filings, and sodium oxalate with oxidants, such as potassium, sodium, barium, and strontium nitrates, and potassium chlorate, and perchlorate, which were usually initiated by the flames from fuses, such as Bickford safety fuse. Sensitivity to such initiation was characterized in terms of the maximum gap between the end of the fuse and the surface of the pyrotechnic charge at which the charge was ignited. It seemed to me that the relationship between particle size, compaction, and sensitivity was similar to the relationship between analogous features of the twigs, shavings, or other

"tinder" and ignitability, which I had noted when passing the Boy Scout second class fir building test in 1927. As I saw it then (in 1941) ignition required that some of the fuel be raised to its "ignition temperature", a concept in which I believed (with some reservations) at that time. This seemed to be more easily accomplished with small elements of fuel in not too intimate contact with others.

We used black gunpowder for various purposes, including augmentation of primer output to ignite flair compositions.

In this connection, I learned that "cannon powder" was the coarsest of those we used because black powder as well as other propellants, burns at the surface of the grains so that the coarser grains burn longer to maintain the generation of gas over the longer time that a cannon projectile spends in the barrel. I later read (in Davis (4)) that the "grains" of smokeless powder for large guns are perforated to provide an increasing surface area as the burning progresses and the holes enlarge so that the gas emission rate (which is proportional to the area of the burning surface) keeps pace with an accelerating projectile.

After a year or so with the Propellant and Pyrotechnic Group, I was transferred to the Research Group of the EAU, (supervised by Harry H. Moore) which, as I remember, took on all tasks assigned to the EAU, which were not obviously within the purview of the Propellant and Pyrotechnic Group or the Fuze Group. The Research Group also was responsible for the design and development of some hydrostatic bomb fuzes for antisubmarine warfare (probably because, at some earlier date, the Fuze Group had been too busy with other projects), an area in which I found myself shortly after my transfer to the Research Group. My attempt to design an improved hydrostatic fuze led to the assignment of an attempt to establish fuze explosive train design criteria. Before asking Mr. Moore for fuze explosive train design criteria, I asked members of the Fuze Group, who had designing fuzes for several years. Their approach as I understood it, was that of adapting a successful explosive train to a new fuze, showing their proposed design to their boss, Mr. Ray Graumann. If he approved, They'd have some made and test them. Although I was to find out, some years later, that this was a reasonably sound approach (since Graumann was a nationally recognized authority on fuze design), it didn't satisfy me, or Mr. Moore, at the time, all of which led to the assignment mentioned above. From the members of the Fuze Group, I learned that the word "fuze" was derived

from "fuse", (I had read in Davis (4)) the distinction between the terms, which is quoted hereinbefore and, they said, "fuze" had been defined "by act of Congress" (as has been quoted, from Davis (4) herein).

About the only "fuze explosive train design criterion" I learned from them was the requirement for "of-line safety" to preclude the transmission of detonation from a detonator to the bursting charge until after a fuze had "armed".

Application if this criterion requires a definition or standard of "detonation". The EAU Fuze Group used the visible damage to the metal parts which had held the explosive charge for this purpose, which, in turn, requires a practiced eye. Members of the Fuze Group could, at a glance, recognize evidence of detonation, and even characterize the detonation as "high order" or "low order". Some even identified certain damage as evidence of "high intensity low order".

I was one of over 1700 engineers and scientists recruited by NOL in 1939, '40, and '41 to meet the increasing demands of the preparedness effort in response to the rising hostilities in Europe and the perceived probability that the US would be involved. The new employees, representing a wide range of technical professions and coming from all over the country, saw things from many perspectives, to which we introduced on another. Few of us found ourselves in a position to apply our previous (specific) experience, but most could apply our general technical backgrounds. Lunch time conversations covered a wide range of subjects, mostly more or less technical. Sometime, in 1941, I remember hearing that "Detonation is a special kind of fire." Somewhere else I heard detonation referred to as a "chain reaction". I felt the need for a more meaningful (to me) definition. It seemed to me that such a definition should be more "scientific" than "a special kind of fire", "a chain reaction", or "explosion", (as it is still defined in dictionaries (1, 2, 13)). I didn't believe that "detonation is a distinct phenomenon in which the chemical transformation is induced in every particle of the mass of explosive at the same instant", as defined in an encyclopedia (14). Davis' (4) description of "Propagation of Explosion" which is quoted herein (a few pages back) was more meaningful to me. Davis (4) included a heuristic description of what he referred to as the "propagation of explosion" in black powder (which, now, seems applicable to other "energetic materials" which have gaseous reaction products). Based on impressions I'd gained, from conversations

with other EAU employees, that the burning rate of black powder (and other propellants and explosives) is proportional to pressure, I determined by a simple integration that the pressure, and hence the burning rate of a confined charge of black powder (or other propellant or explosive) must increase exponentially with the passage of time until its container, such as a bomb case or the paper tube of a firecracker, bursts.

What Davis meant by "powder and explosives" is what aerospace engineers seem to mean by "pyrotechnics" and what others mean by "energetic materials."

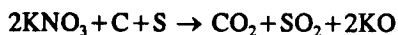
Davis' (4) description provided a perspective of fire (or combustion) including explosion and detonation, which, as Davis pointed out in the paragraph quoted a few pages back, are forms of combustion in that they are dependent upon the transmission of heat. From this explanation, combined with the thermodynamics I had learned in engineering school, I began to see detonation as "The rapid and violent form of combustion in which energy transfer is by mass flow in strong compression waves." Although these words are taken from the opening sentence of "Detonation" by Weldon C. Fickett and William C. Davis (16), (which was published in 1979) they express, more adequately than any that come to mind in 1994, the view I received in 1942 from the book (4) Tenney L. Davis had published the previous year. This view is quite similar to that held today by those who have concerned themselves with detonation, but it is not sufficiently quantitative to serve as a basis for fuze explosive train design criteria. The need for further research was quite apparent.

My assignments, in the Research Group of the EAU, besides the attempt to establish fuze explosive train design criteria, were various, including the adaptation of a motion picture camera (designed for use in the motion picture industry) for "slow motion" recording (from aircraft) of surface effects of underwater explosions, adjusting designs of coil springs, design of loading presses, fuze test gear, blast gages, and mine detonators (to replace those which were adaptations of Nobel's original (1864) blasting cap, (and still in use in the 1940s) with an adaptation of modern (as of the 1940s) commercial blasting caps. When NOL started using "time sheets" to generate records of the distribution of effort among projects, I found myself trying to remember how many hours I had spent, during each past week on each of 42 projects.

Research pursuant to the establishment of fuze explosive train design criteria, at this stage, literature

research, was fit in between other, more urgent efforts. I started with books on desks and shelves in the EAU, including Davis (4), in which I reviewed the parts which have been quoted hereinbefore, and finished reading the 1941 edition, and when it turned up, the 1943 edition. A couple of books on ordnance and explosives, the titles and authors of which I have forgotten, provided a historical perspective, but didn't have much which seemed relevant to fuze design.

The chapters of Davis (4) on BLACK POWDER, PYROTECHNICS, and AROMATIC NITRO COMPOUNDS broadened and sharpened my historical and chemical perspectives of fire (particularly in the forms of explosion and detonation). The use of "Greek fire", a mixture of saltpeter (potassium nitrate) with combustible substance as an incendiary in naval warfare is cited as a progenitor to the discovery that a mixture of potassium nitrate, charcoal, and sulfur is capable of doing useful mechanical work, and the invention of the gun. The chapter traces the evolution of black powder for blasting as well as use as a propellant and includes tables of the proportions of charcoal, sulfur, and saltpeter as described by Marcus Graecus in the 8th century, Roger Bacon in the 13th and others in the 14th, 16th, 17th, and 18th centuries, as well as the stoichiometric equation (2):



for the burning of black powder, and was aware that black powder burns without air because the thermal decomposition of the nitrate releases enough oxygen to oxidize the charcoal, sulfur, and potassium, while the nitrogen forms its own ( $\text{N}_2$ ) molecules.

Davis' (4) chapter on PYROTECHNICS, by which he meant display and amusement fireworks (including such noisemakers as firecrackers, flares, signals, etc.), traces the development of such items from ancient oriental origin to the fireworks we played with as kids on the Fourth of July, and the signals and illuminating flares used by the military, and warning flares used by railroads and highway repair crews. This chapter had been of specific interest to me as a member of the Propellant and Pyrotechnics Group, providing "chemical" and "historical" perspectives of materials with which we were working. Included were tables of compositions for colored lights, flares, fuzes, smokes, marine signals, parade torches, whistles, lances, rockets, Roman candles, stars, fountains, pinwheels, mines, comets, meteors, torpedoes, flash cracker compositions, sparklers, serpents, snakes, etc. (Many of the foregoing terms were, apparently, used in the

sense which had been familiar to me as a kid, shopping in late June and early July in preparation for celebration of the Fourth, rather than in the senses, in which they are used in connection with biology, ordnance, astronomy, or defined in most dictionaries). Consideration of these formulas led to recognition that nitrates other than that of potassium, as well as chlorates perchlorates, etc., have been used as solid providers of oxygen, and increased my awareness that firelight, other than the (black body radiation) of familiar yellow flames, was spectral emission of some elements (such as strontium, which emits red light) in the plasma state and that colored smoke in a colloidal suspension of dye in air.

Davis (4) chapter on AROMATIC NITRO COMPOUNDS, after an introductory paragraph on their usefulness, in which it is stated that they were (when the book was published - in 1941) "the most important class of military high explosives" warns of their toxicity and the fact that they can be absorbed by the skin. A paragraph on the chemistry of these compounds was probably elementary to the graduate students for which the book was written, but for a mechanical engineer, such as I, it was a bit cryptic. I'm not sure, in the 1990s, when I learned that "aromatic compounds" include "benzene rings" "a structural arrangement -- marked by six carbon atoms lined by alternate single and double bonds" (2a), and that a "nitro group" ( $\text{NO}_2$ ) the oxygen atoms are bonded to the nitrogen atom which in an aromatic nitro compound is, in turn bonded to one of the carbon atoms.

Considering the chemistry of aromatic nitro compounds as discussed by Davis (4), and quoted above, from the basic chemical perspective I had acquired in chemistry courses, I saw that, like gunpowder and other pyrotechnics, they contained oxygen sufficient to oxidize at least some of the carbon and hydrogen they contained, but that the oxygen would be available only after decomposition of the nitro groups (or, in the case of black powder, of the potassium nitrate). I can't say, now, when I looked up the heats of formation of the compounds involved, but, when I did, I verified that the reactions were exothermal. These relationships were, of course, obvious to the graduate students in chemistry for which Davis' book (4) was intended, as was the fact that, at the anticipated temperatures of the reaction products (carbon dioxide and water) they were in a gaseous state, so that the product of their pressure and volume was many times those of unreacted solid or liquid unreacted explosives and propellants, as well as



those of gases or explosive mixtures of gases or gases and sols (colloidal suspensions) This, their combustion was considered to be an explosion or detonation if it was fast enough - which, in turn, turns on definitions of explosion and detonation .

## EXPLOSION AND DETONATION

Explosion and detonation are among the many words which, like fire and pyrotechnics have a number of meanings. According to some dictionaries (1,2), they are synonymous, although I doubt that any participant in this workshop considers them to be. Each of the words has a connotation of sudden expansion , and each is derived from a Latin word relating to the sound usually associated with it. Detonation (some meanings of which will be discussed below) is derived from the Latin for thunder while explosion (like applause ) derives from the Latin for clap , but it seems to be mostly commonly used in the sense of bursting of a container such as a boiler or a bomb, but it often means sudden burning as in a dust explosion or that of another explosive mixture of gaseous or finely divided fuel with air.

As observed by chemists and stated in the rule of thumb which has been mentioned in the quotation of Davis' (4) section on Propagation of Explosion that any ---- chemical reaction, doubles its rate with each 10°C (approximate) rise of temperature, so that exothermal reactions (in which heat is evolved) tend to be self accelerating. If, as is usual, their reaction products include one or more gases, the pressure rises, if they are confined, until the container bursts. Since surface or grain burning rates of propellants, explosives and explosive mixtures increase with increasing pressure (17), such burning is self accelerating and the pressure and rate increase, exponentially with time. Either the bursting of a container or self accelerating process is an explosion in one or another of the senses mentioned above. (Self accelerating fire is referred to as thermal explosion ). This association has led to the use of explosion to mean any self accelerating process, such as in population explosion (which seems sudden only from such perspectives as historical or geological ).

In lunchtime conversations, I had hear detonation defined in several sets of terms. Dictionaries and encyclopedias included definitions and descriptions which didn't satisfy me. Davis' (4), discussion (which has been quoted herein) gave me the clearest (though still somewhat fuzzy) view of the process I had

acquired until my literature search in the areas of explosives and detonation extended beyond the shelves and desks of the EAU. Davis' (4), in the section on Propagation of Explosion ,, which has been quoted herein, made the transition to the discussion of detonation with the statement that The explosion of a primary explosive or of a high explosive is believed to be a phenomenon which is dependent upon pressure or, perhaps more properly, on transmission of shock . The propagation of detonation mercury fulminate is described as a reaction which produces hot gas and is so rapid that the advancing front of the mass of hot gas amounts to a pressure wave capable of initiating by its shock the next portion of fulminate . The high velocities of propagation of detonation (3500 meters per second in the fulminate of a blasting cap and much higher in TNT) are mentioned. Although Davis (4) didn't consider shock or detonation waves from physical, thermodynamic, or hydrodynamic perspectives, his discussion left me with the impression that consideration from such perspectives would be appropriate, an impression which was to be verified when I started reading OSRD reports.

As I recall, the other books on the desks and shelves of the EAU, which included a couple of books on ordnance, one, by a hobbyist, on fireworks, and the Dupont Blasters Handbook , considered their subjects from practical , empirical , and historical perspectives, omitting discussion of chemical or physical aspects of their subjects.

On the NOL library, I found the War Department (which, after a decade or so, was to become the Department of the Army) and Bureau of Mines documents which had been cited by Davis (4) and others from these sources and from Picatinny Arsenal, Frankford Arsenal, the Ballistics Research Laboratory (BRL) at Aberdeen, MD., the Naval Powder Factory at Indian Head, Md., the Franklin Institute, the Bureau of Standards, and the British Ministry of Supply and Ordnance Board. I found these documents informative, interesting, and (some of them) quite pertinent to my objective of establishing fuze explosive train design criteria, but none contained much to clarify my views of explosion or detonation except for a few OSRD reports.

## REFERENCES

- (1) Stein, Jess, (editor), The Random House Dictionary of the English Language, Random House, Inc. 1966-1967.
- (2) Webster's Twentieth Century Dictionary of the English Language (unabridged), Publisher's Guild, Inc., New York, N.Y., 1939.
- (2½) McCrone, John C., The Ape that Spoke, William Morrow and Company, Inc., New York, N.Y., 1991.
- (3) Calvin, William H., The Ascent of the Mind, Ice Age Climates and the Evolution of Intelligence, Bantam Books, New York, Toronto, London, Sydney, Auckland, 1990.
- (4) Davis, Tenney L., The Chemistry of Powder and Explosives, John Wiley & Sons, Inc., New York, 1941, 1943.
- (5) Asimov, Isaac, Asimov's Biographical Encyclopedia of Science and Technology, Doubleday & Company, Inc., Garden City, N.Y., 197.
- (6) Gamow, George, One Two Three...Infinity, The Viking Press, New York, 1947.
- (6½) Bradbury, Fahrenheit 451, Simon and Shuster, New York.
- (7) Wells, Robert W., Fire and Ice, Two Deadly Wisconsin Disasters, Fire at Peshtigo, Northword, Madison, WI, 1968.
- (8) Gamow, George, Thirty Years That Shook Physics, Doubleday & Co. (Science Study Series). New York, N.Y. 1966.
- (9) Langdon-Davies, John, Inside the Atom, Harper & Brothers, New York and London, 1933.
- (10) Weast, Robert C. (editor), and Astle, Melvin J. (associate editor), CRC Handbook of Chemistry and Physics, 63rd Edition, CRC Press, Inc., Boca Raton, FL. 1982-1983.
- (11) Eschbach, Ovid W., Handbook of Engineering Fundamentals, Third Edition, Wiley, New York.
- (12) Chapman, D.L., "On the Rate of Explosion of Gases", Philosophical Magazine (5), V. 47, p. 90, 1999.
- (13) Jouguet, E., 4echanique des Rxploszifs" Paris, O. Doin et Fils, Editeurs, 1817.
- (14) The Grolier Society, Grolier Encyclopedia, Vol. 4, 1931-1951.
- (15) Brady, George S., and Clauser, Henry R., Materials Handbook, McGraw-Hill Book Co., New York, etc., etc. 1977.
- (16) Soukhanov, Anne M., (Executive Editor), The American Heritage Dictionary of the English Language, Houghton-Mifflin, Boston, New York, London, 1972.
- (17) Fickett, Wildon, and Davis, William C. Detonation, University of California Press, Berkeley, Los Angeles, London, 1979.
- (18) Smithsonian Tables.
- (19) Henkin, T. "Determination of Explosion Temperatures", OSRD 1986, November 1943. (Later published with McGill, R., in the Journal of Engineering and Industrial Chemistry 44, 1391, 1952.
- (20) Kabik, I., Rosenthal, L. A., and Solem, A.D., "The Response of Electroexplosive Devices to Transient Electrical Pulses" 3rd Electrical Initiator Symposium, Paper #18, 1960.

*[Editor's Note: Time and space precludes completion of Mr. Stresau's paper. He does plan to publish the entire story as a Stresau Laboratories, Inc. report at a later date. Interested readers may contact him at:*  
*Stresau Company*  
*W7882 Stresau Lane*  
*Spooner, WI 54801 J*

## APPENDIX - List of Participants

|  |   |
|--|---|
| <p>Aerojet Propulsion Division ..... Hansen, Jeff</p> <p>Aerospace Corporation, The ..... Gageby, James</p> <p>Aerospace Corporation, The ..... Goldstein, Selma</p> <p>Aerospace Corporation, The ..... Wong, T. Eric</p> <p>American Safety Flight Systems, Inc. .... Ziegler, Ron</p> <p>Analex Corporation ..... Smith, Floyd</p> <p>Analex Corporation ..... Steffes, Paul</p> <p>Attenuation Technology, Inc. .... Dow, Robert L.</p> <p>Boeing Defense &amp; Space Group .. Robinson, Steven P.</p> <p>Conax Florida Corporation ..... Nowakowski, Don</p> <p>Consultant ..... Folsom, Mark</p> <p>Consultant ..... Gans, Werner A.</p> <p>Consultant ..... O'Barr, Gerald L.</p> <p>EG&amp;G Mound Applied Tech. .... Beckman, Thomas M.</p> <p>EG&amp;G Mound Applied Tech. .... Kramer, Daniel</p> <p>EG&amp;G Mound Applied Tech. .... Munger, Alan C.</p> <p>EG&amp;G Mound Applied Tech. .... Spangler, Ed</p> <p>Energetic Materials Technology .... Ostrowski, Peter</p> <p>Ensign Bickford Aerospace Co. .... Graham, John A.</p> <p>Ensign Bickford Aerospace Co. .... Renfro, Steven L.</p> <p>Ensign Bickford Aerospace Co. .... Rhea, Arthur D.</p> <p>Franklin Applied Physics ..... Thompson, Ramie</p> <p>Geo-Centers, Inc. .... Landry, Murphy J.</p> <p>Halliburton Energy Services</p> <p style="padding-left: 20px;">Explosive Products Center ... Barker, James</p> <p>Halliburton Energy Services</p> <p style="padding-left: 20px;">Explosive Products Center ... Motley, Jerry</p> <p>Hercules Aerospace ..... Cole, David A.</p> <p>Hercules Inc. .... McAllister, Pat V.</p> <p>Hi-Shear Technology Corp. .... Novotny, Don</p> <p>Hi-Shear Technology Corp. .... Webster, Richard</p> <p>Inland Fisher Guide Div. of GM ..... Wirrig, Steven T.</p> <p>John Hopkins University - CPIA ..... Filliben, Jeff</p> <p>Los Alamos National Laboratory .... Kennedy, James</p> <p>Martin Marietta Specialty Components ... Hinkle, Lane</p> <p>Martin Marietta Astronautics ..... Wood, Lance</p> <p>McDonnell Douglas ..... Tierney, Michael</p> <p>McDonnell Douglas Aerospace ..... Whalley, Ian</p> <p>McDonnell Douglas Space Sys. ... Parenzan, James E.</p> <p>Morton International Inc. .... Hansen, David</p> <p>Morton International Inc. .... Richardson, Bill</p> <p>NASA Headquarters ..... Schulze, Norman R.</p> <p>NASA Goddard Space Flight Center .. Bajpayee, Jaya</p> <p>NASA Johnson Space Center ..... Hoffman, William</p> <p>NASA Kennedy Space Center ..... Rayburn, Larry</p> <p>NASA Langley Research Center ..... Bement, Larry</p> <p>NASA Lewis Research Center ..... Seeholzer, Tom</p> <p>NASA Stennis Space Center .... St. Cyr, William W.</p> <p>Naval Surface Warfare Center</p> <p style="padding-left: 20px;">Indian Head Division ..... Blachowski, Tom</p> <p>Naval Surface Warfare Center</p> <p style="padding-left: 20px;">Indian Head Division ..... Hinds, Jeffery L.</p> <p>Naval Surface Warfare Center</p> <p style="padding-left: 20px;">Indian Head Division ..... Krivitsky, Darrin</p> <p>Naval Surface Warfare Center</p> <p style="padding-left: 20px;">Indian Head Division ..... Martin, Steve</p> <p>Naval Surface Warfare Center</p> <p style="padding-left: 20px;">Crane Division ..... Schlamp, Jan N.</p> | <p>Olin Rocket Research Co. .... Moran, Joe</p> <p>Olin Rocket Research Co. .... Watson, Bruce</p> <p>Pacific Scientific Corp. .... Cunnington, Rick</p> <p>Pacific Scientific Corp. .... Day, Bob</p> <p>Pacific Scientific Corp. .... Greenslade, John T.</p> <p>Pacific Scientific Corp. .... LaFrance, Bob</p> <p>Pacific Scientific Corp. .... Schuman, Alex</p> <p>Pacific Scientific Corp. .... Smith, Bob</p> <p>Pacific Scientific Corp. .... Spomer, Ed</p> <p>Pacific Scientific Corp. .... Todd, Michael C.</p> <p>Pacific Scientific Corp. .... VonDerAhe, Ken</p> <p>Pacific Scientific Corp. .... Walsh, Tom</p> <p>Quantic Industries, Inc. .... Willis, Kenneth E.</p> <p>Reynolds Industries Systems, Inc. .... Varosh, Ron</p> <p>Rockwell International Corp. .... Cascadden, Raymond</p> <p>Rockwell International Corp. .... Erazo, Anibal</p> <p>Sandia National Laboratories ..... Andrews, Larry A.</p> <p>Sandia National Laboratories ... Bickes Jr., Robert W.</p> <p>Sandia National Laboratories ..... Bonzon, Lloyd L.</p> <p>Sandia National Laboratories .... Brigham, William P.</p> <p>Sandia National Laboratories ..... Chow, Weng W.</p> <p>Sandia National Laboratories ..... Cooper, Paul</p> <p>Sandia National Laboratories ..... Curtis, William</p> <p>Sandia National Laboratories ..... Fleming, Kevin J.</p> <p>Sandia National Laboratories ..... Grubelich, M. C.</p> <p>Sandia National Laboratories ..... Harlan, Jere G.</p> <p>Sandia National Laboratories .... Holswade, Scott C.</p> <p>Sandia National Laboratories ..... Kass, William</p> <p>Sandia National Laboratories ..... Merson, John A.</p> <p>Sandia National Laboratories ..... Metzinger, Kurt</p> <p>Sandia National Laboratories ..... Mitchell, Dennis E.</p> <p>Sandia National Laboratories ..... Salas, F. Jim</p> <p>Sandia National Laboratories ..... Setchell, Robert E.</p> <p>Sandia National Laboratories .... Stichman, Dr. John</p> <p>Sandia National Laboratories ..... Troh, Wayne M.</p> <p>Sandia National Laboratories ..... Williams, T. J.</p> <p>Santa Barbara Research Center .... Gonzales, Roman</p> <p>Santa Barbara Research Center ..... Jeter, James</p> <p>SCB Technologies, Inc. .... McCampbell, C. B.</p> <p>Schimmel Company ..... Schimmel, Morry L.</p> <p>Special Devices, Inc. .... Sipes, William J.</p> <p>Special Devices, Inc. .... Talle, Dennis</p> <p>Stresau Company ..... Stresau, Richard</p> <p>Teledyne McCormick Selph ..... Ingnam, Robert W.</p> <p>Teledyne McCormick Selph ..... Marshall, Clyde</p> <p>Teledyne McCormick Selph ..... Smith, Brian</p> <p>TPL Inc. .... Brown, Ralph</p> <p>United Technologies/USBI ..... Webster, Charles F.</p> <p>Universal Propulsion Co., Inc. .... Barlog, Stan</p> <p>Universal Propulsion Co., Inc. .... Magenot, Michael C.</p> <p>Universal Propulsion Co., Inc. .... Mayville, Wayne</p> <p>Universal Propulsion Co., Inc. .... Wergen, Tom</p> <p>University of Notre Dame ..... Gonthier, Keith A.</p> <p>University of Notre Dame ..... Powers, Joseph M.</p> <p>USAF/30 SW/SESX ..... Gotfraind, Mark</p> <p>USAF/45SPW/SESE ..... Wadzinski, Mike</p> <p>USAF/B-1B Engineering Branch ..... Tipton, Steve</p> <p>USAF/Ogden Air Logistics Center .... Kangas, Charles</p> <p>UTC/Chemical Systems Division ..... Lai, K. S.</p> <p>ZZYZX ..... Potter, Jed</p> |
|--|---|

Larry A. Andrews  
Sandia National Laboratories  
P.O. Box 5800  
Albuquerque, NM 87185-5800

Jaya Bajpayee  
NASA Goddard Space Flight Center  
Wallops Flight Facility - Bldg N-159  
Wallops Island, VA 23337  
(804) 824-2374 (FAX) 824-1518

James Barker  
Halliburton Energy Services  
Explosive Products Center  
2001 S. I35  
Alvarado, TX 76009  
(817) 783-5111 (FAX) 783-5812

Stan Barlog  
Universal Propulsion Co., Inc.  
25401 North Central Ave.  
Phoenix, AZ 85027-7837  
(602) 869-8067 (FAX) 869-8176

Thomas M. Beckman  
EG&G Mound Applied Technologies  
P.O. Box 3000  
Miamisburg, OH 45343-0987  
(513) 865-4551 (FAX) 865-3491

Larry Bement  
NASA Langley Research Center  
Code 433  
Hampton, VA 23681-0001  
(804) 864-7084 (FAX) 864-7009

Robert W. Bickes Jr.  
Sandia National Laboratories  
P.O. Box 5800  
Albuquerque, NM 87185-0326  
(505) 844-0423 (FAX) 844-5924

Tom Blachowski  
Naval Surface Warfare Center  
Indian Head Division - Code 5240E  
101 Strauss Ave.  
Indian Head, MD 20640-5035  
(301) 743-4243 (FAX) 743-4881

Lloyd L. Bonzon  
Sandia National Laboratories  
P.O. Box 5800  
Albuquerque, NM 87185-0327  
(505) 845-8989 (FAX) 844-5924

William P. Brigham  
Sandia National Laboratories  
P.O. Box 5800  
Albuquerque, NM 87185-0327  
(505) 845-9107 (FAX) 844-0820

Ralph Brown  
TPL Inc.

Raymond Cascadden  
Rockwell International Corporation  
201 N. Douglas St.  
El Segundo, CA 90245  
(310) 414-1655 (FAX) 414-2077

Weng W. Chow  
Sandia National Laboratories  
Division 2235  
P.O. Box 5800  
Albuquerque, NM 87185-5800  
(505) 844-9088 (FAX) 844-8168

David A. Cole  
Hercules Aerospace  
P.O. Box 210  
Rocket Center, WV 26726  
(304) 726-5489 (FAX) 726-4730

Paul Cooper  
Sandia National Laboratories  
M/S 1156  
P.O. Box 5800  
Albuquerque, NM 87185-5800  
(505) 845-7210 (FAX) 845-7602

Rick Cunnington  
Pacific Scientific Corp.  
Energy Dynamics Division  
7073 West Willis Road, Box 5002  
Chandler, AZ 85226-5111  
(602) 796-1100 (FAX) 796-0754

William Curtis  
Sandia National Laboratories  
P.O. Box 5800  
Albuquerque, NM 87185  
(505) 845-9649 (FAX) 844-4616

Bob Day  
Pacific Scientific Corp.  
7073 West Willis Road, Box 5002  
Chandler, AZ 85226-5111

Robert L. Dow  
Attenuation Technology, Inc.  
9674 Charles Street  
La Plata, MD 20646  
(301) 934-3725 (FAX) 934-3725

Anibal Erazo  
Rockwell International Corporation  
201 N. Douglas St.  
El Segundo, CA 90245  
(310) 647-2756 (FAX) 647-6824

Jeff Filliben  
John Hopkins University - CPIA  
10630 Little Patuxent Parkway  
Suite 202  
Columbia, MD 21044-3200  
(410) 992-7305 (FAX) 730-4969

Kevin J. Fleming  
Sandia National Laboratories  
P.O. Box 5800  
Albuquerque, NM 87185-0327  
(505) 845-8763 (FAX) 844-0820

Mark Folsom  
Consultant  
25747 Carmel Knolls Drive  
Carmel, CA 93923  
(408) 626-8252 (FAX) 626-1652

James Gageby  
The Aerospace Corporation  
MS M4/907  
2350 E. El Segundo Blvd.  
El Segundo, CA 90245  
(310) 336-7227 (FAX) 336-1474

Werner A. Gans  
Consultant  
1015 Lanark Ct.  
Sunnyvale, CA 94089  
(408) 245-2857

Selma Goldstein  
The Aerospace Corporation  
MS M4-907  
P.O. Box 92957  
Los Angeles, CA 90009-2957  
(310) 336-1013 (FAX) 336-1474

Keith A. Gonthier  
University of Notre Dame  
Aerospace & Mechanical Engineering  
365 Fitzpatrick Hall  
Notre Dame, IN 46556-5637  
(219) 239-6426 (FAX) 239-8341

Roman Gonzales  
Santa Barbara Research Center  
Hughes Aircraft Company  
75 Coromar Drive B30/12  
Goleta, CA 93117  
(805) 562-7705 (FAX) 562-7882

Mark Gotfraind  
U. S. Air Force/30th Space Wing  
30 SW/SESX  
922 N. Brian St.  
Santa Maria, CA 93454  
(805) 928-9637

John A. Graham  
Ensign Bickford Aerospace Co.  
640 Hopmeadow St.  
P.O. Box 427  
Simsbury, CT 06070  
(203) 843-2325

John T. Greenslade  
Pacific Scientific Corp.  
Energy Dynamics Division  
7073 West Willis Road, Box 5002  
Chandler, AZ 85226-5111  
(602) 796-1100 (FAX) 796-0754

M. C. Grubelich  
Sandia National Laboratories  
P.O. Box 5800  
Albuquerque, NM 87185-0326  
(505) 844-9052 (FAX) 844-4709

David Hansen  
Morton International Inc.  
M/S X1830  
3350 Airport Road  
Ogden, UT 84405  
(801) 625-9222 (FAX) 625-4949

Jeff Hansen  
Aerojet Propulsion Division  
Bldg. 2019A2, Dept. 5274  
P.O. Box 13222  
Sacramento, CA 95813-6000  
(916) 355-6102 (FAX) 355-6543

Jere G. Harlan  
Sandia National Laboratories  
P.O. Box 5800  
Albuquerque, NM 87185-0329  
(505) 844-4401 (FAX) 844-4709

Jeffery L. Hinds  
Naval Surface Warfare Center  
Indian Head Division - Code 520  
101 Strauss Ave.  
Indian Head, MD 20640-5035  
(301) 743-6530 (FAX) 743-4881

Lane Hinkle  
Martin Marietta Specialty Components  
P.O. Box 2908  
Largo, FL 34649-2908  
(813) 541-8222 (FAX) 545-6757

William Hoffman  
NASA Johnson Space Center  
Code EP5  
2201 NASA Road One  
Houston, TX 77058  
(713) 483-9056 (FAX) 483-3096

Scott C. Holswade  
Sandia National Laboratories  
P.O. Box 5800  
Albuquerque, NM 87185-0328

Robert W. Ingham  
Teledyne McCormick Selph  
3601 Union Road  
P.O. Box 6  
Hollister, CA 95024-0006  
(408) 637-3731 (FAX) 637-5494

James Jeter  
Santa Barbara Research Center  
Hughes Aircraft Company  
75 Coromar Drive  
Goleta, CA 93117  
(805) 562-7539 (FAX) 562-7740

Charles Kangas  
USAF/Ogden Air Logistics Center  
OO-ALC/LIWCE  
6033 Elm Lane  
Hill AFB, UT 84056  
(801) 777-4135 (FAX) 777-9484

William Kass  
Sandia National Laboratories  
Division 2234  
P.O. Box 5800  
Albuquerque, NM 87185-5800  
(505) 844-6844 (FAX) 844-8168

James E. Kennedy  
Los Alamos National Laboratory  
MS - P950  
Los Alamos, NM 87545  
(505) 667-1468 (FAX) 667-6301

Daniel Kramer  
EG&G Mound Applied Technologies  
P.O. Box 3000  
Miamisburg, OH 45343-0987  
(513) 865-3558 (FAX) 865-3680

Darrin Krivitsky  
Naval Surface Warfare Center  
Indian Head Division - Code 5240E  
101 Strauss Ave.  
Indian Head, MD 20640-5035

Bob LaFrance  
Pacific Scientific Corp.  
Energy Systems Division  
7073 West Willis Road, Box 5002  
Chandler, AZ 85226-5111  
(602) 961-0023 (FAX) 961-0577

K. S. Lai  
UTC/Chemical Systems Division  
P.O. Box 49028  
San Jose, CA 95161-9028  
(408) 776-4327 (FAX) 776-4444

Murphy J. Landry  
Geo-Centers, Inc.  
2201 Buena Vista Dr., SE  
Albuquerque, NM 87106  
(505) 243-3483 (FAX) 242-9497

Michael C. Magenot  
Universal Propulsion Co., Inc.  
25401 North Central Ave.  
Phoenix, AZ 85027-7837

Clyde Marshall  
Teledyne McCormick Selph  
8920 Quartz Ave.  
Northridge, CA 91324  
(818) 718-6643 (FAX) 998-3312

Steve Martin  
Naval Surface Warfare Center  
Indian Head Division  
101 Strauss Ave.  
Indian Head, MD 20640-5000  
(301) 743-4243 (FAX) 743-4881

Wayne Mayville  
Universal Propulsion Co., Inc.  
25401 North Central Ave.  
Phoenix, AZ 85027-7837  
(602) 869-8067 (FAX) 869-8176

Pat V. McAllister  
Hercules Inc.  
M/S N1EA1  
P.O. Box 98  
Magna, UT 84044  
(801) 251-6192 (FAX) 251-6676

C. B. McCampbell  
SCB Technologies, Inc.  
1009 Bradbury Dr. S.E.  
Albuquerque, NM 87106

John A. Merson  
Sandia National Laboratories  
P.O. Box 5800  
Albuquerque, NM 87185-0329  
(505) 844-2756 (FAX) 844-4709

Kurt Metzinger  
Sandia National Laboratories  
Structrual Mechanics Group 1562  
P.O. Box 5800  
Albuquerque, NM 87185-5800  
(505) 844-5077

Dennis E. Mitchell  
Sandia National Laboratories  
P.O. Box 5800  
Albuquerque, NM 87185-0522  
(505) 845-8656 (FAX) 844-3894

Joe Moran  
Olin Rocket Research Co.  
P.O. Box 97009  
Redmond, WA 98073-9709  
(206) 885-5000 (FAX) 882-5744

Jerry Motley  
Halliburton Energy Services  
Explosive Products Center  
2001 S. I35  
Alvarado, TX 76009  
(817) 783-5111 (FAX) 783-5812

Alan C. Munger  
EG&G Mound Applied Technologies  
P.O. Box 3000  
Miamisburg, OH 45343-0987  
(513) 865-3544 (FAX) 865-3491

Don Novotny  
Hi-Shear Technology Corp.  
24225 Garnier Street  
Torrance, CA 90509-5323  
(310) 784-7857 (FAX) 325-5354

Don Nowakowski  
Conax Florida Corporation  
2801 75th Street North  
St. Petersburg, FL 33710  
(813) 345-8000 FAX: 345-4217

Gerald L. O'Barr  
6441 Dennison St.  
San Diego, CA 92122  
(619) 453-0071

Peter Ostrowski  
Energetic Materials Technology  
P.O. Box 6931  
Alexandria, VA 22306-0931  
(703) 780-5854 (FAX) 780-4955

James E. Parenzan  
McDonnell Douglas Space Systems Co.  
MS A3/11-1/L292  
5301 Bolsa Ave.  
Huntington Beach, CA 92647  
(714) 896-5778 (FAX) 896-1597

Jed Potter  
ZZYZX  
25341 Via Oriol  
Valencia, CA 91355  
(805) 259-9491

Joseph M. Powers  
University of Notre Dame  
Aerospace & Mechanical Engineering  
365 Fitzpatrick Hall  
Notre Dame, IN 46556-5637  
(219) 631-5978 (FAX) 631-8341

Larry Rayburn  
NASA Kennedy Space Center  
NASA Shuttle Pyrotechnic Engineering  
Code TV, MS D-23  
Kennedy Space Center, FL 32899  
(407) 861-3652 (FAX) 867-2167

Steven L. Renfro  
Ensign Bickford Aerospace Co.  
640 Hopmeadow St.  
P.O. Box 427  
Simsbury, CT 06070  
(203) 843-2403 (FAX) 843-2621

Arthur D. Rhea  
Ensign Bickford Aerospace Co.  
640 Hopmeadow St.  
P.O. Box 427  
Simsbury, CT 06070  
(203) 843-2360 (FAX) 843-2621

Bill Richardson  
Morton International Inc.  
M/S X1870  
3350 Airport Road  
Ogden, UT 84405  
(801) 625-8222 (FAX) 625-4949

Steven P. Robinson  
Boeing Defense & Space Group  
M/S 81-05  
P.O. Box 3999  
Seattle, WA 98124-2499  
(206) 773-1894 (FAX) 773-4846

William W. St. Cyr  
NASA Stennis Space Center  
Code KA22 Building 1100  
Stennis Space Center, MS 39529-6000  
(601) 688-1134 (FAX) 688-3312

F. Jim Salas  
Sandia National Laboratories  
P.O. Box 5800  
Albuquerque, NM 87185-0329  
(505) 844-3265 (FAX) 844-4709

Morry L. Schimmel  
Schimmel Company  
8127 Amherst Avenue  
St. Louis, MO 63130  
(314) 863-7725 (FAX) 727-8107

Jan N. Schlamp  
Naval Surface Warfare Center  
Code 4073  
300 Highway 361  
Crane, IN 47522-5001  
(812) 854-5431 (FAX) 854-1711

Norman R. Schulze  
National Aeronautics  
and Space Administration  
Code QW  
Washington, DC 20546  
(202) 358-0537 (FAX) 358-2778

Alex Schuman  
Pacific Scientific Corp.  
Energy Dynamics Division  
Box 750  
Litchfield Park, AZ 85340  
(602) 932-8409 (FAX) 932-8949

Tom Seeholzer  
NASA Lewis Research Center  
Code 4330 M/S 86-10  
21000 Brookpark Road  
Cleveland, Ohio 44135  
(216) 433-2523 FAX 433-6382



Robert E. Setchell  
Sandia National Laboratories  
Department 5166  
P.O. Box 5800  
Albuquerque, NM 87185-0445  
(505) 844-3847 (FAX) 844-7431

William J. Sipes  
Special Devices, Inc.  
16830 West Placerita Canyon Road  
Newhall, CA 91321  
(805) 259-0753 (FAX) 254-4721

Bob Smith  
Pacific Scientific Corp.  
102 South Litchfield Road  
Goodyear, AZ 85338-1295  
(602) 932-8450 (FAX) 932-8949

Brian Smith  
Teledyne McCormick Selph  
3601 Union Road  
P.O. Box 6  
Hollister, CA 95024-0006  
(408) 637-3731 (FAX) 637-5494

Floyd Smith  
Analex Corporation  
3001 Aerospace Parkway  
Brookpark, OH 44142-1003  
(216) 977-0201 (FAX) 977-0200

Ed Spangler  
EG&G Mound Applied Technologies  
P.O. Box 3000  
Miamisburg, OH 45343-3000  
(513) 865-3528 (FAX) 865-3491

Ed Spomer  
Pacific Scientific Corp.  
Energy Dynamics Division  
102 South Litchfield Road  
Goodyear, AZ 85338-1295  
(602) 932-8100 (FAX) 932-8949

Paul Steffes  
Analex Corporation  
3001 Aerospace Parkway  
Brookpark, OH 44142-1003  
(216) 977-0123 (FAX) 977-0200

Dr. John Stichman  
Sandia National Laboratories  
Surety Components and  
Instrumentation Center  
P.O. Box 5800  
Albuquerque, NM 87185-5800

Richard Stresau  
Stresau Company  
Star Route  
Spooner, WI 54801  
(715) 635-8497

Dennis Talle  
Special Devices, Inc.  
16830 West Placerita Canyon Road  
Newhall, CA 91321  
(805) 259-0753 (FAX) 254-4721

Ramie Thompson  
Franklin Applied Physics  
98 Highland Ave.  
P.O. Box 313  
Oaks, PA 19456  
(215) 666-6645 (FAX) 666-0173

Michael Tierney  
McDonnell Douglas  
10171 Halawa Dr.  
Huntington Beach, CA 92646  
(714) 963-7242 (FAX) 896-6995

Steve Tipton  
USAF/B-1B Engineering Branch  
Air Logistics Center (AFMC)  
3001 Staff Drive, STE 2AA86A  
Tinker AFB, OK 73145-3006  
(405) 736-7444 (FAX) 736-3714

Michael C. Todd  
Pacific Scientific Corp.  
Energy Systems Division  
7073 West Willis Road, Box 5002  
Chandler, AZ 85226-5111  
(602) 796-1100 (FAX) 796-0754

Wayne M. Troh  
Sandia National Laboratories  
M/S 1512  
P.O. Box 5800  
Albuquerque, NM 87185-5800  
(505) 844-9516 (FAX) 844-8251

Ron Varosh  
Reynolds Industries Systems, Inc.  
3420 Fostoria Way  
San Ramon, CA 94583  
(510) 866-0650 (FAX) 866-0564

Ken VonDerAhe  
Pacific Scientific Corp.  
Energy Systems Division  
7073 West Willis Road, Box 5002  
Chandler, AZ 85226-5111  
(602) 796-1100 (FAX) 796-0754

Mike Wadzinski  
USAF/45SPW/SESE  
1201 Minuteman St.  
Patrick Air Force Base, FL 32925  
(407) 494-7629 (FAX) 494-6535

Tom Walsh  
Pacific Scientific Corp.  
7073 West Willis Road, Box 5002  
Chandler, AZ 85226-5111

Bruce Watson  
Olin Rocket Research Co.  
P.O. Box 97009  
Redmond, WA 98073-9709  
(206) 885-5000 (FAX) 882-5804

Charles F. Webster  
United Technologies/USBI  
M/S EN  
P.O. Box 1900  
Huntsville, AL 35811  
(205) 721-2342 (FAX) 721-2263

Richard Webster  
Hi-Shear Technology Corp.  
24225 Garnier Street  
Torrance, CA 90509-5323  
(310) 784-7867 (FAX) 325-5354

Tom Wergen  
Universal Propulsion Co., Inc.  
25401 North Central Ave.  
Phoenix, AZ 85027-7837  
(602) 869-8067 (FAX) 869-8176

Ian Whalley  
McDonnell Douglas Aerospace  
M/S A3-L292/11-1  
5301 Bolsa Ave.  
Huntington Beach, CA 92647  
(714) 896-6491 (FAX) 896-1106

T. J. Williams  
Sandia National Laboratories  
P.O. Box 5800  
Albuquerque, NM 87185-5800  
(505) 844-3356 (FAX) 844-4616

Kenneth E. Willis  
Quantic Industries, Inc.  
900 Commercial Street  
San Carlos, CA 94070-4084  
(415) 637-3074 (FAX) 592-4669

Steven T. Wirrig  
Inland Fisher Guide Division of GM  
250 Northwoods Blvd. M/S 110  
Vandalia, OH 45377  
(513) 356-2271 (FAX) 356-2280

T. Eric Wong  
The Aerospace Corporation  
MS M4/901  
2350 E. El Segundo Blvd.  
El Segundo, CA 90245  
(310) 336-6190 (FAX) 336-1474

Lance Wood  
Martin Marietta Astronautics  
Mail Stop 5450  
P.O. Box 179  
Denver, CO 80201  
(303) 971-1218 (FAX) 977-1940

Ron Ziegler  
American Safety Flight Systems, Inc.  
11605 Rivera Road, NE  
Albuquerque, NM 87111-5336  
(505) 294-1645 (FAX) 294-1645

# REPORT DOCUMENTATION PAGE

Form Approved  
OMB No. 0704-0188

Public reporting burden for this collection of information is estimated to average 1 hour per response, including the time for reviewing instructions, searching existing data sources, gathering and maintaining the data needed, and completing and reviewing the collection of information. Send comments regarding this burden estimate or any other aspect of this collection of information, including suggestions for reducing this burden, to Washington Headquarters Services, Directorate for Information Operations and Reports, 1215 Jefferson Davis Highway, Suite 1204, Arlington, VA 22202-4302, and to the Office of Management and Budget, Paperwork Reduction Project (0704-0188), Washington, DC 20503.

|   |   |  |  |  |
|---|---|--|--|--|
| 1. AGENCY USE ONLY (Leave blank)  |   | 2. REPORT DATE<br>February 1994                            | 3. REPORT TYPE AND DATES COVERED<br>CP February 8-9, 1995  |  |
| 4. TITLE AND SUBTITLE<br>Second NASA Aerospace Pyrotechnics Systems Workshop  |   |  | 5. FUNDING NUMBERS   |  |
| 6. AUTHOR(S)<br>William W. St. Cyr, compiler  |   |  |  |  |
| 7. PERFORMING ORGANIZATION NAME(S) AND ADDRESS(ES)<br>National Aeronautics and Space Administration<br>John C. Stennis Space Center<br>Code KA60 Building 1100<br>Stennis Space Center, MS 39529-6000   |   |  | 8. PERFORMING ORGANIZATION<br>REPORT NUMBER<br><br>CP 3258 |  |
| 9. SPONSORING/MONITORING AGENCY NAME(S) AND ADDRESS(ES)<br>Office of Safety and Mission Quality<br>Code QW<br>NASA Headquarters<br>Washington, D.C. 20546   |   |  | 10. SPONSORING/MONITORING<br>AGENCY REPORT NUMBER          |  |
| 11. SUPPLEMENTARY NOTES<br>Hosted by Sandia National Laboratories<br>Albuquerque, New Mexico  |   |  |  |  |
| 12a. DISTRIBUTION/AVAILABILITY STATEMENT<br><br>Unlimited   |   |  | 12b. DISTRIBUTION CODE                                     |  |
| 13. ABSTRACT (Maximum 200 words)<br><br>This NASA Conference Publication contains the proceedings of the Second NASA Aerospace Pyrotechnics Systems Workshop held at Sandia National Laboratories, Albuquerque, New Mexico, February 8-9, 1994. The papers are grouped by sessions:<br>Session 1 - Laser Initiation and Laser Systems<br>Session 2 - Electric Initiation<br>Session 3 - Mechanisms & Explosively Actuated Devices<br>Session 4 - Analytical Methods and Studies<br>Session 5 - Miscellaneous<br>A sixth session, a panel discussion and open forum, concluded the workshop. |   |  |  |  |
| 14. SUBJECT TERMS<br>Pyrotechnics, laser ordnance, safety, pyrotechnic database<br>and catalogue, electric initiation, explosively actuated devices, laser<br>safe and arm system, mechanisms, modeling of pyros.   |   |  | 15. NUMBER OF PAGES<br>388                                 |  |
|   |   |  | 16. PRICE CODE   |  |
| 17. SECURITY CLASSIFICATION<br>OF REPORT<br>Unclassified  | 18. SECURITY CLASSIFICATION<br>OF THIS PAGE<br>Unclassified | 19. SECURITY CLASSIFICATION<br>OF ABSTRACT<br>Unclassified | 20. LIMITATION OF ABSTRACT                                 |  |